CHAPTER 12

Behavioral Response to Fire and Smoke

John L. Bryan

Introduction

The determination of the behavioral response of individuals in fire incidents has been examined for approximately 40 years by research studies. Individuals were administered a questionnaire by fire department personnel at the time of a fire incident,[1,2] were mailed questionnaires, or were interviewed following the fire incident. An individual's behavioral response in a fire incident appears to be affected by

1. The variables of the building in which the fire incident occurs
2. The perceived physical cues of the fire severity at the time the individual becomes aware of the fire

The behavioral response of the building occupants may vary if they perceive physical cues (an odor of smoke), in contrast to observed cues (smoke obscuring the means of egress). There is some evidence that the recognition of fire protection systems, provided within the building, may be a factor in an individual's perception of the severity of the fire incident threat. It would appear that the most important individual decisions and behavioral responses usually involve perceived life-threatening situations that occur in the initial stages of the fire incident, prior to fire department arrival. In their studies of health care facilities, Lerup et al.[3] have indicated the importance of the participants initial behavior in the following manner:

> In the process of investigating these case studies we have come to believe that the period between detection of the fire and the arrival of the fire department is the most crucial life saving period in terms of the first compartment. (The area in direct contact with the room of origin and the fire.)[3]

The behavioral response of the individuals intimately involved with the initiation of the fire, or those who were aware of the initial fire cue, often appeared to be a determinant to the outcome of the fire incident. It should be realized that altruistic behavior observed in most fire incidents, with the behavioral response of the occupants in a deliberate, purposeful manner, appears to be the most frequent mode of behavioral response. The nonadaptive flight or panic type behavioral response appears to be an infrequent, unusual, or unique participant behavioral response in most fire incidents.

Awareness of Cues

The manner in which an individual is alerted to the occurrence of a fire may predispose the perception of the threat involved. The alerting means, communication mode, and message content were discussed by Keating and Loftus,[4] in their study on vocal alerting systems in buildings. It would appear that variations in voice quality, pitch, or volume, as well as the content of the message, may provide reinforcing threat cues to occupants.

Proulx and Sime,[5] in their study involving evacuation drills in an underground rapid transit station, found the use of directive public announcements with an alerting alarm bell was the most conducive to creating an immediate effective evacuation. Ramachandran,[6] in his review of the research on human behavior in fires in the United Kingdom since 1969, has summarized the effectiveness of alarm bells as awareness cues in the following manner:

> The response to fire alarm bells and sounders tends to be less than optimum. There is usually skepticism as to whether the noise indicated a fire alarm and, if so, is the alarm merely a system test or drill?[6]

Ramachandran[7] indicated that the development of "informative fire warning systems," which utilize a graphic display with a computer-generated message and a high-pitched alerting tone, has reduced the observed

Dr. John L. Bryan is Professor Emeritus, Department of Fire Protection Engineering at the University of Maryland. Currently a consultant located in Frederick, Maryland, his major interest is in the field of human behavior in fires.

delay times in the initiation of practice evacuations. Cable,[8] in his study of the response times of staff personnel to the fire alarm signal in Veterans Administration hospitals, found the greatest delay in response time with the coded alarm-bell-type systems. Kimura and Sime[9] found, in the evacuation of two lecture halls with college students, the verbal instructions of the lecturer were the determining factor in the choice of the use of the fire exit over the normal entrance and exit. The research literature developed from practice evacuations tends to indicate that the use of verbal directive informative messages may be the most effective in reducing the delay in evacuation initiation.

However, it should be noted that if the verbal directive messages are in conflict with other awareness cues, (e.g., the odor or sight of smoke) the credibility of the message may be questioned and the information disregarded by the occupants. One of the few documented cases of this type of situation occurred in the South Tower of the World Trade Center on April 17, 1975. As reported by Lathrop,[10] the fire occurred at approximately 9:04 a.m. in a trash cart in a storage area on the 5th floor, adjacent to an open stairway door. This allowed the smoke to infiltrate the 9th through 22nd floors. The occupants of these floors moved into the core area of the building. At 9:10 a.m., a verbal message from the building communications center monitoring these core lobby areas advised the occupants to remain calm and return to their office areas. In spite of this announcement, the occupants remained in the core lobby areas and became more concerned about the smoke conditions. Thus, with the occupants on the affected floors becoming more anxious, an evacuation message was announced at 9:16 a.m.

Burns[11] reported on the explosion and fire on February 26, 1993, which severely affected both towers of the World Trade Center, and the Vista Hotel, wherein simultaneous occupant evacuations occurred. The explosion disrupted the structure's communications center, and the occupants, having experienced the explosion, loss of power, and floor areas infiltrated with smoke within minutes, evacuated without the established verbal directional announcements utilized in practice evacuations.

Fahy and Proulx, in their questionnaire study of 406 trained fire wardens located in both towers of the World Trade Center at the time of this explosion and fire, found these individuals reported being alerted in the follow manner:[12]

> Respondents mentioned hearing or feeling the explosion, losing lights or telephones, noticing smoke or dust, hearing sirens and alarms, getting information from others, and seeing other people evacuating the area.

Bryan[1] found that most of the participants in a study of residential fire incidents became aware of the fire incident by the odor of the smoke. However, if the categories "notified by others" and "notified by family" are combined in this residential fire incident study, the process of personal notification becomes the most frequent means of the initial awareness of the fire incident. (See Table 3-12.1.) The noise category included sounds generated from persons moving downstairs, persons moving through corridors, and other related fire incident sounds,

including the breaking of glass and the movement of fire department apparatus.

Table 3-12.2 compares the means of awareness of the British population from Wood's study[2] and the U.S. population from Bryan's study.[1] The number of categories were reduced (from the 11 categories indicated in Table 3-12.1) because the British study had fewer categories. U.S. population responses were adapted to the British categories. There was only one significant difference in the means of awareness between the two populations, with 15 percent of the British population having become aware of the fire incident upon observing flame, as contrasted with 8.1 percent of the U.S. population.

Concerning the awareness of the occupants to smoke detectors, Berry[13] indicated in his study of the National Fire Protection Association–recommended smoke detector noise level of 85 dBA[14] that individuals with hearing impairments, or those taking sleeping pills or medication, may require a detector noise level exceeding 100 dBA. Cohen[15] has indicated that flashing or activated visual light signals are effective indicators of fire alarm system activation in occupancies populated by hearing impaired persons. NFPA *101,® Life Safety Code,®* in 1981, initially permitted the flashing of the exit signs with the activation

Table 3-12.1 *Means of Awareness of the Fire Incident by the Study Population[1]*

Means of Awareness	Participants	Percent
Smelled smoke	148	26.0
Notified by others	121	21.3
Noise	106	18.6
Notified by family	76	13.4
Saw smoke	52	9.1
Saw fire	46	8.1
Explosion	6	1.1
Felt heat	4	0.7
Saw/Heard fire department	4	0.7
Electricity went off	4	0.7
Pet	2	0.3
$N = 11$	569	100.0

Table 3-12.2 *Means of Awareness of the Fire Incident for the British and the U.S. Study Population[1,2]*

Means of Awareness	British Percent	U.S. Percent	$P_1 - P_2$	$SE_{P_1 - P_2}$	CR
Flame	15.0	8.1	6.9	1.64	4.21[a]
Smoke	34.0	35.1	1.1	2.27	0.48
Noises	9.0	11.2	2.2	1.41	1.56
Shouts and told	33.0	34.7	2.7	2.25	1.20
Alarm	7.0	7.4	0.4	1.23	0.33
Other	2.0	2.8	0.8	0.70	1.14
$N = 6$	2193	569			

[a]Critical ratio significant at or above the 1 percent level of confidence.

of an audible fire alarm system. This provision has been continued in the 2000 edition.[16]

Kahn[17] conducted a study with 24 male subjects relative to their being awakened by an audible smoke detector alarm signal and their identification of supplemental fire cues. Kahn found these subjects slept through the alarm signals with a signal-to-noise ratio of 10 dBA at their ears, and consistently failed to identify the awakening smoke detector cue as well as radiant heat and smoke odor cues as fire warnings. Noble et al.[18] have indicated the alarm signal-to-noise ratio is attenuated by physical surroundings. An audible smoke detector or alarm signal may be reduced by 40 dBA in passing through a ceiling or wall, and by 15 dBA in passing through a door. In addition, it was found that the signal could be masked to an ineffective level by a typical residential air conditioner with a noise level of 55 dBA.

The recognition of ambiguous fire incident cues as indicators of a possible emergency condition, appears to be inhibited by the presence of other persons in some occupancies. Latane and Darley,[19] in their experimental studies of the inhibition of adaptive behavioral responses to emergencies, created an experimental situation involving college students. While the students were completing a written questionnaire, the experimenters would introduce smoke into the room through a small vent in the wall. If the subject left the room and reported the smoke, the experiment was terminated. If the subject had not reported the presence of the smoke within a six-minute interval from the time the smoke was first noticed, the experiment was considered completed. Subjects alone in the room reported the smoke in 75 percent of the cases. When two passive subjects were introduced in the room with each subject, only 10 percent of the groups reported the smoke. When the total experimental group consisted of three unknowing subjects, one of the individuals reported the smoke in only 38 percent of the groups. Of the twenty-four persons involved in the eight unknowing subject groups, only one person reported the smoke within the first four minutes of the experiment. In the situations involving subjects alone in a room, 55 percent of the subjects had reported the smoke within two minutes and 75 percent reported smoke in four minutes.

Latane and Darley reported that noticing the smoke was apparently delayed by the presence of other persons, with the median delay of 5 seconds for single subjects and 20 seconds for both of the group conditions. These results would appear to indicate the inhibiting influences that may be imposed on individuals in public places. Latane and Darley reported the behavioral response of nine of the unknowing subjects in the ten passive research situations as follows:

> The other nine stayed in the waiting room as it filled up with smoke, doggedly working on their questionnaire, and waving the fumes away from their faces. They coughed, rubbed their eyes, and opened the window but did not report the smoke.[19]

Latane and Darley suggest that, while trying to interpret ambiguous threat cues as to whether a situation requires a unique response, the individual is influenced by the behavioral response of others who are exposed to the identical cues. If these other individuals remain passive and appear to interpret the situation as a nonemergency, this inhibiting social influence may reinforce this nonemergency interpretation for an individual. This behavioral experiment may help explain the reported tendency of persons (1) to disregard initial ambiguous fire incident cues, or (2) to interpret the cues as a nonemergency condition, when the fire incident occurs with a social audience of other persons, as in a restaurant, motion picture theater, or department store. This experimental study may also be helpful in understanding the incidents reported to fire departments that have been delayed by occupants for periods of minutes or even hours. In the report of the Arundel Park fire,[20] several of the participants indicated that when they reentered the hall after observing the fire from outside the building, they warned other participants and suggested they leave, but they were laughed at and the warning was disregarded.

Latane and Darley indicated that social inhibition, diffusion of responsibility, and mimicking appear to be primarily responsible for the inhibition of adaptive and assistance behavior responses by participants in emergency situations. It would appear that the inhibition of behavioral responses in the early stages of a fire incident (when the fire incident cues are relatively ambiguous) may predispose participants to a nonadaptive type of flight behavior, since the available evacuation time has been expended. In some fire incidents it appears to be difficult to get occupants of a building to evacuate because of the variables of social inhibition and diffused responsibility. The tendency to mimic the interpretation of cues and the behavior responses of others (as established by Latane and Darley) appears to be a frequent occurrence in fire incidents in restaurants, hotels, and other places of public assembly.

Perception of the Fire Incident

Withey[21] has examined seven psychological and physical processes that an individual may utilize in an attempt to perceive, identify, structure, and evaluate the situational fire incident cues. It would appear that six of these individual perceptual processes, as presented in Figure 3-12.1, may be critical factors in the perception of a fire.[22]

Recognition: The process of recognition occurs when the individual identifies the ambiguous fire cues as an indication of a fire incident, and thus becomes aware of the fire. The initial perceptual cues may be very ambiguous, and may not positively indicate a fire incident. The cues are produced by a continuous dynamic physical process, with an increasing intensity due to the fluid mechanics properties of flame, heat, and smoke production. Withey also indicated that the usual mental state and predisposition of an individual is to recognize threat cues in terms of the most probable occurrence, typically as related to a prior personal experience, and in the form of an optimistic favorable outcome. The optimistic outcome aspect of an individual's perception of fire incident cues may be a result of the influence of the individual's concept of a personal invulnerability to risk.
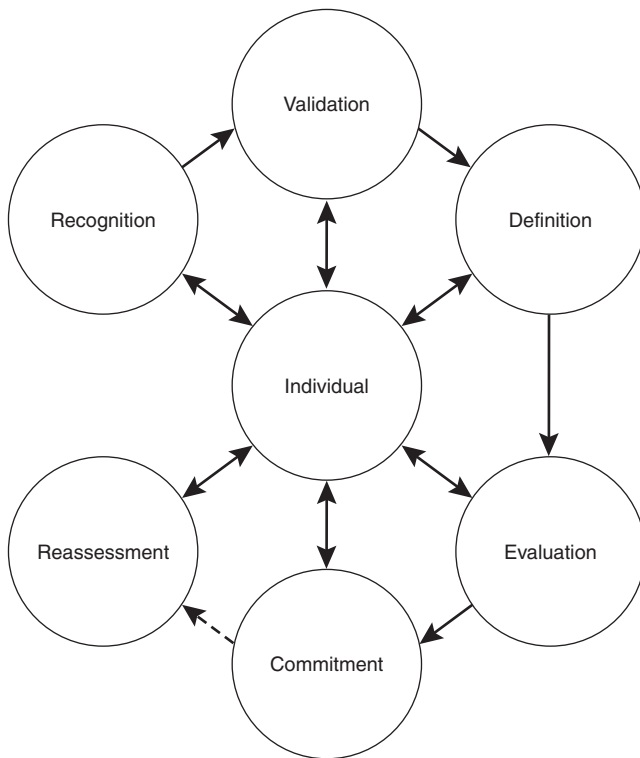
Figure 3-12.1.   *The decision processes of the individual in a fire.*

The concept of threat recognition appears to be a very important problem in fire protection. The decision that initiates the activation of the fire alarm, the evacuation of the building occupants, or suppression of the fire may be delayed or postponed if the individuals involved do not perceive the cues as indicative of an emergency fire situation. Apparently, the ambiguous nature of the fire cues, and the unstructured nature of many public and social groups, require the appearance of significant amounts of smoke, or sudden and threatening flames before most individuals without specialized fire prevention instruction or prior fire incident experiences perceive a threatening fire to be present.

Validation: The process of validation apparently consists of the individual attempting to validate an initial perception of the fire cues, primarily by seeking verbal reassurance of the minor and insignificant character of the fire incident. When the perceived cues are ambiguous, however, the individual often attempts to obtain additional information. Thus, the person is aware that something is happening in the immediate environment, but is not sure exactly how the cues define the event. The process of validation is often conducted by persons exposed to the identical cues. In a study concerned with the individual's perception of cues from the explosion of a fireworks plant, Killian[23] found from the study population of 139 persons that 85 individuals (61 percent) obtained definitive information as to the source and nature

of the explosion or smoke, from someone in person or someone who telephoned.

Latane and Darley[19] established that the physical presence of others during the recognition and validation processes inhibit and structure the behavioral responses of an individual.

Definition: The definition process is considered to be the procedure whereby the individual attempts to relate the information concerning the fire to the perceived and contextual variables, including the qualitative nature of the fire relative to their location, the magnitude of deprivation implied by the fire, and the time context and sequence of the implied deprivation. The generation of stress and anxiety in the individual appears to be most rapid and severe before the individual defines the initial ambiguous cues with structure for the situation. It is often apparent to the individual that the situation requires structure and interpretation before the cues can be defined and assimilated. The role concept of the individual, as well as the physical environment created by the fire incident, appear to be critical factors in the situation, relative to the personalization of the fire threat. The most important physical aspects in the definition process are the generation, intensity, and propagation of smoke, flames, and thermal exposure.

Evaluation: The individual's process of evaluating the fire incident may be described as the cognitive and psychological activities necessary for the individual to respond to the threat. The individual's ability to develop alternate strategies to cope with the fire incident—through psychological and physiological mechanisms that are designed to reduce the stress and anxiety levels of the individual—provide a basis for an initial decision to be formulated for an overt behavioral response. Because of the brief time span involved in the generation and propagation of the fire, it should be remembered that these cognitive processes (including the process of evaluation) may have to be accomplished within several seconds.

Sime[24] has emphasized the importance of the individual's perception of the time available for evacuation or to obtain a refuge, as being an estimation by the individual of the fire threat. Thus, he indicates the perceived time available is dependent upon the information and communication provided to the occupants concerning the location and development of the fire.

The individual's evaluation process may include the formulation of adaptation, escape, or defense procedures. Therefore, the variables of the physical environment in which the fire occurs may be critical in the evaluation process. These determinants and critical variables may be (1) the physical location of the individual in relation to the means of egress, (2) the location and proximity of other members of the population at risk, (3) the physically perceived untenable effects of the fire, and (4) the overt behavioral response of other individuals in the population. During the cognitive process of evaluation, the individual may decide to evacuate the building (flight) or to obtain a fire extinguisher or activate a manual fire alarm station (fight). During the evaluation process, the individual is

very perceptive to the overt actions and communications of the other members of the at-risk population. Thus, the behavioral responses of observed individuals may be mimicked, resulting in mass adaptive or nonadaptive behavior instead of selective individualized behavior.

In his classic studies of nonadaptive group behavior, Mintz[25] developed the concept of this mode of behavior being directly dependent upon the individual's perception of the reward structure of the situation. A heterogeneous population within a building, having perceived and defined a fire threat, would probably initially perceive a reward structure conducive to group and individual cooperative and adaptive behavior responses. Theoretically, all occupants should be able to proceed to and reach the provided means of egress. However, because of the locations of the exits and the relative positions of the individuals within the area, the perceived reward structure for the individuals located farther from the means of egress could provide for the initiation of competitive behavior between occupants. With cooperative behavior, some individuals could perceive that it would be impossible for them to reach an exit in time to escape the deprivation effects of the fire. Once the pattern of competitive behavior becomes observable by one or more individuals, this pattern may become the norm for the group and result in selective, individual competitions to reach the means of egress. Such competitive behavior may be normalized in the group by each individual's perception of the reward structure, or their probability of obtaining the reward. In this fire the reward is to obtain the means of egress.

In the individual's evaluation process, cultural, sociological or economic influences, or the assumption of a particular individual psychological role may be critical to the formulation of behavioral response strategies. The individual in a familiar role, suitable for the fire incident (i.e., those with fire fighting training or experience) and in familiar surroundings, may experience less anxiety and will probably select more adaptive behavior responses than individuals in an unfamiliar role who are confronted with the occurrence of an unfamiliar threat, in unfamiliar surroundings.

Jones and Hewitt[26] conducted detailed interviews with 40 occupants of a 27-story office building who had evacuated the building during a fire incident. (It should be noted that the fire occurred at 9:00 p.m., when the fire management plan was not in effect due to the reduced occupancy of the building.) In this situation it appeared that the leadership and the evacuation group formation were related to the fire training and the normal roles of the occupants. These investigators found the relationship between the occupancy roles and the normal or emergent leadership of the occupants to be the critical factor in a successful evacuation, with the following variables:

the social and organizational characteristics of the occupancy, including what a person knows (or believes) of the situation, whether the person is alone or part of a group, the normal roles that people hold within the occupancy, and the organizational structure or framework. One factor that appears to be related to the chosen evacua-

tion strategy of an occupant is the presence of leadership and the form which that leadership takes.[26]

Horiuchi, Murozaki, and Hokugo[27] reported on a questionnaire study of 458 occupants of an eight-story office building involved in a fire incident. These researchers found significant differences between the normal occupants of the building (familiar with the building) and those occupants attending training sessions in the building (not familiar with the building), relative to their actions, selection of evacuation routes, and effectiveness in achieving an exit. The regular occupants of the building engaged in fire-fighting actions and alerted or assisted other occupants, while the occupants not familiar with the building primarily engaged in evacuation behavior.

Commitment: The process of commitment consists of the mechanisms utilized by the individual to initiate the behavioral responses necessary to achieve the behavioral response strategies that were formulated in the evaluation process. This overt behavioral response to the perceived threat of the fire incident results in completion, partial completion, or noncompletion of the response strategy. Thus, if the response strategy is not completed, the individual immediately becomes involved in the cognitive process of reassessment and commitment. If the behavioral response results in success, however, the anxiety and stress created by the situation are relieved for the individual, even though the fire incident may have increased in severity.

Reassessment: The process of reassessment and overcommitment may be the most stressful of the individual's cognitive processes, because of the failure of previous attempts to achieve the formulated response strategies to the fire incident. More intense psychological and physiological energy is allocated to the behavioral responses, and the individual tends to become less selective in the risks involved in the behavioral response. If successive failures are encountered, the individual becomes more frustrated, anxiety levels increase, and the probability of success decreases. At the Arundel Park fire incident, the number of persons who selected windows as a means of escape from the building increased when the individuals were involved in a secondary evacuation response.[20]

This analysis has been an attempt to understand the cognitive processes of the individual through an examination of the variables related to the processes of recognition, validation, definition, evaluation, commitment, and reassessment. It should be noted that these cognitive processes are dynamic and are constantly being modified in relation to the magnitude, velocity, and intensity of their covert and overt responses. The behavioral responses of the individuals (relative to their psychological and physiological dynamic activity) will probably be below normal during the recognitive process, when the individual is concentrating on the ambiguous perceptual cues. During the process of validation and the definition of the threat, there is usually overt communication and verbalization with adjacent members of the risk population. The period of above normal activity appears to occur

initially during the process of commitment, and often transfers to a hyperactive level during the process of re-assessment and recommitment. It should be remembered that the stress and anxiety generated will tend to increase for the individual as these cognitive and physical behavioral responses result in failure to achieve risk reduction through evacuation or fire control.

The physical variables of the fire incident consist of the flame appearance, the flame, smoke or heat proximity, and the velocity of flame or smoke propagation. These fire incident variables will tend to predispose the individual to a higher level of behavioral response activity, considering the individual's perception of these variables as increasing the personal risk. However, it should be noted that during the process of reassessment and commitment, the individual's physical activity may reach the hyperactive level, or at the other extreme, be expressed as a state of complete physical immobility with a subnormal activity level and a complete loss of the ability to communicate in a coherent manner. These individuals may appear to perceive the fire incident as too severe for their capabilities of adaptability. They appear to be overwhelmed by the stress generation and abandon their attempts to formulate a response strategy. Thus, in ceasing to attempt

any cognitive or physical adaptive behavioral response, they instead adopt a complete cognitive withdrawal from the fire incident environment through psychological withdrawal from reality. A schematic presentation of the dynamics of the behavioral response activity levels of the individual are illustrated in Figure 3-12.2.

Breaux et al.[28] have developed a conceptual model of the cognitive decision processes of the individual in the fire incident. Instead of the six processes adopted from Withey,[21] Breaux et al. have utilized only three processes: recognition/interpretation, behavior (with either action or inaction), and the outcome of the action (that involves the evaluation and long term effects of the behavior.) The evaluation of the behavior is similar to the process of reassessment in Withey's conceptual model. Both the recognition/interpretation process and the behavior process have cognitive inputs that are critical to the decision-making processes. These cognitive inputs involve past experience, the factors immediately arising, and the current state factors, which all impact the recognition/interpretation process. Breaux et al. have emphasized that the individuals in the fire incident may not know precisely at an early stage that they are involved in a fire, and may not know where the fire has developed in relation to their location
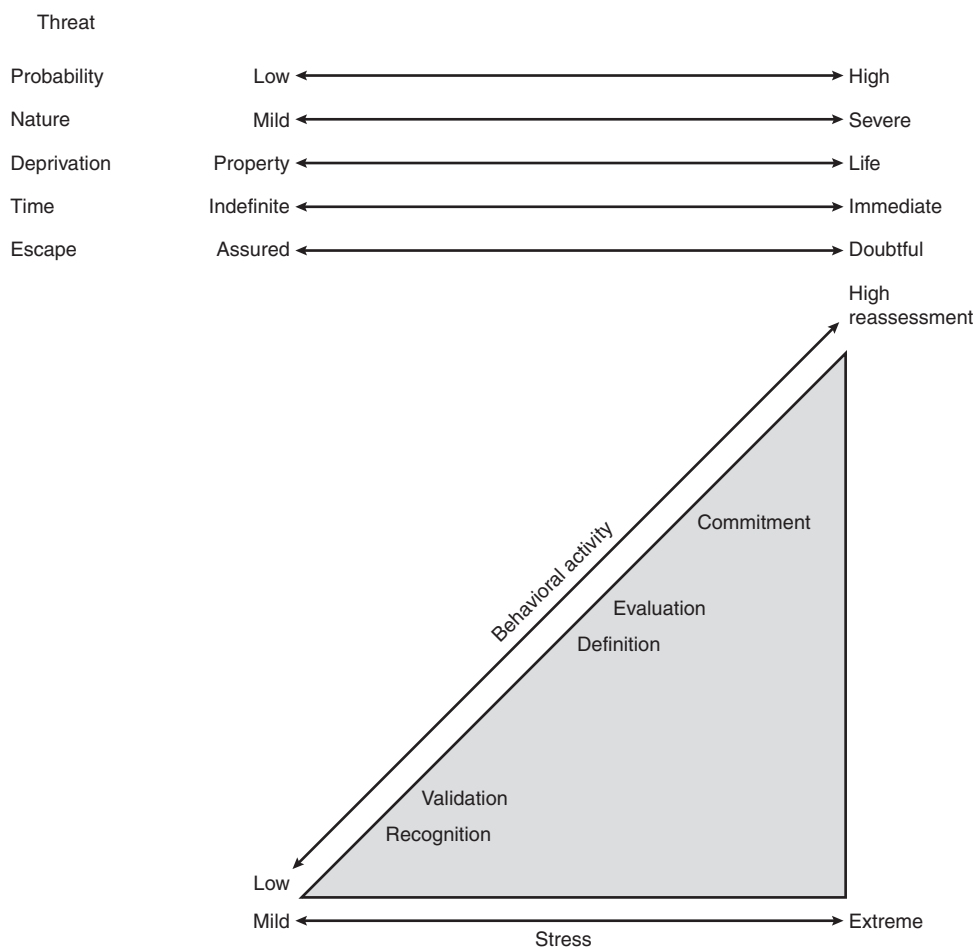

Figure 3-12.2.   *The behavioral activity dynamics of the individual in a fire incident.*
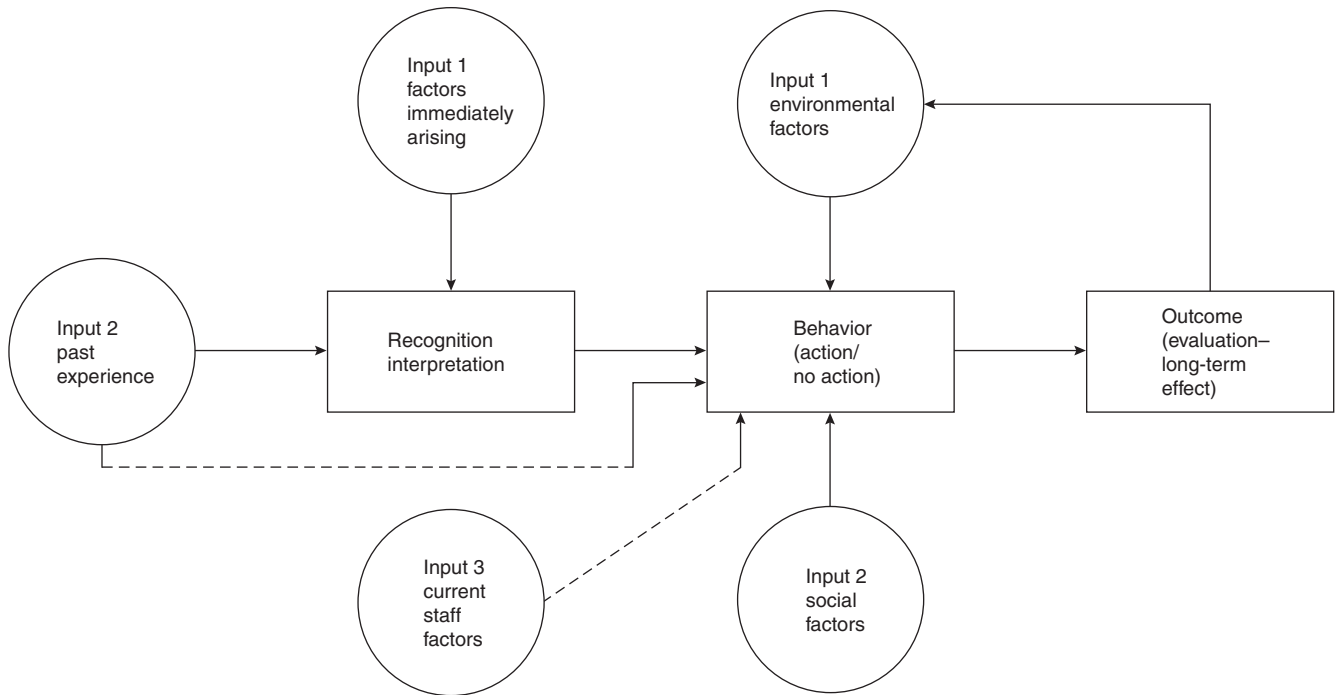
Figure 3-12.3. *Suggested heuristic systems model of human behavior in fire incidents.*

in the building, or their specific location relative to the means of egress. The conceptual model developed by Breaux et al. is shown in Figure 3-12.3.

Bickman et al.[29] have modified the conceptual model of Breaux et al. into one that involves fire as a physical event, with the individual processes of the detection of cues, the definition of the situation, and the coping behavior. Bickman et al. have developed assumptions relative to the behavior responses that increase the probability of detection and the probability of fire suppression, and thus affect the various activities in the coping behavior aspects of their conceptual model.

Proulx[30] has developed a stress model to demonstrate the generation and various levels of stress within the individual involved in the decision process during a fire incident. This stress model is illustrated in Figure 3-12.4, and should be compared with the behavioral activity dynamics of the individual in a fire incident presented in Figure 3-12.2. The left side of Figure 3-12.4 indicates the information to be processed by the individual, and the right side indicates the resulting emotional state. The five loops in the model are described by Proulx in the following manner:

The first loop of the stress model starts with the perception of ambiguous information. This information is decoded in the processing system (PS in the figure) for interpretation. Given that the available information may not allow for a straightforward assessment of the situation, people will at first minimize or deny the situation. These defensive strategies of avoidance lead to an absence of reaction.
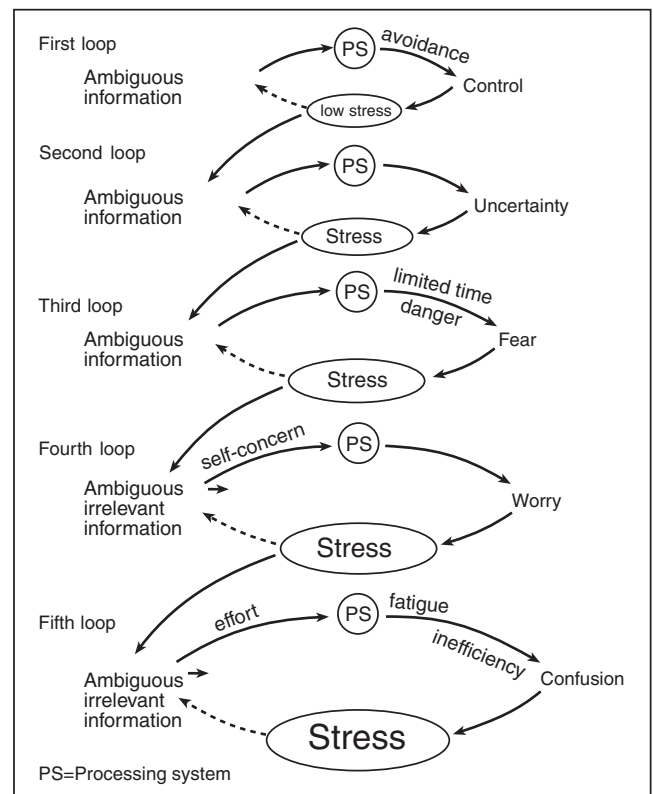

Figure 3-12.4. *Stress model of people in a fire.[30]*

Although individuals may vary considerably in their appraisal of the same event, the repeated perception of ambiguous information will eventually generate a state of uncertainty which will then induce a feeling of stress. Some time can be spent going repeatedly through this second loop of the stress model.

The third loop of the stress model is related to the interpretation of the situation as an emergency. The thicker line around the processing system expresses the pressure of the overload of information with which the person tries to deal at once. The fear felt by the person is a manifestation of a specific appraisal of the environment.

The fourth loop of the model relates to the person's processing of irrelevant information and is represented by the very thick line around the processing system. This irrelevant information creates worry and more stress. The irrelevant information, created by the person, is caused by concern for his or her own performance in coping with the situation. Perceived feelings of arousal and fear, uncertainties regarding how to proceed with the problem, difficulties in interpreting what exactly is going on, and self-estimation of the efficiency of already-applied actions will become additional information to process.

The fifth and last loop of the model supposes an investment of more mental effort to master the problem, momentarily reducing the pressure on the processing system but resulting in fatigue and inefficiency manifested in a state of confusion.[30]

Proulx indicates that definitive, valid, and directive information provided to occupants of a building in a fire incident are the most effective stress reducers and thus tend to minimize the response delays created in the first and second loops of the stress model.

Chubb[31] identified a model of incident command procedure decision processes used by fire department officers, with the possibility that it be used for improvement and training in the decision process for building occupants in a fire situation. The decision model was developed from the theory of naturalistic decision-making, which has evolved from studies of decision-makers in complex, time-critical situations. The critical variables of the naturalistic decision-making theory appear to have many of the environmental and psychological features of the fire situation involving building occupants. Chubb has identified these critical variables as

- Ill-defined goals and ill-structured tasks
- Uncertainty, ambiguity, and missing data
- Shifting and competing goals
- Dynamic and continually changing conditions
- Real-time reactions to changed conditions
- Time stress
- High stakes
- Organizational goals and norms
- Experienced decision-makers[31]

Figure 3-12.5 is an illustration of the recognition-primed decision (RPD) model developed by Klein[32] from the studies of fire department officers. Chubb has correctly indicated that the limitation of this model, when
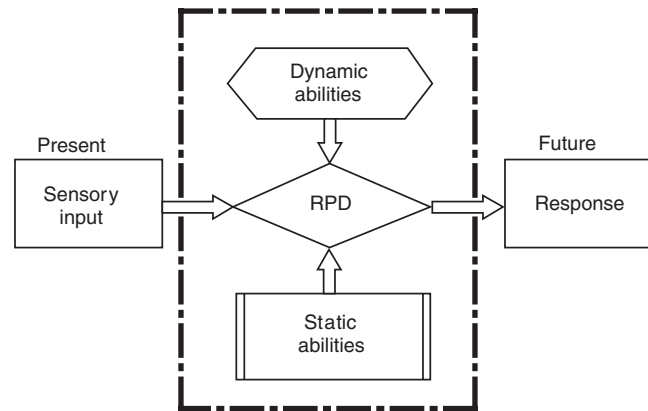

Figure 3-12.5. *Recognition-primed decision model.[31]*

applied to building occupants, is the lack of the fire officers' training and experience in building fires. That is, the static abilities relative to the mental and physical capabilities of building occupants are expected to be more varied and limited than those of fire officers. Chubb indicates that successful recognition-primed decision-making is dependent on the occupant training and practice of the fire safety plans, with the decision support system in the building consisting of egress signs, emergency lighting, and verbal communication systems.

Behavioral Responses of Occupants

A study by Wood[2] involved 952 fire incidents and 2,193 individuals interviewed by fire department personnel at the fire incident scene in Great Britain. Wood found the most frequent behavioral responses to fire could be categorized as evacuation of the building, fighting or containing the fire, and the notification of other individuals or the fire brigade. Bryan[1] found similar types of broad categorization of behavioral response in a United States study primarily concerned with residential occupancies. This residential fire incident study involved interviews of 584 participants in 335 fire incidents, by fire department personnel who used a structured questionnaire at the scene of the fire incident.

Table 3-12.3 presents the initial first actions in the studies of both the British and United States populations. The behavior of the individuals in both studies varied relative to their gender, with the female and male behavior being primarily divided along culturally determined primary group roles. The males were predominantly more active in fighting the fire, while the females were predominantly concerned with alerting others and assisting others in evacuating the building.

There were ten statistically significant differences between the British and United States populations. The United States population was predominant at the five or one percent level of confidence for the first actions of "notified others," "got dressed," "got family," "left area," and "entered the building." A greater percentage of the British population engaged in the first actions of "fought fire," "went to fire area," "closed door to fire area," "pulled fire alarm," and "turned off appliances."

Table 3-12.3   First Actions of the British and U.S. Study Populations[1,2]

Actions	British Percent	U.S. Percent	$P_1 - P_2$	$SE_{P_1 - P_2}$	CR
Notified others	8.1	15.0	6.9	1.38	5.00[a]
Searched for fire	12.2	10.1	2.1	1.51	1.39
Called fire department	10.1	9.0	1.1	1.40	0.79
Got dressed	2.2	8.1	5.9	0.85	6.94[a]
Left building	8.0	7.6	0.4	1.27	0.31
Got family	5.4	7.6	2.2	1.11	1.98[b]
Fought fire	14.9	10.4	4.5	1.63	2.76[a]
Left area	1.8	4.3	2.5	0.70	3.57[a]
Nothing	2.1	2.7	0.6	0.69	0.87
Had others call Fire Department	2.8	2.2	0.6	0.76	0.79
Got personal property	1.2	2.1	0.9	0.55	1.64
Went to fire area	5.6	2.1	3.5	1.01	3.47[a]
Removed fuel	1.2	1.7	0.5	0.53	0.94
Enter building	0.1	1.6	1.5	0.30	5.00[a]
Tried to exit	1.6	1.6	0	0	0
Closed door to fire area	3.1	1.0	2.1	0.76	2.76[a]
Pulled fire alarm	2.7	0.9	1.8	0.70	2.57[b]
Turned off appliances	4.1	0.9	3.2	0.85	3.20[a]
$N = 18$	2193	580			

[a]Critical ratios significant at or above the 1 percent level of confidence.
[b]Critical ratio significant at or above the 5 percent level of confidence.

The general classification of the first, second, and third actions for both the British and United States populations were categorized as "evacuation," "reentry," "fire fighting," "moved through smoke," and "turned back" behavior. The behavioral comparison of the two populations is presented in Table 3-12.4. There was a statistically significant difference between the populations in every behavioral response category except the "moved through smoke" behavior.

An interesting aspect of the actions of the participants involved in the United States study are the modifications in the first, second, and third behavior response actions of the participants. Table 3-12.5 presents these three actions for the total population of 584 individuals in the U.S. study. It should be noted how the action of "notified others" accounted for 15 percent of the first actions and by the time of the third actions, accounted for only 5.8 percent of the behavioral actions. A similar reduction in the frequency of the behavioral response actions can be observed with the action of "searched for the

Table 3-12.4   Human Behavior of the British and U.S. Study Population[1,2]

Behavior	British Percent	U.S. Percent	$P_1 - P_2$	$SE_{P_1 - P_2}$	CR
Evacuation	54.5	80.0	25.5	2.30	11.09[a]
Reentry	43.0	27.9	15.1	2.30	6.57[a]
Fire fighting	14.7	22.9	8.2	1.74	4.71[a]
Moved through smoke	60.0	62.7	2.7	2.29	1.18
Turned back	26.0	18.3	7.7	2.01	3.83[a]
$N = 5$	2193	584			

[a]Critical ratios significant at or above the 1 percent level of confidence.

Table 3-12.5   Compilation of the First, Second, and Third Action of the U.S. Study Populations[1]

Actions	1st Action Percent	2nd Action Percent	3rd Action Percent
Notified others	15.0	9.6	5.8
Searched for fire	10.1	2.4	0.8
Called fire department	9.0	14.6	12.7
Got dressed	8.1	1.8	0.3
Left building	7.6	20.9	35.9
Got family	7.6	5.9	1.4
Fought fire	4.6	5.7	11.5
Got extinguisher	4.6	5.3	1.6
Left area	4.3	2.8	1.1
Woke up	3.1	0	0
Nothing	2.7	0	0
Had others call fire department	2.2	4.0	4.1
Got personal property	2.1	3.8	0.8
Went to fire area	2.1	1.0	0
Removed fuel	1.7	1.0	1.1
Enter building	1.6	0.8	1.1
Tried to exit	1.6	2.4	0.5
Went to fire alarm	1.6	1.8	1.1
Telephoned others—relatives	1.2	0.6	1.1
Tried to extinguish	1.2	1.8	1.9
Closed door to fire area	1.0	0.2	0.3
Pulled fire alarm	0.9	0.6	0.5
Turned off appliances	0.9	0.6	0.3
Check on pets	0.9	1.4	0.5
Await fire department arrival	0	1.0	3.6
Went to balcony	0.2	0.8	2.7
Removed by fire department	0	0	1.6
Open doors—windows	0.2	0.4	1.1
Other	3.9	8.8	6.6
$N = 29$	100.0	100.0	100.0

fire" which is involved with a reduction in the activity from 10.1 percent as the first action to 0.8 percent for the third action. The behavioral actions of "got dressed" and "got family" presented this same tendency toward a reduction in the frequency of the action with the progression during the fire incident. In contrast, an increase in the frequency of the action from the first to the third actions may be noted with the actions of "called fire department," "left building," and "fought fire."

Canter, Breaux, and Sime[33] developed a decomposition diagram of the acts of 41 persons in 14 domestic fires. This study was conducted in the United Kingdom, and the domestic occupancies were similar to those studied by Wood[2] and Bryan.[1] The decomposition diagram is shown in Figure 3-12.6, and should be compared with Tables 3-12.3 through 3-12.5. The sequence of the first, second, and third actions of the U.S. study population is generally similar to the action sequence in Figure 3-12.6.

Behavior According to Gender

The differences between the first behavioral response actions of the occupants according to gender has been examined by Bryan.[1] Table 3-12.6 presents the initial actions of the United States study population relative to the gender of the participants.

Figure 3-12.6. *Decomposition diagram—domestic fires.[33]*

Table 3-12.6 *First Actions of the U.S. Study Population Classified as to the Gender of the Participant[1]*

First Action	Male Percent	Female Percent	$P_1 - P_2$	$SE_{P_1 - P_1}$	CR
Notified others	16.3	13.8	2.5	2.98	0.83
Searched for fire	14.9	6.3	8.6	2.51	3.43[a]
Called fire department	6.1	11.4	5.3	2.41	2.19[b]
Got dressed	5.8	10.1	4.3	2.30	1.87
Left building	4.2	10.4	6.2	2.22	2.79[a]
Got family	3.4	11.0	7.6	2.22	3.42[a]
Fought fire	5.8	3.8	2.0	1.77	1.13
Got extinguishers	6.9	2.8	4.1	1.77	2.31[b]
Left area	4.6	4.1	0.5	1.70	0.29
Woke up	3.8	2.5	1.3	1.45	0.90
Nothing	2.7	2.8	0.1	1.38	0.72
Had others call fire department	3.4	1.3	2.1	1.23	1.71
Got personal property	1.5	2.5	1.0	1.17	0.85
Went to fire area	1.9	2.2	0.3	1.20	0.25
Removed fuel	1.1	2.2	1.1	1.08	1.02
Enter building	2.3	0.9	1.4	1.02	1.37
Tried to exit	1.5	1.6	0.1	1.05	0.09
Went to fire alarm	1.1	1.9	0.8	1.02	0.78
Telephone others—relatives	0.8	1.6	0.8	0.91	0.87
Tried to extinguish	1.9	0.6	1.3	0.91	1.43
Closed door to fire area	0.8	1.3	0.5	0.87	0.57
Pulled fire alarm	1.1	0.6	0.5	0.75	0.66
Turned off appliances	0.8	0.9	0.1	0.79	0.12
Check on pets	0.8	0.9	0.1	0.79	0.12
Other	6.5	2.5	4.0	1.70	2.35[b]
$N = 25$	262	318			

[a]Critical ratios significant at or above the 1 percent level of confidence.

[b]Critical ratios significant at or above the 5 percent level of confidence.

There were significant statistical differences between males and females in the categories of "searched for fire," "called fire department," "got family," and "got extinguishers." Male participants were predominant in fire fighting activities. Thus, 14.9 percent of the males participated in the behavioral response of "searched for fire" as opposed to 6.3 percent of the females, and 6.9 percent of the males were involved in the action of "got extinguishers" as opposed to 2.8 percent of the females. In the United States population, females differed significantly from the males in the warning and evacuation activities—11.4 percent of the females "called fire department" as their initial behavioral response action as opposed to 6.1 percent of the males. In relation to the evacuation behavior, 10.4 percent of the females "left building" as the first behavioral response action, contrasted with 4.2 percent of the males. The cultural role influence on female participants is probably explicitly indicated in the concern for other family members, with the indication that 11 percent of the females "got the family" as the first behavioral response, while only 3.4 percent of the males engaged in this behavioral response. It should be noted that the male actions of "searched for fire" or "fought fire" were matched by the female actions of "called fire department" and "got family." This identical pattern of behavioral responses has also been observed in fire incidents in health care and educational occupancies.

Behavior in Hotel Fire Incidents

The fire protection engineering concepts related to the protection of the occupants of high-rise buildings have been examined and analyzed following the fire in the MGM Grand Hotel in Clark County, Nevada, on November 21, 1980.[34] This hotel fire involved both injuries and fatalities among the guests.

The management of the MGM Grand Hotel, and the Clark County Fire Department under Chief Roy L. Parrish, in cooperation with the National Fire Protection Association (NFPA),[35] conducted an intensive study of the guests registered in the hotel for the evening of November 20 to 21, 1980, to determine how the occupants became aware of the fire incident and their behavioral responses.

The MGM Grand Hotel fire was discovered by an employee of the hotel who entered the deli-restaurant located on the casino level of the hotel at approximately 7:10 a.m. on November 21, 1980. This restaurant area was unoccupied at the time, and the hotel operator was immediately notified to call the fire department. The Clark

County Fire Department received the notification by the direct telephone line call from the hotel at 7:17 a.m., and the first fire company arrived on the scene from a fire station directly across the street on Flamingo Road at approximately 7:18 a.m. The hotel telephone operators were forced from their switchboard positions by the smoke immediately after they had initiated an announcement on the public address system, at approximately 7:20 a.m., for the evacuation of the casino area. The fire reached a flashover condition in the deli area, immediately spread from east to west through the main casino area, and extended out the west portico doors on the casino level immediately following the arrival of the initial fire department personnel.

An addition to the hotel was being constructed adjacent to the west end of the building, and construction workers there participated in warning guests and assisted in the fire fighting and evacuation of guests. The heat and smoke extended from the casino area through seismic joints, elevator shafts, and stairways throughout the 21 residence floors of the hotel. The heat was intense enough on the 26th (top) floor to activate automatic sprinkler heads located in the lobby area adjacent to the elevator shafts.

Due to the rapid early evacuation of the telephone staff, guests in their rooms were not alerted by the hotel public address system or the local fire alarm system.

Guests who became alerted early in the fire incident, or guests already awake and dressed, were able to escape prior to the smoke conditions becoming untenable on the residential floors. Guests alerted later in the progression of the fire incident remained in their rooms or moved to other rooms, often with other occupants. The flame propagation did not extend above the casino level, with the exception of very minor extension into two guests' rooms on the 5th floor. The fire resulted in 85 fatalities to guests and hotel employees in the following areas of the hotel:[34] 14 persons were found on the casino level, 29 persons were found in guest rooms, 21 persons were found in corridors and lobbies, 9 persons were found in the stairways, and 5 persons were found in elevators. The victims were located on the casino level, and the 16th through 25th floors, with the majority of fatalities found between the 20th and the 25th floors.

Figure 3-12.7 is a diagram of the guest floor arrangement and layout of the MGM Grand Hotel which was used in the occupant questionnaire study conducted by the National Fire Protection Association.[35] Of the nine individuals found in the stairways it should be noted that two persons were found in Stairway number 1 at the extreme south end of the south wing on the 17th floor, six persons were found between the 20th and 23rd floors in Stairway number 2 at the central end of the south wing, and one individual was found at the ground-floor level of
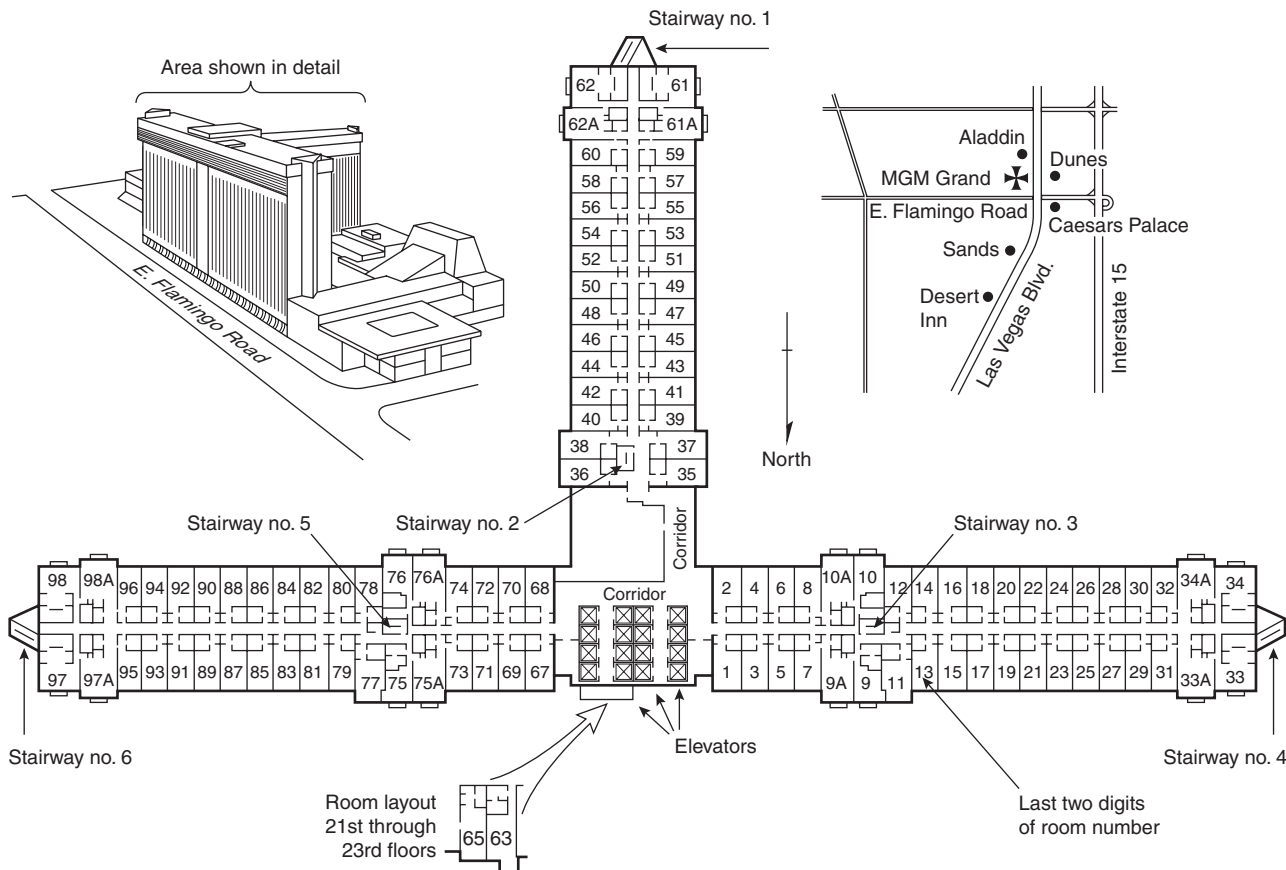

Figure 3-12.7.   *Residential floor diagram of the MGM Grand Hotel.*

Stairway number 4 at the extreme west end of the west wing.

Various estimates have been provided of the number of guests and fire department personnel that suffered injuries at the MGM Grand Hotel fire. Morris[36] indicated that 619 persons were transported to hospitals from the fire scene, and another 150 guests were treated at the Las Vegas Convention Center, where the survivors had been transported. It should be realized that the MGM Grand Hotel fire was a unique fire incident in several aspects. First, it was the second most serious hotel fire in the United States, being surpassed in terms of the loss of life only by the Winecoff Hotel fire in Atlanta, Georgia, on December 7, 1946. Second, it was the first high-rise fire in the United States in which helicopter evacuation was involved for about 300 guests, while the fire department rescued approximately 900 guests.

The Clark County Fire Department obtained from the management of the MGM Grand Hotel a list of the guests registered in the hotel for the evening of November 20 to 21, 1980. This list was transmitted to the NFPA, which prepared a three-page, 28-item questionnaire, with the floor plan of the guest rooms attached as the fourth page. A total of 1960 questionnaires were mailed on December 19, 1980, and 554 questionnaires were returned. Included with the questionnaire was an interview request form by which the respondents indicated their willingness to be interviewed in person about their experience. Of the 554 questionnaires returned, a response rate of approximately 28 percent, 455 individuals (or 82 percent of the response study population) indicated they would be willing to be interviewed.

The ages of the questionnaire respondents ranged from 20 to 84 years, with an average age of 45 years. The questionnaire population consisted of 331 males and 222 females, with one respondent not indicating a gender classification. The population included 103 individuals who indicated they were alone at the time they became aware of the occurrence of the fire within the hotel. The presence of other persons, especially if members of the individual's primary group, has previously seemed to determine the response of some individuals in residential fire incidents.[1]

The initial five behavioral responses of the 554 guests as elicited from the NFPA questionnaire study are presented in Table 3-12.7. The five most frequent first behavioral responses were "dressed," "opened door," "notified roommates," "dressed partially," and "looked out window." The guests involved in the first responses were predominantly engaged in attempting to define and structure the fire cues relative to the severity of the threat to themselves. Approximately 8 percent of the study population initiated or attempted to initiate their evacuation behavior with the first response, as indicated by the actions of "attempted to exit," "went to exit," and "left room." Sixteen individuals, 2.9 percent of the population, initiated actions to improve the room as an area of refuge with the actions "wet towels for face" and "put towels around door." The behavioral responses of the guests in this questionnaire study could be classified as evacuation responses or refuge preparation responses. The responses relating to the evacuation behavior appeared to be initi-

Table 3-12.7 *Compilation of the Initial Five Actions of Guests in the MGM Grand Hotel Fire Incident[35]*

Actions	Percent of Population				
	First	Second	Third	Fourth	Fifth
Dressed	16.8	11.6	6.5	—	—
Opened door	15.9	11.7	6.7	3.4	—
Notified roommates	11.6	3.0	—	—	—
Dressed partially	10.1	7.5	4.5	—	—
Looked out window	9.7	5.7	—	—	—
Got out of bed	4.5	—	—	—	—
Left room	4.3	5.4	8.1	2.4	2.0
Attempted to phone	3.4	3.6	—	2.8	—
Went to exit	2.5	10.3	9.5	16.1	6.7
Put towels around door	1.6	2.5	3.0	6.8	7.7
Felt door for heat	1.3	2.3	—	—	—
Wet towels for face	1.3	3.7	6.3	4.6	7.9
Got out of bath	1.1	—	—	—	—
Attempted to exit	1.1	3.0	5.8	4.3	—
Secured valuables	—	6.8	4.3	—	—
Notified other room	—	3.4	2.2	—	—
Returned to room	—	—	3.9	8.4	4.1
Went down stairs	—	—	3.9	5.4	21.3
Left hotel	—	—	3.4	2.6	2.0
Notified occupants	—	—	3.0	—	—
Went to another exit	—	—	—	3.6	4.8
Went to other room	—	—	—	3.6	3.6
Went to other room/others	—	—	—	3.4	8.7
Looked for exit	—	—	—	2.4	—
Broke window	—	—	—	—	4.3
Offered refuge in room	—	—	—	—	1.8
Went upstairs to roof	—	—	—	—	2.9
Went to balcony	—	—	—	—	1.8
Other	14.8	19.5	28.9	30.2	20.4
Total (percent)	100.0	99.1	96.9	90.4	79.6
Number of guests	554	549	537	501	441

ated early if the means of egress were clear of smoke, or the smoke was determined to be nonthreatening by the guests. However, if the smoke was heavy, the guests appeared to initiate the behavioral response of staying in their rooms or moving to more suitable rooms with responses designed to prevent smoke migration into the rooms and to protect themselves from the smoke.

Examination of Table 3-12.7 indicates the five most frequent behavioral responses reported by guests as second actions were "opened door," "dressed," "went to exit," "dressed partially," and "secured valuables." Approximately 19 percent of the study population reported they were still involved in the dressing actions prior to initiating evacuation or seeking refuge.

Examination of the third behavioral responses of the 537 guests in the study population indicated the responses of the guests generally progressed to evacuation, attempted evacuation, and notification responses. Thus,

approximately 25 percent of the MGM Grand Hotel fire incident study population was involved in evacuation-related behavioral responses, and approximately 10 percent of the guests were involved in attempted evacuations as identified by their third responses of "attempted to exit" and "returned to room." The alerting and notification actions of the guests were involved with the third behavioral responses of "notified occupants" and "notified other room."

The fourth behavioral responses of the guests in the study population indicated a progression of the guests to evacuation, attempted evacuation, and self-protection or room refuge procedural responses. The most frequent action of the guests in their fourth responses was the behavior of "went to exit" (approximately 16 percent of this population). However, combining the guests involved with this action with the guests utilizing the actions of "went down stairs," "went to another exit," "left hotel," and "left room," there were 151 guests (approximately 30 percent of the fourth action guest population) involved in evacuation actions. The process of the guests forming convergence clusters was noted in this hotel fire. This action involved individuals clustering together in rooms as areas of refuge, with the clustered individuals characterized as individuals usually not known to each other prior to the occurrence of the fire incident. The fourth responses of "went to other room" and "went to other room/others," are explicit indicators of the initiation and formation of convergence clusters.

The fifth behavioral responses of the guests were primarily for self-protection, including the improvement of the room as an area of refuge, and evacuation behavior. The primary evacuation behavioral responses would consist of the fifth responses of "went downstairs," "went to exit," and "went to another exit." Thus, the guests involved with evacuation actions consisted of 175 individuals (approximately 40 percent of this study population). The guests who decided not to evacuate and were thus concerned with finding refuge utilized the fifth actions of "went to other room/others," "wet towels for face," "put towels around door," "broke window," "returned to room," "went to other room," "offered refuge in room," and "went to balcony." Approximately 40 percent of the fifth response study population was involved in the finding refuge, and self-protection actions.

Convergence Clusters

The phenomenon of occupant convergence cluster formation in a fire incident was initially noticed in a study of the occupant behavior in a 1979 high-rise apartment building fire.[37] Convergence clusters appear to involve the convergence of the occupants of the building in specific rooms selected as being areas of refuge. In the MGM Grand Hotel fire, the guests tended to select rooms on the north side of the east and west wings, and rooms on the east side of the south wing, due to the prevailing atmospheric conditions and the external smoke migration. In addition, guests reported that people had converged in rooms that had balconies and doors leading to the balconies because of the ease of ventilation, the reduced-smoke exposure, improved visibility, and the communica-

tion advantages the balconies offered. The guests who reported their participation in the convergence behavior in rooms with other persons provided either numerical estimates of the persons occupying the room or suite, or indicated only that "others" or "other persons" were present.

Table 3-12.8 lists the rooms that were identified by guests as being areas of refuge for a total of three or more persons with individuals other than the original occupants of the room. This table also presents the estimates of the length of time the convergence cluster was maintained in the rooms. The duration of the cluster was usually maintained until assistance was obtained for evacuation, or until the occupants were notified by fire or rescue personnel to evacuate. The number of persons shown in the table indicates the total number of persons in the clusters for the total number of rooms identified on the floor. The smallest number of people identified as a single cluster involved three persons, and the largest was 35 persons.

The greatest number of rooms used for convergence clusters, and of course the largest population participating in convergence clusters, was located on the 17th floor of the hotel. No convergence clusters were identified by guests as occurring on the 6th, 21st, or 26th floors. It would appear that convergence clusters may serve as an anxiety and tension-reducing mechanism for individuals

Table 3-12.8   *Compilation of the Time Duration, Room Numbers, and Number of Guests Involved in Convergence Clusters in the MGM Grand Hotel Fire Incident*[35]

Floor	Room Number	Time (Hours)	Persons Number	Persons Percent
7	731	0.6	3	0.7
8	827, 840	1.5–1.75	14[a]	3.3
9	927	2.5	5	1.2
10	1009A, 1025, 1034, 1060	1.2	53	12.7
11	1129, 1115	1.5–2	30[a]	7.2
12	1261, 1225, 1233A	2–3	53	12.7
14	1433A, 1461A, 1451, 1416A	1.5–2	8[a]	1.9
15	1501, 1533A, 1510	2–3	38[a]	9.1
16	1643, 1625, 1633, 1629, 1627, 1615	2–3.5	35[a]	8.4
17	1725, 1775, 1731, 1719 1762, 1756, 1733A	2–2.5	84	20.1
18	1819, 1802, 1850	2–3	20	4.8
19	1929, 1919, 1962A, 1961, 1925	2–3.5	13[a]	3.1
20	2027, 2013, 2030	2–3	13	3.1
22	2213, 2221, 2229	2.5–3.5	25	6.0
23	2329, 2314, 2342, 2331, 2308, 2340	2.5–3.25	20[a]	4.8
24	2446	3.5	4	0.9
25	2512, 2509A	3.5	[a]	0
Total	17 57		418	100.0
Range	7–25 1–7	0.6–3.5	3–84	0–20.1

[a]Persons indicated only as "Others."

confronted with a fire incident perceived as life threatening. The action of "offered refuge in room," which was previously identified in the discussion of the fifth behavioral responses, is a definitive indication of the formation of a convergence cluster.

In addition to the detailed human behavior study of the MGM Grand Hotel fire,[38] the NFPA conducted a similar questionnaire study of the guest's behavior in the Westchase Hilton Hotel fire.[39]

Figure 3-12.8 presents the decomposition diagram for eight multiple-occupancy fires with the acts of 96 persons.[33] These multiple-occupancy fires in the United Kingdom involved hotel occupancies. Figure 3-12.8 and

Table 3-12.7 should be compared to illustrate the similarity of the occupants' behavior in both of these studies.

Nonadaptive Behavior

The classic types of nonadaptive behavior in a fire incident involve the disregard of adaptive actions, behavior that might facilitate the evacuation of others, or inhibit the propagation of the smoke, heat, or flame from a fire incident. Nonadaptive behavior may consist of a single behavioral response, such as leaving the room of fire origin without closing the door to the room, thus allowing the
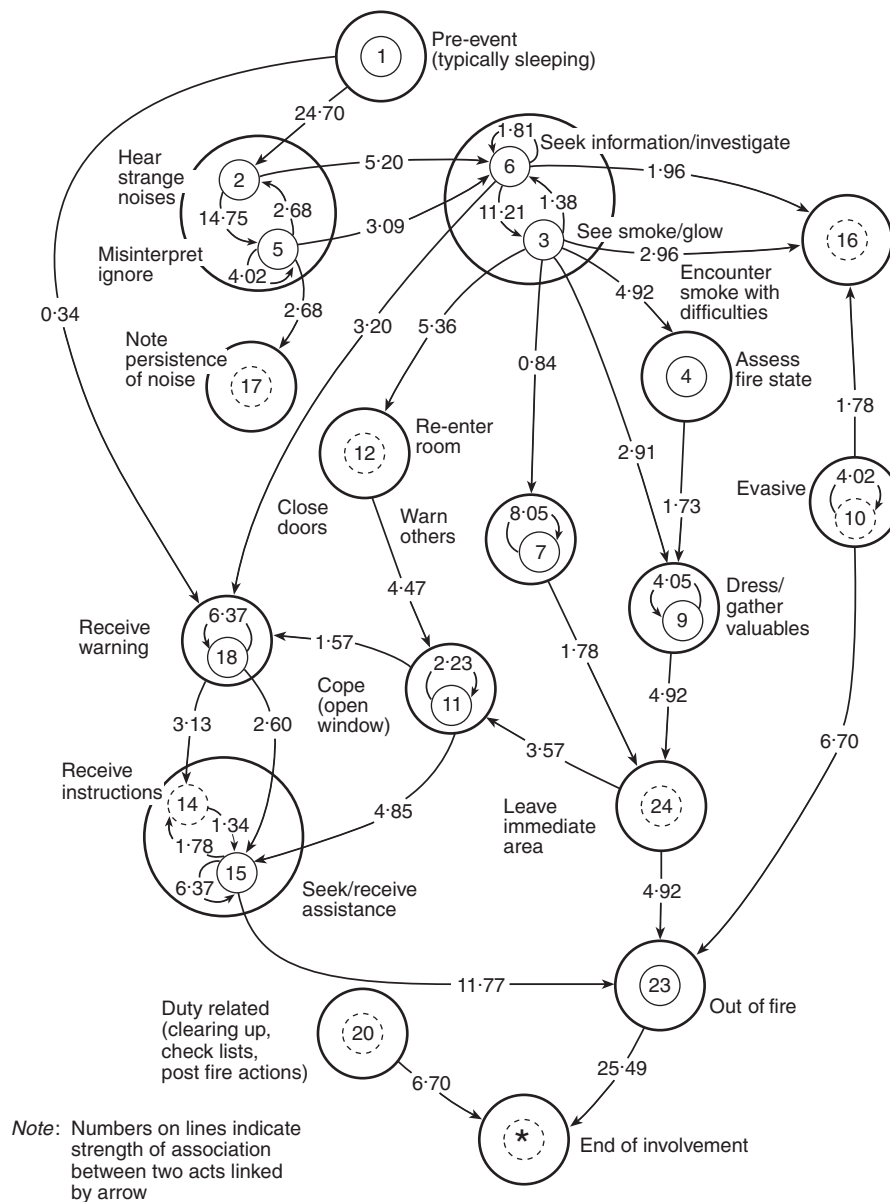
Figure 3-12.8. *Decomposition diagram—multiple-occupancy fires.[33]*

fire to propagate throughout the structure and endanger the lives of other individuals. However, the more generalized concept of nonadaptive behavior consists of a population fleeing the fire incident, without regard for others, and inflicting physical injuries on themselves and others.

Nonadaptive behavior responses may be an omission, such as forgetting to close a door, or may involve a response that, although well meaning and positive in intent, results in negative consequences. When the action of a behavioral response results in the extinguishment of the fire and the reduction of the threat, the behavior may be said to be adaptive. However, when such a behavioral response is ineffective because the fire was more developed than perceived, a more adaptive response might have been to warn others and notify the fire department. Thus, it would appear that some behavior which appears to be nonadaptive, in reality, is behavior that would have appeared to be adaptive if it had only been successful. Injuries suffered by persons in fire incidents may be cues to nonadaptive or risky behavior by the individual.

Panic Behavior

The concept of panic behavior is the nonadaptive behavioral response that is always discussed following fire incidents, such as the Beverly Hills Supper Club fire,[40] where multiple fatalities occurred.

According to most definitions, panic is a flight or fleeing type of behavioral response that also involves extravagant and injudicious effort. Panic is not likely to be limited to a single individual but may be mimicked and adopted by a body of persons. Schultz[41] has defined a panic type of behavior reaction from his simulation experiments:

> A fear-induced flight behavior which is nonrational, nonadaptive, and nonsocial, which serves to reduce the escape possibilities of the group as a whole.[41]

The concept of panic is often used to explain the occurrence of multiple fatalities in fires even when there is no physical, social, or psychological evidence indicating that competitive, injudicious flight behavior actually occurred. Representatives of the media and public officials often label various types of fire incident behavioral responses as panic. The evidence accumulated from interviews with participants and the questionnaires completed by occupants provided no evidence of the classical group type of panic behavior, with competitive flight for the exits in the Beverly Hills Supper Club fire.[42]

Sime[43] has indicated that panic as a concept is primarily a description of the behavior, not an explanation of the behavior. He pointed out that the concept is used to support the introduction of requirements in building laws or ordinances to provide for the fire safety of the building occupants. Sime has also very aptly shown the difference between the use of the concept to describe other persons' behavior in a fire incident, and the use of the concept to describe an individual's behavior which is accompanied by a high state of concern and anxiety. As Sime has indicated, simply because an individual identifies behavior as being associated with a panic reaction does not necessarily identify the behavior as being the classic panic type be-

havioral response. Sime also indicates the outcome of the behavior affects its labeling, and that the actual behavior of people in a fire is most likely to be misinterpreted when the outcome of the fire incident has been unfortunate.

As Sime indicated, the use of the concept of panic must be separated from the use of the terms anxiety or fear. The concept of self-destructive or animalistic panic type behavioral responses to fire incident stimuli, such as the presence of flames or smoke, has not been supported by the research on human behavior in fire incidents. As indicated by Sime,[43] Quarantelli,[44] and others,[1,2,4,45] panic behavior in which the flight response is characterized by actual physical competition between the participants, and personal injuries, is rare.

In his interview study of 100 participants of single-dwelling residential fires, Keating[45] reported no instances of panic behavior and instead found primarily altruistic, helpful behavioral responses.

Ramachandran,[6] in his review of studies on human behavior in fires in the United Kingdom, has developed the following conclusion relative to nonadaptive behavior:

> In the stress of a fire, people often act inappropriately but rarely panic or behave irrationally. Such behavior, to a large extent, is due to the fact that information initially available to people regarding the possible existence of a fire and its size and location is often ambiguous or inadequate.[6]

Reentry Behavior

The study of the 1956 Arundel Park fire documented the initial examination of the phenomenon of reentry behavior.[20] Some codes and regulations affecting the design of the means of egress appeared to assume that pedestrian traffic will only move away from the fire area or floor of the building involved. The Arundel Park study[20] indicated that approximately one-third of the individuals interviewed had reentered the building.

It is apparent that the means of egress components—primarily doors, stairways, and corridors—may be subjected to two-way movement from building occupants or other personnel. The behavioral response of the occupant who after safely leaving the building turns around and reenters has been observed most frequently in the residential fire incident. The occupant is often completely aware of the occurrence of the fire in the building and of the specific portions of the building involved in the area of fire origin and smoke propagation. Table 3-12.9 presents the number of individuals who reentered in the Arundel Park fire from the interviewed population of 61 persons. The reasons for the reentry behavior, and the fact that the reentry participants were predominantly male in this fire incident, should be noted.

The Arundel Park fire incident occurred in an assembly occupancy being utilized for a church-sponsored oyster roast, which is a family event. Thus, the primary group cultural role of father or husband may have been a critical variable in the reentry behavior in the population interviewed and may have resulted in the fact that the reentry participants were mostly male. Reentry behavior should not be considered as nonadaptive behavior since this type of behavior response is often engaged in to assist or rescue

Table 3-12.9 *Reasons for Reentry Behavior by Occupants in the Arundel Park Fire, Classified by Gender of the Occupants[20]*

Gender	Reentered and Left Same Exit	Reentered and Left Different Exit	Stated Reason for Reentrance
M	1		Turn off kitchen stoves
M	1	1	Tell people to leave
M	3	1	To help
M	1		Assist people
M	2	3	Find wife
M	2	2	Assist fire fighting
M & 1 F		5	No stated reason
21 M & 1 F	10	12	

persons remaining or believed to be remaining in the fire incident building. The reentry behavior is often engaged in by parents when children are missing during a fire incident. This reentry behavior is often undertaken in a rational, deliberate, and purposeful manner, without the emotional anxiety or self-anxiety characteristics often associated with nonadaptive behavior. However, reentry behavior has usually been considered nonadaptive since it negatively affects the efficient and effective egress of other persons in the building (i.e., those initially leaving the building are impeded at any egress selected for reentry).

The reasons elicited from participants in reentry behavior in residential occupancies[1] in the United States are presented in Table 3-12.10. It would appear from the total

Table 3-12.10 *Reasons for Reentry of the Population in the Project People Study[1]*

Reasons	Participants	Percent
Fight fire	36	22.2
Obtain personal property	28	17.2
Check on fire	18	11.0
Notify others	13	8.0
Assist fire department	12	7.4
Retrieve pets	12	7.4
Call fire department	9	5.5
Assist evacuation	4	2.5
Taken to hospital	3	1.8
Turn power back on	2	1.2
Rescue from balcony	1	0.6
Help injured family member	1	0.6
Turn off gas	1	0.6
Open windows	1	0.6
Close door	1	0.6
No apparent danger	1	0.6
Entered non-danger area	1	0.6
Responsibility	1	0.6
Due to fire	1	0.6
Told to by others	1	0.6
Not reported	16	9.8
N = 21	163	100.0

Range = 1–36   Percent of Participant Population = 27.9

study population of 584 persons that 162 people or approximately 27.9 percent engaged in reentry behavior. The most frequent reason for reentry behavior in this study was "to fight the fire," followed by "to obtain personal property," "to check on the fire," "to notify others," "to assist the fire department," and "to retrieve pets." These six reentry behavioral response reasons accounted for approximately 73 percent of reentry behavior.

Table 3-12.11 compares the reentry behavior of the British[2] and the United States[1] study populations. It should be noted that all of the behavioral response reasons were significantly different statistically, with the exception of the reason "save personal effects." The United States population was predominant with the reentry reasons of "save personal effects," "call the fire department," "rescue pets," "notify others," "assist fire department," and "assist the evacuation." The British population was predominant with the reentry reasons of "fight the fire," "observe the fire," "shut doors," "await fire department," and "fire not severe."

Occupant Fire Fighting Behavior

Occupants who engaged in fire fighting behavior during fire incidents have been predominantly male. This behavior is now believed to be primarily a culturally determined and assumed aspect of the male role in certain social and occupational situations.

However, in the study of 335 primarily residential fire incidents,[1] it was found that 37.3 percent of those who chose to fight the fire were females, with the youngest participant being a seven-year-old girl. The fire fighting population in this study of 134 persons consisted of 50 females and 84 males. The age range of those who engaged

Table 3-12.11 *Comparison of Reasons for Reentry Behavior of British and U.S. Study Populations[1,2]*

Reasons	British Percent	U.S. Percent	$P_1 - P_2$	$SE_{P_1 - P_2}$	CR
Fight fire	36.0	22.2	13.8	4.02	3.34[a]
Observe fire	19.0	11.0	8.0	3.25	2.46[b]
Save personal effects	13.0	17.2	4.2	2.91	1.44
Shut doors	10.0	0.6	9.4	2.38	3.95[a]
Await fire department	9.0	0	9.0	2.26	3.98[a]
Call fire department	2.0	5.5	3.5	1.32	2.65[a]
Rescue pets	2.0	7.4	5.4	1.40	3.86[a]
Fire not severe	5.0	1.2	3.8	1.74	2.18[b]
Notify others	0	8.0	8.0	0.92	8.69[a]
Assist fire department	0	7.4	7.4	0.88	8.41[a]
Assist evacuation	0	2.5	2.5	0.54	4.63[a]
N = 11	943	163			

[a]Critical ratios significant at or above the 1 percent level.
[b]Critical ratios significant at or above the 5 percent level of confidence.

in the fire fighting behavior varied from the seven-year-old girl to an 80-year-old man. The distribution of the participants relative to sex and age is presented in Table 3-12.12. Approximately 23 percent of the total study population were involved in occupant fire fighting behavior.

The majority of those involved in the fire fighting behavior were between 28 and 37 years old, consisting of approximately 30 percent of the fire fighting behavior population. Statistically significant differences in the behavioral responses of the males and females were shown in the responses of "got extinguisher" and "fought fire." Approximately 15 percent of the male population reacted by obtaining extinguishers. Approximately 26 percent of the male population reported they fought the fire when they first became aware of the fire incident, as opposed to approximately 10 percent of the female occupants. The female members of the population predominantly notified the fire department before initiating the fire fighting type of behavioral response. Approximately 33 percent of the females versus 25 percent of the males reacted to the fire incident by initially notifying the fire department as indicated in Table 3-12.13.

The occupant fire fighting behavioral responses appear most prevalent in occupancies in which the individuals are emotionally or economically involved (primarily their homes) or where such behavior is a result of training or an assigned occupational role. A total of 285 individuals at some time during a fire incident engaged in one of the six actions defined as a fire fighting behavioral response, and a total of 252 individuals participated in one of the four actions relative to notification of the fire department.

In the study by Crossman et al.[46] of residential fire incidents in Berkeley, California, a total of 180 persons were involved in fire fighting behavioral responses. The total of 208 fire incidents for this study included approximately 167 fire incidents, or approximately 80 percent, that had not been reported to the fire department. The majority of the 167 unreported fire incidents had been extinguished

Table 3-12.12   *Gender and Age of U.S. Participants Engaging in Fire Fighting Behavior[1]*

Gender	Participants	Percent
Male	84	62.7
Female	50	37.3
Total	134	100.0
Age		
7–17	8	5.9
18–27	31	23.1
28–37	41	30.6
38–47	27	20.1
48–57	16	11.9
58–67	2	1.5
68–80	3	2.2
Unknown	6	4.7
Total	134	100.00

Percent of Participant Population = 22.9

Table 3-12.13   *Comparison of the Gender of the Participants Engaging in Fire Fighting and Notification of the Fire Department[1]*

Action	Male Percent	Female Percent	$P_1 - P_2$	$SE_{P_1 - P_2}$	CR
Searched for fire	17.2	9.1	8.1	4.23	1.91
Got extinguisher	15.6	6.0	9.6	3.95	2.43[b]
Fought fire	25.6	9.7	15.9	4.83	3.29[a]
Removed fuel	3.4	3.1	0.3	2.17	0.14
Tried to extinguish	5.3	2.8	2.5	2.49	1.00
Went to fire area	3.1	2.8	0.3	2.07	0.14
Total	70.2	33.5	36.7	6.01	6.11[b]
$N =$	184	101			
Called fire department	25.6	33.0	7.4	5.83	1.27
Had others call fire department	9.2	7.5	1.7	3.27	0.52
Went to fire alarm	3.8	3.8	0	0	0
Pulled fire alarm	1.9	1.6	0.3	1.65	0.18
Total	40.5	45.9	5.4	6.31	0.85
$N =$	106	146			

[a]Critical ratio significant at or above the 1 percent level of confidence.
[b]Critical ratio significant at or above the 5 percent level of confidence.

by the occupants of the building involved in the fire incident or the occupants assisted by neighbors. Table 3-12.14 presents the study's percentage distribution of the individuals responsible for extinguishing the fire. Six percent of these fire incidents self-extinguished, and 52 percent of the fires were extinguished by the individual engaged in the activity that created the fire incident. As a means of comparison, the fire incidents in the Project People Study[1] may have consisted of incidents that were judged uncontrollable by the occupants and resulted in the notification of the fire department. It should be remembered that approximately 90 percent of the fire occurrences in the National Fire Prevention and Control Administration National Household Fire Incident Survey[47] had also not been reported to the fire department.

The types of occupancies in which equipment provided within the occupancy was used to fight the fire are shown in Table 3-12.15. The apparently high frequency of residential occupancies, with 64 percent of the occupancies being either single-family dwellings or apartments, may be a variable created by the fire incident population of this study. This residential occupancy distribution may also be representative of many urban areas where the fire problems are essentially concentrated in residential occupancies.

In the Project People Study,[1] 107 of the 584 participants did not voluntarily leave the building after becoming aware of the fire incident. The reasons given for their remaining in the building are presented in Table 3-12.16. Fifty-two occupants, or approximately 49 percent of the population staying in the building, reported that they remained because they intended to engage in fire control or

Table 3-12.14   *Percentage of Occupants Extinguishing Residential Fires in Berkeley, CA[46]*

Fire Suppressed by	Percent
Person engaged in heat-using activity	52.8
Other member(s) of household	28.3
Friends and neighbors	8.9
Fire department	18.9
Burnout	6.1
Total	115.0
Single individual	80.7
Group effort	19.3
Total	100.0

Table 3-12.15   *Occupancies in Which Fire Fighting Equipment Was Utilized by Participants in Fire Fighting Behavior[1]*

Occupancy	Incidents	Percent
Dwelling (1 Family)	23	35.9
Apartment (<29 Units)	18	28.1
Restaurant	3	4.8
Apartment (>20 Units)	3	4.8
Manufacturing	2	4.8
Hotel and motel	2	3.2
School	3	3.2
Billiard center	1	1.5
City club	1	1.5
Hospital	1	1.5
Dwelling (2 Family)	1	1.5
College dormitory	1	1.5
Service station	1	1.5
Office	1	1.5
Photographic laboratory	1	1.5
Other	2	3.2
N = 16	64	100.00

Table 3-12.16   *Elicited Reasons of Participants for Not Voluntarily Leaving the Fire Incident Building[1]*

Reason	Participants	Percent
Fight fire	52	48.7
Notify others	7	6.5
Blocked by smoke	7	6.5
Blocked by fire	5	4.7
Overcome by smoke	5	4.7
Search for fire	3	2.8
Needed help	2	1.9
Secure property	2	1.9
Afraid of fire spread	2	0.9
No fire in area	1	0.9
Help others	1	0.9
Does not know	1	0.9
No response to fire department	1	0.9
Home	1	0.9
Return to area	1	0.9
Not reported	16	15.0
N = 15	107	100.0

Range = 1–52   Percent of Participant Population = 15.6

fire fighting activities. The other most frequent reasons for remaining in the fire incident building were to notify others of the fire occurrence or because the means of egress were obscured by smoke. Approximately 15 percent of the study population voluntarily remained within the fire building.

Occupant Movement through Smoke

The movement of the occupants through smoke is sometimes related to the fire fighting behavior and the alerting of others, and is often a component of the evacuation behavior in many fire incidents.[1,2] The principal variables influencing an occupant's decision to move through smoke appear to be recollection of the location of the exit, and ability to estimate the travel distance required. Secondary variables are the perception of the severity of the smoke (determined by observation of the appearance of the smoke), the smoke density, and the presence or absence of heat with smoke.[38,39] It should be recognized that to achieve evacuation, occupants have moved through smoke for extended distances (over 20 m) under conditions of extremely limited visibility (less than 4 m) at personal risk. Occupants sometimes have also been forced to turn back and not complete the evacuation.

Jin and Yamada[48] reported on a study involving 31 subjects (14 males and 17 females), traveling a maximum distance of 10.5 m in a corridor exposed to smoke from smoldering cedar crib chips. The smoke extinction coefficient varied from 0.1 to 1.2 l/min. The subjects were also exposed to an increasing heat exposure from radiant heaters at the end of the corridor, with a mean temperature at the end of the corridor of 82°C. At five points in the corridor the subjects were stopped and asked arithmetic questions to be solved mentally. Both walking speed in the corridor and the mental arithmetic capability decreased with the increase in smoke density and the increased radiant heat exposure.

Fahy and Proulx[12] in their questionnaire study of 406 trained fire wardens in the World Trade Center explosion and fire found that 94 percent of the respondents in Tower 1 and 70 percent of the respondents in Tower 2 moved through smoke. In addition, the study reported that approximately 75 percent of these individuals turned back during their evacuation because of smoke, crowding, locked doors, breathing difficulty, fear and poor visibility. It was also reported that some occupants continued to move through smoke, even when they perceived the smoke to be worsening and they believed they may have been moving toward the fire.

Table 3-12.17 compares the distance moved through smoke for the 1316 persons in the British study[2] and the 322 persons in the United States study[1] who reported that they moved through smoke. It may be of interest to note that 60 percent of the population in the British study and 62.7 percent of the population in the United States study reported that they moved through smoke. Apparently building occupants will move through smoke in an evacuation process. An important variable may be both the smoke density and the visibility distance available to the occupants during the evacuation process, as well as their familiarity with the means of egress.

Table 3-12.17 *Compilation of the Distance Moved through Smoke for Participants in Both the British and U.S. Study Populations[1,2]*

Distance Moved (feet)	British Percent	U.S. Percent	$P_1 - P_2$	$SE_{P_1 - P_2}$	CR
0–2	3.0	2.3	0.7	1.02	0.69
3–6	18.0	8.4	9.6	2.23	4.30[a]
7–12	30.0	17.1	12.9	2.71	4.76[a]
13–30	19.0	45.5	26.5	2.62	10.11[a]
31–36	5.0	2.0	3.0	1.25	2.40[b]
37–45	4.0	4.1	0.1	1.19	0.08
46–60	5.0	11.0	6.0	1.47	4.08[a]
>60	15.0	9.6	5.4	2.10	2.57[b]
$N =$	1316	322			

[a]Critical ratios significant at or above the 1 percent level of confidence.
[b]Critical ratios significant at or above the 5 percent level of confidence.

Table 3-12.18 *Compilation of the Visibility Distance for the British and the U.S. Populations When They Moved through Smoke[1,2]*

Visibility Distance (feet)	British Percent	U.S. Percent	$P_1 - P_2$	$SE_{P_1 - P_2}$	CR
0–2	12.0	10.2	1.8	1.99	0.90
3–6	25.0	17.2	7.8	2.65	2.94[a]
7–12	27.0	20.2	6.8	2.73	2.49[b]
13–30	11.0	31.7	21.7	2.24	9.69[a]
31–36	3.0	2.2	0.8	1.03	0.78
37–45	3.0	3.7	0.7	1.08	0.65
46–60	3.0	7.4	4.4	1.21	3.64[a]
>60	17.0	7.4	9.6	2.24	4.29[a]
$N =$	1316	322			

[a]Critical ratios significant at or above the 1 percent level of confidence.
[b]Critical ratios significant at or above the 5 percent level of distance.

Table 3-12.18 presents the visibility distance of the British and the United States occupants as they moved through the smoke in evacuating the fire incident buildings. Occupants reported their movement through smoke in relatively high smoke-density conditions, with visibility below 4 m for 64 percent of the British population and for 47.6 percent of the United States population.

Table 3-12.19 relates the distance moved through smoke for the United States population to the visibility distance.[1]

The visibility distance for both the British and the United States populations at the time the participants were forced to turn back is presented in Table 3-12.20. It is interesting to compare Table 3-12.20 with Table 3-12.18 because very few of the participants turned back when the visibility distance exceeded 10 m, with the greater percentage of occupants having turned back at the reduced visibility levels. Comparing the visibility distance below 4 m in Table 3-12.19, it is obvious that 91 percent of the British population who turned back and 76.4 percent of

Table 3-12.19 *Comparison of the Movement through Smoke with the Visibility Distance Significance of These Differences in the Participant Population[1]*

Distance Moved	Participants	Percent
Greater than visibility	170	46.4
Equal to visibility	128	35.0
Less than visibility	68	18.6
$N = 3$	366	100.0

Greater than Visibility Percent	Equal to Visibility Percent	Less than Visibility Percent	$P_1 - P_2$	$SE_{P_1 - P_2}$	CR
46.4	35.0		11.4	5.77	1.97[b]
46.4		18.6	27.8	6.98	3.98[a]
	35.0	18.6	16.4	6.83	2.40[b]
170	128	68			

[a]Critical ratios significant at or above the 1 percent level of distance.
[b]Critical ratios significant at or above the 5 percent level of confidence.

Table 3-12.20 *Compilation of the Visibility Distance for the British and the U.S. Populations at the Time They Initiated the Turned Back Behavior[1,2]*

Visibility Distance (feet)	British Percent	U.S. Percent	$P_1 - P_2$	$SE_{P_1 - P_2}$	CR
0–2	29.0	31.8	2.8	5.31	0.53
3–6	37.0	22.3	14.7	5.57	2.64[a]
7–12	25.0	22.3	2.7	5.02	0.54
13–30	6.0	17.6	11.6	3.07	3.78[a]
31–36	0.5	1.3	0.7	0.90	0.77
37–45	1.0	0	1.0	1.10	0.91
46–60	0.5	4.7	4.2	1.16	3.62[a]
>60	1.0	0	1.0	1.10	0.91
$N =$	570	85			

[a]Critical ratios significant at or above the 1 percent level of confidence.

the United States population initiated their behavior at visibility distances of less than 4 m.

Proulx[49] in the study of the occupant's response to a fire in a 25 story high-rise apartment building received 137 questionnaires returned, with 68 percent of the occupants over 60 years of age. One hundred fourteen of the occupants, or 83 percent, attempted to evacuate during the fire, and 96, or 84 percent, of those attempting to evacuate moved through smoke. Forty-five percent of those moving through smoke indicated they could see "nothing at all" or "little," and 30 percent said they could see 12 to 15 m in the corridor. Of the 114 occupants who attempted to evacuate 61, or 54 percent, were successful, and 53, or 46 percent, were unsuccessful due to the smoke

conditions in the corridors or stairs. Relative to the 53 unsuccessful occupants 29, or 55 percent, returned to their own apartments and 24 occupants, or 45 percent, sought refuge in other apartments.

Heskestad and Pederson[50] have reported on five large "escape through smoke" experiments involving more than 300 persons with various way guidance systems. In all of these experiments the visibility was less the 3 m due to the induced smoke conditions. Two of the experiments involved the test situation modeled on a ship staircase and a ship or hotel corridor. One of these experiments involved an emergency training mock-up, one experiment used a corridor in a health care facility, and one experiment used portions of a passenger ferry. Variables measured during the experiments were the occupants time to travel through the experimental facility and the number of incorrect decisions made during the travel. These experiments found that tactile and audible way guidance systems appear to be as suitable as the visible systems in assisting the individuals movements through smoke.

Jin[51] has reported on his numerous studies involving the effectiveness of guidance sign systems with human subjects in smoke environments. The improvements resulting from these experiments include a pictorial exit sign, flashing exit signs, and a flashing row of lights at floor level indicating the direction of egress travel. The flashing row of lights was effective in a heavy smoke level of 1.0 l/m with the spacing of the lights at 0.5 m and the flashing velocity is 4 m/s.

Handicapped or Impaired Occupants

The problems involving fires in occupancies designed for permanently or temporarily disabled persons, such as nursing homes and hospitals, appear to have been properly alleviated in recent years due to building design, adequate staff training, and preparation to protect the occupants until evacuation is possible.[52] An extensive study of human behavior in health care facilities[53,54] indicated the nursing staff performed their professional roles even in situations with a high degree of personal risk.

The few fire incidents that have been studied, in which handicapped persons have been involved in other occupancies, have primarily been in residential occupancies. In both of these cases the handicapped individuals were assisted in a successful evacuation by other occupants. The one instance involved a wheelchair occupant[38] and the other situation involved a blind occupant.[44]

Pauls[55] has indicated from a number of practice evacuations in high-rise office buildings in Canada that approximately 3 percent of the occupants will be unable to use the stairs due to conditions that permanently or temporarily limit mobility. Paul's population included occupants with heart conditions and individuals recovering from surgery, illnesses, and accidents.

Isner and Klem[56,57] in their reports of the explosion and fire in the World Trade Center indicated that normal power was lost with the occurrence of the explosion at approximately 12:18 p.m., and the emergency generators failed about 20 min. later, with all the remaining power to the World Trade Center complex being disconnected at

approximately 1:32 p.m. Thus, the simultaneous evacuation of both able and disabled occupants from Towers 1 and 2 were conducted in darkness with varying smoke conditions in the stairways. These simultaneous evacuations may have involved the largest number of occupants and the longest evacuation times of any fire-induced evacuations of buildings in the United States.

Juillet,[58] in one of the first documented studies of this type, reported on the interview study of 27 occupants with disabilities who were evacuated from one of the two towers in the World Trade Center during the explosion and fire. Of those interviewed, fourteen had mobility impairments, three had sight or hearing impairments, three were pregnant, two had cardiac conditions, and seven had respiratory conditions. Juillet[59] indicated it was believed the total disabled population in both Towers 1 and 2 at the time of the incident was between 100 and 200 persons, with approximately 100 occupants having been identified previously. The average evacuation time of the 27 study participants was 3.34 hrs, with a reported range of evacuation times from 40 min. to over 9 hrs. The predominate means of evacuation was through the stairs, with assistance from other evacuees or emergency personnel. The altruistic behavior, characteristic in many fire incidents with large populations,[37,38] appeared to have been exhibited in this fire incident with the disabled occupants, as reported by Juillet:

> in the absence of communications by authorities, they gladly accepted assistance—from colleagues and even from complete strangers—in evacuating. These caring groups of people who assisted the disabled protected their "charges" until they were safely evacuated and moved away from the building.[58]

The Fire SERT Centre at The University of Ulster recently completed the most extensive and detailed analytical and experimental studies of the evacuation capabilities of disabled individuals. Boyce, Shields, and Silcock conducted a series of studies in Northern Ireland to determine the number and characteristics of disabled persons who may be expected to frequent public buildings, and to determine the capabilities of these persons to complete an evacuation. The initial study determined the number and types of disabled persons expected to occupy public assembly occupancies.[60] This study found that 12 percent of the mobile population of Northern Ireland out in public are disabled persons and 2 percent of these disabled persons require assistance. Table 3-12.21 presents the number of disabled adults and children by their degree of mobility expressed as a percentage of the total mobile population. Table 3-12.22 illustrates the disabled persons in public who have experienced evacuation difficulties as percentages of the total mobile population. Table 3-12.23 indicates the involvement of disabled persons in social and recreational occupancies relative to their degree of mobility.

Additional valuable data presented in this study involved the frequency with which disabled persons go out in public. In addition, data was presented relative to the severity of disability among disabled adults who live in

Table 3-12.21 *Numbers of Disabled Adults and Children Who Go Out by Degree of Mobility, Expressed as Percentages of the Total Mobile Population (i.e., Able-Bodied People and Mobile Disabled People) in N. Ireland.*[60]

Disability	Adults			Children			Total (adults and children)		
	Unassisted	Assisted	Total	Unassisted	Assisted	Total	Unassisted	Assisted	Total
Locomotion	6.0	1.6	7.6	0.2	0.1	0.3	6.2	1.7	7.9
Wheelchair Users	0.05	0.09	0.14	—	—	—	0.05	0.09	0.14
Zimmer/rollator user	0.13	}	}	—	—	—	0.13	}	}
Walking stick/crutch	1.27	1.52	6.91	—	—	—	1.27	1.52	6.91
No aid	3.99			—	—	—	3.99		
Reaching and Stretching	1.8	0.8	2.6	0.0	0.0	0.1	1.8	0.8	2.6
Dexterity	2.2	0.9	3.0	0.1	0.0	0.1	2.2	0.9	3.1
Seeing	2.0	0.9	2.9	0.04	0.04	0.2	2.1	0.9	3.0
Blind	0.02	0.05	0.06	0.0	0.0	0.01	0.02	0.05	0.07
Hearing	4.2	0.8	5.0	0.1	0.1	0.2	4.3	0.9	5.2
Deaf	0.1	0.1	0.1	0.0	—	0.0	0.1	0.1	0.1
Mental/behavioral	2.0	0.7	2.7	0.3	0.2	0.4	2.3	0.9	3.2

Percentages for each disability do not sum to totals given in Table 2 because many individuals have more than one disability.

Percentages for wheelchair users and walking aid users do not sum to total since some data is missing.

Source: K. E. Boyce, T. J. Shields and G. W. H. Silcock, "Toward the Characterization of Building Occupancies for Fire Safety Engineering: Prevalence, Type, and Mobility of Disabled People," *Fire Technology,* 35, 1, p. 41 (1999).

Table 3-12.22 *Number of Disabled Adults Who Go Out and Experience Difficulty, Expressed as Percentages of Total Mobile Population of N. Ireland*[60]

Action	Go out Unassisted Degree of Difficulty			Assisted Degree of Difficulty			Total Degree of Difficulty		
	Some	Great	Impossible	Some	Great	Impossible	Some	Great	Impossible
Go up and down stairs	2.4	1.1	0.2	0.2	0.6	0.2	2.59	1.69	0.43
Climb outside steps	1.5	0.8	0.2	0.3	0.4	0.2	1.81	1.14	0.40
Cross door saddles	0.1	0.1	0.03	0.2	0.1	0.01	0.32	0.13	0.04
Go through doors	0.1	0.03	0.01	0.1	—	0.01	0.15	0.03	0.02
Turn door knobs	0.3	0.1	0.03	0.2	0.07	0.05	0.43	0.13	0.08

Since these percentages are based on adults, only the actual percentages of the mobile population in N. Ireland who experience difficulty may be higher.

Source: K. E. Boyce, T. J. Shields, and G. W. H. Silcock, "Toward the Characterization of Building Occupancies for Fire Safety Engineering: Prevalence, Type, and Mobility of Disabled People," *Fire Technology,* 35, 1, p. 42 (1999).

communal facilities and go out for meals and drinks, and for adults who are employed. The perceived value of this information and data relative to the application of performance codes was stated as follows:[61]

> The information provided in this analysis has important implications for characterizing building occupancies. It establishes that public buildings are frequented by a significant number of disabled people and that the nature of their disabilities and how well they can be expected to evacuate without assistance during an emergency will be a function of the use of the building or part of the building. Characterizing buildings and characterizing occupants as required by performance-based codes, are not mutually exclusive activities, a fact that has not yet percolated through the design professions.

The second study by Boyce, Shields, and Silcock[62] involved the experimental observations and measurement of the movement of disabled persons on a horizontal corridor, on inclined ramps, and on stairs. The observations included the velocity of movement, rest periods required, assistance required and the physical aids utilized relative to their degree of ambulatory disability. One hundred seven persons completed the horizontal corridor without assistance, 54 males and 53 females, ages 20 to 85. The velocity of this population relative to their ambulatory disability is presented in Table 3-12.24. Sixteen of the 28 manual wheelchair users needed assistance to traverse the 50 m long corridor with the 90 degree turn 8 m from the starting point. Only 34 participants were capable of participating in the stair movement studies involving ascending and descending travel, 30 of these without assistance and 4 with assistance, including three blind persons.

In general the movement velocity was slightly faster in descending travel on ramps while on the stairs the ascending movement was faster, as indicated in a comparison of Tables 3-12.25 and 3-12.26. The authors indicated the following from these experiments:[63]

Table 3-12.23 *Extent of Involvement of Disabled Adults and Children in Various Social and Recreational Activities by Degree of Mobility[60]*

Activity	Adults			Children			Totals		
	Unassisted	Assisted	Total	Unassisted	Assisted	Total	Unassisted	Assisted	All
Participates in theatre, ie, opera, musicals, ballet, cinema	9,756 (6.5)	2,514 (9.6)	12,270 (7.0)	1,028 (14.0)	387 (7.3)	1,415 (11.3)	10,784 (6.9)	2,901 (9.5)	13,685 (7.3)
Goes shopping[a]	1,532 (58.5)	2,233 (40.0)	3,765 (40.1)	153 (81.0)	53 (28.0)	206 (75.7)	2,235 (79.6)	1,330 (23.5)	3,565 (42.1)
Participates indoor sport/spectates sport	13,161 (8.9)	1,006 (4.0)	14,167 (8.1)	3,205 (44.0)	1,084 (20.5)	4,289 (3.4)	16,366 (10.5)	2,090 (6.8)	18,456 (9.9)
Attends ordinary social club	8,052 (5.4)	898 (3.6)	8,950 (5.1)	— —	— —	— —	8,052 (5.4)	898 (3.6)	8,950 (5.1)
Stayed in hotel/other holiday accommodation	40,220 (27.0)	4,437 (17.6)	44,657 (25.6)	— —	— —	— —	40,220 (25.7)	4,437 (14.5)	44,657 (23.9)
Goes out for meals/drinks[a]	1,318 (50.3)	2,032 (36.4)	3,350 (40.9)	— —	— —	— —	1,277 (45.5)	2,032 (35.8)	3,350 (39.6)
Is employed	18,896 (12.7)	229 (0.9)	19,125 (11.0)	— —	— —	— —	18,896 (12.1)	229 (0.7)	19,125 (10.2)
Attends ordinary school	350 (0.2)	0 (0.0)	350 (0.2)	0 (0.0)	0 (0.0)	0 (0.0)	350 (0.2)	0 (0.0)	350 (0.2)
Attends college of further education	316 (0.2)	0 (0.0)	316 (0.2)	0 (0.0)	0 (0.0)	0 (0.0)	316 (0.2)	0 (0.0)	316 (0.2)

[a]Asked of disabled persons living in communal establishments only

Source: K. E. Boyce, T. J. Shields, and G. W. H. Silcock, "Toward the Characterization of Building Occupancies for Fire Safety Engineering: Prevalence, Type, and Mobility of Disabled People," *Fire Technology,* 35, 1, p. 44 (1999).

Table 3-12.24 *Speed on Horizontal by Presence/ Absence of Locomotion Disability and Walking Aid—Unassisted Ambulant[62]*

Subject Group	Mean (m/s)	Standard Deviation (m/s)	Range (m/s)	Interquartile Range (m/s)
All disabled (n = 107)	1.00	0.42	0.10–1.77	0.71–1.28
With locomotion disability (n = 101)	0.80	0.37	0.10–1.68	0.57–1.02
no aid (n = 52)	0.95	0.32	0.24–1.68	0.70–1.02
crutches (n = 6)	0.94	0.30	0.63–1.35	0.67–1.24
walking stick (n = 33)	0.81	0.38	0.26–1.60	0.49–1.08
walking frame or rollator (n = 10)	0.57	0.29	0.10–1.02	0.34–0.83
Without locomotion disability (n = 6)	1.25	0.32	0.82–1.77	1.05–1.34

Source: K. E. Boyce, T. J. Shields, and G. W. H. Silcock, "Toward the Characterization of Building Occupancies for Fire Safety Engineering: Capabilities of Disabled People Moving Horizontally and on an Incline," *Fire Technology,* 35, 1, p. 54 (1999).

Table 3-12.25 *Speed on Stairs (ascent) by Presence/Absence of Locomotion Disability—Unassisted Ambulant[62]*

Subject Group	Mean (m/s)	Standard Deviation (m/s)	Range (m/s)	Interquartile Range (m/s)
With locomotion disability (n = 30)	0.38	0.14	0.13–0.62	0.26–0.52
no aid (n = 19)	0.43	0.13	0.14–0.62	0.35–0.55
crutches (n = 1)	0.22	—	0.13–0.31	0.26–0.45
walking stick (n = 9)	0.35	0.11	0.18–0.49	
rollator (n = 1)	0.14	—	—	—
Without disability (n = 8)	0.70	0.24	0.55–0.82	0.55–0.78

Source: K. E. Boyce, T. J. Shields, and G. W. H. Silcock, "Toward the Characterization of Building Occupancies for Fire Safety Engineering: Capabilities of Disabled People Moving Horizontally and on an Incline," *Fire Technology,* 35, 1, p. 64 (1999).

The abilities of disabled people cover a wide spectrum with respect to movement on horizontal and inclined planes. Given the significant differences in the capabilities of those using different mobility aids and the inherent differences in their spatial requirements, it is suggested that, for evacuation modeling purposes, they be considered separately.

Escape times are usually determined from characteristic travel speeds coupled with pre-movement times. From this study it is apparent that, for some disabled people, it may also be necessary to include periods of rest and time to negotiate changes in direction. This paper's findings should help designers derive characteristic

Table 3-12.26 *Speed on Stairs (descent) by Presence/Absence of Locomotion Disability—Unassisted Ambulant[62]*

Subject Group	Mean (m/s)	Standard Deviation (m/s)	Range (m/s)	Interquartile Range (m/s)
With locomotion disability ($n = 30$)	0.33	0.16	0.11–0.70	0.22–0.45
no aid ($n = 19$)	0.36	0.14	0.13–0.70	0.20–0.47
crutches ($n = 1$)	0.22	—	—	—
walking stick ($n = 9$)	0.32	0.12	0.11–0.49	0.24–0.46
rollator ($n = 1$)	0.16	—	—	—
Without disability ($n = 8$)	0.70	0.26	0.45–1.10	0.53–0.90

Source: K. E. Boyce, T. J. Shields, and G. W. H. Silcock, "Toward the Characterization of Building Occupancies for Fire Safety Engineering: Capabilities of Disabled People Moving Horizontally and on an Incline," *Fire Technology*, 35, 1, p. 65 (1999).

times for disabled people traversing any typical escape route.

The detailed observations made during the movement studies suggest that, in designing accessible escape routes, more attention needs to be focused on the real, rather than the perceived needs of disabled people. Consideration should be given to the nature and position of support systems such as handrails, and the positioning of doors in escape routes, since these will influence the progress and the flight behaviors of some disabled occupants.

The third study by Boyce, Shields, and Silcock[64] was an experimental study of door operation and egress. One hundred four ambulatory disabled persons, 54 male and 50 female, ages 25 to 85 participated in this study. The disabilities of the participants involved 5 using crutches, 28 using a walking stick and 8 using a walker. The time to negotiate a standard single leaf door with a clear width opening of 750 mm is presented in Table 3-12.27, with the type of door operation and the closer force on the door leaf. In addition to the ambulatory disabilities other critical disabilities for this action involved 45 persons with a minor reaching and stretching disability and 58 with a dexterity disability. Table 3-12.28 presents the failure rates and the time to negotiate the door for the seven manual wheelchair users. The manual wheelchair users, in general, took more time to push the door open than to pull the door open. It also took these wheelchair users three to four times longer than the ambulatory disabled persons to negotiate the door.

The fourth study by Boyce, Shields, and Silcock[65] was an experimental study to determine the ability of disabled persons to locate and read three types of exit signs: non-illuminated, internally illuminated and light emitting diode (LED) signs. The signs were placed in a clear atmosphere in a room, 2.3 m from the floor with a maximum viewing distance of 85 m. The distances at which the participants were able to read the exit signs were measured. A total of 118 disabled persons participated in this study, including 25 persons with a vision disability. Table 3-12.29 presents the distances at which the participants could read the signs. The LED signs appeared to be the most visible and legible by the disabled persons with and without vision disabilities.

Klote, Alvord, Levin, and Groner[66] examined the design considerations needed to enable the elevators in tall buildings to be utilized for the evacuation of disabled oc-

Table 3-12.27 *Time to Negotiate Door for Each Door Setting by Mobility Aid—Ambulant Disabled[64]*

Closing Force (N)	No Aid ($n = 63$) Mean (s)	Standard Deviation (s)	Range	Crutch Users ($n = 5$) Mean (s)	Range	Walking Stick Users ($n = 28$) Mean (s)	Standard Deviation (s)	Range (s)	Walking Frame/ Rollator Users ($n = 8$) Mean (s)	Range
Push										
21	3.0	0.8	1.7–4.5	3.7	3.6–3.8	3.7	1.5	2.3–7.4	7.9	2.0–12.8
30	3.5	2.2	1.9–15.0	3.0	2.5–3.2	3.8	1.5	2.5–7.3	6.3	2.2–10.5
42	3.7	1.5	1.6–10.2	3.8	2.9–5.2	4.0	1.6	2.3–7.5	5.2	2.1–10.3
51	4.1	2.4	1.0–14.3	3.6	3.1–3.9	4.3	2.4	1.5–10.7	7.9	2.0–14.3
60	4.0	1.9	1.3–13.0	3.8	3.6–4.1	3.7	1.5	1.7–7.9	5.2	2.0–10.3
70	4.3	2.0	1.7–11.2	3.9	3.3–4.6	4.6	2.1	2.5–11.1	6.2	1.7–11.2
Pull										
21	3.3	1.5	1.5–7.6	2.8	2.2–4.0	3.6	1.4	1.8–7.6	5.7	2.0–8.2
30	3.2	1.0	1.5–5.2	—	—	3.2	0.9	1.8–4.9	5.2	4.3–6.0
42	3.7	1.8	1.4–12.6	4.0	2.9–6.3	3.9	1.4	1.9–6.8	4.7	2.6–6.9
51	3.8	1.6	1.5–10.2	3.6	2.5–4.6	4.6	2.2	1.5–9.5	6.3	2.5–11.2
60	4.1	1.9	1.5–11.4	3.6	2.7–4.7	4.1	1.7	1.4–7.4	8.9	1.9–17.0
70	4.6	2.2	1.5–12.6	4.6	2.6–4.7	4.9	2.3	2.1–9.7	3.2	1.9–6.7

Source: K. E. Boyce, T. J. Shields, and G. W. H. Silcock, "Toward the Characterization of Building Occupancies for Fire Safety Engineering: Capability of Disabled People to Negotiate Doors," *Fire Technology*, 35, 1, p. 73 (1999).

Table 3-12.28 *Percentage Failure and Time to Negotiate Door for Each Door Setting—Manual Wheelchair Users[64]*

Closing Force Leading Edge (N)	No. of Failures (%)	No. (%) Successful	Mean (s)	Median (s)	Range (s)
Push ($n = 7$)					
30	1 (14.3)	6 (85.7)	13.1	7.4	3.6–39.0
42	1 (14.3)	6 (85.7)	13.3	10.7	3.6–36.0
51	2 (28.6)	5 (71.4)	10.0	7.4	3.6–20.5
60	2 (28.6)	5 (71.4)	10.5	10.5	3.5–17.4
70	2 (28.6)	5 (71.4)	11.6	6.7	3.6–26.3
Pull ($n = 7$)					
30	2 (28.6)	5 (71.4)	13.5	11.3	3.7–34.0
42	3 (42.9)	4 (57.1)	12.8	6.8	3.8–34.0
51	3 (42.9)	4 (57.1)	10.5	7.0	3.8–24.0
60	5 (71.4)	2 (28.6)	4.2	4.2	2.8–4.6
70	5 (71.4)	2 (28.6)	4.3	4.3	3.7–5.0

Source: K. E. Boyce, T. J. Shields, and G. W. H. Silcock, "Toward the Characterization of Building Occupancies for Fire Safety Engineering: Capability of Disabled People to Negotiate Doors," *Fire Technology,* 35, 1, p. 74 (1999).

cupants. In the explosion and fire in the World Trade Center with the loss of power in both Towers 1 and 2, including the emergency power, occupants were trapped in elevators in both buildings. Burns[11] indicated Tower 1 had 99 elevator cars, with many of them occupied. One 6-by 8-ft car, when opened, revealed 9 unconscious occupants, after an estimated exposure to the smoke in the shaft for approximately 2 hrs at the 9th floor level. Sherwood[67] reported that one 9- by 12-ft elevator car was stuck for 6 hrs at the 41st floor level of Tower 2 with 72 occupants: 62 elementary-school children and 10 adults.

NFPA *101,*® *Life Safety Code*®[16] in the 1991 edition permitted the use of elevators with fire fighter service from areas of refuge, which were also specified in this edition. In 1997 the *Life Safety Code*® permitted the use of a fire fighter service elevator with special features to be used as a second means of egress from towers with specifications on the occupant load, the provision of automatic sprinklers, the egress arrangement, and capacity.

Summary

Canter et al.[68] have stated the crux of the behavioral response in fire incidents in the following manner: "Behavior in fires can be understood as a logical attempt to deal with a complex, rapidly changing situation in which minimal information for action is available." It is suggested by Swartz[69] that the goals of codes should be "reoriented to increase the likelihood of informed decisions being made by people in fires." The examinations of the behavior in the Beverly Hills Supper Club fire led to the recommendation by Pauls and Jones[70] that "fire safety education should consider and be based on people's erroneous conceptions about distance being related to safety, and the time needed to escape from a fire emergency." Thus, more than a decade of detailed systematic research on human behavior in fires has resulted in the following consensus of the behavior of most persons, by Sime:[43]

Despite the highly stressful environment, people generally respond to emergencies in a 'rational' often altruistic manner, insofar as is possible within the constraints imposed on their knowledge, perceptions and actions by the effects of the fire. In short, "instinctive," "panic" type reactions are not the norm.

There is a complex relationship between the physical and social environment in which the behavior occurs, which is complicated by the individual's perception of the ambiguous fire cues and primarily influenced by the person's relevant training and previous fire experience. It must be recognized that the fire cues are a product of a rapidly changing dynamic process which is constantly altering the decisions of the occupant within the building.

Table 3-12.29 *Distance at Which Subjects Can Read Exit Signs by Presence/Absence of Seeing Disability[65]*

Type of Sign and Subject Group	Mean (m)	Median (m)	Standard Deviation (m)	Range (m)	Interquartile Range (m)
Non-illuminated exit sign					
All disabled ($n = 105$)	13.3	15.0	3.1	1.0–15.0	12.0–15.0
With seeing disability ($n = 25$)	11.4	12.0	4.0	1.0–15.0	9.7–15.0
Without seeing disability ($n = 80$)	13.7	15.0	2.7	6.0–15.0	15.0–15.0
Illuminated exit sign					
All disabled ($n = 118$)	14.2	15.0	2.7	1.0–15.0	15.0–15.0
With seeing disability ($n = 25$)	12.9	15.0	4.6	1.0–15.0	15.0–15.0
Without seeing disability ($n = 93$)	14.5	15.0	1.8	6.0–15.0	15.0–15.0
LED sign					
All disabled ($n = 83$)	14.6	15.0	1.6	5.0–15.0	15.0–15.0
With seeing disability ($n = 23$)	14.0	15.0	2.6	5.0–15.0	15.0–15.0
Without seeing disability ($n = 60$)	14.7	15.0	1.2	7.0–15.0	15.0–15.0

Source: K. E. Boyce, T. J. Shields, and G. W. H. Silcock, "Toward the Characterization of Building Occupancies for Fire Safety Engineering: Capability of People with Disabilities to Read and Locate Exit Signs," *Fire Technology,* 35, 1, p. 83 (1999).

Hazard Calculations

Pauls and Jones[70] have summarized this decision dilemma as follows: "What is an appropriate action at one stage may be quite inappropriate a minute later."

Paulsen[52] has emphasized the limited time constraints imposed on the occupant in a fire incident building as follows:

> With very limited time available in which to decide on a course of action, people involved in fires often face difficult decisions. Decisions may be intellectually difficult in the context of limited knowledge of the engineered safety or the basic configuration of the occupied structure or limited knowledge of the development of the fire itself. Decisions may be difficult because of the sometimes counterinstinctive nature of the correct response, because some additional risk to one's self is incurred by a decision to alert or assist others.

References Cited

1. J.L. Bryan, *Smoke as a Determinant of Human Behavior in Fire Situations,* University of Maryland, College Park (1977).
2. P.G. Wood, *Fire Research Note 953,* Building Research Establishment, Borehamwood, UK (1972).
3. L. Lerup, D. Conrath, and J. Koh Liu, *NBS-GCR-77-93,* National Bureau of Standards, Gaithersburg, MD (1978).
4. J.P. Keating and E.F. Loftus, *Psych. Today,* 14 (1981).
5. G. Proulx and J.D. Sime, "To Prevent Panic in an Underground Emergency: Why Not Tell People the Truth?" *Fire Safety Science—Proceedings of the Third International Symposium,* Elsevier Applied Science, New York, pp. 843–852 (1991).
6. G. Ramachandran, "Human Behavior in Fires—A Review of Research in the United Kingdom," *Fire Technology,* 26, 2, pp. 149–155 (1990).
7. G. Ramachandran, "Informative Fire Warning Systems," *Fire Technology,* 27, 1, pp. 66–81 (1991).
8. E.A. Cable, "Cry Wolf Syndrome: Radical Changes Solve the False Alarm Problem," Department of Veterans Affairs, Albany, NY (1994).
9. M. Kimura and J.D. Sime, "Exit Choice Behavior During the Evacuation of Two Lecture Theatres," *Fire Safety Science—Proceedings of the Second International Symposium,* Hemisphere Publishing Corp., Washington, DC, pp. 541–550 (1989).
10. J.K. Lathrop, "Two Fires Demonstrate Evacuation Problems in High-Rise Buildings," *Fire Journal,* 70, 1, pp. 65–70 (1976).
11. D.J. Burns, "The Reality of Reflex Time," *WNYF,* 54, 3, pp. 26–29 (1993).
12. R.F. Fahy and G. Proulx, "Collective Common Sense: A Study of Human Behavior During The World Trade Center Evacuation," *NFPA Journal,* 87, 2, pp. 61, 64 (1995).
13. C.H. Berry, *Fire J.,* 72, p. 105 (1978).
14. NFPA 74, *Household Fire Warning Equipment,* National Fire Protection Association, Quincy, MA (1975).
15. H. C. Cohen, *Fire J.,* 76, p. 70 (1982).
16. NFPA *101, Life Safety Code,* National Fire Protection Association, Quincy, MA (2000).
17. M.J. Kahn, *Fire Tech.,* 20, p. 20 (1984).
18. E.H. Nober, H. Pierce, A. Well, C.C. Johnson, and C. Clifton, *Fire J.,* 75, p. 86 (1981).
19. B. Latane and J.M. Darley, *J. of Person. and Soc. Psych.,* 10, p. 215 (1968).
20. J.L. Bryan, *A Study of the Survivors' Report on the Panic in the Fire at Arundel Park Hall, Brooklyn, Maryland, on January 29, 1956,* University of Maryland, College Park (1957).
21. S.B. Withey, in *Man and Society in Disaster,* Basic, New York (1962).
22. J.L. Bryan, *Human Behavior Factors and the Fire Occurrence,* University of Maryland, College Park (1971).
23. R.M. Killian, R. Quick, and F. Stockwell, *A Study of Response to the Houston, Texas, Fireworks Explosion,* National Academy of Science, Washington, DC (1956).
24. J.D. Sime, "Perceived Time Available: The Margin of Safety in Fires," *Fire Safety Science—Proceedings of the First International Symposium,* Hemisphere Publishing Corp., Washington, DC, pp. 561–570 (1986).
25. A. Mintz, *J. of Abn. and Soc. Psych.,* 66, p. 150 (1950).
26. B.K. Jones and J.A. Hewitt, "Leadership and Group Formation in High-Rise Building Evacuations," *Fire Safety Science—Proceedings of the First International Symposium,* Hemisphere Publishing Corp., Washington, DC, pp. 513–522 (1986).
27. S. Horiuchi, Y. Murozaki, and A. Hokugo, "A Case Study of Fire and Evacuation in a Multi-Purpose Office Building, Osaka, Japan," *Fire Safety Science—Proceedings of the First International Symposium,* Hemisphere Publishing Corp., Washington, DC, pp. 523–532 (1986).
28. J. Breaux, D. Canter, and J. Sime, *Psychological Aspects of Behavior of People in Fire Situations,* University of Surrey, Guilford, UK (1976).
29. L. Bickman, P. Edelman, and M. McDaniels, *NBS-GCR-78-120,* National Bureau of Standards, Gaithersburg, MD (1977).
30. G. Proulx, "A Stress Model for People Facing a Fire," *Journal of Environmental Psychology,* 13, pp. 137–147 (1993).
31. M. Chubb, "Human Factors Lessons for Public Fire Educators: Lessons from Major Fires," Education Section, National Fire Protection Association, Phoenix (1993).
32. G.A. Klein and D. Klinger, "Naturalistic Decision Making," CSERIAC Gateway, Wright-Patterson AFB, Crew System Ergonomics Information Analysis Center, pp. 1–4 (1991).
33. D. Canter, J. Breaux, and J. Sime, "Domestic, Multiple-Occupancy, and Hospital Fires," in *Fires and Human Behaviour* (David Canter, ed.), John Wiley & Sons, New York, pp. 117–136 (1980).
34. R.L. Best and D.P. Demers, *Fire J.,* 76, p. 19 (1982).
35. J.L. Bryan, *Fire J.,* 76, p. 37 (1982).
36. G.P. Morris, *F. Command,* 68, p. 20 (1981).
37. J.L. Bryan and P.J. DiNenno, *NBS-GCR-79-187,* National Bureau of Standards, Gaithersburg, MD (1979).
38. J.L. Bryan, *An Examination and Analysis of the Dynamics of the Human Behavior in the MGM Grand Hotel Fire,* National Fire Protection Association, Quincy, MA (1983).
39. J.L. Bryan, *An Examination and Analysis of the Dynamics of the Human Behavior in the Westchase Hilton Hotel Fire,* National Fire Protection Association, Quincy, MA (1983).
40. R.L. Best, *Fire J.,* 72, p. 18 (1978).
41. D.P. Schultz, *Contract Report NR 170-274,* University of North Carolina, Charlotte (1968).
42. Kentucky State Police, *Investigative Report to the Governor, Beverly Hills Supper Club Fire,* Kentucky State Police, Frankfort (1977).
43. J.D. Sime, in *Fire and Human Behavior,* John Wiley and Sons, New York (1980).

44. E.L. Quanrantelli, *Panic Behavior in Fire Situations: Findings and a Model from the English Language Research Literature,* Ohio State University, Columbus (1979).

45. J.P. Keating, *Fire J.,* 76, p. 57 (1982).

46. E.R.F. Crossman, W.B. Zachary, and W. Pigman, *UCBFRG/WP 75-5,* University of California, Berkeley (1975).

47. National Fire Prevention and Control Administration, *Highlights of the National Household Fire Survey,* U.S. Fire Administration, Washington, DC (1976).

48. T. Jin and T. Yamada, "Experimental Study of Human Behavior in Smoke-Filled Corridors," *Fire Safety Science—Proceedings of the Second International Symposium,* Hemisphere Publishing Corp., Washington, DC, pp. 511–519 (1989).

49. G. Proulx, "The Impact of Voice Communication Messages During A Residential Highrise Fire," *Human Behavior in Fire Proceedings of the First International Symposium,* Fire SERT Centre, University of Ulster, pp. 265–274 (1998).

50. A.W. Heskestad and K.S. Pederson, "Escape Through Smoke: Assessment of Human Behavior and Performance of Wayguidance Systems," *Human Behavior in Fire Proceedings of the First International Symposium,* Fire SERT Center, University of Ulster, pp. 631–638 (1998).

51. T. Jin, "Studies on Human Behavior and Tenability in Fire Smoke," *Fire Safety Science—Proceedings of the Fifth International Symposium,* International Association for Fire Safety Science, pp. 3–21 (1997).

52. R.L. Paulsen, *Fire Tech.,* 20, p. 15 (1984).

53. J.L. Bryan, P.J. DiNenno, and J.A. Milke, *NBS-GCR-80-297,* National Bureau of Standards, Gaithersburg, MD (1979).

54. J.L. Bryan, J.A. Milke, and P.J. DiNenno, *NBS-GCR-80200,* National Bureau of Standards, Gaithersburg, MD (1979).

55. J.L. Pauls, in *Human Response to Tall Buildings,* Dowden, Hutchinson and Ross, Stroudsburg, Germany (1977).

56. M.S. Isner and T.J. Klem, "Fire Investigation Report, World Trade Center Explosion and Fire, New York, New York, February 26, 1993," National Fire Protection Association, Quincy, MA (1993).

57. M.S. Isner and T.J. Klem, "Explosion and Fire Disrupt World Trade Center," *NFPA Journal,* 87, 6, pp. 91–104 (1993).

58. E. Juillet, "Evacuating People with Disabilities," *Fire Engineering,* 126, 12, pp. 100–103 (1993).

59. E. Juillet, Personal Communication, (Jan. 18, 1994).

60. K.E. Boyce, T.J. Shields, and G.W.H. Silcock, "Toward the Characterization of Building Occupancies for Fire Safety Engineering: Prevalence, Type, and Mobility of Disabled People," *Fire Technology,* 35, 1, pp. 35–50 (1999).

61. K.E. Boyce, T.J. Shields, and G.W.H. Silcock, "Toward the Characterization of Building Occupancies for Fire Safety Engineering: Prevalence, Type, and Mobility of Disabled People," *Fire Technology,* 35, 1, p. 48 (1999).

62. K.E. Boyce, T.J. Shields, and G.W.H. Silcock, "Toward the Characterization of Building Occupancies for Fire Safety Engineering: Capabilities of Disabled People Moving Horizontally and on an Incline," *Fire Technology,* 35, 1, pp. 51–67 (1999).

63. K.E. Boyce, T.J. Shields, and G.W.H. Silcock, "Toward the Characterization of Building Occupancies for Fire Safety Engineering: Capabilities of Disabled People Moving Horizontally and on an Incline," *Fire Technology,* 35, 1, pp. 66–67 (1999).

64. K.E. Boyce, T.J. Shields, and G.W.H. Silcock, "Toward the Characterization of Building Occupancies for Fire Safety Engineering: Capability of Disabled People to Negotiate Doors," *Fire Technology,* 35, 1, pp. 68–78 (1999).

65. K.E. Boyce, T.J. Shields, and G.W.H. Silcock, "Toward the Characterization of Building Occupancies for Fire Safety Engineering: Capability of People with Disabilities to Read and Locate Exit Signs," *Fire Technology,* 35, 1, pp. 79–86 (1999).

66. J.H. Klote, D.M. Alvord, B.M. Levin, and N.E. Groner, "Feasibility and Design Considerations of Emergency Evacuation by Elevators," NISTIR 4870, NIST, Building and Fire Research Laboratory, Gaithersburg, MD (1992).

67. J. Sherwood, "Darkness and Smoke," *WNYF,* 54, 3, pp. 56–60.

68. D. Canter, J. Breaux, and J. Sime, *Human Behavior in Fires,* University of Surrey, Guilford, England (1978).

69. J.A. Swartz, *Fire J.,* 73, p. 73 (1979).

70. J.L. Pauls and B.K. Jones, *Fire J.,* 74, p. 35 (1980).

CHAPTER 13

Movement of People: The Evacuation Timing

Guylène Proulx

Introduction

This chapter is an updated version of the chapter "Movement of People" written originally by Jake Pauls. Most of the initial material is still in the chapter, for example, basic crowd movement characteristics (density, speed, and flow) with some new examples. Extensive descriptions are given of building evacuation models developed by Pauls, based on empirical studies in Canada. The effective-width model for evacuation flow is highlighted, especially in relation to prediction formulas for the total evacuation time of large buildings. Some original material has been included regarding the time delay to start an evacuation, the movement of people with disabilities, and occupant movement in smoke. Although all the answers on these new themes are not yet available, it was felt important to include these issues in this chapter. A limited number of studies have been conducted on these questions; however, with the ever-increasing use of performance-based design, it has become essential for the fire safety engineer to consider their impact on fire safety.

Note of Caution

A caution must be given regarding limitations in the quantitative methods currently available for people's movement in buildings. Some traditional assumptions about people's behavior in fires have been shown to be erroneous by research, especially that conducted during the

Guylène Proulx is a research officer at the Fire Risk Management Program of the National Research Council of Canada, since 1992. She holds a Ph.D. in architectural planning from the University of Montreal specializing in environmental psychology. She focuses her research on investigating human response to alarms, evacuation movement, typical actions taken, timing of escape, time to start evacuation, and social interaction during a fire. She is a member of the National Fire Protection Association (NFPA), the Society of Fire Protection Engineers (SFPE), the Human Factors and Ergonomics Society (HFES), and the International Association for Fire Safety Science (IAFSS).

last three decades. (See Section 3, Chapter 12.) Some models of evacuation behavior, such as the so-called hydraulic model, although applicable to certain situations, should not be applied indiscriminately to any situation. Valuable here are the views of John Archea, abstracted from his remarks (summarized by Pauls[1]) at the International Life Safety and Egress Seminar in 1981.

Most egress rules were developed in their present form some twenty years before research was done.

Research on people's movement falls into two schools: the carrying capacity school which examines exit flow capacity, and the human response school which says that exit capacity may be a necessary condition for safe egress, but it is not a sufficient condition. In the former, the "safe end" of the egress route is emphasized as the key point where egress is to be evaluated. The human response school looks at what happens at the other end of the route—the threatened end of the egress route. The former assumes that people will, upon hearing an alarm, drop what they are doing and immediately evacuate in an orderly fashion, without interacting with each other. Actually, people tend to ignore or downplay the initial fire cues, eventually they investigate conditions, compare with their experience, and then decide on actions that may have little to do with what is assumed in code rules for egress. Such activities take time. Another finding is that familiar entry routes are more likely to be used for evacuation than egress routes that have never been experienced before. Consequently, routes that are being counted on to "drain" the building of its occupants may be disregarded in an actual evacuation.

Traditional exit technology also relies on what is called the "hydraulic model." There are three assumptions in the hydraulic model: occupants are alert, able-bodied, and ambulatory; fire safety depends on the safe end of the evacuation

system; and there is a high-density building population that will tax the capacity of the exit system. There are two phases to evacuation: the time to start and the movement phase. The hydraulic model deals only with the latter. Liquid flow or ball-bearing models do not account for the fact that people will take time to investigate the situation, help one another or that they have different degrees of familiarity with particular routes.

Archea's remarks raise basic questions about long-standing approaches to the design of means of egress. A related chapter, "Behavioral Response to Fire and Smoke" (Section 3, Chapter 12), should be consulted for some of the background research that is helping to describe people's actual behavior when encountering fire. Additional research on the topic of fire-related human behavior, especially the behavior associated with egress, is found in the following literature review.

Literature Review

The following should be regarded as an indicative survey rather than a complete review of technical contributions to the subject of evacuation. Some additional background is provided in reviews by Stahl and Archea,[2] Stahl, Crosson, and Margulis,[3] Paulsen,[4] and Pauls.[5]

Early Committee Documents

The 1935 report *Design and Construction of Building Exits*[6] described committee deliberations; however, it is sometimes incorrectly spoken of as a research document. Because it contains a mix of traditional practice with some empirical studies, the report is often misinterpreted regarding qualitative and quantitative aspects of exit use by crowds; for example, the unit exit width and unrealistically high flow figures, such as 45 persons per min per unit of exit width downstairs, are concepts that predated the 1935 work. These errors influence time-based egress design calculations even today.

Sharing many of the characteristics of the 1935 report, and building upon some of its contents, is its British counterpart, *Post-War Building Studies, No. 29*.[7] This report helped to establish the nominal 2.5-min clearing time for a space (based on a reported successful evacuation time of 2.5 min in the Empire Palace Theatre fire in Edinburgh in 1911), and it suggested the use of very high flows to perform the population capacity calculation (i.e., 40 persons per min per 530 mm or 21 in. of exit width).

General Research on Crowd Movement

The post-war era also marked the beginning of modern studies of crowd movement, notably in Japan by Kikuji Togawa, whose many technical insights and empirical data were reported in 1955.[8] Among his mathematical presentations we find an equation for "time required for escape." It takes into account the flow time for an egress element plus the time needed to traverse some distance in the egress system. This general form of equation appears often in the egress literature.

Post-war publications by Russian experts included highly abstract treatment of evacuation, but did not provide the kind of empirical detail presented by Togawa. Most often referenced is the book titled (in its 1978 English translation) *Planning for Foot Traffic Flow in Buildings*, by Predtechenskii and Milinskii.[9] Their work is little known (and used even less) in North America; however, some of their abstract treatment and graphical techniques have been applied by Kendik,[10,11] using data from evacuation observations in Germany in 1977.

Often mentioned in some egress literature is a small-scale study by an operations research team that worked for the London Transport Board. The team's observations and tests were described in an unpublished research report,[12] and highlights were published by Hankin and Wright.[13] The former unpublished report has been widely circulated, referenced, and misapplied by people who compounded some original defects in the report, such as the failure to distinguish between maximum and mean flows. Again, as with earlier widely referenced but not critically read documents, this has led to overly optimistic predictions of egress time in some calculations. There are other problems inherent as well in applying data from a special-population transit context to the context of evacuation via (unfamiliar) routes, such as exit stairs. Caution on this should also be heeded when applying some of the work by Togawa[8] and Fruin.[14]

John Fruin is a prominent researcher in North America whose well-known book *Pedestrian Planning and Design*[14] is now available in a revised edition. It is a comprehensive reference book on crowd movement. Fruin's work is often referred to in time-based analyses; however, these analyses sometimes tend either to misuse the data for levels of service E and F (which Fruin recommends to be used rarely, if at all, in analysis or design situations) or to combine high-flow density assumptions with relatively high-speed assumptions (an unrealistic combination). Used conservatively (including width deductions for the edge effect also reported by Fruin), there is much similarity between movement characteristics recommended by Fruin and those coming from Pauls' studies.

Between 1972 and 1982, many field observations—mostly unanalyzed and unpublished—were conducted by the National Research Council of Canada. These observations concentrated on people's movement in large assembly-occupancy buildings and large-scale events, such as the 1976 Commonwealth Games in Edmonton. This work provided further empirical underpinning to the effective-width model for crowd flow on egress routes.

The work on evacuation and human behavior in fire has known a renewed of enthusiasm with the arrival of many new researchers in the 1990s. The number of papers on this subject at conferences such as the International Association for Fire Safety Science (IAFSS), Interflam, and First International Symposium on Human Behavior in Fire, and at NFPA's meetings demonstrates the vitality of the field in the last decade.

Research on Tall Buildings

Near the end of the 1960s the matter of high-rise fire safety became a rapidly growing concern to safety officials

and committees working on standards and codes. Among the papers prepared at that time on the matter of evacuation time of tall buildings and the design of exit stairs were ones by Galbreath,[15] Melinek and Booth,[16] and Melinek and Baldwin.[17] These papers contained a reworking of some of the "classical" reports from the 1930s and 1950s to provide formulas relating exit stair width and minimum total evacuation time. Few new data were presented, and the formulas in general seriously underestimated total evacuation times of such buildings.

Beginning in 1969, Pauls began comparatively systematic and detailed observations of many evacuation drills in tall buildings, especially in Ottawa, Canada. Ignoring relatively inaccessible early references, the work is represented in general conference publications and periodical articles[18–20] and in published analyses and applications, especially on the "effective-width model."[21–27] Although dealing largely with evacuation situations where a "hydraulic model" is valid (e.g., there is queuing by people waiting to use egress routes, and much of the activity is relatively simple crowd movement dedicated to egress), this work bridged between movement studies and concurrent studies examining people's behavior in fires (especially in Great Britain and the U.S.). The behavioral studies identified the role played by nonevacuation behavior before, during, and even in place of simple evacuation movement—all of which tend to significantly increase the actual evacuation times of buildings.

Mention should be made of more recent studies of evacuation of tall buildings, mostly in drills but some in connection with serious fires. Many of these studies have been published in conference proceedings. The most highlighted book on this subject is the *Proceedings of the First International Symposium on Human Behaviour in Fire,* 1998, available through FireSERT at the University of Ulster, Belfast, United Kingdom.

By way of a very general and incomplete summary, some conclusions can be drawn regarding movement of people in fire:

1. Panic is very rare even in fires. Normal patterns of behavior, movement route choices, and relationships with others tend to persist during emergency situations.
2. People's behavior tends to be altruistic and reasonable, especially in light of the limited and often ambiguous information available to people at the time of the event.
3. After perceiving a fire cue, such as the fire alarm signal or smelling smoke, people often ignore these initial cues or spend time investigating, seeking information about the nature and seriousness of the situation, which creates a delay time before starting evacuation movement.
4. Faced with ambiguous information and short time for decision making, people are likely to apply a well-run decision plan when choosing an evacuation route, consequently moving toward their most familiar way out of the building.
5. Evacuation, and response to fire generally, is often a social response; people tend to act as a group and to attempt to evacuate with people with whom they have emotional ties.
6. Problems that are encountered during normal building use will tend to persist and exacerbate situations in emergencies. Included are faulty communication, circulation hazards, wayfinding problems.

A key assumption, based on such findings, is that the movement of people observed in normal building use and in evacuation drills is a good basis for predicting their movement in a fire emergency. Specifically, people should not be expected to react faster or move more efficiently in a fire emergency than they do normally. Therefore, much of the evacuation technology, derived from careful documentation of realistic evacuation drills (e.g., without prior warning), is a good basis for developing guidelines for the design and use of emergency egress systems. This is a key to the validity of much of the technology presented in this chapter as well as to the validity of evaluation procedures for egress systems.

Crowd Behavior and Management

Crowd incidents, in which people are seriously injured or killed due to crushing or trampling, are not restricted to emergencies (such as fire), to conditions of crowd violence, or even simply to exuberance of some members of a crowd. Such events can occur, and have occurred, at sports events, religious gatherings, and rock music concerts. Serious injury and even death can occur during entry, occupancy, and evacuation of a building. It can happen under conditions that might, in every other respect, appear to be nearly normal, even to people in close proximity to those hurt in the incident.

An introduction to some problems and solutions for crowd safety has been provided by Pauls[28] and Fruin.[29,30] Pauls notes crowd incidents in Britain, Canada, and the United States and refers to reports such as the one by SCION,[31] prepared after 66 football fans died in a crowd crush on a stairway in 1971 in Ibrox Park, Glasgow (which influenced a U.K. standard for sports grounds);[32] the report of a special committee set up after 11 people were crushed in a crowd waiting to get into a rock concert in Cincinnati in 1980;[33] and a record of a meeting of experts called together by the U.S. National Bureau of Standards (NBS)[34] in response to the Cincinnati committee. Recent contributions to the literature include the reports of British Inquiries into the Hillsborough stadium crush that killed 95 soccer fans in 1989, the Bradford stadium fire, plus crowd incidents in Brussels and Sheffield.[35–38] Crowd safety engineering is also the subject of a book.[39]

Among the NBS report[34] design recommendations, mostly in relation to ingress, some recommendations have wide applicability:

1. Strive for simplicity in all access and movement routes; this lessens the need for directional graphics and ushers.
2. Capacity-handling channels should be continuous walking surfaces, such as ramps. Stairs are satisfactory to shorten channels not subject to heavy pedestrian loads.
3. To the greatest extent possible, ingress systems should be "reversible" and usable whenever emergency egress is necessary.

Among technical papers appended to the NBS report 94 was one by Fruin, entitled "Crowd Disasters—A Sys-

tems Evaluation of Causes and Countermeasures" (which was subsequently republished).[29,40] This paper discusses four fundamental elements—time, space, information and energy—in relation to the following aspects of serious crowd incidents:

1. Rapid accumulation of queuing persons as demand for a facility outstrips its capacity.
2. Pedestrian densities that approach the critical density of about 8 persons/m² (less than 1.5 ft²/person) leave no space between people. Shock waves, causing individuals to move involuntarily as much as 3 m (10 ft) laterally, can be seen moving through crowds in this situation.
3. Competitive rushing by a crowd away from something is termed "panic" by Fruin, and competitive rushing toward some objective (such as in the Cincinnati incident) is termed a "craze."

In relation to the second item on this list and to the unusual physical forces in crowd incidents, Fruin notes[29]

> The combined pressures of massed pedestrians and shock-wave effects through crowds at the critical density level produce forces which are impossible for individuals or even small groups of individuals to resist. Reports of persons being literally lifted out of their shoes and of clothes being torn off are a common result of the forces involved in crowd incidents. Survivors of crowd disasters report difficulty in breathing due to crowd pressures, and asphyxia is a more typical cause of death than trampling by the crowd. In the Glasgow, Scotland, soccer stadium incident in which 66 persons died, the failure of a steel railing under crowd pressures contributed to the piling up of pedestrians. The bending of a steel-pipe railing under crowd pressures was reported at the Cincinnati Coliseum incident. The force required to bend a 50-mm (2-in.) diameter steel railing, applied 0.75 m (30 in.) above the base, is estimated at 500 kg (1100 lb.).

Fruin lists countermeasures for critical density levels, such as provision of adequate pedestrian processing capacity and control of demand (e.g., arrival process). Also recommended are dispersion of routes as well as separation of waiting pedestrians into smaller groups. The U.K. *Guide to Safety at Sports Grounds*[32] calls for systems of rails placed across the tops of wide stairs to break up large mass flows onto stairs into smaller flows that will not tax the stair's capacity so severely, thus reducing crowd forces to safe levels, a method sometimes termed "metering." Under this U.K. guide—made mandatory retroactively through reference in British regulations—such crowd control rails, as well as all guardrails, must be designed to resist loads that are much greater than called for in North American code requirements for guardrails.

Crowd incidents often exhibit what can be termed a failure of front-to-back communication, which was well represented in the rock concert incident at the Toronto's Exhibition Stadium in July 1980.[41] People at the back of a crowd or bulk queue may contribute unknowingly to the forces that can build up in the crowd, forces that can reach crushing levels in the middle of the crowd or at the front, especially where forward movement is stopped by a barrier. The people being crushed are unable to communicate their plight to those at the back. For example, this was exhibited very well during the Hillsborough stadium crush in 1989.[35,42] Thirty minutes away from kickoff, the terrace section (standing spectators) of the Leppings Lane stand was near capacity, although some room was still available in the outer pens. Outside, several thousand fans, some without tickets, were trying to push and force their way forward. With the congestion building up outside to dangerous levels, the police made the decision to open a gate into the stadium. Suddenly the intense pressure from outside was dramatically transferred inside to the narrow confines of a tunnel that was the quickest way to the terrace. The extreme pressure at the back of the crowd pinned the people at the front against the steel-wire fence. Some of the victims trapped were women and children who thought being in front was the safest place to watch the game. Five minutes after it started, the match was interrupted, with visual indication from television coverage that injuries might have occurred on the terrace. In total, 95 people died, suffocated, or were trampled to death, and another 400 were injured.

There is a distinction between "crowd management" and "crowd control." Designers and managers of places where crowds assemble should be aware of this distinction, which is carefully drawn, at least by leading North American crowd behavior experts. To manage a crowd is to make use of design and operating features based on the subtle and beneficial exploitation of people's natural behavior. This requires a good understanding of a crowd's reason for being, and the collective motivation of its members. Crowd control, on the other hand, is a more extreme, disruptive line of defense when crowd management is not successful; it might include dramatic police actions to subdue mob violence with force against force. Unfortunately, little literature exists that can be referenced here for guidance; designers or consultants working on projects subject to use by crowds should seek the advice of experienced facility and event managers as well as use their own powers of observation. Examples of crowd control—which have little to offer designers and managers—may be viewed on television news accounts of riots. Examples of generally very good crowd management can be seen at the Disney complexes.

Basic Movement Characteristics and Relationships

Crowd movement is quantitatively specified using three fundamental characteristics, all of which are expressed as rates. These are density, speed, and flow. Density is the number of persons in a unit area of walkway (e.g., 2.0 persons/m²). Often this characteristic is referred to by using the inverse of density, that is, the area per person or pedestrian module, for example, 0.5 m² (5.4 square ft²) per person. Speed is simply the distance covered by a moving person in a unit of time [e.g., 1.0 m/s (3.3 ft/s)]. The term "flow" is often used in a casual, nontechnical way when the general term "movement" is implied, or

when speed is actually being specified. Flow is specifically the number of people that pass some reference point in a unit of time (e.g., 2.0 persons/s). These three characteristics are related, along with path width, in the fundamental traffic equation (which, incidentally, applies to motor vehicles as well as pedestrians)

$$\text{flow} = \text{speed} \times \text{density} \times \text{width} \quad (1)$$

For example, the density, speed, and flow values shown above are consistent with what would be obtained with this equation, assuming the walkway's width is 1.0 m (3.3 ft). Note that, to be correct, a consistent set of units must be used, and speed must be measured along the slope of the walkway.

Also important is that speed is dependent on density. People can move quickly with a normal gait if there is a great deal of space between them. The closer they are to each other, the more constrained is their movement until, when very close together, they can only shuffle along slowly. Aside from these speed implications, high-density situations are also uncomfortable to varying degrees, depending on culture, social setting, and the relationship to those nearby. Expressed quantitatively, when the pedestrian density is less than about 0.5 persons/m² (21 ft²/person), people are able to move along walkways at about 1.25 m/s (4.1 ft/s), an average unrestricted walking speed. With greater density, speed decreases, and it decreases very markedly with very high densities, reaching a standstill when density reaches 4 or 5 persons/m² (2.1 to 2.6 ft²/person), equivalent to a fairly crowded elevator situation. This is also similar to the situation in a closely packed bulk queue of people anxiously waiting or competing to get through an entrance. Speeds of movement are more variable at low densities. When density is low, it is not necessarily accurate to calculate high speeds of movement. In fact, at low density, the main factors that will determine speed are more likely to be occupants' characteristics such as age, limitations, and grouping. For example, a family group is likely to move at the speed of its slowest member, being a child or a senior person.

On stairs, the speeds of movement are slightly lower and, at low densities, relatively fit people can average about 1.1 m/s (3.6 ft/s) descending along the stair slope [a horizontal speed component of about 0.8 m/s (2.6 ft/s)]. The speed-density relation data from a study by Pauls[23] in uncontrolled total evacuations of tall office buildings are shown in Figure 3-13.1. A curve representing similar speed-density findings reported by Fruin[14] is included in Figure 3-13.1 along with a regression equation for Pauls's data. (Note that Fruin's data were not derived from observations of evacuation in buildings.)

Given these dynamics as illustrated in Figures 3-13.1 and 3-13.2, there is a relatively complex relationship between flow and density. As shown in Figure 3-13.2, flow is small at both low and very high densities, but it attains a peak or optimum value at some intermediate density ranging around 2.0 persons/m², depending on whether people are on a level walkway or on a stairway. Equation 2 describes the flow-density relation obtained empirically for stairs used in total evacuations of tall office buildings.[23]

$$\text{flow} = [1.26(\text{density})] - [0.33(\text{density})^2] \quad (2)$$
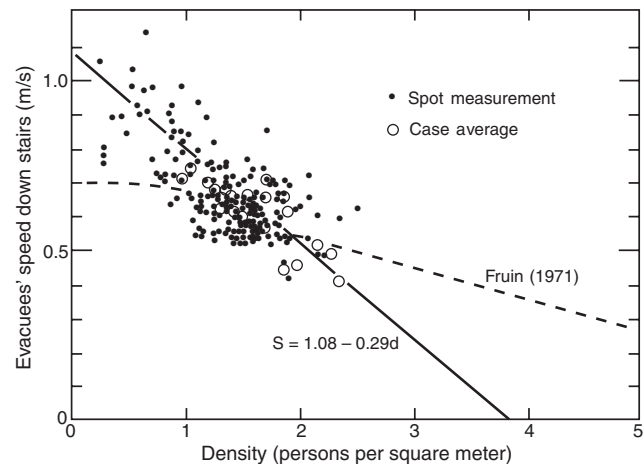
Figure 3-13.1. *Relation between speed and density on stairs in uncontrolled total evacuations.*
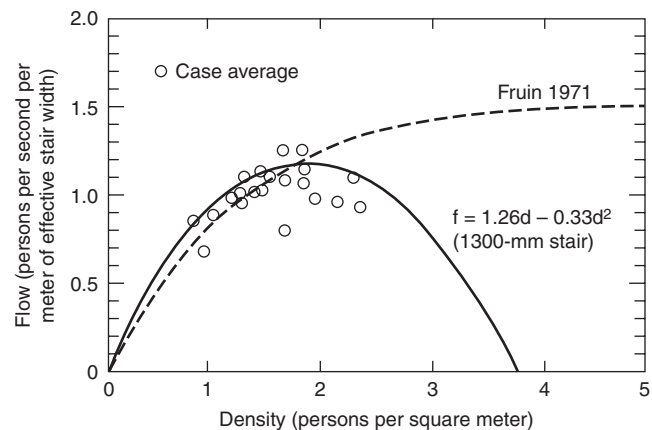
Figure 3-13.2. *Relation between flow and density on stairs in uncontrolled total evacuations.[61]*

These basic characteristics and relationships are often described in publications on pedestrian movement.[14] Little should be made of the differences in the curves at the high-density end in Figure 3-13.2. As seen from the data points in Figure 3-13.1, these conditions are rarely or never observed, and the differences are mainly of academic interest.

Put into simple terms, the optimum flow conditions observed in uncontrolled total evacuation drills on a typical 1120-mm (44-in.) wide exit stair in a well-populated office building evacuation are as follows:

1. Each person would occupy slightly less than two treads.
2. There would be a descent of one storey every 15 seconds.
3. One person per second would pass a fixed point.

Going further, for evacuees on such an optimally-loaded stairway, there would be one evacuee on every other stair, staggered left and right. These conditions are similar to those expected with level of service E, the busiest level of service recommended for stairs by Fruin.[14]

Expressed abstractly, the optimum flow conditions for evacuation downstairs include

1. Density of 2.0 persons/m^2
2. Speed of 0.5 m/s along the stair slope
3. Flow of 1.18 persons/(m·s) of effective stair width

Note that a stair's effective width is 300 mm (12 in.) less than its nominal width (credited in building codes); for example, a nominal width of 1120 mm (44 in.) equates to an effective width of 812 mm (32 in.).[23,24,26] This is described more completely in the following subsection.

Fruin's Levels of Service

Chapter 4 of Fruin's *Pedestrian Planning and Design*[14] is much used as a basis for deciding on appropriate pedestrian values to be used in dynamic exit calculations. The book's central concepts and data are also available in several other publications.[43,44]

Fruin describes six levels of service (A through F) for walkways, stairways, and queuing. Level A provides the highest standard with the least chance of congestion; level F provides the lowest—Fruin notes, an unacceptably low—standard with much congestion. Chapter 4 describes the levels of service in terms of flow as a function of area per persons, or "pedestrian module"—the inverse of crowd density—while Chapter 3 describes how speed varies with the module. For emergency movement and limited space situations, usually of concern to a fire protection engineer, levels of service C, D, and E should be used. Expressed in Fruin's original imperial-units form, pedestrian modules range, respectively, from about 25 to 5 ft^2/person (2.3 to .5 m^2/person) on walkways and 10 to 4 ft^2/person (0.9 to .4 m^2/person) on stairways. Corresponding flows range from 10 to 25 PFM [persons per foot (of effective width) per minute] [.5 to 1.4 persons/(m·s) of effective width] on walkways and 7 to 17 PFM [.4 to .9 person/(m·s)] on stairways (plus or minus 1 PFM [(0.5 person/(m·s)], respectively, depending on whether descent or ascent is required). Speeds of movement, which are more variable at low densities, range in average value from 250 to 100 ft/min (1.27 m/s to .51 m/s) on walkways

and from 115 to 70 ft/min (.58 m/s to .36 m/s) (along the slope) on stairs. It is estimated that ramps with slopes up to about 5 percent do not decrease movement speed; a 10 percent upward slope decreases speed by about 10 percent; an unusually steep 20 percent upward slope leads to a 25 percent reduction in speed.

Fruin also reports reductions in walkway effective width due to edge effects; however, he did not carry his work as far as Pauls did in relation to stairs, nor did he carry out detailed documentation of the effective width of corridors as did Habicht and Braaksma,[45] who reported edge effects of about 150 mm (6 in.) at each corridor wall, edge effects similar to what Pauls found at stair walls.

Evacuation Timing

The level-of-service characteristics, described previously, are stated in terms of rates. Most important, however, is the total time needed for evacuation to be completed. The total time taken for people to move past or through one part of a circulation system, which is the flow time, must be distinguished from the movement time, which is time taken to go from a point of origin to some destination, such as a remote place of safety. The flow time is simply a function of the crowd flow capacity of the usable width of a particular circulation element and the population or number of people to be moved through it. Population, capacity, and flow time are related as follows:

$$\text{population} = \text{flow capacity} \times \text{flow time} \qquad (3)$$

Evacuation time is relatively complex, and it is more difficult to control and predict than is flow time. The total evacuation time contains two major components: (1) the delay time to start evacuation movement and (2) the time needed to travel to a place of safety.

The time available for a safe evacuation of the occupants in the event of a fire is limited to the time when untenability conditions occur in the evacuation route. In a way to visualize the timing of escape, Figure 3-13.3 illustrates the different components of the time available (this
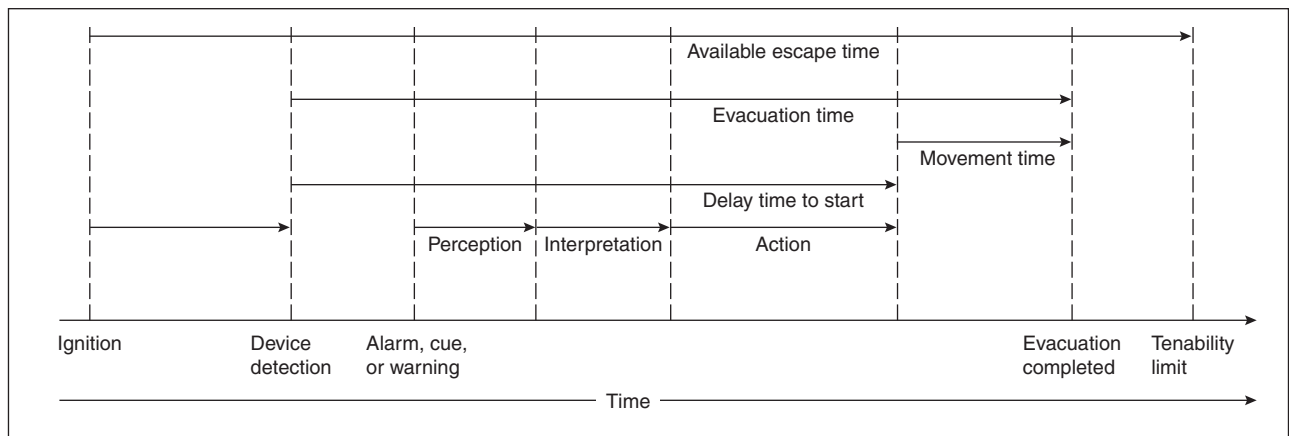
Figure 3-13.3. *Sequence of occupant response to fire.*

figure is largely inspired by British Standard (BS) Draft for Development document DD240, 1997,[46] and the FIRE-CAM occupant response model, 1992[47]).

The time of ignition is the starting time of the fire event. Then a time should be calculated for the detection to take place. Detection could take a few seconds to a few hours, depending on the type of fire and the detection devices in place. An elapsed time should be calculated between detection and alarm activation. In some cases, these two events are almost simultaneous, but there could be a delay, for example, if occupants have to manually activate the fire alarm signal at a pull-station. When the fire alarm signal, or cue, has been perceived, then a time to start should be calculated. The fire alarm may not be activated or may not work, so occupants will eventually perceive some cues from the fire or will receive a warning by others. The delay time to start comprises 3 subcomponents: perception, interpretation, and action. Perception is the time occupants will take to perceive the fire alarm signal; it could also be a fire cue or warning by others. Interpretation of this information will take some time, and different actions will be taken to investigate or search for more information before a decision to evacuate is made. Once the decision to evacuate is made, occupants will engage in other actions before leaving, such as getting dressed, gathering children, or finding valuables. After the perception-interpretation-action process has taken place, then the occupants will start to move. Movement time should be calculated from the flow time through various elements of the egress system and the travel time to move along an egress route. The evacuation time is calculated from the time of alarm signal activation until the last occupant to evacuate has reached a location of safety. This time should be less than the time when untenability occurs (some say half the time).

Delay Time to Start

The time occupants will take to initiate their evacuation movement once they have perceived some cues of the fire can be a difficult figure to estimate. In the past, no such delay was considered, which made calculation easier but provided totally inaccurate evacuation times. Traditionally, it was assumed that as soon as the occupants would perceive fire cues or the fire alarm signal, they would start to evacuate the building. Victims reporting their behavior during fires have always challenged this assumption of immediate response. In the calculation of an expected total time to evacuate a building, it is now a common practice to add some time to account for a delay to start evacuation.

The literature on time delay to start is still scarce, but data from case studies are appearing constantly. It is important to mention that what is called here delay time to start or time to start is considered under "premovement," particularly in the British literature. This denomination of premovement is a bit peculiar, since occupants' behavior during this premovement time is usually to move around trying to figure out the situation. Therefore, there could be a lot of movement during this premovement time; this explains why the expression *delay time to start* is preferred here.

It was suggested in former editions of this chapter that a safe bet to account for the delay time to start would be to double the calculated time to move to obtain the overall time to evacuate. Many fire safety engineers, however, have found this approach too demanding on their design and prefer to add 15 to 30 s to account for the delay time to start. Is 30 s reasonable, or is 3 min more realistic? Instead of picking up numbers in the air, it is important to closely study the available research findings.

The delay time to start has been studied in two ways: during evacuation drills and from fire victim interviews. Some tend to denigrate the fire drill studies, although they are perfectly representative of a fire situation, especially if the drill is nonannounced. Fire drills represent exactly the situation that would face occupants if the fire were located in a remote area or on an upper floor of the building and the only sign of fire would be the sudden sound of the fire alarm signal.

In Canada, Proulx's obtained the time to start of over 500 occupants of 7 mid-rise and high-rise residential buildings during evacuation drills.[48] For ethical reasons, occupants of these residential buildings received a note a few weeks before the exercise informing them that a fire drill would be conducted in their building without informing them of the date and time. Video cameras located in the building corridors recorded the exact time occupants took to leave their apartments. A questionnaire filled out after the drill provided essential information on occupants' perception of the fire alarm, their interpretation of the signal, their actions before leaving their apartment, and their evacuation movement. Around 25 percent of the occupants in each building thought it was a real fire when they heard the fire alarm.

Significant variations were observed for the time to start in the 7 residential buildings studied. A clear distinction was made between buildings with a good or a poorly audible fire alarm signal. From the questionnaires, when over 80 percent of the respondents mentioned that the fire alarm was loud enough in their apartment, it was judged that the building had a good audible fire alarm signal. In 3 of the buildings studied, where the alarm had good audibility, the mean delay time to start evacuation was 2 min 49 s. In these buildings, three-quarters of the evacuation time was used for the delay time to start and one-quarter in movement time. So for an evacuation that lasted in total 4 min, 3 min were spend in time to start and 1 min to move to the outside.

A fourth building where the alarm was judged good by the occupants had 5 min 19 s as a mean time to start evacuation. The latter was a winter evacuation, which required putting on coat, boots, mitts, and hat, which explains the longer time to start. In a fifth building with good alarm, most occupants decided to evacuate onto their balconies instead of the procedure that required occupants to leave to ground level. The mean time for occupants to appear onto their balconies was 2 min 25 s.

Two of the residential buildings studied by Proulx had over 20 percent of the occupants who judged that the alarm was not loud enough inside their suites. These occupants took an extra long time to start, since many started 2 to 3 min after hearing the arriving fire trucks or after firefighters knocked at their door. For these two

buildings, although some started in the initial 2 min, others took as long as 25 min to start, for an overall mean time to start of 9 min.

Some may wonder what were the occupants doing during these 2 to 3 min after hearing the fire alarm (or the fire trucks) before starting to evacuate. From the questionnaires, occupants mentioned that they got dressed, were gathering children, pets, purse, wallet, and keys. Some put away supper, had a look on their balcony, or gave a call to the superintendent before leaving their apartments. Six of these evacuation drills were conducted in the summer on a week day at around 7:30 p.m., and the winter evacuation was on a Saturday at 11:00 a.m. It is not known what would be the delay time to start evacuation at night, but it is likely to be longer than the times observed during the day. It is also interesting to know that in all these evacuation drills, many occupants (maybe as much as half the occupants present) never came out, and many refused to answer the firefighters who knocked at their doors. This behavior might be more prevalent at night.

Evacuation drills were studied by Proulx in three office buildings.[49,50] Occupants received no warning of this exercise, since these Canadian government buildings conduct evacuation drills annually. Data on time to start was gathered using video cameras. The individual time to start of over 1000 occupants was recorded. The mean time to start for the three buildings was 50 s. Although all these office workers had received training and were fully aware of the evacuation procedure, they nevertheless spent time finishing phone calls, saving data on computers, securing files, and gathering belongings before leaving their desks. Many had to be prompted to move by their local fire warden.

In their fascinating evacuation study of a large retail store, Shields, Boyce, and Silcock[51] found that staff response had the most determinant effect on the occupant time to start their evacuation. They conducted an unannounced evacuation drill of a Marks & Spencer's store using video cameras to record behavior and movement, and a questionnaire administered to evacuees after the drill. The fire alarm was activated in the entire store. Although floor staff were not aware of the drill, their fast response was essential in prompting customers movement. The average time to start moving for customers after the sound of the alarm was 25 s with a maximum of 55 s. Cash counters were closed within 30 s of the alarm sounding. Customers in the changing rooms were all evacuated by staff within 60 s. Clearly, the fast staff response during this drill had a major impact on the fast evacuation of the store.

Time to start evacuation was studied in an underground transport system by Proulx and Sime[52]. This study demonstrated the importance of the cue received to prompt evacuation movement. In the underground levels of the station, passengers never started to evacuate after the activation of the fire alarm signal: they kept waiting for their trains, reading, standing, and never made a move to evacuate. When staff appeared to prompt movement, passengers complied immediately. The same response was observed with the use of precise live messages from the voice communication system. The messages informed the passengers of the type of incident and its location, and instructed them on what to do. Only

15 s after the voice communication message, passengers started to move.

The delay time to start has also been studied through reports of fire victims. Although it is recognized that victims may have difficulty reporting accurately the delay time they took before starting to evacuate, there are interview techniques that can help to obtain acceptable estimates.[53,54] In Australia, Brennan used such interview techniques to obtain detailed accounts of fire victims.[55] She studied a severe high-rise office fire that started in a stack of polyurethane-padded chairs stored on the third level of a 14-story building. The fire grew rapidly, emitting a large quantity of smoke. The central fire alarm system never sounded. Victims reported becoming aware of the incident by seeing and smelling smoke or being warned by others. From the interviews, it was estimated that the mean time to start evacuation was approximately 2 min 30 s.

Brennan also studied the occupants' behavior during a high-rise residential fire that occurred at night.[56] From interviews with victims, it was estimated that occupants took around 10 min to start evacuation after hearing the fire alarm and seeing light smoke in the corridor. It should be noted that it is estimated that only half the occupants of that building actually evacuated during that fire.

Studies of two high-rise residential fires in Canada that resulted in six fatalities in stairwells in one case and one fatality in the suite of origin in the other case were studied by Proulx.[57,58] The high-rise fire with six fatalities occurred at night in the winter time. According to the occupant accounts, the fire alarm was not audible in many of the apartments; these occupants learned about the fire from the warning of others. Victims estimated their time to start evacuation at 10 to 30 min for occupants who attempted to evacuate. In the second case study, all occupants heard the fire alarm since there was a sounder in every suite. Occupants waited for instructions from the voice communication system. Evacuees estimated that they took 5 min before starting to evacuate after receiving the evacuation order.

These different studies on the delay time to start show the marked difference in response time according to the type of warning obtained. The time to start will vary according to the information available. The fire alarm signal is probably the less reliable cue of a fire since there are a large number of false alarms, test alarms, or prank alarms in some buildings that have reduced the credibility of this signal as an indication of a real fire.[59] Fire cues, such as smelling something burning or seeing smoke come forth has very ambiguous, initializing investigation response from occupants more than evacuation movement. Obtaining a warning by others appears to be a better indication of an actual problem. Messages delivered through a voice communication system or directly by staff seem to be the signals that are taken most seriously by occupants as indicating a requirement to promptly leave the area.

Building Characteristics and Occupant Characteristics

From the case studies reported above, a marked difference in delay time to start evacuation is found according to the type of occupancy studied. In office buildings,

occupants appear as more readily prepared to move than in residential occupancies. In fact, it is not so much the type of occupancy that makes a difference, but the characteristics of the building and of the occupants. For example, a characteristic of the building that would make a difference in the delay time to start is the visual access to other occupants and what goes on in the building. In a residential building, occupants are by themselves in their suites; they don't have access to the overall behavior of others, and they don't have an overview of the space, such as in an open-plan office or a cinema. This lack of visual access is likely to increase the delay time to start, since occupants will have to take time to obtain more information before making the decision to evacuate. An occupant characteristic that could make a difference is the alertness of the occupant; for example, in an office building, occupants are dressed, awake, and alert. These conditions could be completely different for a family group in a hotel room at night. The time to prepare to start evacuation for a family with children in the middle of the night could be extensive compared to somebody who is at work.

A number of such characteristics that could have an impact on the time delay to start evacuation have been identified and discussed in BS DD240.[46] Here are some of the characteristics with some findings of the most recent work on human behavior in fire. The most salient building characteristics are as follows:

Type of warning system: The fire alarm signal is usually the basic warning system. It is, however, the signal that occupants will take the longest to respond to if they have received no training or if the alarm is often activated for no-fire reasons. The use of a voice communication system with informative live messages is probably the best way to initiate a fast response. Prerecorded messages, in comparison, are rarely as effective in making occupants start to move and less informative in content as live messages. The audibility and the intelligibility of these systems should be assessed to ensure occupants will perceive the information provided. The voice communication system, coupled with closed-circuit TV, could allow an officer to provide precise information to the occupants regarding the unfolding event and instructions tailored to the location of different groups.

Building layout and wayfinding: The way each floor and the whole building are organized has an impact on the possibility for the occupant to have developed a mental map of the space. When looking for information or devising a plan of action, occupants are likely to spend more time obtaining information in a building where wayfinding is difficult.

Visual access: The way the building is designed may or may not provide occupants with visual access to the behavior of others, which could be an important source of information for people. Visual access could also improve the perception of fire cues or strobe lights as well as the location of the closest exit.

Focal point: In buildings where occupants focus their attention on the stage, the screen, or the ambient atmo-

sphere (e.g., at a discotheque or rave party), the animation of this focal point will have to stop and full lighting should resume for occupants to pay attention to the fire situation. Information regarding the expected response of occupants should be provided from a figure of authority at the focal point.

Training: An essential part of a fast occupant response. Training is more a characteristic of the building than of people, since training should be specifically tailored to each building evacuation procedure. Although a person who has received training may transfer this knowledge to another location, it is common to observe that well-trained people did not take any action when the fire alarm rang in another building. Overall, training of the occupants is usually performed only in institutions such as schools and some work environments. In public buildings, occupants are unlikely to be trained for that specific building. Consequently, staff have to be very well trained to efficiently prompt occupant movement. Staff also have to be in sufficient numbers to cover the full space.

Frequency of false alarm: The number of false alarms in a building is an important determinant of the efficiency of this system to warn occupants. A large number of false alarms could be estimated at three or more alarms over a period of 6 months. A fire alarm signal, by itself, rarely triggers evacuation movement, unless training and other information is provided. However, the fire alarm is a very good way to alert occupants and prepare them to receive complementary information or to look for information. If the number of false alarms is important, it could be expected that the delay time to start will be endlessly extended since occupants are unlikely to look for information and will be less receptive to other cues.

Some occupant characteristics are as follows:

Familiarity: Occupants who are familiar with a building, who have participated in evacuation drills, and are aware of the evacuation procedure are more likely to start evacuation rapidly.

Responsibility: In single-family houses, occupants respond rapidly when the smoke alarm goes off because they know they are responsible for it; no one else will take care of that problem. In a public building, such as a museum or a shopping center, visitors don't feel responsible if the fire alarm goes off. They assume that they will be told if something is really happening. The delay to start will depend on the fast and precise voice communication information provided and the staff behavior and instruction.

Social affiliation: Occupants are likely to attempt to gather with people with whom they have emotional ties before starting evacuation, such as a family group. This activity of gathering members may take time, especially if members are not together at the start of the incident.

Commitment: People who are committed to an activity will take a long time to turn their attention toward an unexpected situation. For example, people waiting in line to board a plane, eating in a restaurant, or gambling at the

casino are all committed to these activities and will be reluctant to turn their attention to an alarm bell or some strange smell of smoke. However, at the cinema, if the movie is stopped and lights are turned on, attention of the occupants will be captured right away and information to prompt their time to start can be provided.

Alertness and limitation: A fire in the middle of the night in a hotel or residential building will require a longer time to respond since most occupants will be asleep. Another dimension to this characteristic is the possibility that occupants may have some limitation that will extend their response time. These limitations could be perceptual, physical, or intellectual, or might be due to the consumption of medication, drugs, or alcohol. It is important to estimate the proportion of occupants who will have a longer delay time to start due to alertness conditions or a limitation.

Staff or warden: The speed with which occupants will respond to the fire alarm or other fire cues is largely dependent on their status in the building and the behavior and instruction of staff and wardens. Consequently, the training of staff and wardens is paramount. To be readily recognized, they need to wear distinctive uniforms and show their authority through their behavior. The delay time to start could be dramatically shortened by the behavior and instruction of well-trained staff and wardens.

The preceding building and occupant characteristics should be taken into account when estimating a time delay to start evacuation. In the past, the delay time to start has always been neglected, which usually explains the discrepancy between the calculated evacuation time and the observed evacuation time during fire drills. Some have suggested that the delay time in a real fire should be shorter than in a drill, since signs of the fire should trigger fast occupant response. Interviews with victims show another story. In fact, the initial signs of a fire are usually judged extremely ambiguous, which tend to further increase the delay time to start of occupants.

Delay Time Calculation

For calculation purpose of a total evacuation time, a delay time to start has to be calculated. All researchers in the field of human behavior in fire are hesitant at suggesting numbers because of the limited research findings in this area. Nevertheless, due to the fast development of the performance-based approach to look at new innovative fire safety design systems for buildings, some data to account for the delay time to start evacuation by occupants is essential. In 1997, the British Standards Institute published the Draft for Development DD240.[46] Although initially meant as a British Standard on Fire Safety Engineering, public comments received on the draft code of practice suggested to the relevant committee to publish this document as a Draft for Development, so information contained in DD240 is essentially provisional until a review is conducted. DD240 provides a flexible but formalized framework to fire safety design.

Table 21 of DD240, reproduced here as Table 3-13.1 (with some modification to the terminology), suggests

Table 3-13.1 *Estimated Delay Time to Start Evacuation in Minutes*

Occupancy Type	W1 (min)	W2 (min)	W3 (min)
Offices, commercial and Industrial buildings, schools, colleges and universities (Occupants awake and familiar with the building, the alarm system, and evacuation procedure.)	< 1	3	> 4
Shops, museums, leisure-sport centers, and other assembly buildings (Occupants awake but may be unfamiliar with building, alarm system, and evacuation procedure.)	< 2	3	> 6
Dormitories, residential mid-rise and high-rise (Occupants may be asleep but are predominantly familiar with the building, alarm system, and evacuation procedure.)	< 2	4	> 5
Hotels and boarding houses (Occupants may be asleep and unfamiliar with the building, alarm system, and evacuation procedure.)	< 2	4	> 6
Hospitals, nursing homes, and other institutional establishment (A significant number of occupants may require assistance.)	< 3	5	> 8

W1: live directives using a voice communication system from a control room with closed-circuit television facility, or live directives in conjunction with well-trained, uniformed staff that can be seen and heard by all occupants in the space
W2: nondirective voice messages (prerecorded) and/or informative warning visual display with trained staff
W3: warning system using fire alarm signal and staff with no relevant training

Source: Adapted from *Fire Safety Engineering in Buildings, Part 1: Guide to the Application of Fire Safety Engineering Principles,* Table 21, British Standard Institutue, DD240, London, 1997.

some delay time to start evacuation for different occupancies according to the warning systems available in the building.[46] The time to start depends mainly upon the type of warning system provided in the building, the type of occupancy, and the characteristics of the occupants. (The type of warning considered here offers a slight variation from the same concept presented by DD240.)

Occupants are likely to respond more rapidly to a warning system that will provide more information for decision making. To take into account fire scenario, DD240 suggests that the times given in Table 3-13.1 be

adjusted in relation to the assumed rate of fire growth,

(a) for occupants in a small room/space of fire origin who can clearly see smoke and flames at a distance, adopt the relevant time given for W1,

(b) for occupants in a large room/space of fire origin who can clearly see smoke and flames at a distance, adopt the relevant time given for W2, unless W1 is in operation,

(c) for occupants outside the room/space of fire origin who cannot clearly see smoke and flames, adopt the time given for the warning system in operation.[46]

Further, it should be emphasized that in some types of occupancies such as factories, some time for shutdown of equipment may have to be added to the time given in Table 3-13.1.

Equations for Total Evacuation Time

Several equations for total evacuation time, such as the ones from Togawa[8] or Melinek and Booth[16] appear formidably complex; the calculation benefits they promise are hidden behind scientific notation systems. In using such formidable equations, there is a danger of getting sidetracked by their apparent sophistication. Like computer models, they may tend to keep us from understanding the world as it actually exists; the equations and models can take on a reality of their own. Therefore, the emphasis in this section is on minimizing the complexity of the mathematics and maximizing the awareness, using simple language and graphs, of real processes that many existing models depict incompletely.

Empirical Method by Pauls

While early Canadian research on evacuation did not get into the mathematical abstraction found in some other researchers' work, it did utilize many simple graphic representations of people's movement, merging, and queuing in evacuations of tall buildings.

In contrast to previous contributors to evacuation technology, Pauls began by observing as many evacuation drills as possible in tall office buildings, being careful to record many aspects of each exercise in great detail, and then developing relations that best described what was actually observed.[23,60] This method revealed defects in earlier literature on matters of crowd configuration on stairs, maximum and mean flows, and actual evacuation populations—all of which were sources of error in other predictions.

Altogether, 29 drills were observed in buildings ranging from 8 to 21 stories high, in which traditional, uncontrolled total evacuation procedures were used. Generally, all stairways in each building were monitored at ground-floor discharge points and at selected heights, often through the use of instrumented, moving observers. An average of two stairways were documented for each drill, thus giving 58 cases for analysis. (A smaller number of drills were documented where the procedure involved a selective or sequenced controlled evacuation procedure, with either partial or total evacuation. These controlled evacuations are not covered by any of the equations provided here and are separately discussed under the section titled "Evacuation Procedures in Tall Office Buildings.")

By way of background to the prediction equations developed from Pauls's study, the effective-width model for crowd movement must be defined. This empirically based model describes flow as a linear function of a stair's effective width—the width remaining once edge effects are deducted [150 mm (6 in.) in from each wall boundary and 90 mm (3.5 in.) in from each handrail centerline]. (See Figure 3-13.4.) The effective-width model takes into account the propensity of people to sway laterally—especially when walking slowly in a crowd—and, therefore, to
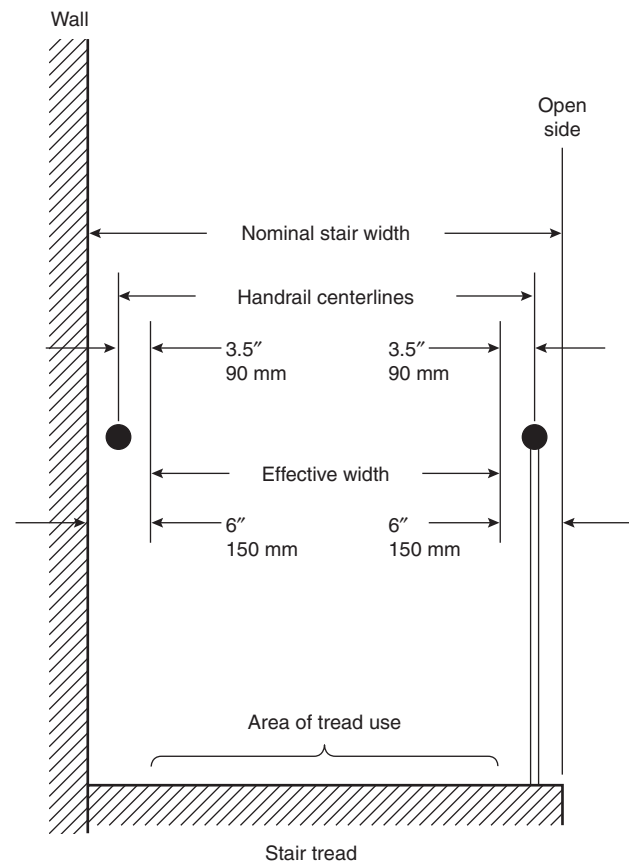
Figure 3-13.4. *Measurement of effective stair width in relation to walls and handrails.*

arrange themselves in a staggered configuration, not in regular lanes, as assumed in the traditional unit-width model based on presumed static dimensions of people's shoulders.[23] For example, a stair designed to provide two of the traditional units of exit width has a nominal width of 1120 mm (44 in.) and an effective width of 820 mm (32 in.), causing crowds to take up a staggered formation.

Another finding underlying the effective-width approach is that mean evacuation flow (per meter of effective stair width) varies in a nonlinear fashion with evacuation population (per meter of effective stair width), as shown in Figure 3-13.5. The regression equation is designated here as Equation 4.

$$f = 0.206\rho^{0.27} \qquad (4)$$

where f and ρ have the metric units shown in Figure 3-13.5.

Other factors besides effective stair width, influencing the mean flow in evacuations are people's use of extra clothing (for protection against precipitation or cold conditions outside a building), plus various building design and use factors, including normal stair use.[23] Regarding building design, the assumed influence of stair-step geometry on crowd flow is considered below.

Equation 5 (with dimensions in mm) and Equation 6 (with dimensions in inches) relate effective stair width, w,
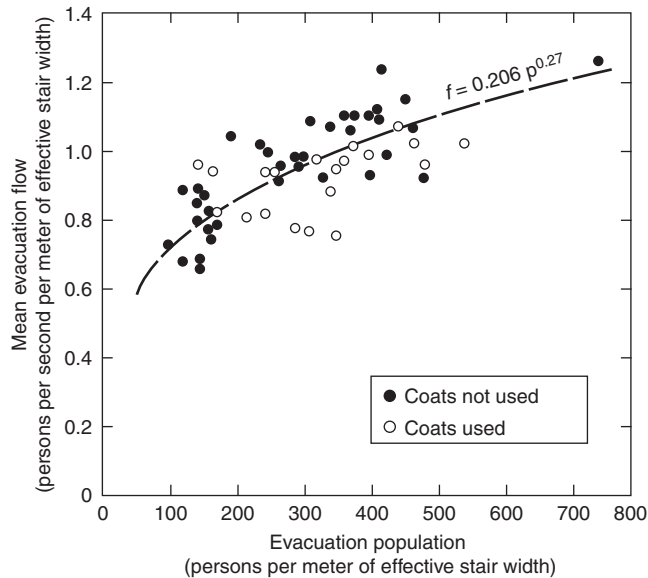
Figure 3-13.5. *Effect of population on flow down stairs in uncontrolled total evacuations.[61]*

actual total population, *P*, and the expected flow time, *t*, in seconds. These equations can be translated into a somewhat more useful form and graphed as shown in Figure 3-13.6, which relates effective stair width per person and the resulting flow time for a crowd moving down stairs. Three curves are provided to show the assumed effect of various step geometries on crowd movement efficiency. It should be noted that some of Pauls's early publications of equations similar to Equations 5 and 6 differ slightly, because they were based on stairs with step geometries approximately described by the highest of the three curves. Equations 5 and 6 relate to the middle curve.

$$w = \frac{8040}{t^{1.37}} P \qquad (5)$$

$$w = \frac{317}{t^{1.37}} P \qquad (6)$$

In relation to evacuation time prediction, the preceding equations and graphs have dealt only with flow time. For uncontrolled total evacuations of tall office buildings, there is a simple way of predicting the time to start needed for flow to build up to half its mean level. This empirically derived time to start is shown in Figure 3-13.7. When added to flow time, based on empirically determined mean flows, the 41 s (0.68 min.) accounts for travel time plus all or part of the other subcomponents of minimum evacuation time discussed previously. The extent to which the 41 s is adequate depends on the experience of the building occupants and the manner in which the evacuation is initiated and run. Evacuations in cases of actual fire or other emergencies are assumed to take longer, as discussed earlier.

From Equation 4, and from the 41 s time to start shown in Figure 3-13.7, the first of two prediction equations shown in Figure 3-13.8 is derived. The prediction
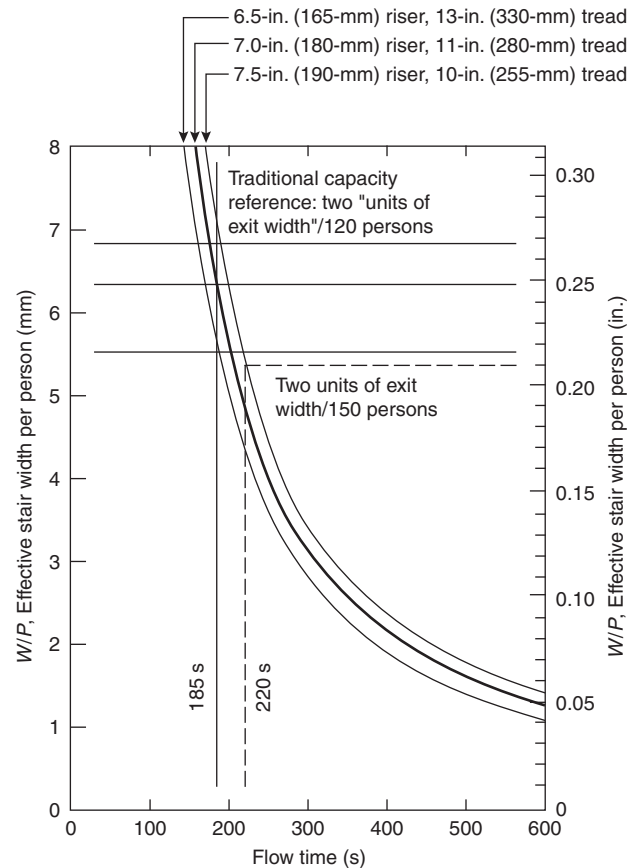
Figure 3-13.6. *Relationship between effective stair width per person and flow time for several step geometries.*
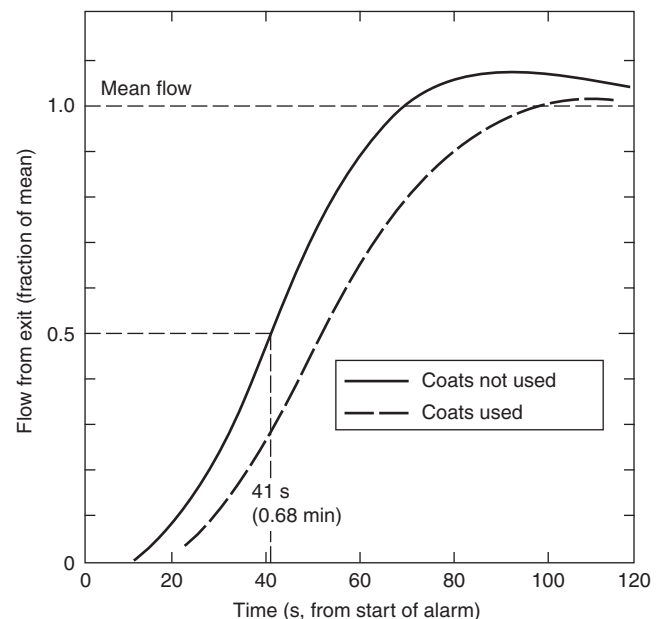
Figure 3-13.7. *Buildup of flow from exits in uncontrolled total evacuations of tall office buildings.*
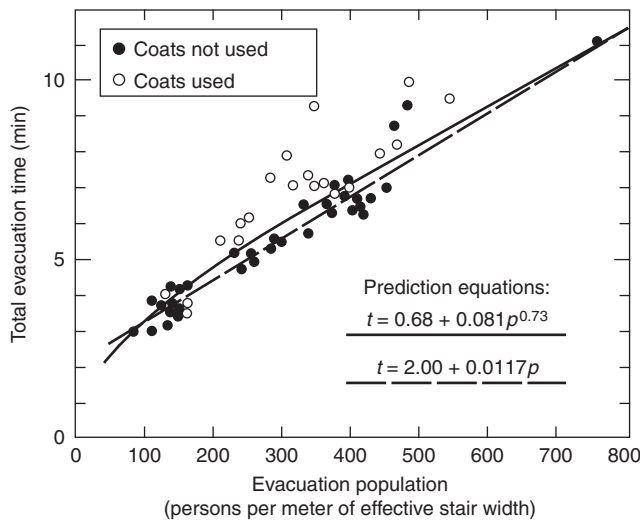
Figure 3-13.8. *Predicted and observed total evacuation times for tall office buildings.*

equations apply to cases where there are no more than 800 persons/m of effective stair width. (The upper equation in Figure 3-13.8 is Equation 7, and the lower one is Equation 8.) Note that there is a good match between the prediction curve (Equation 7) and the observed total evacuation times for the uncontrolled evacuations, especially in those cases where extra outdoor clothing was not used. Using Equation 7, the net error in predicting total evacuation times for 50 cases in buildings 8 to 15 stories high was 0.2 percent. The simplified linear equation, Equation 8, also fits these data very well.

$$T = 0.68 + 0.081p^{0.73} \tag{7}$$

$$T = 2.00 + 0.0117p \tag{8}$$

where T is the minimum time, in minutes, to complete an uncontrolled total evacuation by stairs, and p is the actual evacuation population per meter of effective stair width, measured just above the discharge level of the exit. (Note the upper limit of 800 persons per meter of effective stair width.) This also applies to Equation 4.

Buildings that will be less accurately predicted with Equations 7 and 8 are the taller ones with very low populations on each floor. With such buildings, the total evacuation time is influenced by the travel distance and people's ability to descend stairs quickly, that is, at about 10 s/story, rather than the 15 to 20 s observed in evacuations with higher populations. The observed times departing most from the prediction lines in Figure 3-13.8 were for buildings with 18 to 20 stories.

For buildings with more than 800 persons per meter of effective stair width, Equation 9 provides a good basis for predicting times for uncontrolled total evacuations in tall office buildings.

$$T = 0.70 + 0.0133p \tag{9}$$

Figure 3-13.9 shows Equations 8 and 9, along with prediction lines based on equations proposed by Melinek and
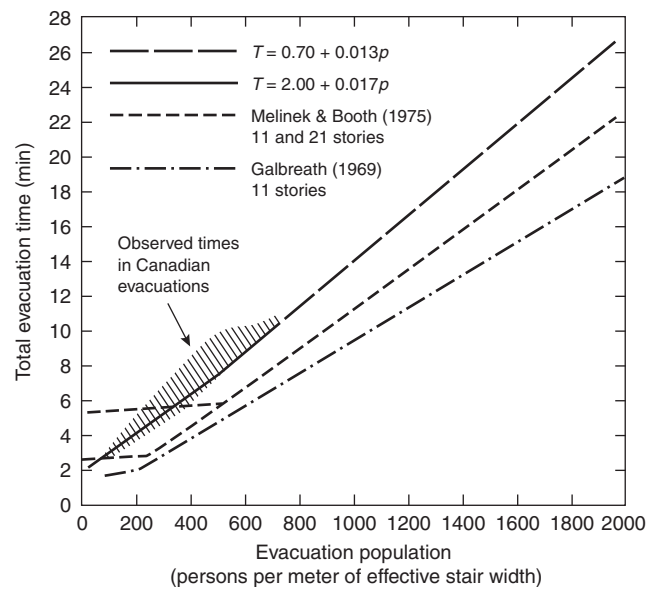
Figure 3-13.9. *Predicted and observed total evacuation times for tall office buildings incorporating results from other investigators.*

Booth[16] and Galbreath,[15] plus a cross-hatched area showing where observed times lie.

Another indication of the accuracy of these prediction equations for uncontrolled total evacuations of office buildings is provided in Figure 3-13.10. This compares predicted and observed evacuation times for approximately 1700 people evacuating an 8-story, 6-exit Canadian office building in March 1983 (in cold-weather conditions), as documented by Public Works Canada.
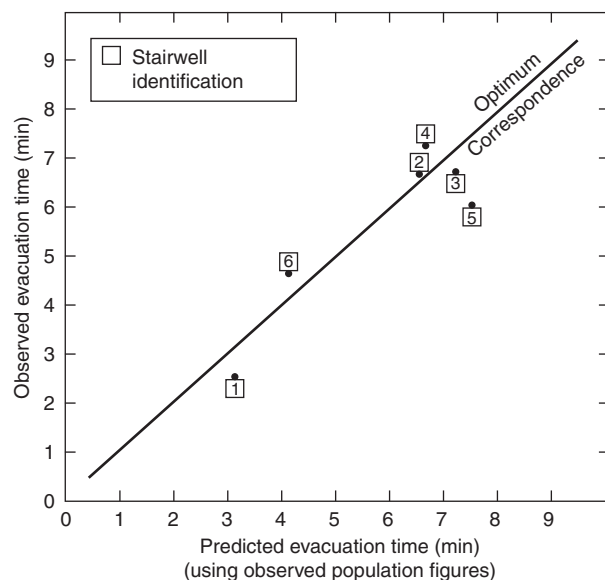
Figure 3-13.10. *Comparison of predicted and observed evacuation times for an office building.*

Actual Populations in Office Buildings

A cautionary note must be given here regarding the prediction of actual populations in buildings. In many buildings with assembly occupancies, the prediction of maximum population will be relatively straightforward, based on seat counts and floor area of waiting spaces [where an area of 0.3 to 0.6 m²/person (3 to 6 ft²/person) is a reasonable assumption]. However, studies in Canadian office buildings strongly support a case for assuming that each actual office building occupant has an average of about 25 m² (268 ft²) of gross rentable area.[23,61] This contrasts sharply with the traditional occupant-load assumption in codes and standards which assume 9.3 m² (100 ft²) of gross rentable area per occupant. Codes and standards give estimates of actual occupants that may be incorrect by a factor of more than 2. Typical workspace counts also overestimate office populations (sometimes by 15 percent).

Evacuation Procedures
in Tall Office Buildings

Evacuations of multistory office buildings can be thought of as being one of two types: uncontrolled total evacuation, and controlled selective evacuation. The former is dependent largely on the nature of evacuation sequencing or deference behavior required, and the latter on the type of control imposed and the availability of a voice communication system to manage the evacuation.

Figures 3-13.11 and 3-13.12 illustrate patterns of evacuee movement, over time and space, for a hypothetical traditional (uncontrolled) total evacuation and a controlled selective evacuation. Traces represent the movement of the last persons to leave each floor. The slopes of the traces represent the speed of movement down an exit stairway; horizontal lines represent queuing. For a more complete discussion of modeling evacuation using such
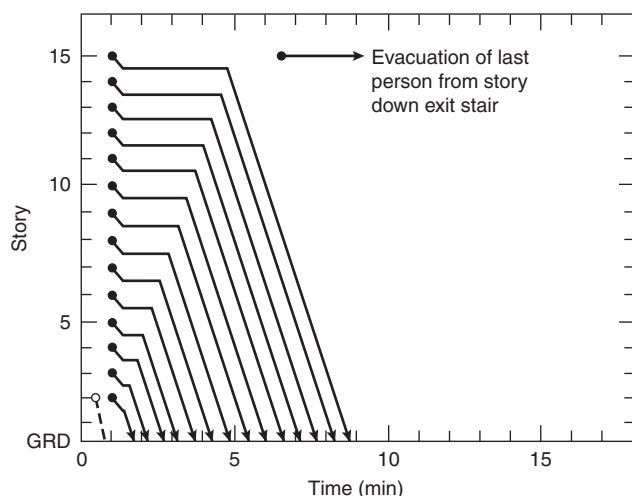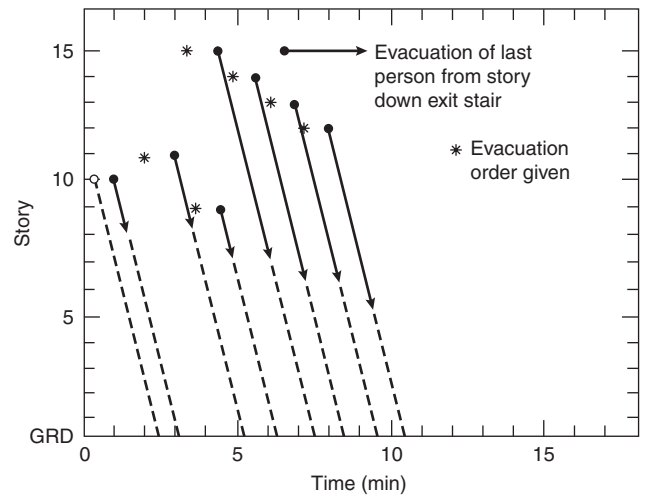
Figure 3-13.12. *Hypothetical controlled selective evacuation of 15-story office building.*

diagrams, including combined use of elevators and stairs, see References 18 and 19.

Based on Canadian observations of 29 evacuation drills in office buildings, ranging from 8 to 21 stories in height, Figure 3-13.11 shows what can be reasonably expected in an uncontrolled total evacuation of a 15-story building occupied by 70 able-bodied persons per floor—a fairly high-population condition that would be expected with about 1400 m² (15,000 ft²) on each floor. It is assumed that there is an equal division of evacuation demand for two standard 1120 mm (44 in.) exit stairs and a mean egress flow of approximately one person per second discharging from each exit. Descent speed is 3.6 floors per minute (about 0.5 m/s along the stair slope), and each evacuee has slightly less than two treads of stair area (0.5 m²/person).

Based on Canadian observations of ten evacuation drills, Figure 3-13.12 depicts a controlled selective evacuation, in this case, a partial evacuation of only the tenth-floor fire area, the floors above, and the ninth floor. Compared to the evacuation depicted in Figure 3-13.11, the movement traces are steeper, indicating faster descent speeds; however, there is also greater space between traces, indicating that densities are lower than depicted in Figure 3-13.11. Resulting flows in each exit are considerably lower.

In both cases, about 9 min are required to move all occupants to areas below a presumed fire area—the tenth floor in the case of Figure 3-13.12. Because of the time required to initiate and control the selective sequential evacuation, it takes approximately the same time to move 490 persons to safety (below the ninth floor) as it does to move all 980 occupants to the ground in the uncontrolled total evacuation depicted in Figure 3-13.11. Rather than jump to the conclusion that uncontrolled total evacuation is better or more efficient, it must be considered that, if there really was a fire on the tenth floor, and if all occupants attempted simultaneous egress, and if the usual rules of deference shown in Figure 3-13.11 applied, occupants of the most immediately threatened floors would
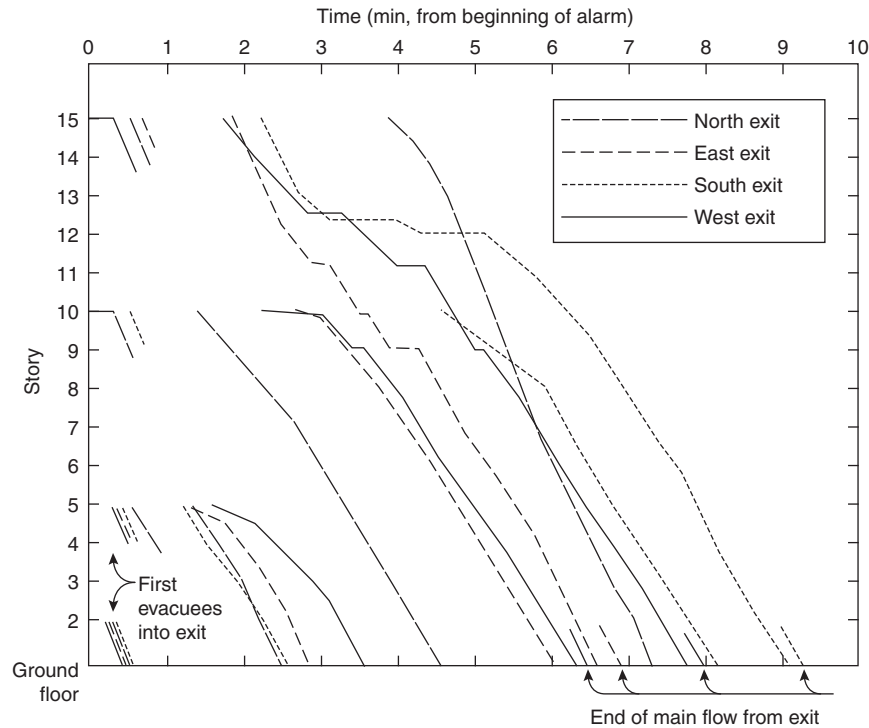

Figure 3-13.11. *Hypothetical uncontrolled total evacuation of a 15-story office building.*

Time (min, from beginning of alarm)

Figure 3-13.13. *Movement of observers with evacuees during an uncontrolled total evacuation.*

have to queue in the vicinity of those floors for several minutes. With the stairwell doors being open on the fire floor, all the upper floors would become contaminated by smoke, and descending occupants from floors above the fire floor would have to move in smoke.

An increasingly common conclusion is that, although uncontrolled total evacuation is not demanding of building management systems, it is too upsetting for occupants who are indiscriminately evacuated (if indeed they can be encouraged, with ambiguous alarm systems, to evacuate at all). On the other hand, the uncontrolled total evacuation process is simple, and there is no need for relatively sophisticated systems and training, which are expensive and may involve a long delay time before occupants who should evacuate become notified to start their evacuation.

Uncontrolled Total Evacuation

One drill case study entailed the 1972 evacuation of 1453 persons, using uncontrolled total evacuation procedures, from a 15-story office building via four 1140-mm exit stairs. The total evacuation time ranged between 6.6 and 9.3 min. The time variation was largely due to unbalanced demand on the four exits—the result of unequally sized catchment areas and an overcompensating attempt to redistribute some of the demand to predesignated exits on several floors. The average total evacuation time was 7.8 min, a figure close to the predicted 7.0 minute time. (See calculations below.) The difference is largely explained by the fact that evacuees experienced slight delays and less efficient movement down stairs because

outdoor clothing was used. The attempt to have people on several floors move to more remote, predesignated, but less familiar exits also added minor delays.

Figure 3-13.13 shows the traces of movement of instrumented observers, using the exit stairs with evacuees, during this uncontrolled total evacuation. In this evacuation, some people were on the fifteenth floor up to 4 min, and their queuing on exit stairs, near this level, lasted up to 4 min from the initiation of the general fire alarm system. It was usually less than 2 min at lower levels. Conditions were much like those noted in relation to Figure 3-13.9; each evacuee occupied an average area equivalent to two stair treads, and descent speed was typically 3.5 stories/min below the seventh floor—conditions that would be unduly arduous or impossible for only a few percent of typical office workers. In the case of this drill, such persons and some assistants (73 persons altogether) descended a central, fifth stairway reserved, in this evacuation, for their use.

The building was recently rebuilt with the same floor areas, but with only the central exit stairway and another one in the largest wing left intact. However, its occupants still are expected to utilize the uncontrolled total evacuation procedure. Given the difficulties of obtaining a balanced use of the remaining exits, it is not unreasonable to predict that the total evacuation time will now be approximately twice what was achieved in the 1972 drill.

Sample computations of uncontrolled total evacuation time: Here it is useful to consider the evacuation time prediction for this building in somewhat greater detail.[24]

This building has a cruciform plan with a total of 33,000 m² (350,000 ft²) of gross rentable area on 14 office floors. One of the four wings is larger in area than the other three; thus, there is unlikely to be an equal population using each exit stairway during an evacuation. For the first computations, the unmodified stairway arrangement will be assumed, with one exit stair at the center of the building and one exit stair at the end of each of the four wings. Subsequent computations will consider the modified case with only two stairways.

For the original, unmodified situation we will assume that the exit stairs have extensive normal use, partly because the building is occupied largely by a single government department. The center stairway has a relatively high level of normal use because of its location near the elevators and its entry door in the ground-floor lobby. The fire emergency procedures call for this stairway to be used only by handicapped persons and others assisting them in emergencies. The stairs have a nominal width of 1140 mm (45 in.) and a dogleg configuration, with two 180-degree turns per story. The step geometry provides a riser height of 180 mm (7 in.) and a tread depth of 250 mm (10 in.). Stair wall finishes have a semirough texture. Assume that the building is slightly more densely occupied than the average noted earlier (specifically, assume one actual occupant for every 22 m² instead of the 25 m² noted in the subsection "Actual Populations in Office Buildings"). Given this kind of information about the office building, as well as the knowledge that the occupants are accustomed to periodic evacuation drills, a prediction of the flow and evacuation time performance when the traditional uncontrolled total evacuation procedure is used can be attempted.

First, an estimate is made of the total number of occupants to be evacuated. At 22 m² per actual occupant and a total gross-rentable office area of 33,000 m², the anticipated evacuation population is 1500 people. It can be assumed that 2 percent of these (i.e., 30 people) cannot or should not evacuate down the stairs in a high-flow situation with relatively able-bodied evacuees and should elect to use the central stairway. Typically, only a few of these people would have such severe mobility impairments that they would need to be assisted by more than one other person to get down the stairs. If an average of one person to assist each of these 30 handicapped patrons is included, the central stairway will then be used by approximately 60 persons; this leaves 1440 persons using the four remaining exit stairs at the building perimeter. As a first approximation, it can be assumed that these stairs will be used equally, even though one of the four wings is larger than the others. Each of the four 1140 mm (45 in.) stairs would thus carry 360 evacuees.

Next, by deducting 300 mm (12 in.) from the nominal stairway width, it can be calculated that each of the stairs has an effective width of 840 mm (33 in.). The anticipated mean evacuation flow can be indirectly calculated using any of a number of methods, such as the methods set out in Equations 4, 5, or 6 and in Figure 3-13.6. The easiest method is to use Figure 3-13.6, interpolating between the two upper curves to account for the step geometry. Each stair provides 2.33 mm (0.09 in.) of effective width per person; thus, we can read off an expected flow time of 390

s, estimated to the closest 10 s (and having two significant figures). The mean flow is obtained simply by dividing the population per stairway (360 persons) by the time (390 s), giving a mean flow of 0.92 person/s.

This uncontrolled evacuation prediction can be adjusted to take into account some modifying factors in addition to the step geometry adjustment[26] already built into Figure 3-13.6 (and further discussed in Pauls).[62] For example, the stair walls are slightly rough; therefore, it is reasonable to expect some reduction in flow.[23] A 4 percent reduction in flow would be a reasonable assumption. The fact that this evacuation was held during somewhat cool weather, and therefore some of the evacuees wear or carry outdoor clothing, should be taken into account. Assume this leads to a 6 percent reduction in the flow. On the positive side, an adjustment for the fact that the building occupants are familiar with evacuation drills and that there is fairly extensive normal use of the stairs (although this is likely to be more the case for the center stairway than for the perimeter stairs) should be considered. There might, in fact, be some confusion as relatively able-bodied people go first to the normally used center stairway only to be redirected to one of the perimeter stairs. There may also be some confusion and delay as the exit stairway in the largest wing develops more extensive queuing at exit doors and, as a result, people either decide on their own to try another stairway or are directed by fire wardens to use another stairway. Thus, on the positive side, it is prudent to assume an adjustment of only 2 percent for normal stair use and familiarity with evacuation drills.

It is sufficiently accurate (given the underdeveloped state of the art) simply to add up the negative and positive factors to give a net adjustment of minus 8 percent for the expected flow. This results in an adjusted flow prediction of 0.83 person/s (50 persons/min) on each of the four perimeter stairs. A well-documented, cool-weather evacuation drill in the same setting had the following mean flows, in person per second: 0.85, 0.83, and 0.80—remarkably similar to the prediction. The differences are largely explainable by the fact that the four stairs were not equally used in the evacuation drill, despite efforts by the building's fire emergency staff to balance usage. Too many evacuees were, in fact, diverted to one of the stairways, which thereby served 448 people. They had been diverted from the largest wing, where the stairs were used by 385 people. The other two stairs served 329 and 291 people, respectively, for a total of 1453, compared with the initial assumption of 1440.

Repeating the above computations, using Figure 3-13.6 and the actual stair populations (448, 385, 329, 291), with the adjustments described above, mean flows of 0.88, 0.84, 0.81, and 0.78 person/s, respectively—all within 4 percent of the observed flows—can be predicted. Thus, it is possible to make some very accurate predictions for the relatively straightforward, traditional, uncontrolled total evacuations of tall office buildings, if we understand some basic factors of building design and use.

As to the matter of minimum total uncontrolled evacuation time, a simple prediction can be made with the 390 s (6.5 min) flow time (read from Figure 3-13.6), which assumes equal usage by 360 people of each of the four perimeter stairs. Adjusting this time by the 8 percent

figure gives an adjusted flow time of 7.0 min. Adding the suggested 0.68 min startup time (the time for flow to build up to half its mean value, read from Figure 3-13.7), a predicted total evacuation time is 7.7 min. Alternatively, without including any adjustments, Figure 3-13.8 or Equations 7 or 8 could be used to calculate an approximate, slightly underestimated total evacuation time in the range of 7.4 to 7.0 min.

The observed total evacuation times were 9.3, 8.2, 7.0, and 6.6 min, respectively, for the stairs, listed in descending order of population. This range of observed times is mainly a result of the nonuniform distribution of evacuees among the four perimeter exits. The average observed time was 7.8 min, compared with the (adjusted) prediction of 7.7 min. In fact, the adjusted predicted times, using the actual populations, are found (using Figure 3-13.6) to be 9.2, 7.9, 7.2, and 6.6 min, respectively, in order of decreasing population, all within 4 percent of observed times.

Finally, the predicted minimum total uncontrolled evacuation time should be computed for the building in its modified form, with only two exit stairs and with a similar total population. Having 1400 people (assuming 100 per floor) equally distributed between the two stairs, each with an effective width of 840 mm (33 in.), would lead to a flow time in excess of the 10-min (600-s) limit of Figure 3-13.6. Because the population per meter of effective stair width, 833, slightly exceeds the 800 limit for most of the formulas suggested, Equation 9 should be used here. Doing so gives an unadjusted minimum total evacuation time of 11.8 min. However, there will be great difficulty achieving balanced usage between the two remaining exit stairs. The central one could easily have a usage 40 percent higher than the other stairway.[23] In this case, (assuming a 817- and 583-person split between the exit stairs) the minimum, unadjusted total evacuation time would be approximately 13.7 min, or about twice what was the case when the building had 5 exits.

These examples demonstrate that traditional total uncontrolled evacuations can be relatively easily understood and predicted in the case of tall office buildings. Such calculation of total evacuation time provides the overall time for occupants to evacuate a building when no particular incident is happening. It should be kept in mind that for a situation where an actual fire is occurring, the time delay to start evacuation would be longer if signs of the fire are present; means of egress could be blocked by smoke, and occupants above the fire floor would be unable to leave. These fire conditions could entirely change the total evacuation time of a high-rise office building.

Controlled Selective Evacuation

The other actual evacuation to be described here occurred in a 21-story office building in 1971 and was one of the first large-scale attempts at a controlled, selective evacuation in Ottawa. (Figure 3-13.14 shows heavier traces depicting actual movement of observers; lighter traces depict the movement pattern predicted several days before the drill, based on estimated populations on individual floors. Given that this was done very early on in the Ottawa study, it shows a remarkably accurate prediction capability.) Although the evacuation drill consisted of the total clearing of the building—some 2100

persons evacuating over a 30-min period—it did utilize the selective, sequential procedure which could have been terminated after 6 min, with the clearing of only the presumed fire floor and two adjacent floors. The drill simulated a worst-case scenario with a fire on the third floor. For this case, a concern for smoke movement to upper floors suggested a procedure that first clears the fire-floor area, then all floors above this, starting with the twenty-first floor and progressing downward.

This evacuation drill, also described in detail by Pauls and Jones,[27] included a dramatic example of what can go wrong when fire safety management personnel misuse the communication systems needed to manage such sequential evacuations. There had been no earlier large-scale attempt to test all aspects of such an evacuation procedure. Due to an incorrectly set switch on a control console, there was a delay in getting the first announcement over the public-address system, following approximately 1.5 min of a standard fire alarm. The first announcement successfully carried over the public address, nearly 3 min into the drill, was made by an obviously flustered, inadequately prepared person who said, "Ladies and gentlemen. We have to evacuate this building. The alarm has been set on the third floor. Please evacuate. Other floors stand by."

This ambiguous announcement was followed by a slightly different one in French—bilingualism being de rigueur in government-occupied buildings in Ottawa. Confusion followed. As many as 350 persons left their floors before they were supposed to, most going down one of the two 1040-mm (41-in.) wide exit stairs. This premature evacuation confused and delayed the intended earlier evacuation of floors 3, 4, and 2. According to a questionnaire returned shortly after the drill by a sample of 176 evacuees (an 88 percent mailback return rate), some people thought they heard the announcer say that a fire had been reported on the third floor. Of the 176 respondents, 43 percent reported interpreting the situation as an actual fire after hearing the first public-address announcement. Regarding their interpretation of the situation before this announcement, with only the ringing of the building's fire alarm system, only 17 percent of the questionnaire respondents thought it was a fire, nearly 60 percent thought it was due to a circuit malfunction, and 16 percent thought it was a drill.

Turning to the conditions faced by evacuees in the two exit stairs, with the confused evacuation procedure, there was extensive queuing and slow progress by some evacuees who prematurely left the twenty-first floor via the south exit. In this exit, some 4 min were required for them to move between the nineteenth and seventeenth floors, and they took 10 min to descend the full distance to the ground. In the other exit, where there was minimal premature evacuation, descent speed was fairly consistent at about 3.8 stories/min, resulting in a 5.3-min descent time from the twenty-first floor.

It is useful to contrast these conditions with what would likely occur in a traditional, uncontrolled total evacuation of the building's 2100 able-bodied occupants via the two 1040-mm stairs. According to Equation 9, an uncontrolled evacuation would take a minimum of nearly 20 min. If all 2100 people were simultaneously standing at their respective floor's exits, there would be only 0.17 m^2 of stair area, or about one-half tread, per person. For evac-
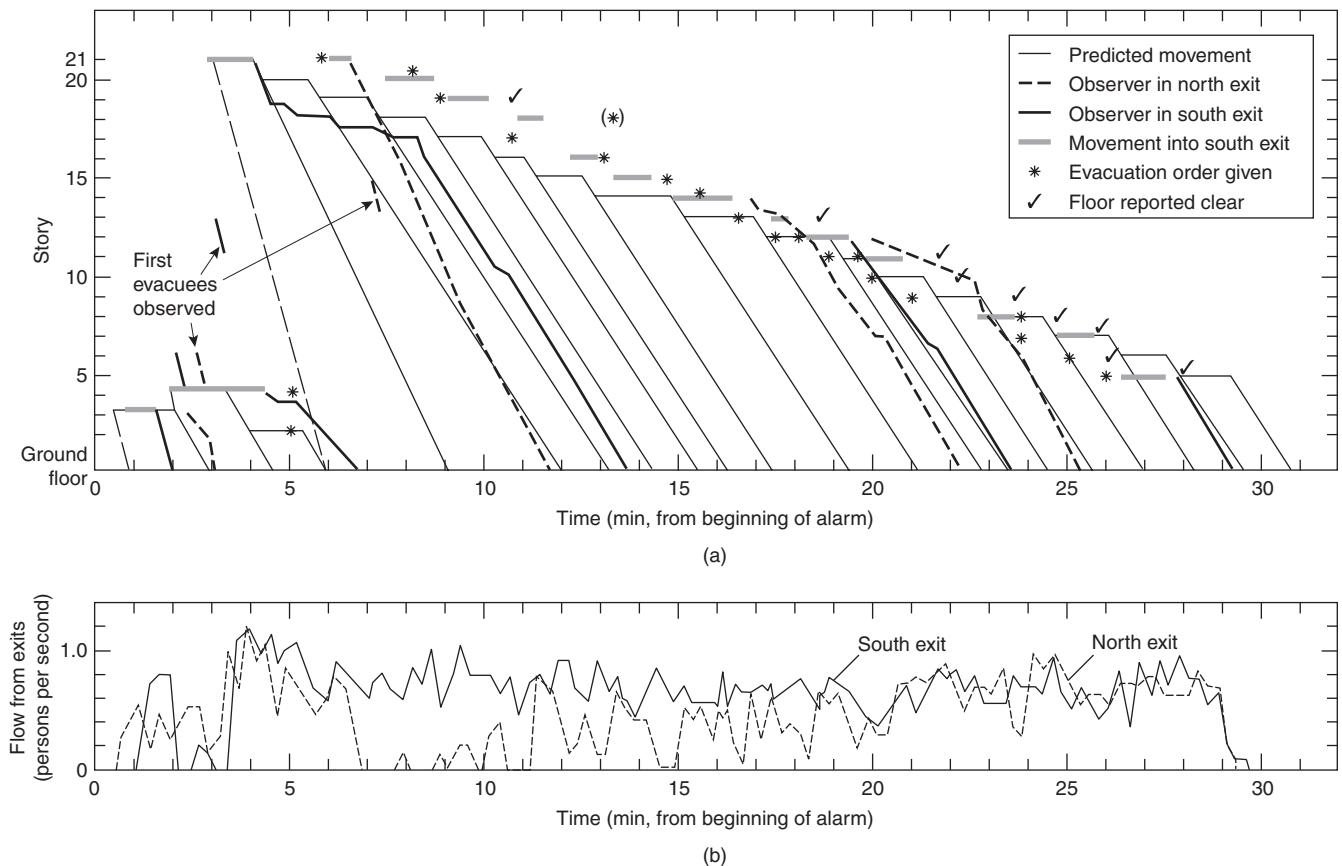
(a)

(b)

Figure 3-13.14. *Predicted and observed movement, plus flow, in a sequential evacuation exercise.*

uees from the highest floors, such queuing might last for 14 of the 20 min.

Whether queuing and evacuation delays create an upsetting situation for the people involved is a good question, and it raises the broader question about how aware typical occupants of high-rise buildings are of the kinds of queuing and movement conditions they might face in a major evacuation. Should they be made aware of such aspects of building safety? By what means? Who has the responsibility for doing it? An important attempt to address this issue was included in the *Report of the Ontario Public Inquiry into Fire Safety in High-rise Buildings.*[63] The report is highly recommended to anyone concerned with fire safety in tall buildings.

Occupants with Disabilities

During the last three decades, there has been a growing effort at providing access for all people in most buildings. It is now well-rooted in the regulation of developed countries to require accessibility to all new or refurbished public buildings. Since most people with disabilities or limitations, as well as the elderly, are determined to stay autonomous and to go out and about, buildings are increasingly occupied by mixed-ability occupants. This phenomenon has to be taken into account in fire safety design.

The prevalence of the population with disabilities appears quite similar among developed countries. The 1991 national census in Canada showed that 15.5 percent reported some level of disability (1 percent were under 15 years old, 7.4 percent were between 15 and 64 years old and 7.1 percent were over 64 years old).[64] Among Canadians with disabilities, 93.7 percent were living in private households, and only 5 percent of them were unable to leave their homes. It is not known how many disabled go out of their home regularly, but among the disabled children under 15 years old, 92 percent were attending school (88 percent were in regular schools), and out of the disabled people between the age of 15 and 64 years of age, 56 percent were holding a job (compared to 81 percent of the able population). The type of limitation identified by disabled adults were limitation in mobility (53 percent), agility (50 percent), intellectual (32 percent), hearing (24 percent), seeing (10 percent), and speaking (9 percent). Many respondents reported more than one disability.

In the United States it was estimated, through the 1994 Survey of Income and Program Participation, that 20.6 percent of the American population had some level of disability.[65] This survey excluded people living in institutions. This high percentage of people with disabilities reflects the passage of the 1990 Americans with Disabilities Act, which brought an increased interest in obtaining accurate statistics and increased awareness of disabled people to identify themselves. From this survey it is estimated that among

the overall population over 6 years old, 3.3 percent used a wheelchair and 9.6 percent used a cane, crutches, or a walker for 6 months or longer. The employment rate for people 21 to 64 years of age was 82.1 percent in the able-bodied population and 52.4 percent among those with a disability.

In the United Kingdom the population census of 1984 showed that 14 percent of the population could be classified as disabled. A detailed survey conducted in Northern Ireland in 1989 estimated that 17 percent of the population could be classified as disabled. Out of this group, 11 percent were confined to their homes while the very large majority were able to go out with assistance or, for most of them, without assistance. An in-depth study of this data showed that disabled people constitute 12 percent of the total mobile population of Northern Ireland who are out and about in the community, and just over 10 percent of that mobile population are disabled people who may be unassisted.[66] Among the disabled people who go out, 55 percent go out every day, and 93 percent go out at least once a week. So it is reasonable to assume that disabled people are regularly visiting public buildings.

In the fire field, so far, efforts have been concentrated in identifying means to provide life safety to people with disabilities. Special procedures have been identified following reports of the experience of occupants with disabilities who survived a fire or went through an evacuation.[67,68] The "egressibility" of occupants with disabilities has become an essential subject to take into account during fire safety design. Egressibility supposes the possibility of everyone leaving a building or reaching an area of safety in case of an emergency. The egressibility concept does not mean that every occupant should egress the same way or through the same route; rather, it intends to promote equivalent opportunity of life safety for everyone.[69]

Different options are being implemented to provide adequate life safety for everyone.[70] The area of refuge concept is one such option. It received limited success during testing,[71] but the area of refuge concept remains an interesting option if supplemented with complementary fire safety provisions. Providing safe elevators in buildings is another option.[72–76] The buddy system, which supposes that one or a few persons are assigned the responsibility to look after or to report the presence of a person with limitation in the case of an emergency, has not proven to be always satisfactory in practice but is used in many work environments. Techniques for carrying mobility impaired persons have been detailed in booklets.[70,77] More evacuation devices are being purchased. These devices can be used with minimum effort to transport people; however, they have to be kept in a convenient place, and some training is needed to use them efficiently. Visual alarms are implemented for the hearing impaired. Another strategy is to keep a list of the people who might have problems evacuating available for the responding firefighters. According to many firefighters, however, most lists are incomplete, since people are free to register on the list. Furthermore, these lists are often out-of-date, as people may have moved in or out of the building without the list being updated. In assessing the effectiveness of the various strategies, it can be seen that no single life safety option or technique will solve all

of the problems. It is more likely that a combination of different options will increase life safety.

All these strategies have pros and cons and should be tailored to specific occupancies. One consideration that has been originally left out is the fact that some occupants with disabilities are likely to attempt to evacuate, no matter the strategy in place. Many disabled people might be mobility-impaired, but usually they are still mobile to some degree—either by themselves, with the aid of a technical device, or with the assistance of others. Consequently, it is essential to obtain some knowledge on the egress capacity of the population with disabilities. The Fire SERT research group at the University of Ulster, Northern Ireland, has developed a substantial body of data on the egress capabilities of disabled people who go out and about in the community. Their results, published in *Fire Technology* (1999), are an essential source of reference to anyone who has to take into account the escape capacities of people with disabilities.[66,78–80] Only partial data of the Fire SERT studies are reported here.

To obtain this data, the Fire SERT group met with 155 disabled participants who regularly visited 5 day centers. Among the disabled people studied, 121 could move without help, and 34 requested assistance throughout the experiment. The movement speeds achieved on a straight horizontal surface are presented in Table 3-13.2.

Table 3-13.2 *Speed on a Horizontal Surface*

Subject Group (number)	Mean (m/s)	Standard Deviation (m/s)	Range (m/s)	Interquartile Range (m/s)
All disabled (*n* = 107)	1.00	0.42	0.10–1.77	0.71–1.28
With locomotion disability (*n* = 101)	0.80	0.37	0.10–1.68	0.57–1.02
no aid (*n* = 52)	0.95	0.32	0.24–1.68	0.70–1.02
crutches (*n* = 6)	0.94	0.30	0.63–1.35	0.67–1.24
walking stick (*n* = 33)	0.81	0.38	0.26–1.60	0.49–1.08
walking frame or rollator (*n* = 10)	0.57	0.29	0.10–1.02	0.34–0.83
Without locomotion disability (*n* = 6)	1.25	0.32	0.82–1.77	1.05–1.34
Electric wheelchair (*n* = 2)	0.89	—	0.85–0.93	—
Manual wheelchair (*n* = 12)	0.69	0.35	0.13–1.35	0.38–0.94
Assisted manual wheelchair (*n* = 16)	1.30	0.34	0.84–1.98	1.02–1.59
Assisted ambulant (*n* = 18)	0.78	0.34	0.21–1.40	0.58–0.92

Table 3-13.3 *Speed on Stairs*

Subject Group (number)	Mean (m/s)	Standard Deviation (m/s)	Range (m/s)	Interquartile Range (m/s)
Ascent				
With locomotion disability				
(*n* = 30)	0.38	0.14	0.13–0.62	0.26–0.52
no aid				
(*n* = 19)	0.43	0.13	0.14–0.62	0.35–0.55
crutches				
(*n* = 1)	0.22	—	0.13–0.31	0.26–0.45
walking stick				
(*n* = 9)	0.35	0.11	0.18–0.49	—
rollator				
(*n* = 1)	0.14	—	—	—
Without disability				
(*n* = 8)	0.70	0.24	0.55–0.82	0.55–0.78
Descent				
With locomotion disability				
(*n* = 30)	0.33	0.16	0.11–0.70	0.22–0.45
No aid				
(*n* = 19)	0.36	0.14	0.13–0.70	0.20–0.47
Crutches				
(*n* = 1)	0.22	—	—	—
Walking stick				
(*n* = 9)	0.32	0.12	0.11–0.49	0.24–0.46
Rollator				
(*n* = 1)	0.16	—	—	—
Without disability				
(*n* = 8)	0.70	0.26	0.45–1.10	0.53–0.90

The speed on stairs was measured for participants who passed a screening test; this reduced the sample to 30 people who could negotiate stairs, although they all had a locomotion disability. Eight people who had no disability were included for comparison, as presented in Table 3-13.3. The researchers observed that participants had to rest repeatedly along the route. Also, more than 35 percent of the participants went up the stairs taking one step at a time; 44 percent went down the stairs the same way. In general, the participants were more confident going up the stairs than they were coming down. Finally, 91 percent of unassisted subjects chose to use the handrail when going up and 94 percent when coming down.

The capacity of disabled people to negotiate doors was also studied by the Fire SERT group. They examined the necessary time for disabled people to go through a door by pulling and pushing the door, which was closing with different forces. Partial results are shown in Table 3-13.4. The researchers observed that the analysis of these data suggests that the ability of disabled people to negotiate doors, subjected to a range of closing forces, may depend on different factors. These include the use of a technical aid such as a walker, since it implies a relatively slow movement speed and particular technique in maneuvering the technical aid though the door; how old the participant was, since this is inherently related to strength; and the presence and severity of a dexterity, or reaching and stretching, disability.

The Fire SERT group also studied the capability of people with disabilities to read and locate exit signs. They compared a nonilluminated exit sign, an internally-illuminated sign, and a light emitting diode (LED). They concluded that for people with seeing impairments, LED signs were the easiest to see and read.[80]

It has been demonstrated that people with intellectual disability can learn to evacuate a building. However, for this skill to be maintained, substantial repeated training is

Table 3-13.4 *Time in Seconds to Negotiate Doors*

Closing Force (*N*)	No Aid (*n* = 63) Mean (s)	Standard Deviation	Range (s)	Crutch Users (*n* = 5) Mean (s)	Range (s)	Walking Stick (*n* = 28) Mean (s)	Standard Deviation	Range (s)	Walking Frame/ Rollator (*n* = 8) Mean (s)	Range (s)
Push										
21	3.0	0.8	1.7–4.5	3.7	3.6–3.8	3.7	1.5	2.3–7.4	7.9	2.0–12.8
30	3.5	2.2	1.9–15.0	3.0	2.5–3.2	3.8	1.5	2.5–7.3	6.3	2.2–10.5
42	3.7	1.5	1.6–10.2	3.8	2.9–5.2	4.0	1.6	2.3–7.5	5.2	2.1–10.3
51	4.1	2.4	1.0–14.3	3.6	3.1–3.9	4.3	2.4	1.5–10.7	7.9	2.0–14.3
60	4.0	1.9	1.3–13.0	3.8	3.6–4.1	3.7	1.5	1.7–7.9	5.2	2.0–10.3
70	4.3	2.0	1.7–11.2	3.9	3.3–4.6	4.6	2.1	2.5–11.1	6.2	1.7–11.2
Pull										
21	3.3	1.5	1.5–7.6	2.8	2.2–4.0	3.6	1.4	1.8–7.6	5.7	2.0–8.2
30	3.2	1.0	1.5–5.2	—	—	3.2	0.9	1.8–4.9	5.2	4.3–6.0
42	3.7	1.8	1.4–12.6	4.0	2.9–6.3	3.9	1.4	1.9–6.8	4.7	2.6–6.9
51	3.8	1.6	1.5–10.2	3.6	2.5–4.6	4.6	2.2	1.5–9.5	6.3	2.5–11.2
60	4.1	1.9	1.5–11.4	3.6	2.7–4.7	4.1	1.7	1.4–7.4	8.9	1.9–17.0
70	4.6	2.2	1.5–12.6	4.6	2.6–4.7	4.9	2.3	2.1–9.7	3.2	1.9–6.7

necessary, with incentives and in a variety of realistic scenarios.[81] The speeds of movement of people with an intellectual disability could be comparable to the speeds of able occupants, although their time delay to start could be very long, especially during night evacuation.

Movement in Smoke

For a long time it was assumed that during an evacuation when occupants encountered smoke, they would stop, turn back, and find another means of egress. It is acknowledged now that many people are prepared to move in smoke. It is estimated that over 60 percent of evacuees in small residential buildings move through smoke to evacuate. A study of the behavior of occupants who evacuated after the bomb blast at the World Trade Center in 1993 showed that 94 percent of the occupants of Tower 1 moved through smoke.[82] Detailed study of the evacuation of two high-rise residential buildings showed that around 96 percent of the occupants located above the fire floor moved through smoke. The only occupants who managed to escape without meeting any smoke were occupants located under the fire floor or occupants who started their evacuation very early during the fire. In fact, movement through smoke is a recurring event in actual fires.[57,58] The fact that movement in smoke is so prevalent during high-rise fire evacuation can be explained by the simultaneous evacuation movement of a large number of occupants. Occupants of the fire floor who evacuate their floor will allow the stairwell to become contaminated when opening the door to that stairwell. Even if the stairwell is pressurized, the repeated movement of occupants from the fire floor to the stairwells and occupants opening doors to the same stairwells on all upper floors will allow this means of egress to become contaminated. In a way, the stairwells of a high-rise building might be the most dangerous place to be during a fire, after the room of fire origin and the fire floor.

Although it seems well known by the public that it is the smoke that kills people in fires,[83] occupants are still prepared to move through smoke to reach safety. The public knowledge that smoke kills does not mean that they are a good judge of the potential lethal effect of smoke. Victims are reporting that they made it through smoke because they moved very fast, or were breathing through a cloth or holding their breath to protect themselves. In fact, these people were extremely lucky because smoke kills, and it kills fast—a couple of breaths could be enough to lose consciousness.

As was discussed in Section 3, Chapter 12, the principal motivation to move through smoke was the knowledge of an exit location and the ability to estimate the travel distance to that exit. Another motivation that can be found in high-rise buildings is the strong desire of occupants to reach ground level. Also, when occupants start their evacuation, it is possible that no smoke was visible, but eventually during their descent, this situation changed (usually within seconds). In these circumstances, some occupants may persist and continue down, others will turn back, while some others may seek refuge.

The presence of smoke has a major impact on occupants' speed of movement. T. Jin in Japan is a pioneer in this field.[84] He tested individual subjects in a 20-m-long corridor filled with two types of smoke analogous to the early stage of a fire, a highly irritant white smoke produced by burning wood cribs and a less irritant black smoke produced by burning kerosene. The visibility in irritant smoke decreased sharply at smoke density extinction coefficient exceeding 0.5 l/m. The occupant speed of movement, which was over 1 m/s at the introduction of smoke, went down to a stop after a few meters in the irritant smoke. Participants could not keep their teary eyes open in irritant smoke. In the nonirritant smoke, participants moved initially at over 1 m/s and slowed down to 0.5 m/s when the extinction coefficient reached 1.0 l/m.

Jensen in Norway tested over 80 subjects in a test facility looking at the performance of different wayguidance systems in smoke.[85] Under smoke optical density of 1.09 and 1.58 l/m, speeds of movement were around 0.2 to 0.4 m/s, which seems to be the ultimate speed of movement in heavy smoke conditions, independent of any egress information system used. Those who have survived catastrophic fires moved on average only 10 m in heavy smoke. At a speed of 0.2 m/s, this equals a time exposure of 50 s.

Tenability studies show that people's movement in smoke before incapacitation varies widely according to a number of factors such as the weight, fitness, and activity of the person or the mix and concentration of the gases developed by the fire. Generally speaking, occupants have only a few minutes available for movement in smoke before incapacitation occurs. Education, training, and evacuation procedures all recommend to avoid moving in smoke, but occupants are still moving in smoke in many fires.

Another problem of movement through smoke is the fast obscuration of the ceiling-mounted luminaires, which gives an impression of total black out. Interviews of fire victims who traveled through smoke are consistent; the occupants insist that the power was out during their evacuation even though no electric fault can be found after the fire. Consequently, it was the smoke density that was obscuring the light fixtures. To alleviate the problem of moving in black-out conditions, the installation of a wayguidance photoluminescent system is gaining popularity. The characteristics of this material to efficiently guide occupants in the dark are particularly interesting. This material could provide support to evacuees where standard lighting and emergency lighting have failed. In the Jensen study,[85] photoluminescent material positioned as a continuous line at floor level and at 1 m from the floor were better than luminaires and lit signs to guide occupants in smoke conditions. In a field study by Proulx,[50] it was found that speeds of movement in a stairwell with a photoluminescent wayguidance system, in black-out conditions, were comparable to speeds of movement in fully-lit stairwells.

Time-Based Egress Analysis

The need to have realistic, verifiable estimates of egress-time criteria and accompanying movement assumptions should be recognized by fire protection engineers and other consultants conducting time-based egress

analyses (sometimes termed "timed exit analyses" or "dynamic exit analyses"). Such analyses are prepared to help get official approval for a building design that otherwise might not meet specific egress requirements in a code. In some cases, the assumptions and calculation methods used in such analyses should be seriously questioned. Currently, authorities having such analyses thrust on them may have difficulty judging their value; they can only fall back on the reputation of the consulting firm and/or the bulk of a report and the apparent (perhaps illusory) sophistication of its calculations.

One should be especially critical of discussions in which egress-time criteria are equated in simple fashion to hazard development times. As noted above in relation to the "life safety evaluation," there should be a factor of safety, especially in view of the incomplete technical grasp of both egress and fire issues at the present time. For example, in a conservative approach, the time available should be at least twice as long as the time required.

This chapter has emphasized egress capacity or flow issues more than travel distance or speed issues. The former are generally more important in building spaces occupied by more than a few persons. Time-based egress analyses usually address both sets of issues and state the total evacuation time for a space as the sum of a flow time and a travel time. In some situations, the travel time component is simply the time taken by the person closest to the exit to move from his or her point of origin to the point considered a place of safety or refuge. Careful judgment is required to predict this speed and the actual flow of those following the first person. A simple, conservative approach would assume a modest speed for the first person, and a speed similar to the congested speed for those following behind. In this case, it is reasonable to predict the minimum total evacuation time (not including communication and decision-making times) as the sum of this first person's travel time and the flow time of those following, based on an assumed mean-flow calculation. (Note that the term *minimum total evacuation time* is used here; some consultants have erroneously reported that their time-based exit analyses predict maximum total evacuation times.)

For example, if the first person is 18.3 mm (60 ft) from a 914-mm- (36-in.-) wide (nominal width) exit door and is followed by 100 people, the two time components are travel time—0.3 min [18 m (60 ft) divided by 61 m (200 ft) per min]—and flow time through the doorway—2.0 min (100 persons divided by 50 persons/min)—for a total of 2.3 min for the minimum total evacuation time. Note that in reality, the first person might walk at a free walking speed; however, it is very unlikely that other people would be close behind. Therefore, it is unreasonable to assume that those immediately behind the fast-walking first person would achieve a mean flow of 50 persons/min, a conservative figure for sustained mean flow through a nominal 914-mm (36-in.) doorway. Further information on reasonable movement rates is provided in Table 3-13.1.

One of the errors in some time-based exit analyses occurs as inconsistent, unrealistic assumptions are made about simultaneous high speed and high density of crowd movement, a combination that appears, according to Equation 1, to give a high flow. (Equation 1, the fundamental equation for traffic movement, describes flow as the product of speed, density, and path width.)

Due to interference among closely spaced people, high densities do not permit high speeds of movement, a fact illustrated by Figure 3-13.1 in relation to crowd movement down stairs. Moreover, optimum flows occur only at speeds that are about 60 percent of the speeds at which individuals can move freely. (See Figure 3-13.2 in relation to stairs and, generally, the subsection "General Research on Crowd Movement.")

The moderate conditions, shown in Table 3-13.5, are reasonable approximations for predicting speeds, densities, and flows in calculations of minimum egress time for many situations (especially in view of the fact that other behavior not involving simple movement directed to the exit will often be a larger factor in determining evacuation time). The figures given for corridors apply to all walkways with level or moderate slope (less than 1:12). The figures for stairs assume relatively good step geometry and handrail provision. The figures are based on work by Fruin[14] and by Pauls (as discussed earlier in this chapter); however, they are simplified and optimistic because there are no reductions for edge effects. Nominal per-foot measurements are used here. The resultant errors will be acceptable so long as egress times calculated using these assumptions are considered minimum times for egress movement only. (Figure 3-13.6 is an example of a more sophisticated approach to stair flow capacity.)

Sample Calculation Using Table 3-13.5

Given a crowd of 170 people using a corridor 1520 mm (5.0 ft) wide leading to a doorway 914 mm (3.0 ft) in nominal width and then a stairway 1220 mm (4.0 ft) in nominal width, what mean flow should be assumed for evacuation purposes? Which of the egress facilities governs this flow? What is expected minimum flow time? And what crowd conditions can be expected in these three facilities?

Using moderate conditions, it is predicted that the corridor will serve 100 persons/min, the doorway will serve 51 persons/min, and the stair will serve 48 persons/min. Therefore, the stair capacity governs the flow. The flow time is expected to be 170 divided by 48, or 3.5 min, a time similar to the implied standard in current egress standards. At a flow of 48 persons/min through each facility

Table 3-13.5 *Crowd Movement Parameters for Various Facilities and Conditions*

Facility	Crowd Condition	Density (ft²)	Speed (ft/min)	Flow (min/ft)
Stair	Minimum	<0.05	150	<5
Stair	Moderate	0.10	120	14
Stair	Optimum	0.19	95	18
Stair	Crush	0.30	<40	<12
Corridor	Minimum	<0.05	250	<12
Corridor	Moderate	0.10	200	20
Corridor	Optimum	0.20	120	24
Corridor	Crush	0.30	<60	<18
Doorway	Moderate	0.10	170	
Doorway	Optimum	0.22	120	
Doorway	Crush	0.30	<50	

For SI units: 1 ft = 0.3048 m; 1 ft² = 0.093 m².

and without any queuing, the corridor will be minimally crowded with an average crowd density of about 0.5 person/m² (0.05 person/ft²), and the doorway and stair will be used at comfortable, moderate levels.

From Figures 3-13.5 and 3-13.6, it can be understood that, with greater population per width of egress facility (and with queuing for the facility), there may be a higher, more efficient flow. In these cases, it may be appropriate to use the optimum values presented in Table 3-13.1; however, caution must be exercised with the localized crowding conditions that may result, especially on stairs and at doors. For example, if there were 800 people using the facilities described in this subsection, the stair would continue to govern the flow time, but with a higher mean flow, the flow time could be 11.1 min. Movement would be restricted to a shuffling pace, with extensive queuing, and a few percent of the people might have difficulty dealing with the sustained high-density conditions.

Movement Assumptions for Simple, First-Approximation Calculations

Although very incomplete, the following will be useful in doing rough, preliminary calculations. Differing crowd compositions and abilities may alter these values up or down by about one-third. Adverse design conditions will reduce effectiveness by as much as one-third. (These values are comparable with those described as "Levels of Service D and E.")[14]

Stairs: A high-quality stairway that allows convenient counterflow and two-abreast movement, with a width of 1220 mm (4 ft) between handrail centerlines—giving an effective width of just over 1 m—will carry a flow of about one person/s under moderate flow conditions. Speed along the slope will be approximately 0.5 m/s (2 ft/s), or one typical office building story every 15 s. Each person will occupy an average of two stair treads.

Level passageways and moderate-slope ramps: A clear width of 1.22 m (4 ft) will permit a flow of 1.33 persons/s under moderate flow conditions. Speed will be approximately 1.0 m/s (3.33 ft/s). Density will be approximately 1 person per 1 m² (10 ft²).

Doorways: A common 910 mm (3 ft) nominal width doorway will permit a flow of 1 person/s under moderate to optimum flow conditions.

The ratio of clear widths for similar flow, comparing stairs and the other facilities, is 4:3; that is, a 1.22-m (4-ft) clear stair width is well matched to a 1-m (3-ft) clear doorway width. Hence the ratios of 4:3 and 3:2 used in common code rules for egress widths are approximately correct and, in the case of the latter 3:2 ratio, err on the side of safety because the code rules are based on stairs' nominal width (not counting handrail incursions or other edge effects).

Other circulation facilities: For completeness, a few other circulation facilities can be noted even though they are not necessarily given egress capacity credit by codes and standards because of a variety of use and mainte-nance difficulties. A 1.22-m (4-ft) nominal width escalator will carry 1.5 persons/s. A typical revolving door will permit a flow of 0.5 person/s. A turnstile will permit a flow of 0.5 to 1.0 person/s depending on ticket or coin collection procedures.

Summary

A quantitative approach to the movement of people must be balanced by a qualitative understanding of the context within which the movement takes place. In cases of fire or other emergencies, egress movement is part of a complex behavior pattern. Calculations addressing time to start and movement directed to egress from a space or building must be considered as providing only minimum evacuation times. Nonetheless, such calculations are useful for making comparisons among design options and for using equivalency approaches to satisfy legal requirements for means of egress.

Calculation methods on movement developed by Pauls and delay time to start developed by Proulx have been emphasized as a result of field studies of evacuation and other movement of people in buildings. Much additional work is required to develop such methods and to revise requirements in codes and standards so that an integrated systematic approach to fire protection, egress provision, and everyday movement safety is the norm.

References Cited

1. J.L. Pauls, "International Life Safety and Egress Seminar, Maryland, November 1981: Summary of Presentations and Discussion," *F. Safety J.,* 5, p. 213 (1983).

2. F.I. Stahl and J.C. Archea, "Assessment of the Technical Literature on Emergency Egress from Buildings." *NBSIR 77-1313,* National Bureau of Standards, Gaithersburg, MD (1977).

3. F.I. Stahl, J.J. Crosson, and S.T. Margulis, "Time-Based Capabilities of Occupants to Escape Fires in Public Buildings: A Review of Code Provisions and Technical Literature." *NBSIR 82-2480,* National Bureau of Standards, Gaithersburg, MD (1982).

4. R.L. Paulsen, Human Behavior and Fire Emergencies: An Annotated Bibliography. *NBSIR 81-2438,* National Bureau of Standards, Gaithersburg, MD (1981).

5. J.L. Pauls, "Development of Knowledge about Means of Egress." *Fire Tech.*, 20, 2, p. 28 (1984).

6. *Design and Construction of Building Exits,* National Bureau of Standards, Washington, DC (1935).

7. *Fire Grading of Buildings, Part III, Personal Safety, Post-War Building Studies,* Her Majesty's Stationery Office, London (1952).

8. K. Togawa, *Report No. 14,* Building Research Institute, Tokyo (1955).

9. V.M. Predtechenskii and A.I. Milinskii, *Planning for Foot Traffic Flow in Buildings,* Amerind Publishing, New Delhi (1978).

10. E. Kendik, "Assessment of Escape Routes in Buildings and a Design Method for Calculating Pedestrian Movement." *Technology Report 85-4,* Society of Fire Protection Engineers, Boston (1985).

11. E. Kendik, *Proceedings of the First International Symposium on Fire Safety Science,* Hemisphere, New York (1984).

12. London Transport Board, *Second Report of the Operational Research Team on the Capacity of Footways,* London Transport Board, London (1958).

13. B.D. Hankin and R.A. Wright, *Oper. Res. Quart.*, pp. 9–81 (1959).

14. J.J. Fruin, *Pedestrian Planning and Design,* revised ed., Elevator World Educational Services Division, Mobile, AL (1987).

15. M. Galbreath, *Fire Research Note 8,* National Research Council of Canada, Ottawa (1969).

16. S.J. Melinek and S. Booth, *Current Paper CP 96/75,* Building Research Establishment, Borehamwood, UK (1975).

17. S.J. Melinek and R. Baldwin, *Current Paper CP 95/75,* Building Research Establishment, Borehamwood, UK (1975).

18. J.L. Pauls, "Movement of People in Building Evacuations," in D.J. Conway (ed.), *Human Response to Tall Buildings,* Chap. 21. Dowden, Hutchinson and Ross, Stroudsburg, PA, pp. 281–292 (1977).

19. J.L. Pauls, "Management of Movement of Building Occupants in Emergencies," in *Proceedings of Second Conference on Designing to Survive Severe Hazards,* Illinois Institute of Technology Research Institute, Chicago, pp. 103–130 (1977).

20. J.L. Pauls, "Evacuation of High Rise Office Buildings." *Buildings,* 84 (May 1978).

21. Board for the Coordination of the Model Codes, *Report on Means of Egress,* Council of American Building Officials, Falls Church, VA (1985).

22. NFPA *101, Code for Safety to Life from Fire in Buildings and Structures,* NFPA, Quincy, MA (1994).

23. J.L. Pauls, "Building Evacuation: Research Findings and Recommendations." in *Fires and Human Behaviour,* John Wiley and Sons, New York, pp. 251–275 (1980).

24. J.L. Pauls, "Effective-Width Model for Evacuation Flow in Buildings," in *Proceedings of Workshop on Engineering Applications of Fire Technology,* National Bureau of Standards, Washington, DC, pp. 215–232 (1980).

25. J.L. Pauls, "Effective-Width Model for Crowd Evacuation Flow on Stairs," *Proceedings of 6th International Fire Protection Engineering Seminar,* Karlsruhe, Germany, pp. 295–306 (1982).

26. J.L. Pauls, "The Movement of People in Buildings and Design Solutions for Means of Egress." *Fire Technology,* 20, 1, pp. 27–47 (1984).

27. J.L. Pauls and B.K. Jones, "Building Evacuation: Research Methods and Case Studies," in *Fires and Human Behaviour,* John Wiley and Sons, New York, pp. 227–249 (1980).

28. J.L. Pauls, *Building Practice Note 35,* National Research Council of Canada, Ottawa (1982).

29. J.J. Fruin, *Audit. News,* 22, p. 4 (1984).

30. J.J. Fruin, *Crowd Dynamics and the Design and Management of Public Places,* Conference, Los Angeles (1985).

31. SCICON, *Safety in Football Stadia: A Method of Assessment, Scientific Control Systems,* London (1972).

32. Home Office/Scottish Home and Health Dept., *Guide to Safety at Sports Grounds (Football),* Her Majesty's Stationery Office, London (1976).

33. *Report of the Task Force on Crowd Control and Safety,* City of Cincinnati (1980).

34. T.F. Ventre, F.I. Stahl, and G.E. Turner, *NBSIR 81-2361,* National Bureau of Standards, Gaithersburg, MD (1981).

35. The Rt. Hon. Lord Justice Taylor, *The Hillsborough Stadium Disaster,* Interim and Final Reports, Her Majesty's Stationery Office, London (1990).

36. T.J. Klem, *Fire J.*, 80, p. 128 (1986).

37. Popplewell, *Committee Report 9585,* Her Majesty's Stationery Office, London (1985).

38. Popplewell, *Committee Report 9710,* Her Majesty's Stationery Office, London (1986).

39. R.A. Smith and J.F. Dickie (eds.), *Engineering for Crowd Safety,* Elsevier, Amsterdam (1993).

40. D.M. Alvord, *NS-GCR 85-496,* National Bureau of Standards, Gaithersburg, MD (1985).

41. J.L. Pauls, "Observations of Crowd Conditions at Rock Concert in Exhibition Stadium, Toronto, 16 July 1980." *Building Research Note No. 185,* National Research Council of Canada, Ottawa (1982).

42. J.M. Lewis and M.L. Kelsey, "The Crowd Crush at Hillsborough: The Collective Behavior of an Entertainment Crush," *Disasters, Collective Behavior, and Social Organisation,* Kent State Univ., OH (1994).

43. J.J. Fruin, *Elev. World,* 33, p. 52 (1985).

44. ITE Technical Council Committee 5-R, *Traffic Eng.*, May 34, (1976).

45. T.A. Habicht and J.P. Braaksmal, *J. Trans. Eng.*, 110, p. 80 (1984).

46. British Standards Institute, *Fire Safety Engineering in Buildings, Part 1: Guide to the Application of Fire Safety Engineering Principles,* DD240, London (1997).

47. G. Proulx and G. Hadjisophocleous, "Occupant Response Model: A Sub-Model for the NRCC Risk-Cost Assessment Model," *Proceedings of the Fourth International Symposium on Fire Safety Science,* Ottawa, Canada (1994).

48. G. Proulx and R.F. Fahy, "The Time Delay to Start Evacuation: Review of Fire Case Studies," *Proceedings of the Fifth International Symposium on Fire Safety Science,* Melbourne, Australia (1997).

49. G. Proulx and J. Pineau, "Differences in the Evacuation Behaviour of Office and Apartment Building Occupants," *Proceedings of the Human Factors and Ergonomics Society 40th Annual Meeting,* Philadelphia (1996).

50. G. Proulx, B. Kyle, and J. Creak, "Effectiveness of a Photoluminescent Wayguidance System," *Fire Tech.* In press (2001).

51. T.J. Shields, K.E. Boyce, and G.W.H. Silcock, "Towards the Characterization of Large Retail Stores," *Proceedings of the First International Symposium on Human Behaviour in Fire,* Belfast, UK (1998).

52. G. Proulx and J.D. Sime, "To Prevent 'Panic' in an Underground Emergency: Why Not Tell People the Truth?," *Proceedings of the Third International Symposium on Fire Safety Science,* Elsevier, London (1991).

53. P. J. Keating and F. E. Loftus, "Post Fire Interviews: Development and Field Validation of the Behavioral Sequence Interview Technique," *NBS-GCR 84-477,* National Bureau of Standards, Washington, DC (1984).

54. A.J. Chapman and D.J. Perry, "Applying the Cognitive Interview Procedure to Child and Adult Eyewitnesses of Road Accidents," *Applied Psychology: An International Review,* 44, 4 (1995).

55. P. Brennan, "Timing Human Response in Real Fires," *Proceedings of the Fifth International Symposium on Fire Safety Science,* Melbourne, Australia (1997).

56. P. Brennan, "Victims and Survivors in Fatal Residential Building Fires," *Proceedings of the First International Symposium on Human Behaviour in Fire,* Belfast, UK (1998).

57. G. Proulx, "Critical Factors in High-Rise Evacuations," *Fire Prevention,* 291, pp. 24–27 (1996).

58. G. Proulx, "The Impact of Voice Communication Messages during a Residential Highrise Fire," *Proceedings of the First International Symposium on Human Behaviour in Fire,* Belfast, UK (1998).

59. G. Proulx, "Occupant Response to Fire Alarm Signals," *NFPA Fire Alarm Code Handbook, Supplement 4,* Quincy, MA (1999).

60. J.L. Pauls, "The 7-11 Stair: Should It Be Required for Residential Construction? (Rebuttal to National Association of Home Builders.)" The Building Official and Code Administrator, May–June 1985, pp. 16–35. *The Building Official and Code Administrator*, 26 (May–June 1985).

61. B.M. Johnson and J.L. Pauls, "Study of Personnel Movement in Office Buildings," *Health Impacts of the Use, Evaluation and Design of Stairways in Office Buildings,* Health and Welfare Canada, Ottawa (1977).

62. J.L. Pauls, "The Stair Event: Some Lessons for Design," *Proceedings of Conference, People and the Man-Made Environment,* Sydney, pp. 99–109 (1980).

63. J.B. Webber, *Report of the Ontario Public Inquiry into Fire Safety in High-Rise Buildings,* Queen's Printer of Ontario, Ontario (1983).

64. Statistics Canada, *1991 Census Handbook, Reference, Catalogue 92-305E,* Statistics Canada, Ottawa (1992).

65. U.S. Census Bureau, "Americans with Disabilities: 1994–95," *Current Population Reports P70-61,* http://www.census.gov: 80/hhes/www/disable/census.html.

66. K.E. Boyce, T.J. Shields, and G.W.H. Silcock, "Toward the Characterization of Building Occupancies for Fire Safety Engineering: Prevalence, Type, and Mobility of Disabled People," *Fire Tech.,* 35, 1, pp. 35–50 (1999).

67. K.E. Dunlop and T.J. Shields, "Real Fire Emergency Evacuation of Disabled People," *CIB W14,* Belfast, UK (1994).

68. E. Juillet, "Evacuating People with Disabilities," *Fire Eng.,* 126, 12, pp. 100–103 (1993).

69. J. Pauls and E. Juillet, "Life Safety of People with Disabilities: How Far Have We Progressed?" in *Proceedings of CIB W14 Symposium and Workshops: Fire Safety Engineering in the Process of Design, Part 1: Symposium: Engineering Fire Safety for People with Mixed Abilities,* Ulster, Northern Ireland, pp. 17–40 (1993).

70. U.S. Fire Administration, *Emergency Procedures for Employees with Disabilities in Office Occupancies,* Emmitsburg, MA (1995).

71. J.H. Klote, H.E. Nelson, S. Deal, and B.M. Levin, "Staging Areas for Persons with Mobility Limitations," *NISTIR 4770,* U.S. Department of Commerce Technology Administration, Gaithersburg, MD (1992).

72. B.J. Semple, "Vertical Exiting: Are Elevators Another Way Out?" *NFPA Journal,* 87, 3, (1993).

73. J.H. Klote and G.T. Tamura, "Design of Elevator Smoke Control Systems for Fire Evacuation," *ASHRAE Transactions,* 97, 2, pp. 634–642 (1991).

74. *Proceedings of the Symposium on Elevators and Fire,* Baltimore, MD, The American Society of Mechanical Engineers, New York, February (1991).

75. N.E. Groner and B.M. Levin, "Human Factors Considerations in the Potential for Using Elevators in Building Emergency Evacuation Plans," *NIST-GCR-92-615,* National Institute of Standards and Technology, Gaithersburg, MD (1992).

76. G.M.E. Cooke, "Assisted Means of Escape of Disabled People from Fires in Tall Buildings," *BRE Information Paper, IP 16/91,* Fire Research Establishment, Garston, UK (1991).

77. B. Johnson, "Evacuation Techniques for Disabled Persons," *National Research Council of Canada,* Springfield Environmental Research Ltd. (1983).

78. K.E. Boyce, T.J. Shields, and G.W.H. Silcock, "Toward the Characterization of Building Occupancies for Fire Safety Engineering: Capabilities of Disabled People Moving Horizontally and on an Incline," *Fire Tech.,* 35, 1, pp. 51–67 (1999).

79. K.E. Boyce, T.J. Shields, and G.W.H. Silcock, "Toward the Characterization of Building Occupancies for Fire Safety Engineering: Capabilities of Disabled People to Negotiate Doors," *Fire Tech.,* 35, 1, pp. 66–78 (1999).

80. K.E. Boyce, T.J. Shields, and G.W.H. Silcock, "Toward the Characterization of Building Occupancies for Fire Safety Engineering: Capabilities of People with Disabilities to Read and Locate Exit Signs," *Fire Tech.,* 35, 1, pp. 79–86 (1999).

81. M. Rowe and J.H. Kedesdy, "Fire Evacuation Skills Training for Institutionalized Mentally Retarded Adults," *Behavioral Residential Treatment,* 3, 2 (1988).

82. F.R. Fahy and G. Proulx, "Collective Common Sense: A Study of Human Behavior during the World Trade Center Evacuation," *NFPA Journal,* 9, 2, pp. 59–67 (1995).

83. G. Proulx, R.F. Fahy, J. Comeletti, M. Appy, and E. Kirtley, "Home Fire Safety Class for Working Adults," *IR 803,* National Research Council of Canada (1999).

84. T. Jin, "Studies on Human Behavior and Tenability in Fire Smoke," *Proceedings of the Fifth International Symposium on Fire Safety Science,* Melbourne, Australia (1997).

85. G. Jensen, "Evacuating in Smoke," *IGS AS,* Trondheim, Norway (1993).

CHAPTER 14

Emergency Movement

Harold E. "Bud" Nelson and Frederick W. Mowrer

Introduction

Prediction of the movement of occupants during egress is an essential aspect of performance-based building fire safety analysis methods. In general, life safety from fire is achieved if the required safe egress time (RSET) is shorter than the available safe egress time (ASET), where the ASET is defined as the time when fire-induced conditions within an occupied space or building become untenable. Methods to evaluate the development of fire-induced conditions and tenability criteria to determine the ASET are addressed in other chapters of this handbook. The RSET can be subdivided into a number of discrete time intervals, the sum of which constitute the total RSET:

$$RSET = t_d + t_a + t_o + t_i + t_e \tag{1}$$

where

t_d = time from fire ignition to detection

t_a = time from detection to notification of occupants of a fire emergency

t_o = time from notification until occupants decide to take action

t_i = time from decision to take action until evacuation commences

t_e = time from the start of evacuation until it is completed

The RSET elements t_d and t_a may involve hardware, such as fire detection devices and fire alarm equipment, and

Harold E. "Bud" Nelson, a senior research engineer at Hughes Associates, Inc., in Columbia, Maryland, is a past president of the SFPE. He has focused on hazard analysis and application of scientific principles to the solution of real-world fire safety problems.

Frederick W. Mowrer is an associate professor in the Department of Fire Protection Engineering at the University of Maryland. He currently serves on the board of directors of the SFPE and is the chair of the SFPE Technical Steering Committee. His research interests include material flammability evaluation, enclosure fire dynamics, and fire risk assessment.

human response, such as discovery of fire, or other indication of fire, and giving the alarm. The elements t_o and t_i relate the individual and collective responses of the occupants until they commence evacuation. The theory and design of detection and alarm systems are covered elsewhere in this handbook. The theory of human response is addressed in Section 3, Chapter 12 "Behavioral Response to Fire and Smoke."

This chapter primarily addresses different methods that can be used to estimate the last of the RSET elements, t_e, the evacuation time. Included in the coverage of this chapter are those human behavioral responses that affect the flow and efficiency of the emergency movement.

This chapter also identifies models that have been developed to evaluate emergency movement in buildings and provides guidance on the criteria for model selection.

Elements of Emergency Movement

Research-based methods for predicting the flow of groups of persons in emergencies have emerged in recent years. The major contributors include Predtechenskii and Milinskii,[1] Fruin,[2] and Pauls.[3,4] The methods developed are, in most cases, compatible and supportive of each other. All are based on the relationship between the speed of movement and population density of the evacuating stream of persons. In general, these methods assume that

1. All persons will start to evacuate at the same instant.
2. Occupant flow will not involve any interruptions caused by decisions of the individuals involved.
3. All or most of the persons involved are free of disabilities that would significantly impede their ability to keep up with the movement of a group.

The approach is often referred to as a hydraulic model of emergency egress.

Separate works by investigators, such as Wood,[5] Bryan,[6] and Keating and Loftus[7] have concentrated on the decisions and resulting actions taken by individuals in actual fires. Sime[8] and MacLennan[9] have examined the

impact of occupant decisions and choices of actions on evacuation time.

In this chapter, the product of hydraulic model calculations is termed modeled evacuation time. Actual egress time is the time required for the occupants to actually leave a building. Generally, the actual egress time will exceed the modeled time. Since the modeled evacuation time is an approximation based on data from evacuation drills and fire experience, it is therefore possible that the modeled evacuation time can exceed the actual evacuation time. The difference between modeled evacuation time and actual evacuation time can be expressed in terms of an apparent evacuation efficiency using the relationship

$$t_e = t_{me}e \tag{2}$$

where

t_{me} = modeled evacuation time (s)
 e = apparent evacuation efficiency

Apparent evacuation efficiency, e, is a function of elements that interfere with the assumed hydraulic evacuation flow. Typical examples of efficiency elements are

1. Delays caused by egress management activities of wardens or others directing the evacuation
2. Time delays involved in stopping and restarting of flows at merging points
3. Delays, self-instituted by individuals, that retard their start or slow their progress
4. Inefficient balance in the use of exit facilities, where some emergency routes are overtaxed while others are underutilized

All of these factors can reduce evacuation efficiency. However, all of the elements will seldom come to bear on a single evacuation.

The first step in appraising emergency movement usually is to calculate the modeled egress time. The use of model calculations provides a reproducible base of reference in appraising the impact of overall systems, individual components, or changes in systems. If, however, the results of the modeled evacuation time are to be compared to a realistically expected evacuation time or to expected fire growth, it is important that the user understand that the modeled evacuation time is seldom achieved in reality. Accurate estimation of expected evacuation time requires the calculation of the modeled evacuation time and an appraisal of evacuation efficiency. (See Equation 2.) The actual time from fire initiation to evacuation includes the expected movement time (t_e) and the other elements in Equation 1 that describe RSET. This chapter separately addresses the use of hydraulic flow calculations to estimate modeled evacuation time and delays in initiation and evacuation efficiency factors.

Hydraulic Flow Calculations

The estimation of modeled evacuation time utilizes a series of expressions that relate data acquired from tests and observations to a hydraulic approximation of human flow. While the expressions indicate absolute relation-

ships, there is considerable variability in the data. Figure 3-14.1, abstracted from Section 3, Chapter 13, shows a typical relationship between the source data and the derived equation. The equations and relationships presented in the following paragraphs can be used independently or collected to solve a complex egress problem. Such a coordinated collection of equations is demonstrated in the sample problem.

Effective Width, W_e

Persons moving through the exit routes of a building maintain a boundary layer clearance from walls and other stationary obstacles they pass. This clearance is needed to accommodate lateral body sway and assure balance.

Discussion of this crowd movement phenomena is found in the works of Pauls,[3] Fruin,[2] and Habicht and Braaksma.[10] The useful (effective) width of an exit path is the clear width of the path less the width of the boundary layers. Figures 3-14.2 and 3-14.3 depict effective width and boundary layer. Table 3-14.1 is a listing of boundary layer widths. The effective width of any portion of an exit route is the clear width of that portion of an exit route less the sum of the boundary layers.

Clear width is measured

1. From wall to wall in corridors or hallways
2. As the width of the treads in stairways
3. As the actual passage width of a door in its open position
4. As the space between the seats along the aisles of assembly arrangement
5. As the space between the most intruding portions of the seats (when unoccupied) in a row of seats in an assembly arrangement

The intrusion of handrails is considered by comparing the effective width without the handrails and the effective width using a clear width from the edge of the handrail. The smaller of the two effective widths then
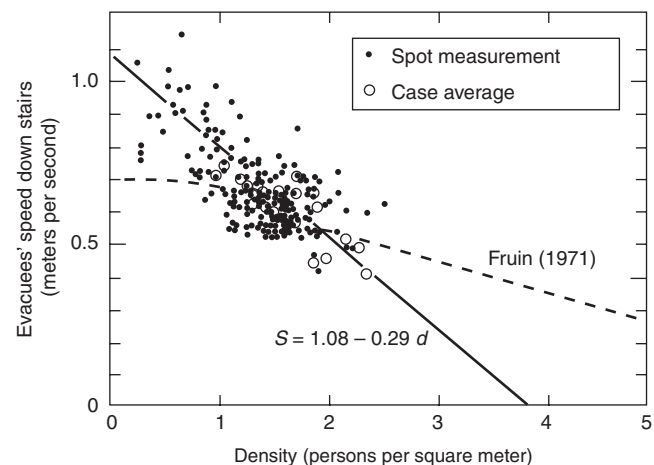

Figure 3-14.1.   *Relation between speed and density on stairs in uncontrolled total evacuations. Dashed line from Fruin.*[2]
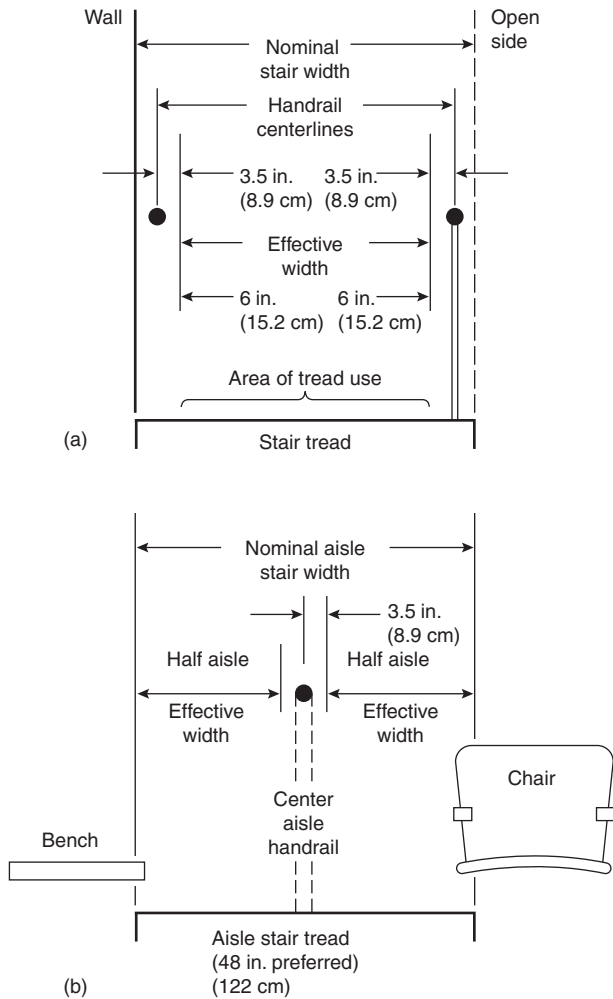
Figure 3-14.2. *Measurements of effective width of stairs in relation to walls, handrails, and seating.*

applies. Using the values in Table 3-14.1, only handrails that protrude more than 2.5 in. need be considered. Minor midbody height or lower intrusions such as panic hardware are treated in the same manner as handrails. Where an exit route becomes either wider or narrower, only that portion of the route has the appropriate greater or lesser clear width.

Density, *D*

Density is the measurement of the degree of crowdedness in an evacuation route and is expressed in persons per unit area. The calculations in this chapter are based on density expressed in persons per square foot (or persons per square meter).

Unless information on the dispersion of occupants indicates otherwise, the density of the first exit element (aisle, corridor, ramp, etc.) is based on all of the served occupants. This information will demonstrate the capacity limits of the route element and produce a value representing the maximum capacity of the element.
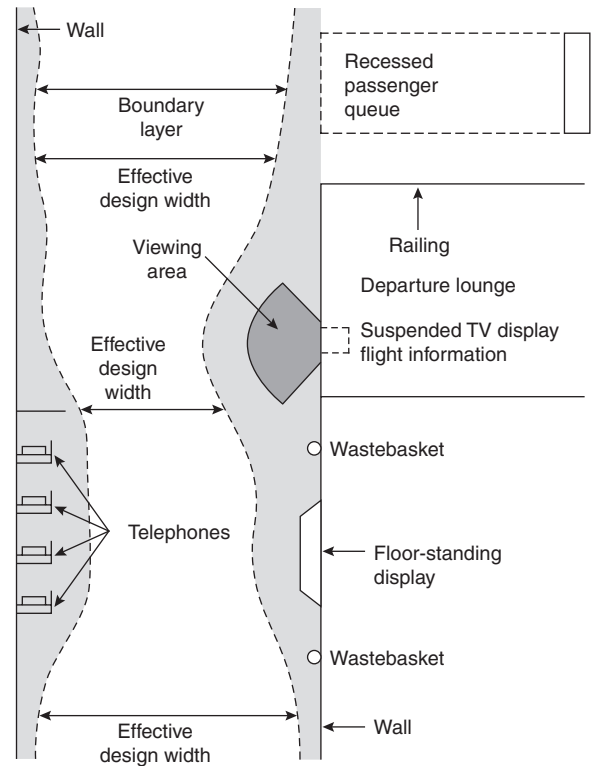
Figure 3-14.3. *Public corridor effective width.*

Table 3-14.1 *Boundary Layer Widths*

Exit Route Element	Boundary Layer	
	(in.)	(cm)
Stairways—wall or side of tread	6	15
Railings, handrails[a]	3.5	9
Theater chairs, stadium benches	0	0
Corridor, ramp walls	8	20
Obstacles	4	10
Wide concourses, passageways	<18	46
Door, archways	6	15

[a]Where handrails are present, use the value if it results in a lesser effective width.

Conversely, if the egressing population is widely dispersed, in terms of reaching the exit route element, the calculation is based on an appropriate time step. At each time increment, the density of the exit route is based on those that have entered the route minus those that have passed from it.

The density factors in subsequent portions of the egress system are determined by calculation. The calculation methods involved are contained in the section of this chapter titled "Transitions."

Speed—Movement Velocity of Exiting Individuals, *S*

Observations and experiments have shown that evacuation flow speed of a group is a function of the population

density. The relationships presented in this section have been derived from Fruin,[2] Pauls,[3] and Predtechenskii and Milinskii.[1]

If the population density is less than about 0.05 persons/ft² (0.54 persons/m²) of exit route (20 ft²/person; 1.85 m²/person), individuals will move at their own pace, independent of the speed of others. If the population density exceeds about 0.35 persons/ft² (3.8 persons/m²), no movement will take place until enough of the crowd has passed from the crowded area to reduce the density.

Between the density limits of 0.05 and 0.35 persons/ft² (0.54 and 3.8 persons/m²) the relationship between speed and density can be considered as a linear function. The equation of this function is

$$S = k - akD \qquad (3)$$

where

S = speed along the line of travel

D = density in persons per unit area

k = constant, as shown in Table 3-14.2

= k_1; and a = 2.86 for speed in ft/min and density in persons/ft²

= k_2; and a = 0.266 for speed in m/s and density in persons/m²

Table 3-14.2 shows evacuation speed constant.

Figure 3-14.4 is a graphic representation of the relationship between speed and density. The speeds determined from Equation 2 are along the line of movement; for stairs the speeds are along the line of the treads. Table 3-14.3 provides convenient multipliers for converting vertical rise of a stairway to a distance along the line of movement. The travel on landings must be added to the values derived from Table 3-14.3.

The maximum speed is that occurring when the density is less than 0.05 persons/ft² (0.54 persons/m²). These maximum speeds are listed in Table 3-14.4.

Within the range listed in Tables 3-14.2, 3-14.3, and 3-14.4, the evacuation speed on stairs varies approximately as the square root of the ratio of tread width to tread height. There is not sufficient data to appraise the likelihood that this relationship holds outside this range.

Table 3-14.2   Constants for Equation 2, Evacuation Speed

Exit Route Element		k_1	k_2
Corridor, Aisle, Ramp, Doorway		275	1.40
Stairs			
Riser (in.)	Tread (in.)		
7.5	10	196	1.00
7.0	11	212	1.08
6.5	12	229	1.16
6.5	13	242	1.23

1 in. = 25.4 mm.
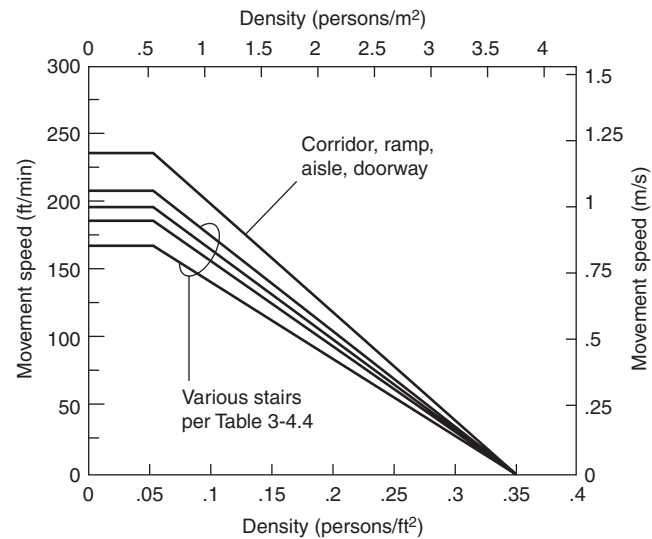
Figure 3-14.4.   *Evacuation speed as a function of density. S = k – akD, where D = density in persons/ft² and k is given in Table 3-14.2. Note that speed is along line of travel.*

Table 3-14.3   *Conversion Factors for Relating Line of Travel Distance to Vertical Travel for Various Stair Configurations*

Stairs Riser (in.)	Tread (in.)	Conversion Factor
7.5	10.0	1.66
7.0	11.0	1.85
6.5	12.0	2.08
6.5	13.0	2.22

Table 3-14.4   *Maximum (Unimpeded) Exit Flow Speeds*

Exit Route Element		Speed (along line of travel)	
		(ft/min)	(m/s)
Corridor, Aisle, Ramp, Doorway		235	1.19
Stairs			
Riser (in.)	Tread (in.)		
7.5	10	167	0.85
7.0	11	187	0.95
6.5	12	196	1.00
6.5	13	207	1.05

Specific Flow, F_s

Specific flow, F_s, is the flow of evacuating persons past a point in the exit route per unit of time per unit of effective width, W_e, of the route involved. Specific flow is expressed in persons/min/ft of effective width (if the value of $k = k_1$ from Table 3-14.2), or persons/s/m of ef-

fective width (if the value of $k = k_2$ from Table 3-14.2). The equation for specific flow is

$$F_s = SD \qquad (4)$$

where

F_s = specific flow
D = density
S = speed of movement

F_s is in persons/min/ft² when density is in persons/ft² and speed in ft/min; F_s is in persons/s/m² when density is in persons/m² and speed in m/s.
    Combining Equations 2 and 3 produces

$$F_s = (1 - aD)kD \qquad (5)$$

where k is as listed in Table 3-14.2.
    The relationship of specific flow to density is shown in Figure 3-14.5. In each case the maximum specific flow occurs when the density is 0.175 persons/ft² (1.9 persons/m²) of exit route space. There is a maximum specific flow associated with each type of exit route element; these are listed in Table 3-14.5.

Calculated Flow, F_c

    The calculated flow, F_c, is the predicted flow rate of persons passing a particular point in an exit route.
    The equation for actual flow is

$$F_c = F_s W_e \qquad (6)$$

where

F_c = calculated flow
F_s = specific flow
W_e = effective width
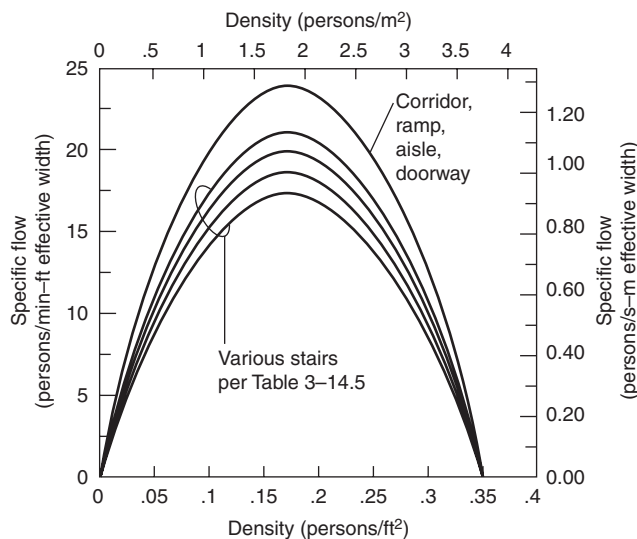
Figure 3-14.5. *Specific flow as a function of density.*

Table 3-14.5 *Maximum Specific Flow, F_{sm}*

Exit Route Element		Maximum Specific Flow	
		Persons/min/ft of Effective Width	Persons/s/m of Effective Width
Corridor, Aisle, Ramp, Doorway		24.0	1.3
Stairs			
Riser (in.)	Tread (in.)		
7.5	10	17.1	0.94
7.0	11	18.5	1.01
6.5	12	20.0	1.09
6.5	13	21.2	1.16

    Combining Equations 4 and 5 produces

$$F_c = (1 - aD)kDW_e \qquad (7)$$

    F_c is in persons/min when $k = k_1$ (from Table 3-14.2), D is persons/ft², and W_e is ft.
    F_c is in persons/s when $k = k_2$ (from Table 3-14.2), D is persons/m², and W_e is m.

Time for Passage, t_p

    Time for passage, t_p, that is, time for a group of persons to pass a point in an exit route, can be expressed as

$$t_p = \frac{P}{F_c} \qquad (8)$$

where t_p is time for passage (t_p is in min where F_c is persons/min; t_p is in s where F_c is persons/s). P is population in persons.
    Combining Equations 6 and 7 yields

$$t_p = \frac{P}{(1 - aD)kDW_e} \qquad (9)$$

Transitions

    Transitions are any points in the exit system where the character or dimension of a route changes or where routes merge. Typical examples of points of transition include the following:

1. Any point where an exit route becomes wider or narrower. For example, a corridor may be narrowed for a short distance by an intruding service counter or similar element. The calculated density, D, and specific flow, F_s, differ before reaching, while passing, and after passing the intrusion.
2. The point where a corridor enters a stairway. There are actually two transitions: one occurs as the egress flow passes through the doorway, the other as the flow leaves the doorway and proceeds onto the stairs.
3. The point where two or more exit flows merge, for example, the meeting of the flow from a cross aisle into a main aisle that serves other sources of exiting

population. It is also the point of entrance into a stairway serving other floors.

The following rules apply to determining the densities and flow rates following the passage of a transition point:

1. The flow after a transition point is a function, within limits, of the flow(s) entering the transition point.
2. The calculated flow, F_c, following a transition point cannot exceed the maximum specific flow, F_{sm}, for the route element involved multiplied by the effective width, W_e, of that element.
3. Within the limits of Rule 2, the specific flow, F_s, of the route departing from a transition point is determined by the following equations:

(a) For cases involving one flow into and one flow out of a transition point,

$$F_{s(\text{out})} = \frac{F_{s(\text{in})}W_{e(\text{in})}}{W_{e(\text{out})}} \qquad (10a)$$

where

$F_{s(\text{out})}$ = specific flow departing from transition point
$F_{s(\text{in})}$ = specific flow arriving at transition point
$W_{e(\text{in})}$ = effective width prior to transition point
$W_{e(\text{out})}$ = effective width after passing transition point

(b) For cases involving two incoming flows and one outflow from a transition point, such as that which occurs with the merger of a flow down a stair and the entering flow at a floor,

$$F_{s(\text{out})} = \frac{F_{s(\text{in}-1)}W_{e(\text{in}-1)} + F_{s(\text{in}-2)}W_{e(\text{in}-2)}}{W_{e(\text{out})}} \qquad (10b)$$

where the subscripts (in – 1) and (in – 2) indicate the values for the two incoming flows.

(c) For cases involving other merger geometries, the following general relationship applies:

$$\begin{aligned}&[F_{s(\text{in}-1)}W_{e(\text{in}-1)}] + \cdots + [F_{s(\text{in}-n)}W_{e(\text{in}-n)}] \\ &= [F_{s(\text{out}-1)}W_{e(\text{out}-1)}] + \cdots + [F_{s(\text{out}-n)}W_{e(\text{out}-n)}]\end{aligned} \qquad (10c)$$

where the letter n in the subscripts (in – n) and (out – n) is a number equal to the total number of routes entering (in – n) or leaving (out – n) the transition point.

4. Where the calculated specific flow, F_s, for the route(s) leaving a transition point, as derived from the equations in rule 3, exceeds the maximum specific flow, F_{sm}, a queue will form at the incoming side of the transition point. The number of persons in the queue will grow at a rate equal to the calculated flow, F_c, in the arriving route minus the calculated flow leaving the route through the transition point.
5. Where the calculated outgoing specific flow, $F_{s(\text{out})}$, is less than the maximum specific flow, F_{sm}, for that route(s), there is no way to predetermine how the incoming routes will merge. The routes may share access through the transition point equally, or there may be total dominance of one route over the other. For conservative calculations, assume that the route of interest is dominated by the other route(s). If all routes are of

concern, it is necessary to conduct a series of calculations to establish the bounds on each route under each condition of dominance.

Impact of Smoke Conditions on Ability to Evacuate

Evacuation Speed in a Smoke-Laden Environment

The emergency movement speeds reported in most sources were derived from experiments and observations conducted in smoke-free environments. While most emergency egress of populations do occur in environments that are smoke free or nearly so, some emergency evacuations involve movement through smoke conditions. Both the density and optic-irritating properties of the smoke can impact movement speed. Jin[11] reports the results and analysis of several series of investigations he conducted, involving human subjects moving through a smoke-laden environment. Jin used two types of smoke, a highly irritating smoke produced by burning wood cribs with narrow spacing between the sticks and a less irritating smoke produced by burning kerosene. The graph in Figure 3-14.6 is typical of the results observed. With the less irritating smoke movement speed decreased gradually as the extinction coefficient increased. With the highly irritating smoke, the evacuation movement speed dropped precipitously once the extinction coefficient reached 0.4/m. Where evacuation through smoke is involved, the movement speed of evacuation should be no greater than that appropriate for the expected density and irritation properties of the smoke. Pending further research the adjustment should be made using the values plotted in Figure 3-14.6.

Probability of Movement through Smoke-Obscured Environment

Table 3-14.6 summarizes data compiled in the United Kingdom[12] and in the United States[13] relating to the visibility distance of smoke and the percentage of building occupants who moved through smoke having the corresponding density. Roughly 40 to 50 percent of occupants
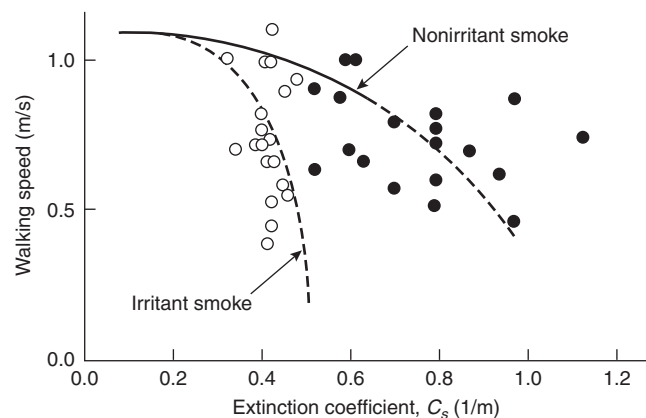

Figure 3-14.6. *Walking speed in fire smoke.*

Table 3-14.6 *Compilation of Visibility Distance for Populations Moving through Smoke*

Visibility Distance		U.K. Sample Population (%)	U.S. Sample Population (%)
(ft)	(m)		
0–2	0–0.6	12.0	10.2
3–6	0.9–1.8	25.0	17.2
7–12	2.1–3.6	27.0	20.2
13–30	4.0–9.1	11.0	31.7
31–36	9.4–11.0	3.0	2.2
37–45	11.3–13.7	3.0	3.7
46–60	14.0–18.3	3.0	7.4
>60	>18.3	17.0	7.4

moved through smoke at visibility distances of less than 12 ft (3.7 m), while 7 to 17 percent of occupants required visibility distances of greater than 60 ft (18.3 m). This range seems to be the demarcation between those occupants willing to move through smoke to an exit (the majority) and those who are reluctant to travel through smoke (the minority). It should be noted that the data in Table 3-14.6 are subjective and are indicative of visibility to both normal objects and backlit exit signs, as the building occupants interviewed were viewing both types of objects while trying to egress.

Users of the data in Table 3-14.6 need to realize that the data in both of the referenced studies was derived, for the most part, from fires in residential properties housing occupants familiar with the means of egress. Also, in the majority of the cases, travel distance through the smoke was 30 ft or less. Additionally, due to the age of the studies (1972 and 1979) these data should be verified with any available more current data.

EXAMPLE:

Consider an office building (Figure 3-14.7) with the following features:

1. There are nine floors, 300 by 80 ft (91 by 24 m).
2. Floor to floor height is 12 ft (3.7 m).
3. Two stairways are located at the ends of the building (no dead ends).

4. Each stair is 44 in. (1.12 m) wide (tread width) with handrails protruding 2.5 in. (63 mm).
5. Stair risers are 7 in. (178 mm) wide and treads are 11 in. (279 mm) high.
6. There are two 4-ft by 8-ft (1.2-m by 2.4-m) landings per floor of stairway travel.
7. There is one, 36-in. (0.91 m) clear width, door at each stairway entrance and exit.
8. The first floor does not exit through stairways.
9. Each floor has a single 8-ft- (2.4-m-) wide corridor extending the full length of each floor. Corridors terminate at stairway entrance doors.
10. There is a population of 300 persons/floor.

SOLUTION A—First Order Approximation:

1. Assumptions.

The prime controlling factor will be either the stairways or the door discharging from them. Queuing will occur; therefore the specific flow, F_s, will be the maximum specific flow, F_{sm}. All occupants start egress at the same time. The population will use all facilities in the optimum balance.

2. Estimate flow capability of a stairway.

From Table 3-14.1, the effective width, W_e, of each stairway is $44 - 12 = 32$ in. (2.66 ft) [813 mm (0.81 m)]. Also, the effective width, W_e, of each door is $36 - 12 = 24$ in. (2 ft) [609 mm (0.61 m)]. The maximum specific flow, F_{sm}, for the stairway (from Table 3-14.5) is 18.5 persons/min/ft (60 persons/min/m) effective width. Specific flow, F_s, equals maximum specific flow, F_{sm}. Therefore, using Equation 6, the flow from each stairway is limited to $18.5 \times 2.66 = 49.2$ persons/min.

3. Estimate flow capacity through a door.

Again from Table 3-14.5, the maximum specific flow through any 36-in. (0.9-m) door is 24 persons/min/ft (78.7 persons/min/m) effective width. Therefore, using Equation 6, the flow through any door is limited to $24 \times 2 = 48$ persons/min. Since the flow capacity of the doors is less than the flow capacity of the stairway served, the flow is controlled by the stairway exit doors (48 persons/stairway exit door/min).
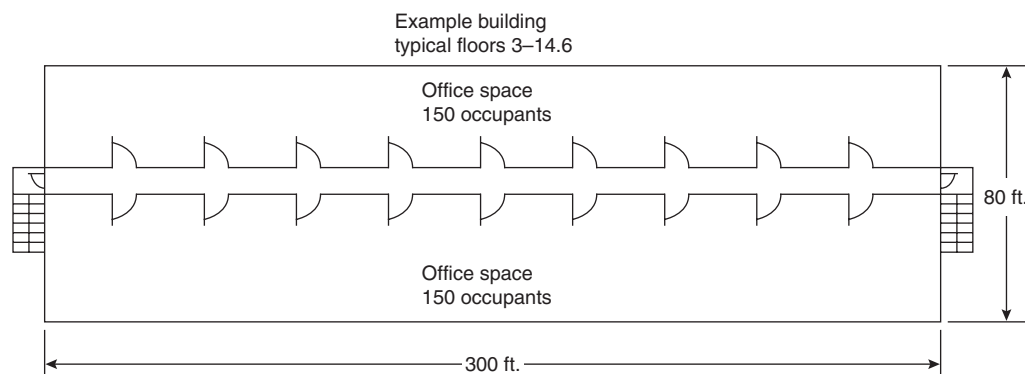
Figure 3-14.7. *Floor plan for example.*

4. Estimate the speed of movement for estimated stairway flow.

From Equation 3 the speed of movement down the stairs is $212 - (2.86 \times 212 \times 0.175) = 105$ ft/min (32 m/min). The travel distance between floors (using the conversion factor from Table 3-14.3) is $12 \times 1.85 = 22.2$ ft (6.8 m) on the stair slope plus 8 ft (2.4 m) travel on each of the two landings, for a total floor-to-floor travel distance of $22.2 + (2 \times 8) = 38.2$ ft (11.6 m). The travel time for a person moving with the flow is $38.2/105 = 0.36$ min/floor.

5. Estimate building evacuation time.

If all of the occupants in the building start evacuation at the same time, each stairway can discharge 48 persons/min. The population of 2400 persons above the first floor will require approximately 25 min to pass through the exit. An additional 0.36 min travel time is required for the movement from the second floor to the exit. The total minimum evacuation time for the 2400 persons located on floors 2 through 9 is estimated at 25.4 min.

SOLUTION B—More Detailed Analysis:

1. Assumptions.

The population will use all exit facilities in the optimum balance; all occupants start egress at the same time.

2. Estimate flow density (D), speed (S), specific flow (F_s), effective width (W_e), and initial calculated flow (F_c) typical for each floor.

Divide each floor in half to produce two exit calculation zones, each 150 ft (45.7 m) long. Determine the density, D, and speed, S, if all occupants try to move through the corridor at the same time, that is, 150 persons moving through 150 ft of an 8-ft- (2.4-m-) wide corridor:

$D = 150$ persons/1200 ft² corridor area $= 0.125$ persons/ft².

From Equation 3, $S = k - akD$.
From Table 3-14.2, $k = 275$.
$S = 275 - (2.86 \times 275 \times 0.125) = 177$ ft/min (54 m/min).
From Equation 5, $F_s = (1 - aD)kD$.
$F_s = [1 - (2.86 \times 0.125)] \times 275 \times 0.125 = 22$ persons/ft (72 persons/m) effective width/min.
From Table 3-14.5, F_s, is less than the maximum specific flow, F_{sm}; therefore, F_s is used for the calculation of calculated flow.
From Table 3-14.1, the effective width of the corridor is $8 - (2 \times 0.5) = 7$ ft (2.13 m)
From Equation 7, calculated flow, $F_c = (1 - aD)kDW_e$.
$F_c = [1 - (2.86 \times 0.125)] \times 275 \times 0.125 \times 7 = 154$ persons/min.

Note: At this stage in the calculation, calculated flow, F_c, is termed initial calculated flow for the exit route element (i.e., corridors) being evaluated. This term is used because the calculated flow rate can be sustained only if the discharge (transition point) from the route can also accommodate the indicated flow rate.

3. Estimate impact of stairway entry doors on exit flow.

Each door has a 36-in. (0.91 m) clear width. From Table 3-14.1, effective width, W_e, is $36 - 12 = 24$ in. (2 ft) (0.605 m).

From Table 3-14.5, the maximum specific flow, F_{sm}, is 24 persons/min/ft effective width.
From Equation 10,

$$F_{s(door)} = [F_{s(corridor)}W_{e(corridor)}]/W_{e(door)}F_{s(door)}$$
$$= (22 \times 7)/2 = 77 \text{ persons/min/ft}$$
$$(25.3 \text{ persons/min/m}) \text{ effective width}$$

Since F_{sm} is less than the calculated F_s, the value of F_{sm} is used. Therefore, the effective value for specific flow is 24.

From Equation 6 the initial calculated flow, $F_c = F_sW_e$ $= 24 \times 2 = 48$ persons/min through a 36-in. (0.91-m) door. Since F_c for the corridor is 154 while F_c for the single exit door is 48, queuing is expected. The calculated rate of queue buildup will be $154 - 48 = 106$ persons/min.

4. Estimate impact of stairway on exit flow.

From Table 3-14.1, effective width, W_e, of the stairway is $44 - 12 = 32$ in. (2.66 ft) (0.81 m).
From Table 3-14.5, the maximum specific flow, F_{sm}, is 18.5 persons/ft (60 persons/m) effective width.
From Equation 10, the specific flow for the stairway, $F_{s(stairway)}$, is $24 \times 2/2.66 = 18.0$ persons/ft (59 persons/m) effective width. In this case, F_s is less than F_{sm} and F_s is used.

The value of 18.0 for F_s applies until the flow down the stairway merges with the flow entering from another floor.

Using Figure 3-14.4 or Equation 5 and Table 3-14.2, the density of the initial stairway flow is approximately 0.146 persons/ft² (1.6 person/m²) of stairway exit route.

From Equation 3 the speed of movement during the initial stairway travel is $212 \times (2.86 \times 212 \times 0.146) = 123$ ft/min (37.5 m/min).

From Solution A, the floor-to-floor travel distance is 38.2 ft (11.6 m). The time required for the flow to travel one floor level is $38.2/123 = 0.31$ min (19 s).

Using Equation 6, the calculated flow, F_c, is $18.0 \times 2.66 = 48$ persons/min.

After 0.31 min, 15 (48×0.31) persons will be in the stairway from each floor feeding to it. If floors 2 through 9 exit all at once, there will be $15 \times 8 = 120$ persons in the stairway. After this time the merging of flows between the flow in the stairway and the incoming flows at stairway entrances will control the rate of movement.

5. Estimate impact of merger of stairway flow and stairway entry flow on exit flow.

From Equation 10,

$$F_{s(out\text{-}stairway)} = \{[F_{s(door)} \times W_{e(door)}] +$$
$$[F_{s(in\text{-}stairway)} \times W_{e(in\text{-}stairway)}]\}/W_{e(out\text{-}stairway)}$$
$$= [(24 \times 2) + (18 \times 2.66)]/2.66$$
$$= 36 \text{ persons/ft effective width}$$

From Table 3-14.5, F_{sm} for the stairway is 18.5 persons/min/ft effective width. Since F_{sm} is less than the calculated F_s, the value of F_{sm} is used.

6. Track egress flow.

Assume all persons start to evacuate at time zero. Initial flow speed is 177 ft/min. Assume that congested flow

will reach the stairway in 30 s. At 30 s, flow starts through stairway doors. F_c through doors is 48 persons/min for the next 19 s. At 49 s, 120 persons are in each stairway and 135 are waiting in a queue at each stairway entrance door.

Note: Progress from this point on depends on which floors take dominance in entering the stairways. Any sequence of entry may occur. To set a boundary, this example estimates the result of a situation where dominance proceeds from the highest to the lowest floor.

The remaining 135 persons waiting at each stairway entrance on the ninth floor enter through the door at the rate of 48 persons/min. The rate of flow through the stairway is regulated by the 48 persons/min rate of flow of the discharge exit doors. The descent rate of the flow is 19 s/floor.

Thus:

at 218 s (3.6 min)	all persons have evacuated the 9th floor
at 237 s (4.0 min)	the end of the flow reaches the 8th floor
at 401 s (6.7 min)	all persons have evacuated the 8th floor
at 420 s (7.0 min)	the end of the flow reaches the 7th floor
at 584 s (9.7 min)	all persons have evacuated the 7th floor
at 603 s (10.1 min)	the end of the flow reaches the 6th floor
at 767 s (12.8 min)	all persons have evacuated the 6th floor
at 786 s (13.1 min)	the end of the flow reaches the 5th floor
at 950 s (15.8 min)	all persons have evacuated the 5th floor
at 969 s (16.2 min)	the end of the flow reaches the 4th floor
at 1133 s (18.9 min)	all persons have evacuated the 4th floor
at 1152 s (19.2 min)	the end of the flow reaches the 3rd floor
at 1316 s (21.9 min)	all persons have evacuated the 3rd floor
at 1335 s (22.3 min)	the end of the flow reaches the 2nd floor
at 1499 s (25.0 min)	all persons have evacuated the 2nd floor
at 1518 s (25.3 min)	all persons have evacuated the building

Evacuation Efficiency Factors

Decisions

Humans require time to make decisions. In general, people are hesitant to undertake overt actions unless they clearly accept the need for such action.

In group situations, group interaction is extremely important to decision making. Latane and Darley[14] pointed out the tendency of many individuals to defer emergency decision making until action is clearly required. More recently MacLennan[9] in his experiments in Australia has classified and is now quantifying this as a

factor he and Sime call "associative." MacLennan has noted that persons in groups often delay response to a warning alarm until it is clear that the group accepts the need to take emergency action. Prior training, organization, and real-time fire information can reduce the delay in the time to take emergency action.

Levin,[15] in analyzing data from many sources related to emergency action in residences, has proposed the division of speed of response into four categories. These categories, which Levin terms ambiguity classes, are based on the initial interpretation of the cues by the individual involved. Levin's classes are

A. Respondent believes that there may be a fire (but is not certain).
B. Respondent believes that it is likely there is a fire.
C. Respondent is sure there is a fire and has seen sufficient smoke to believe that it is a dangerous fire.
D. Respondent has seen flames.

With one major exception, the universal response to ambiguity Class A is to seek information. In the sample studied by Levin, the exception to the general rule occurred with those responsible for persons incapable of taking care of themselves (small children, invalids). These individuals immediately took action to evacuate or otherwise safeguard their charges.

Conversely, in an ambiguity Class D situation emergency action was always taken.

In ambiguity Classes B and C some persons continued to seek information while others undertook other types of emergency action. These actions included attacking the fire, calling the fire department, giving the alarm, and evacuating the building. For the limited number of cases that Levin classified in ambiguity Classes B and C (20 in Class B, and 19 in Class C), the portion of the persons who sought information rather than take emergency action was approximately 50 percent in ambiguity Class B and 35 percent in Class C.

Investigation Time

As noted in the preceding paragraphs, individuals often seek information to clarify the ambiguities inherent in fire situations. This reaction is particularly the case for persons alone or in small groups. Sime[8] has tracked individuals involved in hotel fires, and his data demonstrate significant amounts of apparently nonproductive movement. This movement is assumed to be prompted by individuals seeking information they feel is necessary to make a proper decision. From an engineering standpoint, this response emphasizes the potential of increasing evacuation efficiency by providing clear information to the occupants of a building about the occurrence and location of the fire, and the condition of the exit routes.

Other Actions

When an individual has decided to take action in response to perceived fire danger, that action may or may not contribute to a speedy evacuation. Figure 3-14.8 diagrammatically shows a variety of the types of actions that are likely to occur. In actual fire situations many individuals undertake actions they believe will mitigate the
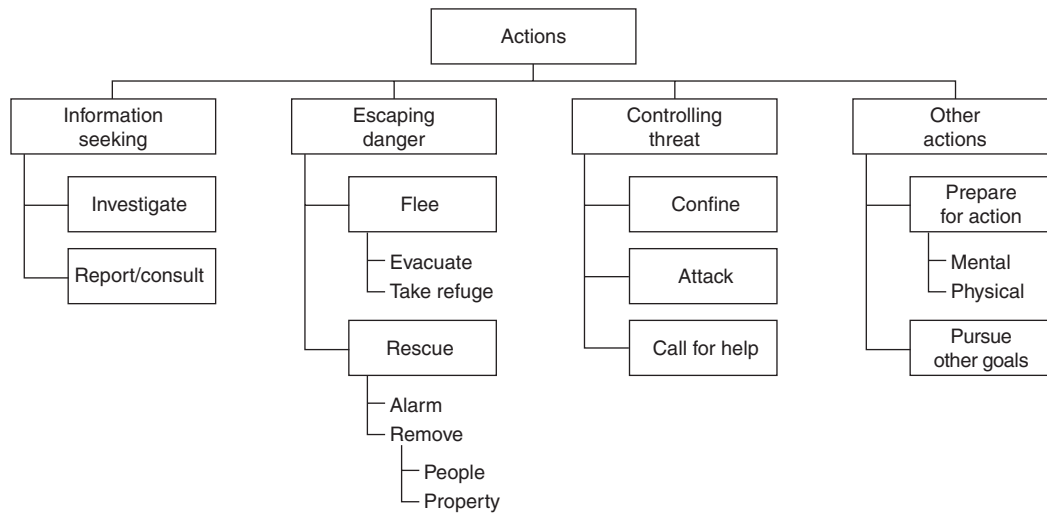
Figure 3-14.8.   *Types of actions.*

fire, help others, or aid in making decisions. Often these actions do not contribute to their evacuation; these alternative actions may be contributing to safety, detrimental to safety, laudable, or mistaken. All actions, however, impact on evacuation efficiency.

Providing real-time information to building occupants and ensuing rapid response of emergency forces can mitigate delays with a minimum of impact on the desirable effects of nonevacuation actions.

Way Finding

Way finding is most important in situations involving a relatively small number of individuals evacuating a location where they are not familiar with the emergency exit system. This situation typically occurs in hotels, multitenant office buildings, and similar structures where persons seldom use the stairways.

The classic solution to the problem of way finding is the provision of exit signs and exit directional signs. Ozel[16] has summarized the current view of researchers in way-finding problems and related these findings to fire evacuation conditions. A person's ability to find his or her way in an emergency relates to how well that person perceives his or her position and surroundings. The term frequently used is *cognitive mapping.* Most people maintain their cognitive mapping images in simple, regularized forms, such as straight lines and rectangles. In this concept, exit signs are only part of the overall ability of a person to perceive a suitable cognitive map.

Other factors that are rated of high importance to way finding include (1) the complexity of the space as related to common layouts or similar types of buildings (e.g., double-loaded corridors terminating at exits are simple while arrangements involving complex curves or unusual angles are complex); and (2) the presence of distinguishing marks or other indications of points of special attention. Of particular importance are both exit routes and dead ends or other spaces that should not be entered in exiting the building.

Way finding affects evacuation efficiency in facilities where the population density is low and the occupants are unfamiliar with the evacuation routes. In such facilities the efficiency is greatest when (1) the routes are simple, and (2) the exit points are evident in both their location and assurance (to the evacuee) that they truly lead to safety.

Way-finding efficiency decreases as the layout complexity increases. Some factors increasing complexity are unusual arrangements of corridors, obtuse angles, concentric corridors, undifferentiated enclosures (where one cannot orient oneself with respect to the exterior), and exit access doors that appear the same as every other door.

Conversely, all aspects that tend to simplify and identify the exit route decrease the time involved in way finding.

Merging Conflicts

Modeled evacuation time calculations assume that the flow of people is similar to that of a hydraulic fluid. As such, the merger of two flows (persons entering at a floor into a stairwell that is already flowing with evacuees from higher floors) is assumed to regulate itself according to the capabilities of the stairwell and the amount of flow from each of the sources.

In emergency evacuation drills MacLennan[9] has observed significant interruption of the continuity of flow when one flow is stopped and another is started at a merger point. The greatest merging flow efficiency occurs when, once a flow uses an exit route to its full capacity, it blocks all other entry until it has cleared past the point of merger. In actual evacuations, however, there is normally a sharing of access at merger points. This situation results in breaks in the egress flow that can have a significant affect on the capacity. MacLennan has seen effects as high as

30 to 50 percent reduction in the stairwell flow from this cause alone.

Wardens

MacLennan's work indicates that the most efficient flow occurs in a situation where all occupants are fully trained and promptly evacuated upon signal without the assistance of wardens.

Where occupants are not so trained it is often necessary to have a trained warden system. While this system is essential, MacLennan's observations indicate that wardens impose a reduction in egress efficiency. The amount of reduction will depend upon the type of organization and the evacuation procedures. The impact on evacuation efficiency is the greatest when wardens hold occupants in a ready position until the wardens are directed from another point to initiate evacuation.

Self-Regulation

In high-density situations (e.g., heavily populated offices, auditoriums, etc.) individuals often withhold themselves from the evacuation procedure until the crowd lessens (i.e., density is reduced). When these persons arrive at critical exit points so that the main crowded path, normally the stairway, is continuously fed by a short queue, their action will have no impact. However, when the self-induced delay reduces the feed of the critical point, a reduction in egress efficiency will occur.

Uneven Use of Exit Facilities

If some exit facilities are used proportionally more than others, the efficiency of the egress system will decrease. Some exit paths will be utilized while others will be overtaxed.

The impact of uneven exit use can be estimated as a function of (1) the distribution of exits relative to the distribution of population, (2) the degree that the exits will be used for either building entry or for common use within the structure, and (3) all of the cognitive mapping factors discussed under "Way Finding."

Evacuation Efficiency Factors—Summary

In his analysis, MacLennan found that large multi-floor office buildings (some high-rise) demonstrated evacuation times in the range of twice the modeled time where a highly organized evacuation system was present; and up to three times the modeled evacuation time when there had been no training and no organization.

It is expected that MacLennan's findings represent reasonable norms but are subject to many variations (e.g., education level, cultural background, age, and gender) that need to be considered in any individual evaluation.

Emergency Movement Models

A number of models have been developed to calculate building emergency movement times. Gwynne and

Galea[17] identified 22 different such models in a review based on available published literature. This includes 16 models that were available at the time of the review and 6 models known to be under development. The 16 available models are as follows:

> BGRAF[18]
> CRISPII[19]
> DONEGAN'S ENTROPY MODEL[20]
> EGRESS[21]
> E-SCAPE[22]
> EVACNET+[23]
> EVACSIM[24]
> EXIT89[25]
> EXITT[26]
> EXODUS[27,28]
> MAGNETMODEL[29]
> PAXPORT[30]
> SIMULEX[31,32]
> TAKAHASHI'S MODEL[33]
> VEGAS[34,35]
> WAYOUT[36]

Gwynne and Galea[17] critically appraised these evacuation models on the basis of four characteristics.

Nature of the Model Application

Three fundamentally different approaches are used in different evacuation models. These include optimization, simulation, and risk assessment. The optimization models generally assume that occupants evacuate a building in the most efficient manner. The evacuation paths and the flow characteristics of people and exits are considered optimal. The population is considered to be a homogeneous ensemble without individual behavior.

The simulation models attempt to represent the behaviors and movements observed in evacuations to realistically represent the actual paths and decisions taken during an evacuation. The behavioral sophistication employed by these models varies greatly, and consequently so does the accuracy of the results.

Risk assessment models attempt to identify fire hazards associated with evacuation. Repeated runs of the model are made to assess statistically significant variations associated with different design changes, including different fire protection measures.

The Enclosure Representation

The enclosure from which the evacuation takes place must be represented in all evacuation models. Two methods are usually used to represent the enclosure: fine networks and course networks. In each case, the enclosure is subdivided. The resolution of the subdivision distinguishes the fine network from the course network. In the course network models, the geometry is defined in terms of partitions based on the actual structure. Typically, each node represents a room or a corridor. Nodes are connected by arcs representing actual connections within the structure.

In the fine network approaches, the entire floor space of the enclosure is covered by a fairly uniform network of tiles or nodes. Nodes are connected with neighboring nodes, with the number of connections depending on the model. In a fine network, a large space may have thousands of nodes; in this way, the geometry of a space, including internal obstructions, can be accurately represented along with the location of each individual during an evacuation.

The Population Perspective

The population in an enclosure can be represented in one of two perspectives: a global or an individual perspective. Models that use the global perspective treat the population as an homogeneous ensemble without individual characteristics. These models represent evacuation on the basis of the number of occupants who escaped, not on the basis of individuals. With the global perspective, only a distributed or average attribute can be assigned to the population.

Models that use the individual perspective allow for personal attributes to be assigned to individual occupants, either by the user of the model or through a random process, in order to represent a diverse population. These personal attributes are then used in the decision-making and movement process of each individual. This process is typically independent of other individuals, although it does not, preclude group interaction and behavior.

The Behavioral Perspective

To consider the decision-making processes of occupants during an evacuation, a model must have a method of determining behavior. This method will be influenced by the representations used for the population and the enclosure and the broad range of potential behaviors of individuals. Some models do not apply any behavioral rules. These models rely completely on the physical movement of the population and the physical representation of the building according to deterministic equations. For models that do consider behavior, the perspective used can be classified into four categories: implicit, rule-based, functional analogy-based, and artificial intelligence-based. Implicit models do not declare behavioral rules, but rather assume the rules to be implicitly represented through methods and data incorporating psychological and sociological influences.

Rule-based models explicitly recognize the behavioral traits of individual occupants and apply a system that allows occupants to make decisions according to a defined set of rules. In the simpler rule-based methods, the same decisions are triggered by the same stimuli in a deterministic way. Other rule-based methods use either a stochastic approach to apply the rules or a combination of deterministic and stochastic approaches.

Functional analogy-based models apply an equation, or a system of equations, to the entire population, based on a field of study believed to be analogous to some aspect of human behavior. In artificial intelligence-based models, artificial intelligence has been applied to mimic human behavior based on various stimuli.

The behavior of people under fire conditions is influenced by their interactions with other people, with the enclosure and with the fire-induced environment. The decision making of people under fire conditions is influenced and complicated by a number of psychological, sociological, and physiological factors. Because of the behavioral and decision-making factors, some of which are not yet well understood, human behavior is the most complex and difficult aspect of evacuation to simulate.

In addition to the models reviewed by Gwynne and Galea[17] is the model EGRESS TIME, contained in the collection of models and procedures FPETOOL.[37] In terms of the characteristics used by Gwynne and Galea,[17] this model would be judged as an optimization model, having a course network, and limited attention to individual population perspectives.

Model Selection Factors

It is beyond the scope of this chapter to review the features, capabilities, uses, limitations, validation, availability, and costs of the evacuation models identified above. Instead, some of the factors that should be considered in the selection of a model for a particular application are presented, based on the foregoing discussion. These factors are presented in the form of a series of questions on a number of topics that a potential user should ask about an evacuation model before deciding to use it for a particular application. These questions are listed by topic.

Evacuation Model Type

Is the model based on optimization, simulation, or risk assessment?
Is the type of model suitable for the application?
What are the limitations of the model with respect to the application?

Enclosure Representation

Is the model based on a fine network or a course network?
How are different spaces and areas within spaces represented?
How are connections between spaces represented?
How are obstructions within a space represented?
How do these representations influence the model results?
How many nodes, connections, and obstructions can the model handle?
How are the data entered to represent spaces, connections, and obstructions?

Population Perspective

Does the model use a global or an individual perspective?
If the perspective is global, what general characteristics of the population are represented?
    If the perspective is individual, what individual characteristics of the population are represented?
    How are the individual or global characteristics of the population entered in the model?

Behavioral Perspective

What type of behavioral perspective does the model employ—none, implicit, rule-based, functional analogy-based, or artificial intelligence-based?

How does the model treat people-people interactions and their effects on behavior?

How does the model treat people-enclosure interactions and their effects on behavior?

How does the model treat people-environment interactions and their effects on behavior?

How does the model address physiological factors that influence decision making?

How does the model address psychological factors that influence decision making?

How does the model address sociological factors that influence decision making?

Model Validation

Has the model been validated? If so, how and to what extent?

How has the model validation been reported?

Model Implementation

Has the model been implemented on a computer?

What computer platforms does the model support?

Model Support

Is the model currently supported by the author(s)?

Is the model supported by another agency?

Is the model still being developed? If so, how are users notified of upgrades?

Model Costs

What is the initial cost of the model?

What are the ongoing costs for upgrades, support, and maintenances

Appropriateness to Task

What inputs does the model require of the user? Are these available?

Does the model consider elements needed for the task at hand, for example,

speed of movement, impact of density on speed?

queuing or other congestion?

merging of flows?

premovement decisions?

decisions/actions during movement?

Does the model produce an output meeting the needs of the task at hand?

Nomenclature

D	density in persons per unit area
e	apparent evacuation efficiency
F	flow
k	constant from Table 3-14.2
P	population
S	speed along the line of travel
t	time
W	width

Subscripts

1	speed in ft/min and density in persons/ft^2
2	speed in m/s and density in persons/m^2
ae	actual evacuation
c	calculated
(corridor)	corridor
(door)	door
d	delay
e	effective
$(in - n)$	prior to point n
me	modeled evacuation
$(out - n)$	after point n
p	passage
s	specific
sm	maximum specific
(stairway)	stairway

References Cited

1. V.M. Predtechenskii and A.I. Milinskii, *Planning for Foot Traffic in Buildings* (translated from the Russian), Stroizdat Publishers, Moscow (1969). English translation published for the National Bureau of Standards and the National Science Foundation, Amerind Publishing Co., New Delhi, India (1978).

2. J.J. Fruin, *Pedestrian Planning Design,* Metropolitan Association of Urban Designers and Environmental Planners, Inc., New York (1971).

3. J.L. Pauls, "Effective-Width Model for Evacuation Flow in Buildings," in *Proceedings, Engineering Applications Workshop,* Society of Fire Protection Engineers, Boston (1980).

4. J.L. Pauls, "Calculating Evacuation Time for Tall Buildings," in *SFPE Symposium: Quantitative Methods for Life Safety Analysis,* Society of Fire Protection Engineers, Boston (1986).

5. P.G. Wood, "The Behavior of People in Fires," *Fire Research Note 953,* Building Research Establishment, Fire Research Station, Borehamwood, United Kingdom (1972).

6. J.L. Bryan, *Smoke as a Determinant of Human Behavior in Fire Situations,* University of Maryland, College Park (1977).

7. J.P. Keating and E.F. Loftus, "Post Fire Interviews: Development and Field Validation of the Behavioral Sequence Interview Technique," *Report GCR-84-477,* National Bureau of Standards, Gaithersburg, MD (1984).

8. J.D. Sime, "Escape from Building Fires: Panic or Affiliation?," Ph.D. Dissertation, University of Surrey, UK (1984).

9. H.A. MacLennan, "Towards an Integrated Egress/Evacuation Model Using an Open System Approach, Fire Safety Science," in *Proceedings of the First International Symposium,* Hemisphere Publishing Corporation, Washington, DC (1986).

10. A.T. Habicht and J.P. Braaksma, "Effective Width of Pedestrian Corridors," *Journal of Transportation Engineering,* 110, 1 (1984).

11. T. Jin, "Studies on Human Behavior and Tenability in Fire Smoke," *Proceedings, 5th International Symposium on Fire Safety Science,* pp. 3–22 (1997).

12. P.G. Wood, *Fire Research Note 953,* Building Research Establishment, Borehamwood, United Kingdom (1972).

13. J.L. Bryan, *Smoke as a Determinant of Human Behavior in Fire Situation,* University of Maryland, College Park (1977).

14. B. Latane and J.M. Darley, "Group Inhibition of Bystander Intervention in Emergencies," *Journal of Personality Psychology,* 10, 3, pp. 215–221 (1968).

15. B.M. Levin, "Design as a Function of Response to Fire Cues," in *Proceedings of American Institute of Architects "Research and Design 85: Architectural Applications of Design and Technology Research,"* Los Angeles (1985).

16. F. Ozel, *Way Finding and Route Selection in Fires,* New Jersey Institute of Technology, Newark, NJ (1986).

17. S. Gwynne and E.R. Galea, "A Review of the Methodologies and Critical Appraisal of Computer Models Used in the Simulation of Evacuation from the Built Environment," Research Report, Society of Fire Protection Engineers, (undated).

18. F. Ozel, "Simulation Modeling of Human Behaviour in Buildings," *Simulation,* pp. 377–384 (1992).

19. J.N. Fraser-Mitchell, "An Object-Oriented Simulation (CRISPII) for Fire Risk Assessment," in *Proceedings of the Fourth International Symposium of Fire Safety Science* (T. Kashiwagi, ed.), pp. 793–804 (1994).

20. H.A. Donegan, A.J. Pollock, and I.R. Taylor, "Egress Complexity of a Building," in *Proceedings of Fourth International Symposium on Fire Safety Science* (T. Kashiwagi, ed.), pp. 601–612 (1994).

21. N. Ketchell, S.S. Cole, and D.M. Webber, "The EGRESS Code for Human Movement and Behaviour in Emergency Evacuation," *Engineering for Crowd Safety* (R.A. Smith and J.F. Dickie, eds.), Elsevier, London, pp. 361–370 (1994).

22. E. Reisser-Weston, "Simulating Human Behaviour in Emergency Situations," *RINA International Conference of Escape, Fire, and Rescue* (1996).

23. T.M. Kisko and R.L. Francis, "EVACNET+: A Computer Program to Determine Optimal Evacuation Plans," *Fire Safety Journal,* 9, pp. 211–220, (1985).

24. L.S. Poon and V.R. Beck, "EVACSIM: Simulation Model of Occupants with Behavioural Attributes in Emergency Evacuation of High Rise Buildings," in *Proceedings of Fourth International Symposium on Fire Safety Science* (T. Kashiwagi, ed.), pp. 681–692 (1994).

25. R.F. Fahy, "An Evacuation Model for High Rise Buildings" in *Proceedings of the Third International Symposium on Fire Safety Science* (G. Cox and B. Langford, eds.), Elsevier, London, pp. 815–823 (1991).

26. B. Levin, "EXITT: A Simulation Model of Occupant Decisions and Actions in Residential Fires," in *Proceedings of the Second International Symposium on Fire Safety Science* (T. Wakamatsu, Y. Hasemi, A. Seizawa, P. Seeger, P. Pagni, and C. Grant, eds.), pp. 561–570 (1989).

27. M. Owen, E.R. Galea, and P.J. Lawrence, "The Exodus Evacuation Model Applied to Building Evacuation Scenarios," *J. of Fire Protection Engr.* 8, 2, pp. 65–86 (1996).

28. E.R. Galea and J.M.P. Galparsoro, "EXODUS: An Evacuation Model for Mass Transport Vehicles," *Fire Safety Journal,* 22, pp. 341–366 (1994).

29. S. Okasaki and S. Matsushita, "A Study of Simulation Model for Pedestrian Movement with Evacuation and Queuing," *Engineering for Crowd Safety* (R.A. Smith and J.F. Dickie, eds.), Elsevier, London, pp. 271–280 (1993).

30. J. Barton and J. Leather, "Paxport: Passenger and Crowd Simulation," *Passenger Terminal* 95, pp. 71–77 (1995).

31. P. Thompson and E. Marchant, "A Computer Model for the Evacuation of Large Building Populations," Fire Safety Journal, 24, pp. 131–148 (1995).

32. P.A. Thompson and E.W. Marchant, "Simulex; Developing New Computing Modelling Techniques For Evaluation," Proceedings of the Fourth International Symposium on Fire Safety Science, (T. Kashiwagi, ed.), International Association for Fire Safety Science, pp. 613–624 (1994).

33. K. Takahashi, T. Tanaka, and S. Kose, "An Evacuation Model for Use in Fire Safety Design of Buildings," in *Proceedings of the Second International Symposium on Fire Safety Science,* (T. Wakamatsu, Y. Hasemi, A. Seizawa, P. Seeger, P. Pagni, and C. Grant, eds.), Hemisphere, pp. 551–560 (1989).

34. G.K. Still, "New Computer System Can Predict Human Response to Building Fires," *Fire,* 84, pp. 40–41 (1993).

35. G.K. Still, "Simulating Egress Using Virtual Reality: A Perspective View of Simulation and Design," *IMAS 94, Fire Safety on Ships* (1994).

36. V.O. Shestopal and S.J. Grubits, "Evacuation Model for Merging Traffic Flows in Multi-Room and Multi-Storey Buildings," in P*roceedings of the Fourth International Symposium on Fire Safety Science,* (T. Kashiwagi, ed.), pp. 625–632, (1994).

37. H.E. Nelson, *FPETOOL: Fire Protection Tools for Hazard Estimation,* NISTIR 4380, National Institute of Standards and Technology, Gaithersburg, MD (1990).

CHAPTER 15

Stochastic Models
of Fire Growth

G. Ramachandran

Introduction

Apart from changes in environmental conditions, such as wind velocity and direction, humidity, and temperature, the spread of fire in a building is governed by physical and chemical processes evolved from a variety of burning materials arranged in different ways. Multiple interactions among these processes at different times during fire growth cause uncertainties in the pattern of fire development. Although different patterns of fire development can be simulated by varying the input values to the parameters of a deterministic model, there is a need to determine the uncertainty (probability) with which each pattern is likely to occur in a real fire in any type of building considered. The likely pattern of fire spread can only be predicted within limits of confidence expressed in probabilistic terms.

Nondeterministic models[1] (or indeterministic models as defined by Kanury[2]), rather than deterministic techniques, offer rational methods of evaluating the uncertainties in the pattern of fire growth and are of two types: (1) probabilistic and (2) stochastic. The first type generally deals with a final outcome, such as area damaged, financial loss, or fire severity, and is considered as a continuous random variable reaching various levels in a fire according to a probability distribution.[3] Large values of the variable follow an extreme value distribution. (See Section 5, Chapter 8.) A semi-probabilistic approach is provided by a fault tree[4] in which the probability of occurrence of a top event (e.g., fire spreading beyond the room of origin) is estimated by assigning discrete (not continuous) probabilities

to sub-events leading to the top event. Models of the first type (i.e., probability distributions and fault trees) do not consider in detail the underlying physical processes and their variation over the duration (time) of fire growth. Such "static" models can provide sufficient tools for fire protection and insurance problems concerned with "collective risk" in a group of buildings.

Stochastic models constitute the subject matter of this chapter, and may be regarded as "dynamic," since they are capable of predicting the course of fire development in a particular building. In these models, the various states, realms, or phases occurring sequentially in space and time during fire growth are specified together with the associated probability distributions. Depending on the nature of these distributions, a fire stays in each state for a random length of time and moves randomly from state to state. The sojourn and transition probabilities may be regarded as "noise" terms superimposed over a deterministic pattern of fire growth.

After describing the basic features of stochastic modeling of fire spread, two types of stochastic models are discussed in detail: (1) Markov chains and (2) networks. Attention is also drawn to the application of other stochastic models, such as random walk, diffusion processes, percolation theory, epidemic models, and branching processes. The next-to-last section in this chapter discusses briefly a new type of stochastic model based on the "stochastic differential equation" which is currently being developed in Australia.

The models discussed in this chapter mainly relate to the growth of fire and not to the spread of smoke or other combustion products.

Dr. G. Ramachandran retired in November 1988 as head of the Operations Research Section at the Fire Research Station, United Kingdom. Since then he has been practicing as a consultant in risk evaluation and insurance. He is a visiting professor at the Universities of Manchester, and Leeds. His research has focused on statistical and economic problems in fire protection and actuarial techniques in fire insurance. In October 1998 he published a book on the economics of fire protection.

Basic Features

Probability Distributions

Consider the burning of a particular object in a room as a random (stochastic) process, with $Q(t)$ denoting the

probability that the object is still burning at time t. In a simple model the process may be assumed to be Poisson,[5] so that $Q(t)$ has the exponential form

$$Q(t) = \exp(-\mu t) \tag{1}$$

In this model the probability of extinction of fire during the short period $(t, t + \partial t)$ denoted by $\mu(t)$ has been assumed to have the constant value μ independent of t. The function $Q(t)$ can also be interpreted as the probability that the duration of burning of the object considered is greater than t. Then, the (cumulative) probability distribution function

$$F(t) = 1 - Q(t) \tag{2}$$

is the probability that the duration of burning is less than or equal to t. The parameter μ is the "instantaneous probability" of extinction of fire, whereas $\lambda(= 1 - \mu)$ is the "instantaneous probability" of fire surviving.

The value of μ will vary depending on whether it is a free-burning fire or a fire extinguished by fire fighting (e.g., by fire brigade or sprinklers). The value of μ for any object burning under specified conditions can be estimated by carrying out replicated extinction experiments with the object. If $\bar{t}$ is the mean (average) duration of burning of the object

$$\mu = 1/\bar{t} \tag{3}$$

according to the properties of an exponential probability distribution. This distribution was implied in Kida's probabilistic analysis of extinction experiments.[6]

Spread to Another Object

In a simple model, as discussed earlier, it can be assumed that a fire involving one object spreads to another object if it survives (i.e., not extinguished) with the probability λ.

$$\lambda + \mu = 1 \tag{4}$$

The model can be expanded to include an (instantaneous) probability w to denote the event of fire not spreading, even though it is not extinguished, that is, the fire continues to burn without spreading. In this case[5]

$$\lambda + \mu + w = 1 \tag{5}$$

and, following the derivation of Equation 1,

$$Q_1(t) = \exp[-(\lambda + \mu)t]$$
$$= \exp(-t + wt) \tag{6}$$

where $Q_1(t)$ is the probability that the fire is burning at time t without spreading. The duration of burning in this case follows an exponential probability distribution with mean duration given by the reciprocal of $(\lambda + \mu)$ or of $(1 - w)$.

The length of time a fire involving an object burns affects future fire spread to another object: heat output (fire severity) increases with time. Equation 5 can, therefore, be modified such that, during a short time interval immediately after time t,

$$\lambda(t) + \mu(t) + w(t) = 1 \tag{7}$$

The instantaneous probabilities $\lambda(t)$, $\mu(t)$, and $w(t)$ are functions of the continuous random variable t. However, in practical problems, one can consider t in minutes and one minute as a short time interval such that the probabilities are denoted by $\lambda(i)$, $\mu(i)$, and $w(i)$ with $i = 1, 2, 3, \ldots$. The probability $w(i)$ applies to a single minute and, hence, it is likely to be small. One can, therefore, write

$$Q_1^1(t + 1) = w(1) \cdot w(2) \cdot \cdots \cdot w(t) \tag{8}$$

to denote the probability of fire burning during the time period $(t + 1)$ without spreading. Equation 8 follows from Equation 6. If $w(i)$ is a constant w as in Equation 6, it may be seen that

$$Q_1^1(t) = w^t \tag{9}$$

General Model

The probability distribution for duration of burning can have other forms, such as uniform and log-normal, although an exponential distribution has been postulated for the sake of simplicity. Following Ramachandran[5] and Aoki,[7] the following probabilities can be defined in the general case for the fire involving the object ignited first:

$q_1(t + 1) =$ probability of burning at the beginning of the $(t + 1)$th period or end of the tth period without spreading before that period

$P_1(t + 1) =$ cumulative probability of becoming extinguished before the end of the $(t + 1)$th period

$S_1(t + 1) =$ cumulative probability of spreading before the end of the $(t + 1)$th period

With subscript 1 denoting the object ignited first, the following equations are easily derived:

$$q_1(t + 1) = q_1(t) \cdot w_1(t) = \prod_{r=1}^{t} w_1(r)$$

as in Equation 8, since $q_1(1) = 1$.

$$P_1(t + 1) = \sum_{r=1}^{t+1} q_1(r) \cdot \mu_1(r)$$

$$S_1(t + 1) = \sum_{r=1}^{t+1} q_1(r) \cdot \lambda_1(r)$$

The parameters $\lambda_1(r)$, $\mu_1(r)$, and $w_1(r)$ are probabilities of spreading, becoming extinguished, and burning without spreading during the rth period.

The following equations with similar definitions can be derived for the second object to which fire can spread from the object first ignited. (The subscript 2 has been used for the second object.)

$$q_2(t + 1) = q_2(t) \cdot w_2(t) + q_1(t) \cdot \lambda_1(t), \; q_2(1) = 0$$

$$P_2(t + 1) = \sum_{r=2}^{t+1} q_2(r) \cdot \mu_2(r)$$

$$S_2(t + 1) = \sum_{r=2}^{t+1} q_2(r) \cdot \lambda_2(r)$$

The probabilities $q_2(t + 1)$, $P_2(t + 1)$, $S_2(t + 1)$ and their associated parameters $w_2(t)$, $\lambda_2(t)$, and $\mu_2(t)$ pertain to the second object and are "conditional," given that the fire has spread to the second object.

In the first of the equations mentioned above it has been assumed that the second object starts burning in the second minute after the ignition of the first object in the first minute. The probability of this event is likely to be low such that $q_2(2)$ has a small value. The time of occurrence of sustained or established burning of the second object depends upon the incubation or latent period beyond which the fire involving the first object becomes capable of spreading to the second object.[8] This time and the spread probability $\lambda_1(r)$ also depend upon the distance between the two objects.[8] Radiation of heat to an object generally decreases in inverse proportion to the square of the distance of the object from the burning object. Fire spread may not occur if the unignited object is located beyond a "critical distance" from the burning object.[9]

As r varies, $q_1(r)$ gives rise to a discrete or continuous probability distribution for the object first ignited. This distribution can be ascertained by carrying out experiments with the two objects considered by varying the distance between them. In the continuous case, if the instantaneous probabilities are assumed as constants, the average duration of burning of the first object before spreading to the second object is an estimate of $(1/1 - w_1)$, assuming an exponential distribution. Applying this result to the discrete case with constant probabilities, for any specified distance between the two objects,

$$q_1(t + 1) = w_1^t$$

as in Equation 9. An exponential distribution with constant probabilities need not be assumed if the mathematical form of $w_1(t)$ and its variation with the distance between the two objects can be established from an analysis of the experimental data. These data would also provide an estimate of $\lambda_1(t)$ for any distance between the object ignited first and the second object. The value of $\mu_1(t)$ can then be obtained from the equation

$$\mu_1(t) = 1 - \lambda_1(t) - w_1(t)$$

It can be verified that, since $q_1(1) = 1$,

$$P_1(t + 1) + S_1(t + 1) = \sum_{r=1}^{t+1} q_1(r)[\mu_1(r) + \lambda_1(r)]$$

$$= \sum_{r=1}^{t+1} q_1(r)[1 - w_1(r)]$$

$$= \sum_{r=1}^{t+1} [q_1(r) - q_1(r + 1)]$$

$$= 1 - q_1(t + 2)$$

As t increases, $q_1(t)$ will decrease toward zero such that the sum of the two cumulative probabilities will tend to unity. Hence, as one would have expected, the probability of burning without spreading will tend to zero with the passage of time, and the fire involving the first object would have either been extinguished or spread to the second object.

In the language of stochastic modeling, the spread probability, $\lambda_1(r)$, is the transition probability at time r, and may be redefined as $\lambda_{12}(r)$ to denote the spread from the object first ignited to the second object. Other objects in a room may be considered as the first or second object such that, in the general case, $\lambda_{ij}(r)$ is the probability of spreading from the ith object to the jth object at time r. Based upon the distances between them, the objects can be arranged in order in a diagram to analyze the sequential spread of fire from object to object at any time r. (See Figure 3-15.1.) This simple analysis may be sufficient for all practical purposes, although a fire from one object can spread to another object directly or indirectly through the ignition of another object.

As t increases, $q_i(t)$ will tend to zero and the cumulative probability of extinguishment, $P_i(t + 1)$, to a limiting value E_i. This value, E_i, denotes the probability of fire being extinguished ultimately, with the spread limited to the ith object. Correspondingly, the cumulative probability of spreading, $S_i(t + 1)$, will tend to $(1 - E_i)$. The following equations may be specified in the limiting case:

$$\begin{aligned} E_1 &= \mu_1 & \lambda_1 &= 1 - \mu_1 \\ E_2 &= \lambda_1 \cdot \mu_2 & \lambda_2 &= 1 - \mu_2 \\ E_3 &= \lambda_1 \cdot \lambda_2 \cdot \mu_3 & \lambda_3 &= 1 - \mu_3 \end{aligned}$$

and so on, such that, in general terms

$$E_i = \lambda_1 \cdot \lambda_2 \ldots \lambda_{i-1} \cdot \mu_i; \quad \lambda_i = 1 - \mu_i \tag{10}$$

$$P_i = \sum_{j=1}^{i} E_j \tag{11}$$

The equations aforementioned provide values for μ_i for $i = 1, 2, 3 \ldots$ which may be regarded as the limiting probability of extinguishment for the ith object, given (conditional) that the fire has spread to this object. The parameter λ_i is the limiting and conditional probability of spread beyond the ith object.

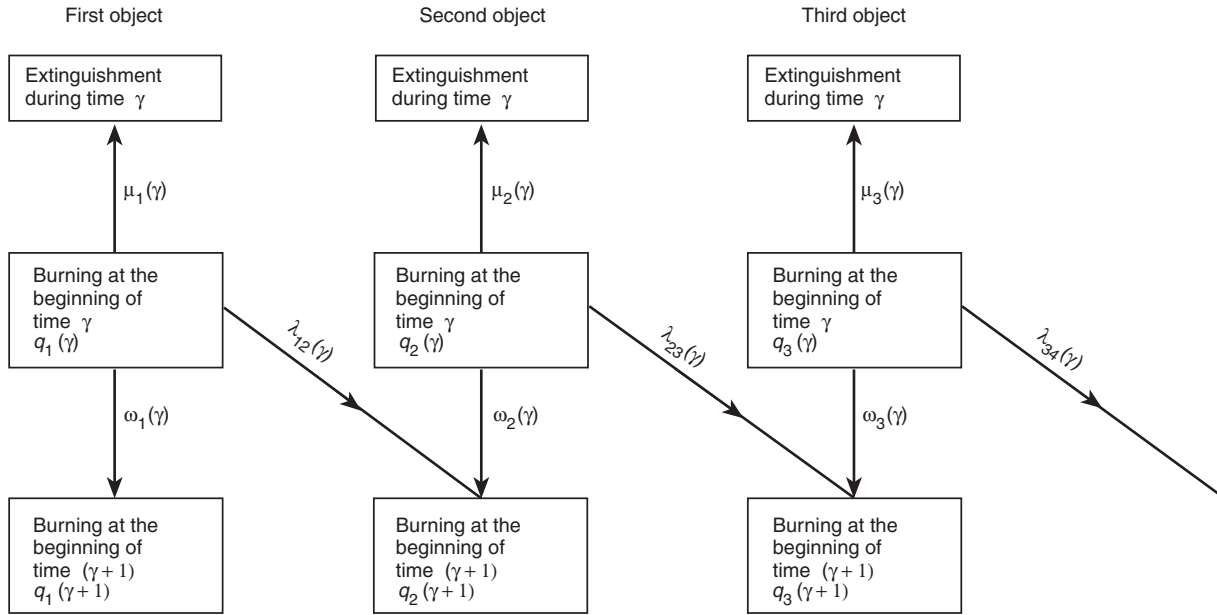The model mentioned above for objects in the room of fire origin can be extended to include structural barriers

Figure 3-15.1. *Probability diagram for spread of fire from object to object at time γ.*

and objects in corridors and other rooms on the same floor or different floors of a building. This procedure involves complex calculations, since a fire in a room can spread to an adjoining room in the same or upper floor; a fire can also spread through several paths. The problem of fire spread throughout a building can be simplified to some extent by applying network models, which are discussed later.

Markov Model

Mathematical Representation

A considerable amount of statistical and experimental data are needed for applying the model for fire spread from object to object. For practical purposes it may be sufficient to consider fire spreading through a number of spatial modules,[10] phases,[11] or realms.[12] These stages of fire growth can generally be defined as *states* such that fire spreads, moves, or makes a transition from state to state.

The movement of fire from state to state is governed by a *transition probability,* which is a function of time since the start of the fire. The fire also spends a certain length of time in each state before making the transition; this duration follows a temporal probability distribution. The state occupied by fire at any moment in time is governed by transition probabilities and temporal probability distributions. Represented mathematically, if the fire is in state a_i at the nth minute, it can be in state a_j at the $(n + 1)^{\text{th}}$ minute, according to the transition probability $\lambda_{ij}(n)$. The transition probabilities are most conveniently handled in matrix form. One may write, dropping (n) for convenience, with m states,

$$P = \begin{bmatrix} \lambda_{11} & \lambda_{12} & \cdot & \cdot & \lambda_{1m} \\ \lambda_{21} & \lambda_{22} & \cdot & \cdot & \lambda_{2m} \\ \cdot & \cdot & \cdot & \cdot & \cdot \\ \cdot & \cdot & \cdot & \cdot & \cdot \\ \lambda_{m1} & \lambda_{m2} & \cdot & \cdot & \lambda_{mm} \end{bmatrix}$$

where

$$\sum_{j=1}^{m} \lambda_{ij} = 1 \qquad i = 1, 2, \ldots, m$$

The probability distribution of the system at time n can be expressed as the vector

$$\mathbf{P} = (q_1 \, q_2 \, q_3 \ldots q_m)$$

where q_i is the probability of the fire burning in the ith state at time n. Since a fire can be in one of the m states at a given time

$$\sum_{i=1}^{m} q_i = 1$$

The mth state may denote the state of fire having been extinguished if such a state is included in the model considered. The vector given by the product $p \cdot \mathbf{P}$ expresses the probabilities of burning in different states one transition (minute) later.

As an example, consider a model of fire growth in a room in which the ith state represents i objects burning. Suppose, with $m = 4$ and no extinguishment, the process

stops with the occurrence of flashover when all four objects are ignited. There is no recession in growth and, hence, there is no transition to a lower state from a higher state. With these assumptions, let the transition matrix be

$$P = \begin{bmatrix} 0.4 & 0.3 & 0.2 & 0.1 \\ 0 & 0.5 & 0.3 & 0.2 \\ 0 & 0 & 0.6 & 0.4 \\ 0 & 0 & 0 & 1 \end{bmatrix}$$

If, at time n, the probabilities of fire burning in different states is given by

$$p_n = (0.1 \quad 0.2 \quad 0.3 \quad 0.4)$$

it can be seen by performing the matrix multiplication, that the probability of fire burning in different states at time $(n + 1)$ is given by

$$p_{n+1} = (0.04 \quad 0.13 \quad 0.26 \quad 0.57)$$

Hence, at time $(n + 1)$, the probability of the fire being in the third state, for example, is 0.26, and the probability of flashover (4th state) is 0.57.

Markov Chains

Markov chains are used for repetitive situations in which there is a set of probabilities that define the likelihood of transition from one state to another. A chain comprises a sequence of such transitions. In a Markov chain, the transition probabilities satisfy the following properties:[4]

1. Each state belongs to a finite set of all possible states.
2. The characteristics of any state do not depend upon any other previous state.
3. For each pair of states (i, j) there is a probability λ_{ij} that state j occurs immediately after state i occurs.

The transition probabilities can be specified in a matrix form P as discussed previously, with the aid of a hypothetical example. Berlin[4] and Watts[10] have illustrated the use of this matrix by modeling a "random walk" among five adjacent spaces.

Markov chains may possess a number of special characteristics, one of which is called an *absorbing state.* The system remains in an absorbing state once it enters this state. A fire burning out (self-termination) and a fire getting extinguished by an extinguishing agent are examples of absorbing states. State i is an absorbing state if row i of the transition matrix has a value of $\lambda_{ij} = 1$ and all other values in the row are zero.

Markov Process

The next step is to consider a slightly more complex model called the *Markov process,* a stochastic or random process where the probability of occurrence of some future state of the system, given its present state, is not altered by information concerning past states. That is, the

history of the process has no influence on its future. This lack of a historical influence is often referred to as a *memoryless* or *Markovian* property of a process.

In a Markov process with stationary transition probabilities, the value of $\lambda_{ij}(n)$ is a constant independent of the time variable n. Following this process Berlin[12] estimated stationary transition probabilities for six realms (states) for residential occupancies: (I) nonfire state, (II) sustained burning, (III) vigorous burning, (IV) interactive burning, (V) remote burning, and (VI) full room involvement. These realms were defined by critical events, such as heat release rate, flame height, and upper room gas temperature. Development of fire over time was considered as a "random walk" through these realms.

Based on data from over a hundred full-scale fire tests, Berlin[12] calculated transition probabilities as in Table 3-15.1. The information in this table indicates that, when a fire is in Realm III, there is a 75 percent chance of growth to Realm IV, and a 25 percent chance of recession to Realm II. Figure 3-15.2 is the transition diagram

Table 3-15.1 *Transition Descriptors for a Typical Room in a Residential Occupancy*

Fire Type: Smoldering fire in a couch with cotton cushions.

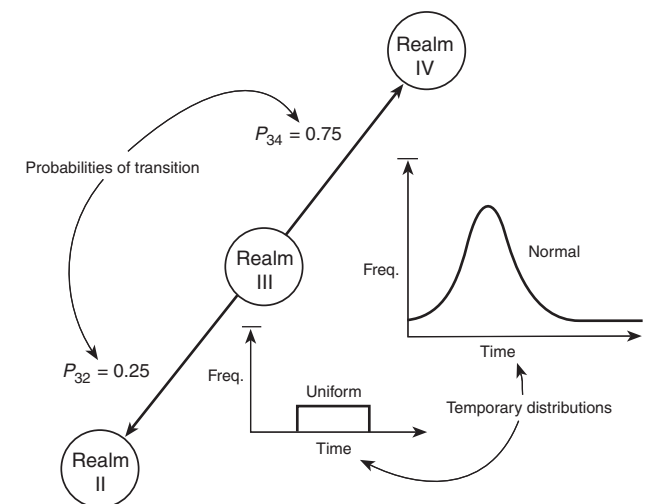| Realm Transition		Transition Probability	Temporal Distribution		
From	To		Type	Mean	Standard Deviation
II	I	0.33	Uniform	2.0	5.0
II	III	0.67	Log-normal	8.45	0.78
III	II	0.25	Uniform	1.0	2.0
III	IV	0.75	Normal	5.55	3.22
IV	III	0.25	Uniform	1.5	9.0
IV	V	0.75	Uniform	0.5	3.5
V	IV	0.08	Uniform	0.6	6.0
V	VI	0.92	Log-normal	5.18	4.18

Figure 3-15.2. *Realm transition descriptors.*

defined by the transition probabilities in Table 3-15.1. Realm I, no fire, is an absorbing state, since all fires eventually terminate in this state. The process also ends when Realm VI (full room involvement) is reached; for this reason, this state also is an absorbing state. Berlin[12] used uniform, normal, and log-normal distributions to describe temporal probability distributions for the different states.

Among many questions asked about fire development using the Markov model is what maximum extent of fire growth represents the most extreme condition. The portion of fires that does not grow beyond Realm II is the probability (0.33) of transition from Realm II to I. If M_3 is the long-run (limiting) probability of fire reaching Realm III, but not growing beyond, then[12]

$$M_3 = \frac{\lambda_{21} + \lambda_{23} \cdot \lambda_{31}}{1 - \lambda_{23} \cdot \lambda_{32}} - \lambda_{21} \qquad (12)$$

Using the figures in Table 3-15.1 and noting that $\lambda_{31} = 0$, it may be seen that $M_3 = 0.07$. Beyond Realm III is more difficult, as described by Berlin.[12] Probabilities of maximum extent of flame development as estimated by Berlin are given in Table 3-15.2. Berlin has also discussed other fire effects, such as probability of self-termination and distribution of fire intensity.

One of the major weaknesses of the Markov model regards the "stationary" nature of the transition probabilities. It is assumed that these probabilities remain unchanged regardless of the number of transitions representing the passage of time. The length of time a fire burns in a given state affects future fire spread. For example, the probability of a wall burn-through increases with fire severity which is a function of time. The time spent by fire in a particular state may also depend on how that state was reached (i.e., whether the fire was growing or receding). Some fires may grow quickly and some grow slowly, depending on high or low heat release. In a Markov model with stationary transition probabilities no distinction is made between a growing fire and a dying fire.

Berlin[12] has estimated that 99 percent of all fires will terminate within twelve transitions. This result is based on the assumption of stationary transition probabilities that may be nearly true for a few fluctuations between the same realms where different materials would be contributing to the burning process. However, the fire will eventually consume all fuels, in which case the probabilities of termination from all realms will be equal to one. Therefore, Berlin's approach represents a worst-case analysis.

Table 3-15.2 *Maximum Extent of Flame Development*

Maximum Flame Extent	Probability of Flame Extent
Realm II	0.33
Realm III	0.07
Realm IV	0.02
Realm V	0.58

State Transition Model

According to Berlin's Markov model, a fire in a particular realm can either grow to a higher realm or recede to a lower realm. There is no transition to the nonfire (absorbing) state (Realm I) from any realm higher than Realm II, except Realm VI (full room involvement) which is also an absorbing state. Receding to a lower state may be true to some extent when describing fire growth in terms of flame spread, but such an assumption is not possible in the case of spatial spread of fire in which, as discussed previously, fire spreads sequentially from one object to another. According to this model, if fire spreads to an object it cannot spread backwards to the object from which it spread. The fire involving an object either spreads forward to other objects, gets extinguished, or stays with the object without spreading.

Complex computational procedures would be involved in a stochastic model for fire spread from object to object in a room or to different rooms. Hence, consistent with the fire statistics available, particularly in the United Kingdom and United States, a simplified model based on the following three main states can be considered for fire development in a room:

S_1 Fire confined to the object first ignited

S_2 Fire spreading beyond the object first ignited but confined to the contents of the room

S_3 Fire spreading beyond room of origin but confined to the building

A fourth state may be added to denote extinguishment or burning out (self-termination) of fire; this is an absorbing state, since a fire process cannot leave this state after entering it. The third state, S_3, is also an absorbing state, since a spreading fire will eventually terminate within the building of origin; spreading beyond the building is not considered.

The three states ($i = 1, 2, 3$) mentioned above generate a state transition model, distinct from Berlin's Markov model. This model was used by Ramachandran[5] for evaluating the transition (spread) probabilities $\lambda_i(t)$ and the probabilities $\mu_i(t)$ for extinguishment or transition to the fourth state. The value of $\lambda_3(t)$ was taken as zero, since fire spread beyond the building was not considered. The probability of burning in a state without spreading was also considered with the aid of the parameter $w_i(t)$ [$= 1 - \lambda_i(t) - \mu_i(t)$]. The duration of burning was divided into subperiods, each of a fixed length of five minutes.

Statistics furnished by fire brigades in the United Kingdom related to fires that were extinguished during each time period since ignition. Hence, Ramachandran[5] used the extreme value technique, with some assumptions, to estimate the number of fires that were burning in a particular stage at the beginning of each subperiod. With the aid of these estimates and the actual numbers of fires that were extinguished, approximate values were obtained for the extinguishment and spread probabilities (as functions of time) and probability distributions of duration of burning in each state. The equations given previously for the general model were utilized for this purpose. Four materials ignited first in the bedroom of a

dwelling were considered for illustrating the application. Tables 3-15.3 and 3-15.4 and Figures 3-15.3 and 3-15.4 are examples extracted from this study. Aoki[7] described fire growth with similar states based on the spatial extent of spread; his analysis was similar to that of Ramachandran[5]

Table 3-15.3   *Bedroom Bedding (Probabilities)*

Period (t) (min)	First State $\mu(t)$	First State $\lambda(t)$	Second State $\mu(t)$	Second State $\lambda(t)$	Third State $\mu(t)$
1–5	0.0055	0.0745	—	—	—
6–10	0.0385	0.1170	0.7026	0.1747	—
11–15	0.0631	0.0602	0.8507	0	0.4894
16–20	0.0407	0.0780	0.8319	0	0.3750
21–25	0.0406	0.1887	0.7576	0.1688	0.8667
26–30	0.1071	0.1730	0.8474	0.0329	0.4878
31–35	0.0723	0.1131	0.8206	0.0676	0.7143
36–40	0.0449	0.1071	0.8218	0.0172	0.5455
41–45	0.0205	0.0758	0.7293	0.2632	0.8333
46–50	0.0160	0.1451	0.8750	0	0.4737
51–55	0.0476	0.2508	0.7350	0.1282	0.5500
56–60	0.0860	0.2308	0.7816	0.0862	0.5417
61–65	0.0861	0.2417	0.7840	0.0800	0.5769
66–70	0.0739	0.1478	0.7444	0.1556	0.6190
71–75	0.0316	0.1519	0.8205	0.1795	0.5455
76–80	0.0233	0.1860	0.6250	0.0833	0.6316
81–85	0.0294	0	0.6774	0	0.4286
86–90	0.0101	0.4950	0.2500	0.3182	0.7500
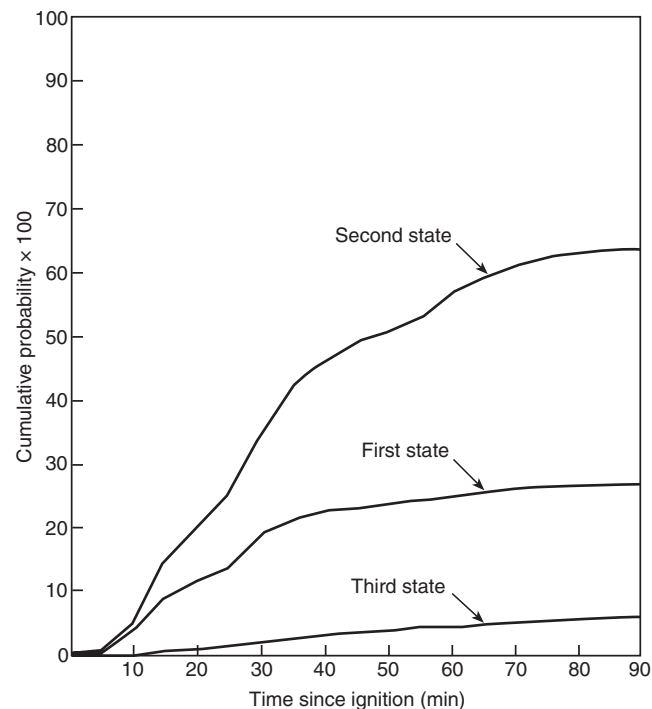
Figure 3-15.3. *Bedding—cumulative probability of extinguishment.*

Table 3-15.4   *Bedroom Bedding (Average Times)*

	First State	Second State	Third State
Duration of burning in the state (min)	24.5	5.9	8.5
Extinguishment time in the state (min)	26.2	32.2	44.1
Time for spreading beyond the state (min)	27.9	38.9	*a*

[a]Spread beyond the third state (building) is not considered.
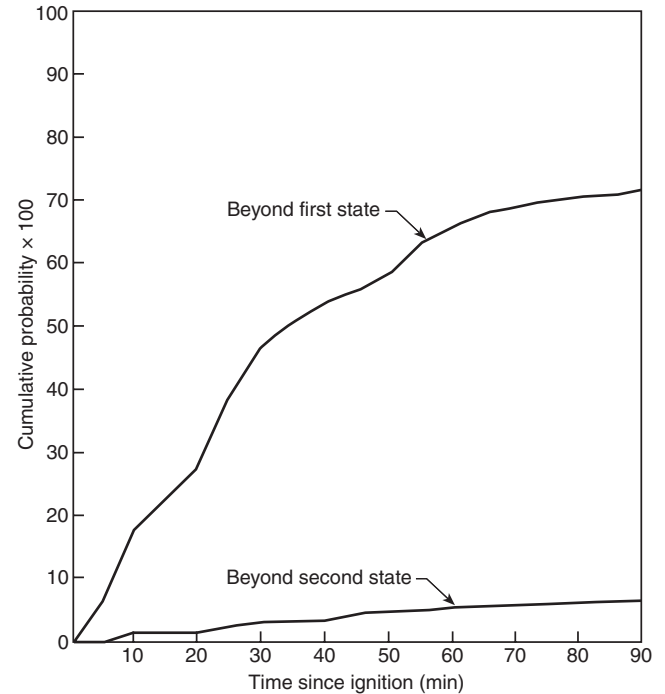
Figure 3-15.4. *Bedding—cumulative probability of spreading.*

and Morishita[11] and considered eight phases of spatial spread of fire, including spread to the ceiling.

In a later study, Ramachandran[3] added another state between S_2 and S_3 to denote the event of fire involving the structural barriers of a room, assumed to occur after fire has spread beyond S_1 and S_2 but still confined to the room. This intermediate state was considered as generally consecutive to S_2, although a fire can spread directly from S_1 and involve the structural boundaries. Fire statistics available in the United Kingdom permit the incorporation of this additional state into a state transition model. As shown in Figure 3-15.5, only the limiting probabilities λ_i and μ_i specified in Equation 10 were estimated.

Fire statistics provided estimates for $E_i (i = 1$ to $4)$, the proportion of fires extinguished in the ith state. The condition that

$$\sum_{j=1}^{4} E_j = 1$$

Sprinklered | States | Nonsprinklered

Figure 3-15.5. *Probability tree—textile industry.*

E_1 = Probability of confinement to items first ignited = μ_1

E_2 = Probability of spreading beyond item first ignited but confinement to contents of room of fire origin = $\lambda_1 \cdot \mu_2$

E_3 = Probability of spreading beyond item first ignited and other contents but confinement to room of fire origin and involvement of structure = $\lambda_1 \cdot \lambda_2 \cdot \mu_3$

E_4 = Probability of spreading beyond room of fire origin but confinement in the building = $\lambda_1 \cdot \lambda_2 \cdot \lambda_3 \cdot \mu_4$ ($\mu_4 = 1$)

follows from the assumption that $\mu_4 = 1$ and, hence, $\lambda_4 = 0$; fire spread beyond the building of origin was not considered.

The parameter μ_1 is the same as λ_{21} in Berlin's model in which the first state (Realm I) is the nonfire state and the second state and above are fire states (Realms II through VI). Also λ_1 is the same as Berlin's λ_{23}, and μ_2 corresponds to λ_{31}. With these changes and the assumption that there is no recession of fire growth ($\lambda_{32} = 0$), the value of M_3 in Equation 12 is equal to

$$E_2 = \lambda_1 \cdot \mu_2$$

as derived from Equation 10.

In Figure 3-15.5, the product $\lambda_1 \cdot \lambda_2 (= E_3 + E_4)$ may be regarded as the probability of flashover, and λ_3 as the probability of failure of the structural boundaries of the room.[13] For the following reasons fire statistics do not provide a valid estimate of λ_3. Figures for the number of fires that spread beyond the room of origin include: (1) fires that spread by destruction of barrier elements (wall, floor, ceiling) as well as (2) those that spread by convection through a door or window left open or through some other opening. In the latter case, the barrier elements would still be structurally sound. A "room," as recorded in fire brigade reports, is not necessarily a "fire compartment." Using a probabilistic model[13] or other methods, the value of λ_3 for any compartment of given fire resistance can be estimated and multiplied by the probability of flashover to provide an estimate of probability of spread beyond the compartment of origin.

The probabilities provided by a stochastic model can be regarded as "noise" terms superimposed over a deterministic trend in fire growth over space and time. The trend can be predicted by a deterministic model, such as an exponential model.[3] Table 3-15.5 is an example based on such a model and fire incidence statistics.[13] The estimates of time in this table have been measured from the time of occurrence of established burning at the end of the first state, denoting confinement of fire to object first ignited. The percentage figures in Table 3-15.5 have provided the probabilities for constructing the probability tree in Figure 3-15.5.

To represent the interaction between human behavior and fire dynamics, Beck[14] developed a series of stochastic

Table 3-15.5 *Textile Industry, U.K., Extent of Fire Spread and Average Area Damaged*

Extent of Spread	Sprinklered[a]			Nonsprinklered		
	Average Area Damaged (m²)	Percentage of Fires	Time (min)	Average Area Damaged (m²)	Percentage of Fires	Time (min)
Confined to item first ignited	4.43	72	0	4.43	49	0
Spread beyond item but confined to room of fire origin						
Contents only	11.82	19	8.4	15.04	23	6.2
Structure involved	75.07	7	24.2	197.41	21	19.4
Spread beyond room	1000.00	2		2000.00	7	
Average	30.69	100		187.08	100	

[a]System operated

state transition models and interrelated deterministic models. His sequential fire growth model was based on the six realms defined by Berlin,[12] with the remote burning state denoting flashover. His results, reproduced in Table 3-15.6, are applicable to office buildings. P_I in this table is the same as E_i in Equation 10. Adopting a different notation and starting with $P_1 = \mu_1$, the conditional probabilities of extinguishment, μ_i, and conditional probabilities of spread, λ_i $(= 1 - \mu_i)$, were calculated according to Equation 10. The probability of a fully developed fire, given a fire defined by P_{FDF}/F, is given by the product $\lambda_1 \cdot \lambda_2 \cdot \lambda_3 \cdot \lambda_4$. The probability of spread beyond the compartment of fire origin, P_{VI}, is given by the product of P_{FDF}/F and λ_5 or by $\lambda_1 \cdot \lambda_2 \cdot \lambda_3 \cdot \lambda_4 \cdot \lambda_5$.

Beard[15] proposed a state transition model by considering a number of "critical events" with directional characteristics that a fire may pass through and the times between critical events. For example, critical heat event CHE2U referred to "fire passing through 2 kW on the way up," whereas CHE2D referred to "fire passing through 2 kW on the way down." The time between two critical events was assumed to have a temporal probability distribution independent of the time between earlier critical events. A particular succession of critical events formed a chain; specific times between critical events were referred to as a *sequence* within the chain. Based on assumed forms for transition probabilities and temporal probability distributions, Monte Carlo simulation was employed to generate randomly particular chains and sequences. A generated sequence to smoke and toxic gases was related to the corresponding sequence for the burning rate. Based on the concentration of carbon monoxide, Beard employed the concept of "fraction of fatality," with fatality resulting at a unit value for this fraction. He applied the model to a particular case involving flaming ignition on a bed in a hospital ward. He concluded that there would be a very large (greater than 80 percent) likelihood of having multiple fatalities if a fire exceeds 50 kW. One of the several assumptions used by him was that the fire did not spread beyond the ward.

Williamson[16] introduced a state transition model for analyzing and reporting the results of fire growth experiments performed under conditions resembling actual fire conditions. Three preflashover states were defined as follows:

J The period of time from the beginning of the experiment to ignition of the specimen

K The period of time from ignition of the specimen until flames touch the ceiling

L The period of time from when the flames first touch the ceiling until full involvement (flashover) occurs

Histograms and cumulative distribution functions of the state durations provided a graphical representation of fire performance. Examples were chosen to illustrate the method. Traditional cellulosic and cementitious walls and ceilings were compared to plastic materials in the same configuration.

Networks

State Transition Model

There is a probability p_f for flashover occurring in a room or compartment which depends on the objects in the room and their spatial arrangement apart from ventilation and other factors. Given flashover, the fire can breach the structural boundaries of the room with a probability p_b and spread beyond the room with a probability $p_s(= p_f \cdot p_b)$. The value of p_b depends on the level of fire severity attained after flashover and the fire resistance of the structural elements, such as walls, ceilings, and floors. The probability of failure of a room or compartment of given fire resistance, p_b, can be estimated from the joint probability distribution of fire severity and fire resistance expressed in units of time.[13] Fire resistance of a compartment will be reduced and the failure probability p_b increased by weakness caused by penetrations, such as piping or cables through walls, doors, windows, or other openings in the structural barriers.

Each room or corridor in a building has, therefore, an independent probability p_s of fire spreading beyond its boundaries. Using these probabilities for different rooms and corridors, fire spread in a building can be considered as a discrete propagation process of burning among points that abstractly express the rooms, spaces, or elements of a building. In a simple analysis, states classified by the burning situation of individual points can be incorporated in a state transition model.[17]

Consider, for example, three adjoining rooms, R_1, R_2, and R_3, that provide the following four states with the fire commencing with the ignition of objects in R_1.

1. Only R_1 is burning.
2. R_1 and R_2 are burning (and not R_3).
3. R_1 and R_3 are burning (and not R_2).
4. All three rooms are burning.

There is no transition from the

1. First to the fourth state
2. Second to the third state
3. Third to the second state
4. Second or third or fourth to the first state (recession of fire growth).

Table 3-15.6   *Probabilities of Extinguishment: Fire-Growth and Suppression Model*

System Configuration	P_I	P_{II}	P_{III}	P_{IV}	P_V	P_{VI}	P_{FDF}/F
No sprinkler	0.5673	0.0038	0.0017	0.3282	0.0666	0.0324	0.0990
Sprinkler	0.5673	0.3827	0.0201	0.0232	0.0045	0.0022	0.0067

A transition from the second to the fourth state involves the spread of fire to R_3 from R_1 or R_2. The probability for this transition is, therefore, the sum of probabilities for spread from R_1 to R_3 and R_2 to R_3. Likewise, the probability of transition from the third to the fourth state is the sum of probabilities for spread from R_1 to R_2 and R_3 to R_2. A fire can burn in the same state without transition to another state. The process terminates when the fourth state is reached.

With the assumptions mentioned above, the following transition matrix can be formed with p_{ij} denoting the probability, p_s, of fire spread from room i to room j per unit time.[17] The unit may be longer than one minute, say, five minutes since one is considering spread from room to room after the occurrence of flashover. The values of p_{ij} may be considered as constants in a state transition model with stationary transition probabilities.

$$\mathbf{P} = \begin{bmatrix} 1 - p_{12} - p_{13} & p_{12} & p_{13} & 0 \\ 0 & 1 - p_{13} - p_{23} & 0 & p_{13} + p_{23} \\ 0 & 0 & 1 - p_{12} - p_{32} & p_{12} + p_{32} \\ 0 & 0 & 0 & 1 \end{bmatrix}$$

During the initial period, since only R_1 is burning, the probability of burning in different states is given by the probability distribution of the system

$$\mathbf{p_0} = (1 \quad 0 \quad 0 \quad 0)$$

The probability distribution of the system after one unit of time is given by

$$\mathbf{p_1} = \mathbf{p_0} \cdot \mathbf{P} = (1 - p_{12} - p_{13} \quad p_{12} \quad p_{13} \quad 0)$$

and after two units of time by the following row vector which, for convenience, has been written as a column vector

$$\mathbf{p_2} = p_1 \cdot P = \begin{bmatrix} (1 - p_{12} - p_{13})^2 \\ 2p_{12}(1 - p_{13}) - p_{12}^2 - p_{12} \cdot p_{23} \\ 2p_{13}(1 - p_{12}) - p_{13}^2 - p_{13} \cdot p_{32} \\ p_{12} \cdot p_{23} + 2p_{12} \cdot p_{13} + p_{13} \cdot p_{32} \end{bmatrix}$$

The probability distributions of the system for later periods can be obtained by repeating the matrix multiplication as described above. This process will generate for each state a probability distribution for burning in that state as a function of time. For the first state (only R_1 burning), for example, the probability after n units of time is $(1 - p_{12} - p_{13})^n$. The probability distributions for the other three states can be obtained by performing the calculations on a computer. The distribution for any state will provide an estimate of average transition time to that state. For estimating the average transition time to the fourth state, denoting the burning of all three rooms, Morishita[17] has proposed a method based on partitioning the matrix **P**. He has also discussed the stochastic process for a system in which extinguishment is attempted. For pur-

poses of illustration he has applied the model to a hypothetical small house.

By carrying out further calculations and adding the corresponding probabilities, cumulative probabilities over time can be estimated for burning in the four states. The cumulative probabilities would generally tend to some limits as the value of n denoting time increases. The limiting value of the cumulative probability for the fourth state (all three rooms burning) and the corresponding time would be of special interest. This probability can be reduced and the associated time increased by (1) increasing the structural fire resistance of the rooms to reduce the probability of barrier failure, p_b, and (2) installing sprinklers to reduce the probability of flashover, p_f. With these safety measures probability of fire spread from room to room, p_s, will be reduced. Consequently the cumulative probability of fire being confined to the room of origin, R_1, will increase; this probability for a duration of t minutes is given by

$$\sum_{n=1}^{t} (1 - p_{12} - p_{13})^n$$

where p_{12} and p_{13} are the probabilities of spreading from R_1 to R_2 and R_3 per unit time.

Network Models

The model described above can be extended to provide cumulative probabilities, at time n or limiting, for the burning of more than three rooms, but this will involve tedious and complex calculations. It would be simpler to consider fire spread between two given rooms through intermediate rooms and corridors in terms of discrete values attached to the probability p_s of spread beyond a room. This probability may be the limiting value for the cumulative probability given by, say, $E_4(= \lambda_1 \cdot \lambda_2 \cdot \lambda_3)$ in Figure 3-15.5. Alternatively, the time taken by fire to breach the boundaries of a room may be ascertained from deterministic (scientific) models and a probability assigned to this time, t_s, used for p_s in the stochastic model. The duration t_s is the sum of t_f representing the time to the occurrence of flashover after the start of established burning and t_b representing the time for which the barriers of the room can withstand fire severity after flashover. The latter time may be the endurance of barrier elements as measured by a standard fire resistance test, such as ASTM E119, *Standard Test Methods for Fire Tests of Building Construction and Materials.* As mentioned earlier $p_s = p_f \cdot p_b$.

Consider, as an example, the simple layout of Figure 3-15.6(a), relating to four rooms, and the corresponding graph shown in part (b), which also shows the probability (p_{ij}) of fire spread between each pair of rooms (i, j). The probability p_{ij} refers to p_s as defined herein, whereas Dusing et al.[18] and Elms and Buchanan[19] have considered only the barrier failure probabilities denoted by p_b, ignoring the probability of flashover denoted by p_f. The specific problem considered by these authors was to compute the probability of fire spread from room 1 to 4, which might follow any of the four paths, that is, $(1) \rightarrow (2) \rightarrow (4); (1) \rightarrow (3) \rightarrow (4); (1) \rightarrow (2) \rightarrow (3) \rightarrow (4);$ and $(1) \rightarrow (3) \rightarrow (2) \rightarrow (4).$

(a) Room layout

(b) Corresponding graph
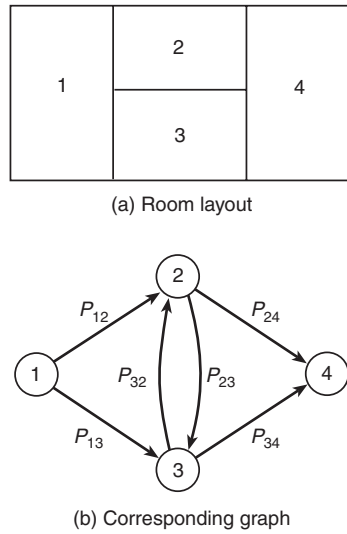
Figure 3-15.6. *Simple diagram for fire spread.*

Figure 3-15.7. *Modified event space tree.*

Using the event space method, Elms and Buchanan[19] considered first all possible "events" or combinations of fire spreading or not spreading along various links. If a_{ij} represents spread of fire along link ij, and $\bar{a}_{ij}$ represents fire not spreading along the link, then one event might be

$$[a_{12}, \bar{a}_{13}, a_{23}, \bar{a}_{32}, \bar{a}_{24}, a_{34}]$$

There will be $2^6 = 64$ events that will be all-exclusive, as any pair of events will contain at least one link for which fire spreads in one event and does not spread in the other. The probability of each event occurring is the product of the probabilities of its elements, assuming that the elements are independent. Thus, for the example given above, the event probability will be

$$p_{12}(1 - p_{13})p_{23}(1 - p_{32})(1 - p_{24})p_{34}$$

and the overall probability is the sum of all 64 event probabilities.

The complete event space can be represented as a tree with 64 branches. The probability of fire spread for each event (branch) is obtained by multiplying all the link probabilities in a branch. However, not all branches have to be computed in full. The computation can be curtailed, while still allowing for all cases. For this purpose, Elms and Buchanan[19] have described a method of constructing the tree and its ordering to identify or search possible paths of links leading to node (room) 4 from node 1. This procedure is known as a "depth-first search" of a graph. In this algorithm, a path is a series of nodes or rooms in a building; the construction of a branch, which is part of a particular event, is based on an underlying path. Each branch allowing fire spread must contain at least one path. Figure 3-15.7 shows the actual tree as it would be computed by the algorithm. The total probability of spread from node 1 to node 4 is given by the sum of all the branch probabilities. The calculation is carried out for each pair of rooms,
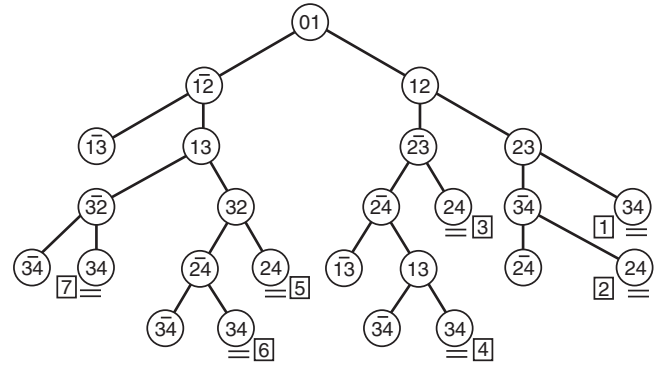
and the results assembled in a "fire spread matrix." The diagonal elements of the matrix are unity.

Various means have been employed to curtail the algorithm to prevent the computer developing excessively lengthy branches that would, as the branch probability decreases with branch length, have little effect on the result. The first means is to restrict the length of a fire spread path to a maximum number of compartments. The second approach is to terminate development of a branch if the cumulative branch probability drops below a certain fraction of the running total of the branch-spread probabilities calculated up to that point. The third means is to terminate development of a branch if the underlying path length becomes greater than a specified amount more than the length of the shortest possible path between the two rooms being considered.

In the computer-based technique of Elms and Buchanan[19] as described above, a building is represented as a network by defining compartments as nodes and the links between these nodes as possible paths for fire spread from compartment to compartment in a multicompartment building. The core of this model is a probabilistic network analysis to compute the probability of fire spreading to any compartment within the building. A series of further refinements were added when the model was applied to analyze the effects of fire resistance ratings on the likely fire damage to buildings.[20]

Time Dimension

Elms and Buchanan[19] did not consider the dimension of time explicitly, although it was implicit in many of their functions. The probability of fire spreading from one compartment to another was considered irrespective of how long it might take. As a result, the analysis did not take into account any intervention (e.g., the fire service). In this respect the model represented a worst-case scenario and assumed that the fire would eventually burn itself out.

The model of Elms and Buchanan[19] was not concerned with the process of fire growth and assumed that the spread was solely a function of the probable effects of a fully developed fire. The probability of flashover was not considered in this model. Platt[21] has proposed a new network model in which fire resistance and severity are

related to real time instead of equating these two parameters to the time based on the ISO standard fire which is not necessarily representative of the real time. The model computes the probability that fire will have spread to any part of a building after an elapsed time t. The essential features of Platt's model[21] are described in the following paragraphs.

The spread of fire to an adjacent compartment may be via the following paths:

1. Through an open doorway
2. Vertical spread via windows
3. Through a barrier, such as a wall, closed door, or ceiling

Two models are considered for estimating fire growth as a function of time. The first model is based on the exponential relationship between fire area and growth time as suggested by Ramachandran.[22] The second model uses the parabolic relationship between rate of heat release and growth time as proposed by Heskestad.[23] This model is used in conjunction with the relationship between compartment temperature and rate of heat flow to provide an estimate of flashover time, which is taken as the time when ceiling temperature reaches 600°C. The temperature is a function of the ventilation characteristics of the compartment, the type of fuel material, its configuration, and the thermal properties of the structural boundaries.

A figure of 49 percent is used to represent the probability that the initial fire will not result in flashover. Subsequent ignitions caused by fire spread are given a 100 percent probability of reaching flashover. This assumption may overestimate the spread of fire, since a barrier may fail in the very latter stages of a fully developed fire, which may not then have the momentum to initiate further ignition.

The real time of the fire duration, t, representing fire severity, s, is estimated by the ratio of fuel load to rate of combustion which is a function of ventilation and dimensional characteristics of the compartment. A formula suggested by CIB[24] is used to estimate the equivalent time, t_e involving the real parameters of the compartment. The approved fire resistance rating (FRR) of a barrier element, modified for weakness and another factor, is multiplied by the ratio (t/t_e) to yield an equivalent FRR denoted by R. R and fire severity, s, are not independent but quite rightly they have been assumed to be independent random variables with log-normal probability distributions. Under this assumption, the probability of fire spread through a barrier is estimated through the safety factor (R/s) which is also a log-normal variate. The probability of fire spread via an open door is assumed to be 100 percent. The probability of fire spreading vertically up the facade of a building via windows is equated to the probability that the height of the external flames is greater than or equal to the height of the spandrel.

A comparison is then made between these values and the design values of the barrier and door fire resistance and the spandrel heights. The output from these comparisons is a series of probabilities that fire will spread via each of the three possible paths described earlier. Combining these individual probabilities gives an overall probability of fire spreading to an adjacent compartment. Repeated for each compartment within the building,

these values collectively form the adjacency fire spread matrix whose values represent the probability that fire will spread from compartment i to an adjacent compartment j. The expected time for fire to spread to an adjacent compartment, given that fire does spread, provides values for the adjacency fire spread time matrix.

By combining the two matrices providing probabilities and expected times for fire spread between adjacent compartments, the analysis computes the probability of fire spreading from an initial compartment i to any compartment j. The fire may spread along any path, but is conditional on having arrived at compartment j in a given time. The resulting matrix (i.e., global fire spread matrix) may be considered as a three-dimensional matrix with each layer being evaluated at a different time. Once the fire spread matrix has been formed, Platt's model[21] is very similar to that of Elms and Buchanan[20] except that, in the former model, the probability of spread is dependent on time, whereas, in the latter model the probability of fire spreading is irrespective of the time taken.

Ling and Williamson[25] have proposed a model in which a floor plan is first transformed into a network similar to the process described by Dusing et al.[18] and Elms and Buchanan.[19] Each link in their network represents a possible route of fire spread, and those links between nodes corresponding to spaces separated by walls with doors are possible exit paths similar to those developed by Berlin et al.[26] The space network is then transformed into a probabilistic fire spread network as in the example in Figure 3-15.8 with four rooms, Rm 1 to Rm 4, and two corridor segments C_1 and C_2. In this figure, Rm 1 has been assumed as the room of fire origin, but it would be a simple modification to reformulate the problem for another room of origin. With Rm 1 and Rm 1′, with a "prime" denoting the preflashover and post-flashover stages, the first link is represented by

$$\text{Rm } 1 \rightarrow \text{Rm } 1'$$
$$(p_f, t_f)$$

where p_f represents the probability of flashover and t_f represents the time to flashover. The nodes denoted by a prime represent a fully developed (i.e., post-flashover) fire in the compartment.
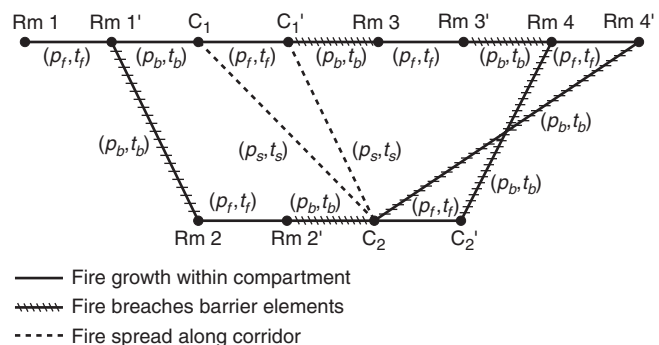
Figure 3-15.8. *Probabilistic network of fire spread of Rm 1 to C_2.*

In Figure 3-15.8, three different types of links are identified. The first corresponds to the fire growth in a compartment, the second to the fire breaching a barrier element, and the third to fire spread along the corridors. To each link i, a pair of numbers (p_i, t_i) is assigned, with p_i representing the distributed probability that a fire will go through link i, and t_i representing the time distribution that it will take for such a fire to go through link i. The section of the corridor, C_1, opposite Rm 1, is treated as a separate fire compartment and is assigned a (p_f, t_f) for the link from C_1 to C_1'. The number pair (p_s, t_s) represents the probability and time for the preflashover spread of fire along the corridor from C_1 to C_2. As a first approximation, p_s may be considered to be governed by the flame spread classification of the corridor's finish materials on the walls and ceiling, as measured by a test method such as the tunnel test in ASTM E84, *Standard Test Method for Surface Burning Characteristics of Building Materials.*

Once full involvement occurs in the section C_1 of the corridor outside Rm 1 (i.e., node C_1' is reached) the fire spread in the corridor is influenced more by the ventilation in the corridor and by the contribution of Rm 1 than by the material properties of the corridor itself. Thus there is a separate link, C_1' to C_2, that has its own (p_s, t_s). The number pair (p_b, t_b) represents the probability of failure of the barrier element, with t_b representing the endurance of the barrier element.

Once one has constructed the probabilistic network, the next step is to solve it by obtaining a listing of possible paths of fire spread with quantitative probabilities and times associated with each path. For this purpose, Ling and Williamson[25] have adopted a method based on "emergency equivalent network," developed by Mirchandani[27] to compute the expected shortest distance through a network. (The word *shortest* has been used instead of *fastest* to be consistent with the literature.) This new equivalent network would yield the same probability of connectivity and the same expected shortest time as the original probabilistic network. In this method, each link has a Bernoulli probability of success and the link delay time is deterministic.

It must be noted that there are multiple links between nodes in the equivalent fire spread network. For example, the door between Rm 1 and the corridor could be either open or closed at the time the fire flashed over in Rm 1. Ling and Williamson[25] assumed, as an example, that there is a 50 percent chance of the door being open and that an open door has zero fire resistance. Furthermore, they assumed that the door, if closed, would have a 5-min fire rating. With further assumptions they constructed the equivalent fire spread network (Figure 3-15.9) with twelve possible paths for the example in Figure 3-15.8 to find the expected shortest time for the fire in Rm 1 to spread to the portion of corridor C_2. This network changes to Figure 3-15.10 with ten possible paths if self-closing 20-min fire-rated doors had been installed in the corridor, assuming that the reliability of the self-closures is perfect and that doorstops had not been allowed. Note that the links have been renumbered for Figure 3-15.10.

For the two equivalent networks shown in Figures 3-15.9 and 3-15.10, all of the possible paths are listed in Tables 3-15.7 and 3-15.8 with increasing time and with all the component links identified. Each of these paths can be described by a fire scenario; for instance, path 1 in Table 3-15.7 consisting of links ℓ_1, ℓ_2, and ℓ_4, would be

"The fire flashes over, escapes from Rm 1 through an open door into the corridor C_1 and spreads along the corridor to C_2."

The probability of that scenario (0.13) is strongly dependent on the probability (0.5) for the occurrence of flashover in Rm 1 and of the probability (0.5) that the door will be open. The time of 17.5 min is composed of the times of 10 min for flashover and 7.5 minutes for fire to spread in the corridor from C_1 to C_2.

Ling and Williamson[25] have derived a formula for calculating from the figures in Tables 3-15.7 and 3-15.8, the probability of connectivity R, which is 0.5 for both the networks (Figures 3-15.9 and 3-15.10). This probability is a direct result of the assumed probability of 0.5 for flashover in the room of fire origin and the occurrence of unity probabilities in the remaining links that make up certain paths through the network. According to another formula, the expected shortest time is 29.6 min for Figure 3-15.9, and increases to 47.1 min for Figure 3-15.10 due to the presence of the 20-min fire-rated door. The equivalent
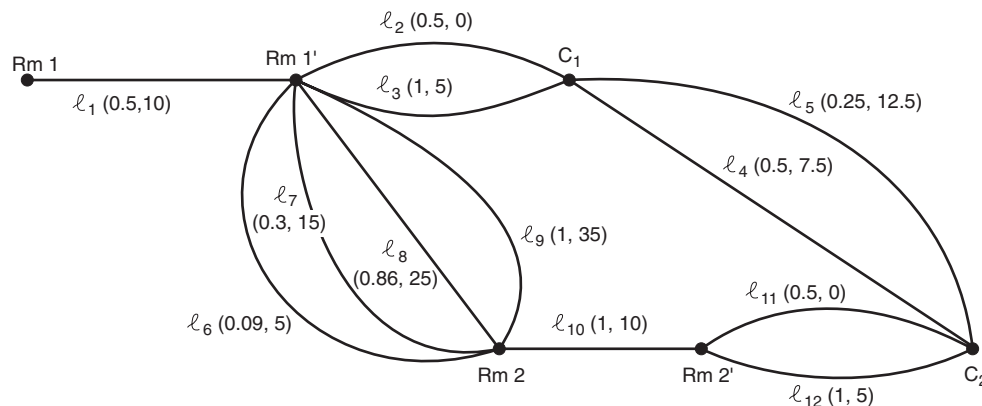
Figure 3-15.9. *Equivalent fire spread network with 5-min unrated doors.*
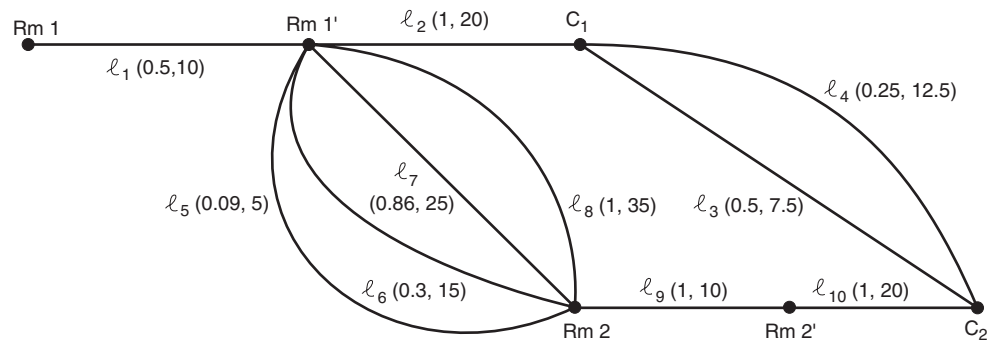
Figure 3-15.10. *Equivalent fire spread network with self-closing 20-min fire-rated doors.*

Table 3-15.7 *Pathways through the Example Fire Spread Equivalent Network Assuming 5-Min Unrated Corridor Doors, as Shown in Figure 3-15.9*

Paths	Component Links	Probability p_i	Time t_i (min)
1	1-2-4	1/8 = 0.13	17.5
2	1-2-5	1/16 = 0.06	22.5
3	1-3-4	1/4 = 0.25	22.5
4	1-6-10-11	1/44 = 0.02	25.0
5	1-3-5	1/8 = 0.13	27.5
7	1-6-10-12	1/22 = 0.05	30.0
8	1-7-10-12	3/40 = 0.08	35.0
9	1-8-10-11	3/14 = 0.21	40.0
10	1-8-10-12	3/7 = 0.43	50.0
11	1-9-10-11	1/4 = 0.25	55.0
12	1-9-10-12	1/2 = 0.50	60.0

Table 3-15.8 *Pathways through the Example Fire Spread Equivalent Network Assuming Self-Closing 20-Min Fire-Rated Corridor Doors, as Shown in Figure 3-15.10*

Paths	Component Links	Probability p_i	Time t_i (min)
1	1-2-3	1/4 = 0.25	37.5
2	1-2-4	1/8 = 0.13	42.5
3	1-5-9-10	1/22 = 0.5	45
4	1-6-9-10	3/20 = 0.15	55
5	1-7-9-10	3/7 = 0.43	65
6	1-8-9-10	1/2 = 0.50	75

fire spread network thus facilitates an evaluation of design changes and affords ready comparison of different strategies to effect such changes.

Random Walk

In a simple stochastic representation, the fire process involving any single material or number of materials can be regarded as a random walk. The fire takes a random step every short period either to spread with a probability λ or to get extinguished (or burnout) with a probability $\mu(= 1 - \lambda)$. The parameter λ denotes the success probability of the fire, whereas μ denotes the success probability of an extinguishing agent. The problem is similar to two gamblers, A (fire) and B (extinguishing agent), playing a sequence of games, the probability of A winning any particular game being λ. If A wins a game he or she acquires a unit stake by destroying, say, a unit of the floor area; if he or she loses the game, no stake is gained. In the latter case, A does not lose his or her own stake to B; an already burned out area is a loss that cannot be regained. Extinguishment can also be considered as an absorbing boundary to the random walk, just as it is an absorbing state in a state transition model.

A random walk will lead to an exponential model described in Equations 1 through 3. In these equations, if one writes $c = \mu - \lambda$ such that $\mu = (1 + c)/2$, since $\mu + \lambda = 1$

$$Q(t) = \exp\left[\frac{-(1 + c)t}{2}\right] \qquad (13)$$

The fire-fighting effort is adequate if c is positive with μ greater than λ and, hence, greater than ½; it is inadequate if c is negative with μ less than λ and, hence, less than ½. If $c = 0$, such that $\mu = \lambda = $ ½, there is an equal balance between fire-fighting efforts and the propensity of fire to spread.

Associated with the random variable t denoting time, there is another random variable x denoting damage which may be expressed in terms of, say, area destroyed. Damage in fire has an exponential relationship with duration of burning,[22] such that the logarithm of x is directly proportional to t as a first approximation. This assumption would lead to Pareto distribution

$$\phi(x) = x^{-w}, \quad x > 1 \qquad (14)$$

denoting the probability of damage exceeding the value x. This distribution is used in economic problems concerned with, for example, income distribution to describe the fact that there are a large number of people with low incomes and a small number of people with high incomes. The damage is small in most of the fires, with high levels of damage occurring only in a small number of fires.

The use of Pareto distribution for fire damage originally proposed by Benckert and Sternberg[28] was later supported by Mandelbrot[29] who derived this distribution following a random walk process. For all classes of Swedish houses outside Stockholm, the value of the exponent w was found to vary between 0.45 and 0.55. A value of $w = 0.5$ in Equation 14 would imply, as discussed with reference to Equation 13, an equal balance between fire-fighting efforts and the propensity of fire to spread and cause damage.

The parameter μ in Equations 1 and 2 is known as the *hazard* or *failure rate* given by the ratio

$$\frac{f(t)}{Q(t)}$$

where $f(t)$ is the probability density function obtained as the derivative of $F(t)$ in Equation 2. A constant value for μ would denote a random failure. For a Pareto distribution in Equation 14, the failure rate is w/x, such that, with a constant value for w, the failure rate would decrease as x increases, indicating that, in terms of damage, a fire can burn forever without getting extinguished. A constant value for μ or w is somewhat unrealistic, particularly for a fire that is fought and extinguished at some stage. A fire will also burn out when all the available fuel is consumed or when it stops spreading due to the arrangement of objects in a room or building. For the reasons mentioned above, although the failure rate can decrease in the early stages of fire development denoting a success for fire spread, it would eventually increase ("wear out failure"), since fire extinguishing efforts would succeed ultimately.[30] There may be a long intermediate stage of steady growth of fire with μ remaining as a constant. The failure rate as a function of time would, hence, resemble a "bathtub" whose cross-section is composed of two curves sloping downwards representing the early and final stages of fire growth, connected at the bottom by a long straight line representing the intermediate stage.

Erving et al.[31] presented an approach to the theory of burning velocity in which a flame front moves forward at a rate determined by the random walk of chemical energy. The flame velocity is estimated by the value of a parameter which is a "collision rate" divided by a "reaction rate," both determined at the point of maximum reaction velocity. Empirical activation energies were given by the authors for certain hydrocarbon flames.

In the context of fire spread, random walk is a one-dimensional process describing the damage by random functions of time rather than by a random function of time and space. The random walk indicates the position of the fire (i.e., damage at any time). At every unit of time, there is a change in position indicated by an increment to the damage or no change due to absorption (extinguishment or burning out). Generally the walk is considered in discrete time. If the walk is continuous in time such that the increments are Gaussian, this leads to a diffusion process.[32] (A diffusion process is an approximation to Brownian motion, a phenomenon well known in many branches of science and technology.) The normal, or diffusion, term is one of two possible components of a general additive stochastic process, the other component being a discontinuous or transition term arising from occurrences of events at random times. The Markov chains discussed earlier belong to the second type of component. A linear superposition of the two components provides a solution to an equation governing a general additive process.

Percolation Process

In random walk and diffusion models, randomness is a property of the moving object, whereas in a percolation process, randomness is a property of the space in which the object moves.[33] Thus the transition the object suffers when at a particular point is random but, if the object ever returns to this point, it would suffer the same transition as before. The process is described by a stochastic field on the space (i.e., a vector field of transition numbers). Percolation process deals with deterministic flow in a random medium, in contrast with random walk and diffusion models which are concerned with random flow in a deterministic medium.

Broadbent and Hammersley[34] considered the walk as taking place on a graph consisting of a number of sites, connected by directed bonds, passage being possible only along such a "bond." If such a graph obeys certain connectivity requirements, it is termed a *crystal.* In a randomized version, each bond of the crystal has an independent probability of being blocked, and it is desired to know what effect this has on the probability of communication from one site A to another site B; this is not the same as from B to A, since communication has a direction.

If fire is considered as the moving object, the movement takes place in a space or medium that has a certain random property although the object (fire) itself has some randomness associated with it. Buildings in an area, for example, are somewhat randomly distributed. Buildings are also connected by directed bonds, with spread (flow) of fire being possible only along the bonds. Each bond has an independent probability of blocking or preventing fire spread; this depends on the nature of a building and its contents, wind conditions, and the distances between buildings. A percolation problem also arises when one considers a network some of whose links, chosen at random, may be blocked, and one wishes to know the effect of this random blockage on flow through the network. Such a problem would be encountered in predicting fire spread in a forest or from building to building in an urban area.

Apparently for the reasons mentioned above, Hori[35] considered percolation process for the modeling of fire spread from building to building. Sasaki and Jin[36] were concerned with the actual application of this model and estimation of probabilities of fire spread. By using the data contained in the fire incidence reports for Tokyo, urban fires were simulated and the average number of burnt buildings per fire estimated. Apart from distances between buildings and wind velocity, the following factors were also regarded as having some effect on the probability of fire spread: building construction, building size and shape, window area, number of windows, indoor construction materials, furniture, walls, fences, gardens, and trees.

For the model, the first factor was classified into three groups: (1) wood construction, (2) mortar (slow burning) construction, and (3) concrete (fireproof) construction. The wind velocity was classified into two groups: (1) 0 to 2.5 m/s and (2) 2.5 to 5.0 m/s. In the former case, fire spread was assumed to be undirectional (isotropic) whereas, in the latter case, the data were subdivided into smaller groups according to the directions of fire spread: the windward direction, the leeward direction, or direction perpendicular to that of the wind (the sideward direction). Fire incidents in which wind velocity was larger than 5.1 m/s were excluded due to their small number. If the number of burnt buildings was i and that of unburnt ones was j, the probability of fire spread was expressed as $i/(i + j)$.

The data were divided by every meter of the distance between buildings, or every 2 m or more in case the data were few. The exponential function $\exp(-cd)$ was used for estimating the probability of spread between two buildings as a function of distance d between them. Using the least square method, the values of c were obtained for different building construction and wind velocity categories. The analysis revealed that building construction was the main factor responsible for fire spread. The simulations did not evaluate the changes in the pattern of spread according to time.

In a recent study, Nahmias et al.[37] have examined the feasibility of applying percolation theory to the spread of fires in forests. For studying the effect of randomness on the propagation of fire the authors have built a square network model containing combustible and noncombustible blocks randomly distributed, with a variable concentration, the parameter q denoting the fraction of noncombustible elements. In the absence of wind, the propagation was found to be consistent with a model of invasion percolation on a square site lattice with nearest neighbor interaction leading to a threshold not far from the theoretical value $q = 0.39$. The threshold was larger with wind blowing on the model. The largest threshold value obtained was $q = 0.65$. The final state of the model after combustion was represented for different values of wind velocity and fraction values q. The observation of this state can bring out the directed, nonlocal, and correlated characters of the contagion.

Epidemic Theory

For predicting fire spread in a large urban area, Albini and Rand[38] have proposed a model that has some similarity with chain-binomial models of Reed and Frost[39] for the spread of an epidemic. The authors envisaged fires in "locales," which may be single buildings or blocks of buildings. A number of these are presumed to be alight initially and randomly distributed and to stay alight for a time T in the absence of fire fighting. At time T, this generation of fires can spread fire and then die out, leaving a second generation to burn for a second period T, and so on.

Fire spread is assumed to take place only at the end of each fire interval. For the $(n + 1)$th interval, the *a priori* probability that any locale is burning is P_n and that it has not yet been burnt is A_n. It follows that

$$A_n = (1 - P_0)(1 - P_1) \ldots (1 - P_n)$$
$$P_{(n+1)} = A_n \cdot B_n$$

where B_n is the probability that during the $(n + 1)$th interval, fire spreads into a "locale" previously unburnt. To obtain B_n, Albini and Rand[38] introduced parameters defining the following three probabilities:

1. Probability that during the $(n + 1)$th interval there are just m locales burning out of N possible locales adjacent to a given locale
2. Probability that at least one of the m burning locales spreads fire
3. *A priori* probability that fire will spread during any interval of duration T from a burning locale to an unburnt neighbor

Based on the aforementioned parameters the authors obtained an upper and lower approximation for B_n and narrow limits for $(1 - A_n)$, the probability of a locale being burnt.

The Albini and Rand[38] model allowing for fire fighting was based on a number of idealizations. First, firefighting effort was assumed to be constant. The authors introduced a parameter M for the fraction of burning locales wherein all fire fighters in a city could extinguish that fraction during the given time interval out of all possible burning locales. Fire fighting was assumed to be continuous throughout the time interval. A fire not extinguished may or may not spread; if extinguished it cannot spread. Under the assumptions mentioned above, the authors have derived an expression for the probability $P_{(n+1)}$ defined earlier. Albini and Rand considered directional spread of fire assuming that from an isolated locale the probability of spread forward and backward was the same and the directional element in the spread arose only from the initial condition. Spatial variation was included in the model by connecting the probability of spread to the probability that any building was itself burning and separated from any of its neighbors not yet burning by less than the appropriate "safe" distance for radiation or brand transfer.

Thomas[40] drew attention to the possible relevance of epidemic theory to fire spread in a building, and compared the model of Albini and Rand[38] with a deterministic epidemic model based on a continuous propensity of fire to spread. He found the results of both models to be in reasonable agreement as to their basic features, but concluded that neither would be appropriate for addressing spread in a single building where the number of "locales" is not large. For such a situation a stochastic treatment is necessary to allow for the finite chance that the initiating fires can burn out before spreading, a chance that is negligible when the number of initial fires is large.

Stochastic Differential Equation

Introduction

Most of the models developed to date use statistical data provided by real fires for quantifying, in terms of

probabilities, uncertainties caused by factors which cannot be controlled. These models do not explicitly consider the underlying physical processes. On the other hand, models such as zone, field, and others involving computational fluid dynamics (CFD) are based on physio-chemical and thermodynamic theories supported by experimental data. These models are essentially deterministic since they do not explicitly consider the uncertainties or randomness affecting the spread of a real fire. In order to avoid complex calculations which cannot be performed even with the aid of advanced computer programs, deterministic models use simplified equations which treat as fixed values parameters which are clearly variables. Exclusion of parameters that can affect fire spread is another source of uncertainty generally ignored by a deterministic model. For these reasons, the development of a real fire is unlikely to follow exactly the pattern predicted by a deterministic model even for the early stage involving the material or object first ignited. More uncertainties are involved when a fire spreads from object to object in a room.

For the reasons mentioned above, there is a need to develop models which couple deterministic and stochastic processes governing the spread of a real fire in a room or building. Ramachandran[41] suggested one such model in which heat output and area damage in a real fire are considered as correlated variables for predicting the rate of fire growth (and "doubling time") according to an exponential model.[22] This method, in conjunction with the probability distribution of area damage, can provide estimates for the time of flashover in a compartment and for the probability of flashover. Another method is to introduce additional parameters in a deterministic model to take account of uncertainties and derive the stochastic version of the deterministic model. One such method, based on the stochastic differential equation,[42] is currently being developed in Australia and has the following basic features.

The Deterministic Model

The deterministic version of the stochastic model derived by Hasofer and Beck[42] for compartment fires is a one-zone model consisting of three variables: the gas temperature T (°C), the rate of fuel burning R (g/min), and the oxygen mass fraction in the compartment x. Eventually x is converted into the percentage oxygen deficiency $D = 23 - 100x$. The initial temperature is $T_0 = 20$°C and the time t is measured in min. The basic laws used to derive the equations are discussed by Dysdale,[43] section 10.3.2.

The following parameters have been used in the model:

Variable parameters

V (volume of compartment) = 21.6 m³

S (inside surface area of compartment) = 46.88 m²

A (area of opening) = 1.6 m²

B_{max} (total fuel mass) = 172.8 kg

R_0 (initial burning rate) = 8.38 g/min

h (height of opening) = 2 m

Fixed Parameters

ρ (gas specific gravity) = 490 g/m³ at 500°C

= 1300 g/m³ at 20°C

C_p (specific heat of gas) = 0.001 kJ/gK

σ (Stefan Boltzmann constant) = 3.4 × 10⁻⁹ kJ/min·m²K⁴

ε (gas emissivity) = 0.015

ν (mass of oxygen used up by 1 g of fuel) = 1.36 g

The values of the variable parameters refer to a flashover fire.

With Q_L denoting the net rate of heat loss from the enclosure, the heat balance equation is

$$C_p \rho V \frac{dT}{dt} = H_B R - Q_L \qquad (15)$$

where H_B is the net combustion heat per gram of fuel, R is the fuel-burning rate, and ρ is taken to be some average gas specific gravity. Rewriting Equation 15

$$\frac{dT}{dt} = \beta R - q(T) \qquad (16)$$

where $\beta = H_B/C_p \rho V$ and $q(T) = Q_L/C_p \rho V$. By expressing the total heat loss rate Q_L as the sum of radiation loss rate and convection loss rate, the following equation has been derived under some assumptions:

$$q(T) = \sum [(T + 273)^4 - (T_0 + 273)^4] + \Phi(T - T_0) \qquad (17)$$

for some values of the calibration parameters Σ and Φ.

Let the oxygen fraction in the incoming air be y (= 0.23). Then, assuming homogenous mixing, the following differential equation is derived for oxygen mass balance:

$$\frac{dD}{dt} = \delta(k_1 - D)R - \mu D \qquad (18)$$

where

$D = 100y - 100x = 23 - 100x$

$\delta = 1/\rho V$

$k_1 = 100(y + \nu)$

$\mu = m_a/\rho V$

The new symbol m_a denotes the ventilation rate in g/min. Equation 18 applies only as long as the oxygen concentration is above 7 percent. When that value is reached, it remains steady at that value until the burning rate starts diminishing.

For the burning rate R, the differential equation

$$\frac{dR}{dt} = \alpha(k - D)z \qquad (19)$$

has been derived under the assumptions that R is an increasing function of the gas temperature T, and R stops increasing when the oxygen fraction falls below 0.126. R rises only slowly for low temperatures. For z, which is

slowly increasing for small T, the following calibration formula has been used:

$$z = 22T\left(1 - \frac{1}{1 + (0.001T)^2}\right) \qquad (20)$$

Equation 19 is applicable as long as there is still some fuel not burning. When most of the combustible material has been consumed, the burning rate quickly decreases exponentially. Equations 16, 18, and 19 require the specification of the initial burning rate, R_0.

The three-variable model described above was calibrated to the output of the National Research Council of Canada (NRCC) model[44] with the particular set of values of the variable and fixed parameters listed earlier, by choosing appropriate values for the calibration parameters. These values were chosen as follows. A discrete version of the NRCC model, at intervals of 0.02 min. was obtained. Denoting the values of the gas temperature, the burning rate, and the oxygen deficiency by T_N, R_N, and D_N, respectively, discrete versions of the model were run with varying values of the parameters. An optimization algorithm was used to obtain the values of the parameters that minimized the distance function

$$\Delta = \sum C_1^2(T_N - T)^2 + C_2^2(R_N - R)^2 + C_3^2(D_N - D)^2 \qquad (21)$$

where $C_1 = 0.001$, $C_2 = 0.008$, and $C_3 = 23$. These values of the Cs were chosen so as to obtain comparable fits for the three variables at their maximum values.

The values of the calibration parameters obtained were as follows:

$\alpha = 2.5$; $\beta = 0.1125$ $\Phi = 0.399$ $\Sigma = 1.875 \times 10^{-10}$

$\delta = 1.5 \times 10^{-5}$ $\mu = 0.58$ $k = 10.4$ $k_1 = 158$

$R_0 = 280$ g/min $B_{max} = 82.5$ kg $\qquad (22)$

The Stochastic Model

The set of three deterministic equations derived in Equations 16, 18, and 19 have been turned into a set of stochastic differential equations by adding on the right hand side forcing functions, which are white noise multiplied by some function of the variables. The purpose of these forcing functions is to model the intrinsic variability of the fire phenomenon due, for example, to the turbulent behavior of the hot gases. The forcing function adopted is a standard Brownian motion differential $d\mathbf{W}$ with independent components (each with mean zero and variance dt) multiplied by an appropriate function of the variables. The standard form for describing the behaviour of a set of n coupled variables is

$$d\mathbf{X} + \boldsymbol{\alpha}(\mathbf{X}, t)\,dt = \boldsymbol{\beta}(\mathbf{X}, t)\,d\mathbf{W} \qquad (23)$$

where $\mathbf{X}$, $\boldsymbol{\alpha}$, and $d\mathbf{W}$ are vectors of length n and $\boldsymbol{\beta}$ is an $n \times n$ matrix. Since the future behavior of the vector $\mathbf{x}$ is independent of its past values, given its present value, it is a Markov vector.

The model does not make $\boldsymbol{\alpha}$ and $\boldsymbol{\beta}$ depend explicitly on the time; they are functions of $\mathbf{x}$ only. It is further assumed that the forcing functions for each of T, D, and R are independent, such that the matrix β is diagonal. An-

other assumption is that the randomness of the fire will increase with increasing temperature. Bearing in mind that the variance of a scalar forcing function differential βdw is $\beta^2 dt$, the following set of stochastic differential equations have been obtained:

$$
\begin{aligned}
dT - \beta R\,dt + q(T)\,dt &= f_1(T)\,d\mathbf{W}_1 \\
dD - \delta(k_1 - D)R\,dt + \mu D\,dt &= f_2(T)\,d\mathbf{W}_2 \qquad (24) \\
dR - \boldsymbol{\alpha}(k - D)z\,dt &= f_3(T)\,d\mathbf{W}_3
\end{aligned}
$$

where $q(T)$ is given by Equation 17 and $z(T)$ by Equation 20. The functions $f_1(T)$, $f_2(T)$, and $f_3(T)$ are appropriately chosen increasing functions of T.

Due to a great paucity of information about the intrinsic variability of enclosure fires, it is presently difficult to determine precise formulas for the functions f_1, f_2, and f_3. Experiments specifically designed to provide data for identifying these functions have been planned to be carried out at the Centre for Environmental Safety and Engineering Risk, Victoria University of Technology, Australia. Statistical variability is another problem whose source is lack of knowledge of the parameters governing the fire. The most important unknown parameter is the initial burning rate which is a nonnegative quantity and, hence, can be assumed to have a lognormal probability distribution. Other parameters affecting the fire are the geometry of the compartment, the size of the openings and whether they are open or shut, and the nature, amount, and position of the fuel load. If these parameters are also unknown, further parameters of the model must be allocated a probability distribution to cater for the added uncertainty. With additional reasonable assumptions regarding the variability of the phenomenon, the probability of extreme values of the fire load can be estimated by a Monte Carlo simulation and used as an input to the probabilistic fire risk analysis of the building under consideration.

Simulation–Illustration

To illustrate the capacity of the model to simulate the intrinsic variability of a fire, a Monte Carlo simulation was performed, using Equation 24 and the parameter values in Equation 22. The functions f_i were chosen as follows:

$$f_1(T) = \frac{\Phi T}{1000} \qquad (25)$$

$$f_2(T) = \frac{15\Phi T}{1000} \qquad (26)$$

$$f_3(T) = \frac{12\Phi T}{10^6} \qquad (27)$$

By varying the parameter Φ, varying degrees of stochasticity may be achieved. Figure 3-15.11 ($\Phi = 50$) and Figure 3-15.12 ($\Phi = 100$) illustrate the type of fire curve obtained.

Since (T, D, R) is a Markov vector and initially all three components increased monotonically, any decrease in the initial burning rate R_0 will just shift the fire curves in Figures 3-15.11 and 3-15.12 to the right. This is illustrated in Figure 3-15.13 for $R_0 = 150$. Thus, choosing a random value for R_0 and a nonzero value for Φ will produce curves similar to Figures 3-15.11 and 3-15.12, but shifted either to the right or to the left.
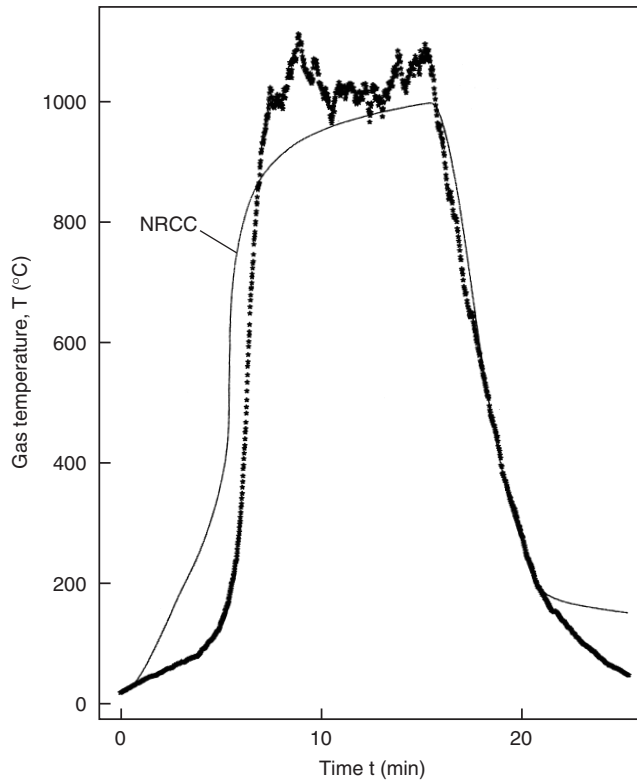
Figure 3-15.11. *Stochastic model. Gas temperature.* $\phi = 50$.
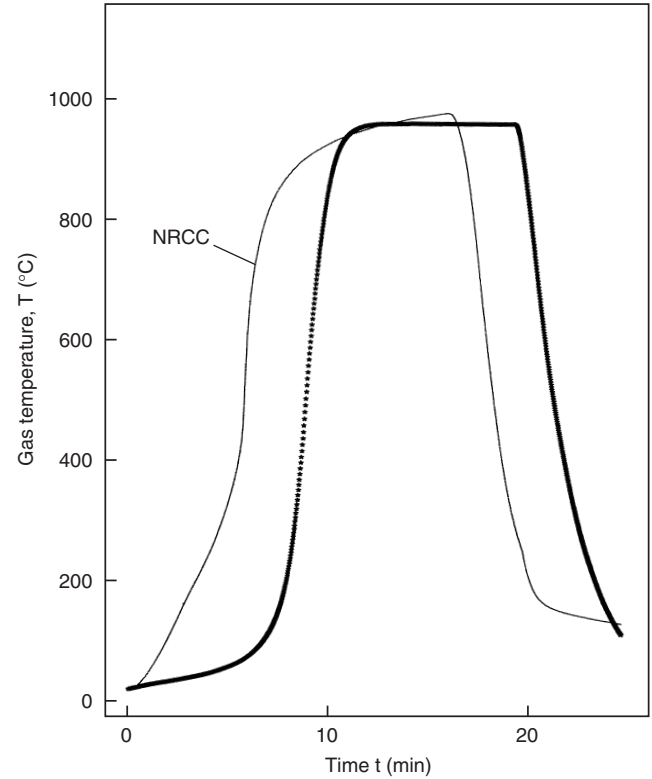
Figure 3-15.13. *Deterministic model. Effect of reducing R_0 to 150.*
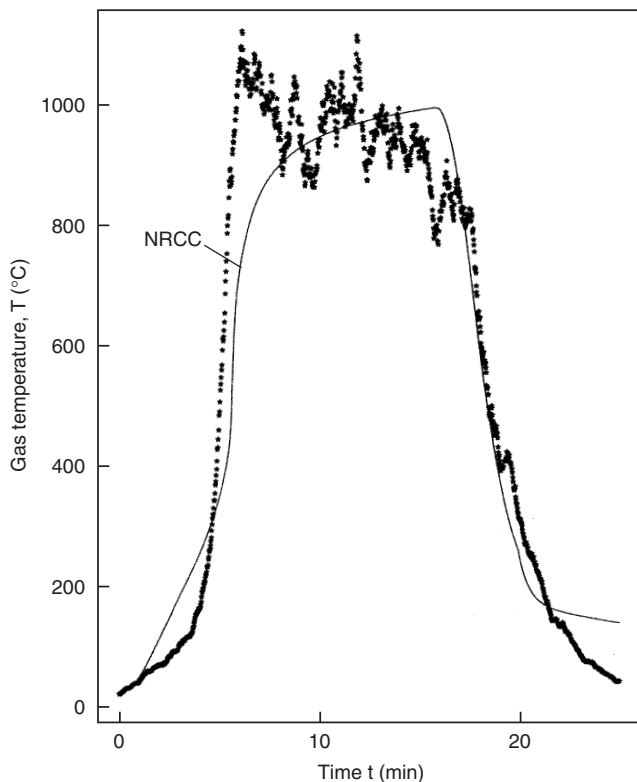
Figure 3-15.12. *Stochastic model. Gas temperature.* $\phi = 100$.

The main projected use of the stochastic fire curves such as Figures 3-15.11 and 3-15.12 is as an input to modules which will calculate the effect of the fire on fire barriers and subsequently trace the possible spread of fire to adjacent compartments. As an illustration of the kind of results obtainable, Hasofer and Beck[42] studied one particular measure of fire severity, normalized heat load, H, proposed by Harmathy and Mehaffy.[45] They obtained histograms of the values of H based on 1500 simulations of the fire curves with $\Phi = 100$ for two cases. In the first case, both the initial burning rate, R_0, and the total fuel mass, B_{max}, were considered as fixed quantities. In this case, in degrees Celsius, the mean of H was 8063.5 and the standard deviation was 849.8. In the second case, R_0 and B_{max} were considered as independent random variables with lognormal distributions. The parameters mean and coefficient of variation had the values of 280 and 0.3 for R_0 and 82.5 and 0.3 for B_{max}. The mean of H increased only slightly to 8222.2, but the standard deviation almost tripled to 2471.6.

A histogram was drawn for the maximum temperature reached, based on 1500 simulations with $\Phi = 100$ and R_0 and B_{max} as independent random variables. This exercise revealed values of 1181.1 and 176.6 for the mean and standard deviation, respectively, of the maximum temperature.

The stochastic model discussed above only takes account of uncertainties governing certain parameters in a deterministic model of fire spread relating to a single material or object. The model does not take account of uncertainties governing the spread of fire from object to object.

However, it may be possible to use the outputs of this model for different objects to construct the matrix of transition probabilities required for a Markov model, discussed earlier, for fire spread from object to object in a room or compartment. Further research in bridging the gap between deterministic fire growth models and stochastic fire growth models is currently being carried out at Victoria University of Technology in Australia.

Other Models

Branching processes[46] can be relevant for fire spread in a building in which a material first ignited (first generation) ignites one or more other materials (second generation), which ignite other materials (third generation), and so on, leading to the spread of fire throughout the building. The number of offsprings (burning materials) vary randomly from one generation to another, depending on the distances between ignited and unignited materials, ventilation, and other factors affecting fire spread. Hence, there is a need to develop a branching process model applicable to random environment.[47]

For predicting the damage to buildings and other properties resulting from incendiary or nuclear attacks, Phung and Willoughby[48] considered two types of stochastic models. In the first model, the entire fire front was regarded as a random walker moving along a linear row of cells or small square areas. In each short time interval the front may be in one of three states: (1) die or stop permanently, (2) spread or move one cell forward, or (3) pause or stay where it is. Simple probability considerations provide an estimate of the probability P_n that, at time t, the fire will be n cell units long after an initial condition of being lit at time zero

$$P_n = \exp\left[-(\lambda + \mu)t\right]\lambda^n t^n$$

The parameters λ and μ are, respectively, the probabilities for forward spread and burnout during a short time interval. The fire will stay where it is, with probability $[1 - (\mu + \lambda)]$.

The second stochastic model of Phung and Willoughby was called *fuel-state* model, because it dealt explicitly with the state of the fuel in each cell. In the burning process, the fuel changes from the unignited to the burnout state passing through the flaming state. A cell will be in one of these three states at any time with probabilities U, F, and B for unignited, flaming, and burnout states, respectively. In a two-dimensional array of cells, the cell dimension can be so chosen that a burning cell can ignite the immediate neighbor cells but not those that are farther away. Under this assumption, an unignited cell can be ignited by one or more of its eight (8) immediate burning neighbors with probability

$$P = 1 - (1 - P_1)(1 - P_2) \ldots (1 - P_8)$$

where P_1, P_2 … P_8 denotes the chances of ignition by the neighbors. These eight spread probabilities are not necessarily symmetrical, due to factors such as wind and topography. Using the formulation described, differential equations are derived for U, F, and B for each cell with the condition $(U + F + B) = 1$, solutions of which can be obtained by numerical calculations using computers, if necessary.

References Cited

1. G. Ramachandran, "Non-Deterministic Modeling of Fire Spread," *Journal of Fire Protection Engineering,* 3(2), pp. 37–48 (1991).

2. A.M. Kanury, "On the Craft of Modeling in Engineering and Science," *Fire Safety Journal,* 12, pp. 65–74 (1987).

3. G. Ramachandran, "Probabilistic Approach to Fire Risk Evaluation," *Fire Technology,* 24, 3, pp. 204–226 (1988).

4. G.N. Berlin, "Probability Models in Fire Protection Engineering," *SFPE Handbook of Fire Protection Engineering* (P.J. DiNenno, et al., eds.), National Fire Protection Association, Quincy, MA (1988).

5. G. Ramachandran, "Stochastic Modeling of Fire Growth," *Fire Safety: Science and Engineering,* ASTM STP 882 (T.A. Harmathy, ed.), American Society for Testing and Materials, Philadelphia, PA, pp. 122–144 (1985).

6. H. Kida, "On the Fluctuations of the Time Required to Extinguish Small Liquid Diffusion Flames with Sprays of Several Salt Solutions," Report of Fire Research Institute of Japan, No. 29, Mitaka, Japan, 25–33 (1969).

7. Y. Aoki, "Studies on Probabilistic Spread of Fire," Research Paper No. 80, Building Research Institute, Tokyo, Japan (1978).

8. G. Ramachandran, "Stochastic Modeling of Fire Growth," CIB Workshop on Mathematical Modeling of Fire Growth, Paris, France (1981).

9. C.R. Theobald, "The Critical Distance for Ignition from Some Items of Furniture," Fire Research Note No. 736, Fire Research Station, Boreham Wood, Herts, U.K. (1968).

10. J.M. Watts, Jr., "Dealing with Uncertainty: Some Applications in Fire Protection Engineering," *Fire Safety Journal,* II, pp. 127–134 (1986).

11. Y. Morishita, "Establishment of Evaluating Method for Fire Safety Performance," *Research Project on Total Evaluating System on Housing Performances,* Building Research Institute, Tokyo, Japan (1977).

12. G.N. Berlin, "Managing the Variability of Fire Behavior," *Fire Technology,* 16, pp. 287–302 (1980).

13. G. Ramachandran, "Probability-Based Fire Safety Code," *Journal of Fire Protection Engineering,* 2(3), pp. 75–91 (1990).

14. V.R. Beck, "A Cost-Effective Decision-Making Model for Building Fire Safety and Protection," *Fire Safety Journal,* 12, pp. 121–138 (1987).

15. A.N. Beard, "A Stochastic Model for the Number of Deaths in a Fire," *Fire Safety Journal,* 4, pp. 169–184 (1981/82).

16. R.B. Williamson, "Fire Performance Under Full-Scale Test Conditions—A State Transition Model," *Sixteenth Symposium (International) on Combustion,* The Combustion Institute, Pittsburgh, PA, pp. 1357–1371 (1976).

17. Y. Morishita, "A Stochastic Model of Fire Spread," *Fire Science and Technology,* 5, 1, pp. 1–10 (1985).

18. J.W.A. Dusing, A.H. Buchanan, and D.G. Elms, "Fire Spread Analysis of Multi-Compartment Buildings," Research Report 79/12, Department of Civil Engineering, University of Canterbury, New Zealand (1979).

19. D.G. Elms and A.H. Buchanan, "Fire Spread Analysis of Buildings," Research Report R35, Building Research Association of New Zealand, Judgeford (1981).

20. D.G. Elms and A.H. Buchanan, "The Effects of Fire Resistance Ratings on Likely Fire Damage in Buildings," Research Report 88/4, Department of Civil Engineering, University of Canterbury, New Zealand (1988).

21. D.G. Platt, "Modeling Fire Spread: A Time-Based Probability Approach," Research Report 89/7, Department of Civil Engineering, University of Canterbury, New Zealand (1989).

22. G. Ramachandran, "Exponential Model of Fire Growth," *Fire Safety Science—Proceedings of the First International Symposium* (C.E. Grant and P.J. Pagni, eds.), Hemisphere Publishing Corporation, New York, pp. 657–666 (1986).

23. G. Heskestad, "Engineering Relations for Fire Plumes," Technology Report 82-8, Society of Fire Protection Engineers, Boston, MA (1982).

24. "Design Guide: Structural Fire Safety, CIB W14 Workshop," *Fire Safety Journal,* 10, 2, pp. 81–138 (1986).

25. W.T.C. Ling and R.B. Williamson, "The Modeling of Fire Spread Through Probabilistic Networks," *Fire Safety Journal,* 9 (1986).

26. G.N. Berlin, A. Dutt, and S.M. Gupta, "Modeling Emergency Evacuation from Group Homes," Annual Conference on Fire Research, National Bureau of Standards, Gaithersburg, MD (1980).

27. P.B. Mirchandani, *Computations and Operations Research,* 3, Pergamon Press, Elmsford, NY, pp. 347–355 (1976).

28. L.G. Benckert and I. Sternberg, "An Attempt to Find an Expression for the Distribution of Fire Damage Amount," *Transactions of the Fifteenth International Congress of Actuaries,* 11, pp. 288–294 (1957).

29. B. Mandelbrot, "Random Walks, Fire Damage Amount and Other Paretian Risk Phenomena," *Operations Research,* 12, pp. 582–585 (1964).

30. G. Ramachandran, "The Poisson Process and Fire Loss Distribution," *Bulletin of the International Statistical Institute,* 43, 2, pp. 234–236 (1969).

31. H. Evring, J.C. Giddings, and L.G. Tensmeyer, "Flame Propagation: The Random Walk of Chemical Energy," *The Journal of Chemical Physics,* 24(4), pp. 857–861 (1956).

32. S. Karlin, *A First Course in Stochastic Processes,* Academic Press, New York (1966).

33. J.M. Hammersley and D.C. Handscomb, "Percolation Processes," *Monte Carlo Methods,* Methuen & Co. Ltd., London, Chapter II (1964).

34. S.R. Broadbent and J.M. Hammersley, "Percolation Processes, 1, Crystals and Mazes," *Proceedings of the Cambridge Philosophical Society,* 53, pp. 629–641 (1957).

35. M. Hori, "Theory of Percolation and Its Applications," *Nippon Tokeigakkai-shi,* 3, p. 19 (1972).

36. H. Sasaki and T. Jin, "Probability of Fire Spread in Urban Fires and Their Simulations," Report No. 47, Fire Research Institute, Tokyo, Japan (1979).

37. J. Nahmias, H. Tephany, and E. Guyon, "Propagation de la Combustion sur un Reseau Heterogene Bidimensionnel," *Revue Phys. Appl.,* 24, pp. 773–777 (1989).

38. F.A. Albini and S. Rand, "Statistical Considerations on the Spread of Fire," IDA Research and Engineering Support Division, Washington, DC (1964).

39. N.J.T. Bailey, "Reed and Frost Model," *The Elements of Stochastic Processes,* John Wiley and Sons, New York, Chapter 12, Section 5 (1964).

40. P.H. Thomas, "Some Possible Applications of the Theory of Stochastic Processes to the Spread of Fire," Internal Note No. 223, Fire Research Station, Boreham Wood, Herts, U.K. (1965).

41. G. Ramachandran, "Heat Output and Fire Area," *Proceedings of the International Conference on Fire Research and Engineering,* Society of Fire Protection Engineers, Orlando, FL, pp. 481–486 (1995).

42. A.M. Hasofer and V.R. Beck, "A Stochastic Model for Compartment Fires." *Fire Safety Journal,* 28, pp. 207–225 (1997).

43. D.D. Drysdale, *An Introduction to Fire Dynamics,* John Wiley and Sons, Chichester, UK (1985).

44. H. Takeda and D. Yung, "Simplified Fire Growth Models for Risk-Cost Assessment in Apartment Buildings," *Journal of Fire Protection Engineering,* 4, 2, pp. 53–66 (1992).

45. T.Z. Harmathy and J.R. Mehaffy, "Normalized Heat Load: A Key Parameter in Fire Safety Design," *Fire and Materials,* 61, pp. 27–31 (1982).

46. T.E. Harris, *The Theory of Branching Processes,* Springer-Verlag, Berlin (1963).

47. W.E. Wilkinson, "Branching Processes in Stochastic Environments," Ph.D. Thesis, University of North Carolina, Chapel Hill (1968).

48. P.D. Phung and A.B. Willoughby, "Prediction Models for Fire Spread Following Nuclear Attacks," Report No. URS641-6, URS Corporation, Burlingame, CA (1965).

CHAPTER 16

Explosion Protection

Robert Zalosh

Introduction

Combustible gases, vapors, and dusts/powders represent explosion hazards when and if they are mixed with air (or some other oxidant) in proportions between the lower and upper flammable limits. The explosion hazard is associated with the premixing of fuel and oxidant in a confined environment prior to the introduction of an ignition source. Upon ignition, flame propagates through the fuel-oxidant mixture, and the confinement prevents the unrestrained expansion of the combustion products. The result is the rapid development of a potentially damaging pressure increase.

Explosion hazard evaluations usually entail (1) recognizing the potential formation of a flammable fuel-air mixture, (2) identifying potential ignition sources present after fuel-air mixture formation, and (3) determining the resulting explosion pressures and their implications with regard to structural damage potential. Explosion protection measures interrupt this sequence of explosion events either by (1) preventing fuel-air mixture formation (e.g., by ventilation or inerting), (2) eliminating potential ignition sources (e.g., by grounding equipment to prevent electrostatic discharges), or (3) limiting pressure buildup (e.g., by explosion venting or explosion suppression). This chapter provides an engineering framework for performing this type of explosion hazard and protection measure evaluation.

Flammability, Explosibility, and Inerting

Gases and Vapors

Flammable limit concentrations for gases and vapors are traditionally determined in a glass test vessel that al-

lows observation of any flame propagation. In some cases, the test vessel is a 5- to 10-cm-diameter, 1.5-m-long, glass tube,[1] while in other cases a 5-liter-capacity (22-cm-diameter) flask is used.[2] A spark situated either at the open lower end of the tube, or near the center of the flask is triggered to determine the flammability of a gas-air mixture of known concentration. If ignition results in flame propagation to the top of the tube, or upward and outward from the center of the flask,[2] the mixture is deemed flammable. The lower flammable limit is the average value of (1) the lowest gas/vapor concentration capable of supporting flame propagation and (2) the largest concentration that does not result in flame propagation. Similarly, the upper flammable limit is average value of (1) the highest gas/vapor concentration for which flame propagation is observed and (2) the lowest concentration at which there is no propagation. The chapter in this handbook entitled "Flammability Limits of Premixed and Diffusion Flames" (Section 2, Chapter 7) has tabulated values of the lower and upper flammable limits reported previously by Zabetakis.[1]

Flammability limit testing is also sometimes performed in pressure vessels that allow pressure increases to indicate flame propagation. Since this type of test is a more direct measure of explosion hazards, the data are usually called explosion limits. In some cases (e.g., methane lower limit and hydrogen upper limit) the flammability limits and explosibility limits are virtually the same, but in other cases (e.g., methane upper limit and hydrogen lower limit) there can be substantial differences. In practice, flammability limits are used when the criterion is the prevention of flame propagation, and explosibility limits are used either when the criterion is the avoidance of a significant overpressure, or when flammability limits are needed at elevated temperatures or pressures.[3] Upper flammable limits are more sensitive to pressure variations than lower limits, except at very low pressures (typically less than one-tenth of an atmosphere) where the two limits suddenly narrow and the gas or vapor becomes nonflammable.[4]

The maximum safe oxygen concentration for explosion prevention via inerting is called the limiting oxidant

Dr. Robert Zalosh is a professor of fire protection engineering at Worcester Polytechnic Institute. He previously worked for Factory Mutual Research Corporation where he initiated the explosion research group and was manager of the applied research department. Professor Zalosh has been a member of the NFPA Committee on Explosion Protection Systems for more than 20 years.

concentration (LOC) in NFPA 69, *Standard on Explosion Prevention Systems*, 1997 edition.[5] Representative values for the limiting oxygen concentration for nitrogen inerting and carbon dioxide inerting are listed in Table 3-16.1. The LOC for carbon dioxide inerting of all of the flammable vapors/gases in Table 3-16.1 except hydrogen is in the range 11.5 to 14.5 volume percent, whereas the corresponding range for nitrogen inerting is 9.5 to 12 volume percent.

The volume percent of inert gas needed to reduce the oxygen concentration to the LOC values shown in Table 3-16.1 is

$$\% \text{ Inert} = 100 - 4.76(\text{LOC})[1 + (F/A)] \qquad (1)$$

where F/A is the fuel/air volumetric ratio for the most challenging gas-air mixture for inerting. Values of F/A can be determined if the complete fuel-air-inert flammability diagram is available. Flammability diagrams for methane and for *n*-hexane are given in the chapter "Flammability Limits of Premixed and Diffusion Flames." The F/A corresponding to the nose of the methane flammability diagram is the stoichiometric ratio of 0.105. The F/A corresponding to the nose of the *n*-hexane flammability diagram is approximately 0.03, which is somewhat greater than the stoichiometric ratio for hexane-air. Since

the worst-case F/A value is $\ll 1$ for most flammable gases and vapors, a reasonably conservative approximation for use in the absence of the complete flammability diagram would be to set $F/A = 0$ in evaluating the volume of inert gas needed via Equation 1.

It is important to recognize that practical applications of flammability/explosibility data for explosion hazard evaluations should account for nonuniform or stratified vapor-air mixtures. The accuracy, response-time, and reliability of the oxygen monitoring instrumentation is another important consideration. Based on these considerations, the guidelines for inerting systems given in NFPA 69 state that the maximum allowable oxygen concentration should be at least 2 volume percent below the LOC when the concentration is continuously monitored. If the oxygen concentration is not continuously monitored, a greater margin of safety is needed.

Combustible Dusts and Powders

Combustible dusts and powders pose a potential explosion hazard when their characteristic particle size is smaller than 100 to 400 micrometers (depending on material combustibility) and they are suspended in air at a concentration between the lower and upper explosive limits. Typical lower explosive limits for dusts with characteristic particle sizes less than about 100 micrometers are in the 30- to 60-g/m^3 range, which is roughly equal to the range for many flammable gases and vapors when expressed in these units. The upper explosive limit for dusts is typically[4] between 2000 and 6000 g/m^3, but it is a difficult measurement to make and an even more difficult measurement to apply as a practical explosion prevention measure.

Contemporary laboratory testing to determine dust explosibility is conducted with a near-spherical vessel of 20- to 30-liter volume. Figure 3-16.1 is a schematic drawing of a typical 20-l spherical apparatus. The weighed dust sample is placed into an auxiliary dust chamber and is air-injected into the sphere via a perforated dispersion

Table 3-16.1 *Limiting Oxygen Concentrations for Fuel-Air Mixtures with Added N_2 or CO_2[5]*

Fuel	Limiting Oxygen Concentration for Nitrogen Inerting	Limiting Oxygen Concentration for Carbon Dioxide Inerting
Gases and vapors		
Acetone	11.5	14
n-Butane	12	14.5
Ethanol	10.5	13
Ethylene	10	11.5
n-Heptane	11.5	14.5
Hydrogen	5.0	5.2
Methane	12	14.5
Methyl Ether	10.5	13
Propane	11.5	14.5
Toluene	9.5	—
Combustible dusts		
Aluminum	5	2
Cellulose Acetate	9	11
Coal, Bituminous	14	17
Coal, Subbituminous	—	15
Corn Starch (17 μm)	9	—
Epoxy Resin	—	12
Nylon	—	13
Polycarbonate	—	15
Silicon	11	12
Stearic Acid and Metal Stearates	10.6	13
Sulfur	—	12
Zinc	9	10
Zirconium	0	0

Figure 3-16.1. *Twenty-liter spherical dust explosion apparatus.*

ring. An electrical spark or pyrotechnic igniter located in the center of the sphere ignites the dust cloud after a suitable time delay for dispersion. ASTM E1515,[6] the American standard for determining the minimum explosible concentration (MEC), specifies using either a 2500 J or 5000 J pyrotechnic igniter in a 20-l test vessel. Results are sensitive to the ignition source used and the level of turbulence in the test vessel at the time of ignition. In some cases, MEC results are so sensitive to the igniter energy that tests are needed in a 1-m³ vessel to minimize ignition energy effects.

Minimum explosible dust concentrations, as determined in a 1-m³ vessel, are shown in Table 3-16.2 for representative industrial and agricultural dusts. More comprehensive tabulations are available.[7,8] The MEC for a given material generally decreases with decreasing particle size, until a limiting size is reached, below which there is no further reduction of the MEC. Apparently, the combustion reaction is limited by the rate of devolatilization (which is dependent on particle surface area) at particle diameters above this limiting size, whereas the flame propagation rate is limited by vapor phase thermochemistry below this limiting size. This explanation is consistent with the equivalence of flammable gas and small-particle combustible dust lower limit concentrations for generically similar materials. For a given material and particle size, the MEC decreases linearly with increasing temperature.[9]

One inherent difficulty in using minimum explosible concentration data is the unknown or deceivingly minimal dust concentrations in many industrial facilities. An example might be a situation in which there is concern about possible explosive dust concentrations in a plastic powder silo. Even if suspended dust concentrations were measured during normal loading and unloading operations, considerably higher concentrations can be generated during upset conditions such as the use of vibrations or air blasts to dislodge powder flow obstructions.

One dust explosion prevention measure for equipment in which dust concentrations cannot be maintained below the MEC, is to use an inert gas to reduce the oxygen concentration. Limiting oxygen concentration data for several dusts are shown in Table 3-16.1. The data for carbon dioxide inerting of organic dusts are in the range 11 volume percent to 15 volume percent, but the LOC values for some of the metals are significantly lower. In fact, the zero LOC for zirconium is indicative of its pyrophoric behavior as a powder. As with the MEC, the LOC for a given dust decreases linearly with increasing temperature, according to the correlations presented by Siwek.[9]

The minimum ignition temperature (MIT) for a dust cloud is usually determined in an apparatus known as the Godbert-Greenwald furnace. A dust sample is air-injected into the top of the preheated vertical tube, and thermocouple measurements indicate whether the dust is ignited before it exits the bottom of the tube. Most of the dusts listed in Table 3-16.2, and in the more extensive tabulation by Eckhoff,[7] have cloud MIT values in the range 440°C to 750°C.

Dust layer ignition temperatures are usually measured using a 5-mm-thick layer of dust deposited on a hot plate with a temperature control. The temperature is in-

Table 3-16.2 *Explosibility Data for Representative Powders and Dusts[7]*

Material	Median Particle Size (μm)	Minimum Explosive Concentration (g/m³)	Minimum Cloud Ignition Temp (°C)	Minimum Layer Ignition Temp (°C)	Minimum Ignition Energy (mJ)	P_{max} (bar·g)	K_{ST} (bar·m/s)
Activated carbon	18	60	790	>450	—	8.8	44
Aluminum	<10	60	560	430	—	11.2	515
Ascorbic acid	39	60	460	Melts	—	9.0	111
Calcium stearate	<10	30	580	>450	16	9.2	99
Coal, bituminous (high volatility)	4	60	510	260	—	9.1	59
Corn starch	<10	—	520	>450	300	10.2	128
Epoxy resin	26	30	510	Melts	—	7.9	129
Fructose	200	60	440	440	180	7.0	28
Methyl cellulose	37	30	410	450	29	10.1	209
Milk powder	165	60	460	330	75	8.1	90
Napthalene	95	15	660	>450	<1	8.5	178
Paper tissue dust	54	30	540	300	—	8.6	52
Phenolic resin	<10	15	610	>450	—	9.3	129
Polyethylene, l.d.	<10	30[a]	420	Melts	—	8.0	156
Polyethylene, l.d.	150	125	480	Melts	—	7.4	54
Polyvinylchloride	25	125	750	>450	>2000	8.2	42
Rubber	80	30	500	230	13	8.5	138
Silicon	<10	125	>850	>450	54	10.2	126
Sugar	10	60	440	Melts	14	8.3	75
Zinc	<10	250	570	440	—	6.7	125

[a]This MEC for polyethylene was determined in a 1.2 liter cylinder.

creased slowly until the dust layer begins to glow. As is evident from the data in Table 3-16.2, the dust layer ignition temperature is often significantly lower than the dust cloud minimum ignition temperature. This is a ramification of the increased heat dissipation rates in a dust cloud compared to the interior of a dust layer.

An important consideration in applying the dust cloud and dust layer ignition temperature data is the frequent occurrence of nonuniform hot wall temperatures. An example is the situation in which a small hot spot is created by mechanical friction, perhaps in a blender or a pulverizer. Data presented by Siwek and Cesana[10] suggest that the small spot (with a temperature of at least 900°C) in a mill or similar process equipment can ignite a dust cloud if the MIT < 600°C as determined in furnace tests.

The minimum ignition energy (MIE) for an electrical spark discharge within a combustible dust cloud is measured via a standardized test conducted in a 1.2-l cylindrical tube, sometimes called a modified Hartmann tube. The International Electrotechnical Commission (IEC) test method described by Siwek and Cesana[10] allows for spark energies in the range from 1 mJ to several hundred mJ. MIE data for the dust samples in Table 3-16.2 range from less than 1 mJ to more than 2000 mJ. For a given material, the MIE is known to be influenced by the following parameters:

- The MIE decreases as the spark duration increases, due to the presence of either inductance or resistance in the capacitive discharge circuit. For example, adding a series inductance in the range 0.1 to 1.0 H, or a series resistance in the range 10^4 to 10^5 Ω, decreases the MIE by an order of magnitude. The practical significance of this is that it takes more spark energy for an electrostatic (capacitive) discharge to ignite a dust cloud than for a spark in electrical equipment due perhaps to actuation of an electromechanical switch. The MIE data in Table 3-16.2 were obtained with long duration inductive discharges.
- The MIE decreases as the dust median particle size increases; Siwek and Cesana[10] show that the variation is to the –2.5 power of particle diameter.
- The MIE varies with dust concentration, but the most sensitive concentration depends on the particular material. The data in Table 3-16.2 are for the most sensitive concentration.
- The MIE decreases with increasing air-dust temperature.
- The MIE and the MIT increase with increasing velocity of the dust-air mixture.

The theoretical spark energy can be calculated for simple electrical discharges. For example, the energy (J) in a purely capacitive discharge is $1/2CV^2$, where C is the capacitance (F), and V is the stored voltage prior to discharge. In the case of a purely inductive circuit, the theoretical spark energy is $1/2Li^2$, where L is the circuit inductance, and i is the current (A). The inductance spark energy can be compared directly to the MIE for a particular dust to assess the likelihood of ignition; the capacitive spark energy comparison should account for the higher ignition energies associated with short duration capacitive discharges. The energy associated with mechanical fric-

tion and impact sparks is much more difficult to determine. Siwek and Cesana[10] state that such sparks will only ignite dusts with MIE values <10 mJ and MIT values <500°C.

EXAMPLE 1:

Coal feed rates and airflow rates at two coal pulverizers are as follows. At Pulverizer A the bituminous coal feed rate is 1.9 kg/s and the airflow rate is 7.1 m^3/s. At Pulverizer B the coal feed rate is 13.9 kg/s and the airflow rate is 7.1 m^3/s.

Are the pulverizer outlet coal dust concentrations within the explosive range? If both coals have a Godbert-Greenwald furnace ignition temperature of 510°C, would you expect a dust explosion to occur if there is a frictional hot spot or a frictional spark in the pulverizer?

SOLUTION:

The pulverizer outlet coal dust concentration during steady-state operation is equal to the coal feed rate divided by the airflow rate. The concentrations for these two pulverizers are 0.27 kg/m^3 for Pulverizer A and 1.96 kg/m^3 for Pulverizer B. The Pulverizer A concentration is well within the explosive limits for typical bituminous coals. The Pulverizer B concentration is close to the reported upper explosive limit for coal (2 to 4 kg/m^3). Since the MIT of both coals is in the range 500 to 600°C, we would expect them to be ignitable by sustained mechanical friction that produces wall temperatures in the range 600 to 900°C depending on the size of the heated area; we would not expect ignition by short-duration mechanical impact sparks because the cloud MIT is greater than 500°C. This suggests that a temperature monitor in the pulverizer could be used to shut down the pulverizer well before the wall temperature approaches 600°C, either from mechanical friction or smoldering coal.

EXAMPLE 2:

An elevated silo with an electrical capacitance of 500 picofarads is used to store a pharmaceutical powder with a minimum ignition energy of 10 mJ for inductive sparks and 50 mJ for capacitive sparks. If the silo is not adequately grounded, what would its minimum voltage have to be in order for an electrostatic spark to ignite the cloud of powder in the silo, or being discharged from the silo?

SOLUTION:

The voltage needed to generate an electrostatic spark of capacitive energy E is equal to $\sqrt{2E/C}$, which in this case is equal to

$$\sqrt{\frac{2(50 \times 10^{-3} \text{ J})}{500 \times 10^{-12} \text{ F}}} = 1.4 \times 10^4 \text{ V} = 14 \text{ kV}$$

A very high voltage of this magnitude may indeed be generated from the continuous impact/friction of the powder during filling and unloading. Although grounding of the silo would prevent high voltage from accumulating on the silo itself, there is also a hazard associated with electrostatic charge accumulation on ungrounded

objects and equipment in the silo, and possibly on the powder itself if it has a high electrical resistivity.

Closed Vessel Deflagrations

Ignition of either a gas-air mixture or a dust cloud in an unvented enclosure will usually result in a deflagration (i.e., flame propagation at subsonic speed away from the ignition site). The pressure developed in the enclosure is dependent on the extent of flame propagation, and the temperature and composition of the burned gas. If the flame has propagated throughout the enclosure, the ratio of the deflagration pressure to the initial pressure in the enclosure can be obtained from the ideal gas equation as it applies to the postdeflagration and predeflagration gas-air mixtures, both of which occupy the same enclosure volume. Thus

$$\frac{P_m}{P_0} = \frac{n_b T_b}{n_0 T_0} \tag{2}$$

where

P_m = pressure developed at the completion of a closed vessel deflagration

P_0 = initial pressure in the enclosure

n_b = number of moles of burned gas at the completion of the deflagration

n_0 = number of moles of gas-air mixture initially in the enclosure

T_b = temperature of the burned gas at the completion of the deflagration

T_0 = initial temperature of the gas-air mixture

Equation 2 is applicable to both gas deflagrations and dust deflagrations. However, in the case of dust deflagrations, the effect of the dust does not appear explicitly in the equation because only the gas temperature and composition determine the deflagration pressure. Conservative estimates of burned gas temperature and composition can be obtained using the assumption that combustion occurs adiabatically at constant volume. Thus, the calculation of deflagration pressures becomes an exercise in thermochemical equilibrium in which the initial fuel-oxidant mixture is specified to react adiabatically at constant volume. Various computer codes can be used to do these calculations.

Calculated results obtained with the STANJAN code (written and distributed by Professor William Reynolds of Stanford University) are shown in Figure 3-16.2(a) for the adiabatic, constant-volume flame temperature, for methane-air, propane-air, and hydrogen-air mixtures of varying concentration. The fuel concentration used in Figure 3-16.2 is the equivalence ratio, defined as the fuel-to-air ratio divided by the stoichiometric fuel-to-air ratio. In terms of fuel volume fraction, x, the equivalence ration is equal to $[x(1 - x_{st})]/[x_{st}(1 - x)]$, where x_{st} is the stoichiometric volume fraction of fuel. The stoichiometric fuel volume fraction for methane–air is 0.095, for propane–air is 0.040, and for hydrogen–air is 0.296. The calculated adiabatic constant-volume flame temperatures shown in Figure 3-16.2(a) are generally 200°C to 400°C higher than the

corresponding adiabatic, isobaric flame temperatures for the same fuel–air concentrations.

Calculated adiabatic constant-volume deflagration pressures for the same fuel-air mixtures are shown in Figure 3-16.2(b). The maximum pressures for each flammable gas occur at fuel equivalence ratios in the range 1.1 to 1.2 (i.e., at slightly richer than stoichiometric concentrations). These worst-case deflagration pressures are in the range 8 to 9.6 atm abs. Theoretical values of P_m at an equivalence ratio of 0.5, which corresponds to the lower flammable limit for methane and propane, are in the range 6 to 6.5 atm abs. Experimental measurements of closed vessel deflagration pressures agree well with the theoretical values of P_m at near-stoichiometric concentrations, but are significantly less than the theoretical values at concentrations near the lower and upper flammable limits. The reasons
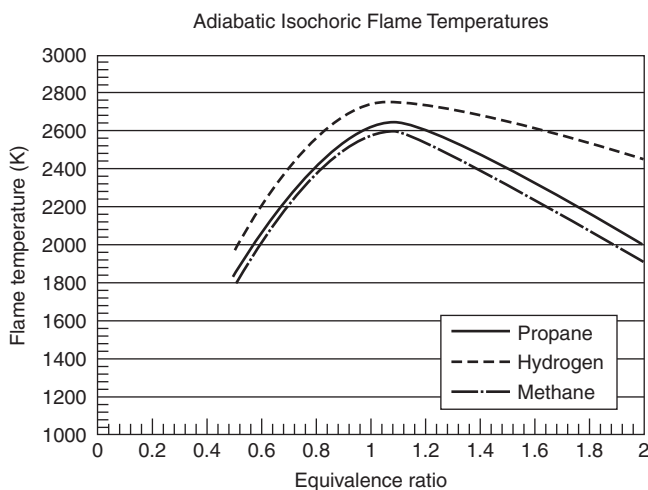
Figure 3-16.2(a). *Calculated adiabatic, constant-volume flame temperatures as a function of equivalence ratio.*
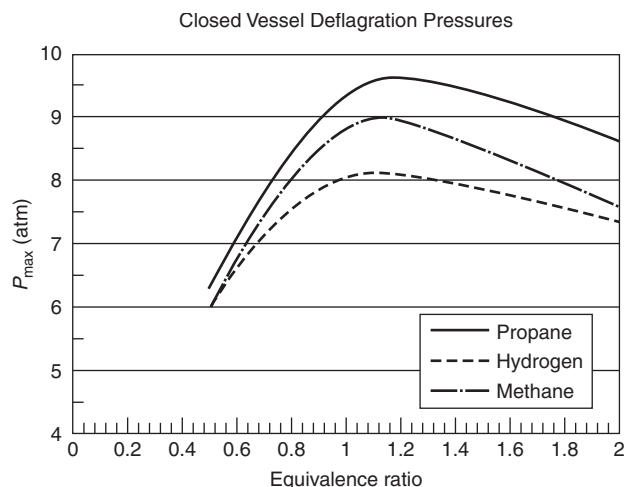
Figure 3-16.2(b). *Flammable gas-air deflagration pressures as a function of fuel equivalence ratio.*

for the deviation at near-limit concentrations are 1) incomplete combustion due to flame propagation through only a portion of the enclosure and 2) slow flame propagation allowing time for heat losses from the burned gas mixture to the enclosure walls. As an example of the incomplete combustion, extensive deflagration testing of lean hydrogen–air mixtures has shown that the fraction of hydrogen burned ranges from zero to one as the hydrogen concentration increases from its lower limit of 4 volume percent to 8 volume percent, and remains equal to approximately one (complete combustion) as the hydrogen concentration ranges from 8 volume percent to about 40 volume percent (equivalence ratio of 1.6).

Measured values of P_{max} (worst-case P_m) are shown in Table 3-16.3 for twelve flammable gases and vapors. All but two values are in the range 6.8 bar to 8.1 bar g. The two exceptions are acetylene (P_{max} = 10.6 bar g) and ammonia (P_{max} = 5.4 bar g).

Theoretical values of P_m can also be calculated for combustible dusts using a thermochemical equilibrium computer code, such as the NASA code CET89, that contains extensive properties for condensed phase materials. Experimental values of P_m depend on particle size as well as dust concentration. The effect of particle size is illustrated by the data in Figure 3-16.3. The value of P_{max} for three of the four dusts is invariant with particle size providing the median particle diameter is no greater than 100 μm. However, for polyvinylchloride (which is significantly less combustible than the other three materials), P_{max} decreases with increasing median particle size for all particles greater than 20 μm, and cannot be ignited at all at particle sizes of 150 μm and larger. The effect of dust concentration on P_{max} is such that the worst-case concentration often occurs at a concentration of about 500 g/m³, which for many organic materials is roughly twice the stoichiometric concentration, and five to ten times the minimum explosible concentration. Values of P_{max} for the twenty dust samples listed in Table 3-16.2 are in the range 6.7 bar g to 11.2 bar g (i.e., about the same range as the values of P_{max} for flammable gases and vapors).

Figure 3-16.3. *Effect of particle size on deflagration pressure and rate-of-pressure rise.[8]*

The rate of pressure rise during a deflagration is primarily dependent on the rate of flame propagation and the vessel size, as well as the flame temperature. Theoretical calculations are usually based on the following assumptions. First, it is assumed that the flame speed is small in comparison to sound speed so that the pressures in the enclosure are spatially uniform at any given time during the deflagration. The rate of flame propagation relative to the unburned gas ahead of the flame front is called the burning velocity, S_u. The mass burning rate is

$$\frac{dm_b}{dt} = -\frac{dm_u}{dt} = \rho_u \chi S_u A_f \qquad (3)$$

where

m_b = mass of burned gas in enclosure at time t

m_u = mass of unburned gas in enclosure at time t

ρ_u = density of unburned gas at time t

A_f = surface area of flame front at time t

χ = ratio of turbulent burning velocity to laminar burning velocity

Flame propagation into a near-stoichiometric gas-air mixture will occur as an expanding spherical flame until the flame approaches the walls of the enclosure. Laminar burning velocities have been measured for worst-case concentrations of many gases and vapors. Values are listed for the twelve gases/vapors in Table 3-16.3. Representative

Table 3-16.3 *Deflagration Parameters for Flammable Gases and Vapors in Air[8]*

Gas or Vapor	P_{max} (bar g)	Laminar Burning Velocity (cm/s)	K_G (bar·m/s)
Acetylene	10.6	166	1415
Ammonia	5.4	—	10
n-Butane	8.0	45	92
Diethyl ether	8.1	47	115
Ethane	7.8	47	106
Hydrogen	6.8	312	550
Isopropyl alcohol	7.8	41	83
Methane	7.1	40	55
Methyl alcohol	7.5	56	75
n-Pentane	7.8	46	104
Propane	7.9	46	100
Toluene	7.8	41	94

values for the alkanes and many other hydrocarbons are 40 to 47 cm/s. Expansion of the burned gas, and the corresponding motion of the unburned gas away from the ignition site as the flame propagates, causes the actual flame velocity relative to a fixed observer (i.e., the flame speed) to be significantly larger than the burning velocity. Before any compression occurs, the flame speed is $(T_b/T_0)S_u$, which is equal to 350 to 440 cm/s for many hydrocarbons at near-stoichiometric concentrations. Turbulent motion of the unburned gas can further increase the burning velocity and flame speed, as represented either by the augmentation factor χ, or by generating wrinkled or distorted flames with corresponding larger flame surface areas, A_f.

A second key assumption invoked in most theoretical models of closed vessel deflagrations is that the fractional pressure rise at any time during the deflagration is equal to the fraction of the total mass burned, that is,

$$\frac{P - P_0}{P_m - P_0} = \frac{m_b}{m_0} \tag{4}$$

where

P = deflagration pressure at time t

m_0 = total mass in the enclosure

The justification for Equation 4 is that it has been verified by more complicated models, such as the Complete Computer Solution described by Bradley and Mitcheson,[11] as well as by experimental data reported in that paper and in Lewis and von Elbe.[12] Equation 4 can also be used to calculate the maximum pressure developed in enclosures that are partially with fuel-air mixtures (i.e., partial volume deflagrations).

The third assumption needed for a closed vessel deflagration model is the type of thermodynamic process undergone by the unburned gas as it is compressed. The most common assumption is that the unburned gas is compressed isentropically [i.e., $P/P_0 = (\rho/\rho_u)^\gamma$], where γ is the ratio of specific heats of the unburned gas (1.4 for most flammable hydrocarbon-air mixtures). Although it is not necessary, it is also common to assume the flame continues to propagate spherically such that its radius at any time t is r_b in a vessel of radius a. The resulting equations for $P(t)$ and $r_b(t)$ are

$$\frac{dP}{dt} = \frac{3\chi S_u}{a} \left(\frac{P}{P_0}\right)^{1/\gamma} (P_m - P_0)\left(\frac{r_b}{a}\right)^2 \tag{5}$$

$$\left(\frac{r_b}{a}\right)^2 = \left[1 - \left(\frac{P_0}{P}\right)^{1/\gamma}\left(\frac{P_m - P}{P_m - P_0}\right)\right]^{2/3} \tag{6}$$

Equations 5 and 6 can be solved simultaneously starting from the initial condition that $r_b/a = \varepsilon$ at $t = 0$, where ε is some small number $\ll 1$ representing the kernel of flame at ignition. An example solution for $P(t)$ and $r_b/a(t)$ for the case $S_u = 45.5$ cm/s, $\chi = 1$, $P_m = 640$ kPa g, $a = 7.15$ m is shown in Figures 3-16.4(a) and 3-16.4(b). The curve in Figure 3-16.4(a) labeled *numerical solution* refers to the numerical integration of Equation 5. The curve labeled *analytical*
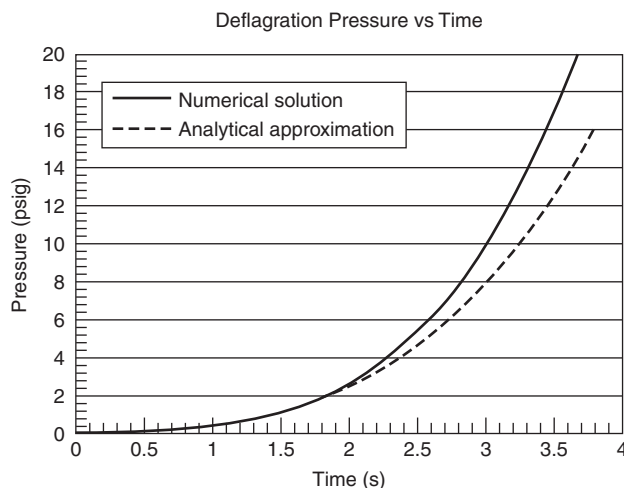
Figure 3-16.4(a). *Pressure versus time for a closed vessel deflagration with $S_u = 45.5$ cm/s, $a = 7.15$ m, and $P_m = 640$ kPa g.*
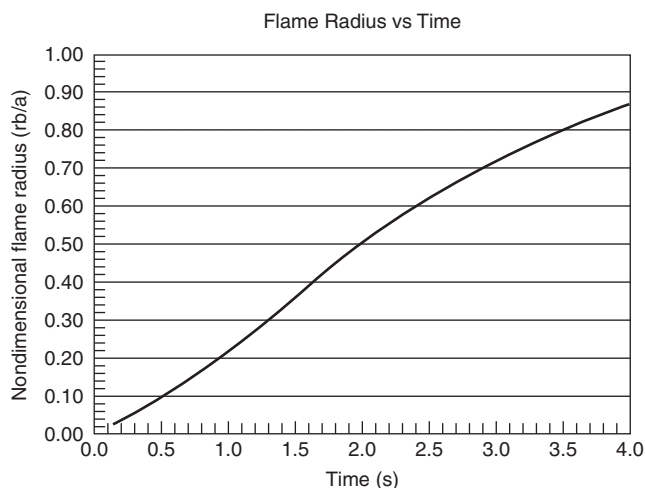
Figure 3-16.4(b). *Calculated nondimensional flame radius during deflagration.*

approximation refers to the following simplified solution for $P(t)$ early in the deflagration when $(P - P_0)/P_0 \ll 1$.

$$\frac{P - P_0}{P_0} = \left(\frac{1}{\gamma} + \frac{P_0}{P_m - P_0}\right)^2 \left(\frac{P_m - P_0}{P_0}\right)^3 \left(\frac{\chi S_u t}{a}\right)^3 \ll 1 \tag{7}$$

The analytical approximation in Figure 3-16.4(a) is virtually identical to the numerical solution when $P < 2$ psig, and only differs by about 20 percent up to $P = 8$ psig. The flame radius at the time $P = 2$ psig is equal to half the enclosure vessel radius, and it is equal to 80 percent of the vessel radius when $P = 16$ psig. Since the pressure ultimately increases to 93 psig in this particular deflagration, it is clear that most of the pressure increase occurs when

the flame has propagated very close to the enclosure wall, such that the entire enclosure is almost filled with flame.

The continued integration of Equation 5 up to $P = P_m$ would require an empirical correlation to account for the variation of S_u with increased pressure and temperature of the unburned gas as it is compressed. Bradley and Mitcheson[11] have carried out nondimensionalized solutions using such correlations. Their results indicate that the time, t_m, at which P reaches P_m can be approximated as

$$t_m = \frac{a}{0.3S_u}$$

where the burning velocity is the mean value of the burning velocities at the beginning and end of the deflagration (i.e., when $P = P_0$ and $P = P_m$). In other words, the mean flame speed, a/t_m, during the deflagration is equal to 3.3 times the mean burning velocity.

Experimental measurements of the rate-of-pressure-rise in a closed vessel explosion are often characterized in terms of the parameter, K_G, defined as

$$K_G = \left(\frac{dP}{dt}\right)_{max} V^{1/3} \tag{8}$$

where V is the vessel volume, and the maximum rate of pressure rise is measured at the inflection point in the P-versus-time curve. Theoretically, there is no inflection point (because there is no heat loss or other mechanism to decelerate the flame), and $(dP/dt)_{max}$ occurs when $P = P_m$. Based on Equation 5, the theoretical relationship between K_G and S_u is

$$K_G = 4.84\chi S_u \left(\frac{P_m}{P_0}\right)^{1/\gamma} (P_m - P_0) \tag{9}$$

Experimentally determined values of K_G listed in Table 3-16.3 for the various gases and vapors indicate that they generally increase as S_u increases, but that they are not necessarily linearly proportional to S_u. This is a manifestation of the fact that the turbulence factor, χ, varies among the individual gases and vapors in a manner that cannot be predicted a priori.

The effect of turbulence on the rate-of-pressure-rise is even more important in the case of dust explosions. There is inherently some level of turbulence in every dust explosion because some type of disturbance or initial motion is needed to generate the dust cloud. One convenient, albeit indirect, measure of the turbulence level is the time delay between the beginning of dust injection and ignition actuation. The turbulent motion in the vessel is a maximum when the dust is first injected, and decays significantly by the time the entire dust cloud has entered the vessel. Figure 3-16.5 shows how the ignition delay time influences the values of P_{max} and $(dP/dt)_{max}$ measured in a 1-m³ vessel with coal dust and with aluminum dust. In view of the importance of this effect, a standardized test method has been developed[13] in the interest of obtaining reproducible results in different test vessels and laboratories. Values of $K_{ST} = [(dP/dt)_{max}]V^{1/3}$ obtained for various dusts using this standardized injection and ig-
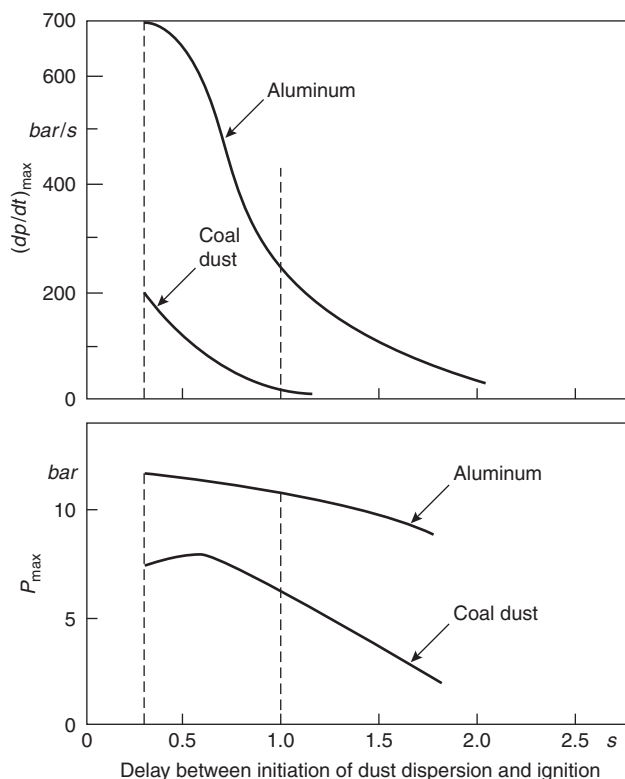
Figure 3-16.5. *Effect of ignition delay time on deflagration pressure and rate-of-pressure-rise.*[7]

nition delay methodology are listed in Table 3-16.2. Except for aluminum, all of the dusts listed have K_{ST} values no greater than 208 bar·m/s. A more direct measure of turbulence level is the root-mean-square fluctuating air velocity in the vessel. Measurements of this rms velocity as a function of time following the initiation of dust injection have been carried out by several researchers and their results are summarized in Eckhoff's textbook.[7] Eckhoff also provides a summary of some theoretical models for closed vessel dust deflagrations that are analogous to the one described for gas explosions, but account for the finite particle burn time and corresponding finite flame thickness in dust explosions.

One special consideration in dust explosions is the propensity for damaging secondary explosions. These secondary dust explosions arise when a gas or dust deflagration in some process equipment causes the equipment to fail (because it cannot withstand the closed vessel deflagration pressure, P_{max}), and produce a strong disturbance in the form of a blast wave and associated air motion. This disturbance often causes the dust that has settled on walls and floors to be put into suspension and form a combustible dust cloud. Even if the subsequent cloud occupies only a small fraction of the building, it is often ignited by the flame that has also emerged from the breached process equipment. If the secondary explosion occurs in an occupied building, it can produce numerous

casualties as well as building structural damage. The quantities of dust needed to generate a particular pressure rise can be estimated using Equation 4.

EXAMPLE 3:

Approximately 200 g of *n*-butane are released into an aerosol can–filling room due to a valve misalignment on one large deodorant can. Suppose the butane mixes in stoichiometric proportions with a portion of the air in the $4 \times 4 \times 3$ m room and is subsequently ignited. What will the peak pressure be in the absence of any explosion venting?

SOLUTION:

Equation 4 can be used to solve this problem if we first calculate the mass of butane needed to fill the entire room with a stoichiometric butane-air mixture. We can do this calculation in terms of the mixture density, ρ_0, and the butane mass fraction as follows:

$$m_0 = \left(\frac{x_{but}M_{but}}{M_{mix}}\right)\rho_0 V$$

where the mixture molecular weight, M_{mix}, is calculated based on the stoichiometric concentration of butane (3.1 volume percent).

$$M_{mix} = x_{but}M_{but} + (1 - x_{but})M_{air}$$
$$= (0.031)(58) + (1 - 0.031)(28.8) = 29.7$$

The mixture density (which is not much different than air density) is calculated from the ideal gas equation:

$$\rho_0 = \frac{M_{mix}P_0}{RT_0} = \frac{(29.7 \text{ kg/kmol})(101 \times 10^3 \text{ Pa})}{(8314 \text{ J/kmol} - \text{K})(298 \text{ K})}$$
$$= 1.21 \text{ kg/m}^3$$

Therefore, $m_0 = \left[\dfrac{(0.031)(58)}{29.7}\right](1.21 \text{ kg/m}^3)(48 \text{ m}^3)$
$$= 3.52 \text{ kg.}$$

and $m_b/m_0 = (0.20 \text{ kg})/(3.52 \text{ kg}) = 0.057.$

Using the value for $P_m - P_0$ for *n*-butane in Table 3-16.3,

$$P - P_0 = (8.0 \text{ bar g})(0.057) = 0.456 \text{ bar g} = 6.6 \text{ psig.}$$

We note that since this pressure is greater than the strength of rooms in industrial facilities, some form of explosion venting and explosion suppression would be needed. We also note that this scenario is entirely possible even though the 200 g of *n*-butane released would be too small to form a flammable mixture if it was dispersed uniformly throughout the 48 m³ enclosure.

EXAMPLE 4:

Determine the value of χ, the ratio of turbulent-to-laminar burning velocity, corresponding to the K_G value listed in Table 3-16.3 for *n*-butane.

SOLUTION:

The value of χ can be calculated using Equation 9 as follows:

$$\chi = \frac{K_G}{4.84 S_u\left(\dfrac{P_m}{P_0}\right)^{1/\gamma}(P_m - P_0)}$$
$$= \frac{92 \text{ bar} - \text{m/s}}{4.84(0.45 \text{ m/s})(9.0)^{1/1.4}(8 \text{ bar})} = 1.10$$

This suggests that the flame speed in the test used to determine K_G was not significantly faster than the speed corresponding to the laminar burning velocity for a worst-case butane-air mixture.

EXAMPLE 5:

A coal-fired power plant has bituminous coal dust layers with a mass-per-floor-area of 1000 g/m² in an enclosure with a 4-m ceiling height. Assume the coal dust layer is dispersed by a primary explosion such that it forms a worst-case dust cloud with a concentration of 500 g/m³ in the lower portion of the enclosure. What would the pressure increase due to a secondary explosion in the enclosure without any explosion venting be?

SOLUTION:

Equation 4 can be used to solve this problem if we use both m_b and m_0 on a per-unit-floor-area basis. Thus, $m_0/A = (500 \text{ g/m}^3)(4 \text{ m}) = 2000 \text{ g/m}^2$, and we are given $m_b/A = 1000 \text{ g/m}^2$. Using the value of $P_m - P_0$ for bituminous coal in Table 3-16.2,

$$P - P_0 = (9.1 \text{ bar g})(1/2) = 4.55 \text{ bar g} = 66 \text{ psig}$$

If the volumetric bulk density of the coal dust layer is equal to a typical value of 500 kg/m³, the corresponding coal dust layer thickness would be

$$\frac{1.00 \text{ kg/m}^2}{500 \text{ kg/m}^3} = 2 \times 10^{-3} \text{ m} = 2 \text{ mm}$$

Detonations

A detonation is an explosion in which the combustion wave (i.e., flame) propagates at supersonic speeds through the unburned fuel. Detonations are fundamentally different than the closed vessel deflagrations described in the previous section of this chapter. Since flames in a deflagration propagate at speeds well below the speed of sound (which is about 340 m/s in room temperature air), the pressure increase during a deflagration occurs virtually uniformly throughout the enclosure as the explosion evolves. In contrast, the pressure rise during a detonation is highly nonuniform and occurs virtually instantaneously as the shock wave propagates through the gas–air mixture. If the flame speed is slightly less than the speed of sound, such that the pressure rise is nonuniform but shock waves do not occur, the explosion is called a quasi-detonation.

The practical significance of this fundamental difference between detonations and deflagrations is that they require different approaches to explosion protection. The sudden, spatially nonuniform pressure rise during a detonation or quasi-detonation precludes the use of explosion venting or explosion suppression systems. Furthermore, the high-peak, short-duration detonative pressure loads warrant special considerations in the evaluation of structural resistance.

The peak pressure during a detonation can be calculated from the classical Chapman-Jouguet theory, which is a combination of thermochemical equilibrium and gas dynamic conservation equations across the detonation front.[12,14] Figure 3-16.6 shows calculated detonation pressures as a function of fuel concentration for seven different flammable gases. Chapman-Jouguet calculations for these and other mixtures can be conducted with both the STANJAN and CET89 computer codes mentioned previously for deflagration calculations. Burgess et al.[14] and others have suggested that a good approximation to the Chapman-Jouguet detonation pressure, P_{CJ}, is $P_{CJ} = 2P_m$ (i.e., twice the closed vessel deflagration pressure). This approximation represents a much simpler alternative to the Chapman-Jouguet theory of calculating detonation pressures. As indicated in Figure 3-16.6, P_{CJ} for a near-stoichiometric gas-air mixture initially at atmospheric pressure is in the range 16 to 20 atmospheres.

The pressure distribution behind the C-J detonation front is shown in Figure 3-16.7 for the case of a detonation wave propagating in both directions away from the initiation site in a tube. Behind the propagating detonation front the pressure decreases to a plateau value equal to about 0.35 P_{CJ}. The speed of propagation is equal to the C-J Mach number times the speed of sound in the unburned gas-air mixture. If the tube has one or more closed ends, the detonation wave will be reflected and propagate in the reverse direction with increased amplitude. If the
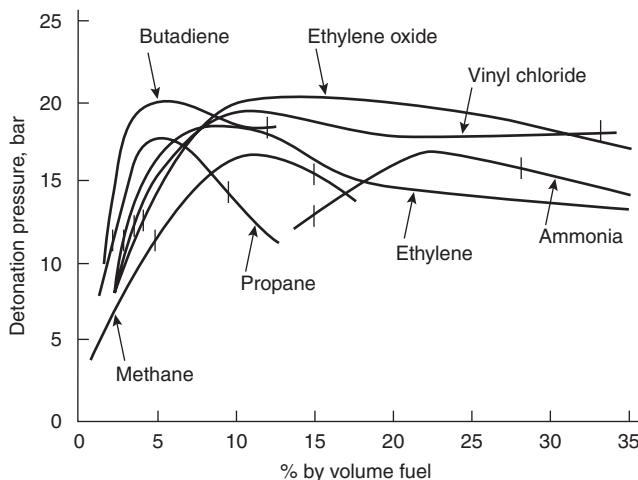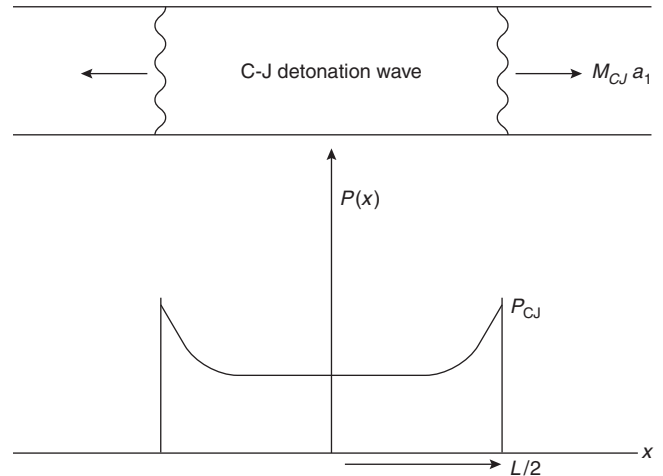
Figure 3-16.7. *Pressure distribution in C-J detonation wave propagating through a tube.*

end wall is rigid, the reflected shock wave for many gas-air mixtures is equal to 2.76 P_{CJ}. If the end wall is open, the detonation wave will be reflected as a rarefaction wave propagating back toward the detonation initiation site.

The structural load associated with a detonation wave depends on the impulse, I_D, per unit area, where

$$I_D(x, t) = \int_{t_a}^{t} [p(x, t) - p_a]\, dt \qquad (10)$$

The detonation front arrival time, t_a, is equal to $x/(M_D a_1)$, where x is the distance from the detonation initiation site, M_D is the detonation Mach number, and a_1 is the speed of sound in the unburned gas-air mixture.

Neglecting any reflected waves, Sichel[15] has shown that a good approximation for I_D is

$$I_D = \frac{0.35 \rho_1 a_1 M_D x}{(\gamma_2 + 1)} \qquad (11)$$

where γ_2 is the ratio of specific heats in the burned gas; in many cases γ_2 is equal to 1.2. The C-J detonation Mach numbers for several stoichiometric gas–air mixtures are listed in Table 3-16.4. They are in the relatively narrow range 4.9 to 5.5. The unburned gas sound speed for most stoichiometric hydrocarbon-air gas mixtures is in the narrow range 330 m/s to 350 m/s, while for hydrogen it is 403 m/s.

An interesting aspect of Equation 11 is that the specific impulse is linearly proportional to the distance from detonation initiation site. Burgess et al.[16] note that pipeline detonations often cause periodic ruptures along the pipeline length, with each break serving as a pressure relief expansion, requiring the pressure duration/impulse to rebuild to the structural failure threshold again by propagating over another length of pipe. Methods to assess the structural damage potential from these impulsive loads generated during detonations are described by Baker et al.[17] One after-the-fact indication of

Figure 3-16.6. *Calculated Chapman-Jouguet detonation pressures.*

Table 3-16.4 *Detonation Mach Numbers and Cell Sizes for Stoichiometric Gas-Air Mixtures*

Gas	C-J Mach Number	Cell Width (cm)[19]
Acetylene	5.46	0.98
n-Butane	—	5.0–6.2
Ethane	—	5.4–6.2
Ethylene	—	2.8
Hydrogen	4.89	1.5
Hydrogen sulfide	—	10
Methane	5.17	28
Propane	5.38	6.9
Propylene	—	5.4

C-J Mach numbers were calculated with the STANJAN computer code.

structural failure due to detonative loads is the occurrence of fragmented structural debris associated with brittle failure, as opposed to the bulging and more ductile failure of structural steel subjected to deflagration pressures beyond the yield point.

In view of the drastically different explosion protection considerations for detonations, it is important to assess the potential for a detonation to occur as opposed to a deflagration. Some guidance, as described below, can be offered for this assessment, but there are no exact criteria to provide an unequivocal answer.

The detonability length scale is the detonation cell width, S_c, shown in Figure 3-16.8. As indicated in Figure 3-16.8, the detonation front consists of a complicated network of curved shock segments that propagate transversely to the detonation propagation direction. The transverse wave structure includes curvilinear triangles with a width S_c. If a smoke foil is inserted on the inner wall of a detonation tube, the detonation cells create a diamond- or fish-scale-shaped pattern on the smoke foil. Detonation cell widths are measured from the traces deposited on these smoke foils as described, for example, by Gelfand et al.[18] The same is true for chemical induction length as a qualitative measure of detonability.

Detonation cell widths can also be correlated with the detonation reaction zone length in a one-dimensional representation of the shock wave initiated chemically reacting flow behind the leading edge of a detonation. This model, which is called a ZND model (the initials stand for three original model developers), requires some chemical kinetics data as well as an assumption about heat losses and drag associated with the tube wall. The calculations and their relationship to cell size are described by Gelfand et al.,[18] by Shepherd,[20] and by Stamps et al.[21]

Detonation cell widths measured or calculated for nine different stoichiometric gas-air mixtures are listed in Table 3-16.4. Values range from about 1 cm for acetylene to about 28 cm for methane. These values were obtained at atmospheric pressure and room temperature. Higher initial pressures and temperatures would result in smaller cell widths. Furthermore, some of the gases listed in Table 3-16.4 have smaller cell widths at some fuel-rich concentrations, with minimum values for a given fuel being as much as 40 percent smaller than the values shown in the table.

OT	Transverse shock
TR	Trailing acoustic wave
OM	Mach stem
O	Triple points
I I I	Reaction zone
:::	Unreacted medium
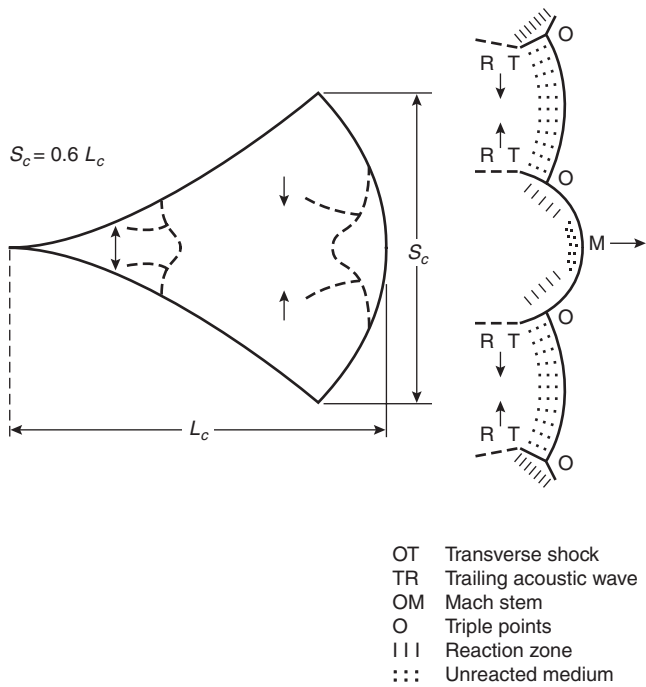
Figure 3-16.8. *Detonation cell structure.[18]*

A sustained detonation can only occur if the characteristic length scale of the gas-air mixture is greater than some multiple of the detonation cell width. The value of the multiplication factor depends on the geometry. In the case of a pipe, the detonation will not propagate down the pipe if the pipe diameter is less than about $S_c/3$. The detonation will not propagate from open end of the pipe into the surrounding gas mixture if the pipe diameter is less than $13\,S_c$.

What is the likelihood of a detonation occurring in an enclosure or cloud larger than the critical size indicated by the detonation cell size? The answer depends on the strength of the ignition source and the presence of either a highly elongated geometry or an exceptionally high level of turbulence for promoting flame acceleration. The minimum ignition source energy required for the direct initiation of a detonation ranges from a low of about 5 kJ for acetylene and hydrogen in air to a high estimated to be 93,000 kJ for methane. Since these initiation energies are many orders of magnitude larger than the energies associated with accidental ignition sources, direct initiation can be precluded from almost all accident initiation scenarios.

In the case of a weak (typically accidental) ignition source in a pipe or some other elongated enclosure, the deflagration-to-detonation transition (DDT) distance depends upon the following parameters.

Mixture reactivity. The more reactive the mixture, the more rapid is the flame acceleration to DDT.

Enclosure or pipe wall roughness and the presence of obstruction. The rougher the pipe interior surface or the more obstructions present, the shorter is the transition length to DDT.

Enclosure or pipe diameter. The larger the pipe or enclosure diameter, the shorter is the transition to DDT.

Initial pressure and temperature. The higher the initial temperature and pressure, the shorter is the transition length to DDT.

Initial turbulence level. The more turbulence or initial gas velocity in the enclosure, the shorter is the DDT transition length.

Figure 3-16.9 illustrates how mixture reactivity influences the DDT length/diameter ratio for the case of a smooth walled 2-inch (5-cm) diameter pipe.[22] The ratio of DDT transition length to pipe diameter is plotted as a function of the ratio of nitrogen/oxygen concentration for methane, for ethane, and for propane at near-worst-case fuel/oxygen ratios that produce stoichiometric combustion with CO formation instead of CO_2. The L_{DDT}/diameter ratio increases rapidly as the nitrogen/oxygen ratio increases for all three alkanes, with the transition length being shortest for propane and longest for methane. In these experiments, the largest N_2/O_2 ratio at which transition occurred (last data point on each curve), was less than the 3.76 ratio corresponding to air. In other words, the L_{DDT}/diameter ratio for these alkanes in air (at a 2-inch pipe diameter) is larger than the largest ratio (120) measurable in these experiments. The three arrows in the graph represent the absence of transition at the indicated N_2/O_2 ratio. These data are consistent with the experimental observations of Flessner and Bjorkland,[23] who did *not* see DDT with gasoline-air mixtures in a 15-cm-diameter, 16-m-long smooth wall pipe, but saw DDT at a distance of 74 pipe diameters when they inserted an expanded metal liner in the pipe entrance to simulate a rough wall section.

Sherman and Berman[24] have developed a semiquantitative methodology to categorize the probability of detonations occurring in specific industrial accident scenarios by subjectively extrapolating the experimental data on the various effects mentioned above. They categorize gas mixture reactivities on the basis of detonation cell size, and they categorize enclosure geometries on the basis of size,

DDT Data For Smooth Tubes
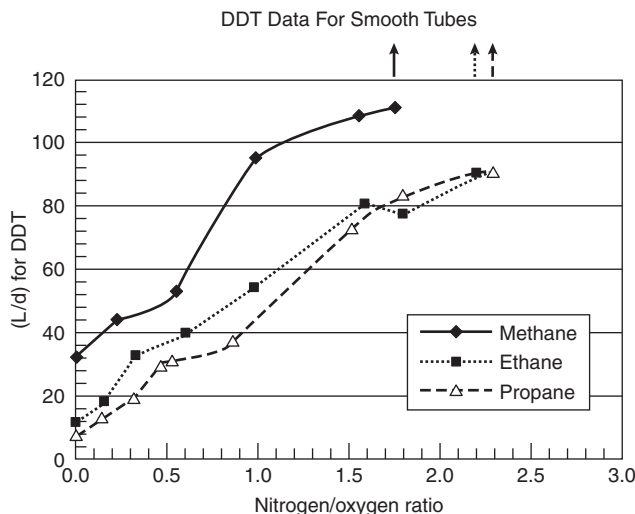
Figure 3-16.9. *Deflagration-to-detonation transition length data.[23]*

confinement, level of obstructions, amount of venting, and so on. They have applied their methodology to the case of a possible hydrogen detonation during hypothesized severe accident scenarios in one particular nuclear plant containment building.

Although most accidental explosions are deflagrations, there are some occasional well-documented accounts of detonation incidents. One excellent example is the Jacobs et al.[25] description of a particularly destructive detonation in a section of a petroleum refinery in which a gas mixture of 3 percent naptha, 19 percent oxygen, and 78 percent inert gas at 105 psig was accidentally allowed to enter several large pieces of process equipment connected by over 1000 ft of piping. Their account of the incident includes a description of the flame propagation path and associated pressures (3000–4000 psi in some locations) developed.

EXAMPLE 6:

A large process oven is heated with a burner utilizing a 1-cm-diameter, 5-m-long fuel line containing a stoichiometric propane-air mixture. What is the likelihood of a detonation occurring in the oven and the fuel line as a result of a delayed ignition after the oven has been inadvertently filled with a fuel-air mixture? How would the situation change if a stoichiometric hydrogen-air mixture replaced the propane-air mixture in the fuel line?

SOLUTION:

From Table 3-16.4, $S_c = 6.9$ cm for a stoichiometric propane-air mixture. Thus, the minimum pipe diameter for detonation propagation in this case is $S_c/3 = 2.3$ cm. Therefore, a sustained propane-air detonation will not propagate through the 1-cm fuel line. If the propane is replaced by hydrogen, $S_c/3 = 0.50$ cm, and a fuel line detonation would be possible, particularly in view of the 500:1 length to diameter ratio.

In order for the detonation to be transmitted into the oven, the fuel line would have to be larger than 13 $S_c = 20$ cm for hydrogen. Thus, the oven should not experience a detonation. Explosion venting could be a viable form of explosion protection for the oven.

EXAMPLE 7:

If a detonation did propagate through a stoichiometric hydrogen-air mixture in the fuel line, what would the specific impulse be on the pipe wall? Neglect any reflected shock wave effects, and use a sound speed of 400 m/s for the unburned stoichiometric hydrogen-air mixture.

SOLUTION:

Before using Equation 11 to evaluate the specific impulse, we need to calculate the molecular weight and density of the stoichiometric hydrogen-air mixture.

$$\rho_{mix} = \frac{M_{mix}}{M_{air}} \rho_{air}$$

$$= \frac{(0.295)(2) + (1 - 0.295)(28.8)}{28.8} (1.2 \text{ kg/m}^3)$$

$$= 0.87 \text{ kg/m}^3$$

Using the C-J detonation Mach number for stoichiometric hydrogen-air listed in Table 3-16.4,

$$I = \frac{0.35(0.87 \text{ kg/m}^3)(400 \text{ m/s})(4.89)(5 \text{ m})}{(1.2 + 1)}$$

$$= 1354 \text{ Pa·s}$$

If we assume the pressure is effectively relieved when the detonation reaches the open end of the tube, the detonation duration in the 5 m long pipe is

$$\frac{5 \text{ m}}{4.89(400 \text{ m/s})} = 2.56 \text{ m·s}$$

The average pressure exerted on the pipe wall is $I/t_{\text{dur}} = 530$ kPa $= 77$ psig. This value is about one-third of the C-J detonation pressure. Structural analysts familiar with dynamic loadings can use these values and the pipe wall properties to determine whether the fuel line should survive the detonation.

Explosion Venting

Explosion venting is the discharge of combustion gases during a deflagration to maintain pressures below the enclosure damage threshold. The enclosure can be a room, a building, or a piece of process equipment. The fuel may be a combustible gas, dust, mist, or hybrid dust-gas mixture. The discharge vent opening is usually covered initially by one or more blowoff panels, rupture discs, or other engineered vent devices. Since explosion vents usually open after the explosion is initiated to limit the pressure rise, they cannot be used for detonations because the maximum pressure occurs instantaneously when the shock front reaches a given location.

The most effective explosion venting systems are those that deploy early in the deflagration, have as large a vent area as possible, and allow unrestricted venting of combustion gases. Early vent deployment requires that the vent release at the lowest possible pressure without interfering with normal operations and pressure fluctuations in the enclosure. In the case of vents on exterior walls and roofs of buildings, the minimum feasible vent release pressure is usually slightly larger than the highest expected differential pressure associated with wind loads (typically 0.14 to 0.21 psig; i.e., 0.96 to 1.44 kPa).

The amount of vent area needed for effective explosion venting depends on the size of the enclosure and the rate of pressure rise within it. According to Equation 5, the rate of pressure rise in an unvented enclosure is proportional to the product of the mixture effective burning velocity and flame surface area, and varies inversely with the enclosure volume. The rate of pressure reduction due to venting is proportional to the product of vent area and gas velocity through the vent. The vent velocity is dependent on the instantaneous pressure in the enclosure and the composition of the vented gas (i.e., the relative proportions of burned and unburned gas). These considerations have been implemented in the formulation of theoretical models, scaling correlations for test data, and guidelines for determining the required vent area.

Theoretical Models

Most of the theoretical models are for vented gas explosions because their effective burning velocities and flame surface areas are more amenable to modeling than those of dust explosions. The two categories of gas explosion models are (1) two-fluid models and (2) computational fluid dynamics (CFD) models. The two-fluid models are conceptually similar to the closed vessel model described previously, but include provisions for modeling the vented flow and various types of flame accelerations and turbulent combustion with possible highly wrinkled flame surface areas. Zalosh[26] has reviewed the status of these models through 1995.

Computational fluid dynamics models are much more sophisticated and complicated than the relatively simple two-fluid models. They solve for the spatial distribution of gas velocities, gas composition, and thermodynamic variables throughout a computational grid that can be either fixed or adaptive to the instantaneous flow and combustion field. Two distinguishing features of each of these models are their formulations for turbulence generation and for turbulent combustion rates. Although they are too complicated and computationally burdensome for routine deflagration vent design, several of these models are being used now for special applications such as offshore platform modules with highly congested equipment. Popat et al.[27] have provided a comparative review of four popular CFD models used in Europe, including their success in pre-test predictions.

Although dust explosions are more difficult to model than gas explosions, there have been several noteworthy efforts summarized by Eckhoff.[7] Some of these explicitly utilize the gas explosion parameters (burning velocity and flame surface area) and provide prescriptions to evaluate them from experimental data. Others use the closed vessel K_{ST} parameter as a representation of the effective burning rate. One recent burning velocity type model developed by Tamanini[28] at FMRC has been utilized to correlate dust-explosion-venting test data.

Test Data and Correlations

Crucial aspects of both vented gas explosion and vented-dust-explosion testing and data correlations are (1) mixture reactivity, (2) turbulence sources (both initial turbulence and obstacle-flame interaction turbulence), (3) vessel volume (scale) effects, and (4) vessel geometry (primarily length/diameter ratio), as well as the vent parameters: vent area, vent release pressure, and vent panel inertia. Vented-gas-explosion testing has the additional complication of various flame instabilities, some of which are dependent on ignition location, enclosure wall lining, and the presence of equipment within the enclosure. Dust-explosion testing has the additional complications of ignition source strength and dust cloud uniformity, as well as the time delay between dust dispersion and ignition.

Rather than attempt to review the numerous vented-explosion test programs, we will briefly focus on the testing that seems to have had the greatest influence on the development of data correlations and our current understanding of vented-explosion phenomenology. In this regard, perhaps the most influential and most extensive testing has been the large-scale testing conducted by Bartknecht and his protégés at the Ciba-Geigy Test Center in Basel, Switzerland. Their test vessels ranged in size from 2.4 m³ to 250 m³, and had a pressure rating of 10 bar so they could be used for both vented and unvented tests.[29] Most of their testing has been with dusts using energetic igniters and worst-case dust concentrations. Their data have been correlated in the various versions of the VDI Guideline for Dust Explosion Venting.[30]

Recent efforts in explosion venting data correlations have utilized nondimensional parameters that lend themselves to data interpolation and extrapolation. The nondimensional pressure parameter is

$$\pi = \frac{\Delta P_{\text{red}}}{\Delta P_{\text{max}}}$$

and the nondimensional vent parameter is

$$\Gamma = \frac{a_{CD} \cdot A_v \cdot P_0}{V^{2/3} \cdot K_{ST}}$$

where

A_v = vent area (m²)

V = enclosure volume (m³)

K_{ST} = ASTM E1226 (20-l vessel) dust reactivity (bar·m/s)

P_{red} = reduced pressure in vented explosion (bar·ga)

P_{max} = unvented explosion pressure (bar·ga)

P_{stat} = vent deployment pressure (bar·ga)

P_0 = initial pressure (= 1 bar·abs)

a_{CD} = vent discharge coefficient × sound speed = $C_D a_1$ = 230 m/s

The current FMRC correlation[31] uses the π parameter and a modified form of the Γ parameter in which a volume-adjusted K_{ST} parameter is used, and P_{max} replaces P_0 in the numerator. The particular correlation of π (Γ) was developed to provide a best fit to the Bartknecht data.

Gas explosion venting correlations relate the pressure parameter, π, to one of two alternate forms of the nondimensional vent parameter.

1. The Swift-Epstein[32] form of the vent parameter is

$$\Gamma_{S\text{-}E} = \frac{\chi S_u A_s}{C_D A_v} \sqrt{\frac{\rho_1}{P_{\text{red}}}}$$

where A_s is the interior surface area of the enclosure, that is, the maximum flame surface area at the time the enclosure is completely filled with flame.

2. The Bradley-Mitcheson[33] form of the vent parameter is

$$\Gamma_{B\text{-}M} = \frac{A_v a_1}{V^{2/3} S_u \left(\dfrac{M_1 T_f}{M_b T_1} \right)}$$

where T_f is the adiabatic isobaric flame temperature and M_b is the burned gas molecular weight. Molkov[34] has subsequently modified the Bradley-Mitcheson vent parameter to include the ratio χ/C_D, and has developed correlations for this ratio that account for turbulent flame stretch.

The turbulence parameter, χ, is particularly difficult to estimate and correlate for the vented gas explosions that produce flame instabilities. These flame instabilities produce complicated pressure-versus-time traces with multiple pressure peaks and oscillations such as shown in Figure 3-16.10. Depending on conditions (as described by Cooper et al.[35]), the maximum pressure during a vented explosion can correspond to any one of the four types of pressure peaks shown in Figure 3-16.10.

Explosion Venting Guidelines

The following vent area guidelines are based on data obtained from numerous tests in relatively large-scale enclosures with near worst-case gas-air or dust-air mixture compositions. The specific test programs are referenced in NFPA 68.[8] In some cases, the data was correlated using the parameters described previously. In other cases (particularly for gas explosions), the data were enveloped rather than correlated. Separate guidelines are offered for low-strength and high-strength enclosures, with the nominal demarcation between the two corresponding to a damage threshold pressure of 1.5 psig (0.1 bar ga). The reason for this demarcation is that the high-strength guidelines were primarily developed from European test programs, which did not include low-pressure tests, while many of the U.S. test programs featured large, low-strength structures.

Low-strength enclosures: The low-strength enclosure guidelines are currently based on the Swift-Epstein correlation parameter described previously. Thus the required vent area required to maintain pressures below the damage threshold, P_{red}, is proportional to the internal surface
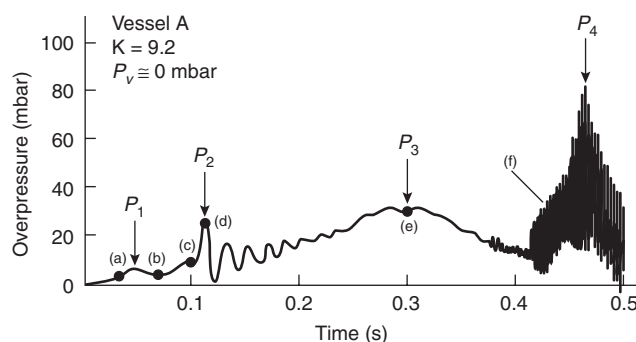
Figure 3-16.10. *Pressure-time profile typical of an explosion in a near-cubic vessel with a low failure pressure explosion relief.*[35]

area of the enclosure. The general form of this venting equation is

$$A_v = \frac{CA_s}{\sqrt{P_{\text{red}}}} \qquad (12)$$

where

A_v = vent area (ft^2 or m^2)

C = fuel characteristic constant (psig$^{1/2}$ or kPa$^{1/2}$) specified in Table 3-16.5

A_s = internal surface area of enclosure (ft^2 or m^2)

P_{red} = overpressure damage threshold (psig or kPa)

The intended range of applicability of Equation 12 is

- 0.35 psig $< P_{\text{red}} < 1.5$ psig
- $P_{\text{red}} - P_{\text{stat}} > 0.35$ psi, where P_{stat} = vent opening pressure
- enclosure length/diameter (hydraulic) < 3

The recommended values of C in Table 3-16.5 represent the highest values inferred on the basis of test data presented in 18 references cited in NFPA 68.[8] Test conditions encompassed both quiescent and initially turbulent fuel-air mixtures in enclosures with volumes ranging from 0.18 to 82.3 m^3.

For a given fuel, most of the data correspond to C values well below those given in Table 3-16.5. For example, the most likely value of C for propane is about one-third of the recommended value of 0.17. On the other hand, it is entirely possible for the recommended C value as used in Equation 12 to underestimate the pressure developed in a vented explosion with an extremely high level of turbulence, such as might occur in a hammermill, for example.

Values of C for other gases should be based on test data. In lieu of such data, a reasonable guess that is consistent with the Swift-Epstein correlation could be made by multiplying the 0.17 psig$^{1/2}$ value for propane (for which the most data are available) by the ratio of the burning velocity of the other gas to that for propane.

High-strength enclosures: The vent area recommended in NFPA 68 for compact ($L/D \leq 2$) high-strength enclosures subject to gas explosions is

$$A_v = \big[(0.127 \log_{10} K_G - 0.0567)P_{\text{red}}^{-0.582} \\ + 0.175 P_{\text{red}}^{-0.572}(P_{\text{stat}} - 0.1)\big]V^{2/3} \qquad (13)$$

where $P_{\text{stat}} \leq 0.5$ bar and $P_{\text{red}} \leq 2$ bar.

Table 3-16.5   *C Values in Swift-Epstein Equation*[8]

Fuel	English Unit C (psig)$^{1/2}$	Metric Unit C (bar)$^{1/2}$
Anhydrous ammonia	0.05	0.013
Methane	0.14	0.037
Gases with S_u values < 60 cm/s	0.17	0.045
Dusts with K_{ST} < 200 bar·m/s	0.10	0.026
Dusts with K_{ST} > 200 and < 300 bar·m/s	0.12	0.030
Dusts with K_{ST} > 300 bar·m/s	0.20	0.051

For enclosures with $L/D > 2$, there is an equation for an incremental vent area to cope with the higher rates of pressure rise in elongated enclosures subject to flame acceleration.

The current (1998) version of NFPA 68 has the same equation for dust explosions in high-strength enclosures as is in VDI 3673. However, the committee has proposed the following new equation for dust explosions in compact enclosures for the 2002 Edition of NFPA 68.

$$A_v = (8.535 \times 10^{-5})(1 + 1.75 P_{\text{stat}})K_{ST}V^{0.75}\sqrt{\frac{(1 - \Pi)}{\Pi}} \qquad (14)$$

where $\Pi = P_{\text{red}}/P_{\text{max}}$ as in the general correlations, V is in m^3 and A_v is in m^2.

An equation for an incremental vent area for enclosures with $L/D > 2$ is also being proposed as of this writing. If approved by NFPA in the fall of 2001, Equation 14 and the auxiliary L/D equation will appear in the next version of NFPA 68, and will be recommended for low-strength as well as high-strength enclosures.

One limitation of all the explosion-vent guidelines as they are currently formulated, is that they do not account for application-specific turbulence levels and equipment obstruction levels. In other words, the implication in using the guidelines is that either the turbulence and equipment levels in the application are comparable to those used in the test data from which the guidelines were based, or else the vent designer is inherently accepting a certain ill-defined level of conservatism by assuming that the application turbulence and equipment obstruction levels are significantly lower than those used in the testing. By the same token, most of the guidelines do not account for the extent of the enclosure filled with combustible mixture. Current research, such as that described by Tamanini[36,37] is providing a basis for overcoming these limitations.

EXAMPLE 8:

Suppose the $4 \times 4 \times 3$ in room of Example 3 has a damage threshold pressure of 1.0 psig. What would be the minimum vent area to maintain pressures under this value for a worst-case butane–air mixture explosion? Assume the gas mixture is initially at rest and the vent release pressure is 0.2 psig.

SOLUTION:

For this room,

$$A_s = 2[4(4) + 4(3) + 4(3)] = 80 \text{ m}^2$$

Since butane has a burning velocity similar to that for propane, from Table 3-16.5, $C = 0.17$. Therefore, using Equation 9,

$$A_v = 80(0.17)/1.0 = 13.6 \text{ m}^2 \ (146 \text{ ft}^2)$$

EXAMPLE 9:

A 400-m^3 electrostatic precipitator used in a power plant firing bituminous coal is to be equipped with lightweight explosion vents. If the damage threshold pressure for the precipitator is 1.2 bar (17.4 psig), its L/D ratio is 1.5, and the vent static release pressure is 0.4 bar (5.8 psig), what is the minimum vent area needed? Assume the bitu-

minous coal has the explosibility parameters listed in Table 3-16.2.

SOLUTION:

From the Table 3-16.2 listing for bituminous coal, K_{ST} = 59 bar·m/s and P_{max} = 9.1 bar g. Therefore, π = 1.2/9.1 = 0.132. Substituting into Equation 14,

$$A_v = (8.535 \times 10^{-5})[1 + 1.75(0.40)](59)(400)^{0.75}\sqrt{\frac{1 - 0.132}{0.132}}$$

$$= 1.96 \text{ m}^2$$

We note that since the vent area is linearly proportional to K_{ST}, which can vary substantially among various coals (and other generic materials for that matter), it is important to base the calculated vent area on data for site-specific samples. Note also that the calculated vent area does not account for the weight (inertia) of the vent panel. A procedure to determine the additional vent area required for heavy vent panels will appear in the next edition of NFPA 68.

Explosion Suppression Systems

An explosion suppression system is designed to detect and suppress an incipient explosion before the pressure rises to the enclosure damage threshold. Suppression is achieved by the rapid discharge of an extinguishing agent from pressurized containers mounted on the protected enclosure. The sequence of events is pictured in Figure 3-16.11. A pressure or flame radiation detector senses the incipient explosion while only a small fraction of the flammable gas or dust has burned. The sensor signal triggers the discharge of suppression agent into the enclosure. When the agent reaches the expanding flame front, it quenches the flame and thereby suppresses the explosion.

One important advantage of explosion suppression systems versus explosion venting is that there is no discharge of flame or fuel. Thus suppression systems can often be used more readily on indoor equipment and on equipment containing toxic materials. One major disadvantage of the system is the high cost associated with both the installation of a complex system and the refilling and resetting of the system after a discharge.

The basic components of an explosion suppression system include detectors, an electrical power supply and control system, and a set of rapid action extinguishing units. Pressure sensing detectors are usually used in applications involving dust explosion hazards, while gas explosion applications can employ either pressure sensors or ultraviolet radiation detectors, depending on the required response line (UV detectors provide the fastest response time) and concerns for spurious activation and/or optical shielding of the detectors. Electrical power supplies and control systems include appropriate interlocks for self-monitoring and for shutting down processes and triggering alarms at system activation. Extinguishing agents traditionally used in explosion suppression systems have been either halogenated hydrocarbons (halons) or chemical powders. Dry chemicals, such as mono-ammonium phosphate and sodium bicarbonate, are still

(a)

(b)
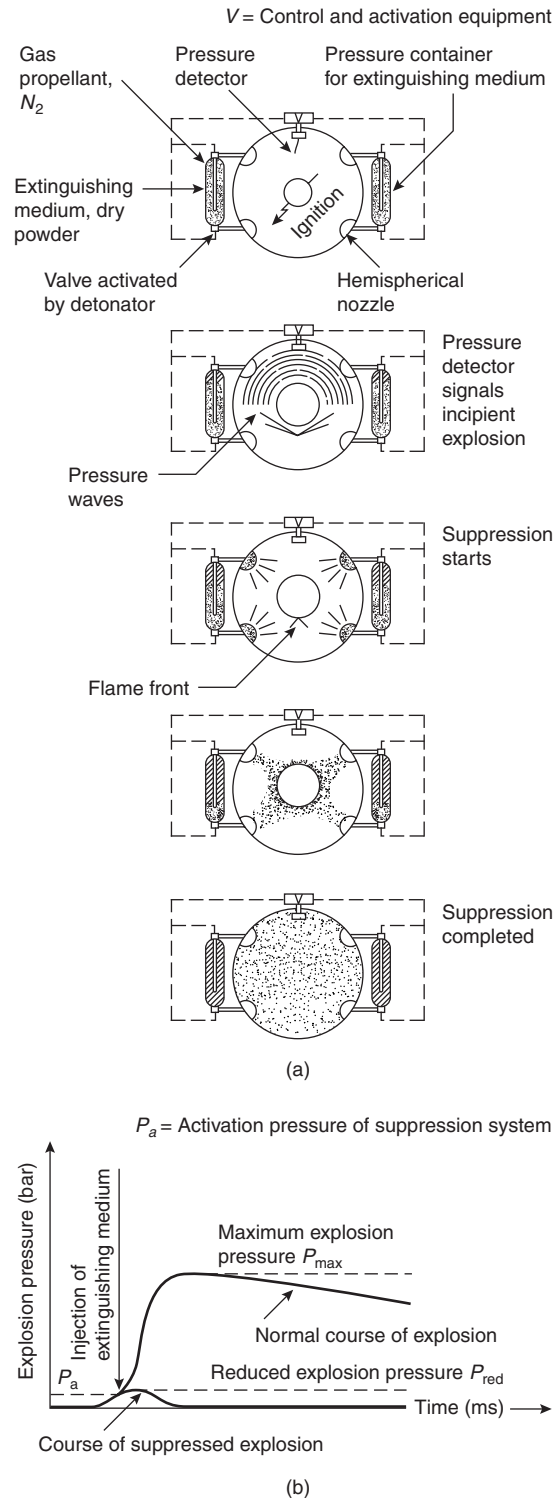
Figure 3-16.11. *(a) Explosion suppression system. (b) Pressure versus time diagram of a normal and a suppressed explosion.*[4]

being used to protect many unoccupied facilities and equipment. However, the recent phaseout of halon production, because of ozone depletion concern, has triggered an ongoing search for new liquid and gaseous

agents (primarily perfluorocarbons and hydrofluorocarbons), and has generated renewed interest in water and aqueous salt solutions for explosion suppression of potentially occupied facilities, such as aerosol propellant filling rooms and gas compressor stations.

Several test programs have provided data on the quantity of agent, activation times and pressures, and method of agent dispersal needed for effective suppression. These programs have encompassed a variety of flammable gases and dusts, have ranged in scale from laboratory vessels[38] to a 500-m³ tanker pump room,[39] and include many tests in the 250-m³ Ciba-Geigy test vessel mentioned previously.[40] The ISO and Factory Mutual standards[41,42] specify that testing should be conducted in a vessel of at least 1-m³ volume, and should include tests with and without suppression agents.

Bartknecht[43] has systematically investigated the effect of enclosure size on the quantity of dry chemical agent needed for effective suppression. His data indicate that the required quantity of agent is proportional to the enclosure volume (i.e., there is a certain critical agent concentration) for volumes under about 5 m³, but that the required amount of agent is proportional to the two-thirds power of the enclosure volume beyond 9 m³. This change in scaling suggests that the dry chemical suppression mechanism changes from advance inerting of unburned fuel ahead of the flame front in small vessels, to actual quenching of the flame front in large vessels. Chatrathi and Going[44] have recently reported on testing using dry chemical suppression agents in both modes: inerted (injected into the vessel with combustible dust) and post-ignition suppression. His inerted test results were used to determine minimum inerting concentrations for mono-ammonium phosphate and sodium bicarbonate.

Recent fundamental research with various suppression agents has elucidated the suppression mechanisms associated with various agents and fuel combinations. Many agents provide the thermal heat sink effect that is the most clearly understood mechanism. Some agents also provide a chemical inhibition effect (via free-radical scavenging), but the magnitude of this effect is dependent upon the flame speed as well as the chemical compositions of the fuel and agent.[45,46]

The importance of the flame speed in assessing suppression agent and system effectiveness can best be appreciated in terms of the components contributing to what Chatrathi and Going[44] call the *total suppressed pressure* (TSP). These components can be expressed in the following equation:

$$TSP = P_A + \Delta P_{inj} + \Delta P_{comb} \qquad (15)$$

where

P_A = deflagration pressure at the time of agent discharge actuation

ΔP_{inj} = incremental pressure associated with the discharge of propellant gas and any gaseous agent into the enclosure

ΔP_{comb} = incremental pressure associated with the combustion that occurs as the agent travels to the flame front and actually suppresses the deflagration

The first term in Equation 15 can be minimized through the selection of fast-acting detectors and the use of very fast opening suppression agent containers. The second term is usually only an important consideration in small enclosures (Chatrathi and Going report that ΔP_{inj} = 1.4 psig when one 2.5 l container, pressurized to 900 psig with nitrogen is injected into a 1-m³ closed vessel). The third term is the most difficult to characterize because it includes consideration of agent dispersal as well as the chemically reacting interaction of the agent with the expanding flame front. In terms of minimizing agent travel time to the flame front, it is clear that the use of a large number of well distributed small agent containers would be preferable to use of fewer large containers. Moore's testing[47] has verified this conjecture. If the agent travel time can be calculated, and the agent is assumed to be instantly effective once it reaches the flame front, the value of ΔP_{comb} can be estimated using Equations 6 and 7.

The ΔP_{comb} term in Equation 15 will inevitably increase with increasing fuel K_{ST} or K_G, as well as with the increasing turbulence level associated with the application explosion scenario. The highest challenge K_{ST} material subjected to explosion suppression tests has been aluminum dust. Early results described by Bartknecht[43] showed the limitations of the first generation suppression systems and agents in suppressing aluminum dust explosions. The recent results of Chatrathi and Going suggest that the TSP of aluminum dust can now be reduced to 10–20 percent of P_{max}. This is significantly larger than the TSP achieved with organic fuels, which is usually less than 5 percent of P_{max}.

The choice of a suitable suppression agent and number/location of agent containers involves some very practical considerations as well as consideration of the maximum pressure developed in the suppressed explosion. Some of these considerations include agent compatibility with process materials, agent toxicity, environmental impact, and agent retention time for applications in which there is a threat of repeated ignitions.

Blast Waves

If explosion prevention and explosion suppression measures are not successful, a blast wave will emanate from the breached enclosure. The blast wave will propagate into the surrounding atmosphere and will decay with distance from the enclosure. One of the most common questions with regard to explosion protection is whether or not the blast wave at a particular location will be sufficiently strong to cause damage or injury. Simplified methodology to address this question is presented here along with reference citations for more thorough and extensive analyses.

If we confine our attention to distances that are large in comparison to the characteristic diameter of the breached enclosure, we can deal with relatively simple far-field blast wave scaling correlations. The characteristic shape of the far-field blast wave is shown in Figure 3-16.12. It consists of a shock wave with a pressure rise, P_s, followed immediately by a rarefaction wave in which the pressure decays to some value below atmo-
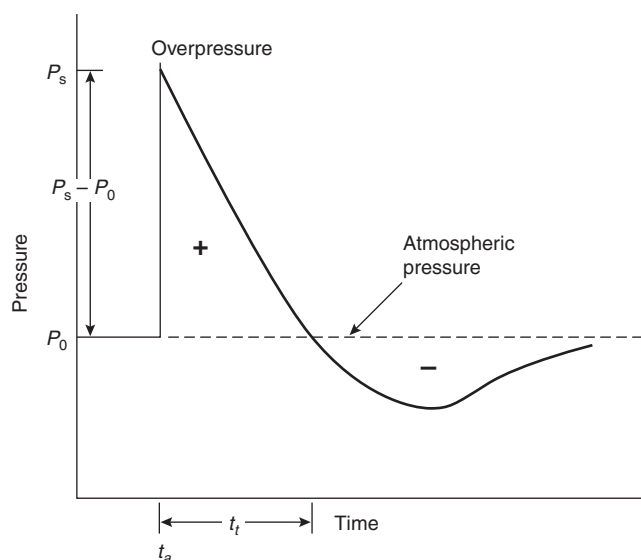
Figure 3-16.12. *Far-field blast wave.[49]*

Figure 3-16.13. *Blast wave pressure versus scaled distance.*

spheric pressure, and then a gradual recovery to atmospheric pressure, P_0. Sometimes the final pressure recovery occurs in the form of a second shock, and the shape takes the form of a slightly deformed letter N, thus leading to the term N *wave.*

Blast wave correlations are often in the form of a nondimensional pressure $(P_s - P_0)/P_0$ and a nondimensional distance from the blast source. The nondimensional distance, $\overline{R}$, is defined as

$$\overline{R} = R\left(\frac{P_0}{E}\right)^{1/3} \qquad (16)$$

where R is the actual distance from the blast source (m), E is the blast wave energy (J), and P_0 is in Pa.

The correlation for nondimensional pressure versus $\overline{R}$ is shown in Figure 3-16.13. The curve labeled PS in Figure 3-16.13 refers to the incident overpressure, while the curve labeled PR refers to the reflected blast wave pressure resulting from a blast wave being reflected head-on from a rigid wall. Neither curve in Figure 3-16.13 accounts for the reflection of the shockwave off the ground surface. The usual procedure for including ground surface reflection is to use twice the calculated blastwave energy when using the correlations in Figure 3-16.13.

The implication in this type of blast wave scaling correlation is that the blast wave is characterized by only one parameter, the blast energy, E. In theoretical models of blast wave pressure, the energy is assumed to be released instantaneously, at a single point. This approach is called ideal blast wave theory. The correlations for ideal blast waves are based on a combination of theory and test data from condensed phase, compact explosives. Baker[17,48] describes the development of these correlations, which include nondimensional blast wave impulses, positive-phase durations, and many other parameters. The impulse is particularly important for doing dynamic structural response analyses, such as those described by Kinney and Graham.[49]
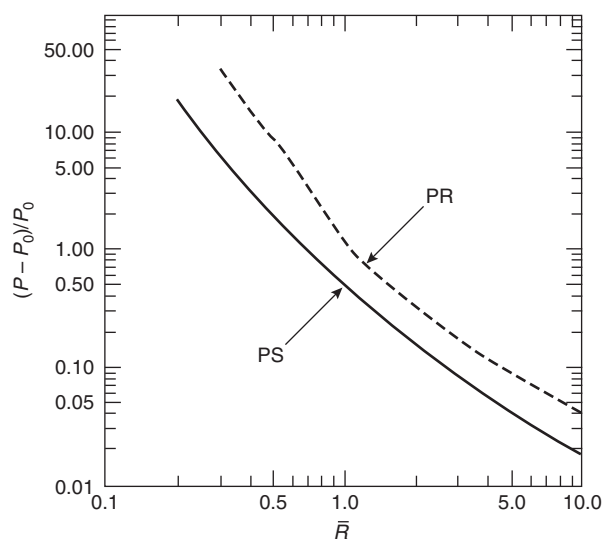
Can the blast waves from various accidental explosions be predicted from these ideal blast wave correlations? In some cases the answer is unequivocally yes. A good example is the blast wave from a ruptured pressure vessel containing a gas that is not ignited upon release. The energy associated from this type of physical explosion is the energy of expansion of the gas as it goes from an initial pressure, P_1, to atmospheric pressure. A perfect gas isentropic expansion representation of this energy is

$$E = \frac{(P_1 - P_0)V}{\gamma - 1} \qquad (17)$$

where V is the vessel volume and γ is the gas ratio of specific heats. Other approaches to this problem, including the assessment of vessel fragment shrapnel effects, are described in the AIChE Consequence Analysis Guidelines.[50]

If the breached vessel fails as a result of an internal combustion explosion, or if the vessel is vented per explosion venting guidelines, the blast wave analysis is considerably more complicated because there is a combustion energy contribution to the total blast wave energy. Correlations to predict blast waves from vented explosions are contained in NFPA 68, and more recent developments, including two-dimensional considerations, are described by Forcier and Zalosh.[51]

Another special consideration in breached vessel blast waves is the blast wave and fragment shrapnel released when a liquefied gas undergoes a boiling liquid expanding vapor explosion (BLEVE) as a result of severe fire exposure. Correlations for BLEVEs are described in *Guidelines for Evaluating the Characteristics of Vapor Cloud Explosions, Flash Fires, and BLEVEs,*[52] and some of the research leading to these correlations are described in Baurer et al.,[53] Hasegawa and Sato,[54,55] and Fay and Lewis.[56] These publications include correlations for the size and radiation emitted from the rising fireball that occurs in most BLEVEs.

One final special consideration is the blast wave associated with vapor cloud explosions. These explosions occur when a very large cloud of flammable gas or vapor is ignited in a highly obstructed environment such as a chemical or petrochemical plant with a high density of process equipment and storage vessels. The strength of the blast wave that occurs in a vapor cloud explosion is dependent on the flame speed that develops and the degree of confinement in and around the vapor cloud.

Early assessments of vapor cloud explosion blast waves were conducted using the idealized blast wave type correlations described here, along with some rough guess at the energy yield (i.e., the fraction of the available combustion energy actually contributing to the blast wave). However, these early efforts were not very successful because 1) most of the interest is in the near-field rather than the far-field, and 2) even the far field assessments were not accurate because the blast wave strength and impulse decays far less rapidly than that of an ideal blasé wave. Two other types of blast wave models are utilized now for vapor cloud explosions. The simpler current approach involves an empirical estimate for the flame speed in different applications, along with results of one-dimensional flame propagation (or piston propagation) nonideal blast wave calculations. This approach, which is still evolving, is described in *Guidelines for Evaluating the Characteristics of Vapor Cloud Explosions, Flash Fires, and BLEVEs*,[52] Strehlow,[57] and van den Berg.[58] The second current approach is to utilize CFD models of the actual two-dimensional or three-dimensional flame propagation, in which the flame speed and acceleration are calculated as part of the solution. The models used for this approach are essentially the same models referenced earlier for CFD calculations of vented gas explosions.[27] Which of these two approaches will see more widespread use in the future depends, in large part, on the availability of faster and more powerful computers, along with the education of potential users of these sophisticated models. In a sense, this issue is only a microcosm of the more general question of what level of modeling will be utilized for performance based explosion hazard assessments.

References Cited

1. M.G. Zabetakis, "Flammability Characteristics of Combustible Gases and Vapors," *U.S. Bureau of Mines Bulletin 627,* Washington (1965).

2. ASTM E 661, "Standard Test Method for Concentration of Limits of Flammability of Chemicals," American Society for Testing and Materials, Philadelphia, PA (1995).

3. ASTM E 918-83, "Standard Practice for Determining Limits of Flammability at Elevated Temperature and Pressure," American Society for Testing and Materials, Philadelphia, PA (1993).

4. M. Hertzberg, "The Flammability Limits of Gases, Vapors, and Dusts: Theory and Experiment," *Fuel-Air Explosions,* p. 3, Univ. of Waterloo Press (1982).

5. NFPA 69, *Standard on Explosion Prevention Systems,* National Fire Protection Association, Quincy, MA (1997).

6. ASTM E 1515-98, "Standard Test Method for Minimum Explosible Concentration of Combustible Dusts," American Society for Testing and Materials (1998).

7. R. Eckhoff, *Dust Explosions in the Process Industries,* 2nd Edition, Butterworth Heinemann (1996).

8. NFPA 68, *Guide for Venting of Deflagrations,* National Fire Protection Association, Quincy, MA (1998).

9. R. Siwek, "Determination of Technical Safety Indices and Factors Influencing Hazard Evaluation of Dusts," *J. Loss Prevention in the Process Industries,* 9, pp. 21–31 (1996).

10. R. Siwek and C. Cesana, "Ignition Behavior of Dusts: Meaning and Interprertation," *Process Safety Progress,* 4, pp. 107–119 (1995).

11. D. Bradley and A. Mitcheson, "Mathematical Solutions for Explosions in Spherical Vessels," *Combustion and Flame,* 26, pp. 201–217 (1976).

12. B. Lewis and G. von Elbe, *Combustion, Flames, and Explosions of Gases,* Academic Press, New York (1961).

13. ASTM E-1226, "Standard Test Method for Pressure and Rate of Pressure Rise for Combustible Dusts," American Society for Testing and Materials, Philadelphia, PA (1988).

14. R. Strehlow, *Combustion Fundamentals,* McGraw-Hill, New York (1984).

15. M. Sichel, "Simplified Calculation of Detonation Induced Impulse," (1980).

16. D.S. Burgess, J.N. Murphy, N.E. Hanna, and R.W. Van Dolah, *Large-Scale Studies of Gas Detonations,* U.S. Bureau of Mines RI 7196, Washington (1971).

17. W.E. Baker, P.A. Cox, P.S. Westine, J.J. Kulesz, and R.A. Strehlow, *Explosion Hazards and Evaluation,* Elsevier, New York (1983).

18. B.E. Gelfand, S.M. Frolov, and M.A. Nettleton, "Gaseous Detonations," *Progress in Energy and Combustion Science,* 17, pp. 327–371 (1991).

19. A. Sulmistras, I.O. Moen, and A.J. Saber, "Detonations in Hydrogen Sulphide-Air Clouds," Defense Research Establishment Suffield, Ralston, Alberta *Report No. 11* 40 (1985).

20. J.E. Shepherd, "Chemical Kinetics of Hydrogen-Air-Diluent Detonations," *Dynamics of Explosions: Progress in Astronautics and Aeronautics,* 106, pp. 263–293 (1986).

21. D.W. Stamps, W.B. Benedick, and S.R. Tieszen, "Hydrogen-Air Diluent Detonation Study for Nuclear Reactor Safety Analysis," *Sandia Report NUREG/CR-5525* (1991).

22. R.P. Lindstedt and H.J. Michels, "Deflagration to Detonation Transition in Mixtures of Alkane LNG/LPG Constituents with O_2/N_2," *Combustion and Flame,* 72, pp. 63–72 (1988).

23. Flessner and Bjorklund, *Coast Guard Report* (1980).

24. M.P. Sherman and M. Berman, "The Possibility of Local Detonations during Degraded-Core Accidents in the Bellefonte Nuclear Power Plant," *Nuclear Technology,* 81, pp. 63–77 (1988).

25. R.B. Jacobs, W.L. Bulkley, J.C. Rhodes, and T.L. Speer, "Gaseous Detonation," *Chemical Engineering Progress,* 53, pp. 565–573 (1957).

26. R. Zalosh, "Review of Gas Deflagration Venting Models," *Proceedings of the First International Seminar on Fire and Explosion Hazard of Substances and Venting of Deflagrations,* All-Russian Research Institute for Fire Protection, pp. 166–181 (1995).

27. N. Popat, C. Catlin, B. Arntzen, R. Lindstedt, B. Hjertager, T. Solberg, O. Saeter, and A. van den Berg, "Investigations to Improve and Assess the Accuracy of Computational Fluid Dynamic Based Explosion Models," *Journal of Hazardous Materials,* 45, pp. 1–25 (1996).

28. F. Tamanini, "Characterization of Mixture Reactivity in Vented Explosions," *14th International Colloquium on the Dynamics of Explosions and Reactive Systems* (1993).

29. W. Bartknecht, "Pressure Venting of Dust Explosions in Large Vessels," *Proceedings of the 20th Annual Loss Prevention Symposium* (1986).

30. VDI 3673, "Pressure Venting of Dust Explosions," *Verein Deutscher Ingenieure,* VDI Verlag GmbH, Dusseldorf, Germany (1995).

31. F. Tamanini and J. Valiulis, "Improved Guidelines for the Sizing of Vents in Dust Explosions," *J. Loss Prevention in the Process Industries,* 9, pp. 105–118 (1996).

32. I. Swift and M. Epstein, "The Performance of Low Pressure Explosion Vents," *20th AlChE Loss Prevention Symposium* (1986).

33. D. Bradley and A. Mitcheson, "The Venting of Gaseous Explosions in Spherical Vessels," *Combustion and Flame,* 32, pp. 221–236 (1978).

34. V. Molkov, A. Korolchenko, A. Ya, and S. Alexandrov, "Venting of Deflagrations in Buildings and Equipment: Universal Correlation," *Proceedings of Fifth International Symposium on Fire Safety Science,* IAFSS, pp. 1249–1260 (1997).

35. M.G. Cooper, M. Fairweather, and J.P. Tite, "On the Mechanisms of Pressure Generation in Vented Explosions," *Combustion and Flame,* 65, pp. 1–14 (1986).

36. F. Tamanini, "Vent Sizing in Partial-Volume Deflagrations and Its Application to the Case of Spray Dryers," *J. Loss Prevention in the Process Industries,* 9, pp. 339–350 (1996).

37. F. Tamanini and J. Chafee, "Mixture Reactivity in Explosions of Stratified Fuel Layers," *Proceedings of the 34th AIChE Loss Prevention Symposium* (2000).

38. M. Hertzberg, K. CashdoUar, L. ZJochower, and D. Ng, "Inhibition and Extinction of Explosions in Heterogeneous Mixtures," *Twentieth International Symposium on Combustion,* pp. 1691–1700 (1984).

39. R. Richards, "Development of Explosion Suppression System Requirements for Shipboard Pump Rooms," *U.S. Coast Guard Report CG-D-79-76, N77S Document #ADA031308,* (1976).

40. P. Moore, "Towards Large Volume Explosion Suppression Systems," *EuropEx Newsletter,* 4, pp. 2–4 (1987).

41. ISO 6184/4, "Explosion Protection Systems—Part 4: Determination of Efficacy of Explosion Suppression Systems," *International Standard ISO 6184/4* (1985).

42. Factory Mutual Approval Standard 5700, "Explosion Suppression Systems," FMRC (1999).

43. W. Bartknecht, *Explosions: Course, Prevention, Protection,* Springer-Verlag, New York (1981).

44. K. Chatrathi and J. Going, "Dust Deflagration Extinction," *Proceedings of the 34th Annual Loss Prevention Symposium* (2000).

45. I. Moen, S. Ward, P. Thibault, J. Lee, R. Kaystautas, T. Dean, and C. Westbrook, "The Influence of Diluents and Inhibitors on Detonations," *Twentieth International Symposium on Combustion,* pp. 1717–1725 (1984).

46. G.W. Gmurczyk and W.L. Grosshandler, "Suppression Effectiveness Studies of Halon-Alternative Agents in a Detonation/Deflagration Tube," *Proceedings of the 1994 Halon Options Technical Working Conference,* New Mexico Engineering Research Institute (1994).

47. P. Moore, "Explosion Suppression Trials," *EuropEx Newsletter,* 1, pp. 3–7 (1986).

48. W.E. Baker, *Explosions in Air,* University of Texas Press, Austin (1973).

49. G. Kinney and K. Graham, *Explosive Shocks in Air,* 2nd Edition, Springer-Verlag (1985).

50. *Guidelines for Consequence Analysis of Chemical Releases,* AIChE Center for Chemical Process Safety (1999).

51. T. Forcier and R. Zalosh, "External Pressures Generated by Vented Gas and Dust Explosions," *J. of Loss Prevention in the Process Industries,* 13, pp. 411–417 (2000).

52. *Guidelines for Evaluating the Characteristics of Vapor Cloud Explosions, Flash Fires, and BLEVEs,* AIChE Center for Chemical Process Safety (1994).

53. B. Baurer, K. Hess, H. Giesbrecht, and W. Louckel, "Modelling of Vapour Cloud Dispersion and Deflagration after Bursting of Tanks Filled with Liquefied Gas," *Proceedings of the 2nd Intemational Symposium on Loss Prevention and Safety Promotion in the Process Industries,* pp. 305–321 (1977).

54. K. Hasegawa and K. Sato, "Study on the Fireball Following Steam Explosion of n-Pentane," *Proceedings of the 2nd International Symposium on Loss Prevention and Safety Promotion in the Process Industries,* pp. 297–304 (1977).

55. K. Hasegawa and K. Sato, "Experimental Investigation of the Unconfined Vapour-Cloud Explosions of Hydrocarbons," *Technical Memorandum No. 12,* Japanese Fire Research Institute (1978).

56. J.A. Fay and D.H. Lewis, Jr., "Unsteady Burning of Unconfined Vapor Clouds," *16th International Symposium on Combustion,* pp. 1397–1405 (1977).

57. R.A. Strehlow, "The Blast Wave from Deflagrative Explosions—An Acoustic Approach," *AlChE Loss Prevention Symposium,* 14, pp. 145–152 (1981).

58. A.C. van den Berg, "The Multi-Energy Method: A Framework for Vapour Cloud Explosion Blast Prediction," *J. of Haz. Matls.,* 12, pp. 1–10 (1985).

Section Four
Design Calculations

Section 4 Design Calculations

CHAPTER 1

Design of Detection Systems

Robert P. Schifiliti, Brian J. Meacham, and Richard L. P. Custer

Introduction

Fire detection and alarm systems are recognized as key features of a building's fire prevention and protection strategy. This chapter presents a systematic technique to be used by fire protection engineers in the design and analysis of detection and alarm systems. The majority of discussion is directed toward systems used in buildings. However, many of the techniques and procedures also apply to systems used to protect planes, ships, outside storage yards, and other nonbuilding environments.

Scientific research on fire growth and the movement of smoke and heat within buildings provides fire protection engineers with information and tools that are useful in the design of fire detection systems. Also, studies of sound production and transmission allow communication systems to be engineered, thus eliminating the uncertainty in locating fire alarm sounders. All of this information allows engineers and designers to design systems that meet specific, identifiable goals.

Sections 1, 2, and 3 of this handbook introduced and discussed a series of concepts and tools for use by fire protection engineers. This chapter shows how some of these tools can be used collectively to design and evaluate detection and alarm systems.

Robert P. Schifiliti, P.E., is a fire protection consultant based in Reading, Massachusetts, and an adjunct associate professor of fire protection engineering at Worcester Polytechnic Institute. He specializes in fire detection and fire alarm system design and analysis.

Brian J. Meacham, Ph.D., P.E., is Principal Risk Consultant and Principal Fire Protection Consult for Arup Fire, located in Massachusetts. Dr. Meacham is a fellow of the Society of Fire Protection Engineers.

Richard Custer, M.Sc., is Technical Director and Principal Fire Analyst for Arup Fire. Mr. Custer is a fellow of the Society of Fire Protection Engineers.

A Note about Precision

When solving multiple equations with numerous variables from many sources, it is often easy to overlook the importance of precision and confidence in the final answer. This acknowledgment is particularly true since engineers have progressed from slide rulers to calculators to computers in a relatively short span of time. Most calculations in this chapter have been done using a computer—most often with a simple spreadsheet. The generally accepted practice for these types of tools is to round off only the final answer to the correct number of significant digits.

The standard and most widely taught rule for rounding is to round off using the same number of significant digits as the least precisely known number used in the calculation. An alternate rule suggests using one more significant figure than suggested by the standard rule. It has been shown that the alternate rule is more accurate and does not lead to loss of data as does the standard rule.[1,2] The alternate rule for rounding has been used in this chapter. For more information or to refresh your knowledge of precision, rounding, and significant figures, consult the references or a standard text on engineering and scientific measurements.

Overview of Design and Analysis

To design a fire detection and alarm system, it is first necessary to establish the system's goals. These goals are established by model codes, the property owner, risk manager, insurance carriers, and/or the authority having jurisdiction. Ultimately, the goals of the system can be put in four basic categories:

1. Life safety
2. Property protection
3. Business protection
4. Environmental concerns

Some designers include heritage conservation in the list of goals. However, the protection of historic property is really another form of property and mission protection, although the methodology and extent for protection may vary.

When designing for life safety, it is necessary to provide early warning of a fire condition. The fire detection and alarm system must provide a warning early enough to allow complete evacuation of the danger zone before conditions become untenable. The fire detectors or fire alarm system may be used to activate other fire protection systems, such as special extinguishing systems and smoke control systems, that are used to help maintain a safe environment during a fire.

In some situations, the life safety mission of a detection system is enhanced by providing information to occupants. This situation is often the case in *stay-in-place* or *defend-in-place* strategies or partial evacuation/relocation strategies. The detection system is used to provide information about the location and extent of the fire. Instructions are then given to the target audience.

Property protection goals are principally economic. The objective is to limit damage to the building structure and contents. Maximum acceptable losses are established by the property owner or risk manager. The goal of the system is to detect a fire soon enough to allow manual or automatic extinguishment before the fire exceeds acceptable damage levels.

Goals for the protection of a mission or business are determined in a manner similar to that used in property protection. Here, fire damages are limited to prevent undesirable effects on the business or mission. Some items that need to be considered are the effects of loss of raw or finished goods, loss of key operations and processes, and loss of business to competitors during downtime. Other concerns include the availability and lead time for obtaining replacement parts. If the equipment to be protected is no longer available or requires several months for replacement, the ability to stay in business during and after an extended period of downtime may be jeopardized.

Protection of the environment is also a fire protection concern. Two examples are (1) toxicity of products of combustion and (2) contamination by fire protection runoff water. Should large quantities of contaminants be expected from a large fire, the goal of the system may well be to detect a fire and initiate appropriate response prior to reaching a predetermined mass loss from burning materials or quantity of fire suppression agent discharged.

Once the overall goals have been set, specific performance and design objectives for a performance-based design can be established.[3–5] Performance-based fire protection design requires that specific performance objectives, rather than generic prescriptive requirements, be met. A typical prescriptive requirement would be to provide a smoke detector for every 84 m^2 (900 ft^2) or 9-m (30-ft) spacing. In prescriptive design, speed of detection and the fire size at detection for such an installation are not known or considered explicitly. In addition, if some action must be taken in response to the alarm in order to control the fire, the expected damage is also unknown.

Implementation of a fire safety performance objective requires that the objective be stated first by the client in terms of acceptable loss. The client loss objectives must then be (1) expressed in engineering terms that can be quantified using fire dynamics, and (2) related to design fires, design fire environments, and the performance characteristics of fire suppression equipment. For example, the client loss objective may be to prevent damage to essential electronic equipment in the compartment of origin. To meet this objective, one must first define what *damage* is. This damage could be expressed in terms of the thickness of the smoke layer. Other criteria, such as temperature or concentration of corrosive combustion products, or a combination of criteria, could also be used.

Based on a study of the likelihood of ignition and fire growth scenarios, a design fire needs to be established. The design fire is characterized by its heat release rate, $\dot{Q}$, at any moment in time; its growth rate, dq/dt; a combustion product rate dcp/dt, such as smoke particulate, toxic or corrosive species, and so forth; and production rate, dp/dt. The design fire may be determined by (1) a combination of small- and large-scale testing specific to the application or (2) analysis of data taken from studies reported in the literature.

For a given fire safety design objective, there will be a point, $\dot{Q}_{do}$, on the design fire curve where the energy and product release rates will produce conditions representative of the design objective. Given that there will be delays in detecting the fire, notifying the occupants, accomplishing evacuation, or initiating suppression actions, the fire will need to be detected at some time in advance of $\dot{Q}_{do}$. In order to account for these delays, a critical fire size, $\dot{Q}_{cr}$, can be defined as the point on the design fire curve at which the fire must be detected in order to meet the design objectives for a given spacing or radial distance from the fire.

There are two types of delays that influence the size of the fire at detection: (1) those that are variable and (2) those that are fixed. Variable delays represent transport lag and are related to radial distance of the detector from the fire, ceiling height, and the convective heat release rate of the fire. Fixed delays are associated with system characteristics, such as alarm verification time. Adding the fixed delays to $\dot{Q}_{cr}$ defines another point on the design fire curve: $\dot{Q}_i$ or the *ideal* fire; that is, the fire that would be detected with no transport delay.

The design fire, $\dot{Q}_{do}$, has been defined as the fire size (in terms of peak heat release and given growth rate history) that corresponds to the maximum acceptable loss fire, and the critical fire, $\dot{Q}_{cr}$, as the maximum fire size at time of detection that allows actions to be taken to limit the continually growing fire to the design fire limit. The time needed to take the limiting actions is the response lag. The total system response time, then, is the amount of time required between the critical fire and the design fire for all the actions to take place before $\dot{Q}_{do}$ is reached, and is the sum of the fixed and variable delays and the response lag. The various design and evaluation points on a design fire curve are shown in Figure 4-1.1.

For example, if the design fire is determined to be 1500 kW and manual suppression will be employed, the critical fire can be selected at a moment in time that permits detection, notification, and response before the 1500 kW fire size is reached. If the total system response
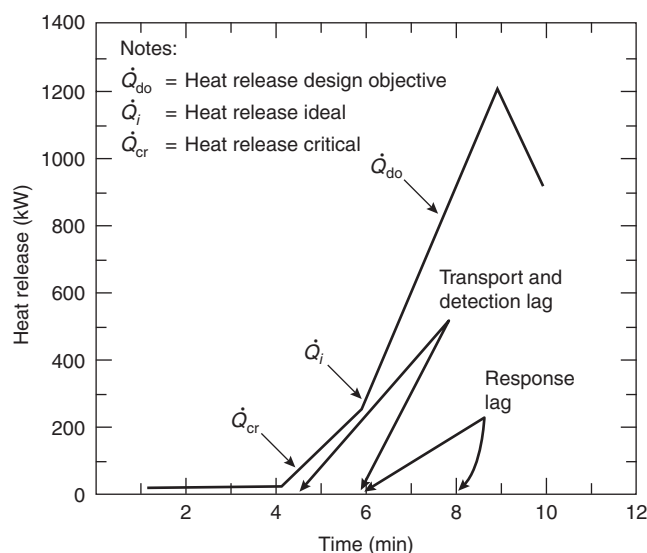
Figure 4-1.1.   *Design fire curve.*

time is estimated to be 3 min, the critical fire would be at the size determined at 3 min prior to reaching 1500 kW using the estimated fire growth rate.

Expressing fire size or fire load as an energy release and growth rate may be thought of in the same way that structural engineers use earthquake zone maps to design for potential earthquakes. Electrical engineers might compare fire loads to fault currents used in designing overcurrent protection devices. At the present time, design fire, critical fire, and total system response time requirements are not established by any building codes. It is the job of the design engineer to work with the building owner and local code officials to establish the performance requirements for a given system application.

Once the goals of a system have been established, several probable fire scenarios should be outlined. The occupancy of the building and the expected fuels should be analyzed to establish an expected fire growth rate and an expected maximum heat release rate. Fire loss reports and fire test data can be used to help estimate heat release rates and the production of smoke and fire gases. It is important that different fire scenarios be evaluated to establish how the system design or response might change as a result of varying fire conditions. Several possible fire scenarios should be outlined using the techniques presented elsewhere in this handbook.

When designing a system, select the most likely fire scenario as the basis of the design. Once the design requirements for spacing and detector type are established, the system's response can be analyzed using the other possible fire scenarios. If the alternate fire scenarios cause the design not to meet the established goals, design changes can be made and retested, if warranted.

The several fire scenarios used when analyzing a system will produce upper and lower bounds or a range of system performance characteristics. The fire scenarios selected should include best and worst case fires as well as several likely scenarios for the particular building characteristics and occupancy.

For the purposes of design or analysis, detection and alarm systems have three basic elements: detection, processing, and signaling. The first, detection, is that part of the system that senses fire. The second element involves the processing of signals from the detection portion of the system. Finally, the processing section of the system activates the signaling portion in order to alert occupants and perform other auxiliary signaling operations. Auxiliary functions may include smoke control, elevator capture, fire department signaling, and door closing.

This chapter focuses on the detection and signaling elements of a fire alarm system. Engineering methods for the design and analysis of heat detector response are presented along with several examples. A method to calculate the audibility of fire alarm sounders is also presented. The selection of a system's control panel and the design of auxiliary functions is beyond the scope of this chapter.

Detection

To design the detection portion of a fire alarm system, it is necessary to determine where fire detectors should be placed in order to respond within the goals established for the system. Several different detector types might respond to the expected fire, so it may be necessary to develop several candidate system designs, using various combinations of detector types in order to optimize the system's performance and cost.

A fire signature[6] is some measurable or sensible phenomenon present during combustion. Table 4-1.1 is a cross-reference of fire signatures and commercially available detector types. The table shows the predominant fire signature to which the detector responds.

Heat Detection

This section discusses an engineering method for determining the placement of heat detectors on a large flat ceiling.

The present practice in designing fire detection systems using heat detectors is to space the detectors at intervals equal to spacings established by tests at Underwriters Laboratories Inc. Listed spacings are determined in full-scale fire tests.[7]

In the Underwriters Laboratories Inc. (UL) test, a burning pan of 190-proof denatured alcohol is located in the center of a test room. Sprinkler heads having a 160°F (71°C) rated operating temperature are located on the ceiling in a square array having 10-ft (3-m) sides. The fire is in the center of the square. The distance between the fire and the ceiling is varied so that the 160°F (71°C) sprinkler head being used operates in approximately 2 min.

As shown in Figure 4-1.2, detectors of the type being tested are located at the corners of squares having 20-, 30-, 40-, and 50-ft (6.1-, 9.1-, 12.2-, and 15.2-m) sides. The spacing of the last detector to operate prior to a sprinkler head operating becomes the detector's listed spacing. A similar test procedure is employed by Factory Mutual Research Corporation (FMRC) to arrive at an approved detector spacing.

Table 4-1.1   *Fire Signatures and Commercially Available Detectors*

Fire Signature/ Detector Type	Electromagnetic Radiation Wave Length 1700 to 2900 Angstroms	Electromagnetic Radiation (thermal) 6500 to 8500	Invisible Products of Combustion Less Than 0.1 Micron	Visible Smoke and Products of Combustion More Than 0.1 Micron	Rapid Change in Temperature	High Temperature
Ultraviolet detector	X					
Infrared detector		X				
Sub-micron particle detector						
Wilson cloud chamber			X			
Infrared particle detector						
Smoke detector						
photoelectric				X		
ionization			X			
photo beam				X		
Rate-of-rise heat detector					X	
Rate anticipation heat detector						X
Fixed temperature heat detector						X

Figure 4-1.2.   *Detector test layout.*

H = Heat detector
S = Sprinkler
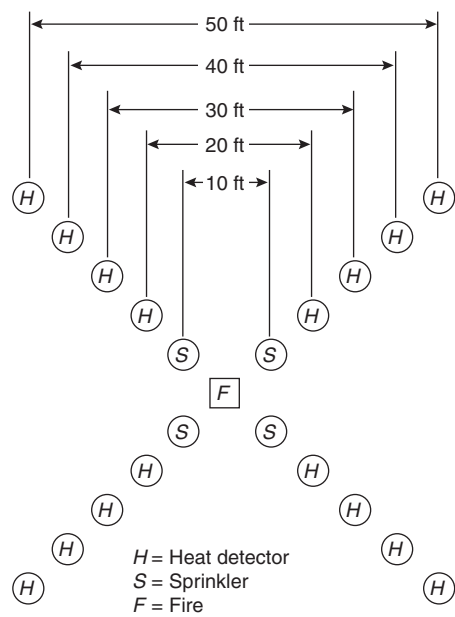F = Fire

Most codes require that detectors be spaced at intervals equal to the UL or FMRC spacing. NFPA 72, National Fire Alarm Code®,[8] 1999 edition, requires that the installed spacing be less than the listed spacing to compensate for high ceilings, beams, and air movement. High ceilings mean that the fire plume will entrain more ambient air as it rises. This condition has the effect of cooling the gases and reducing the concentration of fire products. Beams, joists, walls, or sloped ceilings alter the flow of combustion products. This situation can serve to restrict or enhance the operation of a fire detector. For instance, consider the case where a fire detector is located on a ceiling between two parallel beams and a fire occurs at floor level between the beams. If the distance between the beams is small compared to the horizontal distance from the fire to the detector, the beams will act as a channel directing the flow of hot gas to the detector, thus speeding operation. NFPA 72 allows detector spacing to be increased beyond the listed spacing in areas, such as corridors, with narrow walls to confine the smoke and heat produced by the fire. Systems can be designed using this type of code approach; however, this approach will not permit quantitative assessment of detector response or measure the ability of a given system design to meet specific design goals relating to fire size, allowable damage, or hazard.

The best possible location for a heat detector is directly over the fire. If there are specific hazards to be protected, the design should include detectors directly overhead or inside of the hazard. In areas without specific hazards, detectors should be spaced evenly across the ceiling. When detectors are evenly spaced, as shown in Figure 4-1.3, the point that is farthest from any detector will be in the middle of four detectors. The spacing between detectors is

$$S = 2^{1/2}r \qquad (1)$$

For a given detector, the problem is to determine the maximum distance the detector can be located from the fire and still respond within the design goals of the system. This requires a method for predicting detector response, based on fire size and growth rate, ceiling height, and detector characteristics.

Fire plume and ceiling-jet models can be used to estimate the temperature and velocity of fire gases flowing past a detector. The heat transfer can be calculated, and the response of the detector can be modeled.
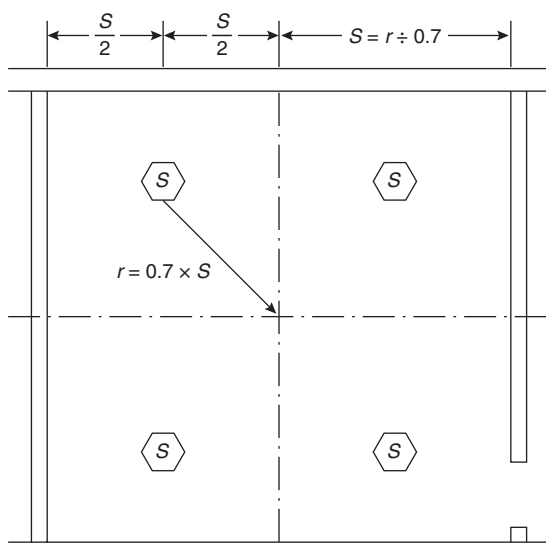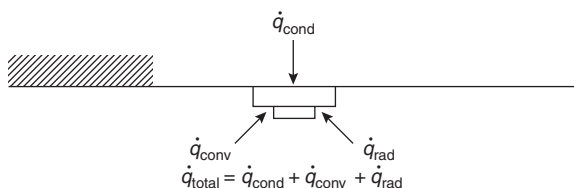
Figure 4-1.3. *Detector spacing.*

Figure 4-1.4. *Heat transfer to a ceiling-mounted detector.*

Figure 4-1.4 describes the heat transfer taking place between a heat detector and its environment. The total heat transfer rate to the unit, $\dot{q}_{total}$, can be expressed by the relationship

$$\dot{q}_{total} = \dot{q}_{cond} + \dot{q}_{conv} + \dot{q}_{rad} \quad \text{(kW or Btu/s)} \qquad (2)$$

where

$\dot{q}_{cond}$ = conduction

$\dot{q}_{conv}$ = convection

$\dot{q}_{rad}$ = radiation heat transfer rates

During the initial stage of fire growth, radiation heat transfer can be neglected. Also, the elements of most commercially available heat detectors are thermally isolated from the remainder of the unit. In these cases, it can be assumed that the heat lost from the heat-sensitive element by conduction to other parts of the detector, and to the ceiling by conduction, is negligible in comparison to the convection heat transfer taking place. This exclusion leaves a net rate of heat transfer to the detector equal to $\dot{q}_{conv}$. The convective heat transfer rate to the detector is described by

$$\dot{q} = \dot{q}_{conv} = hA(T_g - T_d) \quad \text{(kW or Btu/s)} \qquad (3)$$

where

h = convective heat transfer coefficient in kW/(m²·°C) or Btu/(s·ft²·°F)

A = area being heated

T_d = detector temperature

T_g = temperature of the gas heating the detector

Treating the detector element as a lumped mass, m (kg or lbm), the change in its temperature is found by

$$\frac{dT_d}{dt} = \frac{\dot{q}}{mc} \quad \text{deg/s} \qquad (4)$$

where c is the specific heat of the element being heated and has units of kJ/(kg·°C) or Btu/(lbm·°F) and $\dot{q}$ is the heat transfer rate. This equation leads to the following relationship for the change in temperature of the detector with respect to time:

$$\frac{dT_d}{dt} = \frac{hA(T_g - T_d)}{mc} \qquad (5)$$

Heskestad and Smith[9] have proposed use of a time constant, τ, to describe the convective heat transfer to a particular detector element:

$$\tau = \frac{mc}{hA} \quad \text{s} \qquad (6)$$

$$\frac{dT_d}{dt} = \frac{T_g - T_d}{\tau} \qquad (7)$$

Note that τ is a function of the mass, area, and specific heat of the particular detector element being studied. For a given fire-gas temperature and velocity and a particular detector design, an increase in mass increases τ. A larger τ results in slower heating of the element.

The convective heat transfer coefficient, h, is a function of the velocity of the gases flowing past the detector element and the shape of the detector element. For a given detector, if the gas velocity is constant, h is constant. It has been shown[10] that the convective heat transfer coefficient for spheres, cylinders, and other objects similar to a sprinkler or heat detector element is approximately proportional to the square root of the Reynolds number, Re:

$$\text{Re} = \frac{ud}{v} \qquad (8)$$

where

u = gas velocity

d = diameter of a cylinder or sphere exposed to convective heating

v = kinematic viscosity of the gas

For a given detector, this equation means that h and, hence, τ, is approximately proportional to the square root of the velocity of the gases passing the detector. This relationship can be expressed as a characteristic response time index, RTI, for a given detector:

$$\tau u^{1/2} \simeq \tau_0 u_0^{1/2} = \text{RTI} \qquad (9)$$

Thus, if τ_0 is measured in the laboratory at some reference velocity u_0, this expression is used to determine the τ at any other gas velocity, u, for that detector. The product, $\tau u^{1/2}$, is the response time index, RTI.

The use of RTI as a heat transfer function is a simplification. The determination of RTI assumes that τ (and therefore h) is proportional to the square root of the gas velocity, regardless of the magnitude of the velocity. The flow of gases past irregularly shaped objects such as detectors and sprinklers is very complex. Even the flow past cylinders is too complex to use a simple relationship for the heat transfer coefficient (i.e., constant RTI). Hollman showed that the heat transfer coefficient (and therefore τ) is actually proportional to the Reynolds number raised to a fractional power, n, that varies from 0.330 to 0.805 depending on the value of the Reynolds number.[10] For values of Re between 40 and 4000, which is probably the range for most fire detection scenarios, the value of n is given as 0.466. This value is close to 0.5 (square root), but may explain some of the variation found in the experimental determination of τ and RTI.

Plunge tests performed on a variety of heat detectors by Bissell[11] show variations in τ and RTI, while other tests produced reasonable results for a variety of test parameters. It is possible that further analysis may show that an RTI based on $n = 0.5$ is reasonable and that the potential errors are insignificant in the context of fire and detector modeling. On the contrary, it may be found that some other value for n produces better results.

The exponent n may vary over ranges of Reynolds numbers less than those reported by Hollman. Some detector geometries are aerodynamically designed to channel fire gases to the detector element. The ability to affect the gas flow is a function of both the flow velocity and whether the flow is turbulent or laminar. These effects introduce additional variables that complicate the determination of a heat transfer function.

An added source of error in heat transfer modeling is that the temperature-sensing element of a heat detector is never completely isolated from the detector body. This setup results in conductive heat loss that may not be accounted for when using only one time constant. Kokkala has shown that for some detectors as much as 10 percent of the heat gained by convection is lost by conduction to the detector body.[12] A two-time-constant approach, similar to the C parameter used in modeling the response of sprinkler heads, is suggested by Kokkala. In a plunge test, the velocity may be high enough so that the conduction heat loss is negligible when compared to the heat gain by convection. In actual fire conditions, this conduction heat loss may contribute to the variation in RTI as it is currently used.

The magnitude of the potential error resulting from the assumption that RTI is constant has not been investigated. Future research and analysis should also consider the possibility that it might be best to test and report several discrete values for τ (hence h).[13] An example is using a plunge test to find τ at three different velocities. The slow, medium, and fast velocities should be representative of the range of possible fire-gas velocities.

A continuous curve of τ versus u for every model detector would be ideal. However, the economic feasibility of testing must be considered. At the present time, heat detectors are tested in ovens to determine their operating

temperatures, and are tested in full-scale fire tests to determine their listed spacing (relative sensitivity). A single oven could be used to test for operating temperature and τ at several different velocities as discussed above. This type of testing would be more repeatable (precise), have a lower environmental impact, and give results that can be directly used by engineers in performance-based analysis and design. The test data could be used to calculate a listed spacing comparable to that determined in the present full-scale test so that current code-based design methods could continue to be used.

The remainder of the calculations in this chapter will be made using RTI as a heat transfer function. The user will readily see how other functions, when available, can be incorporated into the equations to effect other solutions.

Heskestad and Smith[9] developed a test apparatus at Factory Mutual Research Corporation to determine the RTI of sprinkler heads. In the test, called a *plunge test*, the sprinkler head is suddenly lowered into the flow of a hot gas. The temperature and velocity of the gas are known and are constant during the test. The equation for the change in the detector temperature is then

$$\frac{dT_d}{dt} = \left(\frac{1}{\tau}\right)(T_g - T_d) \tag{10}$$

Since the gas temperature is constant during the test, the solution to this equation is

$$T_d - T_a = (T_g - T_a)\left[1 - \exp\left(\frac{-t}{\tau}\right)\right] \tag{11}$$

where T_a is the ambient, or initial, temperature of the sprinkler or detector at time $t = 0$. T_d is the temperature of the detector at time t. Rearranging the equation gives

$$\tau = \frac{t}{\ln\left[(T_g - T_a)/(T_g - T_d)\right]} \tag{12}$$

By measuring the response time, t_r, of the unit in the plunge test, this equation can be used to calculate τ_0 at the test velocity u_0. This calculation is done by substituting the response temperature and time for T_d and t. The sensitivity of the detector or sprinkler can then be expressed as

$$\tau_0(\text{at } u_0) = \frac{t_r}{\ln\left[(T_g - T_a)/(T_g - T_r)\right]} \text{ (s)} \tag{13}$$

In terms of the response time index, this equation becomes

$$\text{RTI} = \frac{t_r u_0^{1/2}}{\ln\left[(T_g - T_a)/(T_g - T_r)\right]} \tag{14}$$

The RTI has units of $m^{1/2}s^{1/2}$ or $ft^{1/2}s^{1/2}$.

A plunge test can be used to determine the RTI for a heat detector or a sprinkler. Knowing the RTI, the change in temperature of similar units can be calculated for any history of fire gases flowing past it. The form of the heat transfer equation is

$$\frac{dT_d}{dt} = \frac{u^{1/2}(T_g - T_d)}{\text{RTI}} \tag{15}$$

This equation is used to calculate the temperature of a fixed-temperature heat detector or sprinkler exposed to

fire gases. The equation can be used to determine the time at which the unit reaches its operating temperature.

The use of a lumped mass model may not hold for rate-of-rise heat detectors and rate-compensated heat detectors. The heat transferred to a fixed-temperature heat detector either heats a sensing element until it melts, or it heats two dissimilar metals of a snap disk. In each case, the element itself is exposed to the hot gases. This result is not true for rate-of-rise heat detectors or rate-compensated heat detectors.

Most commercial rate-of-rise heat detectors operate when the expansion of air in a chamber exceeds the rate at which the air can escape through a small vent hole. For this type of detector, it is also necessary to model heat transfer from the detector body to the air in its chamber. Then, the expansion of the air and its escape through a vent hole must be accounted for. The response time index determined in a plunge test may not be constant as fire-gas velocities or temperatures vary. Hence, RTI is only an approximation of how the detector responds. Also, it has been hypothesized, but not tested, that rate-of-rise detectors may be modeled by simply comparing the rate of change of gas temperature to their rated response threshold.[13] This hypothesis may be true since their rated response in degrees per minute or degrees per second is actually the measured rate of gas temperature change in the test apparatus. Thus, it would be expected that if the velocity of the fire gases was on the same order of magnitude as in the test, the rate of change of gas temperature would be the measure for detector response.

A rate-compensated detector consists of a metallic shell surrounding two bowed metal struts. There are electrical contacts on the struts. The struts and shell expand at different rates as the detector is heated. When heated fast, the outer shell expands and causes the bowed struts to straighten and close the contacts, signaling an alarm. This condition usually occurs at temperatures below the rated operating temperature. However, if the unit is heated more slowly, the difference between the expansion rates of the inner and outer parts is such that the contacts close at or near the unit's rated temperature. For rates of temperature rise up to approximately 22°C/min (40°F/min), rate-compensated detectors tend to respond when the surrounding gas temperature reaches the unit's rated operating temperature.[14]

Obviously, the rate-compensated type of heat detector cannot be treated as a lumped mass when calculating its response to a fire. However, at rates of temperature rise less than approximately 22°C/min (40°F/min), they can be modeled by simply assuming that they respond when the surrounding gas temperature reaches their operating temperature.

From the discussion above, it is evident that the response of fixed-temperature heat detectors can be modeled. It is necessary to know the temperature at which the detector is rated to operate. For rate-of-rise heat detectors, it is necessary to know the rate of change in the detector's temperature at which it will alarm. The RTI or τ_0 and u_0 for the detector are also needed.

In order to calculate the response of a heat detector, it is necessary to know the temperature and velocity of the gases flowing past it. Some fire plume models or ceiling-jet models may give functional relationships for temperature and velocity that can be substituted into the heat transfer equation and integrated. Other models may not be suitable for an analytical solution. In this case, the fire model should be used to produce data on time-versus-temperature and time-versus-gas velocities. These data can then be used to numerically solve the detector heat transfer equation.

Most fire and ceiling-jet models do not model the temperature and velocity profile as a function of distance from the ceiling. This lapse introduces error and uncertainty in the results. Marrion[15] showed that maximum temperature and velocity occurs between 1 and 3 in. (25 and 76 mm) below the ceiling for small (5- to 7-in. [127 to 178 mm] diameter) gasoline pan fires with a ceiling clearance of about 14 ft (4.3 m). Others have reported maximums at a distance down from the ceiling of approximately one-tenth the distance from the fuel to the ceiling. Alpert[16] reports ceiling jet thickness to be approximately 5 to 12 percent of the ceiling to fuel distance. Users are cautioned when modeling detector mechanisms that are not within this range.

When the responses of multiple detectors or sprinklers are modeled, no provisions are made to account for sprinkler spray cooling of the room, and therefore, the activation of additional elements (beyond the first) may be inaccurately predicted. For more information on this topic the reader is referred to the references for works by Cooper, Delichatsios and Alpert, and Heskestad.[17–19]

Heat Detection—Steady-State Fires

Alpert[16] presented the following series of equations to calculate temperature and velocity of fire gases in a ceiling jet as a function of heat release rate and position for steady-state fires:

$$T_g - T_a = \frac{[5.38(\dot{Q}/r)^{2/3}]}{H} \,°C = \frac{[4.74(\dot{Q}/r)^{2/3}]}{H} \,°F$$

where $r/H > 0.18$, and

$$T_g - T_a = \frac{(16.9\dot{Q}^{2/3})}{H^{5/3}} \,°C = \frac{(14.9\dot{Q}^{2/3})}{H^{5/3}} \,°F$$

where $r/H \le 0.18$, and

$$u = \frac{(0.20\dot{Q}^{1/3}H^{1/2})}{r^{5/6}} \,\text{m/s} = \frac{(0.25\dot{Q}^{1/3}H^{1/2})}{r^{5/6}} \,\text{ft/s}$$

where $r/H > 0.15$, and

$$u = 0.95\left(\frac{\dot{Q}}{H}\right)^{1/3} \,\text{m/s} = 1.2\left(\frac{\dot{Q}}{H}\right)^{1/3} \,\text{ft/s}$$

where $r/H \le 0.15$.

In the above series of equations,

T_g = maximum, near ceiling, fire-gas temperature in °C or °F

T_a = ambient temperature in °C or °F

$\dot{Q}$ = total heat release rate of the fire in kW or BTU/min

r = radial distance from the axis of the fire plume in m or ft

H = height above the origin of the fire in m or ft

u = maximum, near ceiling, fire-gas velocity in m/s or ft/s

This model assumes that the temperature and velocity of the fire gases at a point away from the source are related to the instantaneous heat release rate of the fire. This assumption neglects the time required for transport of the fire gases from the source to the detector. Also, because the correlations are based on the total heat release rate rather than only the convective heat release rate, errors will be introduced when the convective fraction differs from that in the tests used to develop the correlations.

For a constant gas temperature and constant gas velocity, the basic heat transfer equation can be solved:

$$\frac{dT_d}{dt} = \frac{T_g - T_d}{\tau} \qquad (7)$$

$$dT_d = \int_0^t \frac{1}{\tau}(T_g - T_d)\,dt$$

$$\Delta T_d = T_d - T_a = (T_g - T_a)\left[1 - \exp\left(\frac{-t}{\tau}\right)\right] °\mathrm{C}$$

or, substituting the equation for RTI

$$\Delta T_d = T_d - T_a = (T_g - T_a)\left[1 - \exp\left(\frac{-tu^{1/2}}{\mathrm{RTI}}\right)\right] °\mathrm{C}$$

The response of heat detectors to fires with ceiling jets having a near constant gas temperature and velocity can be modeled using the above equations.

EXAMPLE 1:
A 4-m^2 pool of kerosene is burning under a flat ceiling that is 6 m high. The ambient temperature is 20°C. What would be the temperature of a ceiling-mounted heat detector having an RTI of 55 m$^{1/2}$s$^{1/2}$ after a 30-s exposure if it were located 6 m from the center of the plume?

SOLUTION:
From Table 3-4.11 in this handbook the chemical heat of combustion of kerosene is 40.3 kJ/g. The convective heat of combustion is listed as 26.2 kJ/g, which is a convective fraction of about 65 percent. For Alpert's correlations we must use the total heat release rate, hence the total or chemical heat of combustion. This calculation assumes that the convective fraction will be approximately the same as the convective fraction in the experimental data Alpert used to develop the correlations for temperature and velocity. From Table 3-4.5 the mass burning rate is given as approximately 67 g/m^2·s. The total heat release rate is

$$\dot{Q} = H_c \dot{m}'' A \text{ kW}$$

$$\dot{Q} = 40.3(67)4 \text{ kW}$$

$$\dot{Q} = 10,800 \text{ kW}$$

An r/H ratio greater than 0.18 indicates that the detector is located in the ceiling jet temperature profile. In this example,

$$\frac{r}{H} = \frac{6}{6} = 1 > 0.18$$

Therefore,

$$T_g - T_a = \frac{[5.38(\dot{Q}/r)^{2/3}]}{H} °\mathrm{C}$$

$$T_g - 20 = \frac{[5.38(10,800/6)^{2/3}]}{6} °\mathrm{C}$$

$$T_g - 20 = 132.7°\mathrm{C}$$

$$T_g = 153°\mathrm{C}$$

The velocity of the fire gases in the ceiling jet is given by

$$u = \frac{(0.20\dot{Q}^{1/3}H^{1/2})}{r^{5/6}} \text{ m/s}$$

$$u = \frac{[0.20(10.800)^{1/3}(6)^{1/2}]}{6^{5/6}} \text{ m/s}$$

$$u = 2.4 \text{ m/s}$$

The resulting detector temperature after 120 s is now calculated:

$$\Delta T_d = T_d - T_a = (T_g - T_a)\left[1 - \exp\left(\frac{-tu^{1/2}}{\mathrm{RTI}}\right)\right] °\mathrm{C}$$

$$\Delta T_d = (153 - 20)\left[1 - \exp\left(\frac{-30(2.4)^{1/2}}{55}\right)\right] °\mathrm{C}$$

$$\Delta T_d = 76°\mathrm{C}$$

$$T_d = 76 + T_a = 76 + 20 = 96°\mathrm{C}$$

EXAMPLE 2:
What would be the response time of the detector in the above example if its temperature rating was 57°C?

SOLUTION:

$$\Delta T_d = T_d - T_a = (T_g - T_a)\left[1 - \exp\left(\frac{-tu^{1/2}}{\mathrm{RTI}}\right)\right] °\mathrm{C}$$

Rearranging and substituting the rated response temperature T_r for T_d, and response time t_r for t,

$$t_r = \frac{\mathrm{RTI}}{u^{1/2}} \ln\left(\frac{T_g - T_a}{T_g - T_r}\right) °\mathrm{C}$$

$$t_r = \frac{55}{2.4^{1/2}} \ln\left(\frac{153 - 20}{153 - 57}\right) °\mathrm{C}$$

$$t_r = 12 \text{ s}$$

Heat Detection, Growing Fires, and Quasi-Steady-State Modeling

A growing fire can be modeled by assuming the fire to be composed of a series of increasing steady heat release rates. This model is referred to as quasi-steady-state modeling. The first step is to break the heat release rate curve into a series of small time intervals. For each interval, use the average heat release rate for that interval to calculate the fire-gas temperature and velocity. Then, starting at ambient temperature, calculate the change and resulting temperature of the detector at the end of the first interval. Using that new detector temperature at the start of the next interval, use the next gas temperature and ve-

locity to calculate the detector temperature at the end of the interval. Continue until you have reached the time of interest or until the detector temperature exceeds its operating temperature.

EXAMPLE 3:

A stack of wood pallets is burning under a flat ceiling that is 6 m high. Table 4-1.2, showing heat release rates, is given below. The ambient temperature is 20°C. What would be the temperature of a ceiling-mounted heat detector having an RTI of 55 $m^{1/2} \cdot s^{1/2}$ after a 180-s exposure if it were located 6 m from the center of the plume?

SOLUTION:

As in the previous examples, the detector is located in the developed ceiling jet. The first step is to calculate the change in temperature and the velocity for each heat release rate in the table. For the period 0 to 10 s, the heat release rate is given as 5 kW. The change in temperature and the velocity of the ceiling jet at the detector are

$$T_g - T_a = \frac{\left[5.38 \left(\frac{\dot{Q}}{r} \right)^{2/3} \right]}{H} °C$$

$$T_{g,1} - T_a = \frac{\left[5.38 \left(\frac{5}{6} \right)^{2/3} \right]}{6} = 0.794°C$$

$$T_{g,1} = 20.794°C$$

$$u = \frac{(0.20 \dot{Q}^{1/3} H^{1/2})}{r^{5/6}} \text{ m/s}$$

$$u_1 = \frac{[0.20(5)^{1/3}(6)^{1/2}]}{6^{5/6}} = 0.188 \text{ m/s}$$

Next calculate the change in detector temperature ΔT_d as a result of that exposure by assuming the temperature and velocity to be steady over short intervals.

$$\frac{dT_d}{dt} = \frac{T_g - T_d}{\tau} = \frac{u^{1/2}(T_g - T_d)}{RTI}$$

$$\Delta T_d = T_{d,n} - T_{d,n-1} = \frac{u_n^{1/2}(T_{g,n} - T_{d,n-1})}{RTI} \Delta t°C$$

$$T_{d,n} = \left[\frac{u^{1/2}(T_{g,n} - T_{d,n-1})}{RTI} \Delta t \right] + T_{d,n-1} °C$$

Initially, the detector is not exposed to hot gases and is at ambient temperature. For the first step or interval, the detector is exposed and the resulting detector temperature at the end of the interval ($T_{d,1}$) is calculated.

$$T_{d,1} = \left[\frac{u^{1/2}(T_{g,1} - T_{d,0})}{RTI} \Delta t \right] + T_{d,0} °C$$

$$T_{d,1} = \left[\frac{(0.188)^{1/2}(20.794 - 20)}{55} 10 \right] + 20 = 20.063°C$$

To simplify the process, set up a table or a spreadsheet, as shown in Table 4-1.3, to complete the calculations. Rounding to two significant digits is done last. After 120 seconds of exposure the detector temperature is approximately 32°C. If the dectector were rated at 57°C, it would not have responded.

Heat Detection—Potential Errors: Steady-State and Quasi-Steady-State Modeling

There are many sources of potential error in these calculations. These include the following: uncertainty in the operating temperature, uncertainty in the ambient temperature, and inaccuracies in the fire-gas temperature and velocity correlations. Because the magnitude of these potential errors is unknown or unreported, a tolerance or confidence interval for the answer cannot be estimated.

In addition, it has been assumed that use of the ceiling-jet model is valid for the examples above. The model assumes an infinite ceiling for the ceiling jet to flow outward without encountering walls and developing a layer. In the first example, the gas velocity was 2.4 m/s, and the calculation was done for a period of 120 s. The leading edge of the ceiling jet would then be approximately 48 m (2.4 m/s × 120 s) from the fire location. This dimension can be used

Table 4-1.2   *Example 3—Heat Release Rates*

Δt	$\dot{Q}$	Δt	$\dot{Q}$
0	0	100	469
10	5	110	567
20	19	120	675
30	42	130	792
40	75	140	919
50	117	150	1055
60	169	160	1200
70	230	170	1355
80	300	180	1519
90	380		

Table 4-1.3   *Example 3—Spreadsheet Calculations*

t	$\dot{Q}$	ΔT_g	T_g	u	ΔT_d	T_d
0	0	0		0	0	20
10	5	0.794	20.794	0.188	0.063	20.063
20	19	1.934	21.934	0.294	0.184	20.247
30	42	3.281	23.281	0.383	0.341	20.588
40	75	4.830	24.830	0.464	0.525	21.114
50	117	6.496	26.496	0.538	0.718	21.832
60	169	8.301	28.301	0.609	0.918	22.749
70	230	10.194	30.194	0.674	1.112	23.861
80	300	12.170	32.170	0.737	1.297	25.158
90	380	14.247	34.247	0.797	1.476	26.633
100	469	16.393	36.393	0.855	1.641	28.274
110	567	18.603	38.603	0.911	1.792	30.066
120	675	20.896	40.896	0.965	1.935	32.001

as a test to determine if additional error is possible because limitations of the model have been exceeded.

Evans and Stroup[20] published a computer program called DETACT-QS, which uses Alpert's equations to calculate the response of heat detectors. That program requires the following input: ceiling height, H; ambient temperature, T_a; distance from fire axis to detector, r; detector response or activation temperature, T_r; and detector response time index (RTI). The user must also input history of time versus heat release rate for the fire. The program uses the quasi-steady-state method demonstrated above to calculate the detector response.

Heat Detection—Power-Law Fires

Heskestad and Delichatsios[8] presented functional relationships for modeling the temperature and velocity of fires whose heat release rates grow according to the power-law relationship:

$$\dot{Q} = \alpha t^p \text{ kW}$$

where

α = constant for a particular fuel describing the growth of the fire (kW/s²)

t = time (s)

p = positive exponent

$\dot{Q}$ = heat release rate (kW)

NFPA 72, Appendix B, uses a constant called the *fire growth time*, t_g, in lieu of α to describe the fire intensity. The fire growth time is defined as the time at which a power-law fire would reach a heat release rate of 1055 kW (1000 Btu/s). In terms of t_g, the power-law equation becomes

$$\dot{Q} = \left(\frac{1055}{t_g^2}\right) t^p \text{ kW}$$

The nondimensional functional relationships given by Heskestad and Delichatsios[21] for temperature and velocity of fire gases in a ceiling jet are

$$u_p^* = \frac{u}{(A^{1/(3+p)}\alpha^{1/(3+p)}H^{(p-1)/(3+p)})}$$
$$u_p^* = f\left(t_p^*, \frac{r}{H}\right) \tag{16}$$

$$\Delta T_p^* = \frac{\Delta T}{A^{2/(3+p)}(T_a/g)\alpha^{2/(3+p)}H^{-(5-p)/(3+p)}}$$
$$\Delta T_p^* = g\left(t_p^*, \frac{r}{H}\right) \tag{17}$$

where

$$A = \frac{g}{C_p T_a \rho_0} \tag{18}$$

$$t_p^* = \frac{t}{A^{-1/(3+p)}\alpha^{-1(3+p)}H^{4/(3+p)}} \tag{19}$$

All variables are described in this chapter's nomenclature section.

For $p = 2$ power-law fires, the above nondimensional equations reduce to the following:

$$u_2^* = \frac{u}{(A^{1/5}\alpha^{1/5}H^{1/5})}$$

$$\Delta T_2^* = \frac{\Delta T}{A^{2/5}(T_a/g)\alpha^{2/5}H^{-3/5}}$$

$$t_2^* = \frac{t}{A^{-1/5}\alpha^{-1/5}H^{4/5}}$$

Heskestad and Delichatsios[21] presented correlations to the functional relationships for fires whose release rates vary according to the power-law equation, with $p = 2$. These fires are referred to as t^2 fires. It has been shown[22,23] that the $p = 2$ power-law fire growth model can be used to model the heat release rate of a wide range of fuels. The original correlations were used in several publications and popular calculation programs for ceiling-jet and heat-detector modeling, including the first two editions of this handbook.[8,9,20,23–26]

Subsequently Heskestad and Delichatsios found that an incorrect value for the heat of combustion of wood resulted in the correlations being in error. All examples in this chapter that use these correlations have been updated or replaced. The corrected data correlations are as follows:[27]

$$t_{2f}^* = 0.861\left(1 + \frac{r}{H}\right)$$

t_{2f}^* is the nondimensional time at which the heat front reaches the detector. When $t_2^* < t_{2f}^*$, the heat front has not reached the detector position. Therefore, $\Delta T_2^* = 0$.

For $t_2^* \geq t_{2f}^*$,

$$\Delta T_2^* = \left[\frac{(t_2^* - t_{2f}^*)}{(0.146 + 0.242r/H)}\right]^{4/3}$$

This relationship may also be expressed as

$$\Delta T_2^* = \left[\frac{(t_2^* - t_{2f}^*)}{D}\right]^{4/3}$$

where

$$D = 0.146 + 0.242\frac{r}{H}$$

$$\frac{u_2^*}{(\Delta T_2^*)^{1/2}} = 0.59\left(\frac{r}{H}\right)^{-0.63}$$

The above correlations assume that the convective heat release rate is approximately 75 percent of the total heat release rate. The following equations are more useful forms and are used with the nondimensional equations for ΔT_2^* and u_2^* by first multiplying α by the convective fraction X:

$$\alpha_c = X\alpha \text{ kW/s}^2$$

$$t_{2f}^* = 0.813\left(1 + \frac{r}{H}\right) \tag{20}$$

$$\Delta T_2^* = 0$$

when $t_2^* < t_{2f}^*$.

For $t_2^* < t_{2f}^*$,

$$\Delta T_2^* = \left[\frac{(t_2^* - t_{2f}^*)}{(0.126 + 0.210r/H)} \right]^{4/3} \qquad (21)$$

This may also be expressed as

$$\Delta T_2^* = \left[\frac{(t_2^* - t_{2f}^*)}{D} \right]^{4/3}$$

where

$$D = 0.126 + 0.210\frac{r}{H} \qquad (22)$$

$$\frac{u_2^*}{(\Delta T_2^*)^{1/2}} = 0.59\left(\frac{r}{H}\right)^{-0.63} \qquad (23)$$

Beyler found that these correlations for temperature and velocity could be substituted into the heat transfer equation and integrated.[28] Beyler's analytical solution was published in *Fire Technology*[29] and is repeated here.

The analytical solution for the instantaneous rate of change of detector temperature is

$$\frac{dT_d(t)}{dt} = \frac{4}{3}\frac{\Delta T}{\Delta T_2^*} \Delta T_2^{*1/4} \frac{(1 - e^{-Y})}{(t/t_2^*)D} \qquad (24)$$

The analytical solution for change in detector temperature is

$$\Delta T_d = T_d(t) - T_d(0) = \frac{\Delta T}{\Delta T_2^*} \Delta T_2^* \left[1 - \frac{(1 - e^{-Y})}{Y} \right] \qquad (25)$$

where

$$Y = \frac{3}{4}\sqrt{\frac{u}{u_2^*}}\sqrt{\frac{u_2^*}{(\Delta T_2^*)^{1/2}}}\left(\frac{\Delta T_2^*}{\mathrm{RTI}}\right)\left(\frac{t}{t_2^*}\right)D \qquad (26)$$

and as previously defined,

$$D = 0.126 + 0.210\frac{r}{H} \qquad (22)$$

In a design situation, the objective is to determine the spacing of detectors required to respond to a specific fire scenario. The detector must respond when the fire reaches a certain threshold heat release rate or in a specified amount of time. Time and heat release rate are interchanged using the fire growth model. The steps in solving this type of problem using the $p = 2$ power-law model are outlined below and are discussed in more detail in the examples following this section. The referenced equation numbers assume that the correlations used are the ones for a variable convective fraction. The procedure would be the same if using the correlations for the fixed, 75 percent convective fractions except that α is not multiplied by the convective fraction when used in the equations. For design problems,

1. Determine the environmental conditions of the area being considered.
    a. ambient temperature, T_a (convert to absolute temperature)
    b. ceiling height or height above fuel, H
2. Estimate the fire growth characteristic α or t_g for the fuel expected to be burning. If t_g is used, calculate the

corresponding α. Multiply α by the convective fraction to get α_c before using in the equations.
3. Establish the goals of the system: required response time t_r or maximum permitted threshold heat release rate $\dot{Q}_T$.
4. Select the detector type to be used. For fixed-temperature units, this choice establishes the detector response temperature T_r and its RTI, or τ_0 and u_0.
5. Make a first estimate of the distance, r, from the fire to the detector necessary to meet the system goals.
6. Assume that the fire starts obeying the power-law model at time $t = 0$.
7. Set the initial temperature of the detector and its surroundings at ambient temperature.
8. Using Equation 20, calculate the nondimensional time, t_{2f}^*, at which the initial heat front reaches the detector.
9. Calculate the factor A defined in Equation 18.
10. If the equations for a variable convective fraction are used, multiply α by the convective fraction X to get α_c and use result that with the required response time in Equation 19 to calculate the corresponding value of t_2^*.
11. If t_2^* is greater than t_{2f}^*, continue with Step 12. If not, try a new detector position, r, closer to the fire and return to Step 8.
12. Calculate the ratio u/u_2^* using Equation 16.
13. Calculate the ratio $\Delta T/\Delta T_2^*$ using Equation 17.
14. Use Equation 21 to calculate ΔT_2^*.
15. Equation 23 is used to calculate the ratio $u_2^*/(\Delta T_2^*)^{1/2}$.
16. Use Equations 22 and 26 to calculate D and Y.
17. Equation 25 can now be used to calculate the resulting temperature of the detector.
18. If the temperature of the detector is below its operating temperature, this procedure must be repeated using a smaller r. If the temperature of the detector exceeds its operating temperature, a larger r can be used.
19. Repeat this procedure until the detector temperature is about equal to its operating temperature. The required spacing of detectors is then $S = 1.41r$.

This same procedure is used to estimate the response of rate-of-rise heat detectors. The difference is that in Step 17, Equation 24 is used to calculate rate of change of the detector temperature. This result is then compared to the rate at which the detector is designed to respond.

The discussion and procedure so far has centered around the solution of a design problem. The question asked was, How far apart must detectors of a specific design be spaced to respond within specific goals to a certain set of environmental conditions and a specific fire scenario?

The second type of problem that must be addressed is the analysis of an existing system or the analysis of a proposed design. Here the spacing of detectors or sprinklers is known. The engineer must still estimate the burning characteristics of the fuel and the environmental conditions of the space being analyzed. The equations can then be solved in a reverse fashion to determine the rate of heat release or the time to detector response. The technique is as follows:

1. Determine the environmental conditions of the area being considered.
    a. ambient temperature, T_a (convert to absolute temperature)

b. ceiling height or height above fuel, H
2. Estimate the fire growth characteristic α or t_g for the fuel expected to be burning. If t_g is used, calculate the corresponding α. Multiply α by the convective fraction to get α_c before using in the equations.
3. Determine the spacing of the existing detectors or sprinklers. The protection radius is then $r = S/\sqrt{2}$.
4. Determine the detector's rated response temperature and its RTI, or τ_0 and u_0.
5. Make a first estimate of the response time of the detector or estimate the heat release rate at detector response and calculate the corresponding response time using the power-law equation.
6. Assume that the fire starts obeying the power-law model at time $t = 0$.
7. Set the initial temperature of the detector and its surroundings at ambient temperature.
8. Using Equation 20, calculate the nondimensional time, t_{2f}^*, at which the initial heat front reaches the detector.
9. Calculate the factor A defined in Equation 18.
10. Use the estimated response time along with Equation 19 to calculate the corresponding value of t_2^*.
11. If t_2^* is greater than t_{2f}^*, continue with Step 12. If not, try a longer estimated response time or a larger estimated heat release rate and return to Step 8.
12. Calculate the ratio u/u_2^* using Equation 16.
13. Calculate the ratio $\Delta T/\Delta T_2^*$ using Equation 17.
14. Use Equation 21 to calculate ΔT_2^*.
15. Equation 23 is used to calculate the ratio $u_2^*/(\Delta T_2^*)^{1/2}$.
16. Use Equations 22 and 26 to calculate D and Y.
17. Equation 25 can now be used to calculate the resulting temperature of the detector.
18. If the temperature of the detector is below its operating temperature, this procedure must be repeated using a longer estimated response time. If the temperature of the detector exceeds its operating temperature, a smaller t_r can be used.
19. Repeat this procedure until the detector temperature is about equal to its operating temperature. The resulting response time, t_r, can be used to calculate either the total heat release rate or the convective heat release rate at response using the power-law equation.

As in the design problem, this technique can be used to estimate the response of existing systems of rate-of-rise heat detectors. The difference is that in Step 4 the set point or rate of temperature rise at which the detector will respond must be determined from the manufacturer's data. In Step 17, Equation 24 is used to determine the rate at which the temperature of the detector is changing.

Heat Detection—Potential Errors:

Power-Law Fire Modeling

When the exact conditions of velocity and temperature of fire gases flowing past a detector are not known, errors are introduced in the design and analysis of fire detector response. Graphs in Heskestad and Delichatsios' report show the errors in calculated fire-gas temperatures and velocities.[22] An exact treatment of these errors is beyond the scope of this chapter, though some discussion is warranted.

Plots of actual data and calculated data show that errors in ΔT_2^* can be as much as 50 percent, though generally there appears to be much better agreement.[22,23] The maximum errors occur at r/H values of about 0.37. All other plots of actual and calculated data, for various r/H, show much smaller errors. In terms of the actual change in temperature over ambient, the maximum errors are on the order of 5 to 10°C. The larger errors occur with faster fires and lower ceilings.

At $r/H = 0.37$, the errors are conservative when the equations are used in a design problem. That is, the equations predicted lower temperatures. Plots of data for other values of r/H indicate that the equations predict slightly higher temperatures.

Errors in fire-gas velocities are related to the errors in temperatures. The equations show that the velocity of the fire gases is proportional to the square root of the change in temperature of the fire gases.[22] In terms of heat transfer to a detector, the detector's change in temperature is proportional to the change in gas temperature and the square root of the fire-gas velocity. Hence, the expected errors bear the same relationships.

Based on the discussion above, errors in predicted temperatures and velocities of fire gases will be greatest for fast fires and low ceilings. Sample calculations simulating these conditions show errors in calculated detector spacings on the order of plus or minus 1 m, or less.[23]

Similar to Alpert's steady-state model, the power-law ceiling-jet model assumes a flat infinite ceiling. If the leading edge of the ceiling jet has passed the detector position and not reached a wall or other obstruction, then the model is within its stated parameters. The nondimensional time that the heat front reaches some position, r/H, is given by the equation for t_{2f}^*. The corresponding nondimensional time at response is given by the equation for t_2^*. Setting these equal to each other and solving for r at $t = t_r$ gives the radial distance from the fire to the leading edge of the heat front. Using the equations for a user-entered convective fraction,

$$t_{2f}^* = 0.813\left(1 + \frac{r}{H}\right)$$

and

$$t_2^* = \frac{t_r}{A^{-1/5}\alpha_c^{-1/5}H^{4/5}}$$

$$t_{2f}^* = t_2^*$$

$$0.813\left(1 + \frac{r}{H}\right) = \frac{t_r}{A^{-1/5}\alpha_c^{-1/5}H^{4/5}}$$

$$r = \frac{(t_r/A^{-1/5}\alpha_c^{-1/5}H^{4/5})/0.813 - 1}{H} = \frac{t_2^*/0.813 - 1}{H}$$

Selection of Data for Design and Analysis

In order to calculate the required spacing of heat detectors or sprinklers to respond to a given fire, the following information is required:

1. *System goals:* desired fire size (heat release rate) at response or time to detector response from the start of open flaming

2. Fire growth constant α or t_g
3. Ambient temperature
4. Height above the fuel or ceiling height

In addition to the above, the heat capacity of air at constant pressure, C_p, the density of air, ρ_0, and the gravitational constant, g, are used in the calculations. It is also necessary to know the characteristics of the detector for which the spacing calculations are being made. Specifically, the response temperature and the RTI of the detector must be known.

Establishing system goals is not within the scope of this chapter. However, it should be pointed out that, no matter what the goals are, they must be expressed in terms of heat release rate or time to detector response. The system's goals may actually be to limit damages to some dollar value, provide adequate escape time, or limit the production of toxic gases. In order to calculate required detector spacing using this system, these goals would have to be translated. For instance, as the fire grows, at what time or heat release rate must the detector respond so that the fire department can be summoned and extinguish the fire before damage levels are exceeded or conditions become untenable due to toxic gases?

Table 4-1.4 is a list of furniture calorimeter tests done at the National Bureau of Standards.[16,24] The tests provide

Table 4-1.4   Summary of NBS Calorimeter Tests

Test No.	Description	Fire Growth Time (s) (t_g)	α (kW/s²)	Virtual Time (s)	Maximum Heat Release Rate (kW)
Test 15	Metal wardrobe 41.4 kg (total)	50	0.4220	10	750
Test 18	Chair F33 (trial loveseat) 39.2 kg	400	0.0066	140	950
Test 19	Chair F21 28.15 kg (initial stage of fire growth)	175	0.0344	110	350
Test 19	Chair F21 28.15 kg (later stage of fire growth)	50	0.4220	190	2000
Test 21	Metal wardrobe 40.8 kg (total) (average growth)	250	0.0169	10	250
Test 21	Metal wardrobe 40.8 kg (total) (later growth)	120	0.0733	60	250
Test 21	Metal wardrobe 40.8 kg (total) (initial growth)	100	0.1055	30	140
Test 22	Chair F24 28.3 kg	350	0.0086	400	700
Test 23	Chair F23 31.2 kg	400	0.0066	100	700
Test 24	Chair F22 31.9 kg	2000	0.0003	150	300
Test 25	Chair F26 19.2 kg	200	0.0264	90	800
Test 26	Chair F27 29.0 kg	200	0.0264	360	900
Test 27	Chair F29 14.0 kg	100	0.1055	70	1850
Test 28	Chair F28 29.2 kg	425	0.0058	90	700
Test 29	Chair F25 27.8 kg (later stage of fire growth)	60	0.2931	175	700
Test 29	Chair F25 27.8 kg (initial stage of fire growth)	100	0.1055	100	2000
Test 30	Chair F30 25.2 kg	60	0.2931	70	950
Test 31	Chair F31 (loveseat) 39.6 kg	60	0.2931	145	2600
Test 37	Chair F31 (loveseat) 40.40 kg	80	0.1648	100	2750
Test 38	Chair F32 (sofa) 51.5 kg	100	0.1055	50	3000
Test 39	½-in. Plywood wardrobe w/ fabrics 68.8 kg	35	0.8612	20	3250
Test 40	½-in. Plywood wardrobe w/ fabrics 68.32 kg	35	0.8612	40	3500
Test 41	⅛-in. Plywood wardrobe w/ fabrics 36.0 kg	40	0.6594	40	6000
Test 42	⅛-in. Ply. wardrobe w/ fire-ret. (int. fin. initial)	70	0.2153	50	2000
Test 42	⅛-in. Ply. wardrobe w/ fire-ret. (int. fin. later)	30	1.1722	100	5000
Test 43	Repeat of ½-in. Plywood wardrobe 67.62 kg	30	1.1722	50	3000
Test 44	⅛-in. Ply. wardrobe w/ F-R., latex paint 37.26 kg	90	0.1302	30	2900
Test 45	Chair F21 28.34 kg (large hood)	100	0.1055	120	2100
Test 46	Chair F21 28.34 kg	45	0.5210	130	2600
Test 47	Chair adj. back metal frame, foam cush. 20.8 kg	170	0.0365	30	250
Test 48	Easychair CO7 11.52 kg	175	0.0344	90	950
Test 49	Easychair 15.68 kg (F-34)	200	0.0264	50	200
Test 50	Chair metal frame minimum cushion 16.52 kg	200	0.0264	120	3000
Test 51	Chair molded fiberglass no cushion 5.28 kg	120	0.0733	20	35
Test 52	Molded plastic patient chair 11.26 kg	275	0.0140	2090	700
Test 53	Chair metal frame w/ padded seat and back 15.5 kg	350	0.0086	50	280
Test 54	Loveseat metal frame w/ foam cushions 27.26 kg	500	0.0042	210	300
Test 55	Group chair metal frame w/ foam cushion 6.08 kg	Never exceeded 50 kW heat release rate			
Test 56	Chair wood frame w/ latex foam cushions 11.2 kg	500	0.0042	50	85
Test 57	Loveseat wood frame w/ foam cushions 54.60 kg	350	0.0086	500	1000
Test 61	Wardrobe ¾-in. particleboard 120.33 kg	150	0.0469	0	1200
Test 62	Bookcase plywood w/ aluminum frame 30.39 kg	65	0.2497	40	25
Test 64	Easychair molded flexible urethane frame 15.98 kg	1000	0.0011	750	450
Test 66	Easychair 23.02 kg	75	0.1876	3700	600
Test 67	Mattress and boxspring 62.36 kg (later fire growth)	350	0.0086	400	500
Test 67	Mattress and boxspring 62.36 kg (initial fire growth)	1100	0.0009	90	400

a database of heat release rate, particulate production, and radiation from a variety of common furnishings. The table provides the corresponding α or t_g for the calorimeter tests.[23] The virtual time data in the table is the approximate time at which the heat release rate in the test began to follow the $p = 2$ power-law model ($\dot{Q} = \alpha t^2$ kW). Prior to this time, the behavior of the fire cannot be predicted with this model. Figure 4-1.5 shows some test data along with a power-law curve superimposed.

The data in Table 4-1.4 can be used to select α or t_g for use in spacing calculations. However, in many cases the data in this table will not match the scenario being studied. If the heat-release-rate-versus-time history can be obtained or approximated for the expected fuel, the α or t_g can be calculated using curve fitting techniques.[23]

In most cases, since the exact fuel that will be involved in a fire cannot be known, the rigorous calculation of α is not warranted. Engineering judgment can be used to select an α or t_g that approximates the severity of the fire. The data in Table 4-1.4 suggest a range of 50 to 500 s for t_g. Only a few rapidly developing fires had a t_g below 50 s. Three slow fires had values above 500 s for t_g.

Table 4-1.4 also lists the maximum heat release rate reached during the power-law growth. The heat release rate model $\dot{Q} = \alpha t^2$ does not predict when a fuel package stops following the model or when the fuel is depleted. This task is an important point often missed by many designers. A simple test is to calculate the mass of fuel consumed from $t = 0$ to the time of interest. For $p = 2$ power-law fire growth rate, the total energy consumed is

$$E = \int_{t=0}^{t} \dot{Q} = \int_{t=0}^{t} \alpha t^2 \text{ kJ}$$

$$E = \frac{\alpha t^3}{3} \text{ kJ}$$

Knowing the heat of combustion, H_c, for the fuel permits calculation of the mass of fuel necessary to release a given amount of energy in the time period:

$$E = mH_c \text{ kJ}$$

$$m = \frac{E}{H_c} \text{ g or kg (depending on the units for } H_c)$$

When doing a design or analysis, try several different fire growth rates to determine the effect of their variance on the calculations. In some cases, the effect will be minimal. In other cases, this type of sensitivity analysis will show that a more thorough analysis of the possible fuels and fire scenarios is warranted.

The selection of an ambient temperature can have a measurable effect on the calculations. The calculations assume that the detector or sprinkler starts out at the same temperature as the ambient air when the fire starts. Hence, if a temperature of 20°C is assumed for the spacing calculations and the actual temperature at the time of the fire is 10°C, the system's goals will not be met. For design calculations to be conservative, the lowest expected ambient temperature should be used.
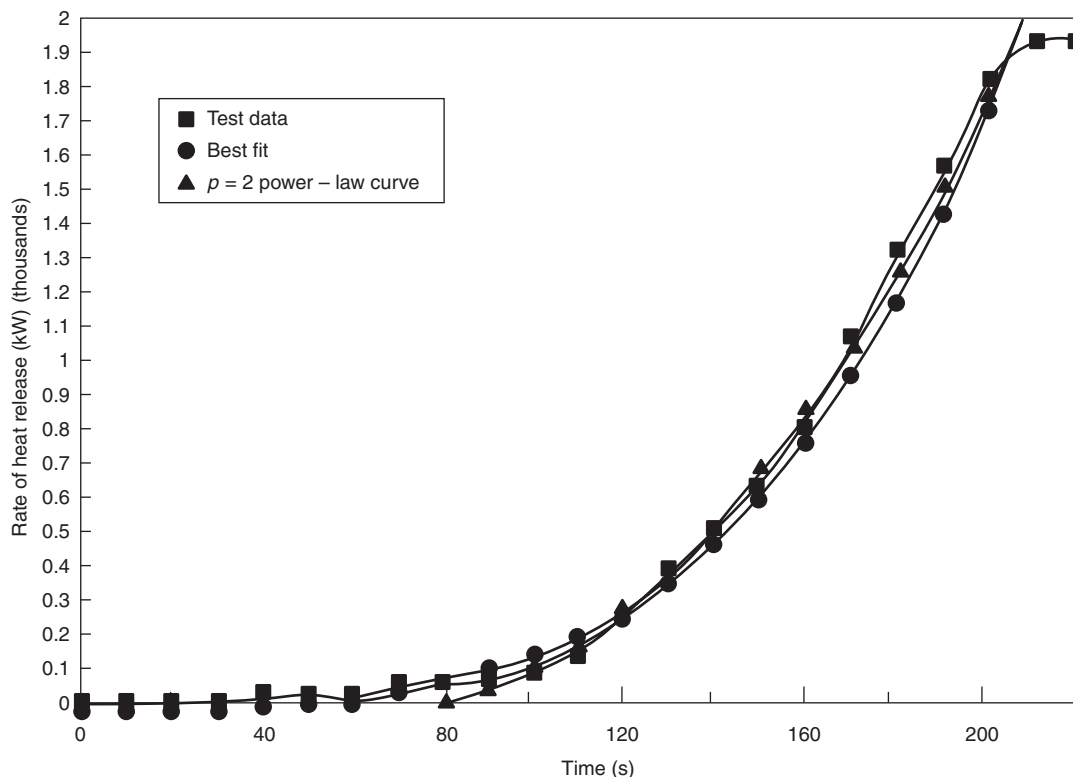

Figure 4-1.5.   *Test 27 chair.*

The relationships presented by Heskestad and Delichatsios[21] are correlated to fire test data using the ceiling height above the fuel surface for H. If this height varies, the larger value of H will produce more conservative results in the calculations for detector spacing or response. The most conservative results are obtained when the floor-to-ceiling height is used, since this height is the maximum vertical distance from fuel to detector.

The values for C_p, ρ_0, and g should be 1.040 kJ/(kg·K), 1.1 kg/m³, and 9.81 m/s², respectively. Slight variations in these constants have negligible effects on the calculations.

As previously mentioned, the design or analysis calculations are done for a particular detector or sprinkler. Therefore, it is necessary to know the unit's operating temperature. The response time index or τ_0 and u_0 are also needed. Operating temperature is obtained from manufacturer's data. The detector's sensitivity is best determined by conducting a plunge test.[9]

In the absence of plunge test data, a detector's UL-listed spacing can be used as a measure of detector sensitivity. Heskestad and Delichatsios analyzed UL test data and calculated time constants, τ_0, for various combinations of UL-listed spacing and detector operating temperature.[22] The Appendix Subcommittee of NFPA 72 expanded the table to include a larger selection of detectors.[8] That table is reproduced here as Table 4-1.5.

Heat Detection Design and Analysis Examples Using the Power-Law Fire Model

Analysis and design problems will be used to show how fire protection engineers can use the techniques presented in this chapter. The examples show the sensitivity of these techniques to changes in variables and input parameters. A design problem is first worked by hand to solve the equations presented earlier in the section on heat detection. The remaining examples were worked using a spreadsheet written to solve the equations.

Table 4-1.5   Time Constants for Any Listed Detector τ_0 (s)[a]

Listed Spacing (ft)	UL (°F)						FMRC All Temp.
	128°	135°	145°	160°	170°	196°	
10	400	330	262	195	160	97	195
15	250	190	156	110	89	45	110
20	165	135	105	70	52	17	79
25	124	100	78	48	32		48
30	95	80	61	36	22		36
40	71	57	41	18			
50	59	44	30				
70	36	24	9				

These time constants are based on an analysis of the Underwriters Laboratories Inc. and Factory Mutual Research Corporation listing test procedures. Plunge test results performed on the detector to be used will give a more accurate time constant.

[a]At a reference velocity of 5 ft/s

(Reproduced from NFPA 72–1993, Appendix B.[8])

EXAMPLE 4:

A fire detection system is being designed for an unsprinklered manufacturing building. The area being considered has a large, flat ceiling 5.0 m high. Ambient temperature is normally 20°C, but on weekends it is cut back to 10°C. It will be assumed that the fire scenario involves the ignition of a stack of wood pallets. The pallets are stacked 1.5 m (5 ft) high. Fire tests[8] show that this type of fire follows the $p = 2$ power-law equation with a t_g of approximately 150 s. The corresponding α can be calculated:

$$\dot{Q} = \alpha t^2 \text{ kW}$$

$$\alpha = \frac{1055}{t_g^2} = \frac{1055}{150^2} = 0.047 \text{ kW/s}^2$$

The goal is to detect the fire before it reaches a total heat release rate of 2500 kW. Fixed-temperature heat detectors will be used. The detectors have a 57°C (135°F) operating temperature and a UL-listed spacing of 30 ft. From Table 4-1.5 the time constant is found to be 80 s. This time constant is referenced to a gas velocity of 1.5 m/s and can be used with Equation 9 to calculate the detector's RTI.

First, use the power-law equation to calculate the time that the fire would reach a total heat release rate of 2500 kW:

$$\dot{Q} = \alpha t^2 \text{ kW}$$

$$t = \sqrt{\frac{\dot{Q}}{\alpha}} = \sqrt{\frac{2500}{0.047}} = 231 \text{ s}$$

The RTI is calculated using Equation 9 and a reference velocity, u_0, of 1.5 m/s (5 ft/s):

$$\text{RTI} = \tau_0 u_0^{1/2} = 80\sqrt{1.5} = 98 \text{ m}^{1/2}\text{s}^{1/2}$$

As described previously in Step 5 for design of a proposed system, it is necessary to make a first guess at the required detector spacing. In this case, try using $r = 6.0$ m. Use Equation 20 to calculate the nondimensional time, t_{2f}^*, at which the initial heat front reaches the detector. Use the distance from the top of the fuel package to the ceiling for H.

$$t_{2f}^* = 0.813\left(1 + \frac{r}{H}\right)$$

$$t_{2f}^* = 0.813\left(1 + \frac{6.0}{3.5}\right) = 2.207$$

Next, Equation 18 is used to calculate A. Note that in this equation the ambient temperature, T_a, must be expressed as an absolute temperature. In this case add 273 to °C to get K (Kelvin).

$$A = \frac{g}{C_p T_a \rho_0}$$

$$A = \frac{9.81}{1.040(10 + 273)1.1} = 0.030$$

The nondimensional time corresponding to the required response time is now calculated. However, first we must calculate α_c:

$$\alpha_c = X\alpha = 0.70(0.047) = 0.033 \text{ kW/s}^2$$

$$t_2^* = \frac{t}{A^{-1/5}\alpha_c^{-1/5}H^{4/5}}$$

$$t_2^* = \frac{231}{(0.030)^{-1/5}(0.033)^{-1/5}(3.5)^{4/5}} = 21.256$$

Since $t_2^* > t_{2f}^*$, we know that the heat front has passed the detector location. Next, the ratio of the velocity to the nondimensional velocity is calculated:

$$u_2^* = \frac{u}{(A^{1/5}\alpha_c^{1/5}H^{1/5})}$$

$$\frac{u}{u_2^*} = A^{1/5}\alpha_c^{1/5}H^{1/5}$$

$$\frac{u}{u_2^*} = (0.030)^{1/5}(0.033)^{1/5}(3.5)^{1/5} = 0.322$$

The ratio of the change in gas temperature to the nondimensional gas temperature is calculated:

$$\Delta T_2^* = \frac{\Delta T}{A^{2/5}(T_a/g)\alpha_c^{2/5}H^{-3/5}}$$

$$\frac{\Delta T}{\Delta T_2^*} = A^{2/5}\left(\frac{T_a}{g}\right)\alpha_c^{2/5}H^{-3/5}$$

$$\frac{\Delta T}{\Delta T_2^*} = (0.030)^{2/5}\left(\frac{283}{9.81}\right)(0.033)^{2/5}(3.5)^{-3/5} = 0.855$$

The nondimensional change in gas temperature is now calculated:

$$D = 0.126 + 0.210\left(\frac{6.0}{3.5}\right) = 0.486$$

$$\Delta T_2^* = \left[\frac{(t_2^* - t_{2f}^*)}{D}\right]^{4/3}$$

$$\Delta T_2^* = \left[\frac{(21.256 - 2.207)}{0.486}\right]^{4/3} = 133.142$$

Next, the ratio $u_2^*/(\Delta T_2^*)^{1/2}$ is calculated:

$$\frac{u_2^*}{(\Delta T_2^*)^{1/2}} = 0.59\left(\frac{r}{H}\right)^{-0.63}$$

$$\frac{u_2^*}{(\Delta T_2^*)^{1/2}} = 0.59\left(\frac{6.0}{3.5}\right)^{-0.63} = 0.420$$

Y is now calculated:

$$Y = \frac{3}{4}\sqrt{\frac{u}{u_2^*}}\sqrt{\frac{u_2^*}{(\Delta T_2)^{1/2}}}\left(\frac{\Delta T_2^*}{\text{RTI}}\right)\left(\frac{t}{t_2^*}\right)D$$

$$Y = \frac{3}{4}\sqrt{0.322}\sqrt{0.420}\left(\frac{133.142}{98}\right)\left(\frac{231}{21.256}\right)(0.486) = 1.979$$

The resulting temperature of the detector at $t = 231$ s, $T_d(t)$, can now be calculated. Assume that the temperature of the detector at the start of the fire, $T_d(0)$, is the same as ambient temperature, T_a.

$$\Delta T_d = T_d(t) - T_d(0) = \frac{\Delta T}{\Delta T_2^*}\Delta T_2^*\left[1 - \left(\frac{1 - e^Y}{Y}\right)\right]$$

$$\Delta T_d = T_d(t) - T_d(0)$$

$$= 0.855(133.142)\left[1 - \left(\frac{1 - e^{-1.979}}{1.979}\right)\right]$$

$$\Delta T_d = T_d(t) - T_d(0) = 64.264$$
$$T_d(t) = \Delta T_d + T_d(0) = 64.264 + 10 = 74.264 = 74°C$$

After 231 s, when the heat release rate has reached 2500 kW, the detector located 6 m from the fire axis has reached an approximate temperature of 74°C. Note that the answer has been rounded to two significant digits, one more than the least precision of any of the variables. This rule is the alternate rule for rounding as discussed in the introduction of this chapter.

The detector actuation temperature is 57°C. This result indicates that the detector has responded before the fire has reached 2500 kW. Since the calculated temperature is higher than the actuation temperature, a larger r can be tried. The calculations should be repeated until the calculated detector temperature is approximately equal to the actuation temperature.

For this example the answer converges on a radial distance of approximately 7.4 m. The spacing between detectors is

$$S = r\sqrt{2} = 7.4\sqrt{2} = 10.5 \text{ m}$$

EXAMPLE 5:
This example will show how an existing heat detection system or a proposed design can be analyzed to determine its response time or fire size at response. The scenario used in Example 4 will be repeated, except that the manufacturing building has an existing system of heat detectors, which are spaced evenly on the ceiling at 15.0-m intervals. The detector characteristics are the same as above. The actuation temperature is 57°C and the RTI is 98 $\text{m}^{1/2}\cdot\text{s}^{1/2}$. The ceiling height is 5 m, and the height of the pallets is 1.5 m. Ambient temperature is 10°C. α is 0.047 kW/s^2 ($t_g = 150$ s) and α_c is 0.033 kW/s^2.

The maximum radial distance from the fire axis to a detector is calculated first, using Equation 5.

$$S = r\sqrt{2} \text{ m}$$

$$r = \frac{S}{\sqrt{2}} = \frac{15.0}{\sqrt{2}} = 10.6 \text{ m}$$

The next step in the analysis is to estimate the response time of the detector or the fire size at response. In the design above, the fire grew to about 2500 kW in 231 s when the detector at a distance of 7 m responded. The radial distance in this example is larger and should result in

a slower response and larger fire size at response. A first guess at response time might be 6 min or 360 s. The fire size (total heat release rate) at 360 s is

$$\dot{Q} = \alpha t^2 \text{ kW}$$

$$\dot{Q} = 0.047(360)^2 = 6091 \text{ kW}$$

The remaining calculations for the resulting detector temperature are similar to those in Example 4. Rather than show the detail, a spreadsheet was used to complete the calculations. The resulting detector temperature at 360 s was calculated to be approximately 84°C.

This result indicates that the detector response time is less than the estimated 6 min. Therefore, a smaller response must be tried. If the calculated temperature were lower than the actuation temperature, a larger t would be tried. The calculations are repeated until the calculated detector temperature is approximately equal to the actuation temperature. In this case, the response time converges at 295 s. This result corresponds to a fire size at response of 4070 kW. It is at this time and heat release rate that the detector temperature reaches its actuation temperature of 57°C.

This example assumes that the fire continues to follow the power-law relationship through the burning period. If there is not enough fuel available, it is possible for the heat release rate curve to flatten out before reaching 4070 kW. These calculations do not predict when this development will happen. These calculations also do not predict how the detector temperature changes after the fire stops following the power-law relationship. It may be that sufficient heat continues to be released and the detector eventually responds. It is also possible for the fire gases to cool sufficiently to preclude detector actuation unless additional fuel becomes involved in the fire.

Comparing Example 4 with Example 5 shows how detector spacing affects response time. A difference in spacing of 4.4 m (15 − 10.6 m) results in a difference of approximately 64 s in the detector response time. Because the fire is accelerating according to the $p = 2$ power-law relationship, the resulting difference in fire size at response is 1570 kW.

EXAMPLE 6:

A warehouse is used to store sofas and other furniture. The sofas are similar to one tested by the National Bureau of Standards in their furniture calorimeter.[30] Burning characteristics are assumed to be similar to the sofa used in Test 38:[23,30] $\alpha = 0.1055$ kW/s^2, $t_g = 100$ s; peak heat release rate = 3000 kW. The sofas are stored one or two high. Assume a convective fraction of 65 percent.

The building has a flat roof and ceiling. The distance from the floor to the ceiling is 4.6 m. When the sofas are stacked two high, the distance from the top of the fuel package to the ceiling is 2.4 m. Ambient temperature in the warehouse is kept above 10°C. (See Figure 4-1.6.)

Based on maximum allowable property loss goals established by the owner, it is desirable to detect a fire and notify the fire department prior to a second fuel package becoming involved. The original NBS report[30] contains data on radiation measured during Test 38. This informa-
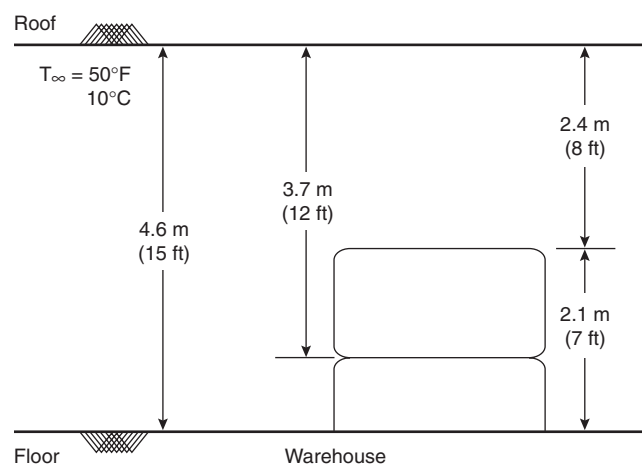

Figure 4-1.6. *Example 6—Warehouse.*

tion can be used along with other techniques presented in this handbook to determine when a second item might ignite. For instance, it might be determined that furniture across a 2-m aisle might ignite when the fire reaches a total heat release rate of 3000 kW. The objective would then be to detect the fire soon enough so that the fire can be extinguished or controlled before the fire reaches total 3000 kW. In this example, it is assumed that the fire must be detected when it reaches a total heat release rate of about 2000 kW.

The fire detection system will consist of fixed-temperature heat detectors connected to a control panel that is, in turn, connected to the local fire department. The detector to be used has a fixed temperature rating of 57°C and an RTI of 42 m$^{1/2}$·s$^{1/2}$.

The problem is determining the spacing of detectors required to detect this fire. When the computer program runs, the user is prompted for all of the above information. In this example, the data are fixed except for the distance from the ceiling to the flame origin. If the distance between the top of the fuel and the ceiling (2.4 m) is used, the calculations indicate that the detectors must be spaced 7.3 m apart to respond when the fire reaches a heat output of 2000 kW.

For a worst-case analysis, the distance from the floor to the ceiling (4.6 m) is used. This distance results in a required detector spacing of 5.9 m.

A more realistic worst-case scenario would be when the sofas are not stacked two high. With one sofa on the floor, the distance from the fuel to the ceiling would be about 3.7 m. The required detector spacing would then be 6.5 m.

These results are summarized in Table 4-1.6. This table clearly shows the relationship between ceiling height and detector response. The greater the distance from the fire to the ceiling, the closer the detectors must be spaced to respond within the goals of the system. Designs based on the floor-to-ceiling distance are conservative and representative of a worst-case condition. More realistic designs are based on the most probable or the greatest expected vertical clearance between fuel and detector.

Table 4-1.6 *Example 6—Ceiling Height or Height above Fuel versus Detector Spacing*

Ceiling Height, H (m)	Required Spacing, S (m)
2.4	10.3
3.7	9.2
4.6	8.4

Table 4-1.7 *Example 7—Ceiling Height or Height above Fuel versus Response Time*

Ceiling Height, H (m)	Response Time, t_r (s)
2.4	140
3.7	150
4.6	160

EXAMPLE 7:

For the same conditions in Example 6, if the detector spacing is fixed at 10.3 m ($r = 7.3$ m), how does the ceiling height affect the response time of the system?

Using the spreadsheet, the results, after rounding, are summarized in Table 4-1.7.

EXAMPLE 8:

This example will show how to select a detector type to economically meet the system's goals. The fire scenario and goals used in Examples 6 and 7 will be used: $H = 2.4$ m; $T_a = 10°C$; RTI = 42 $m^{1/2} \cdot s^{1/2}$; X = 65 percent, $t_g = 100$ s.

In Example 6, it was found that heat detectors with a fixed temperature rating of 57°C and an RTI of 42 $m^{1/2} \cdot s^{1/2}$ must be spaced 10.3 m apart to meet the system's goals—a response at 2000 kW. Here, the spacing of rate-of-rise heat detectors will be estimated.

The detector to be used is rated to respond when its temperature increases at a rate of 11°C/min or more. The detector's RTI will be assumed to be the same as the detector in Example 6. The calculation procedure is the same as for fixed temperature detectors except that, in the last step, the equation for the rate of temperature change is used:

$$\frac{dT_d(t)}{dt} = \frac{4}{3} \frac{\Delta T}{\Delta T_2^*} \Delta T_2^{*\,1/4} \frac{(1 - e^{-\Upsilon})}{(t/t_2^*)D}$$

Solving the equations, it is found that the rate-of-rise heat detectors can be spaced up to 25 m apart and respond at approximately 2000 kW total heat release rate.

If the total area of the warehouse is 5000 m^2, approximately 48 fixed-temperature heat detectors would be required to meet the established goals. The same goals can be met with approximately 8 rate-of-rise heat detectors. Additional detectors might be required due to of obstructing beams or walls. It should also be pointed out that the use of m^2 for calculating the required number of units is only an estimate. The detector does not cover an area that is 625 m^2 (25 m × 25 m). It is covering a circular

area having a radius no more than about 17.7 m. That is, all points on the ceiling must be within the protection radius of a detector for the calculations to be valid. If one used a "rated area" for a detector rather than a radial measurement, it could be concluded that a single detector in this example could cover a space that was 125 m long if it were only 5 m wide.

By trying different detector types or detectors with higher sensitivities, project goals might be met with a fewer number of detectors. The scenario in this example shows that, to detect the same fire, a much greater number of fixed-temperature heat detectors than rate-of-rise heat detectors is required. This conclusion is not always the case. Many fires will develop slowly and cause high ceiling temperatures without ever exceeding the rate of temperature rise necessary to actuate a rate-of-rise heat detector. As a backup, most commercially available rate-of-rise heat detectors have a fixed-temperature element also. The rate-of-rise element and the fixed-temperature element should be considered separately when designing or analyzing a system.

EXAMPLE 9:

In this example, a combination fixed-temperature and rate-of-rise heat detector will be analyzed and the response of the two elements will be compared. For an installed spacing of 10.0 m ($r = 0.707$ m), the effect of fire growth rate on response time will be shown. The following conditions from examples 6, 7, and 8 will be repeated: $H = 2.4$ m; $T_a = 10°C$; RTI = 42 $m^{1/2} \cdot s^{1/2}$; X = 65 percent. The fixed-temperature element response threshold is $T_r = 57°C$, and the rate-of-rise threshold is $dTr/dt = 11°C/min$.

The results are shown in Table 4-1.8 and Figure 4-1.7. For fire growth times up to $t_g = 509$ s, the rate-of-rise element responds faster. For fires that grow slower (increasing t_g), the fixed-temperature element will respond faster.

For larger installed spacings, such as the 25-m spacing calculated in the previous example for the spacing of the rate-of-rise detector, the crossover point occurs sooner. The results for a 25-m spacing are shown in Table 4-1.9 and Figure 4-1.8. For fire growth times up to $t_g = 228$ s, the rate-of-rise element responds faster. For fires that grow slower (increasing t_g), the fixed-temperature element will respond faster.

Table 4-1.8 *Response Time as a Function of Fire Growth Time, t_g*

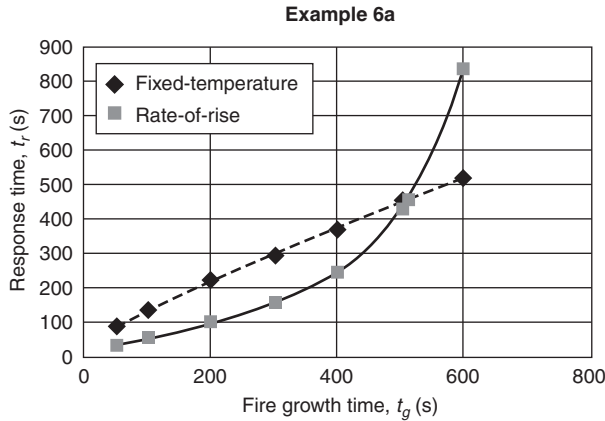| t_g	Response Time, t_r (s)	
	Fixed-Temperature	Rate-of-Rise
50	85	31
100	135	53
200	219	98
300	297	155
400	373	241
500	447	426
509	454	454
600	521	835

Example 6a

Figure 4-1.7. *Response time as a function of fire growth time, t_g.*

Table 4-1.9 *Response Time as a Function of Fire Growth Time, t_g*

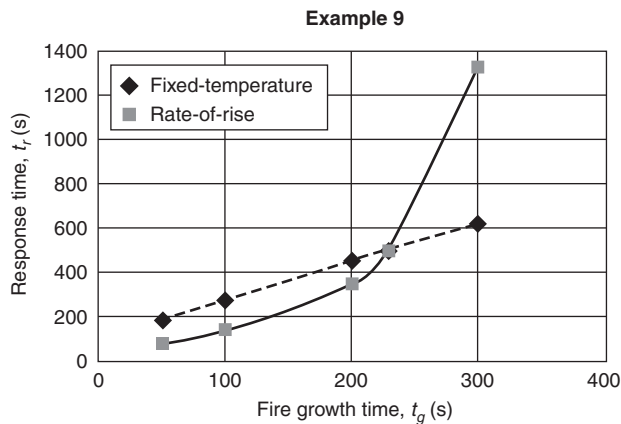|	Response Time, t_r (s)	
t_g	Fixed-Temperature	Rate-of-Rise
50	168	77
100	269	140
200	448	355
228	497	497
300	619	1330

Example 9

Figure 4-1.8. *Response time as a function of fire growth time, t_g.*

EXAMPLE 10:

In this example, the effects of fire growth rate on detector spacing will be examined. The scenario used in Examples 6 through 9 will be used again. The following conditions from these examples will be repeated:

$H = 2.4$ m; $T_a = 10°C$; RTI = 42 m$^{1/2}·$s$^{1/2}$; X = 65 percent. The fixed temperature element response threshold is $T_r = 57°C$ and the rate-of-rise threshold is $dT_r/dt = 11°C$/min.

In Examples 6, 7, and 8, the rate of fire growth followed the power-law equation with an α of 0.1055 kW/s^2 or $t_g = 100$ s. Calculations were done for several values of t_g. The results are summarized in Table 4-1.10 and Figure 4-1.9.

For fixed-temperature detectors, if the fire grows at a faster rate (smaller t_g), a smaller spacing is required to meet the system's goals. If the fire grows at a slower rate, a larger detector spacing is allowed. This relationship clearly shows the effects of thermal lag on detector response. At slow rates of growth, the detector is immersed in the hot fire gases and, despite thermal lag, has time to absorb the heat before the fire reaches the maximum permissible heat release rate. The effects of thermal lag are less important at slow rates of fire growth.

The rate-of-rise detector also experiences thermal lag. However, the curve peaks at approximately $t_g = 110$ m$^{1/2}·$s$^{1/2}$ and $S = 25$ m. For the rate-of-rise detector, as

Table 4-1.10 *Required Detector Spacing as a Function of Fire Growth Time, t_g*

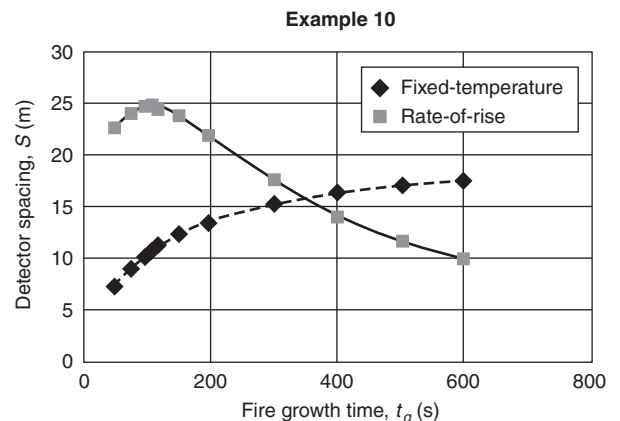|	Required Spacing (m)	
t_g	Fixed-Temperature	Rate-of-Rise
50	7.2	23
75	9	24
100	10	25
110	11	25
120	11	24
150	12	24
200	14	22
300	15	18
400	16	14
500	17	12
600	18	10

Example 10

Figure 4-1.9. *Required detector spacing as a function of fire growth time, t_g.*

the fire growth rate slows (larger t_g), thermal lag decreases as it did for the fixed temperature detector. However, as the rate of fire growth slows, so does the rate of change of the detector's temperature. For this particular detector and fire scenario, at fire growth times greater than about 110 s, the detector spacing must be reduced so that the threshold rate of change of the detector temperature is reached before the maximum permissible heat release rate is reached.

EXAMPLE 11:

In this example a detector is exposed to the ceiling jet for a fire with $t_g = 150$ s and a 75 percent convective fraction. Ambient temperature is 10°C. The ceiling is 4 m high, and the detector is located at a radial distance of 5 m from the fire. The RTI of the detector is 50. Plot the detector temperature and the fire-gas temperature at the detector location for t up to 240 s.

The detector remains at ambient temperature until the ceiling jet first reaches the detector position. At what time does the ceiling jet first reach the detector? This result is found by setting $t_{2f}^* = t_2^*$ and solving for t. First, α_c is calculated:

$$\alpha = \frac{t_g^2}{1055} = \frac{1055}{150^2} = 0.047 \text{ kW/s}^2$$

$$\alpha_c = X\alpha = 0.75(0.047) = 0.035 \text{ kW/s}^2$$

$$t_{2f}^* = t_2^*$$

$$0.813\left(1 + \frac{r}{H}\right) = \frac{t}{A^{-1/5}\alpha_c^{-1/5}H^{4/5}}$$

$$t = 0.813\left(1 + \frac{r}{H}\right) = A^{-1/5}\alpha_c^{-1/5}H^{4/5} \text{ s}$$

$$t = 0.813\left(1 + \frac{5}{4}\right) = (0.030^{-1/5})(0.035^{-1/5})(4^{4/5})$$

$$= 21.86 = 22 \text{ s}$$

The heat front reaches the detector at about 22 s, and heating begins. Prior to this point, the detector and gas temperature surrounding the detector are at ambient temperature.

The method to calculate the detector temperature is the same as in previous examples. To calculate the change in ceiling-jet gas temperature, combine the following equations and solve to ΔT:

$$\Delta T_2^* = \frac{\Delta T}{A^{2/5}(T_a/g)\alpha_c^{2/5}H^{-3/5}}$$

and

$$\Delta T_2^* = \left[\frac{(t_2^* - t_{2f}^*)}{(0.126 + 0.210r/H)}\right]^{4/3}$$

$$\Delta T = A^{2/5}\left(\frac{T_a}{g}\right)\alpha_c^{2/5}H^{-3/5}\left[\frac{(t_2^* - t_{2f}^*)}{(0.126 + 0.210r/H)}\right]^{4/3}$$

A spreadsheet solution is shown in Table 4-1.11 and graphed in Figure 4-1.10.

EXAMPLE 12:

A sprinkler system is being installed in a large exhibition hall. The building has a flat roof deck supported by open space frame trusses. The distance from the underside of the roof deck to the floor is 12 m. Ambient temperatures do not usually fall below 5°C.

Table 4-1.11 *Example 11—Ceiling Jet and Detector Temperature as a Function of Time*

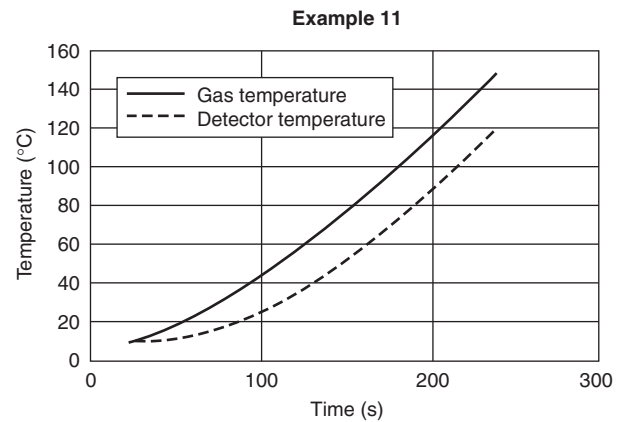| t (s)	T_g (s)	T_d (s)
22	10	10
30	12	10
40	15	10
50	19	11
60	24	13
70	29	15
80	34	18
90	39	21
100	45	25
110	51	30
120	58	35
130	64	40
140	71	46
150	78	52
160	85	59
170	93	66
180	100	73
190	108	81
200	116	88
210	124	96
220	132	104
230	140	112
240	148	120

Figure 4-1.10. *Example 11—Ceiling jet and detector temperature as a function of time.*

Three different designs for the sprinkler system have been proposed. All three are designed to provide the same water density over a specified area. Each proposal uses a sprinkler with a temperature rating of 74°C and an RTI of 110 $m^{1/2} \cdot s^{1/2}$. The only difference among the three systems is the spacing of the sprinklers and the branch lines that feed them. The first proposal uses a square array with a spacing of 3.0 m. The second and third proposals are based on square array spacings of 3.7 m and 4.6 m, respectively.

What effect will the three different spacings have on the size of the fire when the system responds? Assume two different fire scenarios. In the first, the fire grows at a moderate rate with $t_g = 200$ s. The second fire scenario has a slower fire growth rate with $t_g = 500$ s. For both, assume a convective fraction of 75 percent. Results of the calculations are shown in Table 4-1.12 after rounding.

The calculations show an increase of about 25 percent in the fire size at response when the spacing is increased 50 percent from 3.0 to 4.6 m. The increased spacing may result in a lower system cost. However, closer spacings mean that the sprinkler system will probably respond sooner. The fire protection engineer can use this type of analysis to assist in choosing a system that best meets the project's overall goals.

EXAMPLE 13:

A fire impacting elevator machinery can result in passengers or fire fighters being carried to a fire floor or being trapped between floors. Elevator safety codes generally do not require any sprinkler protection or detection at the top of shafts since the fuel load is typically insufficient to actuate a sprinkler or affect persons in the cars.

Smoke detection is used in elevator lobbies and machine rooms to recall elevators to a safe level when smoke threatens the elevator shaft. The presence of sprinklers in the elevator machine room presents another risk: the possibility of water discharge on energized controllers and motors and on the elevator brakes. To reduce this risk, in addition to smoke detection, heat detectors may be used to ensure that equipment is de-energized upon or prior to the discharge of water. To accomplish this task, some codes may require a heat detector with a lower temperature rating and a lower RTI within 0.61 m of every sprinkler in an elevator machine room. Are these requirements sufficient to assure response before the sprinkler to a range of possible fire scenarios?

SOLUTION:

For this example, use an ambient temperature of 15°C and a ceiling height or clearance of 4 m. Assume the actuation temperature of the sprinklers is 74°C and the actuation temperature of the heat detectors is 57°C. The RTI of the sprinklers is 110 $m^{1/2} \cdot s^{1/2}$, and the RTI of the detectors is 42 $m^{1/2} \cdot s^{1/2}$. Spacing of the sprinklers is 3.0 m. Calculate the response of the sprinkler and the heat detector to a fast fire, $t_g = 50$ s, and a slow fire, $t_g = 600$ s. Assume a 75 percent convective fraction.

A sprinkler spacing of 3.0 m results in a worst case radial distance of 2.12 m. The heat detector could be an additional 0.61 m beyond at $r = 2.73$ m. The results of the calculations are summarized in Table 4-1.13.

These calculations show that the heat detector will respond before the sprinkler. Depending on the actual conditions, additional calculations should be tried for different fire scenarios and for changes in other variables such as RTI, ambient temperature, ceiling clearance, and so forth.

Smoke Detection

In order to determine whether or not a smoke detector will respond to a given $\dot{Q}_{cr}$, a large number of factors must be evaluated. These include the following: smoke aerosol characteristics, aerosol transport, detector aerodynamics, and sensor response.

Smoke aerosol characteristics at the point of generation are a function of the fuel composition, the combustion state (smoldering or flaming), and the degree of vitiation of the combustion air. The characteristics considered include particle size and distribution, particle number or concentration at various sizes, composition, color, and refractive index. Given the dynamic nature of fire growth and spread and fuels involved, ventilation conditions will change over time, thus affecting the smoke produced.

Transport considerations include (1) changes to the aerosol characteristics that occur with time and distance from the source and (2) transport time. Changes in the aerosol largely relate to the particle size and concentration, and result from the processes of sedimentation, agglomeration, and coagulation. Transport time is a function of the characteristics of the travel path from the source to the detector, which include ceiling height and configuration (sloped, beamed, etc.), intervening barriers such as doors, and buoyancy effects such as layering and thermal inversions.

Table 4-1.12 *Example 12—Effects of Sprinkler Spacing on Fire Size at Response and Time to Response*

	$t_g = 200$ s		$t_g = 200$ s	
S (m)	t_r (s)	$\dot{Q}_T$ (kW)	t_r (s)	$\dot{Q}$ (kW)
3.0	350	3300	800	2700
3.7	370	3600	840	3000
4.6	400	4100	890	3400

Table 4-1.13 *Example 13—Sprinkler and Heat Detector Response to Different Fire Growth Rates*

	Response Time (s)	
	$t_g = 50$ s	$t_g = 600$ s
Sprinkler	65	370
Heat Detector	50	300

Once smoke reaches the detector, other factors become important, namely the aerodynamic characteristics of the detector and the type of sensor. The aerodynamics of the detector relate to the ease with which smoke can pass through the detector housing and enter the sensor. In addition, the location of the entry portion of the housing relative to the velocity profile of the detector normal to the plane of the ceiling is also a factor. Finally, different sensing modes (e.g., ionization or photoelectric) will respond differently, depending on the characteristics of the transported aerosol. Within the family of photoelectric devices, there will be variations depending upon the wavelengths of light and the scattering angles employed. Also, algorithms used to sample and weight the sensor's response are introduced by the manufacturer and affect the detector's response.

Standard practice for the design of smoke detection systems is much the same as that for heat detection systems. Recommended spacing criteria are established based on detector response to a specific parameter, such as the optical density within an enclosure. A variety of smoke tests are used to verify that the detector responds between defined upper and lower activation thresholds and within required response times to a range of different types of smoke. This information translates into recommended spacing criteria that is intended to ensure that the detector responds within defined parameters. In some cases, the recommended spacing can be increased, or must be decreased, depending on factors such as compartment configuration and air flow velocity.[8]

In applications where estimating the response of a detector is not critical, the recommended spacing criteria provide sufficient information for the design of a basic smoke detection system. If the design requires detector response within a certain time frame, optical density, specified heat release rate, or temperature rise, then additional analysis may be required. In this case, information concerning the expected fuel, fire growth, sensor, and compartment characteristics is required. The following examples show various performance-based approaches to evaluating smoke detector response.

Modeling Smoke Detector Response—General

The response of smoke detectors to fire conditions is not easily modeled. The response characteristics of smoke detectors vary widely compared with thermal detectors. In addition, less is known about the production and transport of smoke in the early stages of a fire. Natural and forced air currents have a larger effect on the movement of smoke at the time of interest (very early in the fire) than they do on the stronger thermal currents required to alarm heat detectors.

A comparison of how smoke detectors operate with the smoke measurement methods most often employed and reported by researchers shows that smoke measurements do not generally include the factors that we need to model smoke detector response.[13] Thus, there is a gap between the data generated by fire researchers and the data needed to model smoke detector response.

For example, fire researchers most often measure and report data on heat release rate, temperature and velocity of fire gases, and the optical density or obscuration per unit distance of the smoke at various locations. Of these, only optical density and obscuration relate to smoke. Although called *obscuration,* it is more accurately called *attenuation* since the light beam may be absorbed, reflected, or refracted by the smoke. These are calculated as follows:

Percent obscuration, O:

$$O = 100\left(I - \frac{I}{I_0}\right)$$

Percent obscuration per unit distance, O_u

$$O_u = 100\left[1 - \left(\frac{I}{I_0}\right)^{1/l}\right]$$

Optical density, D

$$D = \log_{10}\left(\frac{I_0}{I}\right) = -\log_{10}\left(\frac{I}{I_0}\right)$$

Optical density per unit distance, D_u (m^{-1})

$$D_u = \frac{D}{l} = \frac{1}{l}\log_{10}\left(\frac{I_0}{I}\right) = -\frac{1}{l}\log_{10}\left(\frac{I}{I_0}\right) \text{ m}^{-1}$$

where I_0 is the initial intensity of a light beam reaching a photocell, I is the intensity of the light beam in the presence of smoke, and l is the distance between the source and the photocell.

Optical density and obscuration are useful data for evaluating visibility. However, the only commercially available smoke detector that operates by sensing the attenuation of a light beam is the projected-beam-type smoke detector. Further, these measurements are sensitive to the wavelength of light used. Thus, to be valuable for estimating the response of a projected-beam smoke detector, the data must be measured and reported using the same wavelength as the light source used by the detector.

The two most common types of smoke detectors are ionization type and photoelectric type. Neither type operates using light attenuation. Without a correlation between the optical density data and the response characteristics of a particular detector, accurate modeling is not possible.

In addition, detectors often use complex response algorithms rather than simple threshold or rate-of-change response levels. The algorithms are used to reduce false and nuisance alarms and to enhance fire signature matching. These algorithms vary from detector to detector and are generally not published by the manufacturers. Thus, even if correlations between optical density and the response of scattering- and ionization-type smoke detectors were available, the actual response of each model is affected by the signal sampling algorithm.

Nevertheless, there are methods that can be used to grossly estimate smoke detector response. These estima-

tion methods may not provide accurate prediction of time to detector response because the potential errors in the estimation methods are not generally known and the response algorithms for a particular detector are not known. Without knowledge of the accuracy of the models and the potential errors, these estimation methods should not be used to compare detector response to other model calculations such as egress time calculations or time to untenability. Estimation methods are best used to compare changes in the response of a particular detector as a result of changes in spacing or location, while holding all other variables constant.

In addition to these estimation methods, actual fire tests with detectors present may provide information to compare smoke detector response to other factors such as egress time, structural response, heat release rate, and so forth. Product performance tests may be sources of data. Although, the actual response may not be reported in manufacturer's literature, the minimum and maximum permissible performance imposed by the test standard provides ranges of possible response.

Modeling Smoke Detector Response—Light Obscuration Smoke Detectors

For projected-beam-type detectors, fire or smoke models that calculate the optical density per unit length, D_u, in a space or the total optical density in the path of the detector, D, may be used to determine when the detector would respond. Manufacturer specifications will typically indicate at what levels of total obscuration or total optical density the detectors respond. Projected-beam smoke detectors generally have adjustable response thresholds.

Many fire models estimate the unit optical density, D_u, in a uniform upper layer or volume. This method is referred to as zone modeling. The optical density over the entire length of the beam is then determined by multiplying D_u by the path length, l. The path length is the distance between the source and receiver or the projected-beam smoke detector. This method assumes homogenous distribution of smoke throughout the path, an assumption which may not be valid.

Another method to model the response of projected-beam obscuration-type detectors is to calculate the unit optical density, D_u, at several discrete points or in several discrete segments between the source and the receiver of the projected-beam smoke detector. This approach is a form of field modeling. The optical density per unit length is then multiplied by the length of that particular segment. The total optical density of the path is then the sum of all of the densities for the individual segments.

Modeling Smoke Detector Response—Light Scattering (Photoelectric) Smoke Detectors

The amount of light scattered by smoke is very complex and is related to factors such as the particle number density and size distribution, refractive index, the wavelength of the light source, and the angle between the source and the receiver. Some of these variables can be de-

scribed by the manufacturer for a particular detector. Some require information about the smoke produced by the fuel and its transport to the detector location.

Information about smoke properties related to light scattering is presently limited to a few types of fuels and is not readily available to practicing fire protection engineers. In addition, the data may not be in a useable format. For instance, the data must match the wavelength of the light source used in the detector being modeled. Scattering data at other wavelengths introduces errors and uncertainties.

Meacham has shown that it is possible to model the response of light-scattering detectors using information about smoke properties obtained by small-scale testing of various fuels.[31,32] However, the recommended test methods have not been further developed, tested, or incorporated into fire test programs.

At the present time, there are no practical methods available to directly model the response of light-scattering-type detectors. However, obscuration or optical density modeling, as discussed above for obscuration-type detectors, can be used in a limited way to estimate scattering-type smoke detector response.

A scattering-type detector responds at different optical densities for different types of smoke. For example, a scattering-type smoke detector that responds at an optical density of .029 m^{-1} (2.0%/ft obscuration) to smoke produced by a smoldering gray cotton lamp wick may not respond until an optical density of 0.15 m^{-1} (10%/ft) is reached for smoke from a kerosene fire. At the response threshold, both types of smoke are scattering the same amount of light to the receiver of the scattering photoelectric smoke detector. There are many factors involved in this effect. One is that the darker smoke from the kerosene fire does not reflect as much light as the lighter colored smoke from the lamp wick.

Another way to understand the differing response of a scattering-type detector to two types of smoke is to consider the amount of light being scattered when both smoke samples have the same optical density. Both samples of smoke equally block our vision of the light reflected by an object. One type of smoke may be composed of large, highly reflective smoke particles that cause the incident light to scatter in many directions. Thus, it reduces the amount of light in the forward direction. The other type of smoke may consist of a smaller number of larger particles that absorb light more readily than they reflect it. Though they have equal optical densities, one is more likely to scatter light and set off a scattering-type detector.

In order to model the response of a scattering-type detector using obscuration or optical density, it is necessary to know the optical density required for a particular type of smoke to alarm a particular model detector. For example, many manufacturers label their smoke detectors with a unit optical density, D_u, or unit obscuration, O_u, based on a calibration test that is part of UL standard number 268.[33] That number indicates the unit optical density required for that detector to respond to smoke having very specific characteristics. The optical density required to alarm a particular detector as quoted by the manufacturer is just

one value for a given particle size distribution, concentration, color, and so on used in the laboratory calibration test of that model detector. If the smoke and conditions are similar to that used in the test of the detector, the specified alarm threshold can be used in calculations.

It is not sufficient to have data for a particular fuel and detector combination. It is known that smoke changes as it moves away from a fire.[34] There may be changes in the number, size, shape, and velocity of the particles. The optical density at response to any smoke signature other than the laboratory calibration test will be different and will vary with different fuels and burning modes.

Threshold response data to various fuels for a particular detector are not readily available. Some manufacturers may provide data if available and when requested. Product performance and safety tests as well as fire tests with detectors present are useful sources of limiting performance data. Product standards typically test detectors in rooms with specified fuels and smoke buildup rates and velocities. The detectors must respond at certain levels or within certain time limits. While the exact performance data may not be made available, the test limits are useful for estimating the range of possible detector response.

Modeling Smoke Detector Response—
Ionization Smoke Detectors

The signal produced by the chamber of an ionization detector has been shown to be proportional to the product of the number of particles and their diameter.[35–38] The exact signal produced by an ionization smoke detector is given by a more complex equation in the literature and requires an additional number called the chamber constant. The chamber constant varies with each different model of detector.

Given the quantity and size distribution of smoke particles and the chamber constant (from the manufacturer), it is possible to model the ionization smoke detector. Unfortunately, there are no fire models that provide the required detector model input. In addition, manufacturer specifications do not presently include chamber constants.

Newman modified the chamber theory to account for ionization detector sensitivity to the small electrical charge carried by some fire aerosols.[39] Newman also developed a method to model ionization smoke detector sensitivity as a function of the soot yielded by a particular fuel. Using his method, the change in a detector's signal, ΔI, can be related to the optical density of smoke measured at a particular wavelength, $D_{u\lambda}$.

To use the method proposed by Newman it is necessary to know what change in detector chamber signal, ΔI, will cause a detector or system to alarm. Although manufacturers do not presently provide this data, they may be persuaded to do so in the future.

Newman's work was done using a small-scale apparatus and three ionization smoke detectors. A wider range of tests, including some full-scale testing, is needed to verify this method. Presently, the only way to model ionization detector response is to use the optical density esti-

mations as discussed for scattering-type photoelectric smoke detectors.

Modeling Smoke Detector Response—
Entry Resistance

In addition to smoke characteristics and the detector's operating mechanism, the ability to get the smoke into the chamber affects the response of the unit. For spot-type photoelectric- and ionization-type smoke detectors, entry resistance is caused by bug screens, chamber design, and the detector's aerodynamic characteristics.

In a scenario where the optical density at the detector location is increasing with time, the optical density inside the detector chamber will always be less than that outside the detector chamber. Similarly, if a detector is placed in a smoke stream having a constant optical density, there will be a time delay before the optical density inside the chamber approaches that outside the detector. As with heat transfer to heat detectors, smoke entry resistance can be characterized by a detector time constant, τ:

$$\frac{dD_{ui}}{dt} = \frac{1}{\tau}(D_u - D_{ui}) \text{ s}^{-1} \cdot \text{m}^{-1}$$

where

D_{ui} (m^{-1}) = optical density per unit length inside the detector chamber

D_u (m^{-1}) = optical density per unit length outside the detector

τ = detector time constant (s)

If the time constant and the rate of change of optical density outside the detector are constant, then this equation can be solved. Further, substituting D_{ur} for the optical density outside the detector at response and D_{uo} for the optical density required inside the detector to produce response yields the following:[40,41]

$$D_{ur} = D_{uo} + \tau\left(\frac{dD_u}{dt}\right)\left\{1 - \exp\left[-D_{ur}\frac{1}{\tau}\left(\frac{dD_u}{dt}\right)\right]\right\} \text{ m}^{-1}$$

Heskestad proposed that the time constant could be represented by the following:

$$\tau = \frac{L}{u} \text{ s}$$

where L is the detector's characteristic length and u is the velocity of the ceiling jet flowing past the detector.

The characteristic length is thought to be a property of the detector that is independent of the smoke and ceiling-jet properties. It is interpreted as the distance the smoke would travel at the velocity u before the optical density inside the detector reaches the value outside of the detector. Combining the equations,

$$D_{ur} = D_{uo} + \frac{L}{u}\left(\frac{dD_u}{dt}\right)\left\{1 - \exp\left[-D_{ur}\frac{u}{L}\left(\frac{dD_u}{dt}\right)\right]\right\} \text{ m}^{-1}$$

The exponential term is small compared to the rest of the equation, allowing the equation to be simplified.[40] Simplification of the equation is not necessary when calculations are made using a computer. However, the simplified form clearly shows the effect of entry resistance:

$$D_{ur} = D_{uo} + \tau\left(\frac{dD_u}{dt}\right) \text{ m}^{-1}$$

or

$$D_{ur} = D_{uo} + \frac{L}{u}\left(\frac{dD_u}{dt}\right) \text{ m}^{-1}$$

This form of the entry resistance equation clearly shows that when the optical density outside a detector is increasing with time, the optical density inside the detector will lag behind if there is any entry resistance.

Heskestad and, later, Bjorkman et al.[42] have plotted test data to determine the L number for a variety of smoke detectors. Additional work has been done by Marrion and by Oldweiler to study the effects of detector position and gas velocity on the L number.[15,43]

Bjorkman et al., Marrion, and Oldweiler all observed variations in L that may be attributed to a dependence on velocity. Marrion's and Oldweiler's data also imply that there may also be a dependence on the characteristics of the smoke. Table 4-1.14 below summarizes the results from the works cited above.

Examination of the data and analysis work cited above shows that more work needs to be done to study the effects of low velocities and smoke characteristics on detector entry characteristics. The sharp increase in L at lower velocities appears to indicate that entry resistance may be related to smoke particle size. It is also possible that L is a function of the smoke momentum at low velocities. Thus, the time lag would be inversely proportional to the velocity squared.

Table 4-1.14 *Range of Characteristic Length (L) Numbers*

Researcher	Ionization Detector L (m)	Scattering Detector L (m)
Heskestad[40]	1.8	15[a]
Bjorkman et al.[42]	3.2 ± 0.2[b]	5.3 ± 2.7[c]
Marrion[15]	Not tested	7.2,[d] 11.0–13.0,[e] 18.4[f]
Oldweiler[43]	4.0–9.5,[g] 4.3–14.2[h]	Not tested

[a]older style detector with more elaborate labyrinth

[b]L determined by best fit for three test velocities

[c]L based on a single test velocity and a limited number of tests (complete equation used)

[d]low L number at low test velocity

[e]range of L for several fuels and detector positions

[f]L increased by adding "fence" to further restrict smoke entry

[g]range of L for a variety of velocities using simplified equation for entry resistance

[h]range of L for a variety of velocities using simplified equation for entry resistance

Engineers can use L as a measure of entry resistance and the resulting time lag. However, in scenarios where the ceiling-jet velocity is low, there will be greater uncertainty in the results.

Without validation of L as a measure of lag time, manufacturers and test laboratories are not measuring or reporting L in their literature. Nevertheless, the range of L numbers reported in Table 4-1.14 can be used to estimate possible errors in detector response time.

Smoke Detection Calculation Examples

EXAMPLE 14:

The smoke level measured outside of a detector at the time of response in a laboratory calibration test is listed on manufacturers' specifications as the optical density or obscuration required to alarm the unit. Because of entry resistance, the smoke level inside the detector will be less. The specified response is for a particular type of smoke and is measured in a laboratory test apparatus. An example of one calibration test is the gray smoke test listed in the UL 268 smoke detector test standard.[33]

In the test, the smoke detector response threshold must not exceed 0.0581 m^{-1} (4.0%/ft). Velocity in the test chamber is 9.8 m/min. The test starts with clear air. A smoldering cotton lamp wick is used to increase the optical density in the test chamber. The rate of increase of optical density in the chamber must fall within the following limits:

$$3.7 \times 10^{-3} \le \frac{dD_u}{dt} \le 5.3 \times 10^{-3} \text{ m}^{-1}\cdot\text{min}^{-1}$$

What is the range of optical density inside of the detector at the time of response (D_{uo}) if the detector has an L of 3 m? What would it be if the detector had an L of 14 m?

SOLUTION:

For $L = 3$ m and $dDu/dt = 3.7 \times 10^{-3}$ m$^{-1}\cdot$min^{-1},

$$D_{ur} = D_{uo} + \frac{L}{u}\left(\frac{dD_u}{dt}\right) \text{ m}^{-1}$$

$$D_{uo} = D_{ur} - \frac{L}{u}\left(\frac{dD_u}{dt}\right) \text{ m}^{-1}$$

$$D_{uo} = 0.0581 - \frac{3}{9.8}(3.7 \times 10^{-3}) = 0.057 \text{ m}^{-1}$$

For $L = 3$ m and $dD_u/dt = 5.3 \times 10^{-3}$ m$^{-1}\cdot$min^{-1},

$$D_{uo} = 0.0581 - \frac{3}{9.8}(5.3 \times 10^{-3}) = 0.056 \text{ m}^{-1}$$

For $L = 14$ m and $dD_u/dt = 3.7 \times 10^{-3}$ m$^{-1}\cdot$min^{-1},

$$D_{uo} = 0.0581 - \frac{14}{9.8}(3.7 \times 10^{-3}) = 0.053 \text{ m}^{-1}$$

For $L = 14$ m and $dD_u/dt = 5.3 \times 10^{-3}$ m$^{-1}\cdot$min^{-1},

$$D_{uo} = 0.0581 - \frac{14}{9.8}(5.3 \times 10^{-3}) = 0.051 \text{ m}^{-1}$$

These calculations indicate that the actual quantity of this particular type of smoke required to alarm the detector varies from 0.051 to 0.057 m^{-1} or from 3.5 to 3.9 percent/ft.

Smoke production and characteristics. The fuel characteristics of primary concern for smoke detection are (1) material and (2) mode of combustion. These two parameters are important for determining pertinent features of expected products of combustion, such as particle size, distribution, concentration, and refractive index. The importance of these features with regard to smoke detection are well documented[6,31,32] and are discussed by Mulholland in Section 2, Chapter 13.[34] Assuming a well-mixed smoke-filled volume, data on smoke characteristics for given fuels can provide an estimation of detector response.

EXAMPLE 15:
The design objective is to detect the smoke from a flaming 200-g (0.5-lb) polyurethane pillow in less than 2 min. The pillow is located in a 36 m^2 room with a ceiling height of 2.5 m (8 ft). Assume that the pillow is burning at a steady rate of 50 g/min. Can the design objective be met? What assumptions are required?

SOLUTION:
The total mass loss at 2 min is 100 g. Given this information, the optical density in the room can be calculated from the relationship (see Section 2, Chapter 13):

$$D_u = \frac{D_m M}{V_c} \tag{29}$$

where D_m [mass optical density (m^2/g)] can be taken from Table 2-13.5 in Section 2, Chapter 13 as 0.22 m^2/g.

$$D_u = \frac{(0.22\ m^2/g)(100\ g)}{(36\ m^2)(2.5\ m)} = 0.244\ m^{-1}$$

Assuming the detector will respond at the UL upper sensitivity limit of 0.14 m^{-1} (black smoke),[33] it can be assumed that the detector will respond within 2 min. This approach is simplified, however, and assumes that the smoke is confined to the room, is well mixed, can reach the ceiling level, and can enter the detector.

EXAMPLE 16:
Polyurethane mattresses are stored in a room that is 50 m × 75 m × 10 m high. A goal has been set to detect a flaming fire before approximately 350 g of fuel has been consumed. Using a projected beam smoke detector with sensitivity settings that can vary from 20 percent to 70 percent total obscuration in 10 percent increments, what is the minimum sensitivity setting for response to this fire? Assume the smoke is mixed evenly throughout the space.

SOLUTION:
The mass optical density, D_m, for a flaming polyurethane mattress is given in this handbook on p. 2-264 as 0.22 m^2/g. The volume of the room is 37,500 m^3.

From the equation for mass optical density, calculate the resulting unit optical density in the room when 350 g of fuel is consumed:

$$D_m = \frac{D_u V}{\Delta m}\ m^2/g$$

$$D_u = \frac{\Delta m D_m}{V}\ m^{-1}$$

$$D_u = \frac{350(0.22)}{37,500} = 0.002\ m^{-1}$$

Knowing D_u and assuming the path length of the beam to be 75 m, the ratio of light reaching the receiver of the unit can be calculated:

$$\frac{I}{I_0} = 10^{-D_u l}$$

$$\frac{I}{I_0} = 10^{-0.002(75)} = 0.708$$

Next, the percent obscuration caused by the smoke is calculated:

$$O = 100\left(1 - \frac{I}{I_0}\right)$$

$$O = 100(1 - 0.708) = 29.2$$

Thus, a projected beam smoke detector would have to be set to respond at about 30 percent total obscuration or less to meet the design objective.

Discussion related to the use of D_m. The previous two examples used the mass optical density, D_m, to calculate the expected optical density, D_u, in a space when a certain mass of fuel was consumed. D_m data are typically measured in small-scale tests due to the need for accurate measurements of mass loss and optical density. The use of D_m from small-scale tests to calculate the resulting D_u in a large-scale scenario introduces error. Some comparisons show qualitative correlation. However, it has been reported that the correlation breaks down with complex fires.[34]

Stratification. In the context of this chapter, smoke dilution refers to a reduction in the quantity of smoke available for detection at the location of the detector. This dilution can occur either through natural convection (entrainment in the plume or the ceiling jet) or by effects of a heating or ventilation system. In many cases, forced ventilation systems with high exchange rates cause the most concern. In the early stages of fire development, when smoke production rate is small and the plume is weak, smoke can easily be drawn out of the room and away from area smoke detectors. In addition, high velocity air flows out of supply and into return vents creating defined patterns of air movement within a room. Such flows can either keep smoke away from detectors that are located outside of these paths, or, in some cases, inhibit smoke from entering a detector located directly in the air flow path.

Although there currently are no quantitative methods for estimating either smoke dilution or air flow effects on smoke detector siting, these factors must be considered qualitatively. It should be clear, however, that the air flow effects become larger as the required fire size at detection, $\dot{Q}_{cr}$, gets smaller. If the application warrants, it

may be useful to obtain velocity profiles of the air movement within a room or to perform small-scale smoke tests under various conditions to aid in the smoke detector placement analysis.

The potential for smoke stratification is another concern in the detection of low-energy fires and fires in rooms or volumes with very high ceilings. Stratification occurs when the temperature within the plume equals that of the surrounding air, and there is insufficient thermal energy from the fire to force the smoke higher. Once this point of equilibrium is reached, the smoke layer will maintain its height above the fire, regardless of the ceiling height, until additional energy is provided.

Unlike the effects of air flow on smoke dilution, stratification effects can be calculated using the relationship[44]

$$\dot{q}_{\text{conv}} > 0.352 H^{5/2} T_s^{3/2} \qquad (27)$$

where

$\dot{q}_{\text{conv}}$ = convective heat release rate in W

H = distance from the top of the fuel package (base of the fire) to the ceiling level in m

T_s = difference in ambient gas temperature in °C between the fuel location and ceiling level

This same relationship can also be found in NFPA 92B, *Guide for Smoke Management Systems in Malls, Atria, and Large Areas,* 1991 edition.[45]

EXAMPLE 17:
The design objective is to detect the pyrolysis of overheated PVC cable insulation in a 7-m (23-ft) high, 100-m² (1076-ft²) room. The room is air conditioned, with a temperature differential of 10°C (18°F) between the base of the switch equipment and the ceiling. The proposed design has smoke detectors mounted at the ceiling level. Assuming the critical fire size is 1000 W, will there be sufficient thermal energy to force the smoke to the ceiling level?

SOLUTION:
In this case, one can rearrange Equation 27 and solve for H:

$$H < \left(\frac{\dot{q}_{\text{conv}}}{0.352 T_s^{3/2}} \right)^{2/5}$$

where $\dot{Q}_{\text{cr}} = 1000$ W, and $T_s = 10$°C (18°F). This result indicates that the highest level of smoke rise is estimated to be 6 m (20 ft). As a result, the design objective may not be achieved by the proposed design. This approach is also valid for evaluating the effects of stratification in a high-ceiling room where a larger fire might be expected. However, the effects of heating and air conditioning systems and warm or cold walls are not considered.

EXAMPLE 18:
The design objective is to detect the flaming combustion of a chair located in the lobby of an office building in order to initiate smoke management functions. The lobby is located at the lowest level of a 20-m (64-ft) high atrium. The atrium has offices on three sides and a glass facade to

the outside on the other. The atrium is air conditioned, with a temperature differential of 20°C (36°F) between the lobby and the ceiling level. The proposed design is for smoke detectors to be mounted at the ceiling level. Is there sufficient thermal energy to force the smoke to the ceiling level?

SOLUTION:
First, a value for $\dot{Q}_{\text{cr}}$ must be selected for the burning chair. From an analysis of the chair and a review of published heat release data, it is determined that the chair most closely resembles the metal frame chair with padded seat used in Test 53 of the NIST furniture heat release rate tests.[8] This chair had a maximum heat release rate of 280 kW, which can be used as $\dot{q}_{\text{conv}}$ (or in this case $\dot{Q}_{\text{cr}}$, the critical fire) in Equation 27. Equation 27 can then be rearranged to solve for H:

$$H < \dot{Q}_{\text{cr}} / (0.352 T_s^{3/2})^{2/5}$$

where $\dot{Q}_{\text{cr}} = 280{,}000$ W and $T_s = 20$°C (36°F). In this case, the highest point of smoke rise is estimated to be 38 m (125 ft). Thus, the smoke would be expected to reach the ceiling-mounted detector.

It should be noted that air flow concerns were not considered in Examples 12, 13, and 14. In some cases, a system supplying air at a low level and exhausting at an upper level may actually help transport the smoke to the upper levels of a room, where in other cases it may serve to inhibit smoke movement. It should also be noted that, simply because the smoke reaches the level of the detector, there is no guarantee that it can enter the sensor chamber.

Velocity analog. Spot-type smoke detectors, whether commercial or residential, or ionization- or light-scattering type, all require smoke to enter the detection chamber in order to be sensed. This requirement is another factor that must be considered when attempting to estimate smoke detector response. Smoke entry into the detector can be affected in several ways, for example, due to insect screens, chamber configuration, and proximity of the detector to the ceiling.

As previously discussed in this chapter, Heskestad[46] introduced the concept of smoke detector lag to explain the difference between the optical density outside (D_{ur}) and inside (D_{uo}) of a detector at the time of activation. Although studies of this relationship have provided useful information concerning smoke detector lag,[15,41] the difficulty in quantifying L for different detectors and relating it to siting requirements has limited its usefulness. In its stead, the concept of critical velocity (u_c) has been introduced.[4,47]

Critical velocity, in this context, refers to the lowest gas velocity required for smoke entry into the sensor chamber at a level to sound an alarm at a given threshold. Experimental work has shown this requirement to be in the range of 0.15 m/s for the detectors tested in one study.[47] When velocities fell below this value, the smoke level outside the detector at the time a specified analog output level was reached rose dramatically compared to levels when the velocity was above the critical value. This figure can be useful for design and evaluation purposes, as it is close to the low-velocity value (0.16 m/s) at which a detector must respond in the UL smoke detector sensi-

tivity chamber in order to be listed.[33] Thus, the location of a velocity of 0.16 m/s in the ceiling jet for a given fire and ceiling height can be considered as a first approximation design radius for detector siting purposes. It should be noted that the ceiling-jet velocity correlations assume a horizontal, smooth ceiling. A detailed discussion of ceiling-jet flows by Evans is presented in Section 2, Chapter 2. The critical velocity approach can be illustrated with a simplified example.

EXAMPLE 19:

The new owners of a hotel have established a fire detection design objective that the smoke detection system in the grand ballroom must be able to detect a 50-kW fire. The ballroom is 50 m (160 ft) long by 30 m (96 ft) wide with a 7.1-m (23-ft) high smooth ceiling. The existing smoke detectors are installed at a listed spacing of 10 m on center and have a critical velocity of 0.15 m/s. Assuming the fire starts at a point equally spaced between the existing smoke detectors, will the velocity of the ceiling jet from a 50-kW fire be sufficient to force smoke into the detection chamber? Assume there will be no ventilation system effects.

SOLUTION:

The stated design objective is to detect a 50-kW fire. Because it is not stated whether the fire is steady state or growing, this solution will assume a steady-state fire of 50 kW. This assumption allows the use of Alpert's[16] velocity correlations for a steady-state fire. Alpert provides two equations that can be used: one for $r/H = 0.15$, and the other for $r/H > 0.15$. This correlation is generally considered to be valid when r/H is between 0.15 and 2.1. Therefore, the ratio r/H must be determined first. In addition, the fire source should be at a distance of at least 1.8 times the ceiling height from the nearest enclosure wall.

The installed spacing is 10 m (32 ft) on center. Using the relationship $S = 2^{1/2}r$, the radial distance is found to be approximately 7.1 m (23 ft). Given that H is also 7.1 m (23 ft), the ratio r/H is found to be 1.0. This value is greater than 0.15; thus the following equation can be used:

$$U = \frac{0.195\dot{Q}^{1/3}H^{1/2}}{r^{5/6}}$$

By entering the values of $\dot{Q} = 50$ kW, $H = 7.1$ m (23 ft), and $r = 7.1$ m (23 ft), a velocity of 0.37 m/s is calculated. This indicates that, for a steady-state 50-kW fire, there will be sufficient velocity to force smoke into the detectors at their existing locations.

However, if the 50 kW fire as stated is the design fire, $\dot{Q}_{do}$, and it was determined that the critical fire, $\dot{Q}_{cr}$, was only 5 kW, the resulting velocity using the steady-state correlation at 5 kW would be 0.17 m/s—very close to the critical velocity of 0.16 m/s. Furthermore, with a relatively small fire and a relatively high ceiling, stratification is likely to be a factor and should be considered. Assuming the room is air conditioned, with a temperature differential of 10°C from the top of the fuel package to the ceiling level, the smoke from a 5-kW fire would stratify at a level of about 7.3 m (23.4 ft)—very close to the ceiling height of 7.1 m (23 ft). Given probable dilution of smoke and errors

in approximations, it could be considered unlikely that a 5-kW fire would be detected under the defined conditions.

In addition to illustrating how the concept of critical velocity can be used for the design of smoke detection systems, it clearly points out the need to adequately define performance and design objectives, and to select correlations that fit those objectives. First, the objectives should be stated in terms of both the design fire and the critical fire. A 50-kW design fire is significantly different from a 50-kW critical fire, and the design for one may not meet the requirements for the other. Second, care should be taken in selecting a ceiling-jet velocity correlation that most closely fits the design objectives. Unless the hazard analysis indicates that the maximum fire size of $\dot{Q}_{do}$ will be 50 kW, it may be better to apply a ceiling-jet velocity correlation, based on a growing fire. In this case, the fire growth rate must also be estimated as part of the evaluation. The following example shows the importance of these factors by using the same ballroom as described in Example 19, and provides more specific performance and design parameters.

EXAMPLE 20:

After additional consultation, the owners of the hotel described in Example 19 have modified their objectives as follows: assuming that a fire will begin in a chair, the smoke detection system for the grand ballroom must be able to detect the fire and initiate an internal response before it spreads beyond the chair of origin. The typical fuel load within the room consists of metal-framed chairs with padded seats and backs, and plywood tables with cotton tablecloths.

The response time from when the alarm signal is indicated at the annunciator until the first staff member arrives is estimated to be 60 s. The delay time from detector activation until alarm initiation, as measured at the sensor, is 10 s. Because of the potential for nuisance alarms, the detection system employs an alarm verification feature that has a minimum delay time of 15 s and a maximum delay time of 60 s.

The existing smoke detectors are installed at a UL-listed spacing of 10 m on center and have a critical velocity of 0.15 m/s. Assuming the fire starts at a point equally spaced between the existing smoke detectors, and there are no ventilation system effects, can the existing smoke detection system be expected to meet the design objectives?

SOLUTION:

The complete solution to a problem like this one may require several steps; for example, determination of the design fire, determination of the critical fire, estimation of ceiling jet velocity at $\dot{Q}_{cr}$, estimation of smoke production or optical density, and analysis of possible stratification effects. In all cases, however, determination of the design fire and the critical fire is essential.

Given that the goal is to detect the fire while in the chair of origin, a first step might be to estimate the fire size within the chair that could ignite the cotton tablecloth. From analysis of the chair and a review of published heat release data, it is determined that the chair most closely resembles the metal frame chair with padded seat and back used in Test 53 of the NIST furniture heat release rate

tests.[8] This chair had a maximum heat release rate of 280 kW; a fire growth rate of ≈ 0.0086 kW/s^2; a growth time, t_g, of 350 s; and a virtual start time, t_v, of 50 s.

Assuming that the fire would likely grow up the seatback of the chair and that the seatback is located approximately 0.5 m from the tablecloth, an estimate of the energy output required for ignition of the tablecloth can be made. In this case, using the radiant ignition routine in FIREFORM[48] and assuming the fuel being easy to ignite (ignition flux of 10 kW/m^2) with a separation distance of 0.5 m, it is estimated that the tablecloth will ignite when the total energy output from the burning chair reaches 139 kW. These parameters define the design fire.

The next step is to calculate the time for the design fire to reach the threshold limit of 139 kW. Using the relationship $\dot{Q} = \alpha t^2$, a time of 118 s (about 2 min) is calculated. This calculation is growth time of the fire after it begins to follow an exponential growth rate until the design fire size is reached. Given that the fire would probably start as smoldering combustion, the actual growth time could be considerably larger (1 to 2 hr possible).

The critical fire size can then be estimated by subtracting the various response times and estimating the heat release rate at that moment in time. In this regard, reasonable time delays should be used based on the information provided. The focus should be on obtaining the "most reasonable" worst-case delay for the situation. From the problem statement, this delay is estimated based on the response times given, using the following equation:

$$t_{\text{response}} = t_{\text{transport}} + t_{\text{verify}} + t_{\text{system}} + t_{\text{staff}}$$

where the following assumptions are made:

transport = smoke transport time (unknown)

verify = verification time (60 s maximum)

system = system response time (10 s)

staff = staff response time (60 s)

Momentarily ignoring the smoke transport time and assuming prompt staff response, the result is a maximum detection system response time of 130 s. However, in an actual fire situation, the smoke detector verification time should be at its minimum of 15 s, and not at its maximum of 60 s. Making this assumption, the total response time (still ignoring smoke transport time) is 85 s. This result is less than the 127 s time to ignition of the tablecloth and is used to help define the critical fire size ($\dot{Q}_{\text{cr}}$).

Here, the 85 s is subtracted from the 127 s (that defines the design fire), and the relationship $\dot{Q} = \alpha t^2$ is used to calculate the heat release rate at that moment in time. The result is a heat release rate of 15 kW. Assuming no smoke transport time, this result would be the critical fire size at which detection must occur in order to detect the fire and cause the required response before the design fire size is reached.

The next step is to factor in a lag due to the smoke transport time. In order to account for smoke transport lag, Brozovsky[47] suggests a safety factor that is equivalent to a heat release rate that is 80 percent of the maximum

fire size at the time of detection. This factor would result in a critical fire size of 12 kW and a corresponding response time of 37 s. These values can then be used to determine if the ceiling-jet velocity will exceed 0.16 m/s.

Although several simplifications have been made, this example outlines a methodology for estimating the potential for detector response, given the concepts of design fire and critical fire. In addition, the cross-checking utilized points out the importance of understanding the limitations and boundary conditions of correlations and empirical relationships; i.e., simply because one condition can be met, it does not automatically mean that all others will be met as well, and the complete scenario should be considered. Engineering of smoke detection, especially for low-energy fires, can be a difficult task, and the application of any method for this purpose should include clear statements of all assumptions made.

Temperature approximation method for modeling smoke detection. The temperature approximation theory is another method used to estimate the optical density produced by flaming fires. The theory hypothesizes that the mass concentration of smoke particles at a point is proportional to the change in temperature due to the fire (at that point).[49] The following assumptions are necessary:

1. Particle size distribution is constant in space and time.
2. Mass generation rate is proportional to mass burning rate.
3. There is no heat transfer between particles or between the particles and the confining surfaces.
4. The smoke does not continue to react as it travels.

Heskestad then hypothesized that the ratio of optical density to temperature rise would be a constant for a particular fuel and burning mode (flaming, smoldering, vertical combustion, horizontal combustion, etc.). There are actually three parts to this hypothesis.

The first is that each fuel and burning mode results in a unique optical density required to alarm a particular model and type of detector. This aspect was discussed previously regarding photoelectric, ionization, and projected-beam smoke detectors. This phenomenon is regularly observed, explained by theory, and accepted by the scientific and engineering community.

The second part of the hypothesis is that for each fuel and burning mode the optical density at a point is proportional to the mass concentration of particles:

$$D_u \propto C$$

The final part of the hypothesis is that, for each fuel and burning mode, the mass concentration of particles is proportional to the change in temperature at a point:

$$C \propto \Delta T$$

Combining these proportionalities, optical density is proportional to the change in gas temperature for a given fuel and combustion mode:

$$D_u \propto \Delta T$$

Therefore, the ratio of optical density to temperature rise is constant for a given fuel:

$$\frac{D_u}{\Delta T_g} = \text{CONSTANT}$$

This hypothesis assumes that the only way to move the smoke particles from the source to the detector at the ceiling is by buoyant forces.

Heskestad and Delichatsios examined experimental data for obscuration and temperature rise at various locations on a ceiling for different fuels. They concluded that while the data showed some variation in time at different radial positions relative to the fire source, the ratio could be approximated as a constant. Table 4-1.15 lists the ratios recommended by Heskestad and Delichatsios for various fuels.

Examining the original data, the last column has been added to show the range of values for each fuel. Averages have also been calculated and listed in the last row of the table for reference.

Others experiments have resulted in data that differ from that of Heskestad and Delichatsios. Bjorkman et al. reported values for polyurethane that are approximately one half that reported by Heskestad and Delichatsios.[42] The data produced by Heskestad and Delichatsios show the ratio of optical density to temperature rise was not constant. The authors concluded that the variation was the result of slowly changing characteristics of the smoke particles as they left the flaming source and traveled in the plume and ceiling jet. Nevertheless, they concluded that a constant value could be used as a rough approximation to allow engineers to model optical density produced by a fire. Although it has not yet been done, it is possible to examine their original data and place error bars on the values recommended in Table 4-1.15.

A fire model can be used to calculate the temperature rise at a smoke detector location or in a layer. Then, using the ratios reported by researchers, the optical density at that location as a function of time can be approximated.

Discussion related to the use of fire models for heat and smoke detector modeling. Some computer fire models or sets of computational tools include routines for calculating heat or smoke detector response. It is important for users to understand the underlying detector models being used so that limitations and potential errors can be understood. For heat detection, most computational tools use a lumped mass model as described in this chapter. However, for smoke detection some use a temperature rise model, and some use a mass optical density or specific extinction area model. The specific extinction area σ_f is similar to the mass optical density except that it is based on calculations using the natural log, e, rather than $\log_{10}$. Most do not include entry resistance modeling. Some permit the use of fuel-specific parameters for smoke yield and mass optical density. Others use preset values.

Radiant Energy Detection

During the combustion process, electromagnetic radiation is emitted over a broad range of the spectrum. Currently, however, fire detection devices operate only in one of three bands: ultraviolet (UV), visible, or infrared (IR), where the wavelengths are defined within the following ranges:[8]

Ultraviolet	0.1	to	0.35 microns
Visible	0.35	to	0.75 microns
Infrared	0.75	to	220 microns

Selection of a specific sensor type for fire detection is based on a number of factors, including fuel characteristics, fire growth rate, ambient conditions, resulting control or extinguishing functions, and environmental conditions in the detection area. More specifically, it includes evaluation of the radiant energy absorption of the atmosphere, presence of nonfire-related radiation sources, the electromagnetic energy of the spark, ember or fire to be detected, the distance from the fire source to the sensor, and characteristics of the sensor.

These factors are important for several reasons. First, a radiation sensor is primarily a *line-of-sight* device, and must "see" the fire source. If there are other radiation sources in the area, or if atmospheric conditions are such that a large fraction of the radiation may be absorbed in the atmosphere, the type, location, and spacing of the sensors may be affected. In addition, the sensors react to specific wavelengths, and the fuel must emit radiation in the sensors' bandwidth. For example, an infrared detection device with a single sensor tuned to 4.3 microns (the CO_2 emission peak) cannot be expected to detect a noncarbon-based fire. Furthermore, the sensor must be able to respond reliably within the required time, especially when activating an explosion suppression system or similar fast-response extinguishing or control system.

Once the background information has been determined, the detection system can be designed. Standard practice for the design of radiant energy detection devices is based on application of generalized fire size versus distance curves that are derived using the inverse square law:[8]

Table 4-1.15 *Ratios Recommended by Heskestad and Delichatsios for Various Fuels*

Material	$10^2 D_u/\Delta T$ (1/ft°F)	Range of Values
Wood	0.02	0.015–0.055
Cotton	0.01/0.02	0.005–0.03
Paper	0.03	Data not available
Polyurethane	0.4	0.2–0.55
Polyester	0.3	Data not available
PVC	0.5/1.0	0.1–1.0
Foam rubber PU	1.3	Data not available
Average	0.4	0.005–1.3

$$S = \frac{kP \exp^{\zeta d}}{d^2}$$

where

S = radiant power reaching the detector (W)

k = proportionality constant for the detector

P = radiant power emitted by the fire

ζ = the extinction coefficient of air

d = the distance between the fire and the detector

This relationship is used to produce sensor response information for specific fuels. By then plotting the normalized fire size versus the normalized distance, the resulting curve defines the maximum distance at which the tested sensor can be expected to consistently detect a fire of a defined size (usually provided in m²). By testing a sensor using various fuels, a family of curves can be developed to assist in system design. These curves (sometimes given in tabular form) are usually provided by the sensor manufacturer.

Before applying the distance obtained from such a curve, one must also consider the sensors' field of view. Because the radiation sensor is a line-of-sight device, the sensitivity of the device to a defined fire size decreases as the fire location is moved off the optical axis of the device. This result means that a fire of X m², which is detectable at a distance Y m on axis from the sensor, may not be detectable at the same distance Y m if it is located 30 degrees off axis. Limitations of viewing angles are also provided by manufacturers.

Ambient conditions should also be considered as part of the evaluation and design process. Factors, such as humidity and dust, can affect the absorption of radiation in the atmosphere, thus limiting the amount of radiation reaching the sensor for a given fire size. Similarly, temperature can affect the relative sensitivity of a sensor. As the ambient temperature increases, the relative sensitivity can decrease. Even if the decrease is small, it can affect the response of the sensor to the expected fire.

Radiation Detection Example

EXAMPLE 21:

The design objective is to detect a 1.0 m² (11 ft²) pool fire of JP4 aircraft fuel in a large hangar in order to activate a fixed suppression system. The hangar dimensions are 50 m (160 ft) by 80 m (257 ft) with a 20-m (64-ft) ceiling height. The ambient temperature at the ceiling level varies between 15°C (59°F) and 60°C (140°F), depending on time of day and season. The humidity also varies by season, with relative humidity of 90 percent possible. What steps should be taken during system design?

SOLUTION:

The first step should be selection of a detection device. Because the hazard is carbon based, IR detection at 4.3 microns is suitable. Also, because IR detectors generally provide a larger surveillance area per device than UV detectors, they could be more cost effective than UV detection in this case.

One should then determine possible sources of interfering radiation and select a device that is resistant to these extraneous sources. Such resistance to false response can be obtained by filtering, use of multiple sensors (e.g., two- or three-channel detector), or a combination.

The next step is to review the manufacturer's data to determine mounting criteria based on the size of the critical fire [1.0 m² (11 ft²)]. Generally, this step begins with the fire size versus distance curve or table. If only a curve is provided, one must then determine the mounting height and lateral distance limits of the detector. Lateral distances are important as related to the sensors' field of view.

Given this information, a device layout design can be made. This design should consider all possible obstructions, and result in all parts of the hangar being monitored. One such design is illustrated in Figure 4-1.11.

As part of the layout, one should consider the possible effects of reduced device sensitivity due to angular displacement, temperature, and humidity. Because manufacturers' criteria vary on these parameters, typical values are used in this solution to illustrate their effects.
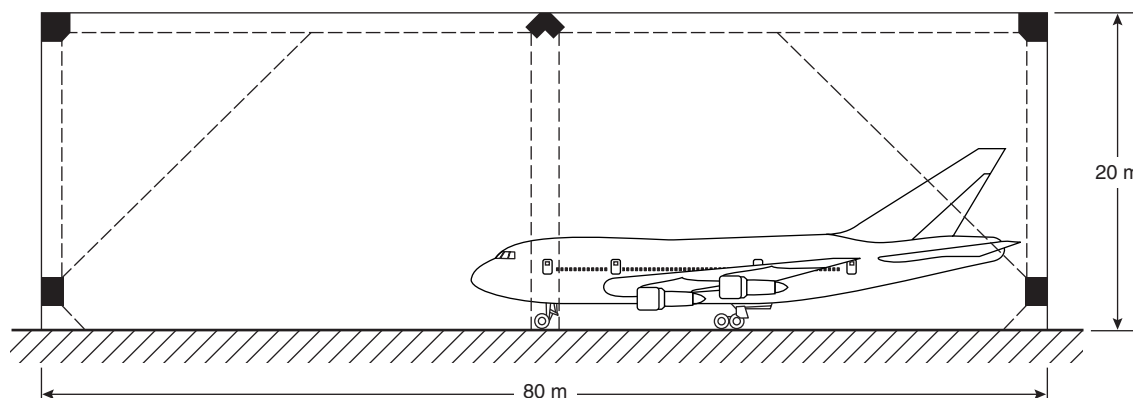

Figure 4-1.11. *IR detector layout for an aircraft hangar.*

For example, the proposed layout has devices utilizing a field of view of 45 degrees. Assuming the nominal sensitivity is such that a 1.0 m^2 (11 ft^2) fire can be detected at 40 m (128 ft), and there is a reduction in sensitivity of 30 percent due to angular displacement, the distance at which a 1.0 m^2 (11 ft^2) fire can be detected at 45 degrees is reduced to 28 m (90 ft). If the manufacturers' data indicate a further reduction in sensitivity for temperature, for example 3 percent at 50°C (122°F), the distance is reduced to about 26.8 m (86 ft). If there are further reductions due to humidity, for example a 3 percent reduction at 90 percent relative humidity, the resulting detection distance at 45 degrees is about 25.6 m (82 ft).

In this example, the viewing distance at 45 degrees is a maximum of 20 m (64 ft), and the design can be considered valid. Had the sensitivity decreased such that the distance dropped below 20 m (64 ft), an alternative layout or different devices must be used. In all cases, the manufacturers' literature should be consulted to determine all pertinent increases or reductions in detector sensitivity due to fuel, distance, angular displacement, and environmental conditions.

Designing Fire Alarm Audibility

In most cases, the purpose of a fire detection and alarm system is to alert the occupants of a building that an emergency exists and to initiate evacuation. In situations such as high-rise or industrial buildings, it may be desirable to provide the occupants with more information, such as the nature and location of the fire. In either case, the purpose of the system is defeated if the signal is not heard and understood by the occupants.

This section demonstrates a method for fire protection engineers to estimate the relative effectiveness and cost of various fire alarm alerting systems during the design process. In the past, the selection and location of fire alarm devices has been based on experience and engineering judgment. The use of this simplified methodology can save thousands of dollars in retrofit costs required to correct deficiencies in an alarm system.

The transmission of sound from a source to a target is a function of many factors, such as humidity; air viscosity and temperature; the frequency of the signal; the location of the source relative to the target; the construction of walls, floors, and ceilings; and the furnishings in the area. *Architectural Acoustics*[50] contains a good discussion of these and many other factors affecting sound transmission and loss.

Sound power and sound pressure levels are expressed in decibels (dB) relative to a reference. It is assumed that the reader is familiar with this system of measurement. Throughout this chapter sound power level (SWL or L_W) in decibels is referenced to 10^{-12} W. Sound pressure level (SPL or L_p) in decibels is referenced to 2×10^{-5} Pa. This discussion also assumes that the reader is familiar with the concept of A-weighting. The purpose of A-weighting is to adjust sound pressure level measurements to correspond as closely as possible to the way humans perceive the loudness of the many different frequencies we hear. For instance, a 1000-Hz signal at an SPL of 20 dB would be clearly audible. A 100-Hz signal at the same SPL would not be heard. A-weighting allows a single number to describe the SPL produced by a signal containing frequencies between 20 and 20,000 Hz. The weighting of the various frequencies is established by an internationally accepted A-weighting curve.[51]

Typical fire alerting systems consist of a combination of audible and visual signals activated by fire detection systems. The audible devices are usually horns, bells, chimes, or speakers. The visual indicators are usually strobe lights, incandescent lamps, or, occasionally, revolving beacons.

In residential occupancies, fire alerting systems should be capable of awakening a sleeping person and informing him or her that a fire emergency exists. Several studies have been done to establish the sound pressure level required to achieve this goal.[52,53] These studies suggest an SPL between 55 and 70 dBA will awaken a college-age person with normal hearing. The minimum required SPL is also a function of the background noise or signal-to-noise ratio. These levels establish the SPL required to alert or be audible. They do not address the problem of how the person will perceive the sound or react to it.

Until recently, fire codes did not set forth the SPL that a fire alarm system must produce within a building. NFPA 72[8] requires signals to be 15 dBA above ambient in areas where people may be sleeping. British standards require fire alarm signals to produce a sound pressure level of 65 dBA or 5 dBA above ambient noise in areas where occupants are not sleeping.[54] A sound pressure level of 75 dBA at the head of the bed is required in occupancies where people may be sleeping.

The audible design requirements listed above and the remaining discussion and examples in this section all use dBA as a measure of audibility. However, it should be pointed out that for a sound to be perceived as audible, it need only penetrate or be greater than the background noise level at one particular frequency bandwidth. For example, certain facilities such as manufacturing plants may have a background noise level in excess of 85 dBA. An installed fire alarm may produce only 75 dBA at a certain location. Nevertheless, occupants will hear and respond to the fire alarm system. Why? The reason is because the background noise that contributes to the 85 dBA is mostly low frequency sound and the fire alarm is mostly high and midrange frequencies. Figure 4-1.12 illustrates this concept. Like two picket fences, one behind the other, only one picket or octave band must be taller for us to perceive the presence of the second fence or signal. While the balance of this section uses dBA, the procedure and methods apply equally well to work done in a single frequency band.

Visual signals are located to assist people in deciphering potentially confusing alarm signals. The visual signals also help alert occupants in high background noise environments.

Butler, Bowyer, and Kew[51] have described a method to estimate sound pressure levels at some location remote from the sound source. Formulas presented in their
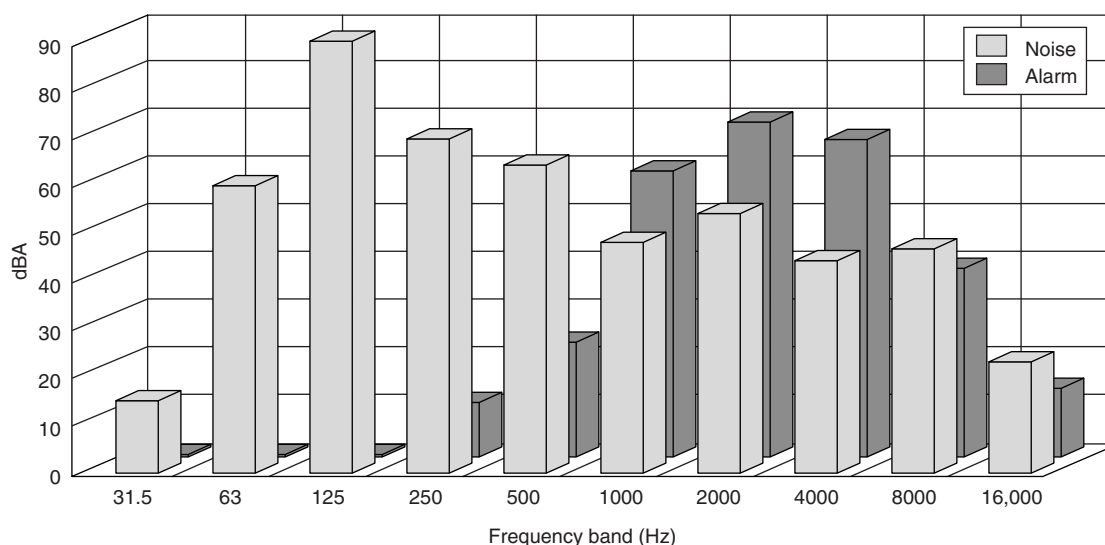
Figure 4-1.12. *Penetration of noise by alarm.*

study are analogous to standard sound attenuation for-
mulas found in other references.[50,55] They have been
simplified by replacing complex terms with constants
for which they have provided tables of data (see Tables
4-1.16 through 4-1.29). The equations and data presented
in their study provide a straightforward method for ana-
lyzing proposed designs. The same equations and data
can be used to determine the power requirement and
maximum allowable spacing of signaling devices re-
quired to achieve a specified sound pressure level. The
technique presented in their study is suitable for acousti-
cally simple buildings only. Complex building arrange-
ments and materials may require a more rigorous
analysis using other methodologies which are beyond
the scope of this chapter.

To demonstrate how signaling systems can be de-
signed and analyzed, two scenarios will be considered.
Both scenarios are based on a typical dormitory or office
layout. The building has long corridors with rooms of
equal size on each side. Each room is approximately 5 m
wide by 6 m deep. The walls consist of two layers of
Sheetrock (total of 25.4 mm thick) separated by wood
studs. The wall cavities contain 75-mm-thick mineral
fiber insulation. The floors are concrete with carpeting.
The ceiling is 3 m high and consists of acoustical tiles. The

room doors are solid core with good edge seals. The alert-
ing systems will be designed to achieve a 75 dBA sound
pressure level at the farthest point in the rooms.

In the first scenario, wall-mounted fire alarm
speaker/light combinations are spaced equally in the cor-
ridor. Calculations determine the maximum allowable
spacing of the speakers in order to achieve the design goal
of 75 dBA in the rooms.

In the second scenario, speakers are placed in each
room as well as in the corridor. Calculations determine
the size of the speaker and the power needed to drive
that speaker to achieve the design goal of 75 dB. Calcula-
tions are also presented to determine the required spac-
ing of speakers in the corridor to achieve a sound level of
65 dB.

**Table 4-1.16   Adjustment for Mounting Position of
Sounder (C_1)**

Sounder Position	C_1
Wall/ceiling mounted (more than 1 m from any other major surface)	+5
Wall/ceiling mounted (closer than 1 m to one other major surface)	+7

**Table 4-1.17   Adjustment for Distance (C_2) with
Distance from Source (m)**

Distance from Source (m)	C_2
1	−11
2	−17
3	−21
6	−27
12	−33
15	−35
20	−37
25	−39
30	−41
40	−43
50	−45
60	−47
80	−49
100	−51

Unless otherwise noted, the following formulas and data are from Butler, Bowyer, and Kew.[51]

Scenario A:

In this scenario, the fire alerting system, or sounder, will consist of wall-mounted speaker/light combinations in the corridors only.

L_W is the sound power level of a horn, bell, speaker, or any sounder (dBA referenced to 10^{-12} W).

$$L_W = L + 20 \log_{10} r + 11 \text{ dB}$$

where L is the manufacturer's stated output in dBA at a distance r meters. A typical compression driver-type fire alarm speaker powered at 2 W has an L equal to 94 dBA at 3.05 m.[56] Therefore,

$$L_W = 94 + 20 \log_{10} (3.05) + 11$$
$$L_W = 115 \text{ dB}$$

L_{P1} is the sound pressure level (dBA referenced to 2×10^{-5} Pa) produced outside of a room wall from one speaker.

$$L_{P1} = L_W + C_3 + C_4 + C_5$$

where

C_3 = correction for the number of directions that the sounder propagates

C_4 = correction for the characteristics of the corridor walls, ceiling, and floor

C_5 = function of the distance from the sounder to the center of the bedroom wall

From Table 4-1.18[51] C_3 is -3 dB, because the speaker propagates in two directions along the corridor; from Table 4-1.19 C_4 is -9 dB, because the floor and ceiling are acoustically soft; and C_5 is unknown since the required spacing of the corridor speakers has not yet been determined. Table 4-1.20 provides C_5 values for determined distances.

A worst-case condition exists for a room located farthest from a speaker. In this situation the room is located equally between two speakers. Since each unit propagates sound to the room, the sound pressure level outside of the room is higher than if there were only one speaker. The sound pressure level is not double that for a single

Table 4-1.18   Adjustment for Number of Directions of Sound Propagation (C_3)

Number of Directions	C_3
Single direction (e.g., positioned at one end of a corridor)	0
Two-directional (e.g., positioned in the length of a corridor)	−3
Three-directional (e.g., positioned at a T junction of corridors)	−5

Table 4-1.19   Adjustment Based on the Finishes in the Corridor (C_4)

Surface Finishes	C_4
Hard (e.g., walls and ceiling with solid surfaces and tarazzo floor)	0
Medium (e.g., acoustic ceiling, plastered solid walls with 5% coverage of soft surfaces and floor of composite tiles)	−8
Soft (e.g., acoustic ceiling, plastered solid walls with 5% coverage of soft surfaces and carpets on felt on concrete floor)	−9

Table 4-1.20   Adjustment for Distance from Source to Mid-Point of the Partition (C_5)

Distance from Source (m)	C_5
1	0
3	−4
6	−8
10	−10
12	−11
15	−12
20	−14
30	−15
50	−17

Table 4-1.21   Addition of Two Sound Pressure Levels

Difference between the Two Levels (dB to Be Added)	Add to the Higher Level (dB)
0	3
1	2
2	2
3	2
4	2
5	1
6	1
7	1
8 or more	0

speaker. For equally spaced sounders, Table 4-1.21 indicates to add 3 dB to the level expected from a single unit. Therefore,

$$L_{P1} = 115 - 3 - 9 + C_5 + 3$$
$$L_{P1} = 106 + C_5$$

L_{P2} is the sound pressure level at the farthest point in a room. To achieve the established goals, L_{P2} must be 75 dBA. In this situation, with the speaker located outside of the occupied space,

$$L_{P2} = L_{P1} - R + C_2 + C_6 + C_7 + 11 \text{ dBA}$$

Table 4-1.22 *Factor for Area of Partition between Sounder and Receiver (C_6)*

Partition area (m²)	C_6
2	+3
4	+6
8	+9
10	+10
15	+11.5
20	+13
30	+15
50	+17
80	+19
100	+20
200	+23

where

R = average sound reduction index for the wall

C_2 = function of the distance from the wall to the point of interest

C_6 = function of the area of the room wall (see Table 4-1.22)

C_7 = function of the frequency of the sound reaching the wall (see Table 4-1.23)

Table 4-1.23 *Adjustment for Frequency of Maximum Output of Sounders (C_7)*

Frequency of Sounder	C_7
500 Hz	0
1000 Hz	−3
2000 Hz	−5
4000 Hz	−9

In this case, from data presented by Butler, Bowyer, and Kew,[51] the sound reduction index R for the wall is about 40 dB. (See Table 4-1.24.) This value is based on incident sound in the range of 100 to 3150 Hz. Sound attenuation through the door is about 26 dB. (See Table 4-1.24.) The average sound reduction index, R, for the combined door and wall is 34 dB, if the door is 10 percent of the area. (See Table 4-1.25.) C_2 is found to be −27 dB, because there are 6.5 m from the center of the wall to the corner of the room. (See Table 4-1.25.) Since the wall is 15 m², C_6 is +11.5 dB. (See Table 4-1.22.) If it is assumed that the sound reaching the wall is a maximum at a frequency of 2000 Hz, $C_7 = 15$ dB. (See Table 4-1.23.) Therefore,

$$L_{P2} = (106 + C_5) - 34 - 27 + 11.5 - 5 + 11 \text{ dBA}$$

$$L_{P2} = 62.5 + C_5 \text{ dBA}$$

Table 4-1.24 *Second Reduction Indices (dB) for a Selection of Typical Structures (100–3150-Hz Frequency Range)*

Building Element	Weight of partition (kg/m²)	Average Attenuation (dB)
Walls and Partitions		
1. 100-mm-dense concrete with or without plaster	250	45
2. 150-mm "no fines" concrete with 12-mm plaster on both faces	250	45
3. 115-mm brickwork with 12-mm plaster on both faces	250	45
4. 115-mm brickwork unplastered	195	42
5. 300-mm lightweight concrete precast blocks with well-grouted joints	190	42
6. 75-mm clinker blockwork with 12-mm plaster on both faces	115	40
7. 50-mm-dense concrete	120	40
8. 25.4-mm plasterboard (2 layers) separated by timber studding (75 mm) and mineral fiber blanket	—	40
9. 200-mm lightweight concrete precast blocks with well-grouted joints	122	40
10. 150-mm lightweight concrete precast blocks with well-grouted joints	93	37
11. 50-mm clinker blocks with 12-mm plaster on both faces	—	35
12. 63-mm hollow clay blocks with 12-mm plaster on both faces	—	35
13. 9.5-mm plasterboard (2 layers) separated by timber studding (75-mm with 12-mm) on plaster on both faces	—	35
14. 6-mm plywood/hardboard (2 layers) separated by timber studding (50- and 50-mm) mineral fiber blanket	—	30
15. 19-mm chipboard on a supporting frame	—	25
16. 0.8-mm sheet steel	—	25
17. 21-mm tongued and grooved softwood boards tightly clamped on a support frame	—	20
18. 3.2-mm hardboard (2 layers) separated by 44-mm polystyrene core	—	20
Doors		
19. Flush panel, hollow core, hung with one large air gap	9	14
20. Flush panel, hollow core, hung with edge sealing	9	20
21. Solid hardwood, hung with edge sealing	28	26
Windows		
22. Single glass in heavy frame	15	24
23. Double-glazed 9-mm panes in separate frames 50-mm cavity	62	34
24. Double-glazed 6-mm panes in separate frames 100-mm cavity	112	38
25. Double-glazed 6-mm and 9-mm panes in separate frames 200-mm cavity, absorbent blanket in reveals	215	58

Table 4-1.25 *Average Sound Reduction Indices (dB) of Partitions Incorporating a Door of 26-dB Attenuation (i.e., heavy door with edge sealing) (100–3150-Hz Frequency Range)*

Door Representing Percentage of Total Area of Partition	Sound reduction index of partition without glazing					
	25 dB	30 dB	35 dB	40 dB	45 dB	50 dB
100%	26	26	26	26	26	26
50%	25	27	28	28	28	28
25%	25	28	30	31	31	31
10%	25	28	32	34	35	35
5%	25	28	33	36	38	38

Table 4-1.26 *Average Sound Reduction Indices (dB) of Partitions Incorporating a Door of 14-dB Attenuation (i.e., one with large air gaps) (100–3150-Hz frequency range)*

Door Representing Percentage of Total Area of Partition	Sound reduction index of partition without glazing					
	25 dB	30 dB	35 dB	40 dB	45 dB	50 dB
100%	14	14	14	14	14	14
50%	16	16	16	16	17	17
25%	19	19	19	19	20	20
10%	21	23	23	23	23	23
5%	23	25	26	26	26	26

If there were no loss of sound pressure level between the speaker and the room wall due to distance, C_5 would be zero and L_{P2} would be 62.5 dBA. This result shows that even if the two speakers were right outside the room, the goal of 75 dBA in the room would not be met. In fact, the resultant noise level in the room would be slightly less than the 65 dBA required by British standards[54] to alert nonsleeping persons. The sound level of 62.5 dBA would exceed the 55 dBA reported by Nober et al.[32] to alert sleeping college-age persons in a quiet ambient setting.

To meet the goal of 75 dBA in the room, either the sound system or the environment would have to be changed. Fire alarm speakers are normally available with multiple power taps such as 4, 2, 1, 1/2, and 1/4 W. A single unit may allow choice of two or three different power levels, which allows balancing of the system after installation.

If a 4-W power input were used, this would be a doubling of the 2 W originally tried in the previous calculation. Because decibels are logarithmic, a doubling of power results in a change of 3 dB in L_W ($10 \times \log_{10} 2 = 3$). This action alone would not be sufficient to meet the 75-dBA goal. In addition, the higher sound pressure level in the immediate vicinity of the speaker might be discomforting. If the fire alarm system were also used for voice communication, a speaker tapped at 4 W in a small corridor might sound very distorted and be unintelligible.

It is also possible to change the sound pressure level in dBA by changing the frequency of the source. In general, the higher the frequency, the higher the attenuation as the sound waves pass through a wall. Hence, a lower frequency would increase the sound pressure level in the room. In the calculations above, it was assumed that the predominant frequency of the source was 2000 Hz. This frequency resulted in a C_7 of -5 dBA. According to Table 4-1.23, if this frequency were 500 Hz, C_7 would be 0 dBA. This adjustment would increase the SPL in the room by 5 dBA.

Changes could be made to the building design that would make it possible to meet the design goal. For instance, the use of a lighter-weight door or one without good edge sealing could increase sound transmission to the room by as much as 12 dBA. (See Tables 4-1.26 through 4-1.29.) However, changes such as this one

Table 4-1.27 *Average Sound Reduction Indices (dB) of Partitions Incorporating a Door of 20-dB Attenuation (i.e., light door with edge sealing) (100–3150-Hz frequency range)*

Door Representing Percentage of Total Area of Partition	Sound reduction index of partition without glazing					
	25 dB	30 dB	35 dB	40 dB	45 dB	50 dB
100%	20	20	20	20	20	20
50%	21	22	22	22	22	23
25%	23	24	25	25	25	26
10%	24	27	28	29	29	29
5%	24	28	30	32	32	32

Table 4-1.28 *Combined Sound Reduction Indices for Combination of Standard Doors and Glazing (100–3150-Hz frequency range)*

Area of (24 dB) Glazing (m²)	Sound Reduction Index for Standard Size Door (1.54 m²)		
	14 dB	20 dB	26 dB
	Insulation Values for Combined Door and Glazing		
1	16	21	25
2	17	22	25
4	18	22	24
6	19	23	24
8	20	23	24
10	20	23	24
12	21	23	24
16	21	23	24
20	22	23	24

would tend to defeat other goals such as fire resistance and resistance to smoke spread. If the floor and ceiling were hard surfaces without carpeting or tiles, C_4 could be increased from -9 to 0 dBA. (See Table 4-1.30.) Changes

Table 4-1.29 *Average Sound Reduction Indices for a Partition Whose Surface Is a Combination of Glass, Door, and Wall Partition (100–3150-Hz frequency range)*

Door + Glazing as Percentage of Total Partition Area	Sound Reduction Value of Partition without Glazing or Door											
	30 dB			35 dB			40 dB			45 dB		
	Insulation Value of Combined Door and Glazing (dB) (from Table 4-1.27)											
	15	20	25	15	20	25	15	20	25	15	20	25
5	26	28	30	28	31	33	28	32	36	28	33	37
10	24	27	29	24	29	32	25	30	34	25	30	35
20	22	25	28	21	26	31	22	27	32	22	27	32
30	20	24	28	20	25	29	20	25	30	20	25	30
50	18	23	27	18	23	28	18	23	28	18	23	28
75	16	21	26	16	21	26	16	21	26	16	21	26
100	15	20	25	15	20	15	15	20	25	15	20	25

Table 4-1.30 *Average Sound Reduction Indices (dB) of Partitions Incorporating Single Glazing (100–3150-Hz frequency range)*

Percentage of Glazing (24 dB)	25 dB	30 dB	35 dB	40 dB	45 dB	50 dB
100%	24	24	24	24	24	24
75%	24	25	25	25	25	25
50%	24	26	27	27	27	27
33%	25	27	28	29	29	29
25%	25	27	29	30	30	30
10%	25	29	31	33	34	35
5%	25	29	33	35	36	37
2½%	25	30	34	37	39	40
—	25	30	35	40	45	50

such as this would probably be resisted for reasons other than fire safety.

The only remaining alternative is to provide speakers in each of the rooms.

Scenario B:

In this case, a speaker in each room powered at only 1/4 W will be tried in addition to the speaker in the corridor. The problem, then, is to select a speaker with a sound power output that can meet the goal of 75 dB at the pillow.

L = ? at r = 3.05 m (3.05 m is a commonly used reference point.)

$$L_W = L + 20 \log_{10} r + 11 \text{ dB}$$
$$L_W = L + 20 \log_{10} (3.05) + 11 \text{ dB}$$
$$L_W = L + 21 \text{ dB}$$

L_{P2} is the sound level at the bed. In this case, with the speaker in the occupied space,

$$L_{P2} = L_W + C_1 + C_2 \text{ dBA}$$

where C_1 is a correction for how close the sounder is to an adjacent surface, and C_2 is a correction for the distance from the speaker to the bed. In this case, the speaker is on the wall and close to the ceiling. Therefore,[51] C_1 is +7 dB, and C_2 is −27 dB (approximately 6.5 m from the speaker to the bed). (See Tables 4-1.16 and 4-1.17.) Therefore,

$$L_{P2} = (L + 21) + 7 - 27 \text{ dBA}$$
$$L_{P2} = L + 1 \text{ dBA}$$

To get L_{P2} = 75 dBA, L must be at least 74 dBA. The smallest and least expensive fire alarm speaker available is a 4-in. paper cone speaker. A typical speaker of this size and type, powered at 1/4 W, has an L equal to 75 dB at 3.05 m.[58] This speaker would meet the design goal in the room, without even considering any sound contribution from corridor-mounted speakers.

For the corridor speakers in Scenario B, L_{P1} is the sound pressure level at a point farthest from a speaker.

$$L_{P1} = L_W + C_3 + C_4 + C_5 \text{ dBA}$$

where C_3 and C_4 are the same as in Scenario A (−3 and −9 dB, respectively). C_5 is a function of the spacing, which is to be determined. If a single corridor speaker tapped at only 1/4 W is used, with an L of 85 dB at 3.05 m,[56]

$$L_W = L + 20 \log_{10} r + 11 \text{ dB}$$
$$L_W = 85 + 20 \log_{10} (3.05) + 11 \text{ dB}$$
$$L_W = 106 \text{ dB}$$
$$L_{P1} = 106 - 3 - 9 + C_5 \text{ dBA}$$
$$L_{P1} = 94 + C_5$$

The goal is to maintain a 65-dBA sound pressure level in the corridors (L_{P1}).

Therefore, C_5 must be −29 dBA or more for L_{P1} to be 65 dBA or higher. From Table 4-1.20,[51] it is found that distance of 50 m between source and target in the corridor could be exceeded and still meet the 65-dBA goal.

Cost Analysis

Scenario A:

For comparison purposes, assume that sufficient changes could be made to the building and alarm system to allow speakers to be mounted in the corridor only at a spacing of 3 m. A typical dormitory with about 30 bedrooms per floor requires approximately 24 speakers per floor in the corridors. In a building with seven floors, this requirement amounts to 168 speakers. At 2 W per speaker, the result would be 336 W. This setup requires three 125-W power amplifiers at an installed cost of about $1400.00 each. This amount does not include other fixed costs, such as control equipment and detectors, that are the same for each of the scenarios.

Assume each corridor unit to be a speaker/light combination. The average installed cost, including backbox, wiring back to a control panel on the first level, and conduit, would total to about $135.00 per unit. The total cost is then

$$\text{TOTAL} = (3 \times \$1400.00) + (168 \times \$140.00)$$
$$\text{TOTAL} = \$27{,}720$$

Scenario B:

In this case, there are thirty 4-in paper cone speakers per floor at an average cost of $100.00, installed. Assume a total of four speaker/light units per floor in the corridors. The calculations show that the system goals are met with only one or two units in the corridors. However, the halls may be split by smoke doors or they may be irregular in shape. Also, system reliability is increased by using more than one unit.

Each bedroom speaker and corridor speaker is powered at 1/4 W. For seven floors, this setup gives a total power requirement of 59.5 W. Therefore, one 60-W amplifier, at a unit cost of $1125.00, is needed. The total cost is then

$$\text{TOTAL} = \$1125.00 + (7 \times 30 \times \$100.00)$$
$$+ (7 \times 4 \times \$135.00)$$
$$\text{TOTAL} = \$25{,}905.00$$

Summary

The estimates show the relative costs of the different scenarios, not the actual costs. The real costs of the systems are affected by factors such as whether the building is new or existing. If existing, the price is affected by the extent of other renovations. Also, the estimates do not reflect the cost of other parts of the system. The balance of the system includes such items as smoke and heat detectors, equipment for elevator capture, and air handler controls.

The relative costs of the two systems in Scenarios A and B under "Cost Analysis" differ by only 7 percent. In a building of this size and type, such a small margin cannot be considered significant enough to conclude that one system is more economical than the other.

The small difference in the costs of the two systems is due to the additional cost of amplifiers needed to power the system that has only corridor units. The total number of units (corridor + room) in Scenario B is 70 more than in Scenario A. The reduced power requirement offsets the added cost of their installation.

Scenario A has a higher equipment cost but a lower installation cost than Scenario B. This result means that the relative costs of the two systems will be slightly sensitive to the type of equipment used and the cost of installation labor. By changing the figures used in the cost estimates, it can be shown that the variance is only a few percent and probably not significant.

If the building were four stories or less in height, the difference in relative cost reduces to about two percent. Again, this amount is not considered to be a significant difference.

By increasing the size of the building to twelve stories, Scenario B becomes significantly less expensive than Scenario A. Above this height, the combined use of room and corridor units becomes increasingly economically attractive.

Changing the size of each floor has about the same effect as changing the height of the building. Therefore, increasing the floor area makes Scenario B more viable. A reduction in floor area and building height does not make the corridor-only system attractive, unless the building is only a few stories in height. Then, a voice system is probably not needed. From an economics standpoint, a corridor-only horn/light system is probably best, since the cost of these units is generally less than that of speakers. Again, this conclusion assumes that sufficient changes could be made to the building design to increase the level of sound penetrating the corridor walls.

Obviously, if the sound loss from the corridor to the individual rooms is less, Scenario A starts to look better. This situation has the effect of raising the height above which Scenario B becomes significantly less expensive. However, changing construction features to reduce sound loss may reduce the passive fire resistance of the structure below an acceptable level as well as decrease the privacy level.

There are other factors to consider when choosing between different systems. In Scenario A, the quantity of speakers in the corridors and the high power levels driving each speaker (2 W each) can cause sound distortion. Voice messages may not be intelligible in the bedrooms even though there is enough sound to wake a sleeping occupant. Also, the high sound levels (106 dBA plus) in the corridors approach uncomfortable levels.

It is clear from the discussions above that a system with room speakers in conjunction with corridor units is the most desirable case. That system has the added advantage of eliminating most of the uncertainties in the design of the system. It is easier and more accurate to calculate sound levels at a point in the same room as the sound source than it is to estimate sound losses through composite walls.

This cost-benefit analysis shows that a fire alarm alerting system with units in each office or bedroom can be installed at about the same cost or less than a corridor-

only system. In addition, there is a higher confidence level that the system with the sounders in each room will perform its intended function: to awaken and alert sleeping occupants.

Designing Fire Alarm Visibility

Visual alarm notification is an important part of a fire alarm system. This visual aspect is especially important in cases where the ambient noise level is high, building occupants may be sleeping, or building occupants or their visitors may have hearing impairments. In these cases, it should be expected that the visual alarm will be required to alert occupants and initiate evacuation or relocation. As such, one first needs to determine a suitable intensity required to obtain this function.

In many cases, a suitable intensity can be obtained from regulatory documents, such as building codes, fire codes, or the Americans with Disabilities Act. These references typically give a required appliance intensity and a maximum size space that can be covered by an appliance with that intensity. If additional guidance is needed, reference can be made to appropriate documentation on alerting of persons by visual means.[57] It is also possible that a reference may cite a required level of illumination to alert someone. This requirement should not be confused with the intensity of the lamp providing the signal. The two are related by the inverse square law where E is the illumination (lumens per unit area), I is the intensity of the light source (candela), and d is the on-axis distance between the light source and the point where the illumination is measured. See Figure 4-1.13.

$$E = \frac{I}{d^2}$$

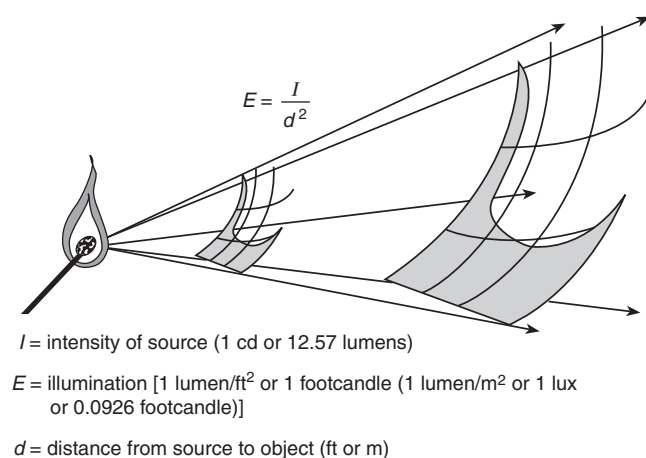In cases where flashing signals are required, the source strength or output is cited as *effective intensity*. Effective intensity is used to equate the perceived brightness of a flashing light to that of a steady light. It can be calculated using the relationship,[58]

$$I_e = \frac{\left(\int_{t_1}^{t_2} I \, dt\right)}{(a + t_2 - t_1)} \qquad (28)$$

where

I_e = effective intensity

I = instantaneous intensity

t_1 = the time (s) of the beginning of that part of the flash where I exceeds I_e

t_2 = the time (s) of the ending of that part of the flash where I exceeds I_e

In the United States, the value of 0.2 is usually used for the constant a. This relationship is shown graphically in Figure 4-1.14.

If the duration of the flash is less than one millisecond, Equation 28 can be further simplified to[58]

$$I_e = 5 \int I \, dt$$

where the integration is performed over the complete flash cycle.

As part of a test program to determine signaling applications for the hearing impaired, UL determined that an illumination of 0.398 lumens/m² (0.037 lumens/ft²) as viewed on axis from a single flashing light source located in the center of one wall of a 6.1 m by 6.1 m (20 ft by 20 ft) room was the minimum required by their objective. It was also determined that, by increasing the "square" dimensions in increments of 3 m (10 ft) in both directions (length
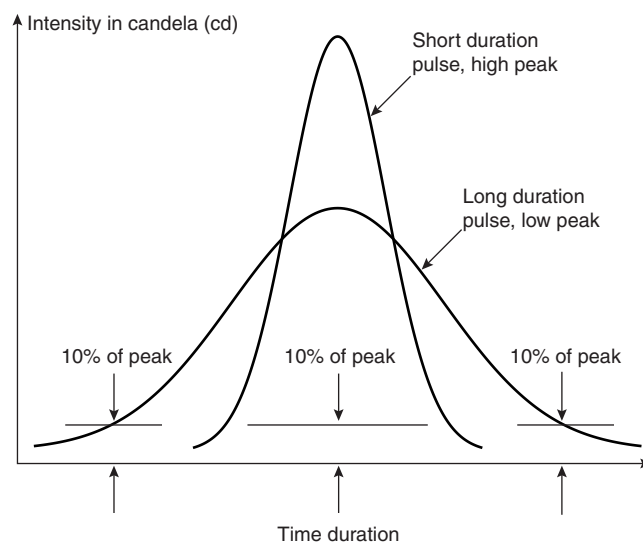

$E = \dfrac{I}{d^2}$

I = intensity of source (1 cd or 12.57 lumens)

E = illumination [1 lumen/ft² or 1 footcandle (1 lumen/m² or 1 lux or 0.0926 footcandle)]

d = distance from source to object (ft or m)

Figure 4-1.13. *Relationship between intensity of lamp and level of illumination required to alert someone.*

Figure 4-1.14. *Peak versus effective intensity. (Source: R.P. Schifiliti Associates, Inc., Reading, MA)*

and width), the minimum illumination value of 0.398 lumens/m² could be used to extrapolate the required signal intensity as the room size increased.

For example, if the room size were increased to 12.2 m by 12.2 m (40 ft by 40 ft), the effective intensity, cd eff, of the flashing strobe signal could be determined using the inverse square law and solving for *I:*

$$E = \frac{I}{d^2} ; \text{therefore}$$

$$I = Ed^2 = (0.398 \text{ lumens/m}^2)(12.2 \text{ m}^2) = 59.2 \text{ candela}$$

Thus, one signal rated at 60 cd eff would be sufficient for the space. Using the same approach, but smaller squares, one would also find that two signals rated at 30 cd eff, or four signals rated at 15 cd eff each, would also be applicable.

Designers should check with the authority having jurisdiction or the current edition of NFPA 72 regarding the use of multiple flashing lights.

EXAMPLE 22:

The design objective is to evaluate the visual alarm notification system installed in a large open space for suitability in providing signals for the hearing impaired. The space is 21 m (70 ft) by 37 m (120 ft), with a 6.5-m (20-ft) ceiling height. The notification appliances are located 2 m (6.5 ft) above floor level and are spaced as shown in Figure 4-1.15. The signals are rated at 45 cd eff each. Is the required illumination of 0.398 lumens/m² currently provided?

SOLUTION:

The first step is to section off the space into blocks that are anticipated to be covered for each signal. In this case, the result is six blocks, each 12.2 m (40 ft) long by 10.5 m (34 ft) wide. This step is illustrated in Figure 4-1.16.

Given these dimensions, one could calculate the illumination at point A, where

$$E = \frac{45 \text{ cd}}{(10.5 \text{ m})^2} = 0.41 \text{ lumens/m}^2$$

This is greater than the minimum required illumination of 0.398 lumens/m². However, application of this method requires the blocks of coverage by a signal to be
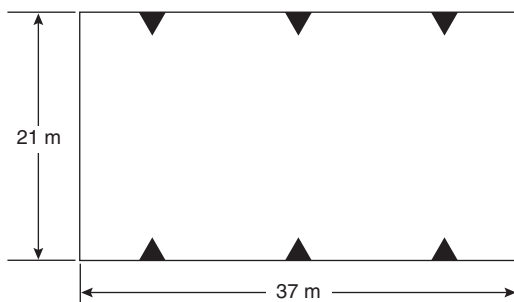

Figure 4-1.15. *Notification appliance (▲) locations.*
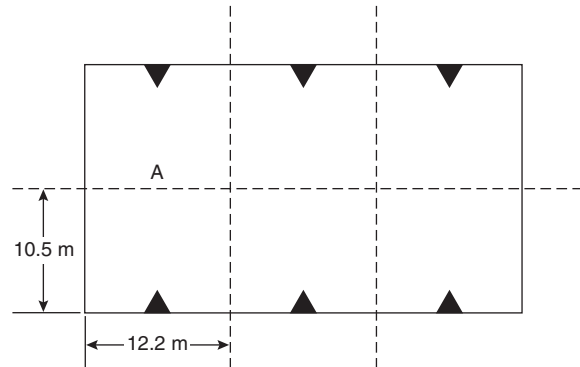

Figure 4-1.16. *Sections for anticipated signal (▲) coverage.*

square, with the lateral distance (90 degrees) being equal to one-half the coverage distance on-axis. In this case, the lateral distance is 12.2 m (40 ft), and this is the figure that should be used to calculate the illumination throughout the entire block. In doing this, one finds that the illumination provided is

$$E = \frac{45 \text{ cd eff}}{(12.2 \text{ m})^2} = 0.29 \text{ lumens/m}^2$$

which is below the minimum required 0.398 lumens/m². This outcome results in areas of the space not having the required illumination. This outcome is illustrated in Figure 4-1.17.

To determine what intensity is required for the signals in order to provide the required 0.398 lumens/m², the inverse square law can be applied using the value $d = 12.3$ m. This application results in a required incident intensity of 60 cd eff for each existing signal location.

By applying this method of dividing spaces into squares and applying the inverse square law, the intensity of signals and their required spacing can be calculated for spaces of any shape and size. Tradeoffs can be made between the number of signals and the intensity of signals to best fit the application (e.g., one signal of 60 cd eff versus four properly spaced signals of 15 cd eff each).

In cases where a minimum required illumination at all points in a space is specified (as opposed to the minimum effective intensity on-axis within a square), the illumination can be calculated using the inverse square law, the cosine law, and the cosine cubed law. In this case, the inverse square law provides the illumination on-axis, application of the cosine law provides the illumination at a perpendicular surface within the same plane as the signal, and application of the cosine cubed law provides the illumination at parallel surfaces within the same plane as the signal.

With this information, it should be possible to calculate visual fire alarm signals for most situations. In all cases, a value for the required effective intensity at some point within the room is required. If not provided at the beginning of the design process, one should determine an effective intensity based on the specific application and the condition of the occupants being alerted.
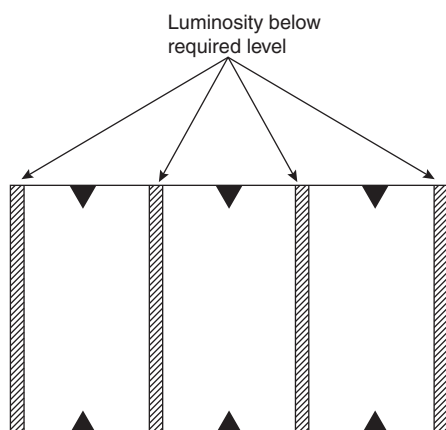
Figure 4-1.17. *Diagram of subadequate luminosity intensity.*

Nomenclature

α fire intensity coefficient (Btu/s^3 or kW/s^2)

A area (m^2 or ft^2)

A $g/(C_p T_a \rho_0)$ [m^4/(s^2·kJ) or ft^4/(s^2·Btu)]

c specific heat of detector element [Btu/(lbm·R) or kJ/(kg·K)]

C_p specific heat of air [Btu/(lbm·R) or kJ/(kg·K)]

d diameter of sphere or cylinder (m or ft)

D $0.188 + 0.313\, r/H$

Δt change in time (s)

ΔT increase above ambient in temperature of gas surrounding a detector (°C or °F)

ΔT_d increase above ambient in temperature of a detector (°C or °F)

ΔT_p^* change in reduced gas temperature

f functional relationship

g functional relationship

g gravitational constant (m/s^2 or ft/s^2)

h_c convective heat transfer coefficient [kW/(m^2·°C) or Btu/(ft^2·s·°F)]

H ceiling height or height above fire (m or ft)

ΔH_c heat of combustion (kJ/mol)

H_f heat of formation (kJ/mol)

L_P sound pressure level

L_W sound power level

m mass (lbm or kg)

p positive exponent

$\dot{q}$ heat release rate (Btu/s or kW)

$\dot{q}_{cond}$ heat transferred by conduction (Btu/s or kW)

$\dot{q}_{conv}$ heat transferred by convection (Btu/s or kW)

$\dot{q}_{rad}$ heat transferred by radiation (Btu/s or kW)

$\dot{q}_{total}$ total heat transfer (Btu/s or kW)

$\dot{Q}$ heat release rate (Btu/s or kW)

$\dot{Q}_{cr}$ critical heat release rate

$\dot{Q}_{do}$ design heat release rate

$\dot{Q}_i$ ideal heat release rate

$\dot{Q}_p$ predicted heat release rate (Btu/s or kW)

$\dot{Q}_T$ threshold heat release rate at response (Btu/s or kW)

r radial distance from fire plume axis (m or ft)

ρ_0 density of ambient air (kg/m^3 or lb/ft^3)

Re   Reynolds number

RTI   response time index (m$^{1/2}$·s$^{1/2}$ or ft$^{1/2}$·s$^{1/2}$)

S spacing of detectors or sprinkler heads (m or ft)

t time (s)

t_c critical time—time at which fire would reach a heat release rate of 1000 Btu/s (1055 kW) (s)

t_r response time (s)

t_v virtual time of origin (s)

t_{2f} arrival time of heat front (for $p = 2$ power-law fire) at a point r/H (s)

t_{2f}^* reduced arrival time of heat front (for $p = 2$ power-law fire) at a point r/H (s)

t_p^* reduced time

T temperature (°C or °F)

T_a ambient temperature (°C or °F)

T_d detector temperature (°C or °F)

T_g temperature of fire gases (°C or °F)

T_s rated operating temperature of a detector or sprinkler (°C or °F)

U velocity (m/s)

u instantaneous velocity of fire gases (m/s or ft/s)

u_0 velocity at which τ_0 was measured (m/s or ft/s)

u_p^* reduced gas velocity

v kinematic viscosity (m^2/s or ft^2/s)

x vectorial observation point (m or ft)

Y defined in Equation 27

τ detector time constant—$mc/(hA)$ (s)

τ_0 measured at reference velocity u_0 (s)

References Cited

1. C. Mulliss and W. Lee, "On the Standard Rounding Rule for Multiplication and Division," *Chinese Journal of Physics,* 36, 3, pp. 479–487 (1998).

2. W. Lee, C. Mulliss, and H.-C. Chiu, "On the Standard Rounding Rule for Addition and Subtraction," *Chinese Journal of Physics,* 38, 1, pp. 36–41 (2000).

3. R. Custer, "Selection and Specification of the 'Design Fire' for Performance-Based Fire Protection Design," in *Proceedings, SFPE Engineering Seminar,* Phoenix, AZ, Society of Fire Protection Engineers, Boston (1993).

4. R. Custer, B. Meacham, and C. Wood, "Performance-Based Design Techniques for Detection and Special Suppression Applications," in *Proceedings of the SFPE Engineering Seminars on Advances in Detection and Suppression Technology,* San Francisco, Society of Fire Protection Engineers, Boston (1994).

5. SFPE Engineering Guide to Performance-Based Fire Protection. Society of Fire Protection Engineers. Published by National Fire Protection Association, Quincy, MA (2000).

6. R. Custer and R. Bright, "Fire Detection: The State-of-the-Art," *NBS Tech. Note 839,* National Bureau of Standards, Washington, DC (1974).

7. UL 521, *Standard for Safety Heat Detectors for Fire Protective Signaling Systems,* Underwriters Laboratories Inc., Northbrook, IL (1993).

8. NFPA 72, *National Fire Alarm Code,* NFPA, Quincy, MA (1999).

9. G. Heskestad and H. Smith, *FMRC Serial Number 22485,* Factory Mutual Research Corp., Norwood, MA (1976).

10. J.P. Hollman, *Heat Transfer,* McGraw-Hill, New York (1976).

11. W. Bissell, "An Investigation into the Use of the Factory Mutual Plunge Tunnel and the Resulting RTI for Fixed Temperature Fire Detectors," Master's Thesis, Worcester Polytechnic Institute, Worcester, MA (1988).

12. M. Kokkala, "Thermal Properties of Heat Detectors and Sprinklers," *Nordtest Brand Symposium,* Boras, Sweden (1986).

13. R.P. Schifiliti and W.E. Pucci, "Fire Detection Modeling: State of the Art," The Fire Detection Institute, Bloomfield, CT (1996).

14. "Discussion of a New Principle in Fire Detection, Rate Compensation," Fenwal, Inc., Ashland, MA (1951).

15. C. E. Marrion, "Lag Time Modeling and Effects of Ceiling Jet Velocity on the Placement of Optical Smoke Detectors," Master's Thesis, Worcester Polytechnic Institute, Center for Firesafety Studies, Worcester, MA (1989).

16. R. Alpert, *Fire Tech.,* 8, p. 3 (1972).

17. L.Y. Cooper, "Interaction of an Isolated Sprinkler and a Two Layer Compartment Fire Environment," National Institute of Standards and Technology, Gaithersburg, MD (1991).

18. M. Delichatsios and R. L. Alpert, "Calculated Interaction of Water Droplet Sprays with Fire Plumes in Compartments," *NBS-GCR 86-520,* Center for Fire Research, National Bureau of Standards, Washington, DC (1986).

19. G. Heskestad, "Sprinkler/Hot Layer Interaction," *NIST-GCR 91-590,* National Institute of Standards and Technology, Gaithersburg, MD (1991).

20. D.D. Evans and D.W. Stroup, "Methods to Calculate the Response Time of Heat and Smoke Detectors Installed Below Large Unobstructed Ceilings," *NBSIR 85-3167,* National Bureau of Standards, Gaithersburg, MD (1985).

21. G. Heskestad and M.A. Delichatsios, "The Initial Convective Flow in Fire," *17th Symposium on Combustion,* Combustion Institute, Pittsburgh, PA (1978).

22. G. Heskestad and M.A. Delichatsios, "Environments of Fire Detectors—Phase I: Effect of Fire Size, Ceiling Height, and Material," Volume I: "Measurements" (NBS-GCR-77-86), (1977), Volume II: "Analysis" (NBS-GCR-77-95), National Technical Information Service (NTIS), Springfield, VA (1977).

23. R.P. Schifiliti, "Use of Fire Plume Theory in the Design and Analysis of Fire Detector and Sprinkler Response," Master's Thesis, Worcester Polytechnic Institute, Center for Firesafety Studies, Worcester, MA (1986).

24. D.W. Stroup, D.D. Evans, and P. Martin, *NBS Special Publication 712,* National Bureau of Standards, Gaithersburg, MD (1986).

25. *SFPE Handbook of Fire Protection Engineering,* NFPA, Quincy, MA (1988 and 1995).

26. NFPA 72, *National Fire Alarm Code,* NFPA, Quincy, MA, 1984 through 1996 editions.

27. G. Heskestad and M. Delichatsios, "Update: The Initial Convective Flow in Fire," *Fire Safety Journal,* 15, pp. 471–475 (1989).

28. C. Beyler, personal communication (1985).

29. C. Beyler, "A Design Method for Flaming Fire Detection," *Fire Technology,* 20, 4, pp. 9–16 (1984).

30. J.R. Lawson, W.D. Walton, and W.H. Twilley, *NBSIR 83-2787,* National Bureau of Standards, Washington, DC (1983).

31. B.J. Meacham, "Characterization of Smoke from Burning Materials for the Evaluation of Light Scattering-Type Smoke Detector Response," Master's Thesis, Worcester Polytechnic Institute, Center for Firesafety Studies, Worcester, MA (1991).

32. B.J. Meacham and V. Motevalli, "Characterization of Smoke from Smoldering Combustion for the Evaluation of Light Scattering-Type Smoke Detector Response," *J. of Fire Protection Engineering, SFPE,* 4, 1, p. 17 (1992).

33. UL 268, *Standard for Safety Smoke Detectors for Fire Protective Signaling Systems,* Underwriters Laboratories, Inc., Northbrook, IL (1989).

34. G. Mulholland, "Smoke Production and Properties," *SFPE Handbook of Fire Protection Engineering,* 2nd ed., Quincy, MA (1995).

35. J. Hoseman, "Uber Verfahren zur Bestimmung der Korngrossenverteilung Hokkonzentrierter Polydispersionen von MiePartikeln," Ph.D. Thesis, Aachen, Germany (1970).

36. C.D. Litton, "A Mathematical Model for Ionization Type Smoke Detectors and the Reduced Source Approximation," *Fire Technology,* 13, 4, pp. 266–281 (1977).

37. R.W. Bukowski and G.W. Mulholland, "Smoke Detector Design and Smoke Properties," TN 973, U.S. Department of Commerce, National Bureau of Standards, Washington, DC (1978).

38. C. Helsper, H. Fissan, J. Muggli, and A. Scheidweiler, "Verification of Ionization Chamber Theory," *Fire Technology,* 19, 1, p. 14 (1983).

39. J. Newman, "Modified Theory for the Characterization of Ionization Smoke Detectors," in *Fire Safety Science—Proceedings of the Fourth International Symposium,* International Association for Fire Safety Science, Ottawa, Ontario (1994).

40. G. Heskestad, "Generalized Characteristics of Smoke Entry and Response for Products-of-Combustion Detectors," in *Proceedings, 7th International Conference on Problems of Automatic Fire Detection,* Rheinisch-Westfalischen Technischen Hochschule, Aachen, Germany (1975).

41. M. Kokkala et al., "Measurements of the Characteristic Lengths of Smoke Detectors," *Fire Technology,* 28, 2, p. 99 (1992).

42. J. Bjorkman, O. Huttunen, and M. Kokkala, "Paloilmaisimien toimintaa kuvaavat laskentamallit (Calculation Models for Fire Detector Response)," *Research Notes 1036,* Technical Research Center of Finland (1989).

43. A. Oldweiler, "Investigation of the Smoke Detector L Number in the UL Smoke Box," Master's Thesis, Worcester Polytechnic Institute, Worcester, MA (1995).

44. M.A. Delichatsios, "Categorization of Cable Flammability, Detection of Smoldering, and Flaming Cable Fires," Interim Report, Factory Mutual Research Corporation, Norwood, MA (1980).

45. NFPA 92B, *Guide for Smoke Management Systems in Malls, Atria, and Large Areas,* NFPA, Quincy, MA (1991).

46. G. Heskestad, *FMRC Serial Number 21017,* Factory Mutual Research Corp., Norwood, MA (1974).

47. E.L. Brozovsky, "A Preliminary Approach to Siting Smoke Detectors Based on Design Fire Size and Detector Aerosol Entry Lag Time," Master's Thesis, Worcester Polytechnic Institute, Center for Firesafety Studies, Worcester, MA (1991).

48. S. Deal, "Technical Reference Guide for FPEtool Version 3.2," *NISTIR 5486,* National Institute for Standards and Technology, Gaithersburg, MD (1994).

49. G. Heskestad and M.A. Delichatsios, "Environments of Fire Detectors, Phase I: Effects of Fire Size, Ceiling Heights, and Material," Volume II, *Analysis Technical Report Serial Number 11427,* RC-T-11, Factory Mutual Research Corp., Norwood, MA (1977).

50. K.B. Ginn, *Architectural Acoustics,* Bruel and Kjaer (1978).

51. H. Butler, A. Bowyer, and J. Kew, "Locating Fire Alarm Sounders for Audibility," Building Services Research and Information Association, Bracknell, UK (1981).

52. E.H. Nober, H. Pierce, A. Well, and C.C. Johnson, *NBS-GCR-83-284,* National Bureau of Standards, Washington, DC (1980).

53. M.J. Kahn, "Detection Times to Fire-Related Stimuli by Sleeping Subjects," *NBS-GCR-83-435,* National Bureau of Standards, Washington, DC (1983).

54. *British Standard Code of Practice CP3,* British Standards Institution, London (1972).

55. C. Davis and D. Davis, *Sound System Engineering,* Howard H. Sams and Co., Inc., Indianapolis, IN (1975).

56. *Product Catalog,* Fire Control Instruments, Newton, MA (1986).

57. UL 1971, *Standard for Safety Signaling Devices for the Hearing Impaired,* Underwriters Laboratories, Inc., Northbrook, IL (1992).

58. "Nomenclature and Definitions for Illuminating Engineering," *IES RP-16-1987,* Illuminating Society of North America, New York (1987).

Additional Reading

V. Babrauskas, J.R. Lawson, W.D. Walton, and W.H. Twilley, *NB-SIR 82-2604,* National Bureau of Standards, Washington, DC (1982).

CHAPTER 2

Hydraulics

John J. Titus

Introduction

Hydraulics may be regarded as the application of knowledge about how fluids behave to the solution of practical problems in fluid flow. It is generally held to describe the behavior and effects of water in motion in both closed conduits and open channels. In the field of fire protection we are concerned primarily with the closed conduit flow regime. In this chapter we will restrict our discussion to the behavior and properties of water flowing in pipes as the phenomenon of paramount interest.

Fluid Statics

Physical Properties of Fluids

Solution of any flow problem requires a basic knowledge of the physical properties of the fluid being considered. A brief description of the most basic properties follows.

1. Density:
$$\rho = \frac{m}{V}$$

The density of a fluid is the mass of the fluid per unit volume, expressed in SI units as kg/m^3 and in English, or U.S. customary, units as $slugs/ft^3$ (or $lbf \cdot s^2/ft^4$). The density of water at 4°C (~40°F) is $1000 \ kg/m^3$ ($1.94 \ lbf \cdot s/ft^4$).

2. Specific weight:
$$\gamma = \rho g$$

As the representation of the force exerted by gravity on a unit volume of fluid, specific weight takes on units of weight per unit volume. At 4°C, the specific weight of water is $9.81 \ kN/m^3$ ($62.4 \ lb/ft^3$).[1]

John J. Titus, P.E., is a former research associate at the Center for Fire-safety Studies at Worcester Polytechnic Institute, Worcester, Massachusetts. He has been active in engineering design and contracting of fire suppression and detection systems since 1971. Mr. Titus is a partner in MBS Fire Technology, Inc., a fire protection engineering consulting firm based in central Massachusetts.

3. Specific gravity (relative density): Specific gravity is the ratio of a liquid's density or specific weight to that of water at 4°C.

4. Viscosity: The term *viscosity* refers to a proportionality constant in the equation relating cross-sectional velocity variations (or rate of fluid deformation) to shear stresses developed in the fluid flow. (See the section of this chapter titled "Fluid Energy Losses in Pipe Flows.") Viscosity can be considered a measure of a fluid's resistance to deformation or shear or, alternatively, its readiness to flow when acted upon by an external force. In engineering analyses it is useful to think of viscosity as a momentum diffusivity term.

Viscosity is commonly expressed in one of two forms: absolute (or dynamic) viscosity, μ, which is the proportionality constant referred to above, or kinematic viscosity, ν, which is related to the absolute viscosity by the equality

$$\nu = \frac{\mu}{\rho}$$

A wide variety of units is used to express viscosity, depending not only on U.S. customary or SI formulations but also on older English and metric conventions as well as on the type of instrument used to measure this fluid property. A unit based on the c.g.s. (centimeter, gram, second) convention of the old metric system has gained wide favor in the representation of absolute viscosity. This unit, called the *poise,* has dimensions of dyne·seconds per square centimeter or grams per centimeter·second. The centipoise, which equals 0.01 poise, is the form of preference since the viscosity of water at 20°C (68°F) equals one centipoise to a very close approximation. In the English system the unit of viscosity is pound-seconds per square foot. One $lb \cdot s/ft^2$ equals 478.8 poise.

5. Fluid pressure: Pressure is a force per unit area that arises when a fluid is subjected to a compressive stress. Units may be $Newtons/m^2$, lb/ft^2, $lb/in.^2$, or the equiva-

lent. Pascal's law states that the pressure in a fluid at rest is the same in all directions, a condition different from that for a stressed solid where the stress on a plane depends upon the orientation of that plane. For an infinitesimal fluid element in a larger static body of fluid, a free body diagram of the vertical forces may be drawn as in Figure 4-2.1. The pressure difference $[(p + dp) - p]$ is due only to the weight of the fluid element. Since the weight of the element is given by $mg = \rho g\, dz\, dA$, a summing of forces in the vertical direction gives

$$dp\, dA = -\rho g\, dz\, dA \tag{1a}$$

$$dp = -\rho g\, dz \tag{1b}$$

In integral form, Equation 1b becomes

$$\int_1^2 \frac{dp}{\rho g} = -\int_1^2 dz = -(z_2 - z_1) \tag{2}$$

where the path endpoints 1 and 2 refer to different elevation levels.

To integrate Equation 2, it is necessary to establish a functional relation between pressure p and the term ρg. Where density varies with pressure, the fluid is considered compressible, and the functional relation may be complex. For fluids that may be considered incompressible, such as water, ρ is a constant at any specified temperature. Equation 2 then becomes

$$p_2 - p_1 = -\rho g(z_2 - z_1) \tag{3}$$

The term $(z_2 - z_1)$ may be called a static *pressure head,* which can be expressed in feet, inches, or meters of water, or some height unit of any liquid. A simplified form of Equation 3 is often written

$$\rho = \gamma h \tag{4}$$

where h = elevation of the column of liquid above a reference surface (i.e., $z_2 - z_1$). For water at 60°F (15.6°C), γ is taken equal to 62.4 lb/ft³ (16.02 kg/m³). The pressure corresponding to a head of h feet, then, is 0.433h lb/in.² (psi), or approximately 3 kPa per meter elevation. The head corresponding to a pressure of one psi (0.07 bar) is, inversely, 2.3 ft (0.7 m). Note that Equation 4 is valid only for a homogeneous, noncompressible fluid at rest, and that regardless of the shape of the container, points in the same horizontal plane experience the same pressure.

The vertical distance h is termed the *head* of a fluid. A pressure due only to the weight of a column of fluid is called a static pressure and can be measured by a standard Bourdon-type gage (see Figure 4-2.4). Such a measure is generally referred to as gage pressure. The term *absolute pressure* takes into account the pressure exerted by the atmosphere as well, which at sea level is approximately 14.7 psi (1 bar), equivalent to a 33.9-ft- (10.3-m-) high column of water. A pressure less than atmospheric is called a vacuum pressure, a perfect vacuum being zero absolute pressure. Since most fluid properties of interest are not significantly affected by small changes in atmospheric pressure, most fluids calculations are in terms of gage pressure, although this fact is not often indicated in standard calculation nomenclature. When they are explicitly identified, gage pressure is denoted by the term psig and absolute pressure by psia. If not stated otherwise, psi may be taken to designate gage pressure.

Pressure Measuring Devices

1. Manometer tube: Pressure measurement in a manometer tube is obtained by measuring the vertical displacement of a relatively heavy fluid (usually mercury), which will rise a smaller vertical distance than water in proportion to the ratio of its specific weight to that of water. Depending on the actual arrangement of the manometer tubing, a gage equation can be written to solve for the pressure head. For the manometer shown in Figure 4-2.2, the gage equation is written by proceeding from the open
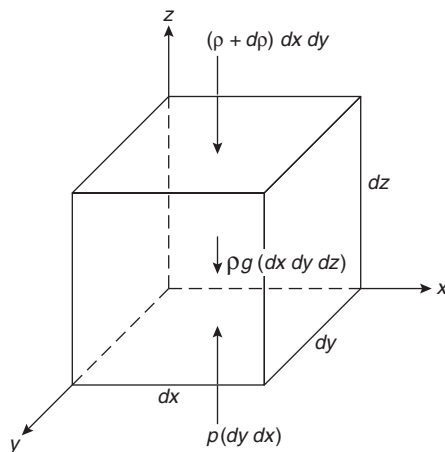

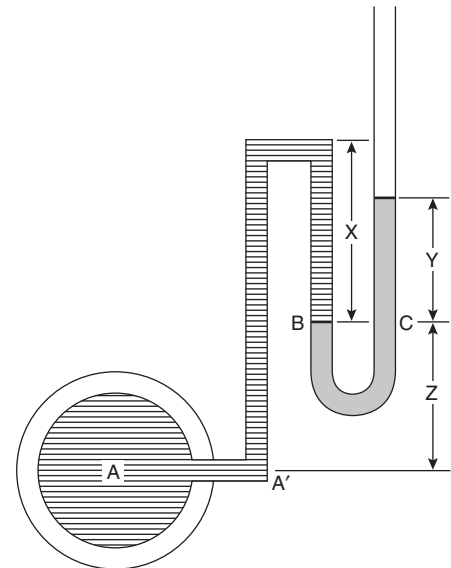**Figure 4-2.1.** *Notation for basic equation of fluid statics.*

Figure 4-2.2. *Manometer.*

end through the tube to point A', adding terms when descending a column and subtracting when ascending. Using mercury as the manometer fluid, we can write

$$(y + z)\gamma_{Hg} - z\gamma_{Hg} - x\gamma + (x + z)\gamma = p_A \qquad (5)$$

Combining terms, generalizing the result, and expressing in terms of feet of water (head),

$$\frac{P_A}{\gamma} = ys + z \qquad (6)$$

where s is the specific gravity of the manometer fluid.

2. Piezometer tube (Figure 4-2.3): Literally a *pressure measuring tube*, a piezometer consists essentially of a narrow tube rising from a container enclosing a fluid under pressure. Through the relation among pressure, height, and specific weight, the height to which the fluid rises in the tube represents the pressure of the contained fluid. While useful for some laboratory work, piezometer tubes are not generally feasible in practical applications.

3. Bourdon gauge (Figure 4-2.4): The standard pressure measuring device used in a wide variety of fluid pressure measurement applications is the Bourdon gauge. The gauge contains a curved tube of elliptical cross section that undergoes a change in curvature with change in pressure. A dial hand, connected to the inner tube through a linkage system, indicates gauge pressure on a numerical dial face. Bourdon gauges are factory calibrated and reasonably accurate instruments if not damaged by pressure surge or impact force. A field reading, unless known to be correct, cannot be assumed to be accurate and should be checked by independent means.

Forces on Submerged Plane Areas
Due to Fluid Pressure

It is sometimes of interest to determine the magnitude of the resultant force on a submerged area and the location of the center of pressure where the resultant force
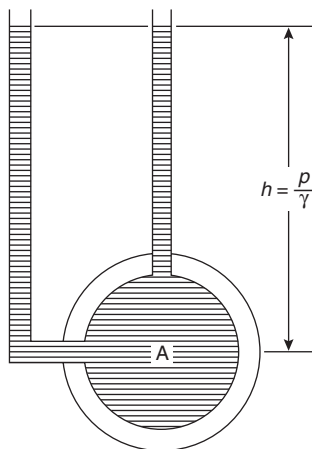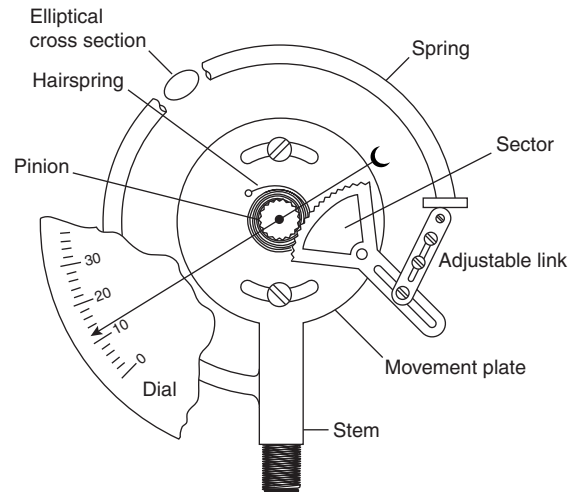

Figure 4-2.4.   *Standard Bourdon gauge.*

can be assumed to act. Consider the following example of a tank that has a rectangular window in an inclined wall (Figure 4-2.5). The magnitude of the resultant force can be determined from

$$F_R = \gamma h_c A \qquad (7)$$

The center of pressure of the area is the point at which the resultant force can be considered to act. Its location is determined from the relation

$$l_p = l_c + \frac{I}{l_c A} \qquad (8)$$

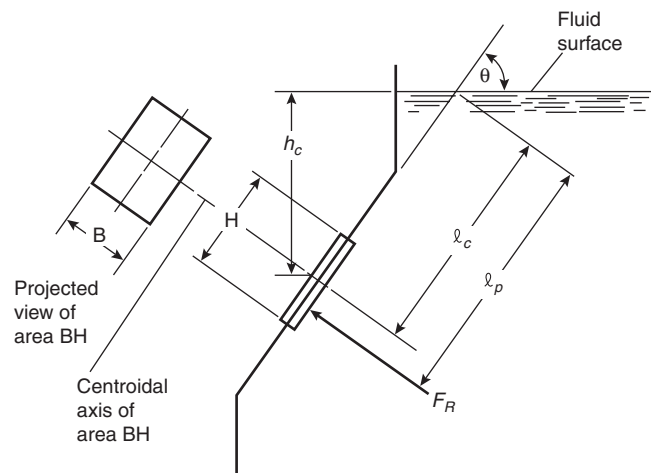where I = the moment of inertia of the area about its centroidal axis.

Figure 4-2.3.   *Piezometer.*

Figure 4-2.5.   *Tank with a rectanglar window in an inclined wall.*

For a vertical wall, the center of pressure is located at a distance $d/3$ from the bottom (where d is the total depth below the free surface), and at a distance $l/3$ from the bottom of an inclined wall or area (where l is the length of the face of the wall).

Conservation Laws in Fluid Flows

Fluid flow may be characterized as uniform or nonuniform, steady or unsteady, compressible or incompressible, laminar or turbulent, rotational or irrotational, and one-, two-, or three-dimensional or some combination thereof. Real flows may be modeled as approximations of ideal flows when real properties do not depart significantly from the ideal characteristics defined by these terms.

For example, uniform flow occurs when the average velocity of a fluid does not change in either magnitude or direction anywhere along the flow path. Thus, liquid flow in a constant head pipeline of unchanging diameter is considered uniform flow. Steady flow, on the other hand, is determined with reference to a stationary point in the flow path. For steady flow to occur, the velocity of flow at that point must remain constant with time. This condition implies that the fluid density, the pressure head, and the volume rate of flow also are invariant with time. Thus, liquid flow in a constant head pipeline of varying diameter may be considered steady, nonuniform flow. It is important to note that a flow may be considered uniform (no change in magnitude or direction of the velocity) in a curved pipeline as long as the reference direction of the velocity vector is taken in the direction of the flow. We can then say that the velocity of the fluid does not change direction with respect to its enclosing boundaries.

We can also consider this flow one-dimensional whenever it is permissible to say that velocities or accelerations normal to the general direction of the flow are negligible. Clearly, real flow in a real-world structure has three dimensions, but a one-dimensional analysis is highly desirable as it represents a considerable mathematical simplification. Fortunately, a very large number of practical engineering flow problems involving water can be modeled as one-dimensional, steady flow problems, particularly many pipeline flows. In such cases it is possible to apply basic physical principles of conservation of mass and conservation of energy in the direction of flow to obtain the energy balance at any point in the flow. In fire flow hydraulics, it is common practice to introduce additional simplifying assumptions, such as the requirements that the fluid be incompressible and that flow properties be invariant with temperature and pressure. It then follows directly that with no flow additions or subtractions, the volumetric flow rate at any point in a fluid stream must be a constant. This statement of mass conservation, known as the equation of continuity, can be expressed mathematically as

$$\rho_1 A_1 v_1 = \rho_2 A_2 v_2 = \text{constant} \qquad (9)$$

If the fluid is considered incompressible, as is the case with water, Equation 9 becomes

$$A_1 v_1 = A_2 v_2 = \text{constant} = Q \qquad (9a)$$

By applying the principal of conservation of energy to a flowing fluid, an expression can be derived that gives the theoretical net energy balance of the fluid at any point along its flow path. This is known as the Bernoulli equation, which can be written as

$$\frac{p_1}{\gamma} + \frac{v_1^2}{2g} + z_1 = \frac{p_2}{\gamma} + \frac{v_2^2}{2g} + z_2 \qquad (10)$$

In this form, units are ft lb/lb of fluid or, simply, ft of fluid. Each term thus represents a fluid head. Multiplying each term by the specific weight, γ, converts the equation to units of pressure. Changes in internal energy of the fluid are ignored and are assumed to be negligible. The form of Equation 10 suggests that the flow of liquid (or transport of fluid energy) results from three principal causes: pressure difference, gravity, and inertia. Equation 10 expresses an ideal condition fulfilled by the three components of head corresponding to these three causes. The assumption of incompressibility (i.e., constant density) requires that the product of the velocity of flow and the cross-sectional area of the flow of any conserved portion of the stream be constant; the ideal flow streamlines, therefore, converge as the velocity increases and diverge as the velocity decreases. If it could be assumed that the total Bernoulli head were, indeed, constant or, equivalently, if it were possible to obtain total head simply as a function of the coordinates of the moving fluid element, then many hydrokinetic problems could be solved theoretically by mathematically manipulating and extrapolating the Bernoulli equation. Unfortunately, this is not the case. Other energy transfers are possible, and these require use of a more general form of the equation. In addition to the pressure, velocity, and position (elevation) energies possessed by the fluid at sections 1 and 2, energy may be added to the fluid (work done on the fluid by a pump), lost by the fluid (through friction), or extracted from the fluid (work done by the fluid). Therefore, we write the Bernoulli energy conservation expression in the more general form

$$\left(\frac{p_1}{\gamma} + \frac{v_1^2}{2g} + z_1 \right) + h_A - h_L - h_E = \left(\frac{p_2}{\gamma} + \frac{v_2^2}{2g} + z_2 \right) \qquad (10a)$$

| Energy at Section 1 | Energy Added | Energy Lost | Energy Extracted | Energy at Section 2 |

EXAMPLE 1:

Water flows from a reservoir through a pipeline as shown in the following diagram. The flow is considered frictionless and discharges freely at point *C*.
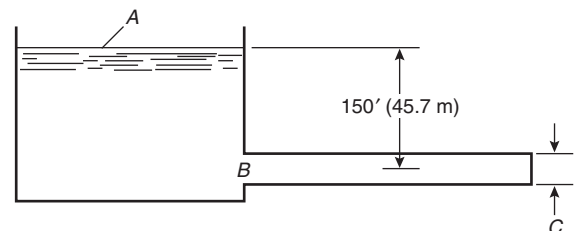
(a) What is the total head (total specific energy) at point *B*?

(b) What is the discharge velocity at point *C*?

SOLUTION:

(a) At *A*, both the velocity and gage pressures are considered to be zero. By Bernoulli, then, the total head would be written as

$$h_A = 0 + 0 + 150 \text{ ft} = 150 \text{ ft}$$

or, in SI unit equivalents,

$$h_A = 0 + 0 + 45.7 \text{ m} = 45.7 \text{ m}$$

At *B*, the fluid has a nonzero velocity head and is under hydrostatic pressure. As long as we consider the flow frictionless, the total head is constant. Therefore,

$$h_B = h_A = 150 \text{ ft} \ (45.7 \text{ m})$$

(b) At *C*, the pressure head is again zero, since the discharge is at atmospheric pressure. Once more by Bernoulli,

$$h_C = 0 + \frac{v^2}{2g} + 0$$

$$v^2 = 2(32.2)(150)$$

$$v = 98.3 \text{ ft/s}$$

or, in SI unit equivalents,

$$v^2 = 2(9.81)(45.7)$$

$$v = 29.9 \text{ m/s}$$

Note that we could calculate the actual values of the pressure and velocity heads at point *B* if we had more information about the system. For example, we could determine $\dot{Q}$, the discharge at point *C*, knowing the area and type of discharge opening (see the section of this chapter titled "Free Discharge at an Opening"). This determination is simply an application of the continuity equation. Knowing the pipeline diameter at point *B* allows us to apply continuity constraints once again to calculate v_B from which the velocity head may be determined. The pressure head at *B* is simply a function of the weight of the vertical column of water.

The components of the Bernoulli equation may be expressed graphically in terms of energy levels existing at any points in the flow regime. In Figure 4-2.6 a simple system representing a realistic flow is shown. Water flows from a reservoir (with presumed constant surface elevation) to atmosphere. The flow is accompanied by losses of energy represented by h_L. The losses may occur in many places such as at valves, bends, and sudden changes in pipe diameter. Generally, the most important loss is that due to friction between the moving fluid and the pipe wall. Since there are always energy losses in real flows, the total energy of the system decreases in the direction of flow. The line connecting all points representing the total energy is called the *energy gradient* (EG). It must always decrease in the direction of flow unless energy is added to the system, such as by a pump. The *hydraulic gradient* (HG) connects the points representing the sum of static pressure and elevation energies (i.e., the heights to which water in piezometer tubes would rise). Note that the hydraulic gradient may increase in the direction of flow if velocity head is converted to pressure head at any point (such as at an increase in pipe diameter). Thus, the relationship between the energy and hydraulic gradients can be written as

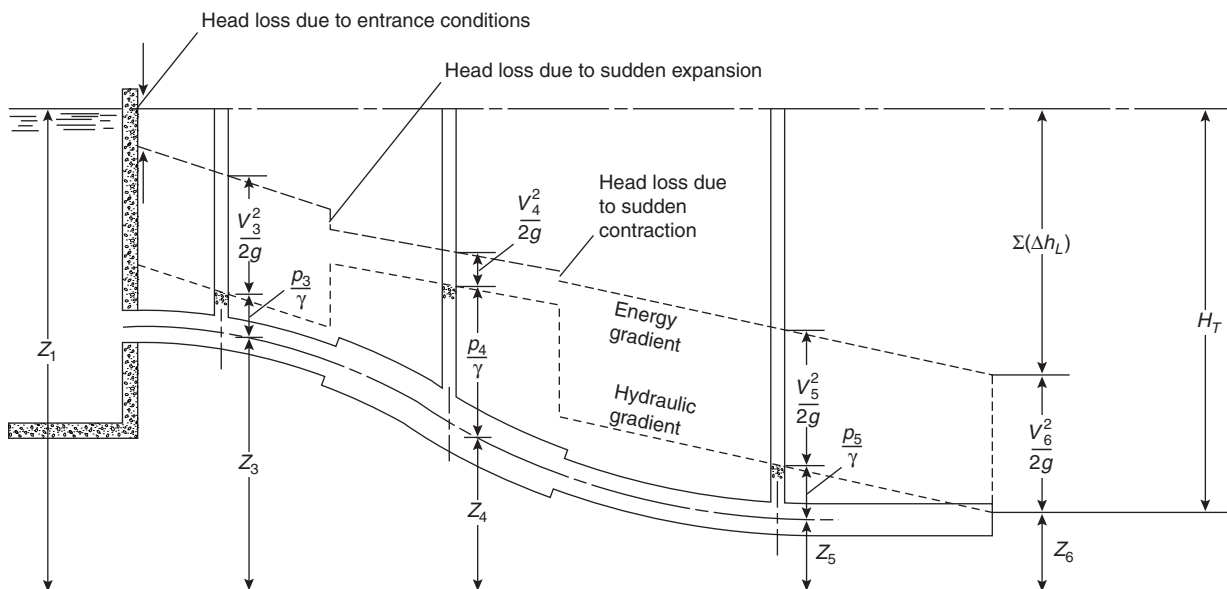$$\text{EG} = \text{HG} + \frac{v^2}{2g} \tag{11}$$

Figure 4-2.6.   *Realistic flow characteristics.*

Fluid Energy Losses in Pipe Flows

General Considerations

That part of hydraulics which treats fluid energy losses due to friction in piping is well known and well utilized in fire protection engineering. Losses to friction are due to shear stresses set up within a moving fluid in a conduit by an imposed pressure gradient. Flow driven by the pressure force is restrained by drag forces acting at the conduit wall. To better visualize this phenomenon, it is useful to introduce the concept of the boundary layer. For many fluids, such as air or water, motion through a stationary conduit or pipe is characterized in most practical situations by a nearly constant velocity cross section everywhere except in a very thin layer near the wall of the pipe. This layer thickness may be as little as 0.1 mm but may vary significantly with the nature of the fluid, the velocity of flow, and the surface roughness of the conduit. We may visualize boundary layer flow (see Figure 4-2.7) in terms of a velocity profile. Theory* holds that a very thin (molecular) layer of fluid sticks to the conduit wall. The tendency of the next fluid layer to move due to an imposed force creates a shearing stress, τ, between the layers. If the boundary is thought of as many fluid lamina sliding on each other, then we can expect the velocities of these lamina to increase with distance y from the wall until, at the edge of the boundary layer, the local velocity reaches the free-stream velocity of the fluid. The factor relating the velocity profile to the developed stress in the fluid is termed the fluid viscosity. The relationship was expressed mathematically by Newton as

$$\tau = \mu \frac{du}{dy} \tag{12}$$

The smaller the value of fluid viscosity, the thinner the boundary layer will be. The first layer of fluid sticks or adheres to the surface of the conduit while lamina above it successively slide on each other, exerting drag forces that, for most fluids, are proportional to the viscosity (so-called Newtonian fluids). The rate of change of the velocity between successive lamina is a measure of the unit shearing force between them. A curve joining the tips of velocity vectors plotted for the different lamina in the boundary layer is called a velocity profile. Laminar (smooth, streamline) flow [see Figure 4-2.8(a)] is characterized by a parabolic velocity profile with maximum velocity attained at the theoretical centerline of the flow. Turbulent flow, by contrast, is rough (nonstreamline) flow [see Figure 4-2.8(b)], characterized by an essentially uniform average velocity across the flow section, with only a very thin boundary layer close to the wall where viscous forces predominate. The velocities associated with laminar flows are generally so low as to be impracticable from a design standpoint. Most flows of interest, therefore, are turbulent, and the use of an assumed uniform or average velocity to calculate kinetic energy and velocity pressures
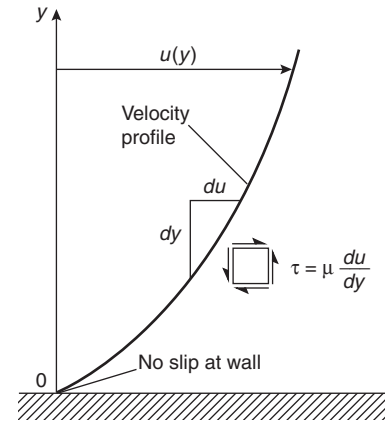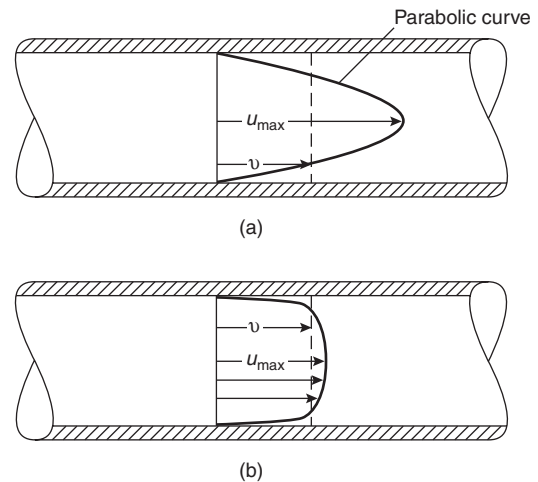

Figure 4-2.7.   *Velocity profile.*

Figure 4-2.8.   *Laminar (a) and turbulent (b) pipe flow velocity profiles for the same volume.*

does not introduce significant error. In those atypical situations where relatively large velocity heads are involved (such as where a pump adds a large amount of energy), a correction factor may be used to relate the actual average kinetic energy to the kinetic energy calculated using average velocity. From continuity considerations,

$$\text{KE} = \int_A \rho u^3 \, dA = \alpha \rho \int_A v^3 \, dA \tag{13}$$

where

KE = true kinetic energy of the flow

v = average velocity of flow

α = kinetic energy correction factor

For incompressible fluids

$$\alpha = \frac{1}{A} \int_A \left(\frac{u}{v}\right)^3 \, dA \tag{14}$$

---

*Early theoretical development of the boundary layer concept is due primarily to Prandtl.[2,3]

and has the value of approximately 1.1 for most turbulent flow problems. Since the velocity head in water distribution piping is small, this correction factor is usually ignored.

While the development of boundary layer theory and the theory of viscous forces has led to an improved theoretical understanding of the mechanics of pipe flows, most flows of interest in fire protection cannot be fully analyzed from theoretical considerations alone. Fire protection flows are almost always turbulent flows. Despite a great expenditure of effort to develop a general predictive theory of turbulent flow phenomena, a fully descriptive theory does not yet exist. While it is postulated that head losses arise because of friction between the fluid and the pipe wall, there is an additional head loss contribution due to turbulence within the fluid. In turbulent flows the rate of head loss, unfortunately, is not simply a function of velocity but depends also on pipe wall roughness. It is further complicated by the changing interaction between these variables at different velocities and roughness element sizes. Within the last century, however, a large body of empirical flow data has been collected, analyzed, and reduced by several investigators. The major features and limits of applicability of the more important results are presented in the following paragraphs.

Fluid Flow Energy Loss Equations

Theoretical development of the physical relationships describing pipe flows dates from about the middle of the nineteenth century, when Chezy postulated a fundamental proportionality between volumetric flow and pipe size based on the continuity equation. His formula is commonly given as

$$Q = \frac{\pi D^2}{4} v = \frac{\pi D^2}{4} \frac{C}{2} \sqrt{DS} \tag{15}$$

and may also be written as

$$S = \left(\frac{8Q}{\pi C}\right)^2 D^{-5} \tag{16}$$

where D and S are pipe diameter and slope of the energy grade line, respectively. The factor C is a proportionality factor incorporating a significant degree of physical uncertainty. Since, by definition

$$S = \frac{h_L}{L}$$

we may write

$$h_L = \left(\frac{8}{\pi C}\right)^2 \frac{L}{D^5} Q^2 \tag{17}$$

as an expression for pipe flow head loss as a function of pipe diameter and discharge. Use of this equation was limited by uncertainties relating to evaluations of the C-factor, which is not, in fact, a constant for a given size conduit or wall condition as was originally thought.

A theoretically more satisfying approach was taken by Darcy, Weisbach, and others. Their formula, which

bears the names of the two primary investigators, is generally written as

$$h_L = f \frac{L}{D} \frac{v^2}{2g} \tag{18}$$

It postulates a basic proportionality between head loss and the kinetic energy of the flow, as well as to pipe length and diameter. The proportionality factor f, known as the friction factor, became the subject of extensive theoretical and experimental investigation. The value of f for laminar flow can be shown theoretically to be a simple linear function of the Reynolds number, Re, where Re = $D_e v \rho / \mu$. The term D_e is the equivalent flow diameter, which is the actual inside diameter of a circular pipe flowing full. The equivalent diameter, D_e, can be found from the hydraulic radius, r_h, which is defined as the area in flow divided by the wetted perimeter. The wetted perimeter does not include the free fluid surface.

$$D_e = 4r_h$$

For Re less than about 2000 (corresponding to low velocity flows or fluids of high viscosity) the relation is

$$f = \frac{64}{Re} \tag{19}$$

In turbulent flows the roughness of the pipe walls becomes a much more significant factor, and a simple expression to determine f is unavailable.

A systematic investigation of the actual characterisitics of piping inner wall surfaces was first performed by Nikuradse in 1933. To simulate varying degrees of roughness in commercial pipes due to corrosion or surface finish, Nikuradse glued sand grains of known sizes to the inside walls of test pipes. The resulting logarithmic plot of friction factor versus Re is shown in Figure 4-2.9. Although the tests are from Nikuradse, the plot is called Stanton's diagram in recognition of his earlier (1914) elucidation of the relation between friction factor and Reynolds number. Note that at sufficiently high Re, the friction factor depends almost entirely on pipe roughness and is essentially independent of Re. In these plots the roughness parameter is expressed as the ratio of the root mean square grain diameter to the pipe diameter. The resulting ratio is termed the relative roughness and is represented mathematically as ε/D. Typical roughnesses of new commercial pipe is shown in Table 4-2.1. Several later investigators developed mathematical formulas for expressing Nikuradse's results. Chief among them were Colebrook, Moody, and VonKarman.

Moody plotted various equations on a graph similar to the earlier work of Stanton. The resulting Moody diagram (Figure 4-2.10) is widely used today in conjunction with the Darcy-Weisbach equation to compute friction losses for water flowing in pipe. Figure 4-2.11 (page 4-53) presents relative roughness values for use with the Moody diagram over a wide range of conditions. Other diagrams have been developed for use with the Darcy-Weisbach equation[4,5] when parameters other than h_L are sought. Essentially, the alternative graphical formulations employ a rearrangement of variables to facilitate solving for some other unknown such as Q or D.
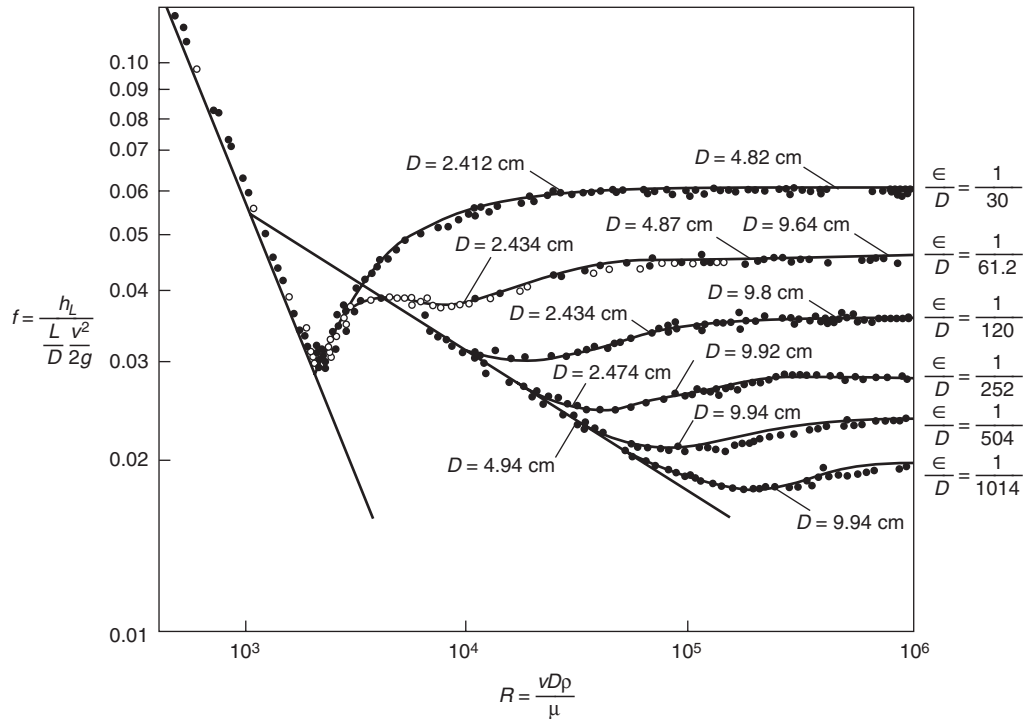
Figure 4-2.9. *Nikuradse's sand-roughened-pipe tests.*

Table 4-2.1 *Values of Absolute Roughness of New Clean Commercial Pipes*

Type of Pipe or Tubing	ε ft (0.3048 m) × 10^6		Probable Maximum Variation of *f* from Design (%)
	Range	Design	
Asphalted cast iron	400	400	−5 to +5
Brass and copper	5	5	−5 to +5
Concrete	1,000–10,000	4,000	−35 to +50
Cast iron	850	850	−10 to +15
Galvanized iron	500	500	0 to +10
Wrought iron	150	150	−5 to +10
Steel	150	150	−5 to +10
Riveted steel	3,000–30,000	6,000	−25 to +75
Wood stave	600–3,000	2,000	−35 to +20

Source: *Pipe Friction Manual, 3d ed.* Hydraulic Institute, *(1961).*

Both experimental and theoretical investigations have yielded uncertain results in the region known as the *critical zone*, wherein the flow changes from laminar to turbulent. Uncertainty may be expected since the transition point is difficult to define precisely and, in fact, varies over a considerable range of Re depending upon the direction of the transition (i.e., flow going from laminar to turbulent or from turbulent to laminar) and the local conditions affecting flow stability. As a practical consideration, however, this uncertainty is of little importance, since most real flows of interest fall well into the turbulent range.

Colebrook developed an empirical transition function for the region between smooth flow and complete turbulence. Flow in this region is sometimes referred to as hydraulically smooth or turbulent smooth. The equation has been presented in various forms, the following expression being commonly used:

$$\frac{1}{\sqrt{f}} = -0.86 \ln\left(\frac{\varepsilon/D}{3.7} + \frac{2.51}{\text{Re}\,\sqrt{f}}\right) \tag{20}$$

An alternate and equivalent expression is

$$f = \left[1.14 - 2\log\left(\frac{\varepsilon}{D} + \frac{9.35}{\text{Re}\sqrt{f}}\right)\right]^{-2} \tag{20a}$$

This relation forms the primary basis for the Moody diagram.

VonKarman used boundary layer theory to derive an expression characterizing the friction factor for fully turbulent flow within rough-walled pipes. The final numerical form of the equation,

$$\frac{1}{\sqrt{f}} = 1.4 + 2\log\frac{D}{\varepsilon} \tag{21}$$

was adjusted to agree more closely with Nikuradse's experimental results. As pipe roughness decreases, this expression approaches Colebrook's equation.

Perhaps the most widely used flow-energy loss relation is the empirically based Hazen-Williams formula, developed near the turn of the century from observations of
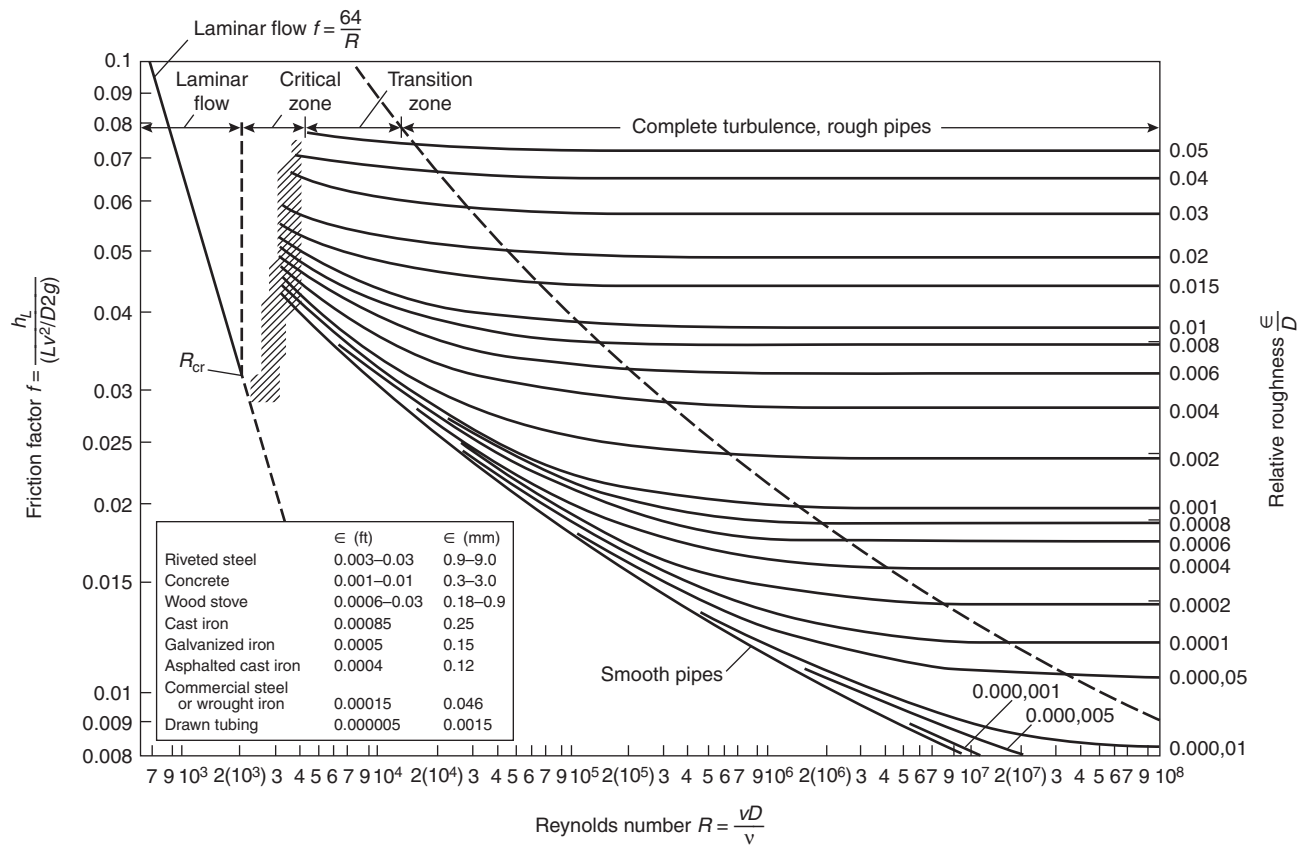
Figure 4-2.10.   *Moody diagram.*

a very large number of pipeline flows. The Hazen-Williams equation was originally written in the form

$$V = 0.113CD^{0.63}S^{0.54} \tag{22}$$

where V is the average velocity in feet per second, S is the slope of the energy grade line—that is, the loss of energy per unit length of the pipe—and D is the actual internal pipe diameter in inches. The coefficient C is a *friction* factor introduced as a constant to represent the roughness of the pipe walls. Table 4-2.2 presents a representative list of C coefficients for various piping materials. Note that the value of C can vary significantly with the piping material, the age of the pipe, and the corrosive qualities of the water.

The Hazen-Williams formula is also encountered in the form

$$Q = 0.285CD^{2.63}S^{0.54} \tag{22a}$$

where Q is volumetric flow rate in gpm and D is in inches. Yet another form, also in the same units for Q and D, is widely used in automatic sprinkler system design. It is arranged to solve for the pressure drop in psi per linear foot of pipe

$$p = \frac{4.52Q^{1.85}}{C^{1.85}D^{4.87}} \tag{22b}$$

In SI units

$$p = \frac{6.05Q^{1.85}}{C^{1.85}D^{4.87}} \times 10^5 \tag{22c}$$

where the units of Q are $L/\min$, D is in mm, and p is in bars per meter of pipe.

Many manufacturers of fire protection equipment, many fire underwriters, and others have published Hazen-Williams-based pipe friction loss data (usually in tabular format) over applicable ranges of pipe sizes, flow rates, and C-factors. A useful calculation aid in a more compact format is the Hazen-Williams nomograph (Figure 4-2.12), which is reproduced here in its generalized form.

The Hazen-Williams formula may be used only for water at or around 60°F (15.6°C), as it does not contain any terms relating to the physical properties of the fluid. The formula does not actually have a sound theoretical basis, but still gives acceptable results in practice with a judicious choice of the C coefficient. Fundamentally, the C-factor is a proportionality constant and, as such, its *true* value depends as much upon the values chosen for the exponents as it does upon actual pipe roughness. The suggested values are the result of curve-fitting exercises and cannot be expected to accurately and evenly represent flow parameter relationships across the full range of
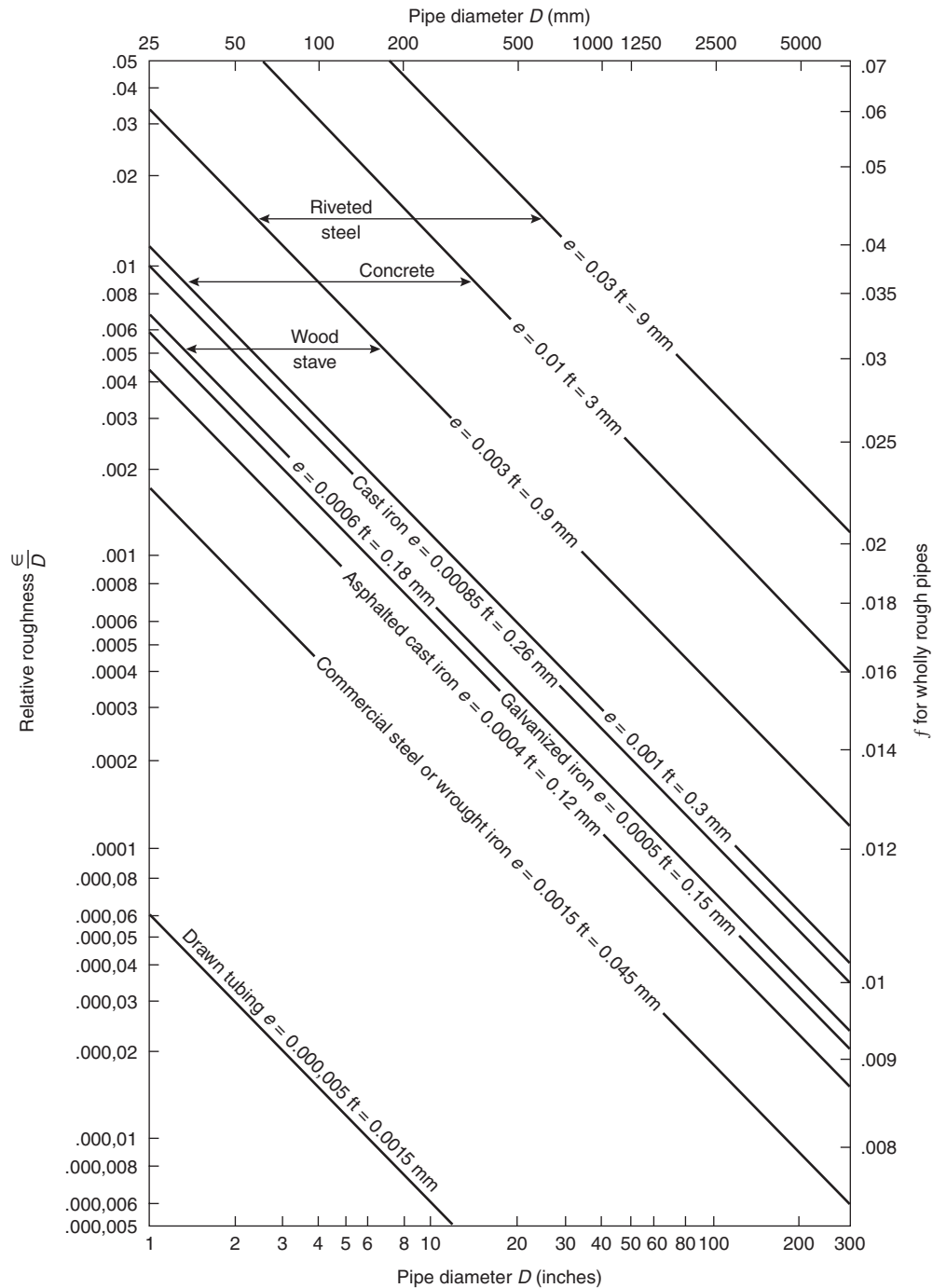
Pipe diameter *D* (mm)

Figure 4-2.11. *Relative roughness chart.*

observed flow velocities. Allowing the desirability of retaining constant exponents for *D* and *S* (i.e., a presumed theoretically stable correlation among all flow parameters in the equation), the value of *C* for any given flow scenario becomes a narrowly bounded variable that reflects the pipe roughness. Although as in the Chezy formula *C* is not actually a constant, for practical use it is assigned a constant value for a given presumed roughness. Unfortunately, as Table 4-2.2 shows, the Hazen-Williams equation is a much better model of smooth pipe flow than of rough pipe flow. As long as the flow velocity is close to that at which *C* was measured and as long as the pipe roughness is not excessive, the Hazen-Williams relation can be expected to give reliable results. It has

Table 4-2.2　Values of C in Hazen-Williams Formula[a]

Type of Pipe	C values for certain pipe diameters					
	2.5 cm (1 in.)	7.6 cm (3 in.)	15.2 cm (6 in.)	30.5 cm (12 in.)	61 cm (24 in.)	122 cm (48 in.)
Uncoated cast iron—smooth and new		121	125	130	132	134
Coated cast iron—smooth and new		129	133	138	140	141
30 years old						
Trend 1—slight attack		100	106	112	117	120
Trend 2—moderate attack		83	90	97	102	107
Trend 3—appreciable attack		59	70	78	83	89
Trend 4—severe attack		41	50	58	66	73
60 years old						
Trend 1—slight attack		90	97	102	107	112
Trend 2—moderate attack		69	79	85	92	96
Trend 3—appreciable attack		49	58	66	72	78
Trend 4—severe attack		30	39	48	56	62
100 years old						
Trend 1—slight attack		81	89	95	100	104
Trend 2—moderate attack		61	70	78	83	89
Trend 3—appreciable attack		40	49	57	64	71
Trend 4—severe attack		21	30	39	46	51
Miscellaneous						
Newly scraped mains		109	116	121	125	127
Newly brushed mains		97	104	108	112	115
Coated spun iron—smooth and new		137	142	145	148	148
Old—take as coated cast iron of same age						
Galvanized iron—smooth and new	120	129	133			
Wrought iron—smooth and new	129	137	142			
Coated steel—smooth and new	129	137	142	145	148	148
Uncoated steel—smooth and new	134	142	145	147	150	150
Coated asbestos-cement—clean		142	149	150	152	
Uncoated asbestos-cement—clean		142	145	147	150	
Spun cement-lined and spun bitumen-lined—clean		147	149	150	152	153
Smooth pipe (including lead, brass, copper, polythene, and smooth PVC)—clean	140	147	149	150	152	153
PVC wavy—clean	134	142	145	147	150	150
Concrete—Scobey						
Class 1—C_s = 0.27; clean		69	79	84	90	95
Class 2—C_s = 0.31; clean		95	102	106	110	113
Class 3—C_s = 0.345; clean		109	116	121	125	127
Class 4—C_s = 0.37; clean		121	125	130	132	134
Best—C_s = 040; clean		129	133	138	140	141
Tate relined pipes—clean		109	116	121	125	127
Prestressed concrete pipes—clean				147	150	150

[a]The above table has been compiled from an examination of 372 records. It is emphasized that the Hazen-Williams formula is not suitable for the coefficient C values appreciably below 100, but the values in the above table are approximately correct at a velocity of 0.9 m/s (3 ft/s).
For other velocities the following approximate corrections should be applied to the values of C in the table above.

Values of C at 0.9 m/s	Velocities below 0.9 m/s for Each Halving, Rehalving of Velocity Relative to 0.9 m/s	Velocities above 0.9 m/s for Each Doubling, Redoubling of Velocity Relative to 0.9 m/s
C below 100	Add 5 percent to C	Subtract 5 percent from C
C from 100 to 130	Add 3 percent to C	Subtract 3 percent from C
C from 130 to 140	Add 1 percent to C	Subtract 1 percent from C
C above 140	Subtract 1 percent from C	Add 1 percent to C

Excerpted from *Journal AWWA*, 73, 5 (1981), by permission. Copyright © 1981, The American Water Works Association.

been noted, however, that in rough pipes head loss varies with flow (and velocity) to the power of 2 rather than the power of 1.85 characteristic of smooth pipes.[6] This observation introduces a significant element of uncertainty into the hydraulic analysis of rough pipe with higher velocity flows.

EXAMPLE 2:
　Water at 50°F (10°C) flows through 4 in. (102 mm) Schedule 40 welded steel pipe at a rate of 500 gpm (1892.7 l/m). Compare the friction head losses calculated by the Darcy-Weisbach and Hazen-Williams equations for flow through 100 ft of pipe.
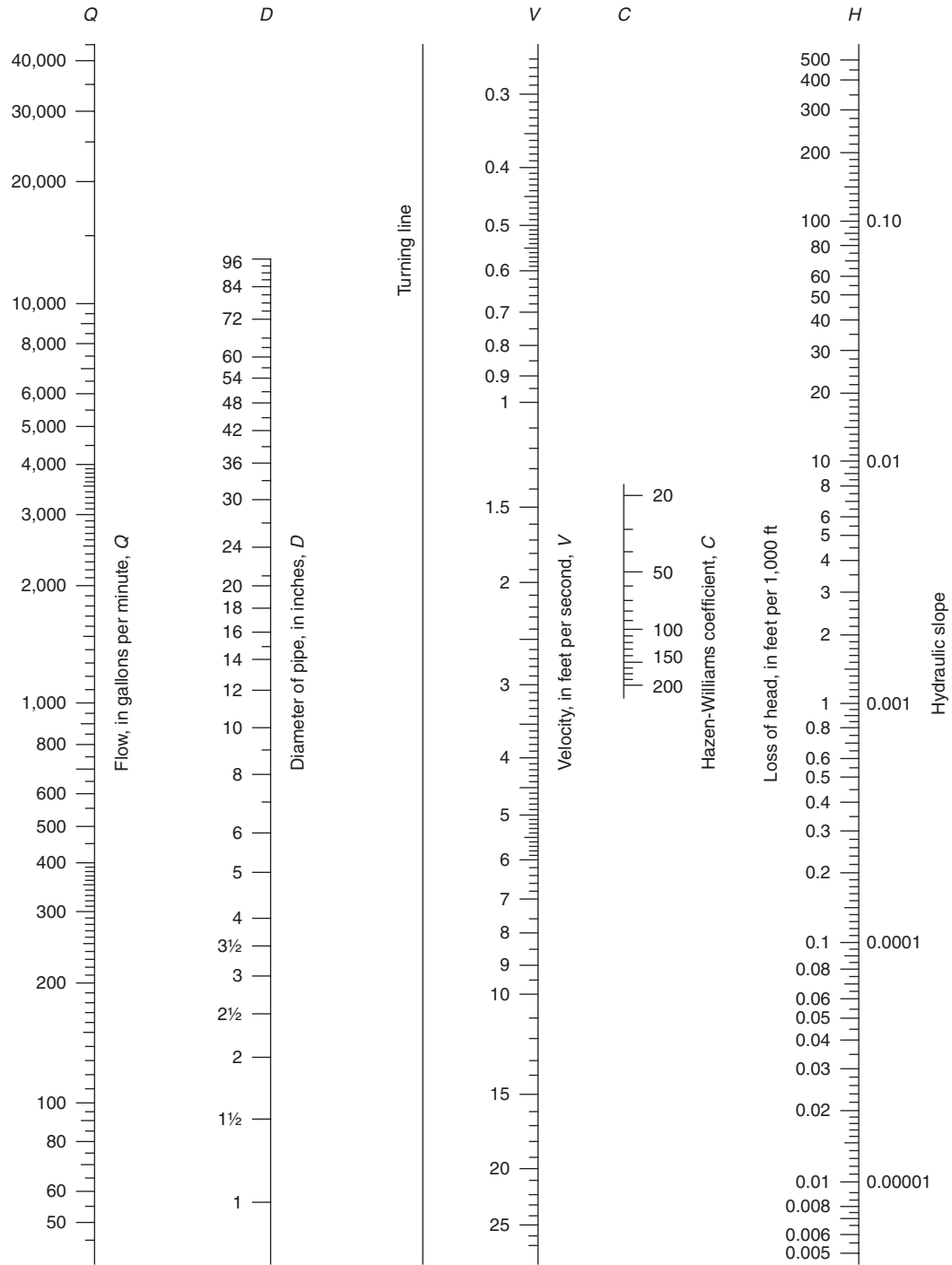
Q	D		V	C	H	

Figure 4-2.12. *Nomograph for solution of the Hazen-Williams formula.*

SOLUTION:

Basic Data:

For 50°F water, $\nu = 1.41 \times 10^{-5}$ ft²/s

pipe flow area = 0.0884 ft²

$\varepsilon = 0.0002$

pipe inside diameter = 0.3355 ft = 4.026 in.

Using the Darcy approach, we first determine Re, ε/D, and then enter the Moody diagram (Figure 4-2.10).

Flow quantity = Q = 500 gpm ≡ 1.1140 cfs (31.54 l/s)

Velocity = $v = \dfrac{Q}{A} = \dfrac{1.1140}{0.0884} = 12.60$ fps (3.8 m/s)

$$\text{Re} = \frac{Dv}{\nu} = \frac{0.3355(12.60)}{1.41 \times 10^{-5}} = 3.0 \times 10^5$$

$$\frac{\varepsilon}{D} = \frac{0.0002}{0.3355} = 0.0006$$

From the Moody friction chart, $f = 0.0188$.

From Equation 18

$$h_L = \frac{0.0188(100)(12.60)^2}{2(0.3355)(32.2)} = 13.8 \text{ ft} = 5.98 \text{ psi } (0.41 \text{ bar})$$

The Hazen-Williams approach—Equation 22b—does not take into account any variability in the physical properties of water. It is more straightforward to apply but will likely be less accurate. If we assume a C-factor of 100 and solve directly for pressure drop in psi per 100 ft we obtain

$$\Delta p = \frac{4.52(100)(500)^{1.85}}{(100)^{1.85}(4.026)^{4.87}} = 10.06 \text{ psi } (0.69 \text{ bar})$$

If we assume $C = 140$,

$$\Delta p = 5.40 \text{ psi } (0.37 \text{ bar})$$

a drop of nearly 50 percent and much closer to the Darcy result.

Accuracy in using Hazen-Williams clearly depends on a careful choice of C-factor. The Darcy result is not nearly so sensitive to choice of specific roughness ε.

Minor Losses

Flows through pipe fittings, valves, or other pipeline fixtures generate additional turbulence and, therefore, additional energy losses. These losses, although termed minor, can be very significant fractions of the total energy loss due to friction in a piping system. In particular, losses due to pipeline obstructions such as swing-type check valves and certain types of flow meters are equivalent to many feet (or meters) of straight pipe losses. Thus, in some instances minor losses may have to be considered major, particularly in systems where there are many fittings, valves, or other appurtenances. Empirical methods are used to determine these losses for a range of flow or obstruction geometries. One common method is to define a *minor loss coefficient* to express head loss as a function of velocity head. Thus,

$$h_L = k \frac{v^2}{2g} \tag{23}$$

where k is a dimensionless loss coefficient. It is sometimes convenient to express such losses in terms of *equivalent length of straight pipe*, or as pipe diameters that produce the same head loss. Thus, by Darcy-Weisbach,

$$\frac{L}{D} = \frac{k}{f} \tag{24}$$

Table 4-2.3 shows local loss coefficients for a number of fittings and flow patterns. Wherever possible manufacturers' data should be used, particularly for valves because of the wide variety of designs even for valves of the same generic type. Such data are often published in the form of flow coefficient or C_v values, which may be used in the equation

$$Q = C_v \sqrt{h_L} \tag{25}$$

C_v is determined from the relation

$$C_v = \pi D^2 \sqrt{\frac{g}{8k}} \tag{26}$$

which results directly from a combination of the continuity equation with the equations above.

EXAMPLE 3:

Table 4-2.4 lists a number of equivalent lengths of standard Schedule 40 pipe for screwed steel fittings and valves. Using the table determine the equivalent length of the 2-in.-diameter pipe network shown below.
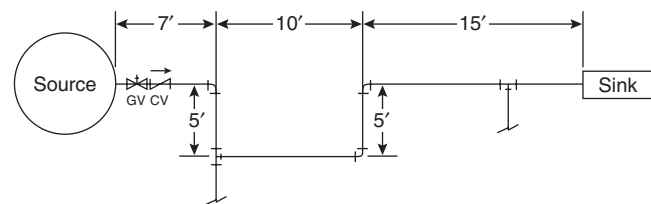
SOLUTION:

The line comprises

1 check valve	19.0 ft (5.7 m)
3 90° standard elbows	$3 \times 8.5 = 25.5$ ft (7.7 m)
1 tee (flow through run)	7.7 ft (2.4 m)
1 tee (flow through branch or stem)	12.0 ft (3.7 m)
1 gate valve	1.5 ft (0.5 m)
straight pipe	42.0 ft (12.8 m)
	$L_e = 107.7$ ft (32.8 m)

The Darcy equation for determining friction losses through the network would then have the form

$$h_L = \frac{fL_e v^2}{2Dg}$$

Alternately, the loss coefficient approach may be used, where

$$h_L = k \frac{v^2}{2g}$$

This method must be used to find entrance and exit losses. For this example, however, we either refer to manufacturer's data for valve and fitting C_v values or calculate k from the relation
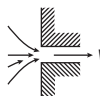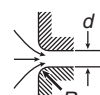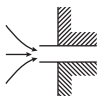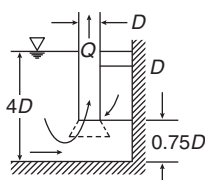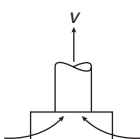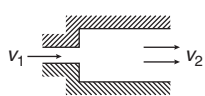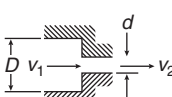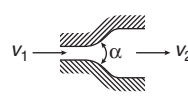
$$k = \frac{fL_e}{D}$$

Energy Losses in Pipe Networks

Flow networks may consist of pipes arranged in series, parallel, or some more complicated configuration. In

Table 4-2.3 *Local Loss Coefficients*

Use the equation $h_L = kv^2/2g$ unless otherwise indicated. Energy loss E_L equals h_v head loss in feet.

1		Perpendicular square entrance: $k = 0.50$ if edge is sharp

2

Perpendicular rounded entrance:

$R/d =$	0.50	0.1	0.2	0.3	0.4
$k =$	0.25	0.17	0.08	0.05	0.04

3

Perpendicular re-entrant entrance:
$k = 0.8$

4

Additional loss due to skewed entrance:
$k = 0.505 + 0.303 \sin \alpha + 0.226 \sin^2 \alpha$

5

Suction pipe in sump with conical mouthpiece:

$$E_L = D + \frac{5.6Q}{\sqrt{2g}D^{1.5}} - \frac{v^2}{2g}$$

Without mouthpiece:

$$E_L = 0.53\,D + \frac{4Q}{\sqrt{2g}D^{1.5}} - \frac{v^2}{2g}$$

Width of sump shown: $3.5D$ (After I. Vágás)

6

Strainer bucket:
$k = 10$ with foot value
$k = 5.5$ without foot value

(By Agroskin)

7

Standard tee, entrance to minor line:
$k = 1.8$

8

Sudden expansion:

$$E_L = \left(1 - \frac{v2}{v1}\right)^2 \frac{v_1^2}{2g} \quad \text{or} \quad E_L = \left(\frac{v1}{v2} - 1\right)^2 \frac{v_2^2}{2g}$$

9

Sudden contraction:
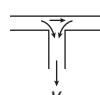
$(d/D)^2 =$	0.01	0.1	0.2	0.4	0.6	0.8
$k =$	0.5	0.5	0.42	0.33	0.25	0.15

10

Diffusor:
$E_L = k(v_1^2 - v_2^2)/2g$

$\alpha° =$	20	40	60	80
$k =$	0.20	0.28	0.32	0.35

(Continued)

Design Calculations

Table 4-2.3 Local Loss Coefficients (Continued)
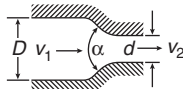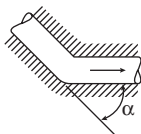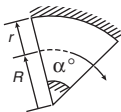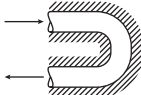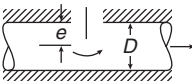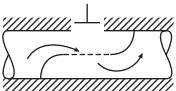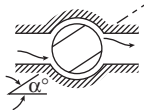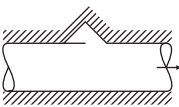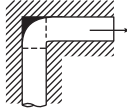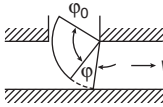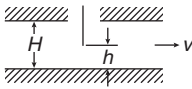
11		Confusor:

$E_L = k(v_1^2 - v_2^2)/2g$

$\alpha° =$	6	10	20	40	60	80	100	120	140
k for $D = 3d$	0.12	0.16	0.39	0.80	1.0	1.06	1.04	1.04	1.04
$D = 1.5d$	0.12	0.16	0.39	0.96	1.22	1.16	1.10	1.06	1.04

12

Sharp elbow:
$k = 67.6 \times 10^{-6}(\alpha°)^{2.17}$

(By Gibson)

13

Bends:
$k = [0.13 + 1.85(r/R)^{3.5}]\sqrt{\alpha°/180°}$

(By Hinds)

14

Close return bend:
$k = 2.2$

15

Gate valve:

$e/D =$	0	1/4	3/8	1/2	5/8	3/4	7/8
$k =$	0.15	0.26	0.81	2.06	5.52	17.0	97.8

16

Global value:
$k = 10$ when fully open

17

Rotary valve:

$\alpha° =$	5	10	20	30	40	50	60	70	80
$k =$	0.05	0.29	1.56	5.47	17.3	52.6	206	485	∞

(By Agroskin)

18

Check valves:
Swing type $k = 2.5$ when fully open
Ball type $k = 70.0$
Lift type $k = 12.0$

19

Angle valve:
$k = 5.0$ if fully open

20

Segment gate in rectangular conduit:

$k = 0.3 + 1.3\left[\left(\dfrac{1}{n}\right)\right]^2$

where $n = \varphi/\varphi_0$ = the rate of opening with respect to the central angle

(By Abelyev)

21

Sluice gate in rectangular conduit:

$k = 0.3 + 1.9\left[\left(\dfrac{1}{n}\right) - n\right]^2$

where $n = h/H$

(By Burkov)

Table 4-2.4 *Typical Equivalent Lengths of Schedule 40 Straight Pipe for Screwed Steel Fittings and Valves (for any fluid in turbulent flow)*

Fitting Type	Equivalent Length (ft) Pipe Size		
	1" (25.7 mm)	2" (50.8 mm)	4" (101.6 mm)
Regular 90° elbow	5.2	8.5	13.0
Long radius 90° elbow	2.7	3.6	4.6
Regular 45° elbow	1.3	2.7	5.5
Tee, flow through line (run)	3.2	7.7	17.0
Tee, flow through stem	6.6	12.0	21.0
180° return bend	5.2	8.5	13.0
Globe valve	29.0	54.0	110.0
Gate valve	0.84	1.5	2.5
Angle valve	17.0	18.0	18.0
Swing check valve	11.0	19.0	38.0
Coupling or union	0.29	0.45	0.65

Figure 4-2.13. *Energy losses in pipe network: (a) pipes in series, (b) pipes in parallel.*

any case, an evaluation of friction losses for the flows is based on energy conservation principles applied to the flow junction points. Methods of solution depend on the particular piping configuration. In general, however, they involve establishing a sufficient number of simultaneous equations or employing a friction loss formula where the friction coefficient depends only on the roughness of the pipe (e.g., Darcy or Hazen-Williams).

Pipes in series: When two pipes of different sizes or roughnesses are connected in series [Figure 4-2.13(a)], head loss for a given discharge, or discharge for a given head loss, may be calculated by applying the energy equation between the bounding points, taking into account all losses in the interval. Thus, head losses are cumulative.

Series pipes may be treated as a single pipe of constant diameter to simplify the calculation of friction losses. The approach involves determining an equivalent length of a constant diameter pipe which has the same friction loss and discharge characteristics as the actual series pipe system. Minor losses due to valves and fittings are also included. Using the previous example once again, we note that application of the continuity equation to the solution allows the head loss to be expressed in terms of only one pipe size.

The lost head in equivalent feet of 6-in. pipe is then given in Darcy-Weisbach form by

$$h_L = f\left(\frac{L_e}{D}\right)\left(\frac{v^2}{2g}\right)$$

L_e can be obtained if f is known. Exact hydraulic equivalence in the velocity head terms depends upon f being a constant over the range of velocities applicable to the problem. In fact, f is not a constant over wide ranges of velocity. Since it varies only slightly with Reynolds number, however, solutions are sufficiently accurate.

Pipes in parallel: Two or more pipes connected as in Figure 4-2.13(b), so that flow is first divided among the pipes and is then rejoined, comprise a parallel pipe sys-

tem. Flows in pipes arranged in parallel are also determined by application of energy conservation principles—specifically, energy losses through all pipes connecting common junction points must be equal. Each leg of the parallel network is treated as a series piping system and converted to a single equivalent length pipe. The friction losses through the equivalent length parallel pipes are then considered equal and the respective flows determined by proportional distribution. For a given Q, an outline of the procedure is as follows:
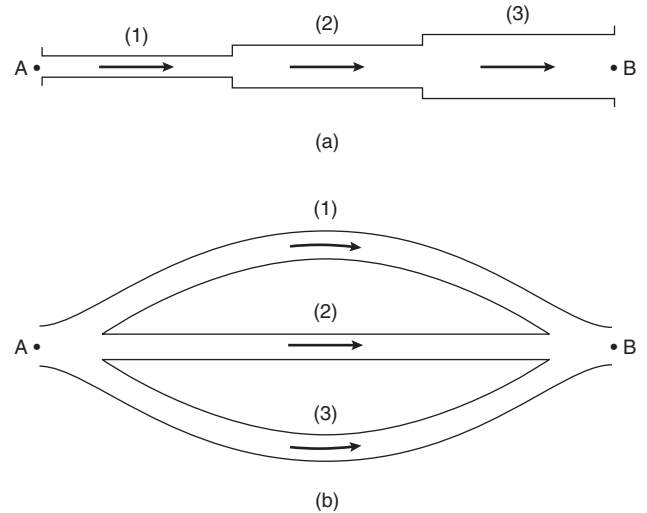
1. Express each branch of the parallel system as an equivalent length of a single pipe size, including all minor losses between the bounding junction points.
2. Assume a discharge Q_1' through pipe branch 1.
3. Solve for h_L, using Q_1'.
4. Using h_L, find Q_2' and Q_3' for the remaining branches.
5. Knowing the proportional distribution of flow among the legs, Q_1', Q_2', and Q_3' are adjusted so that their sum equals the known Q; thus,

$$Q_1 = \frac{Q_1'}{\sum Q'}Q \quad Q_2 = \frac{Q_2'}{\sum Q'}Q \quad Q_3 = \frac{Q_3'}{\sum Q'}Q \quad (27)$$

6. h_{L_1}, h_{L_2}, and h_{L_3} are computed for the values of Q_1, Q_2, and Q_3 as a check for correctness.

For judicious choice of assumed discharges, solutions are obtained rapidly that agree within a few percent, well within the range of accuracy of the assumed friction factors.

In the case where the head loss is known between points A and B, Q for each branch is found simply by solution of the equation for pipe discharge. The discharges are added to obtain the total flow through the system.

Compound piping networks: Energy loss calculations in compound piping configurations or networks employ

the same basic physical principles as for single pipes. That is, conservation of energy and conservation of mass (continuity) must be satisfied throughout the network. In particular, at each pipe junction

$$\sum Q = Q_1 + Q_2 + \cdots + Q_n = 0 \tag{28}$$

and around each closed loop or circuit

$$\sum h_L = h_{L_1} + h_{L_2} + \cdots + h_{L_n} = 0 \tag{29}$$

The general solution procedure involves setting up a sufficient number of independent equations of these two types and solving simultaneously for the unknowns. For complicated networks straightforward algebraic solution is clearly impractical. A very widely used relaxation method for systematic solution of large networks was developed by Hardy Cross in 1928. The method is well suited for solution by hand and is readily adaptable for machine computation.

We have seen that loss of head in a pipe may be represented generally by an equation of the form $h_L = KQ^n$ (where, for the Hazen-Williams formula, $n = 1.85$). For any single pipe in a network, we may write

$$Q = Q_0 + \Delta \tag{30}$$

where

Q = corrected flow
Q_0 = assumed flow
Δ = flow correction

The problem, so stated, reduces to finding Q to a desired degree of accuracy by successive evaluations of Δ based on updated estimates of Q_0. We solve for Δ as follows:

$$h_L = KQ^n = K(Q_0 + \Delta)^n$$
$$= K(Q_0^n + nQ_0^{n-1}\Delta + \cdots) \tag{31}$$

If Δ is small relative to Q_0, the higher-order terms in the expansion may be neglected. Since, for any circuit, $\Sigma h_L = 0$, we may write

$$\sum KQ^n = 0 = \sum [KQ_0^n + KnQ_0^{n-1}\Delta] \tag{32}$$

to a good approximation. Solving for Δ we have

$$\Delta = \frac{-\sum KQ_0^n}{n\sum KQ_0^{n-1}} = \frac{\sum h_{L_0}}{n\sum (h_{L_0}/Q_0)} \tag{33}$$

The overall formulation is made algebraically consistent by designating clockwise flows positive and counterclockwise flows negative. The calculation procedure is controlled by the requirement that the algebraic sum of all assumed flows must equal zero at each pipe junction. The originally assumed flows are repeatedly and cyclically corrected until the Δ values are negligible, indicating that a hydraulic balance has been reached. Note that pipes common to two circuits are corrected twice in each cycle,

once for each circuit. For a system where total head loss is known, flows can be balanced by correcting assumed head losses instead of flows.

Several other methods exist for determining flows and head losses in compound pipe networks. Many can be performed manually, although computer analysis is desirable and necessary for the more complex methods, particularly those involving unsteady flow. For a review of alternative methods, the reader is referred to Stephenson[7] and Walski.[6]

Flow Measurement and Discharge

Flow Measuring Devices

This section deals primarily with the basic principles of operation of some flow measuring devices in common use and, in particular, with the pitot tube and the pipeline differential flow meters that have been standardized by the ASME (American Society of Mechanical Engineers): namely, the Venturi, the flow nozzle, and the square-edge thin-plate concentric orifice.

In general, an incompressible fluid of density ρ, viscosity μ, flows with average velocity v through a metering element of diameter d. The metering element is located in a horizontal metering tube of roughness ε and diameter D. The flow through the element produces a pressure differential Δp sensed by pressure taps located a distance L apart. It can be shown by dimensional analysis that the fundamental parameters involved in fluid metering, namely L, ε, v, ρ, μ, d, D, and Δp, yield relational solutions conventionally formulated as follows:

$$\frac{d\rho v}{\mu} = \mathrm{Re}_d \qquad \text{metering element Reynolds number}$$

$$\frac{L}{D} \qquad \text{tap location ratio}$$

$$\frac{d}{D} = \beta \qquad \text{beta ratio}$$

$$\frac{\varepsilon}{D} \qquad \text{relative roughness}$$

$$\frac{v}{\sqrt{2g\Delta p/\rho}} = \overline{K} \qquad \text{flow coefficient (pressure coefficient)}$$

Since $v = \overline{K}\sqrt{2g\Delta p/\rho}$, the continuity equation allows the volumetric flow rate measured by the meter to be expressed as

$$Q = \overline{K}A_d\sqrt{2g\Delta p/\gamma} \tag{34}$$

where A_d is the flow area of the metering element.

Typically, flow meter calculations are based on the idealized flow of a one-dimensional, frictionless, incompressible fluid in a horizontal metering tube. Real conditions require corrections to the ideal formulation. Conventional corrections for the effects of variations from ideal geometry and flow velocity profile are achieved through the use of modification factors. Thus, in Equation 34 above, $\overline{K}$ in-

cludes pressure and flow modifications which are conventionally defined as

$$\overline{K} = CE \qquad (35)$$

where C = coefficient of discharge defined as the ratio of actual flow rate to ideal rate and

$$E = \frac{1}{\sqrt{1 - \beta^4}}$$

and is known as the velocity of approach factor, since it accounts for the one-dimensional kinetic energy at the inlet tap.

The general volumetric flow metering equation is, then,

$$Q = \overline{K}A_d\sqrt{\frac{2g\Delta p}{\gamma}} = CEA_d\sqrt{\frac{2g\Delta p}{\gamma}} \qquad (36)$$

Venturi flow meter: Figure 4-2.14 shows a schematically typical Venturi-type flow tube. The divergent cone section reduces the overall pressure loss of the meter. Pressure is sensed through a series of holes in the inlet cone and throat. These holes lead to an annular chamber, and the two chambers are connected to a pressure differential sensor such as a U-tube manometer. ASME standardized discharge coefficients are given in Table 4-2.5. Venturi tubes must be individually calibrated to obtain these coefficients outside the tabulated limits.
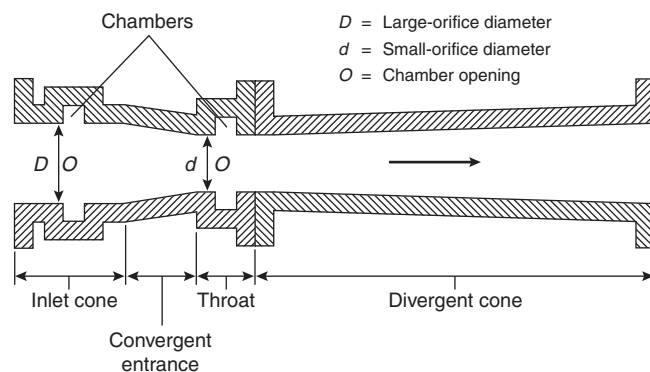
Figure 4-2.14. *Venturi tube.*

Table 4-2.5 *ASME Coefficients for Venturi Tubes*

Type of Inlet Cone	Re₂		Value of C	Tolerance (%)
	Minimum	Maximum		
Machined		1,000,000	0.995	±1.00
Rough welded sheet metal	500,000	2,000,000	0.985	±1.50
Rough cast			0.984	±0.70

Determination of volumetric flow rate is a simple calculation employing the general flow metering formula—Equation 36—where C is the applicable tabulated value based on Re_d, and E is calculated directly from the beta ratio.

ASME flow nozzle: This nozzle is depicted in Figure 4-2.15. The pressure differential is sensed by either throat taps or pipe wall taps appropriately located. Coefficients of discharge for ASME flow nozzles may be accurately computed from the following equation:

$$C = 0.9975 - 0.00653\left(\frac{10^6}{\text{Re}_d}\right)^a \qquad (37)$$

where

$a = \dfrac{1}{2}$ for $\text{Re}_d < 10^6$

$a = \dfrac{1}{5}$ for $\text{Re}_d < 10^6$

Volumetric flow rates are calculated in the same manner as for the Venturi tube.

ASME orifice meters: Fluid flowing through a thin, square-edged orifice plate experiences a contraction of the flow stream some distance downstream from the orifice. The minimum area of flow is called the *vena contracta* and its location is a function of the beta ratio. Figure 4-2.16 shows the relative pressure difference due to the presence of the orifice plate and the location of the *vena contracta* with respect to beta. By inspection of Figure 4-2.16 it is clear that the actual location of the pressure taps is critical. Three distinct arrangements for tap locations are specified by the ASME for accurately measuring the pressure differential. These types of tap arrangements are called the flange, *vena contracta,* and the 1*D* and ½*D*. Each has certain advantages and disadvantages and affects the value of the discharge coefficient.
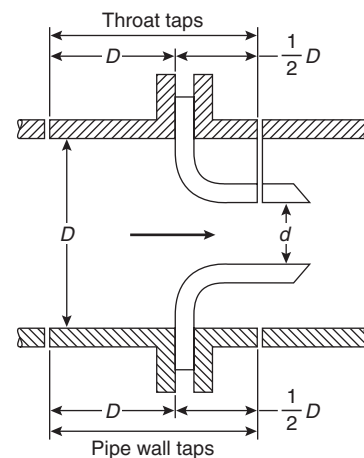
Figure 4-2.15. *ASME flow nozzle.*
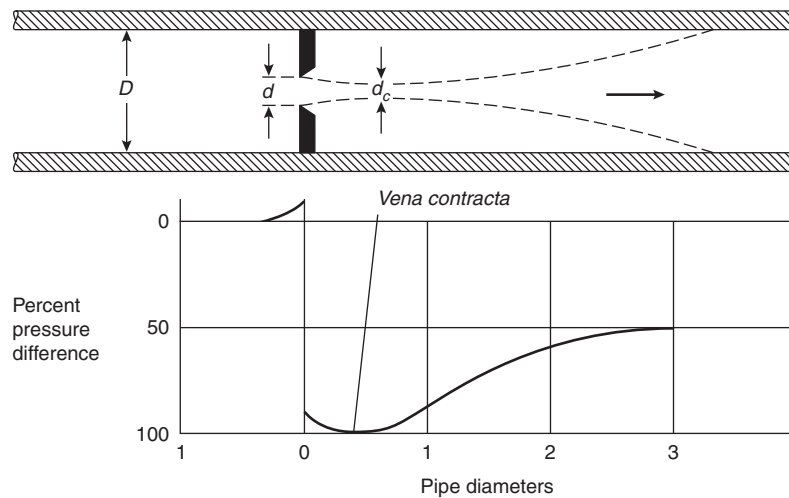
Figure 4-2.16. *Relative pressure changes due to flow through an orifice.*

Discharge coefficients for orifice metering plates may be calculated from the equation

$$C = C_o + \frac{\Delta C}{\text{Re}_d^\alpha} \tag{38}$$

where C_o and α are obtained from Table 4-2.6. Since the jet contraction downstream of the orifice can amount to nearly half of the orifice area, orifice discharge coefficients are in the order of 0.6 compared to the near-unity coefficients obtained with Venturi tubes and flow nozzles.

Pitot tube: A pitot tube is a device designed to sense stagnation or total pressure for the determination of velocity and volumetric flow rate. A number of commercial devices are available, some of which include a static pressure tap, that are designed for insertion into a water main under pressure through a standard pipe tap or corporation cock. The installed pitot tube measures velocity at a point in the fluid. Conventional practice assumes that the conversion of kinetic energy to flow work in the tube is frictionless. Thus, applying the energy equation to the generalized pitot tube diagram (Figure 4-2.17) we obtain

$$\frac{u_s^2 - u_i^2}{2g} + \frac{p_s - p_0}{\rho_0 g} = 0 \tag{39}$$

where

u_s = stagnation point velocity
u_i = ideal streamtube velocity
p_s = stagnation pressure
p_0 = static pressure

Since, by definition $u_s = 0$, solving for u_i we obtain

$$u_i = \sqrt{\frac{2g(p_s - p_0)}{\gamma_0}} = \sqrt{\frac{2g\Delta p}{\gamma_0}} \tag{40}$$

Typically, a pipe coefficient, C_p, which is independent of the geometry of the velocity profile, is defined as

$$C_p = \frac{\text{average velocity}}{\text{centerline velocity}}$$

For typical velocity profiles, C_p varies from about 0.75 to 0.97 but usually lies within a narrower range of about 0.80 to 0.90. Knowing the centerline velocity, the flow can be obtained simply by

$$Q = C_p A v_{\text{CL}} \tag{41}$$

In situations where pipe velocity profiles are unknown, and therefore average velocities are not available, it may be necessary to obtain velocity measurements at many individual points. Given n velocities, the flow is then

$$Q = \sum_{i=1}^{n} v_i A_i \tag{42}$$

where

v_i = velocity at the ith point
A_i = area of annular ring of flow cross section for which velocity v_i is accurate

Detailed procedures for obtaining accurate pitot traverses are available in the literature along with suggestions for assessing the reliability of water audits, C-factor tests, and so forth, based on pitot gage measurements.[4,6] See the next section for a discussion of discharge measurements using pitot tubes.

Free Discharge at an Opening

Flow discharging to the atmosphere from a tank, hydrant, nozzle, or open conduit is affected by the area and shape of the opening. The total energy of the fluid is converted into kinetic energy at the orifice according to an

Table 4-2.6 *Values of C_o, ΔC, and α for Use in Equation 38*

β	D = 2 in. = 50 mm		D = 4 in. = 100 mm		D = 8 in. = 200 mm		D = 16. in. = 400 mm	
	C_o	ΔC	C_o	ΔC	C_o	ΔC	C_o	ΔC
				Flange taps α = 1				
0.20	0.5972	127	0.5946	200	0.5951	327	0.5955	551
0.30	0.5978	144	0.5977	209	0.5978	307	0.5980	457
0.40	0.6014	181	0.6005	256	0.6002	362	0.6001	514
0.50	0.6050	260	0.6034	386	0.6026	584	0.6022	903
0.60	0.6078	392	0.6055	622	0.6040	1015	0.6032	1710
0.70	0.6068	573	0.6030	953	0.6006	1637	0.5991	2898
				Vena contracta taps α = ½				
0.20	0.5938	1.61	0.5928	1.61	0.5925	1.61	0.5924	1.61
0.30	0.5939	1.78	0.5934	1.78	0.5933	1.78	0.5932	1.78
0.40	0.5970	2.01	0.5954	2.01	0.5953	2.01	0.5953	2.01
0.50	0.5994	2.29	0.5992	2.29	0.5992	2.29	0.5991	2.29
0.60	0.6042	2.68	0.6041	2.68	0.6041	2.69	0.6041	2.70
0.70	0.6069	3.34	0.6068	3.37	0.6067	3.44	0.6068	3.57
				1D and ½D taps α = ½				
0.20	0.5909	2.03	0.5922	1.41	0.5936	1.10	0.5948	0.94
0.30	0.5915	2.02	0.5930	1.50	0.5944	1.24	0.5956	1.12
0.40	0.5936	2.17	0.5951	1.72	0.5963	1.49	0.5974	1.38
0.50	0.5979	2.40	0.5978	1.99	0.5999	1.79	0.6007	1.69
0.60	0.6036	2.67	0.6040	2.31	0.6044	2.12	0.6048	2.11
0.70	0.6078	3.19	0.6072	2.98	0.6068	3.07	0.6064	3.51
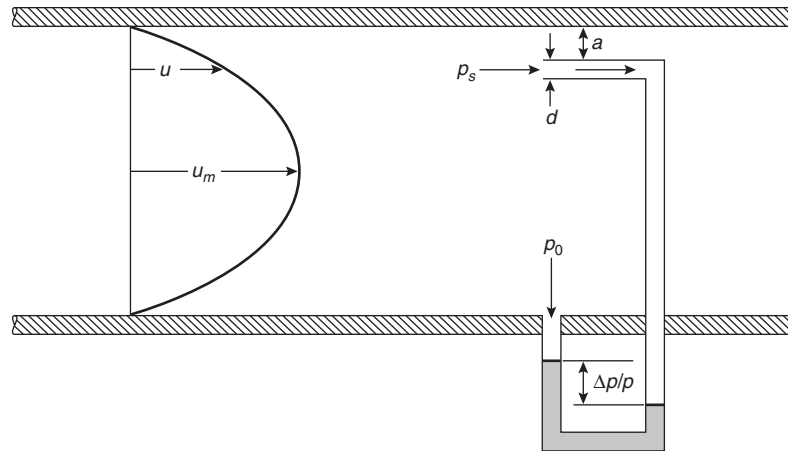
Figure 4-2.17. *Pitot tube study.*

appropriate form of the Bernoulli equation. In the most general case of a closed pressurized tank,

$$\frac{v_0^2}{2g} = z_1 + \frac{p_1}{\rho} \tag{43}$$

$$v_0 = \left[2g\left(z_1 + \frac{p_1}{\rho} \right) \right]^{1/2} \tag{44}$$

Accounting for losses at the point of discharge,

$$v_0 = C_v\sqrt{2gh} \tag{45}$$

where C_v, the coefficient of velocity, is determined from the coefficients of discharge and contraction

$$C_v = \frac{C_d}{C_c}$$

Table 4-2.7   *Orifice Coefficients for Water*

Illustration	Description	C_d	C_c	C_v
A	Sharp-edged	0.62	0.63	0.98
B	Round-edged	0.98	1.00	0.98
C	Short tube (fluid separates from walls)	0.61	1.00	0.61
D	Short tube (no separation)	0.82	1.00	0.82
E	Short tube with rounded entrance	0.97	0.99	0.98
F	Reentrant tube, length less than one-half of pipe diameter	0.54	0.55	0.99
G	Reentrant tube, length 2 to 3 pipe diameters	0.72	1.00	0.72
Not shown	Smooth, well-tapered nozzle	0.98	0.99	0.99

Commonly used values of orifice coefficients for water are given in Table 4-2.7. The orifice discharge can then be expressed as

$$Q_o = C_d A_o \sqrt{2gh} \qquad (46)$$

and the head loss due to turbulence at the orifice as

$$h_L = \left(\frac{1}{C_v^2} - 1\right)\frac{v_0^2}{2g} \qquad (47)$$

where

$$\left(\frac{1}{C_v^2} - 1\right) = \text{minor loss } k\text{-factor}$$

For the general case of a tank of varying cross-sectional area being replenished with inflow, $\dot{Q}_{IN}$, the time to empty from height z_1 to z_2 is given by

$$t = \int_{z_1}^{z_2} \frac{A_t\,dz}{c_d A_o \sqrt{2gh} - \dot{Q}_{IN}} \qquad (48)$$

where A_t is expressed as a function of z.

For a tank of constant cross section this simplifies to

$$t = \frac{2A_t\left(\sqrt{z_1} - \sqrt{z_2}\right)}{C_d A_o \sqrt{2g}} \qquad (49)$$

EXAMPLE 4:

A 15-ft-diameter tank discharges water at 50°F through a 2-in.-diameter sharp-edged orifice. If the initial water depth in the tank is 10 ft and the tank is continuously pressurized to 50 psig, how long will it take to empty the tank?
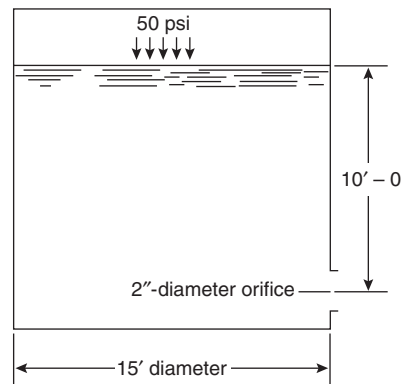
SOLUTION:

At 50°F (10°C),

$$\gamma = 62.4 \text{ lbm/ft}^3 \text{ (16.02 kgm/m}^3\text{)}$$

For the orifice:

$$A_o = \frac{\pi D^2}{4} = 3.14 \text{ ft}^2 \text{ (0.29 m}^2\text{)}$$

$$C_d = 0.62 \text{ (sharp-edged orifice)}$$

For the tank:

$$A_t = \frac{\pi D^2}{4} = 176.7 \text{ ft}^2 \text{ (16.4 m}^2\text{)}$$

$$h_0 = 10 + \frac{50(144)}{62.4} = 125.38 \text{ ft (38.2 m)}$$

$$h_1 = 0 + \frac{50(144)}{62.4} = 115.38 \text{ ft (35.2 m)}$$

The total pressure head on the discharging fluid results from both an elevation and a static pressure head. Therefore,

$$t = \frac{2A_t\left[(z_0 = p_0/\gamma)^{1/2} - (z_1 + p_1/\gamma)^{1/2}\right]}{C_d A_o \sqrt{2g}}$$

$$t = 10.4 \text{ s}$$

Discharge stream coordinates are given by

$$x = v_0 t = v_0 \sqrt{\frac{2y}{g}} = 2C_v\sqrt{zy} \qquad (50a)$$

$$y = \frac{gt^2}{2} \qquad (50b)$$

For the simpler case of a hydrant discharging to atmosphere, the flow can be determined by an appropriate form of Equation 36,

$$Q = 29.8D^2 C_d\sqrt{p} \qquad (51)$$

where

Q = discharge (gpm)

D = outlet diameter (in.)

p = pressure detected by pitot gage (psi)

C_d = coefficient based on hydrant outlet geometry (usually taken to be 0.90 for full flow across a standard 2½-in. outlet)

In the absence of a pitot gage, hydrant flows may be estimated by observing the trajectory of the discharge stream. The horizontal component of the velocity does not change appreciably over time, thus allowing calculation of the velocity based on the height of the outlet and the distance traveled by the stream. Figure 4-2.18 presents the basic parameters. The velocity determined in this manner is at the *vena contracta* and is given by

$$v = \frac{x}{\sqrt{2y/g}} \qquad (52)$$

The discharge is simply the product of this velocity and the area of the *vena contracta*. The method is relatively inaccurate due to the obvious difficulty of measuring the
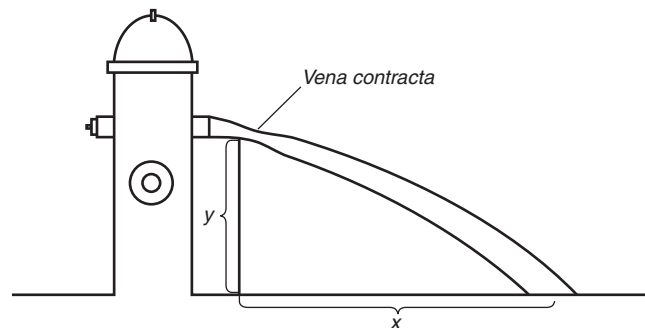
Figure 4-2.18. *Determining discharge by the trajectory method.*

required area and the distance *x.* It is a useful bounding guide, however, in the absence of precision measuring devices.

WATER HAMMER*

Water hammer in a pipeline is caused by a sudden stoppage of flow and is characterized by loud noise and vibration. The kinetic energy from the interrupted flow is transferred to the walls of the enclosing pipe or equipment, which expand under the increased pressure. Such pressures, or shock waves, can be severe enough to destroy the equipment and the pipeline itself.

Density changes due to pressure are assumed zero for nearly all hydraulic calculations, as water is considered incompressible for practical purposes even though it is about 100 times more compressible than steel. When shock waves arise in confined water, however, the compressibility of water becomes very significant, and water's elastic properties must be taken into account. The primary property of interest is the bulk modulus of elasticity, *E,* which is defined as the ratio of pressure change to the corresponding change of volume as determined by compression tests on volumes. (The bulk modulus is analogous to Young's modulus in solid mechanics, which is the ratio of linear stresses to linear strains as determined by tension tests.) The formula expressing the relationship between pressure and volume is

$$\Delta p = -E\frac{\Delta V}{V_0} \qquad (53)$$

where the minus sign indicates that a positive change in pressure produces a decrease in volume. A modulus of compressibility, *K,* is also defined as the inverse of *E.*

Under normal conditions, water confined and flowing under pressure in a pipeline exerts pressure on the pipe walls according to the pressure-energy term of the energy equation. Any change in discharge within the system (due to valve closure, pump stoppage, etc.) results in a change of flow momentum. By virtue of the impulse-momentum relation, the momentum change will cause an impulse force to be created. This force in a pipeline is commonly referred to as water hammer.

The theory of water hammer, as developed by Zhukovsky, can be briefly illustrated as follows: a valve in a pipeline is closed instantaneously; the fluid impacts the closed gate and is decelerated to zero velocity, thereby creating a pressure shock. By Newton, pressure shocks in fluids of infinite extent travel at a velocity given by

$$c^* = \sqrt{\frac{KE}{\rho}} \qquad (54)$$

where c^* is called the celerity (velocity) of the shock wave, *KE* is the kinetic energy of the fluid, and ρ is the fluid density. The pipe, however, is also elastic. Therefore, if the fluid in the pipe is compressed, the pipe will expand. The

*This discussion is patterned after the theory of water hammer as developed by N. J. Zhukovsky and as presented in Andrew L. Simon's *Practical Hydraulics,* 2nd ed.[4]

modulus of elasticity, E_c, of a system composed of fluid and pipe may be determined from the equation

$$\frac{1}{E_c} = \frac{1}{E} + \frac{D}{E_p w} \tag{55}$$

where

D = pipe diameter
w = thickness of the pipe wall
E_p = modulus of elasticity of the pipe material

Table 4-2.8 gives the modulus of elasticity for common pipe materials. The celerity of a shock wave in a pipe system of finite extent can then be computed from

$$\frac{c}{c^*} = \frac{1}{\sqrt{1 + ED/(E_p w)}} \tag{56}$$

which is plotted in Figure 4-2.19. The graph indicates the considerable influence of pipe rigidity on the velocity of the shock.

The shock waves that travel upstream and downstream from the valve closure eventually reach points in the system that correspond to large stationary energy stores (e.g., reservoirs) or other sudden closure points, which may vary in their ability to absorb or reflect the shock wave. If the shock is absorbed into a larger energy field it will disappear, and it will do so in time

$$t = \frac{L}{c} \tag{57}$$

where L is the distance from the energy reservoir to the shock wave point of origin. At the instant of shock absorption the compressed fluid, no longer balanced, begins to flow backward, creating a relief pressure shock that travels back to the valve. The time period T that the initial shock or impulse pressure acts on the valve is, therefore, the time required for the pressure wave to travel away from and back to the valve:

$$T = 2t = \frac{2L}{c} \tag{58}$$

Table 4-2.8 Modulus of Elasticity E_p of Various Pipe Materials

Pipe Material	E_p		
	(psi)	(lb/ft²)	(kg/m²)
Lead	0.045×10^6	6.48×10^6	31.64×10^6
Lucite (at 73°F)	0.4×10^6	57.6×10^6	281.23×10^6
Rubber (vulcanized)	2×10^6	288×10^6	1406×10^6
Aluminum	10×10^6	1440×10^6	7030×10^6
Glass (silica)	10×10^6	1440×10^6	7030×10^6
Brass, bronze	13×10^6	1872×10^6	8489×10^6
Copper	14×10^6	2016×10^6	9842×10^6
Cast iron, gray	16×10^6	2304×10^6	$11,249 \times 10^6$
Cast iron, malleable	23×10^6	3312×10^6	$16,170 \times 10^6$
Steel	28×10^6	4023×10^6	$19,685 \times 10^6$
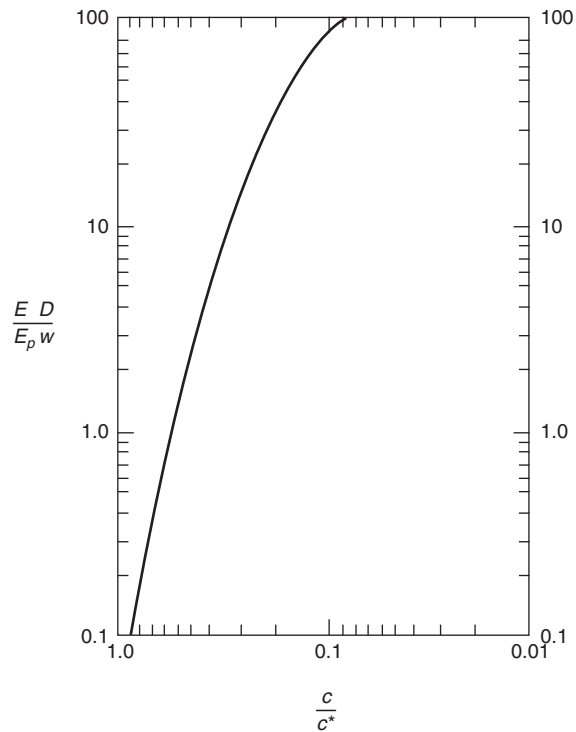
Figure 4-2.19. Celerity of pressure waves in pipes, c equals celerity in elastic pipe; c* equals celerity in fluid of infinite extent.

At time T, all the fluid is moving backward at some velocity v. Since the valve is closed, there is no supply for this flow. A negative pressure shock is created at the valve. The shock travels to and back from the reservoir, as the flow is reversed. Such oscillations of pressure and periodic flow reversals persist until the kinetic energy is dissipated by friction. The process described will occur both upstream and downstream from the point of origin, though the initial shock will be positive upstream and negative downstream and the periodicities would not likely be equal.

The theoretical magnitude of the pressure shock at instantaneous valve closure can be determined directly from

$$p^* = \rho c \Delta v \tag{59}$$

and the pressure will oscillate in the pipe within the range

$$p = p_0 \pm p^* \tag{60}$$

In actuality, the time of closure of a valve is not zero but some finite time period which we may call T_c. The water hammer pressure increases gradually with the rate of closure of the valve. Depending on whether T_c is smaller or larger than T, we distinguish between quick and slow closure. For $T_c < T$, the shock pressure will attain its maximum value p^*. (In this sense, quick closure is equivalent to instantaneous closure.) For $T_c > T$, maximum pressure

will be somewhat less than p^* and may be calculated by the Allievi formula

$$p = p_0\left(\frac{N}{2} + \sqrt{\frac{N^2}{4} + N}\right) \qquad (61)$$

in which

$$N = \left(\frac{Lv\rho}{p_0 T_c}\right)^2 \qquad (61a)$$

In general the calculation of water hammer pressure rises, regardless of method, will tend to underestimate the actual values. Real systems will tend to experience superimposition of positive or negative pressure waves due to complex piping configurations. Discontinuities introduced by a variety of auxiliary valving and metering equipment complicate the analysis considerably. Other methods are available for analyzing water hammer effects on systems that may not be reasonably handled by the above idealized method.[8] Since water hammer can be extremely detrimental, often resulting in complete loss of the system, it is desirable to perform an analysis wherever such effects are of concern. Control over the development of damaging shock waves is achieved through use of slow-closing valves, pressure relief valves, or shock-absorbing devices.

Pumps

Pump Operating Characteristics

Pumps are mechanical devices that convert electrical or mechanical energy into hydraulic energy. There are many classes of pumps—for example, reciprocating, rotary, jet, ram, centrifugal—each class referring to different ways pumps move liquids. A common class of pump is the centrifugal and it is usually the only type we are concerned with in fire protection applications. Based on the way in which the impeller (the rotating component) imparts energy to the water, centrifugal pumps may be divided into several categories. Turbine or radial flow centrifugal pumps force water outward at right angles to the rotating axis. Mixed flow pumps force water in both radial and axial directions. Propeller pumps move water in the axial direction only. Any of these types may be single or multistage, where stage refers to the number of impellers on the pump's rotating shaft. The orientation of the shaft may be vertical or horizontal. The following discussion, while broadly applicable, is directed mainly to centrifugal pumps.

Figure 4-2.20 illustrates several of the terms commonly used to describe pump performance conditions. In general, pumping of liquids requires that the pressure at any point in the intake line be greater than the vapor
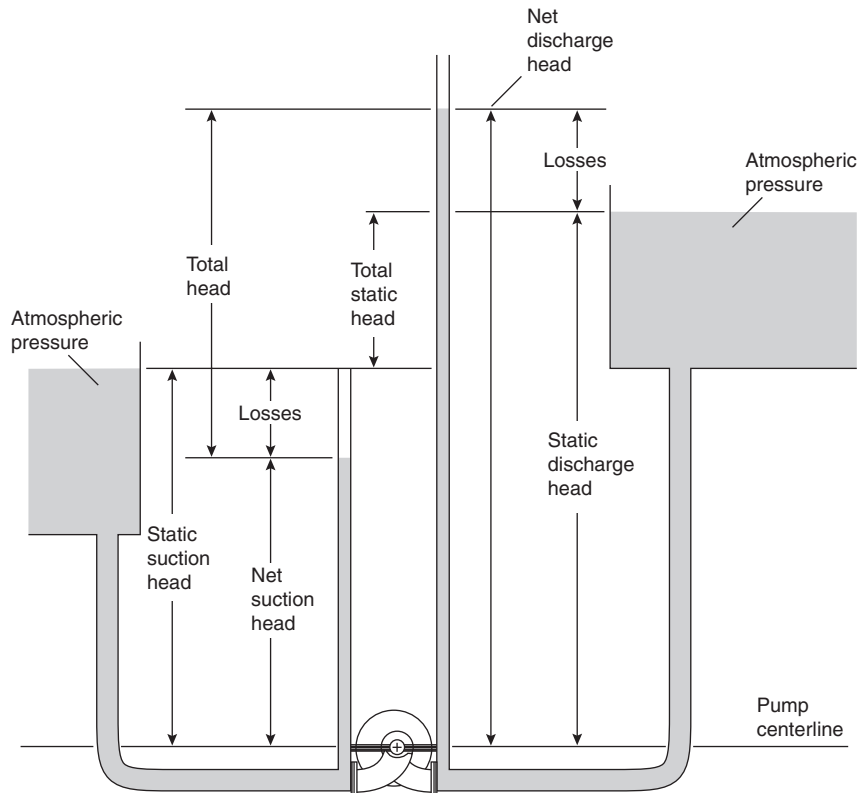
Figure 4-2.20.   *Pump head definitions.*

pressure of the liquid to avoid loss of prime and the highly destructive phenomenon known as cavitation. The pressure gradient that causes a liquid to move through the intake line to the pump impeller is termed the net positive suction head (NPSH). In pump selection, it is essential to determine that the *available* NPSH of the system exceeds the *required* NPSH for the pump under consideration. Required NPSH depends upon many factors relating to pump geometry and construction and intake system operating conditions, but it is defined simply as the difference between net suction head and vapor pressure at a given flow, or the energy needed to fill the pump on the intake side and overcome intake system head losses. If the net suction head is less than the vapor pressure of the water, the water will vaporize in the pump, producing cavitation. Small vapor bubbles formed in the low-pressure region will collapse violently upon entering regions of high pressure, causing localized stress concentrations and vibrations, ultimately leading to mechanical failure.

The required net positive suction head ($NPSH_{req}$) for any pump can be obtained from the manufacturer. The available net positive suction head ($NPSH_{av}$) must be calculated for each system. Because the total energy of a system is constant, the available NPSH may be determined at any point in the system. The general expression at the pump centerline follows from Bernoulli as

$$NPSH_{av} = \frac{(p_{gauge} + p_{atm})}{\rho g} + z - h_L - \frac{p_{vp}}{\rho g} \qquad (62)$$

where

h_L = friction head loss in intake system piping (in feet of water)

p_{vp} = vapor pressure (0.256 psia for water at 20°C)

Knowing the pressure and pipe friction loss terms, the pump can be set at a height, z, which will ensure that $NPSH_{av} > NPSH_{req}$.

Where a free surface exists on the intake side (such as at the surface of an intake reservoir) and the velocity at a point on the surface is negligible, the above expression simplifies to

$$NPSH_{av} = z - h_L + \frac{(p_{atm} - p_{vp})}{\rho g} \qquad (63)$$

For pumps of relatively low heads and large discharge capacities (common in fire protection applications) the available NPSH may be less than zero (h_L is large). These pumps should be installed well below the reservoir water level to eliminate the possibility of cavitation. For this reason and also to avoid accidental loss of prime, authorities having jurisdiction generally require *positive suction* installation. In such instances the pump should be of the vertical shaft type so that the motor can be installed at an elevation above any possible flood level.

The useful work done by a pump is the product of the weight of the liquid pumped and the head developed by the pump. The work per unit time in this context is the hydraulic horsepower, commonly called the water horse-

power (WHP). For discharge, Q, in gpm, total dynamic head, h, in feet, and specific weight, γ, for water at 20°C (68°F),

$$WHP = \frac{Qh}{3960} \qquad (64)$$

The power required to actually drive the pump is the brake horsepower (BHP). The difference between water horsepower and brake horsepower is the power lost within the pump due to mechanical and hydraulic friction. The ratio of WHP to BHP is the pump efficiency, η_p. Similarly, the ratio of BHP to electrical or engine horsepower (EHP) is the motor efficiency, η_m. The overall efficiency is, then, the pump efficiency multiplied by the motor efficiency:

$$\eta = (\eta_p)(\eta_m) = \frac{WHP}{BHP} \cdot \frac{BHP}{EHP} \qquad (65)$$

Although WHP should be calculated using the specific weight of the fluid at known conditions of temperature and pressure, the variation for water is very small; it should be noted that pump motor sizes are chosen from standard available sizes in any case.

The interrelations of head, capacity, power, and efficiency for a given pump are known as the characteristics of the pump. They can be expressed graphically in the form of pump characteristic curves. Figure 4-2.21 shows a standard plot of the several variables at constant impeller speed (N). Note that the point of maximum operating efficiency on the head-capacity curve corresponds to the maximum value of the efficiency curve. The actual operating point of the pump, however, depends on the system demand (or system head) curve. The system head loss for any flow rate is the sum of the system friction head loss at that rate plus the total static head to be overcome in the system. Figure 4-2.22 illustrates the relationship. Recall from Figure 4-2.20 that the total static head is the difference in elevation between the discharge level and the suc-
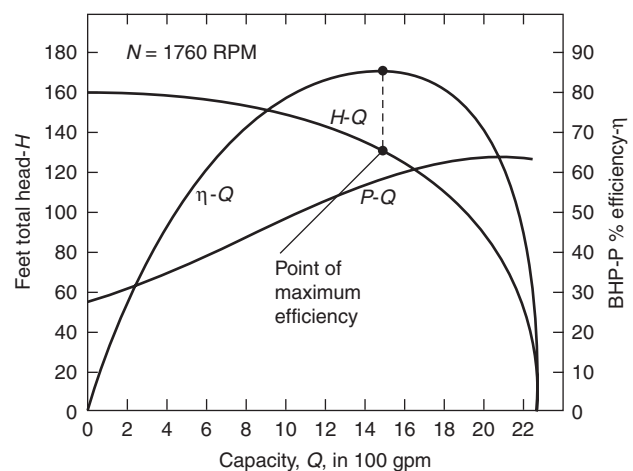
Figure 4-2.21. *Centrifugal pump characteristics.*
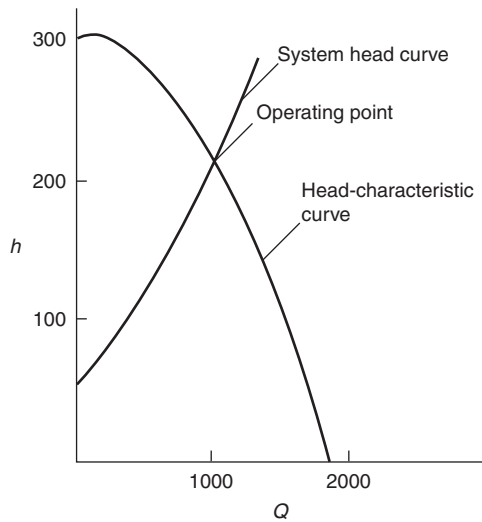
Figure 4-2.22. *Graphical determination of operating point.*

tion level. System friction losses may be determined by calculations methods given in previous sections.

Pump Selection

Economical pump selection for fire protection applications requires consideration of the following factors:

1. The maximum discharge rate required under the most demanding design conditions
2. The total head-capacity relation (characteristic curve)
3. The suction head—in particular, the net positive suction head available
4. Pump speed and power source requirements
5. Pump spatial and environmental requirements
6. The maximum allowable system head downstream of the pump discharge

The usual design condition is that a system will be given or will be chosen from a very limited range of possibilities, and the proper pump must be selected. As shown in Figure 4-2.22, when the system demand curve and the pump head-capacity curve are superimposed, their intersection will determine the operating point of the pump. This point also locates the efficiency and, therefore, the power requirements. It is often economically desirable to select a pump such that its operating point is at or near its peak efficiency. In many fire protection applications, however, a pump may be called upon to operate very infrequently. Power consumption may, therefore, not be a significant factor relative to initial cost. Common practice in fire protection applications is to select a pump to operate at 150 percent of rated capacity at 65 percent of rated head (see NFPA 20[8])—that is, an operating point farther out along the characteristic curve. A pump is chosen such that its operating point so defined meets or exceeds the system demand curve at that point.

If the pump is to be used as a *booster* to increase supply main pressure, care must be exercised to select a pump having a maximum discharge head at zero flow (also known as *churn* head), which, when added to the maximum main's supply head, does not exceed the maximum allowable working pressure on the system. The maximum allowable working pressure prescribed by NFPA 13, for example, is 175 psig.[9]

Centrifugal Pump Affinity Relations

The abstract concept of *pump specific speed* has been developed to simplify the description of pump performance characteristics. It consolidates the discharge, head, and speed (rpm) at optimum performance into a single number. For a single stage, single suction pump, specific speed may be calculated from

$$N_s = \frac{NQ^{1/2}}{H^{3/4}} \tag{66}$$

where Q (in gpm) is taken at pump rpm, N, and total dynamic head, H. The specific speed of a pump is not actually a speed for that pump in any physical sense; it is defined as the speed in revolutions per minute at which a homologous (geometrically similar) pump would run if constructed to deliver 1 gpm against 1 ft total head at its peak efficiency. For pump impeller designs of identical proportions but different sizes, the specific speed is a constant performance index. That is, the performance of any impeller can be predicted from knowledge of the performance of any other geometrically similar impeller.

Changing the impeller diameter results in changes in discharge, total head, and delivered power. These changes occur according to the follow relations:

$$\frac{Q_1}{Q_2} = \left(\frac{D_1}{D_2}\right)^3 \frac{n_1}{n_2} \tag{67a}$$

$$\frac{H_1}{H_2} = \left(\frac{D_1}{D_2}\right)^2 \left(\frac{n_1}{n_2}\right)^2 \tag{67b}$$

$$\frac{Q_1}{Q_2} = \left(\frac{H_1}{H_2}\right)^{1/2} \left(\frac{D_1}{D_2}\right)^2 \tag{67c}$$

$$\frac{\text{BHP}_1}{\text{BHP}_2} = \left(\frac{D_1}{D_2}\right)^5 \frac{\rho_1}{\rho_2} \frac{n_1^3}{n_2^3} \tag{67d}$$

Since

$$\frac{N_1}{N_2} = \frac{D_1}{D_2} \tag{68}$$

a change in motor speed only will yield similar results. That is, a change in impeller size has the same effect on pump performance as a change in speed provided, of course, that there is no marked change in operating efficiency.

EXAMPLE 5:

A 6-in. (152.4-mm) pump operating at 1770 rpm discharges 1500 gpm (5678 l/m) of water at 40°F against a 120-ft (36.6-m) head.

(a) What discharge capacity and total head can be expected from a homologous 8-in. (203-mm) pump operating at 1170 rpm?

(b) If the pumps operate at an overall 80 percent efficiency, what is the 8-in. (203-mm) pump power requirement?

SOLUTION:

(a) From Equation 67b,

$$H_2 = \left[\frac{8^2(1170)^2}{(6)^2(1770)^2} \right](120) = 93.2 \text{ ft (28.4 m)}$$

From Equation 67a,

$$Q_2 = \left[\frac{(8)^3(1170)}{(6)^3(1770)} \right](1500) = 2350 \text{ gpm (8895.5 l/m)}$$

(b) From Equation 64,

$$\text{WHP} = \frac{2350(93.2)}{3960} = 55.3 \text{ HP}$$

Therefore,

$$\text{BHP} = \frac{55.3}{0.8} = 69.1 \text{ HP}$$

The motor chosen would be the next highest standard horsepower rating.

If more discharge or more head is required than a single pump can provide, two or more pumps may be combined to provide the necessary output. For example, when discharge is too little, pumps may be installed in parallel, sharing the same suction and inlet conditions. Figure 4-2.23 illustrates the principle. If a pump provides sufficient discharge but too little head, a second pump may be installed in series, the output of the first pump being fed directly into the suction of the second pump. Figure 4-2.24 depicts the series arrangement. A variety of compound arrangements are possible, depending on details of actual supply and demand, with economics being the prime arbiter.

Figure 4-2.24.   *Two pumps combined in series.*

Nomenclature

A	area
C	proportionality constant or flow coefficient, Hazen-Williams *C*-factor
c	celerity of a shock wave
D	pipe diameter
d	element diameter
E	velocity of approach factor, bulk modulus of elasticity
f	Darcy-Weisbach friction loss factor
g	gravitational acceleration constant, 9.8 m/s²
H	head of water
h	head
h_c	height of centroid
h_L	head loss
I	moment of inertia
K	proportionality constant or flow coefficient
k	proportionality constant or flow coefficient
L	length of conduit (in friction loss equations)
l	length or distance
m	mass

Figure 4-2.23.   *Two pumps combined in parallel.*

N pump rpm

p pressure

Q volumetric discharge rate

Re   Reynolds number

S slope of energy gradient

s specific gravity

u stream velocity at a given point in flow cross section

V volume

v average stream velocity

z height above a reference datum (potential head)

α kinetic energy correction factor

β beta ratio

γ specific weight

Δ increment

ε pipe wall absolute roughness

η efficiency

μ absolute (dynamic) viscosity

ν kinematic viscosity

ρ density

τ fluid shear stress

References Cited

1. H.E. Hickey, *Hydraulics for Fire Protection,* National Fire Protection Association, Quincy, MA (1980).
2. R.P. Benedict, *Fundamentals of Pipe Flow,* Wiley-Interscience, New York (1980).
3. V.L. Streeter and E.G. Wylie, *Fluid Mechanics,* McGraw-Hill, New York (1979).
4. A.L. Simon, *Practical Hydraulics,* John Wiley & Sons, New York (1981).
5. F.M. White, *Fluid Mechanics,* McGraw-Hill, New York (1986).
6. T.M. Walski, *Analysis of Water Distribution Systems,* Van Nostrand Reinhold, New York (1984).
7. D. Stephenson, *Pipeflow Analysis,* Elsevier, Amsterdam (1984).
8. NFPA 20, *Installation of Centrifugal Fire Pumps,* National Fire Protection Association, Quincy, MA (1993).
9. NFPA 13, *Installation of Sprinkler Systems,* National Fire Protection Association, Quincy, MA (1994).

Additional Readings

R.A. Granger, *Fluid Mechanics,* Holt, Rinehart and Winston (CBS College Pub.), New York (1985).

N.H.C. Hwang, *Fundamentals of Hydraulic Engineering Systems,* Prentice-Hall, Englewood Cliffs, NJ (1981).

I.J. Karassik, ed., *Pump Handbook,* McGraw-Hill, New York (1986).

J.W. Murdock, *Fluid Mechanics and Its Applications,* Houghton Mifflin, Boston (1976).

CHAPTER 3

Automatic Sprinkler System Calculations

Russell P. Fleming

Introduction

Applications Where Water Is Appropriate

Water is the most commonly used fire extinguishing agent, mainly due to the fact that it is widely available and inexpensive. It also has very desirable fire extinguishing characteristics such as a high specific heat and high latent heat of vaporization. A single gallon of water can absorb 9280 Btus (2586.5 kJ) of heat as it increases from a 70°F (21°C) room temperature to become steam at 212°F (100°C).

Water is not the perfect extinguishing agent, however, and is considered inappropriate for the protection of certain water reactive materials. In some cases, the use of water can produce heat, flammable or toxic gases, or explosions. The quantities of such products must be considered, however, because application of sufficient water can overcome the reaction of minor amounts of these materials.

Another drawback of water is that it is more dense than most hydrocarbon fuels, and immiscible as well. Therefore, water will not provide an effective cover for burning hydrocarbons, or mix with them and dilute them to the point of not sustaining combustion. Instead, the hydrocarbons will float on top of the water, continuing to burn and possibly spread. To combat such fires, foam solutions can be introduced into the water to provide an effective cover and smother the fire. Applying water in a fine mist has also been successful.

However, even when water from sprinklers will not suppress the fire, its cooling ability can protect structural elements of a building by containing the fire until it can be extinguished by other means.

Russell P. Fleming, P.E., is vice president of engineering, National Fire Sprinkler Association, Patterson, New York. Mr. Fleming has served as a member of more than a dozen NFPA technical committees, including the Committee on Automatic Sprinklers. He currently serves on the Board of Directors of NFPA.

Types of Sprinkler Systems

Automatic sprinkler systems are considered to be the most effective and economical way to apply water to suppress a fire. There are four basic types of sprinkler systems:

1. A *wet pipe* system is by far the most common type of sprinkler system. It consists of a network of piping containing water under pressure. Automatic sprinklers are connected to the piping such that each sprinkler protects an assigned building area. The application of heat to any sprinkler will cause that single sprinkler to operate, permitting water to discharge over its area of protection.

2. A *dry pipe* system is similar to a wet system, except that water is held back from the piping network by a special dry pipe valve. The valve is kept closed by air or nitrogen pressure maintained in the piping. The operation of one or more sprinklers will allow the air pressure to escape, causing operation of the dry valve, which then permits water to flow into the piping to suppress the fire. Dry systems are used where the water in the piping would be subject to freezing.

3. A *deluge* system is one that does not use automatic sprinklers, but rather open sprinklers. A special deluge valve holds back the water from the piping, and is activated by a separate fire detection system. When activated, the deluge valve admits water to the piping network, and water flows simultaneously from all of the open sprinklers. Deluge systems are used for protection against rapidly spreading, high hazard fires.

4. A *preaction* system is similar to a deluge system except that automatic sprinklers are used, and a small air pressure is usually maintained in the piping network to ensure that the system is air tight. As with a deluge system, a separate detection system is used to activate a deluge valve, admitting water to the piping. However, because automatic sprinklers are used, the water is usually stopped from flowing unless heat from the fire has also activated one or more sprinklers. Some

special arrangements of preaction systems permit variations on detection system interaction with sprinkler operation. Preaction systems are generally used where there is special concern for accidental discharge of water, as in valuable computer areas.

These four basic types of systems differ in terms of the most fundamental aspect of how the water is put into the area of the fire. There are many other types of sprinkler systems, classified according to the hazard they protect (such as residential, in-rack, or exposure protection); additives to the system (such as antifreeze or foam); or special connections to the system (such as multipurpose piping). However, all sprinkler systems can still be categorized as one of the basic four types.

Applicable Standards

NFPA 13, *Standard for the Installation of Sprinkler Systems* (hereafter referred to as NFPA 13), is a design and installation standard for automatic sprinkler systems, referenced by most building codes in the United States and Canada.[1] This standard, in turn, references other NFPA standards for details as to water supply components, including NFPA 14, *Standard for the Installation of Standpipe and Hose Systems;* NFPA 20, *Standard for the Installation of Centrifugal Fire Pumps* (hereafter referred to as NFPA 20); NFPA 22, *Standard for Water Tanks for Private Fire Protection* (hereafter referred to as NFPA 22); and NFPA 24, *Standard for the Installation of Private Fire Service Mains and Their Appurtenances.*

For protection of warehouse storage, NFPA 13 traditionally referenced special storage standards that contained sprinkler system design criteria, including NFPA 231, *Standard for General Storage Materials* (hereafter referred to as NFPA 231); NFPA 231C, *Standard for Rack Storage of Materials* (hereafter referred to as NFPA 231C); NFPA 231D, *Standard for Rubber Tire Storage;* and NFPA 231F, *Standard for Roll Paper Storage.* However, beginning with the 1999 edition of NFPA 13 these standards were all merged into NFPA 13 to produce a consolidated sprinkler system design and installation standard.

Other NFPA standards contain design criteria for special types of occupancies or systems, including NFPA 13D, *Standard for the Installation of Sprinkler Systems in One- and Two-Family Dwellings and Manufactured Homes* (hereafter referred to as NFPA 13D); NFPA 15, *Standard for Water Spray Fixed Systems for Fire Protection;* NFPA 16, *Standard for the Installation of Foam-Water Sprinkler and Foam-Water Spray Systems;* NFPA 30, *Flammable and Combustible Liquids Code;* NFPA 30B, *Code for the Manufacture and Storage of Aerosol Products;* and NFPA 409, *Standard on Aircraft Hangars.*

Limits of Calculation
in an Empirical Design Process

Engineering calculations are best performed in areas where an understanding exists as to relationships between parameters. This is not the case with the technology of automatic sprinkler systems. Calculation methods are widely used with regard to only one aspect of sprinkler systems: water flow through piping. There are only very rudimentary calculation methods available with regard to the most fundamental aspect of sprinkler systems, i.e., the ability of water spray to suppress fires.

The reason that calculation methods are not used is simply the complexity of the mechanisms by which water suppresses fires. Water-based fire suppression has to this point not been thoroughly characterized to permit application of mathematical modeling techniques. As a result, the fire suppression aspects of sprinkler system design are empirical at best.

Some, but not all, of the current sprinkler system design criteria are based on full-scale testing, including the criteria originally developed for NFPA 231C and 13D, and parts of NFPA 13, such as the material on the use of large drop and ESFR (early suppression fast response) sprinklers. Most of the NFPA 13 protection criteria, however, are the result of evolution and application of experienced judgment. In the 1970s, the capabilities of pipe schedule systems, which had demonstrated a hundred years of satisfactory performance, were codified into a system of area/density curves. This permitted the introduction of hydraulic calculations to what had become a cookbook-type method of designing sprinkler systems. It allowed system designers to take advantage of strong water supplies to produce more economical systems. It also permitted the determination of specific flows and pressures available at various points of the system, opening the door to the use of "special sprinklers." Special sprinklers are approved for use on the basis of their ability to accomplish specific protection goals, but are not interchangeable since there is no standardization of minimum flows and pressures.

Because of this history, the calculation methods available to the fire protection engineer in standard sprinkler system design are only ancillary to the true function of a sprinkler system. The sections that follow in this chapter address hydraulic calculations of flow through piping, simple calculations commonly performed in determining water supply requirements, and optional calculations that may be performed with regard to hanging and bracing of system piping. The final section of this chapter deals with the performance of a system relative to a fire, and the material contained therein is totally outside the realm of standard practice. This material is not sufficiently complete to permit a full design approach, but only isolated bits of total system performance.

Hydraulic Calculations

Density-Based Sprinkler Demand

Occupancy hazard classification is the most critical aspect of the sprinkler system design process. If the hazard is underestimated, it is possible for fire to overpower the sprinklers, conceivably resulting in a large loss of property or life. Hazard classification is not an area in which calculation methods are presently in use, however. The proper classification of hazard requires experienced judgment and familiarity with relevant NFPA standards.

Once the hazard or commodity classification is determined and a sprinkler spacing and piping layout has

been proposed in conformance with the requirements of the standard, the system designer can begin a series of calculations to demonstrate that the delivery of a prescribed rate of water application will be accomplished for the maximum number of sprinklers that might be reasonably expected to operate. This number of sprinklers, which must be supplied regardless of the location of the fire within the building, is the basis of the concept of the remote design area. The designer needs to demonstrate that the shape and location of the sprinkler arrangement in the design area will be adequately supplied with water in the event of a fire.

Prior to locating the design area, there is the question of how many sprinklers are to be included. This question is primarily addressed by the occupancy hazard classification, but the designer also has some freedom to decide this matter.

Figure 7-2.3.1.2 of the 1999 edition of NFPA 13 and corresponding figures in NFPA 231 and 231C contain area/density curves from which the designer can select a design area and density appropriate for the occupancy hazard classification. Any point on or to the right of the curve in the figure(s) is acceptable. The designer may select a high density over a small area, or a low density over a large area. In either event, the fire is expected to be controlled by the sprinklers within that design area, without opening any additional sprinklers.

EXAMPLE 1:

Using the sample area/density curve shown in Figure 4-3.1, many different design criteria could be selected, ranging from a density of 0.1 gpm/ft² (3.7 mm/min) over 5000 ft² (500 m²) to 0.17 gpm/ft² (6.9 mm/min) over 1500 ft² (139 m²). Either of these two points, or any point to the right of the curve [such as 0.16 gpm/ft² (6.5 mm/min) over 3000 ft² (276 m²)] would be considered acceptable. A selection of 0.15 gpm/ft² (6.1 mm/min) over 2400 ft² (221 m²) is indicated.
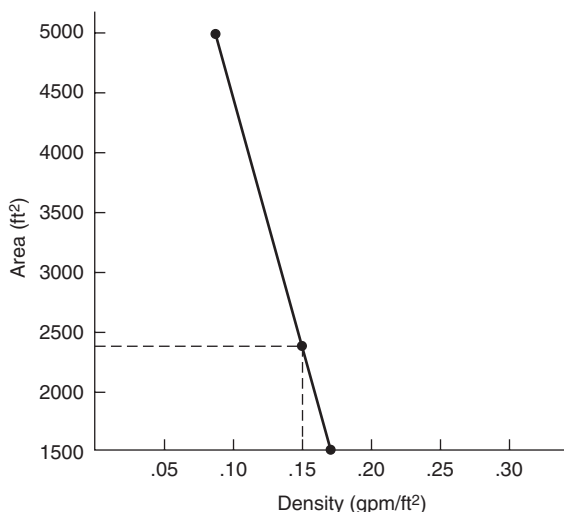
Figure 4-3.1.   *Sample area/density curve.*

Water is provided only for the number of sprinklers in the design area, since no water is needed for the sprinklers that are not expected to open. The actual number of sprinklers in the design area depends, of course, on the spacing of the sprinklers. NFPA 13 requires that the design area be divided by the maximum sprinkler spacing used, and that any fractional result be rounded up to the next whole sprinkler.

EXAMPLE 2:

Based on the point selected from the sample area/density curve above and the proposed maximum spacing of sprinklers, the number of sprinklers to be included in the design area can be determined. If sprinklers are spaced at 12 × 15 ft (3.66 × 4.57 m) so as to each protect an area of 180 ft² (16.72 m²), the design area of 2400 ft² (221 m²) would include

$$\frac{2400}{180} = 13.33 = 14 \text{ sprinklers}$$

The remote design area is required to have a rectangular shape, with the long side along the run of the branch lines. The length of the design area (needed to determine how many sprinklers along a branch line are contained within it) is found by multiplying the square root of the design area by a factor of 1.2. Again, any fractional result is rounded to the next whole sprinkler.

EXAMPLE 3:

If the 14 sprinklers from Example 2 were spaced 12 ft (3.66 m) along branch lines 15 ft (4.57 m) apart, the length of the rectangular area along the branch lines would be

$$\frac{1.2(2400)^{1/2}}{12} = \frac{1.2(49)}{12} = 4.9 = 5 \text{ sprinklers}$$

If the sprinklers were spaced 15 ft (4.57 m) along branch lines 12 ft (3.66 m) apart, the same length of the design area would include only 4 sprinklers.

NFPA 13 (1999) contains some exceptions to this method of locating a remote design area and determining the number of sprinklers to be supplied. Chapter 7 of the standard has special modifications to the design area based on factors such as the use of a dry system, the use of quick response sprinklers under flat smooth ceilings of limited height, and the existence of nonsprinklered combustible concealed spaces within the building. The chapter also contains a room design method, which can reduce the number of sprinklers expected to operate in a highly compartmented occupancy. Also, beginning in 1985, the standard adopted a four sprinkler design area for dwelling units and their adjacent corridors when residential sprinklers are installed in accordance with their listing requirements.

Figures in the appendix to Chapter 8 of NFPA 13 (1999 edition) show the normal documentation and the step-by-step calculation procedure for a sample sprinkler system. The starting point is the most remote sprinkler in the design area. For tree systems, in which each sprinkler is supplied from only one direction, the most remote sprinkler is generally the end sprinkler on the farthest branch line from the system riser. This sprinkler, and all

others as a result, must be provided with a sufficient flow of water to meet the density appropriate for the point selected on the area/density curve.

Where a sprinkler protects an irregular area, NFPA 13 prescribes that the area of coverage for the sprinkler must be based on the largest sides of its coverage. In other words, the area which a sprinkler protects for calculation purposes is equal to

$$\text{area of coverage} = S \times L$$

where S is twice the larger of the distances to the next sprinkler (or wall for an end sprinkler) in both the upstream and downstream directions, and L is twice the larger of the distances to adjacent branch lines (or wall in the case of the last branch line) on either side. This reflects the need to flow more water with increasing distance from the sprinkler, since increased flow tends to expand the effective spray umbrella of the sprinkler.

The minimum flow from a sprinkler must be the product of the area of coverage multiplied by the minimum required density

$$Q = \text{area of coverage} \times \text{density}$$

Most of the special listed sprinklers and residential sprinklers have a minimum flow requirement associated with their listings, which is often based on the spacing at which they are used. These minimum flow considerations override the minimum flow based on the area/density method.

EXAMPLE 4:

If a standard spray sprinkler protects an area extending to 7 ft (2.1 m) on the north side (half the distance to the next branch line), 5 ft (1.5 m) on the south side (to a wall), 6 ft (1.8 m) on the west side (half the distance to the next sprinkler on the branch line), and 4 ft (1.2 m) on the east side (to a wall), the minimum flow required for the sprinkler to achieve the density requirement selected in Example 1 can be found by completing two steps. The first step involves determining the area of coverage. In this case

$$S \times L = 2(6 \text{ ft}) \times 2(7 \text{ ft}) = 12 \text{ ft} \times 14 \text{ ft}$$
$$= 168 \text{ ft}^2 \ (15.6 \text{ m}^2)$$

The second step involves multiplying this coverage area by the required density

$$Q = A \times \rho = 168 \text{ ft}^2 \times 0.15 \text{ gpm/ft}^2$$
$$= 25.2 \text{ gpm} \ (95.4 \text{ lpm})$$

**Pressure Requirements
of the Most Remote Sprinkler**

When flow through a sprinkler orifice takes place, the energy of the water changes from the potential energy of pressure to the kinetic energy of flow. A formula can be derived from the basic energy equations to determine how much water will flow through an orifice based on the water pressure inside the piping at the orifice:

$$Q = 29.83 c_d d^2 P^{1/2}$$

However, this formula contains a factor, c_d, which is a discharge coefficient characteristic of the orifice and which must be determined experimentally. For sprinklers, the product testing laboratories determine the orifice discharge coefficient at the time of listing of a particular model of sprinkler. To simplify things, all factors other than pressure are lumped into what is experimentally determined as the *K*-factor of a sprinkler, such that

$$Q = K \times P^{1/2}$$

where K has units of gpm/(psi)$^{1/2}$ [lpm/(bar)$^{1/2}$].

If the required minimum flow at the most remote sprinkler is known, determined by either the area/density method or the special sprinkler listing, the minimum pressure needed at the most remote sprinkler can easily be found.

Since $\qquad Q = K(P)^{1/2}, \qquad$ then $P = (Q/K)^2$

NFPA 13 sets a minimum pressure of 7 psi (0.48 bar) at the end sprinkler in any event, so that a proper spray umbrella is ensured.

EXAMPLE 5:

The pressure required at the sprinkler in Example 4 can be determined using the above formula if the *K*-factor is known. The *K*-factor to be used for a standard orifice (nominal ½-in.) sprinkler is 5.6.

$$P = \left(\frac{Q}{K}\right)^2 = \left(\frac{25.2}{5.6}\right)^2 = 20.2 \text{ psi } (1.4 \text{ bar})$$

Once the minimum pressure at the most remote sprinkler is determined, the hydraulic calculation method proceeds backward toward the source of supply. If the sprinkler spacing is regular, it can be assumed that all other sprinklers within the design area will be flowing at least as much water, and the minimum density is assured. If spacing is irregular or sprinklers with different *K*-factors are used, care must be taken that each sprinkler is provided with sufficient flow.

As the calculations proceed toward the system riser, the minimum pressure requirements increase, because additional pressures are needed at these points if elevation and friction losses are to be overcome while still maintaining the minimum needed pressure at the most remote sprinkler. These losses are determined as discussed below, and their values added to the total pressure requirements. Total flow requirements also increase backward toward the source of supply, until calculations get beyond the design area. Then there is no flow added other than hose stream allowances.

It should be noted that each sprinkler closer to the source of supply will show a successively greater flow rate, since a higher total pressure is available at that point in the system piping. This effect on the total water demand is

termed hydraulic increase, and is the reason why the total water demand of a system is not simply equal to the product of the minimum density and the design area. When calculations are complete, the system demand will be known, stated in the form of a specific flow at a specific pressure.

Pressure Losses through Piping, Fittings, and Valves

Friction losses resulting from water flow through piping can be estimated by several engineering approaches, but NFPA 13 specifies the use of the Hazen-Williams method. This approach is based on the formula developed empirically by Hazen and Williams:

$$p = \frac{4.52Q^{185}}{C^{1.85}d^{4.87}}$$

where

p = friction loss per ft of pipe in psi

Q = flow rate in gpm

d = internal pipe diameter in inches

C = Hazen-Williams coefficient

The choice of C is critical to the accuracy of the friction loss determination, and is therefore stipulated by NFPA 13. The values assigned for use are intended to simulate the expected interior roughness of aged pipe. (See Table 4-3.1.)

Rather than make the Hazen-Williams calculation for each section of piping, it has become standard practice, when doing hand calculations, to use a friction loss table, which contains all values of p for various values of Q and various pipe sizes. In many cases the tables are based on the use of Schedule 40 steel pipe for wet systems. The use of other pipe schedules, pipe materials, or system types may require the use of multiplying factors.

Once the value of friction loss per foot is determined using either the previous equation or friction loss tables, the total friction loss through a section of pipe is found by multiplying p by the length of pipe, L. Since NFPA 13 uses p to designate loss per foot, total friction loss in a length of pipe can be designated by p_f, where

$$p_f = p \times L$$

In the analysis of complex piping arrangements, it is sometimes convenient to lump the values of all factors in the Hazen-Williams equation (except flow) for a given piece of pipe into a constant, K, identified as a friction loss coeffi-

cient. To avoid confusion with the nozzle coefficient K, this coefficient can be identified as FLC, friction loss coefficient.

$$\text{FLC} = \frac{(L \times 4.52)}{(C^{1.85}d^{4.87})}$$

The value of p_f is therefore equal to

$$p_f = \text{FLC} \times Q^{1.85}$$

EXAMPLE 6:

If the most remote sprinkler on a branch line requires a minimum flow of 25.2 gpm (92.1 lpm) (for a minimum pressure of 20.2 psi [1.4 bar]) as shown in Examples 4 and 5, and the second sprinkler on the line is connected by a 12-ft (3.6-m) length of 1 in. (25.4 mm) Schedule 40 steel pipe, with both sprinklers mounted directly in fittings on the pipe (no drops or sprigs), the minimum pressure required at the second sprinkler can be found by determining the friction loss caused by a flow of 25.2 gpm (92.1 lpm) through the piping to the end sprinkler. No fitting losses need to be considered if it is a straight run of pipe, since NFPA 13 permits the fitting directly attached to each sprinkler to be ignored.

Using the Hazen-Williams equation with values of 25.2 for Q, 120 for C, and 1.049 for d (the inside diameter of Schedule 40 steel 1-in. pipe) results in a value of $p = 0.20$ psi (0.012 bar) per foot of pipe. Multiplying by the 12-ft (3.6-m) length results in a total friction loss of $p_f = 2.4$ psi (0.17 bar). The total pressure required at the second sprinkler on the line is therefore 20.2 psi + 2.4 psi = 22.6 psi (1.6 bar). This will result in a flow from the second sprinkler of $Q = K(P)^{1/2} = 26.6$ gpm (100.7 lpm).

Minor losses through fittings and valves are not friction losses but energy losses, caused by turbulence in the water flow which increase as the velocity of flow increases. Nevertheless, it has become standard practice to simplify calculation of such losses through the use of "equivalent lengths," which are added to the actual pipe length in determining the pipe friction loss. NFPA 13 contains a table of equivalent pipe lengths for this purpose. (See Table 4-3.2.) As an example, if a 2-in. (50.8-mm) 90-degree long turn elbow is assigned an equivalent length of 3 ft (0.914 m), this means that the energy loss associated with turbulence through the elbow is expected to approximate the energy loss to friction through 0.914 m of 50.8 mm pipe. As with the friction loss tables, the equivalent pipe length chart is based on the use of steel pipe with a C-factor of 120, and the use of other piping materials requires multiplying factors. The equivalent pipe length for pipes having C values other then 120 should be adjusted using the following multiplication factors: 0.713 for a C value of 100; 1.16 for a C value of 130; 1.33 for a C value of 140; 1.51 for a C value of 150.

EXAMPLE 7:

If the 12-ft (3.6-m) length of 1-in. (25.4-mm) pipe in Example 6 had contained 4 elbows so as to avoid a building column, the pressure loss from those elbows could be approximated by adding an equivalent length of pipe to the friction loss calculation. Table 4-3.2 gives a value of 2 ft (0.610 m) as the appropriate equivalent length for standard elbows in 1 in. (25.4 mm) Schedule 40 steel pipe. For

Table 4-3.1   *C Values for Pipes*

Type of Pipe	Assigned C Factor
Steel pipe—dry and preaction systems	100
Steel pipe—wet and deluge systems	120
Galvanized steel pipe—all systems	120
Cement lined cast or ductile iron	140
Copper tube	150
Plastic (listed)	150

Table 4-3.2 *Equivalent Pipe Length Chart (for C = 120)*

Fittings and Valves	Fittings and Valves Expressed in Equivalent Feet of Pipe													
	¾ in.	1 in.	1¼ in.	1½ in.	2 in.	2½ in.	3 in.	3½ in.	4 in.	5 in.	6 in.	8 in.	10 in.	12 in.
45° Elbow	1	1	1	2	2	3	3	3	4	5	7	9	11	13
90° Standard Elbow	2	2	3	4	5	6	7	8	10	12	14	18	22	27
90° Long Turn Elbow	1	2	2	2	3	4	5	5	6	8	9	13	16	18
Tee or Cross (Flow Turned 90°)	3	5	6	8	10	12	15	17	20	25	30	35	50	60
Butterfly Valve	—	—	—	—	6	7	10	—	12	9	10	12	19	21
Gate Valve	—	—	—	—	1	1	1	1	2	2	3	4	5	6
Swing Check[a]	—	5	7	9	11	14	16	19	22	27	32	45	55	65

For SI Units: 1 ft = 0.3048 m.

[a]Due to the variations in design of swing check valves, the pipe equivalents indicated in the above chart are to be considered average.

4 elbows, the equivalent fitting length would be 8 ft (2.4 m). Added to the actual pipe length of 12 ft (3.6 m), the total equivalent length would be 20 ft (6 m). This results in a new value of $p_f = 20$-ft · 0.20 psi/ft = 4.0 psi (0.28 bar). The total pressure at the second sprinkler would then be equal to 20.2 psi + 4.0 psi = 24.2 psi (1.67 bar). The total flow from the second sprinkler in this case would be $Q = K(P)^{1/2} = 27.5$ gpm (100.4 lpm).

Some types of standard valves, such as swing check valves, are included in the equivalent pipe length chart, Table 4-3.2. Equivalent lengths for pressure losses through system alarm, dry, and deluge valves are determined by the approval laboratories at the time of product listing.

Use of Velocity Pressures

The value of pressure, *P*, in the sprinkler orifice flow formula can be considered either the total pressure, P_t, or the normal pressure, P_n, since NFPA 13 permits the use of velocity pressures at the discretion of the designer. Total pressure, normal pressure, and velocity pressure, P_v, have the following relationship:

$$P_n = P_t - P_v$$

Total pressure is the counterpart of total energy or total head, and can be considered the pressure that would act against an orifice if all of the energy of the water in the pipe at that point were focused toward flow out of the orifice. This is the case where there is no flow past the orifice in the piping. Where flow does take place in the piping past an orifice, however, normal pressure is that portion of the total pressure which is actually acting normal to the direction of flow in the piping, and therefore acting in the direction of flow through the orifice. The amount by which normal pressure is less than total pressure is velocity pressure, which is acting in the direction of flow in the piping. Velocity pressure corresponds to velocity energy, which is the energy of motion. There is no factor in the above expression for elevation head, because the flow from an orifice can be considered to take place in a datum plane.

When velocity pressures are used in calculations, it is recognized that some of the energy of the water is in the form of velocity head, which is not acting normal to the pipe walls (where it would help push water out the orifice), but rather in the downstream direction. Thus, for every sprinkler (except the end sprinkler on a line), slightly less flow takes place than what would be calculated from the use of the formula $Q = K(P_t)^{1/2}$. (See Figure 4-3.2.)

NFPA 13 permits the velocity pressure effects to be ignored, however, since they are usually rather minor, and since ignoring the effects of velocity pressure tends to produce a more conservative design.

If velocity pressures are considered, normal pressure rather than total pressure is used when determining flow through any sprinkler except the end sprinkler on a branch line, and through any branch line except the end branch line on a cross main. The velocity pressure, P_v, which is subtracted from the total pressure in order to determine the normal pressure, is determined as

$$P_v = \frac{v^2}{2g} \times 0.433 \text{ psi/ft (0.098 bar/m)}$$

or

$$P_v = 0.001123Q^2/d^4$$
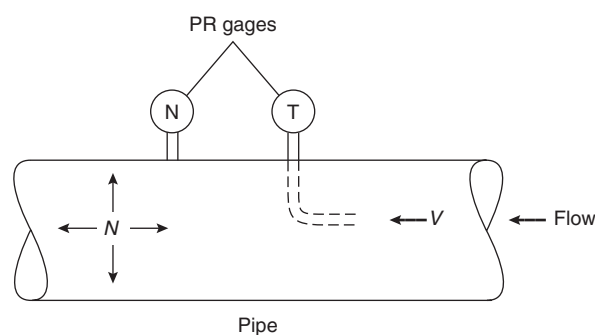
Figure 4-3.2. *Velocity and normal pressures in piping.*

where Q is the upstream flow through the piping to an orifice (or branch line) in gpm and d is the actual internal diameter of the upstream pipe in inches.

Because NFPA 13 mandates the use of the upstream flow, an iterative approach to determining the velocity pressure is necessary. The upstream flow cannot be known unless the flow from the sprinkler (or branch line) in question is known, and the flow from the sprinkler (or branch line) is affected by the velocity pressure resulting from the upstream flow.

EXAMPLE 8:

If the pipe on the upsteam side of the second sprinkler in Example 6 were 3 in. Schedule 40 steel pipe with an inside diameter of 1.38 in. (35 mm), the flow from the second sprinkler would be considered to be 26.6 gpm (100.2 lpm) as determined at the end of Example 6, if velocity pressures were not included.

If velocity pressures were to be considered, an upstream flow would first be assumed. Since the end sprinkler had a minimum flow of 25.2 gpm (95.2 lpm) and the upstream flow would consist of the combined flow rates of the two sprinklers, an estimate of 52 gpm (196.8 lpm) might appear reasonable. Substituting this flow and the pipe diameter into the equation for velocity pressure gives

$$P_v = \frac{0.001123Q^2}{d^4}$$
$$= \frac{0.001123(52)^2}{(1.38)^4}$$
$$= 0.8 \text{ psi } (0.06 \text{ bar})$$

This means that the actual pressure acting on the orifice of the second sprinkler is equal to

$$P_n = P_t - P_v$$
$$= 22.6 \text{ psi} - 0.8 \text{ psi}$$
$$= 21.8 \text{ psi } (1.50 \text{ bar})$$

This would result in a flow from the second sprinkler of

$$Q = K(P)^{1/2}$$
$$= 26.1 \text{ gpm } (98.7 \text{ lpm})$$

Combining this flow with the known flow from the end sprinkler results in a total upstream flow of 51.3 gpm (194.2 lpm). To determine if the initial guess was close enough, determine the velocity pressure that would result from an upstream flow of 51.3 gpm (194.2 lpm). This calculation also results in a velocity pressure of 0.8 psi (0.06 bar), and the process is therefore complete. It can be seen that the second sprinkler apparently flows 0.5 gpm (1.9 lpm) less through the consideration of velocity pressures.

Elevation Losses

Variation of pressure within a fluid at rest is related to the density or unit (specific) weight of the fluid. The unit weight of a fluid is equal to its density multiplied by the acceleration of gravity. The unit weight of water is 62.4 lbs/ft³ (1000 kg/m³).

This means that one cubic foot of water at rest weighs 62.4 pounds (1000 kg). The cubic foot of water, or any other water column one foot high, thus results in a static pressure at its base of 62.4 pounds per square foot (304.66 kg/m²). Divided by 144 sq in. per sq ft (1.020×10^4 kg/m³ bar), this is a pressure of 0.433 pounds per sq in. per ft (0.099 bar/m) of water column.

A column of water 10 ft (3.048 m) high similarly exerts a pressure of 10 ft $\times$ 62.4 lbs/ft² $\times$ 1 ft/144 in.² = 4.33 psi (3.048 m $\times$ 999.5 kg/m² ÷ 1.020×10^4 kg/m² bar = 0.299 bar). The static pressure at the top of both columns of water is equal to zero (gauge pressure), or atmospheric pressure.

On this basis, additional pressure must be available within a sprinkler system water supply to overcome the pressure loss associated with elevation. This pressure is equal to 0.433 psi per foot (0.099 bar/m) of elevation of the sprinklers above the level where the water supply information is known.

Sometimes the additional pressure needed to overcome elevation is added at the point where the elevation change takes place within the system. If significant elevation changes take place within a portion of the system that is likely to be considered as a representative flowing orifice (such as a single branch line along a cross main that is equivalent to other lines in the remote design area), then it is considered more accurate to wait until calculations have been completed, and simply add an elevation pressure increase to account for the total height of the highest sprinklers above the supply point.

EXAMPLE 9:

The pressure that must be added to a system supply to compensate for the fact that the sprinklers are located 120 ft (36.6 m) above the supply can be found by multiplying the total elevation difference by 0.433 psi/ft (0.099 bar/m).

$$120 \text{ ft} \times 0.433 \text{ psi/ft} = 52 \text{ psi } (3.62 \text{ bar})$$

Loops and Grids

Hydraulic calculations become more complicated when piping is configured in loops or grids, such that water feeding any given sprinkler or branch line can be supplied through more than one route. A number of computer programs that handle the repetitive calculations have therefore been developed specifically for fire protection systems, and are being marketed commercially.

Determining the flow split that takes place in the various parts of any loop or grid is accomplished by applying the basic principles of conservation of mass and conservation of energy. For a single loop, it should be recognized that the energy loss across each of the two legs from one end of the system to the other must be equal. Otherwise, a circulation would take place within the loop itself. Also, mass is conserved by the fact that the sum of the two individual flows through the paths is equal to the total flow into (and out of) the loop. (See Figure 4-3.3.)
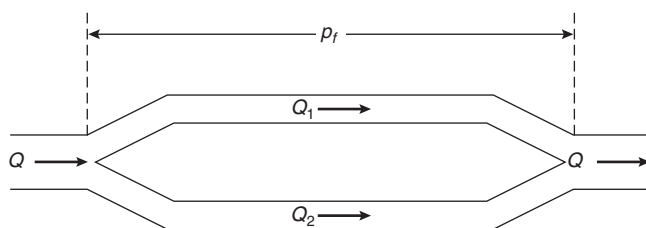
Figure 4-3.3. *Example of a simple loop configuration.*

Applying the Hazen-Williams formula to each leg of the loop

$$p_f = L_1 \frac{4.52 Q_1^{1.85}}{C_1^{1.85} d_1^{4.87}} = L_2 \frac{4.52 Q_2^{1.85}}{C_2^{1.85} d_2^{1.85}}$$

Substituting the term FLC for all terms except Q,

$$p_f = \text{FLC}_1 Q_1^{1.85} = \text{FLC}_2 Q_2^{1.85}$$

This simplifies to become

$$\left(\frac{Q_1}{Q_2}\right)^{1.85} = \frac{\text{FLC}_2}{\text{FLC}_1}$$

Since Q_1 and Q_2 combine to create a total flow of Q, the flow through one leg can be determined as

$$Q_1 = \frac{Q}{[(\text{FLC}_1/\text{FLC}_2)^{0.54} + 1]}$$

For the simplest of looped systems, a single loop, hand calculations are not complex. Sometimes, seemingly complex piping systems can be simplified by substituting an "equivalent pipe" for two or more pipes in series or in parallel.

For pipes in series

$$\text{FLC}_e = \text{FLC}_1 + \text{FLC}_2 + \text{FLC}_3 + \cdots$$

For pipes in parallel

$$\left(\frac{1}{\text{FLC}_e}\right)^{0.54} = \left(\frac{1}{\text{FLC}_1}\right)^{0.54} + \left(\frac{1}{\text{FLC}_2}\right)^{0.54} + \cdots$$

For gridded systems, which involve flow through multiple loops, computers are generally used since it becomes necessary to solve a system of nonlinear equations. When hand calculations are performed, the Hardy Cross[2] method of balancing heads is generally employed. This method involves assuming a flow distribution within the piping network, then applying successive corrective flows until differences in pressure losses through the various routes are nearly equal.

The Hardy Cross solution procedure applied to sprinkler system piping is as follows:

1. Identify all loop circuits and the significant parameters associated with each line of the loop, such as pipe length, diameter, and Hazen-Williams coefficient. Reduce the number of individual pipes where possible by finding the equivalent pipe for pipes in series or parallel.
2. Evaluate each parameter in the proper units. Minor losses through fittings should be converted to equivalent pipe lengths. A value of all parameters except flow for each pipe section should be calculated (FLC).
3. Assume a reasonable distribution of flows that satisfies continuity, proceeding loop by loop.
4. Compute the pressure (or head) loss due to friction, p_f, in each pipe using the FLC in the Hazen-Williams formula.
5. Sum the friction losses around each loop with due regard to sign. (Assume clockwise positive, for example.) Flows are correct when the sum of the losses, dp_f, is equal to zero.
6. If the sum of the losses is not zero for each loop, divide each pipe's friction loss by the presumed flow for the pipe, p_f/Q.
7. Calculate a correction flow for each loop as

$$dQ = \frac{-dp_f}{[1.85\Sigma(p_f/Q)]}$$

8. Add the correction flow values to each pipe in the loop as required, thereby increasing or decreasing the earlier assumed flows. For cases where a single pipe is in two loops, the algebraic difference between the two values of dQ must be applied as the correction to the assumed flow.
9. With a new set of assumed flows, repeat steps 4 through 7 until the values of dQ are sufficiently small.
10. As a final check, calculate the pressure loss by any route from the initial to the final junction. A second calculation along another route should give the same value within the range of accuracy expected.

NFPA 13 requires that pressures be shown to balance within 0.5 psi (0.03 bar) at hydraulic junction points. In other words, the designer (or computer program) must continue to make successive guesses as to how much flow takes place in each piece of pipe until the pressure loss from the design area back to the source of supply is approximately the same (within 0.5 psi [0.03 bar]) regardless of the path chosen.

EXAMPLE 10:
For the small two-loop grid shown in Figure 4-3.4, the total flow in and out is 100 gpm (378.5 lpm). It is necessary to determine the flow taking place through each pipe section. The system has already been simplified by finding the equivalent pipe for all pipes in series and in parallel. The following values of FLC have been calculated:

Pipe 1 FLC = 0.001
Pipe 2 FLC = 0.002
Pipe 3 FLC = 0.003
Pipe 4 FLC = 0.001
Pipe 5 FLC = 0.004
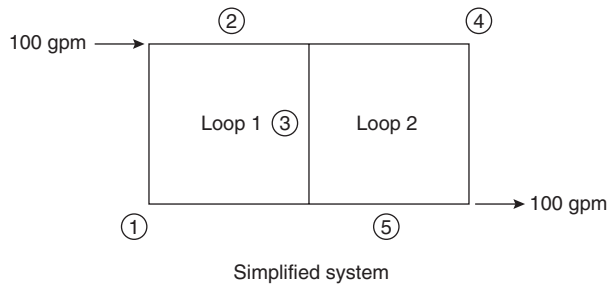
Figure 4-3.4. *Simplified system, pipe in series.*

Original flow assumptions

Figure 4-3.5. *Original flow assumptions.*

Under step 3 of the Hardy Cross procedure, flows that would satisfy conservation of mass are assumed. (See Figure 4-3.5.) Steps 4 through 9 are then carried out in a tabular approach. (See Table 4-3.3.)

Making these adjustments to again balance flows, a second set of iterations can be made. (See Table 4-3.4.) For pipe segment 3, the new flow is the algebraic sum of the original flow plus the flow corrections from both loops. (See Figures 4-3.6 and 4-3.7.)

In starting the third iteration, it can be seen that the pressure losses around both loops are balanced within 0.5 psi. (See Table 4-3.5.) Therefore, the flow split assumed after two iterations can be accepted. As a final check, step 10 of the above procedure calls for a calculation of the total pressure loss through two different routes, requiring that they balance within 0.5 psi (0.03 bar):

Route through pipes 1 and 5:

$$FLC_1, (Q_1)^{1.85} + FLC_2(Q_2)^{1.85}$$
$$= 0.001(54.0)^{1.85} + 0.004(35.9)^{1.85}$$
$$= 1.6 + 3.0 = 4.6 \text{ psi (0.32 bar)}$$

Route through Pipes 2 and 4:

$$0.002(46.0)^{1.85} + 0.001(64.1)^{1.85} = 2.4 + 2.2$$
$$= 4.6 \text{ psi (0.32 bar)}$$

This is acceptable. Note that it required only two iterations to achieve a successful solution despite the fact that the initial flow assumption called for reverse flow in pipe 3. The initial assumption was for a clockwise flow of 5 gpm (18.9 lpm) in pipe 3, but the final solution shows a counterclockwise flow of 18.1 gpm (68.5 lpm).

Table 4-3.3   *First Iteration*

Loop	Pipe	Q	FLC	p_f	dp_f	(p_f/Q)	$dQ = -dp_f/1.85[\sum(p_f/Q)]$	$Q + dQ$
1	1	−40	0.001	−0.92		0.023	$dQ = -16.4$	−56.4
	2	60	0.002	3.90		0.065		+43.6
	3	5	0.003	0.06		0.012		−11.4
					= 3.04	0.100		
2	3	−5	0.003	−0.06		0.012	$dQ = 11.2$	+6.2
	4	55	0.001	1.66		0.030		+66.2
	5	−45	0.004	−4.58		0.102		+33.8
					= −2.98	0.144		

Table 4-3.4   *Second Iteration*

Loop	Pipe	Q	FLC	p_f	dp_f	(p_f/Q)	$dQ = -dp_f/1.85[\sum(p_f/Q)]$	$Q + dQ$
1	1	−56.4	0.001	−1.74		0.031		−54.0
	2	43.6	0.002	2.16		0.050		+46.0
	3	−22.6	0.003	−0.96		0.042	$dQ = 2.4$	−20.2
					= −0.54	0.123		
2	3	22.6	0.003	0.96		0.042		+20.5
	4	66.2	0.001	2.34		0.035		+64.1
	5	−33.8	0.004	−2.69		0.080	$dQ = -2.1$	+35.9
					= 0.61	0.157		
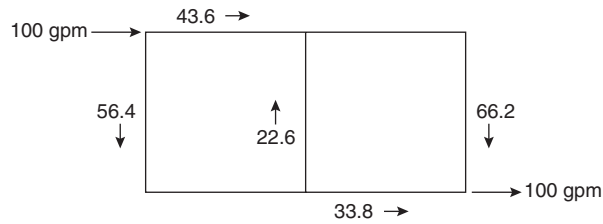
Figure 4-3.6. *Corrected flows after first iteration.*
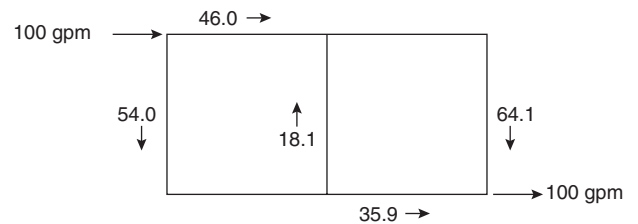
Figure 4-3.7. *Corrected flows after second iteration.*

Table 4-3.5 *Third Iteration*

Loop	Pipe	Q	FLC	p_f	dp_f	(p_f/Q)	$dQ = -dp_f/1.85[\sum(p_f/Q)]$	Q + dQ
1	1	−54.0	0.001	−1.60				
	2	46.0	0.002	2.38				
	3	−18.1	0.003	−0.64				
					= 0.14			
2	3	18.1	0.003	0.64				
	4	64.1	0.001	2.20				
	5	−35.9	0.004	−3.01				
					= −0.17			

Water Supply Calculations

Determination of Available Supply Curve

Testing a public or private water supply permits an evaluation of the strength of the supply in terms of both quantity of flow and available pressures. The strength of a water supply is the key to whether it will adequately serve a sprinkler system.

Each test of a water supply must provide at least two pieces of information—a static pressure and a residual pressure at a known flow. The static pressure is the "no flow" condition, although it must be recognized that rarely is any public water supply in a true no flow condition. But this condition does represent a situation where the fire protection system is not creating an additional flow demand beyond that which is ordinarily placed on the system. The residual pressure reading is taken with an additional flow being taken from the system, preferably a flow that approximates the likely maximum system demand.

Between the two (or more) points, a representation of the water supply (termed a water supply curve) can be made. For the most part, this water supply curve is a fingerprint of the system supply and piping arrangements, since the static pressure tends to represent the effect of elevated tanks and operating pumps in the system, and the drop to the residual pressure represents the friction and minor losses through the piping network that result from the increased flow during the test.

The static pressure is read directly from a gauge attached to a hydrant. The residual pressure is read from the same gauge while a flow is taken from another hydrant, preferably downstream. A pitot tube is usually used in combination with observed characteristics of the nozzle though which flow is taken in order to determine the amount of flow. Chapter 7 of NFPA 13 provides more thorough information on this type of testing.

Figure A-8-3.2(d) of NFPA 13 (1999 edition) is an example of a plot of water supply information. The static pressure is plotted along the *y*-axis, reflecting a given pressure under zero flow conditions. The residual pressure at the known flow is also plotted, and a straight line is drawn between these two points. Note that the *x*-axis is not linear, but rather shows flow as a function of the 1.85 power. This corresponds to the exponent for flow in the Hazen-Williams equation. Using this semi-exponential graph paper demonstrates that the residual pressure effect is the result of friction loss through the system, and permits the water supply curve to be plotted as a straight line. Since the drop in residual pressure is proportional to flow to the 1.85 power, the available pressure at any flow can be read directly from the water supply curve.

For adequate design, the system demand point, including hose stream allowance, should lie below the water supply curve.

EXAMPLE 11:
If a water supply is determined by test to have a static pressure of 100 psi (6.9 bar) and a residual pressure of 80 psi (5.5 bar) at a flow of 1000 gpm (3785 lpm), the pressure available at a flow of 450 gpm (1703 lpm) can be approximated by plotting the two known data points on the hydraulic graph paper as shown in Figure 4-3.8. At a flow of 450 gpm (1703 lpm), a pressure of 90 psi (6.2 bar) is indicated.
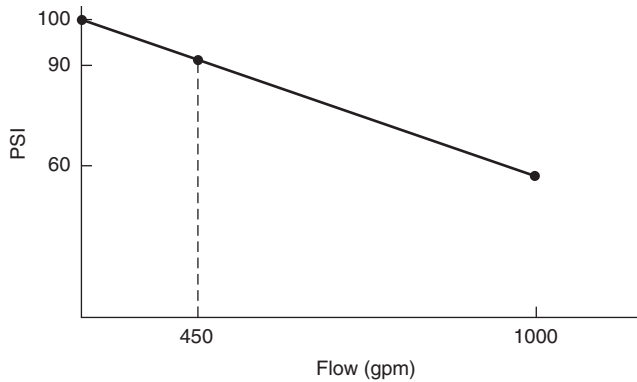
Figure 4-3.8. *Pressure available from 450 gpm flow water supply.*

Figure 4-3.9. *Pump performance curve.*

Pump Selection and Testing

Specific requirements for pumps used in sprinkler systems are contained in NFPA 20, which is cross-referenced by NFPA 13.

Fire pumps provide a means of making up for pressure deficiencies where an adequate volume of water is available at a suitable net positive suction pressure. Plumbing codes sometimes set a minimum allowable net positive suction pressure of 10 to 20 psi (0.69 to 1.38 bar). If insufficient water is available at such pressures, then it becomes necessary to use a stored water supply.

Listed fire pumps are available with either diesel or electric drivers, and with capacities ranging from 25 to 5000 gpm (95 to 18,927 lpm), although fire pumps are most commonly found with capacities ranging from 250 to 2500 gpm (946 to 9463 lpm) in increments of 250 up to 1500 gpm (946 up to 5678 lpm) and 500 gpm (1893 lpm) beyond that point. Each pump is specified with a rated flow and rated pressure. Rated pressures vary extensively, since manufacturers can control this feature with small changes to impeller design.

Pump affinity laws govern the relationship between impeller diameter, D, pump speed, N, flow, Q, pressure head, H, and brake horsepower, bhp. The first set of affinity laws assumes a constant impeller diameter.

$$\frac{Q_1}{Q_2} = \frac{N_1}{N_2} \qquad \frac{H_1}{H_2} = \frac{N_1}{N_2} \qquad \frac{bhp_1}{bhp_2} = \frac{N_1}{N_2}$$

These affinity laws are commonly used when correcting the output of a pump to its rated speed.

The second set of the affinity laws assumes constant speed with change in impeller diameter, D.

$$\frac{Q_1}{Q_2} = \frac{D_1}{D_2} \qquad \frac{H_1}{H_2} = \frac{D_1}{D_2} \qquad \frac{bhp_1}{bhp_2} = \frac{D_1}{D_2}$$

Pumps are selected to fit the system demands on the basis of three key points relative to their rated flow and rated pressure. (See Figure 4-3.9.) NFPA 20 specifies that each horizontal fire pump must meet these characteristics, and the approval laboratories ensure these points are met:
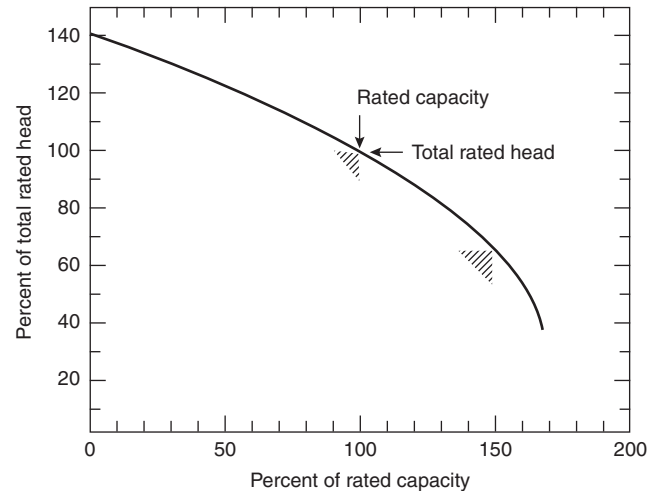
1. A minimum of 100 percent of rated pressure at 100 percent of rated flow.
2. A minimum of 65 percent of rated pressure at 150 percent of rated flow.
3. A maximum of 140 percent of rated pressure at 0 percent of rated flow (churn).

Even before a specific fire pump has been tested, therefore, the pump specifier knows that a given pump can be expected to provide certain performance levels. It is usually possible to have more than one option when choosing pumps, since the designer is not limited to using a specific point on the pump performance curve.

There are limits to flexibility in pump selection, however. For example, it is not permitted to install a pump in a situation where it would be expected to operate with a flow exceeding 150 percent of rated capacity, since the performance is not a known factor, and indeed available pressure is usually quick to drop off beyond this point.

NFPA 20 gives the following guidance on what part of the pump curve to use:[1]

A centrifugal fire pump should be selected in the range of operation from 90 percent to 150 percent of its rated capacity. The performance of the pump when applied at capacities over 140 percent of rated capacity may be adversely affected by the suction conditions. Application of the pump at capacities less than 90 percent of the rated capacity is not recommended.

The selection and application of the fire pump should not be confused with pump operating conditions. With proper suction conditions, the pump can operate at any point on its characteristic curve from shutoff to 150 percent of its rated capacity.

For design capacities below the rated capacity, the rated pressure should be used. For design capacities between 100 and 150 percent of rated capacity, the pressure

used should be found by the relationship made apparent by similar triangles.

$$\frac{0.35P}{0.5Q} = \frac{P' - 0.65P}{1.5Q - Q'}$$

where P and Q are the rated pressure and capacity, and P' is the minimum available pressure at capacity, Q', where $Q < Q' < 1.5Q$.

EXAMPLE 12:

A pump is to be selected to meet a demand of 600 gpm (2271 lpm) at 85 psi (5.86 bar). To determine whether a pump rated for 500 gpm (1893 lpm) at 100 psi (6.90 bar) would be able to meet this point without having an actual pump performance curve to work from, the above formula can be applied, with $P = 100$, $Q = 500$, and $Q' = 600$.

Inserting these values gives

$$\frac{(0.35)(100)}{(0.5)(500)} = \frac{[P' - (0.65)(100)]}{[(1.5)(500) - 600]}$$

$$\frac{35}{250} = \frac{(P' - 65)}{(750 - 600)}$$

$$P' = 65 + 21 = 86 \text{ psi (5.93 bar)}$$

Since the value of P' so calculated is greater than the 85 psi (5.86 bar) required, the pump will be able to meet the demand point.

Tank Sizing

Tank selection and sizing are relatively easy compared to pump selection. The most basic question is whether to use an elevated storage (gravity) tank, a pressure tank, or a suction tank in combination with a pump. Following that is a choice of materials. NFPA 22 is the governing standard for water tanks for fire protection, and includes a description of the types of tanks as well as detailed design and connection requirements.

From a calculation standpoint, tanks must be sized to provide the minimum durations specified by NFPA 13 or other applicable standards for the system design. Required pressures must still be available when the tanks are at the worst possible water level condition (i.e., nearly empty).

If the tank is intended to provide the needed supply without the use of a pump, the energy for the system must be available from the height of a gravity tank or the air pressure of a pressure tank.

An important factor in gravity tank calculations is the requirement that the pressure available from elevation [calculated using 0.433 psi per foot (0.099 bar/m)] must be determined using the lowest expected level of water in the tank. This is normally the point at which the tank would be considered empty.

In sizing pressure tanks, the percentage of air in the tanks must be controlled so as to ensure that the last water leaving the tank will be at an adequate pressure. While a common rule of thumb has been that the tank should be one-third air at a minimum pressure of 75 psi (5.17 bar), this rule does not hold true for systems with high pres-

sure demands or where the tank is located a considerable distance below the level of the highest sprinkler.

For pipe schedule systems, two formulas have traditionally been used, based on whether the tank is located above the level of the highest sprinkler or some distance below.

For the tank above the highest sprinkler

$$P = \frac{30}{A} - 15$$

For the tank below the highest sprinkler

$$P = \left(\frac{30}{A} - 15\right) + \left(\frac{0.434H}{A}\right)$$

where

A = proportion of air in the tank

P = air pressure carried in the tank in psi

H = height of the highest sprinkler above the tank bottom in feet

It can be seen that these formulas are based simply on the need to provide a minimum pressure of 15 psi (1.03 bar) to the system at the level of the highest sprinkler, and an assumption of 15 psi (1.03 bar) atmospheric pressure.

Using the same approximation for atmospheric pressure, a more generalized formula has come into use for hydraulically designed systems:

$$P_i = \frac{P_f + 15}{A} - 15$$

where

P_i = tank air pressure to be used

P_f = system pressure required per hydraulic calculations

A = proportion of air in the tank

EXAMPLE 13:

A pressure tank is to be used to provide a 30-min-water supply to a system with a hydraulically calculated demand of 140 gpm (530 lpm) at a pressure of 118 psi (8.14 bar). Since there are sprinklers located adjacent to the tank, it is important that air pressure in the tank not exceed 175 psi (12.0 bar). To determine the minimum size tank that can be used, it is important not only to consider the total amount of water needed, but also the amount of air necessary to keep the pressures within the stated limits.

The above equation for hydraulically designed systems can be used to solve for A.

If

$$P_i = \left[\frac{(P_f + 15)}{A}\right] - 15$$

then

$$A = \frac{(P_f + 15)}{(P_i + 15)}$$

$$A = \frac{(118 + 15)}{(175 + 15)} = \frac{133}{190} = 0.70$$

This means that the tank will need to be 70 percent air if the air pressure in the tank is to be kept to 175 psi (12.0 bar).

The minimum water supply required is 30 min × 140 gpm = 4200 gallons (15,898 l).

Thus, the minimum tank volume will be such that 4200 gallons (15,898 l) can be held in the remaining 30 percent of volume.

$$0.3V = 4200 \text{ gal} \quad V = \frac{4200}{0.3} = 14,000 \text{ gal tank (53,000 l)}$$

Hanging and Bracing Methods

Hangers and Hanger Supports

NFPA 13 contains a great deal of specific guidance relative to hanger spacing and sizing based on pipe sizes. It should also be recognized that the standard allows a performance-based approach. Different criteria exist for the hanger itself and the support from the building structure.

Any hanger and installation method is acceptable if certified by a registered professional engineer for the following:

1. Hangers are capable of supporting five times the weight of the water-filled pipe plus 250 pounds (114 kg) at each point of piping support.
2. Points of support are sufficient to support the sprinkler system.
3. Ferrous materials are used for hanger components.

The building structure itself must be capable of supporting the weight of the water-filled pipe plus 250 pounds (114 kg) applied at the point of hanging.

The 250 pound (114 kg) weight is intended to represent the extra loading that would occur if a relatively heavy individual were to hang on the piping.

Trapeze Hangers

Trapeze hangers are used where structural members are not located, so as to provide direct support of sprinkler lines or mains. This can occur when sprinkler lines or mains run parallel to structural members such as joists or trusses.

A special section of NFPA 13 addresses the sizing of trapeze hangers. Because they are considered part of the support structure, the criteria within NFPA 13 are based on the ability of the hangers to support the weight of 15 ft (5 m) of water-filled pipe plus 250 pounds (114 kg) applied at the point of hanging. An allowable stress of 15,000 psi (111 bar) is used for steel members. Two tables are provided in the standard, one of which presents required section moduli based on the span of the trapeze and the size and type of pipe to be supported, and the other of which presents the available section moduli of standard pipes and angles typically used as trapeze hangers.

In using the tables, the standard allows the effective span of the trapeze hanger to be reduced if the load is not at the midpoint of the span. The equivalent length of trapeze is determined from the formula

$$L = \frac{4ab}{(a+b)}$$

where L is the equivalent length, a is the distance from one support to the load, and b is the distance from the other support to the load.

EXAMPLE 14:

A trapeze hanger is required for a main running parallel to two beams spaced 10 ft (3.048 m) apart. If the main is located 1 ft 6 in. (0.457 m) from one of the beams, the equivalent span of trapeze hanger required can be determined by using the formula

$$L = \frac{4(1.5 \text{ ft})(8.5 \text{ ft})}{(1.5 \text{ ft} + 8.5 \text{ ft})} = 5.1 \text{ ft (1.554 m)}$$

Earthquake Braces

Protection for sprinkler systems in earthquake areas is provided in several ways. Flexibility and clearances are added to the system where necessary to avoid the development of stresses that could rupture the piping. Too much flexibility could also be dangerous, however, since the momentum of the unrestrained piping during shaking could result in breakage of the piping under its own weight or upon collision with other building components. Therefore, bracing is required for large piping (including all mains) and for the ends of branch lines.

Calculating loads for earthquake braces is based on the assumption that the normal hangers provided to the system are capable of handling vertical forces, and that horizontal forces can be conservatively approximated by a constant acceleration equal to one-half that of gravity.

$$a_h = 0.5g$$

NFPA 13 contains a table of factors that can be applied if building codes require the use of other horizontal acceleration values.

Since the braces can be called upon to act in both tension and compression, it is necessary not only to size the brace member to handle the expected force applied by the weight of the pipe in its zone of influence, but also to avoid a member that could fail as a long column under buckling.

The ability of the brace to resist buckling is determined through an application of Euler's formula with a maximum slenderness ratio of 300. This corresponds to the maximum slenderness ratio generally used under steel construction codes for secondary framing members. This is expressed as

$$\frac{\ell}{r} \leq 300$$

where ℓ = length of the brace and r = least radius of gyration for the brace.

The least radius of gyration for some common shapes is as follows:

pipe $\quad r = \dfrac{(r_0^2 + r_i^2)^{1/2}}{2}$

rod $\quad r = \dfrac{r}{2}$

flat $\quad r = 0.29h$

Special care must be taken in the design of earth-quake braces so that the load applied to any brace does not exceed the capability of the fasteners of that brace to the piping system or the building structure, and that the braces are attached only to structural members capable capable of supporting the expected loads.

Performance Calculations

Sprinkler Response as a Detector

Automatic sprinklers serve a dual function as both heat detectors and water distribution nozzles. As such, the response of sprinklers can be estimated using the same methods as for response of heat detectors. (See Section 4, Chapter 1.) Care should be taken, however, since the use of such calculations for estimating sprinkler actuation times has not been fully established. Factors, such as sprinkler orientation, air flow deflection, radiation effects, heat of fusion of solder links, and convection within glass bulbs, are all considered to introduce minor errors into the calculation process. Heat conduction to the sprinkler frame and distance of the sensing mechanism below the ceiling have been demonstrated to be significant factors affecting response, but are ignored in some computer models.

Nevertheless, modeling of sprinkler response can be useful, particularly when used on a comparative basis. Beginning with the 1991 edition, an exception within Section 4-1.1 of NFPA 13 permitted variations from the rules on clearance between sprinklers and ceilings " . . . provided the use of tests or calculations demonstrate comparable sensitivity and performance."

EXAMPLE 15:

Nonmetallic piping extending 15 in. (0.38 m) below the concrete ceiling of a 10-ft- (3.048 m-) high basement 100 ft by 100 ft (30.48 × 30.48 m) in size makes it difficult to place standard upright sprinklers within the 12 in. (0.30 m) required by NFPA 13 for unobstructed construction. Using the LAVENT[9] computer model, and assuming RTI values of 400 ft$^{1/2}$·s$^{1/2}$ (221 m$^{1/2}$·s$^{1/2}$) for standard sprinklers and 100 ft$^{1/2}$·s$^{1/2}$ (55 m$^{1/2}$·s$^{1/2}$) for quick-response sprinklers, it can be demonstrated that the comparable level of sensitivity can be maintained at a distance of 18 in. (0.457 m) below the ceiling. Temperature rating is assumed to be 165°F, and maximum lateral distance to a sprinkler is 8.2 ft (2.50 m) (10 ft × 13 ft [3.048 m × 3.962 m] spacing). Assuming the default fire (empty wood pallets stored 5 ft [1.52 m] high), for example, the time of actuation for the standard sprinkler is calculated to be 200 s, as compared to 172 s for the quick-response sprinkler. Since the noncombustible construction minimizes concern relative to the fire control performance for the structure, the sprinklers can be located below the piping obstructions.

Dry System Water Delivery Time

Total water delivery time consists of two parts. The first part is the trip time taken for the system air pressure to bleed down to the point where the system dry valve opens to admit water to the piping. The second part is the transit time for the water to flow through the piping from the dry valve to the open sprinkler. In other words

water delivery time = trip time + transit time

where water delivery time commences with the opening of the first sprinkler.

NFPA 13 does not contain a maximum water delivery time requirement if system volume is held to no more than 750 gal (2839 l). Larger systems are permitted only if water delivery time is within 60 s. As such, the rule of thumb for dry system operation is that no more than a 60 s water delivery time should be tolerated, and that systems should be divided into smaller systems if necessary to achieve this 1-min response. Dry system response is simulated in field testing by the opening of an inspector's test connection. The test connection is required to be at the most remote point of the system from the dry valve, and is required to have an orifice opening of a size simulating a single sprinkler.

The water delivery time of the system is recorded as part of the dry pipe valve trip test that is conducted using the inspector's test connection. However, it is not a realistic indication of actual water delivery time for two reasons:

1. The first sprinkler to open on the system is likely to be closer to the system dry valve, reducing water transit time.
2. If additional sprinklers open, the trip time will be reduced since additional orifices are able to expel air. Water transit time may also be reduced since it is easier to expel the air ahead of the incoming water.

Factory Mutual Research Corporation (FMRC) researchers have shown[3] that it is possible to calculate system trip time using the relation

$$t = 0.0352 \frac{V_T}{A_n T_0^{1/2}} \ln \left(\frac{p_{a0}}{p_a} \right)$$

where

t = time in seconds

V_T = dry volume of sprinkler system in cubic feet

T_0 = air temperature in Rankine degrees

A_n = flow area of open sprinklers in square feet

p_{a0} = initial air pressure (absolute)

p_a = trip pressure (absolute)

Calculating water transit time is more difficult, but may be accomplished using a mathematical model developed by FMRC researchers. The model requires the system to be divided into sections, and may therefore produce slightly different results, depending on user input.

Droplet Size and Motion

For geometrically similar sprinklers, the median droplet diameter in the sprinkler spray has been found to be inversely proportional to the $1/3$ power of water pressure and

directly proportional to the $2/3$ power of sprinkler orifice diameter such that

$$d_m \propto \frac{D^{2/3}}{P^{1/3}} \propto \frac{D^2}{Q^{2/3}}$$

where

d_m = mean droplet diameter

D = orifice diameter

P = pressure

Q = rate of water flow

Total droplet surface area has been found to be proportional to the total water discharge rate divided by the median droplet diameter

$$A_S \propto \frac{Q}{d_m}$$

where A_S is the total droplet surface area.

Combining these relationships, it can be seen that

$$A_S \propto (Q^3 p D^{-2})^{1/3}$$

When a droplet with an initial velocity vector of $\mathbf{U}$ is driven into a rising fire plume, the one-dimensional representation of its motion has been represented as[4]

$$\frac{m_1 d\mathbf{U}}{dt} = m_1 g - \frac{C_D \rho_g (\mathbf{U} + V)^2}{2S}$$

where

$\mathbf{U}$ = velocity of the water droplet

V = velocity of the fire plume

m = mass of the droplet

ρ_g = density of the gas

g = acceleration of gravity

C_D = coefficient of drag

S_f = frontal surface area of the droplet

The first term on the right side of the equation represents the force of gravity, while the second term represents the force of drag caused by gas resistance. The drag coefficient for particle motion has been found empirically to be a function of the Reynolds number (Re) as[5]

$$C_D = 18.5\ \text{Re}^{-0.6} \qquad \text{for Re} < 600$$
$$C_D = 0.44 \qquad\qquad \text{for Re} > 600$$

Spray Density and Cooling

The heat absorption rate of a sprinkler spray is expected to depend on the total surface area of the water droplets, A_S, and the temperature of the ceiling gas layer in excess of the droplet temperature, T. With water temperature close to ambient temperature, T can be considered excess gas temperature above ambient.

Chow[6] has developed a model for estimating the evaporation heat loss due to a sprinkler water spray in a smoke layer. Sample calculations indicate that evaporation heat loss is only significant for droplet diameters less

than 0.5 mm. For the droplet velocities and smoke layer depths analyzed, it was found that the heat loss to evaporation would be small (10 to 25 percent), compared to the heat loss from convective cooling of the droplets.

Factory Mutual Research Corporation researchers[7] have developed empirical correlations for the heat absorption rate of sprinkler spray in room fires, as well as convective heat loss through the room opening, such that

$$\dot{Q} = \dot{Q}_{\text{cool}} + \dot{Q}_c + \dot{Q}_l$$

where

$\dot{Q}$ = total heat release rate of the fire

$\dot{Q}_{\text{cool}}$ = heat absorption rate of the sprinkler spray

$\dot{Q}_c$ = convective heat loss rate through the room opening

$\dot{Q}_l$ = sum of the heat loss rate to the walls and ceiling, $\dot{Q}_s$, the heat loss rate to the floor, $\dot{Q}_f$, and the radiative heat loss rate through the opening, $\dot{Q}_r$

Test data indicated that

$$\dot{Q}_{\text{cool}}/\dot{Q} = 0.000039\Lambda^3 - 0.003\Lambda^2 + 0.082\Lambda$$

for $\qquad 0 < \Lambda \le 33\ l/(\text{min} \times \text{kW}^{1/2} \times \text{m}^{5/4})$

where Λ is a correlation factor incorporating heat losses to the room boundaries and through openings as well as to account for water droplet surface area.

$$\Lambda = (AH^{1/2}\dot{Q}_l)^{-1/2}(W^3 P D^{-2})^{1/3}$$

for $\qquad P = \dfrac{p}{(17.2\ \text{kPa})} \quad$ and $\quad D = \dfrac{d}{0.0111\ \text{m}}$

where

A = area of the room opening in meters

H = height of the room opening in meters

P = water pressure at the sprinkler in bar

d = sprinkler nozzle diameter in meters

W = water discharge in liters per minute

The above correlations apply to room geometry with length-to-width ratio of 1.2 to 2 and opening size of 1.70 to 2.97 m².

Suppression by Sprinkler Sprays

Researchers at the National Institute of Standards and Technology (NIST) have developed a "zeroth order" model of the effectiveness of sprinklers in reducing the heat release rate of furnishing fires.[8] Based on measurements of wood crib fire suppression with pendant spray sprinklers, the model is claimed to be conservative. The model assumes that all fuels have the same degree of resistance to suppression as a wood crib, despite the fact that tests have shown furnishings with large burning surface areas can be extinguished easily compared to the deep-seated fires encountered with wood cribs.

The recommended equation, which relates to fire suppression for a 610-mm-high crib, has also been checked for validity with 305-mm crib results. The equation is

$$\dot{Q}(t - t_{\text{act}}) = \dot{Q}(t_{\text{act}})\exp\left[\frac{-(t - t_{\text{act}})}{3.0(\dot{w}'')^{-1.85}}\right]$$

where

$\dot{Q}$ = the heat release rate (kW)

t = any time following t_{act} of the sprinklers (s)

$\dot{w}''$ = the spray density (mm/s)

The NIST researchers claim the equation is appropriate for use where the fuel is not shielded from the water spray, and the application density is at least 0.07 mm/s [4.2 mm/min. (0.1 gpm/ft²)]. The method does not account for variations in spray densities or suppression capabilities of individual sprinklers.

The model must be used with caution, since it was developed on the basis of fully involved cribs. It does not consider the possibility that the fire could continue to grow in intensity following initial sprinkler discharge, and, for that reason, should be restricted to use in light hazard applications.

Sprinklers are assumed to operate within a room of a light hazard occupancy when the total heat release rate of the fire is 500 kW. The significance of an initial application rate of 0.3 gpm/ft² (0.205 mm/s) as compared to the minimum design density of 0.1 gpm/ft² (0.07 mm/s) can be evaluated by the expected fire size after 30 s. With the minimum density of 0.07 mm/s (0.1 gpm/ft²), the fire size is conservatively estimated as 465 kW after 30 s. With the higher density of 0.205 mm/s (0.3 gpm/ft²), the fire size is expected to be reduced to 293 kW after 30 s. Corresponding values after 60 s are 432 kW and 172 kW, respectively.

Nomenclature

C coefficient of friction

FLC friction loss coefficient

Q flow (gpm)

$\dot{w}''$ spray density (mm/s)

References Cited

1. *NFPA Codes and Standards,* National Fire Protection Association, Quincy, MA.
2. H. Cross, *Analysis of Flow in Networks of Conduits or Conductors,* Univ. of Illinois Engineering Experiment Station, Urbana, IL (1936).
3. G. Heskested and H. Kung, *FMRC Serial No. 15918,* Factory Mutual Research Corp., Norwood, MA (1973).
4. C. Yao and A.S. Kalelkar, *Fire Tech.,* 6, 4 (1970).
5. C.L. Beyler, "The Interaction of Fire and Sprinklers," *NBS GCR 77-105,* National Bureau of Standards, Washington, DC (1977).
6. W.K. Chow, "On the Evaporation Effect of a Sprinkler Water Spray," *Fire Tech.,* pp. 364–373 (1989).
7. H.Z. You, H.C. Kung, and Z. Han, "Spray Cooling in Room Fires," *NBS GCR 86-515,* National Bureau of Standards, Washington, DC (1986).
8. D.D. Evans, "Sprinkler Fire Suppression Algorithm for HAZARD," *NISTIR 5254,* National Institute of Standards and Technology, Gaithersburg, MD (1993).
9. W.D. Davis and L.Y. Cooper, "Estimating the Environment and Response of Sprinkler Links in Compartment Fires with Draft Curtains and Fusible-Link Actuated Ceiling Vents, Part 2: User Guide for the Computer Code LAVENT," *NISTIR/89-4122,* National Institute of Standards and Technology, Gaithersburg, MD (1989).

CHAPTER 4

Foam Agents and AFFF System Design Considerations

Joseph L. Scheffey

Introduction

Foams have been developed almost entirely from experimental work. While the technologies are rather mature, no fundamental explanations of foam extinguishment performance have been developed based on first principles. As a result, foams are characterized by (1) fire tests for which there is no general international agreement and (2) physical and chemical properties which may or may not correlate with empirical results. This chapter reviews the important parameters associated with foam agents, test methods used to evaluate foams, and relevant data in the literature that can be used to evaluate designs for special hazards. Because of their superior performance in extinguishing hydrocarbon fuel fires, the emphasis is on film-forming foams and thin pool fires (e.g., from spills). Situations involving fuels "in depth" are not evaluated in detail here.

Fire-fighting foam consists of air-filled bubbles formed from aqueous solutions. The solutions are created by mixing a foam concentrate with water in the appropriate proportions (typically 1, 3, or 6 percent concentrate to water). The solution is then aerated to form the bubble structure. Some foams, notably those that are protein-based, form thick, viscous foam blankets on hydrocarbon fuel surfaces. Other foams, such as film-formers, are much less viscous and spread rapidly on the fuel surface. The film-formers are capable of producing a vapor-sealing film of surface-active water solution on most of the hydrocarbon fuels of interest.

Since the foam is lighter than the aqueous solution that drains from the bubble structure, and lighter than flammable or combustible liquids, it floats on the fuel surface. The floating foam produces an air-excluding layer of aqueous agent, which suppresses and prevents combustion by halting fuel vaporization at the fuel surface. If the entire surface is covered with foam, the fuel vapor will be completely suppressed, and the fire will be extinguished. Low-expansion foams (i.e., foam volume: solution volume of $\leq 10:1$) are quite effective on two-dimensional (pool) flammable and combustible liquid fires, but not particularly effective on three-dimensional fuel fires. This is particularly true of three-dimensional fires involving a low flashpoint fuel. Typically, an auxiliary agent, such as dry chemical, is used with foam where a three-dimensional fire (running fuel or pressurized spray) is anticipated.

Description of Foam Agents

There are no universally agreed-on definitions of foam agents or terms associated with fire-fighting foam. For example, where foam is referenced in NFPA standards, definitions vary from document to document. Because foams vary in performance, in terms of application rates and quantities required for extinguishment, agent definitions can be cast to accentuate positive attributes, such as "rapid knockdown" or "superior burnback resistance." Geyer et al. have described the composition of various foam agents, paraphrased as follows.[1]

1. *Protein foam.* Protein foam is a "mechanical" foam produced by combining (proportioning) foam concentrate and water and discharging the resulting solution through a mixing chamber. The mixing chamber introduces (aspirates) air, which expands the solution to create foam bubbles. The liquid concentrate consists primarily of hydrolyzed proteins in combination with iron salts. Hoof and horn meal and hydrolyzed feather meal are examples of proteinaceous materials used in protein-foam concentrates. No aqueous film is formed on the fuel surface with this type of agent.

Joseph L. Scheffey, P.E., is director of Fire Protection RDT&E for Hughes Associates, Inc., Baltimore, Maryland.

2. *Fluoroprotein.* These agents are basically protein foams with fluorocarbon surface-active agents added. The varying degrees of performance are achieved by using different proportions of the base protein hydrolyzates and the fluorinated surfactants. While fluoroprotein foams generally have good fuel shedding capabilities and dry chemical compatibility, the solution that drains out from the expanded foam does not form a film on hydrocarbon fuels. However, the addition of the fluorinated surfactants may act to reduce the surface tension of the solution. This reduction may, in turn, decrease the viscosity of the expanded solution, thus promoting more rapid fire control when compared to protein foams.

3. *Aqueous film-forming foam (AFFF).* These agents are synthetically formed by combining fluorine-free hydrocarbon foaming compounds with highly fluorinated surfactants. When mixed with water, the resulting solution achieves the optimum surface and interfacial tension characteristics needed to produce a film that will spread across a hydrocarbon fuel. The foam produced from this agent will extinguish in the same vapor-excluding fashion as other foams. Further, the solution that results from normal drainage or foam breakdown produces an aqueous "film" that spreads rapidly and is highly stable on the liquid hydrocarbon fuel surface. It is this film formation characteristic that is the significant distinguishing feature of AFFF.

These definitions are by no means all-inclusive. For example, film-forming fluoroprotein (FFFP) foam is an agent that is produced by increasing the quantity and quality of the surfactants added to a protein hydrolyzate. By doing this, the surface tension of the resulting solution, which drains from the expanded foam, is reduced to the point where it may spread across the surface of a liquid hydrocarbon fuel. An alcohol-resistant concentrate is formulated to produce a floating polymeric skin for foam buildup on water-miscible fuels. This polymeric skin protects the foam from breakdown by polar solvents, for example, acetone, methanol, and ethanol.

The descriptions show that there are distinct chemical differences between protein-based foams and AFFF. In general, the surfactants used in aqueous foams are long-chained compounds that have a hydrophobic or hydrophilic (i.e., water repelling or water attracting, respectively) group at one end.[2] The molecular structure of a typical AFFF fluorinated surfactant is shown in Figure 4-4.1.[3] In this molecule, the perfluoroctyl group on the left is the hydrophobic group, while the propyltrimethylammonium group is the hydrophilic group. When these compounds are dissolved into solution with water, they will tend to group near the surface of the solution, aligned so that their hydrophobic ends are facing toward the air/solution interface. The advantage of this is that the perfluoroctyl group found in these compounds is also oliophobic (i.e., oil repelling) as well as hydrophobic.[4]

AFFF concentrates also contain hydrocarbon surfactants. These compounds are less hydrophobic than those containing the perfluoroctyl group. However, they do provide greater stability once the solution is expanded into a foam. As a result, the surface tension of the solution is reduced below that of water; the expanded foam produced from the solution is resistive to breakdown from heat, fuels, or dry chemical extinguishing agents; and the solution that drains out from the expanded foam is able to form a film on hydrocarbon fuels.

The importance of both the film formation and foam bubble characteristics of AFFF, resulting from the combination of fluorocarbon and hydrocarbon surfactants, was evaluated in early work by Tuve et al.[5] When a highly expanded, stiff formulation of AFFF was used, these researchers found it difficult to obtain good fire extinguishment and vapor sealing characteristics. The foam resisted flow, and drainage of the aqueous solution (film) was slow. The drainage was corrected by expanding the foam to a lesser degree. This pioneering AFFF formulation, with an expansion ratio of 8 : 1 and 25 percent drainage time of 6 min, appeared to offer the best compromise in characteristics. It provided a readily flowable foam that sealed up against obstructions, promoted the rapid formation of a surface-active film barrier on the fuel, and provided a sufficiently stable foam to resist burnback.

Fire Extinguishment and Spreading Theory

As noted by Friedman in his review of suppression theory, the mechanisms of foam fire extinguishment on two-dimensional pool fires have not been developed.[6] Usually, the fire extinguishment is described simply as a factor of the cessation of fuel vaporization at the fuel surface. As the fuel vapor decreases, the size of the combustion zone decreases. When the area is totally covered, extinguishment occurs. Cooling must occur to bring the vapor pressure of the fuel below that of its boiling point. Once the fuel is cooled, a layer of foam must then be applied either manually, or by spreading, to prevent combustion. Hanauska et al. have proposed fundamental extinguishment parameters, summarized in the following text.[7] A similar foam extinguishment model has been proposed by Persson and Dahlberg.[8]

Foam Loss Mechanisms

Fire extinguishment by foams can be summarized as shown in Figure 4-4.2. Foam having a temperature, T_i,

$$\begin{bmatrix} \begin{matrix} & F & F & F & F & F & F & F & F & & CH_3 \\ & | & | & | & | & | & | & | & | & & | \\ F - & C - C - C - C - C - C - C - C & - SO_2\,N\,(CH_2)_3 - N - CH_3 \\ & | & | & | & | & | & | & | & | & & | \\ & F & F & F & F & F & F & F & F & & CH_3 \end{matrix} \end{bmatrix}^{+} \; I^{-}$$
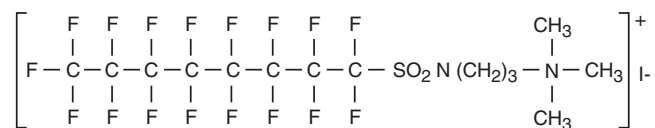
Perfluoroctylsulfommide - N - Propyltrimethylammonium Iodide

Figure 4-4.1. *Typical AFFF fluorosurfactant molecule.[3]*
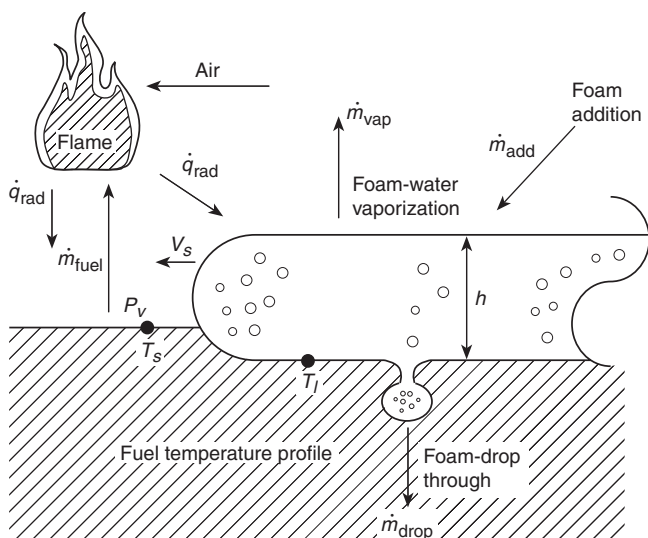
Figure 4-4.2. *Illustration of the significant parameters affecting a foam's hydrocarbon fuel fire extinguishment capability.*

and depth, h, spreads at a rate of V_s along a fuel of temperature, T_s, and vapor pressure, P_v. Fuel is volatized by the fire at a rate of $\dot{m}_{fuel}$, which is a function of the radiative feedback, $\dot{q}_{rad}$. The foam is added by the discharge application, $\dot{m}_{add}$, and lost through evaporation, $\dot{m}_{vap}$, and drop-through, $\dot{m}_{drop}$.

The total mass loss of the foam is a function of the loss due to drop-through and the mass loss due to vaporization. The mass loss due to drop-through is at least partially dependent on the drainage of liquid from the foam. Evaporation of the liquid results primarily from radiant energy from the fire. Assuming that most of the radiation results in direct evaporation of the foam, the evaporation of foam can be characterized by

$$\dot{m}''_{vap} = \frac{\dot{q}''_{rad}}{\Delta H_v} \tag{1}$$

where ΔH_v is the combined latent and sensible heats of vaporization. Using a rough estimate of $\dot{q}''$ from large pool fires of 45–185 kW/m^{2} yields an evaporation rate of 18 and 72 g·m[2]/s, assuming a heat of vaporization of 2563 kJ/kg. (See Section 2, Chapter 2.) To account for reflective and absorbed losses, Persson[9] has proposed a calculation method

$$\dot{m}''_{vap} = \dot{q}''_{rad} k_e \tag{2}$$

where k_e is an experimentally derived constant using different fluxes from a radiant exposure. For q''_{rad} values of 45 and 185 kW/m^{2}, Equation 2 yields values for $\dot{m}''_{vap}$ of 11 and 46 g·m[2]/s, respectively. Since the estimated $\dot{m}''_{vap}$ values based on Equation 1 at the same heat fluxes were 18 and 72 g·m[2]/s, the experimental mass loss rate results are about 62 percent lower than the theoretical loss. The difference between values is attributable to neglect-

ing the reflected and absorbed losses in Equation 1. This indicates that about 48 percent of the radiant flux to the foam surface is either reflected from or absorbed into the foam blanket. The division between these two heat-transfer mechanisms is not clear and is an area for further study.

Foam loss can likewise be described theoretically, based on the downward force of gravity and the opposing forces due to surface tension and buoyancy. Alternately, a model mass loss due to drainage can be expressed as a time-averaged constant

$$\dot{m}_{drain} = k_d \tag{3}$$

where k_d is an experimentally determined drainage coefficient. From the data of Persson, the drainage coefficient can be estimated to be 17 to 25 g·m[2]/s.[9] The drainage rate was found to be relatively independent of the radiant heat flux to the foam, but highly dependent on the expansion ratio. Foams with lower expansion ratios will drain faster. For example, decreasing the expansion ratio by about half (11.3 to 5.3) increased the drainage rate by a factor of about 2 (55 to 105 g/min). Decreasing the expansion ratio changes fundamental parameters of the foam, which allows it to drain faster.

Experimental work on the foam model, particularly with regard to the effects of incident heat flux on the foam blanket, are continuing in the United States and Europe. Lattimer et al.[10] designed a test apparatus that was used to measure the behavior of foam when exposed to irradiance levels of 0–50 kW/m^{2}. The apparatus provided data on evaporation rate, drainage rate, foam destruction rate, foam temperature, heat penetration, and time to fuel ignition. The performance of a single AFFF formulation was characterized.

Evaporation rates were measured primarily to be a function of irradiance, making it possible to predict evaporation using the irradiance from the fire and an effective heat of vaporization. The AFFF foam evaluated in this study was determined to have an effective heat of vaporization of 4.87 ±0.75 MJ/kg. This result is slightly higher than that found by Ikasson and Persson,[11] 4.0 MJ/kg. Different AFFF formulations may explain this difference.

Foam drainage rate was measured to be insensitive to the irradiance level or the presence of a fuel layer below the foam. This was consistent with the findings of the Swedish researchers. For foams with expansion ratios ranging from 6.0–9.7, drain rate was determined to be a function of foam mass per unit area. A single curve was developed to characterize the drain rate for all foams with a thickness equal to or less than 75 mm. The drainage rate was measured to be constant down to a foam mass per unit area of 3.0 kg/m^{2} and decreased linearly to zero by 1.5 kg/m^{2}. The steady-state drain-rate level decreased from 40 g·m[2]/s to 28 g·m[2]/s by increasing the expansion ratios from 6.0 to 9.7, respectively.

The drainage rate of low-expansion ratio foams (3.3) was as much as 4–10 times higher than levels measured at higher expansion ratios. The high level was attributed to the fluidity of the foam, which is affected by solution density in foam, breaking and coalescing of bubbles, and so-

lution viscosity. Measurements of foam fluidity for different AFFF foam expansion ratios and temperatures are necessary to further understand these trends in the data at low expansion ratios.

Foam depletion rate was measured primarily to be a function of the irradiance level incident on the foam. As irradiance increased, the foam depletion rate increased. Foam depletion rate was independent of the initial foam height and expansion ratio.

Heat penetration through the foam was measured to be a function of foam height and foam mass. For all of the different tests where heat penetration was measured, the data indicate that heat begins penetrating through the foam when the foam becomes approximately 50 ± 7 mm thick and has a foam mass of 4.2 ± 1.2 kg/m^2.

Ignition time in tests with JP-5 fuel layers was measured to be a function of both irradiance and initial foam height. Increases in irradiance and decreases in initial foam height were determined to decrease the time to ignition. This result was found to be independent of expansion ratio and initial fuel temperature. At ignition, nearly all of the AFFF (less than 0.8 kg/m^2) had been lost from the fuel surface.

Additional small-scale testing needs to be performed to quantify the foam losses and foam spread characteristics of other foam concentrates. Foam loss and spread data are expected to be concentrate dependent, and these data are necessary to further validate the performance of the foam extinguishment model.

Foam drainage is a complicated phenomenon that is highly time dependent. Besides the forces associated with the bubble structure, drainage is dependent on the continual changing geometries of the cells and other variable conditions, such as collapsing cells. Even though all aspects of this problem cannot be fully detailed, simplified models have been created that predict the drainage rate for foams. Kraynik has developed one such model that considers the drainage from a column of persistent foam.[12] The model contains no empirical parameters and assumes the foam is dry with very thin walls such that the liquid contained in the cell walls is negligible. In relaxing the assumptions, this basic model might ultimately be used to assess the effect of various fundamental parameters on foam drainage.

Foam Spread over Liquid Fuels

In order to predict the extinguishment of a liquid pool fire by fire-fighting foam, it is necessary to describe the process of spreading the foam over the liquid fuel surface. This process of foam spread on a liquid fuel is similar to the spread of a less dense liquid (such as oil) on a more dense liquid (such as water). This phenomenological approach to the spread of foam on a liquid pool fire is appropriate to the extent that foam can be treated as a liquid. Kraynik characterizes foams macroscopically as being Bingham fluids with a finite shear stress and non-newtonian viscosity.[13] That is, foam displays an infinite viscosity up to some initial shear rate above which it displays a shear-rate dependent viscosity.

Since fuels typically have low viscosities (especially compared to foam viscosities at relatively low shear rates), it may be appropriate to model foam spread across a fuel surface using models developed for oil spread on water. These models assume that the oil spreads as a fluid with a viscosity much higher than the water on which it is spreading. The process of oil spread on water has been described in detail by Fay,[14] and Fay and Hoult.[15] Their phenomenologically based model describes three regimes of spread characterized by combinations of spreading forces and retarding forces. The first regime is the gravity-inertia regime, where the outward spread of the oil is driven by a gravity force and retarded by the inertia required to accelerate the oil. The second regime is the gravity-viscous regime, where the gravity-induced spreading is retarded by viscous dissipation in the water. Since the oil is much more viscous than the water, they assume that there is slug flow in the oil and that the viscous drag force is dominated by the velocity gradient in the water. The third regime is characterized by a surface-tension spreading force opposed by the viscous retarding force. By setting the spreading and retarding forces equal in each of the regimes, they developed equations to estimate the length of the spread as a function of time.

By treating the spread of foam on fuel as similar to the spread of oil on water, the equations developed by Fay and Hoult might be used to describe the spread of a foam blanket over a fuel pool as a function of time.[14] Since foam generally has a much higher viscosity than the fuel on which it is spreading, the assumption of slug flow made for the oil by Fay and Hoult should be reasonably valid for foam spread on fuel as well.[14] The equations are

gravity-inertia regime:
$$l = \left(\Delta g V t^2 \right)^{1/4}$$

gravity-viscous regime:
$$l = \left(\frac{\Delta g V^2 t^{3/2}}{\nu^{1/2}} \right)^{1/6} \quad (4)$$

surface-tension-viscous regime:
$$l = \left(\frac{\sigma^2 t^3}{\rho^2 \nu} \right)^{1/4}$$

where
l = length of spread (cm)
$\Delta = (\rho_{fuel} - \rho_{foam})/\rho_{fuel}$
g = acceleration of gravity (981 cm/s^2)
V = foam volume (cm^3)
t = time (s)
ν = kinematic viscosity of fuel (cm^2/s)
σ = spreading coefficient (dynes/cm)
ρ = density of fuel or foam (g/cm^3)

Equation 4 represents an untested theoretical model of foam spread. The equation includes the parameters that are known or suspected to affect foam spread. They are presented here as an initial effort to understand foam flow based on first principles. They are not yet developed

for engineering use. The following discussion expands on this theory.

The transition from gravity-dominated spread to surface-tension-dominated spread can be shown to occur at a critical thickness of the foam layer, h_c, given by

$$h_c = \left(\frac{\sigma}{g\Delta\rho_{foam}}\right)^{1/2} \quad (5)$$

The transition from inertia to viscous-dominated retarding force occurs when the foam thickness, h, is equal to the viscous boundary layer thickness, δ, of the fuel, with

$$h = \frac{V}{l^2}$$
$$\delta = (\nu t)^{1/2} \quad (6)$$

The equations for length of spread can be used to generate preliminary estimates of the spread distance and area coverage for the placement of a volume of foam on a fuel surface. The equations are only estimates because they consider a force balance between just the dominant forces for each regime. All forces are actually present in each regime. Also, the densities of both fluids are considered to be very nearly equal for the development of the equation for the gravity-viscous regime. This is the case for oil spread on water, but may not be the case for foam on fuel.

Using approximations for fuel and foam characteristics, it can be shown that a positive spreading coefficient does not begin to affect the spread of foam until the foam layer has become very thin. For the placement of a volume of foam on a fuel, this may not occur until after significant time has passed, relative to the time scale for knockdown desired in many fire protection situations.

The equations for foam spread on fuel include many of the parameters known to be important to foam spread. However, the equations are independent of the foam viscosity. Observations indicate that low-viscosity nonrigid foams, such as AFFF, spread faster than high-viscosity rigid protein foams. The inclusion in the model of a term to account for this is desirable.

The equations for spread length so far have assumed that the foam spreads over the fuel as plug flow, with no relative movement within the foam itself. It is easy to conceive that the foam has the capability to flow over itself. The relative movement within the foam is equivalent to the foam flowing over a solid surface. The total foam flow might ultimately be modeled as the combination of the foam plug over the fuel and the flow within the foam layer itself.

According to Cann et al., several regimes exist for spread of a liquid on a solid that are similar to those described for spread of a liquid on a liquid.[16] Most of this spread occurs in a gravity-viscous force regime, where the spread is given by

$$l = \frac{kt}{\mu} \quad (7)$$

where k is an empirically determined constant, and μ is the foam viscosity.

Thus, the spread of foam over fuel can be characterized by two scenarios: (1) high-viscosity liquid spreading over a low-viscosity liquid and (2) a liquid spreading over a "solid." The spread of foam can be described by modifying Equation 4, as follows:

gravity-inertia regime: $\quad l = \left(\Delta g V t^2\right)^{1/4} + \frac{kt}{\mu}$

gravity-viscous regime: $\quad l = \left(\frac{\Delta g V^2 t^{3/2}}{\nu^{1/2}}\right)^{1/6} + \frac{kt}{\mu} \quad (8)$

surface-tension regime: $\quad l = \left(\frac{\sigma^2 t^3}{\rho^2\nu}\right)^{1/4} + \frac{kt}{\mu}$

Kraynik describes foams as being characterized by a yield stress and shear thinning viscosity.[13] Thus, the foam viscosity in the equations above is not a constant but is a function of the shear rate. The stress in the foam is a result of the gravity-induced pressure gradient. As the foam flows out and becomes thin, the stress will be reduced. When the stress falls below the yield stress, the viscosity will become infinite and the second term, kt/μ, in the spread length equations will go to zero. The foam will flow simply as plug flow. Above the yield stress, the foam will have a finite viscosity, but this viscosity will be dependent on the yield stress.

An AFFF agent that is very free flowing will have a relatively small yield stress and will retain the second term in the spread length equations until it has flowed out to a very thin layer. A protein foam that is relatively stiff will have a large yield stress, and the second term will go to zero before the foam has spread very far. Above the yield stress, the viscosity of the AFFF will be lower than that of a protein foam, and the second term will provide a greater contribution to foam spread. The rheological properties described appear to have a significant impact on foam spread; however, the properties are not a part of any current specification and are rarely measured.

Foam Extinguishment Modeling

At present, modeling of foam extinguishment cannot be performed because of the large number of remaining uncertainties. A model would have to take into account the addition of foam to the fuel surface, the spread of foam on the fuel surface, and the foam loss mechanisms of evaporation and drop-through. The foam spread length equations can be used to estimate the area of foam coverage at a specific time and for a specific quantity of foam. Modeling at this time is limited because of the lack of established values for k_e (Equation 2) and k_d (Equation 3). Also, the yield stress and viscosity relationships for firefighting foams have not been quantified. Experimental work is needed to complete this modeling effort. Also, the actual method of application (e.g., from a handline nozzle or fixed device such as a sprinkler) must ultimately be

taken into account. Even so, preliminary calculations using this methodology are encouraging and support continued development.[7]

Surface Tension and Spreading Coefficient

Film-forming foams are defined by the ability of the aqueous solution draining from the foam to spread spontaneously across the surface of a hydrocarbon fuel. The fundamental relationship used to describe the spreading coefficient is

$$S_{a/b} = \gamma_b - \gamma_a - \gamma_l \tag{9}$$

where

$S_{a/b}$ = spreading coefficient (dynes/cm)

γ_b = surface tension of the lower liquid phase of a hydrocarbon fuel (dynes/cm)

γ_a = surface tension of the upper layer of liquid using AFFF solution (dynes/cm)

γ_l = interfacial tension between liquids a and b (dynes/cm)

Surface tension and interfacial tension can be measured using methods such as those described in ASTMD-1331, *Standard Test Methods for Surface and Interfacial Tension of Solutions of Surface-Active Agents.* Reagent-grade cyclohexane is typically used as a reference fuel. A du Nouy tensiometer, having a torsion balance with a 4- or 6-cm-circumference platinum-iridium ring, is lowered into the liquid and slowly pulled out until the liquid detaches from the ring's surface. The force recorded at the point where this separation occurs is the surface tension (dynes/cm) of the pure liquid. Similarly, the interfacial tension is the measurement of tension when the ring is pulled through the boundary layer between two liquids.

The Naval Research Laboratory developed some of the earliest quantitative data on the spreading coefficient of AFFF on hydrocarbons, as shown in Tables 4-4.1 and 4-4.2.[17] As fuel temperature increases, the surface tensions of both the fuel and solution decrease. The spreading coefficient may go to zero or go negative.[17,18]

While it has been shown that film-forming foams are superior fire extinguishing agents compared to other foams, there are no one-to-one correlations between bench-scale surface-tension/spreading coefficient data and fire control, extinguishment, and burnback resistance times. Both Scheffey et al.[19] and Geyer[20] have demonstrated that there is no direct correlation between fire extinguishment and spreading coefficient. As such, spreading coefficient data alone cannot be used as a relative predictor of fire performance.

Since the surface tensions of most AFFFs are approximately equal, there must be a balance between the surface tension of the fuel and the interfacial tension of the two liquids to create a positive spreading coefficient. It can be seen then that, while both the surface tension of the solution and the interfacial tension between the liquids have an impact on the spreading coefficient, the interfa-

Table 4-4.1 *Surface Tension of Hydrocarbon Liquids and Fuels[17]*

Hydrocarbon Liquid	Grade	Surface Tension at 25°C (dynes/cm)
Cyclohexane	Certified A.C.S.	24.2
n-Heptane	Certified spectroanalyzed	19.8
n-Heptane	Commercial	20.9
Isooctane	Certified A.C.S.	18.3
Avgas	115/145	19.4[a] 19.5[b]
JP-4	Navy specification	22.4[a] 22.8[b]
JP-5	Navy specification	25.6[a] 25.8[b]
Motor fuel	Regular	20.5[a] 21.5[b]
Naphtha	Stove and lighting	20.6

[a]Sample 1
[b]Sample 2

cial tension is usually the determining factor. For fuels, such as avgas or *n*-heptane, which have surface tensions in the range of 19 to 20 dynes/cm, either the foam surface tension or the interfacial tension, or both, must be reduced. Normally, the changes resulting from a modification of the formulation will be more significant for the interfacial-tension value than they will be for the foam surface-tension value. Still, a relationship between the two values does exist.[4] Therefore, in reducing the sum of the values to obtain a positive spreading coefficient, a delicate balance must be maintained.

Maintaining this balance and achieving a positive spreading coefficient is accomplished by controlling the amount and type of fluorinated surfactants used to formulate the agent. This at first seems beneficial, since a positive number on a low surface-tension fuel will ensure an even larger value with higher surface-tension fuels (e.g., JP-5 or motor gasoline). But, in reducing the interfacial tension, the agent may lose some of its fuel-shedding capabilities. The effects of adding too much fluorosurfactant to an aqueous solution and the result on foam bubble stability are described by Rosen[4] and Aubert et al.[2] This could be a problem that manifests itself only during actual fire testing. The type and amount of fluorosurfactants also affect the spreading coefficient.[19]

Despite the lack of one-to-one correlations between surface-tension spreading coefficient data and fire control, extinguishment, and burnback results, these criteria are useful in categorizing film-forming agents. The spreading coefficient test is used throughout the world as a standard indicator of aqueous film-forming foams. Although undocumented, it is believed that film formation results in improved viscosity (or associated mechanisms that improve spreading), ultimately resulting in superior extinguishing performance.

Table 4-4.2 *Interfacial Tensions, Spreading Coefficients, and Film Formation Observations for Various Surfactant Solution-Hydrocarbon Liquid Combinations[17]*

Surfactant Solution	Hydrocarbon Liquid	Interfacial Tension (dynes/cm)	Spreading Coefficient (dynes/cm)	Film Formed
FC-194 (lot 107) (solution surface tension of 15.5 dynes/cm at 25°C)	Cyclohexane	4.3	4.4	Yes
	n-Heptane, certified	5.5	−1.2	No
	n-Heptane, commercial	4.3	1.1	Yes (very slow spread)
	Avgas[a]	4.6	−0.7	No
	JP-4[a]	3.6	3.3	Yes
	JP-5[a]	4.9	5.2	Yes
	Motor Fuel[a]	3.7	1.3	Yes
FC-195 (lot 9) (solution surface tension of 15.6 dynes/cm at 25°C)	Cyclohexane	3.2	5.4	Yes
	n-Heptane, certified	4.2	0.0	Yes (slow spread)
	Isooctane	2.5	0.2	Yes (slow spread)
	Avgas[a]	0.5	3.3	Yes
	JP-4[b]	3.6	3.6	Yes
	JP-5[b]	4.9	5.3	Yes
	Motor fuel[a]	2.6	2.3	Yes
FC-195 (lot 10) (solution surface tension of 16.4 dynes/cm at 25°C)	Naphtha	2.8	2.2	Yes
	Cyclohexane	1.5	6.3	Yes
	n-Heptane, certified	3.2	0.6	Yes
	Isooctane	2.8	−1.3	No
	Avgas[a]	2.1	1.0	Yes
	JP-4[a]	2.7	3.3	Yes
	JP-5[a]	4.2	5.0	Yes
	Motor fuel[a]	1.2	2.9	Yes
	Naphtha	0.8	3.4	Yes (slow spread)

[a]Sample 1
[b]Sample 2

Assessment of Fire Extinguishing and Burnback Performance

Standard Test Methods

Since a theory of foam spreading has not been developed, performance of foams is measured using fire tests. The use of bench-scale burning fuel trays (e.g., less than 1 m diameter) results in varying fuel burning rates. This was observed by Chiesa and Alger when they attempted to use a 15-cm by 45-cm pan for foam performance evaluation.[21] Data from their experiments are shown in Figure 4-4.3, which correlates control times observed when foam samples were tested using bench-scale apparatus (laboratory) and 4.6-m² (50-ft²) fire tests (field method). Equal control times correspond to a 45-degree line. Since the majority of the points fall below this line, the laboratory test is more severe (about 35 percent) than the field test.

Fire test methods used by regulatory authorities for certification are usually on the order of 2.6 to 9.3 m² (28 to 100 ft²). Foams must also meet additional test parameters related to storage, proportioning, and equipment factors.

Underwriters Laboratories Standard 162: Underwriters Laboratories (UL) 162, *Standard for Foam Equipment and Liquid Concentrates,* is the principle test standard for the listing of foam concentrates and equipment in the United States. Test procedures outlined in this standard have been developed to evaluate specific agent/proportioner/discharge device combinations. When a foam concentrate is submitted for testing, it must be accompanied by the discharge device and proportioning equipment with which it is to be listed. Listed products, including the agent, discharge device, and proportioner, are then described in the UL *Fire Protection Equipment Directory.*

Listed with a system, foam liquid concentrates are associated with discharge devices classified as Type I, II, or III. Type I devices deliver foam gently onto the flammable liquid fuel surface, for example, a foam trough along the inside of a tank wall. These devices are no longer evaluated in UL 162. Type II discharge devices deliver foam onto the liquid surface in a manner that results in submergence of the foam below the fuel surface, and restricted agitation at the fuel surface. Examples include subsurface injection systems, tank wall–mounted foam chambers, and applications where foam is bounced off the wall of a tank. Type III discharge devices deliver foam
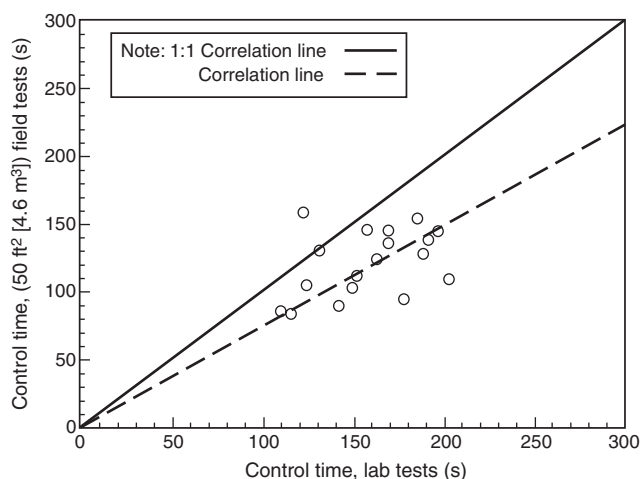
Figure 4-4.3. *Correlation of control times observed in laboratory and field tests of foam.[21]*

directly onto the liquid surface and cause general agitation at the fuel surface, for example, by using hand-held nozzles. The flammable liquid fire tests in UL 162 include methods for sprinklers, subsurface injection, and topside discharge devices, including nozzles.

Class B fire test requirements for Types II and III discharge devices and sprinklers are shown in Table 4-4.3. Commercial grade *n*-heptane is placed in a square test pan. The area of the pan is a minimum of 4.6 m² (50 ft²). The application rates ("densities" in UL 162, *Standard for*

Foam Equipment and Liquid Concentrates) for various concentrates are outlined in Table 4-4.3.

In the test fire, the fuel is ignited and allowed to burn for 60 s. Foam is then discharged for the duration specified in Table 4-4.3. The foam blanket resulting from the foam discharge must spread over and completely cover the fuel surface, and the fire must be completely extinguished before the end of the foam discharge period.

After all the foam is discharged, the foam blanket formed on top of the fuel is left undisturbed for the period specified in Table 4-4.3. During the time the foam blanket is left undisturbed, a lighted torch is passed approximately 25.4 mm (1 in.) above the entire foam blanket in an attempt to reignite the fuel. The fuel must not reignite, candle, flame, or flash over while the torch is being passed over the fuel. However, candling, flaming, or flashover that self-extinguishes is acceptable, provided that the phenomenon does not remain in one area for more than 30 s.

After the attempts to reignite the fuel with the lighted torch are completed, a 305-mm- (12-in.-) diameter section of stovepipe is lowered into the foam blanket. The portion of the foam blanket that is enclosed by the stovepipe is removed with as little disturbance as possible to the blanket outside the stovepipe. The cleared fuel area inside the stovepipe is ignited and allowed to burn for 1 min. The stovepipe is then slowly removed from the pan while the fuel continues to burn. After the stovepipe is removed, the foam blanket must either restrict the spread of fire for 5 min to an area not larger than 0.9 m² (10 ft²), or flow over and reclose the burning area.

When the UL 162 test is passed, the agent, proportioning device, and discharge device become listed. The

Table 4-4.3   *Foam Application Rates and Duration to Burnback Ignition in UL 162 for Hydrocarbon Fuels*

Application	Foam Concentrate	Fuel Group	Test Application Density [lpm/m² (gpm/ft²)]	Time of Foam Applicaton (min)	Maximum Extinguishment Density [l/m² (gal/ft²)]	Duration until Burnback Ignition (min)	Minimum Application Rate [lpm/m² (gpm/ft²)]
Type III discharge outlets	P, FP, S, FFFP[a]	Hydrocarbon	2.5 (0.06)	5	12.2 (0.03)	15	6.6 (0.16)
	AFFF, FFFP[a]	Hydrocarbon	1.6 (0.04)	3	4.9 (0.12)	9	4.1 (0.10)
Type II discharge outlets	P, FP, S, FFFP[a]	Hydrocarbon	2.5 (0.06)	5	12.2 (0.3)	15	4.1 (0.10)
	AFFF, FFFP[a]	Hydrocarbon	1.6 (0.04)	3	4.9 (0.12)	9	41. (0.10)
	All	Polar	[b]	5	—	15	[c]
Foam-Water sprinklers	P, FP, S	Hydrocarbon	6.6 (0.16)	5	30 (0.8)	15	6.6 (0.16)
Standard orifice sprinkler and spray systems	AFFF, FFFP	Hydrocarbon	4.1 (0.10)	5	20.4 (0.5)	15	6.6 (0.16)
		Polar	[b]	5	—	15	[d]

P = Protein   FFFP = Film-forming fluoroprotein   FP = Fluroprotein   AFFF = Aqueous film-forming fluoroprotein   S = Synthetic

[a]Film-forming fluoroprotein is to be tested at application densities of 2.5 and 1.6 Lpm/m² (0.06 and 0.04 gpm/ft²).

[b]Application rate may vary among polar groups, as specified by the manufacturer.

[c]0.01 or 1.67 times test application rate, whichever is greater.

[d]0.16 or 1.6 times test application rate, whichever is greater.

Source: UL 162, *Standard for Foam Equipment and Liquid Concentrates,* March 1994.

fact that foam concentrate has a UL label does not mean it has been tested under all potential end-use conditions. The UL *Fire Protection Equipment Directory* must be referenced to determine with what equipment the concentrate has been tested and approved.

UL 162, *Standard for Foam Equipment and Liquid Concentrates,* is not an agent specification; therefore, there are no requirements for physical properties, such as film formation and sealability and corrosion resistance. Neither are there any provisions to test, on a large scale, the degree of dry chemical compatibility of an agent, or the effects of aging or mixing with agents of another manufacturer. Requirements for a positive spreading coefficient (greater than zero using cyclohexane) for film-forming foams recently have been implemented.[22]

U.S. military specification: The U.S. Military Specification, MIL-F-24385, is the AFFF procurement specification for the U.S. military and federal government. The U.S. military, in all likelihood, is the largest user of foam in the world. It is important to recognize that MIL-F-24385 is a procurement specification as well as a performance specification. Hence, there are requirements for packaging, initial qualification inspection, and quality conformance inspection, in addition to fire performance criteria. Equipment designs unique to the military, in particular U.S. Navy ships, also impact on the specification requirements (e.g., use of seawater solutions and misproportioning-related fire tests). These requirements have been developed based on research and testing at the Naval Research Laboratory and actual operational experience with protein and film-forming foams.

Table 4-4.4 summarizes the important fire extinguishment, burnback resistance, film formation, and foam quality requirements established by MIL-F-24385. The fire tests are conducted using 2.6 m² (28 ft²) and 4.6 m² (50 ft²) circular fire test pans. There are specific requirements to conduct a fire test of the agent after it has been subjected to an accelerated aging process (simulating prolonged storage) and after intentionally misproportioning the concentrate with water. In particular, the requirement to conduct a fire test of the agent at one-half of its design concentration is one of the most difficult tests. The 2.6-m² (28 ft²) half-strength fire test must be extinguished in 45 s, only 15 s greater than allowed when the full-strength solution is used.

The physical and chemical properties evaluated for MIL-F-24385 agents are outlined in Table 4-4.5, along with the rationale for each test. These procedures have been developed based on experience and specific military requirements. For example, MIL-F-24385 requires that the agent be compatible with dry chemical agents. Dry chemical agents may be used as "secondary" agents in aviation and shipboard machinery space fires, for example, to combat three-dimensional fuel fires, where AFFF alone may have limited effectiveness. MIL-F-24385 requires that an agent's compatibility with potassium bicarbonate dry chemical agent (PKP) be demonstrated. The burnback time of the foam in the presence of the dry chemical is measured. Also, the concentrate of one manufacturer

Table 4-4.4   *Summary of the U.S. Military AFFF Specification (MIL-F-24385, Revision F) Key Performance Requirements*

Test Parameter	Revision F
Fire extinguishment	
2.6-m² (28-ft²) fire test	
Application rate	2.9 lpm/m² (0.71 gpm/ft²)
Maximum extinguishment time	30 s
Maximum extinguishment density	1.45 l/m² (0.036 gal/ft²)
4.6-m² (50-ft²) fire test[a]	
Application rate	1.6 lpm/m² (0.04 gpm/ft²)
Minimum 40-s summation	320 s
Maximum extinguishment time	50 s
Maximum extinguishment density	1.34 l/m² (0.033 gal/ft²)
Fire extinguishment—over- and under-proportioning [2.6-m² (28-ft²) Test]	
One-half strength	
Maximum extinguishment time	45 s
Maximum extinguishment density	2.2 l/m² (0.054 gal/ft²)
Quintuple (5 ×) strength	
Maximum extinguishment time	55 s
Maximum extinguishment density	2.7 l/m² (0.066 gal/ft²)
Burnback resistance	
2.6-m² (28-ft²) fire test	25% maximum at 360 s[b]
4.6-m² (50-ft²) fire test	25% maximum at 360 s
Foam quality	
Expansion ratio	6.0 : 1 minimum
25% drainage	150 s minimum
Film formation	
Spreading coefficient	
Fuel	Cyclohexane
Minimum value	3 dynes/cm
Ignition resistance test	
Fuel	Cyclohexane
Pass/fail criteria	No ignition

[a]Saltwater only
[b]300 s for one-half-strength solutions; 200 s for quintuple-strength solutions

must be compatible with concentrates of the same type furnished by other manufacturers, as determined by fire tests and accelerated aging tests.

Standards outside the United States: The number of standards developed for foams outside the United States is quite substantial. A brief review of the literature yielded over 17 different standards and test methods.[23] Developments in the European community are reviewed here to provide examples of differences in test standards.

The International Civil Aviation Organization (ICAO) develops crash fire-fighting and rescue documents for its member bodies. The ICAO *Airport Services Guide,* Part 1, "Rescue and Firefighting," describes airport levels of protection to be provided and extinguishing

Table 4-4.5 *Physical/Chemical Properties and Procurement Requirements of the AFFF Mil Spec*

Requirement	Rationale
Refractive index	Enable use of refractometer to measure solution concentrations in field; this is most common method recommended in NF PA 412[a]
Viscosity	Ensures accurate proportioning when proportioning pumps are used; for example, balance pressure proportioner or positive displacement injection pumps
pH	Ensures concentrate will be neither excessively basic or acidic; intention is to prevent corrosion in plumbing systems
Corrosivity	Limits corrosion of, and deposit buildup on, metallic components (various metals for 28 days)
Total halides/ chlorides	Limits corrosion of, and deposit buildup on, metallic components
Environmental impact	Biodegradability, fish kill, BOD/COD[b]
Accelerated aging	Film formation capabilities, fire performance, foam quality; ensures a long shelf life
Seawater compatibility	Ensures satisfactory fire performance when mixed with brackish or saltwater
Interagent compatibility	Allows premixed or storage tanks to be topped off with different manufacturers' agents, without affecting fire performance
Reduced- and over-concentration Fire test	Ensures satisfactory fire performance when agents are proportioned inaccurately
Compatibility with dry chemical (PKP) agents	Ensures satisfactory fire performance when used in conjunction with supplementary agents
Torque to remove cap	Able to remove without wrench
Packaging requirements	Strength, color, size, stackable, minimum pour, and vent-opening tamperproof seal; ensures uniformity of containers and ease of handling
Initial qualification inspection	Establish initial conformance with requirements
Quality conformance inspection (each lot)	Ensures continued conformance with requirements

[a]NFPA 412, *Standard for Evaluating Aircraft Rescue and Fire-Fighting Foam Equipment,* 1998 edition.
[b]BOD/COD: Biological oxygen demand/chemical oxygen demand

agent characteristics. Minimum usable amounts of extinguishing agents are based on two levels of performance: Level A and Level B. The amounts of water specified for foam production are predicted on an application rate of 8.2 lpm/m^2 (0.20 gpm/ft^2) for Level A, and 5.5 lpm/m^2 (0.13 gpm/ft^2) for Level B. Agents that meet performance

Level B require less agent for fire extinguishment. ICAO foam test criteria are described in Table 4-4.6. Foams meeting performance Level B have an extinguishment application density of 2.5 l/m^2 (0.061 gal/ft^2). There are no surface-tension, interfacial-tension, and spreading coefficient requirements.

The International Organization for Standardization (ISO) has issued a draft specification for low-expansion foams, EN 1568-3.[24] The specification includes definitions for protein, fluoroprotein, synthetic, alcohol resistant, AFFF, and FFFP concentrates. A positive spreading coefficient is required for film-forming foams when cyclohexane is used as the test fuel. There are toxicity, corrosion, sedimentation, viscosity, expansion, and drainage criteria. The fire test uses a 2.4-m- (8-ft-) diameter circular pan with heptane as the fuel. The UNI 86 foam nozzle is used for either a "forceful" or "gentle" application method at a flow rate of 11.4 lpm (3 gpm). The application rate is 2.4 lpm/m^2 (0.06 gpm/ft^2). For the greatest performance level, a 3-min extinguishment time is required. This extinguishment time results in an extinguishment application density of 7.6 l/m^2 (0.19 gal/ft^2).

The proposed ISO/EN requirements for extinguishing and burnback are summarized in Table 4-4.7. There are three levels of extinguishment performance and four levels of burnback performance. For extinguishing performance, Class I is the highest class and Class III the lowest class. For burnback resistance, Level A is the highest level and Level D the lowest level.

Typical performance classes and levels for different concentrates are provided. Typical anticipated performance for AFFF is noted as Level IC, and Level IB for alcohol-type AFFF. For a fluoroprotein foam, performance is expected to be Level IIA for both alcohol-type and hydrocarbon-only concentrates.

Table 4-4.6 *ICAO Foam Test Requirements*

Fire Tests	Performance Level A	Performance Level B
1. Nozzle (air aspirated)		
(a) Branch pipe	UNI 86 foam nozzle	UNI 86 foam nozzle
(b) Nozzle pressure	700 kPa (100 psi)	700 kPa (100 psi)
(c) Application rate	4.1 lpm/m^2 (0.10 gpm/ft^2)	2.5 lpm/m^2 (0.06 gpm/ft^2)
(d) Discharge rate	11.4 lpm (3.0 gpm)	11.4 lpm (3.0 gpm)
2. Fire size	$\cong$ 2.8 m^2 ($\cong$ 30 ft^2) (circular)	$\cong$ 4.5 m^2 ($\cong$ 48 ft^2) (circular)
3. Fuel (on water surface)	Kerosene	Kerosene
4. Preburn time	60 s	60 s
5. Fire performance		
(a) Extinguishing time	$\leq$60 s	$\leq$60 s
(b) Total application time	120 s	120 s
(c) 25% reignition time	$\geq$5 min	$\geq$5 min

Table 4-4.7 *Maximum Extinction Times and Minimum Burnback Times from Proposed ISO/EN Specification*

Extinguishing Performance Class	Burnback Resistance Level	Gentle Application Test		Forceful Application Test	
		Extinction Time (min) Not More Than	Burnback Time (min) Not Less Than	Extinction Time (min) Not More Than	Burnback Time (min) Not Less Than
I	A	—	—	3	10
	B	5	15	3	Not tested
	C	5	10	3	Not tested
	D	5	5	3	Not tested
II	A	—	—	4	10
	B	5	15	4	Not tested
	C	5	10	4	Not tested
	D	5	5	4	Not tested
III	B	5	15	Not tested	Not tested
	C	5	10	Not tested	Not tested
	D	5	5	Not tested	Not tested

Comparison of small-scale tests: Table 4-4.8 outlines the large number of variables associated with foam performance and testing. These include factors such as foam bubble stability and fluidity, actual fire test parameters (e.g., fuel, foam application method and rate), and environmental effects. Even the fundamental methods of measuring foam performance (i.e., knockdown, control, and extinguishment) vary. For example, Johnson reported that FFFP fails the proposed ISO/EN gentle application tests because small flames persist along a small area of the tray rim.[25] As a result, the foam committees have proposed redefining extinction to include flames.

Given the variations and lack of fundamental foam spreading theory, it follows that tests and specifications for various foams and international standards have different requirements. The differences are reflected in Table 4-4.9, which compares four key parameters of MIL-F-24385, UL 162, ICAO, and ISO/EN standards for manual application (e.g., handline or turret nozzles). There is no uniform agreement among test fuel, application rate, the allowance to move the nozzle, and the extinguishment application density for AFFF. There is a factor of six difference between the lowest permitted extinguishment application density (MIL-F-24385) and the highest (ISO/EN). This significant difference is attributed, at least in part, to the fixed nozzle requirement in the ISO/EN specification.

No study has been performed to correlate test methods; given the significant differences in performance characteristics and requirements, it is unlikely that correlation between these test methods could be established, even when considering AFFF only. An AFFF that meets the ICAO standard could not be said to meet MIL-F-24385 without actual test data. The problem of correlating differences in small-scale tests was demonstrated by UL in a comparison of UL, MIL-F-24385, O-F-555B (U.S. government protein foam specification), and United Kingdom test methods.[26] In those tests, differences between different classes of agents (protein vs. AFFF) and between agents within a class (e.g., AFFF) were demonstrated. No correlations between test standards could be established.

The problem of correlation is compounded when a single test method is used in an attempt to assess different classes of foam (e.g., protein and AFFF). Attempts to use a single test method are problematic because of the inherent difference between these foams. That is, protein foams require air aspiration so that the foam floats on the fuel surface. This stiff, "drier" foam is viscous and does not inherently spread well without outside forces (e.g., nozzle stream force). AFFF, because of its film-formation characteristics, does not require the degree of aspiration that protein foams require. This heavier, "wetter" foam is inherently less viscous, which contributes to improved spreading and fluidity on fuel surfaces. This is related, at least in part, to the degree of aspiration of the foam. A more exact description of foam aspiration is appropriate. Thomas has described two levels of foam aspiration: (1) primary aspirated and (2) secondary aspirated.[27] Primary aspirated foam occurs when a foam solution is applied by means of a special nozzle designed to mix air with the solution within the nozzle. The consequence is foam bubbles of general uniformity. *Air-aspirated* foam refers to this primary aspirated foam. Secondary aspirated foam results when a foam solution is applied using a nozzle that does not mix air with the solution within the nozzle. Air is, however, drawn into the solution in-flight or at impact at the fire. Secondary aspirated foam is more commonly referred to as *non-air-aspirated* foam.

The correlation between foam solution viscosity and extinguishment time has been shown by Fiala, but the entire foam spreading and extinguishment theory has yet to be demonstrated based on first principles.[28] Thus, the test standards reference bench-scale methods that measure a factor of foam fluidity (e.g., spreading coefficient), but fail to recognize the total foam spreading system, including viscous effects. Fundamental understanding of foam mechanisms would promote the development of bench- and small-scale test apparatuses that potentially have greater direct correlation for predicting large-scale results.

There has been some criticism of the human element involved in many of the test methods. The human factor occurs when an operator is allowed to apply foam from a

Table 4-4.8 *Variables Associated with Foam Performance and Testing*

I. Physical/chemical properties of foam solution
  A. Bubble stability
    1. Measures
      a. Expansion ratio
      b. Drainage rate
    2. Variables
      a. Water temperature
      b. Water hardness/salinity
      c. Water contamination
  B. Fluidity of foam
    1. Measures
      a. Viscosity
      b. Spreading rate
      c. Film formation
    2. Variables
      a. Fuel type and temperature
      b. Foam bubble stability
  C. Compatibility with auxillary agents
    1. Measures—fire and burnback test
    2. Variables
      a. Other foam agentsl
      b. Dry chemical agents
  D. Effects of aging
    1. Measures—fire and burnback test
    2. Variable—shelf life of agent
II. Test methods to characterize foam performance
  A. Fuel
    1. Measures
      a. Vapor pressure
      b. Flash point
      c. Surface tension
      d. Temperature
    2. Variables
      a. Volatility
      b. Depth and size
      c. Initial temperature of air and fuel temperature
      d. Time fuel has been burning (e.g., short versus long, and depth of hot layer)
  B. Foam application method
    1. Measures
      a. Stream reach
      b. Aspiration of foam
      c. Foam stability, e.g., contamination by fuel
      d. Water content of foam
      e. Proportioning rate
    2. Variables
      a. Aspiration
        (1) Effect on stream reach
        (2) Degree to which foam is aspirated and the need to aspirate based on foam type

II B. 2. Variables (continued)
      b. Fixed versus mobile device
      c. Application technique
        (1) Indirect, for example, against backboard or sidewall
        (2) Direct
          (a) Gentle
          (b) Forceful
          (c) Subsurface injection
      d. Application location
        (1) High—need to penetrate plume
        (2) Low
      e. Application rate of foam
      f. Wind (as it affects stream reach)
        (1) Crosswind
        (2) With and against
      g. Effect of reduced or increased concentration due to improper proportioning
  C. Fire configuration
    1. Measures
      a. Fuel burning rate, radiation feedback to fire
      b. Propensity for reignition
      c. Surface tension
    2. Variables
      a. Pan/containment geometry
      b. Two-dimensional (pool) versus three-dimensional (running fuel/atomized pray)
      c. Presence and temperature of freeboard
      d. Wind (as it affects flame tilt and reradiation)
      e. Surface on which there is fuel
        (1) Rough
        (2) Smooth
        (3) Water substrate—"peeling" effect of fuel
  D. Measurement of results
    1. Measures
      a. Time to knockdown, control, extinguish, and burnback
        (1) Actual or estimated time by visual observations
        (2) ummation values, that is, summation of control at 10, 20, 30, and 40 sec
      b. Heat flux during extinguishment and burnback
    2. Variables—qualitative and quantitative methods to determine fire knockdown, extinguishment, and burnback
      a. 90 percent control—measure of ability of foam to quickly control the fire
      b. 99 percent (virtual extinguishment)—all but the last flame or edge extinguished
      c. Extinguishment—100 percent
      d. Burnback—25 percent, 50 percent

hand-held nozzle onto the burning test fire. Personnel are also called upon in some tests to qualitatively assess the percentage of fire involvement in the test pan during the burnback procedure. Using a fixed nozzle during a specification test eliminates the human element during extinguishment. For sprinkler applications, using a fixed nozzle is entirely appropriate and should yield results comparable to actual installations. For applications where movement is actually involved (e.g., fire-fighting hand-lines, crash-rescue truck turrets, and movable monitors on ships and at petrochemical facilities), the extinguishment densities in the fixed test application will generally exceed the densities found in actual applications in the field. (See Table 4-4.9 for differences in extinguishing densities for manual versus fixed applications.) Removal of the human element is certainly advisable from a test repeatability standpoint. However, removing the human element from approval fire tests has proved difficult. Both

Table 4-4.9 *Examples of Extinguishment Application Densities of Various Test Standards*

Test Standard	Fuel	Application Rate [lpm/m² (gpm/ft²)]	Nozzle Movement Permitted	Extinguishment Application Density [l/m² (gal/ft²)]
MIL SPEC	Motor gasoline	1.6 (0.04)	Yes	1.34 (0.033)
UL 162	Heptane	1.6 (0.04)	Yes	4.9 (0.12)
ICAO	Kerosene	2.5 (0.06)	Yes (horizontal plane)	2.6 (0.061)
ISO/EN— Forceful	Heptane	2.5 (0.06)	No	7.6 (0.19)

U.S. and Canadian military authorities have investigated the use of fixed nozzles. Both organizations concluded that tests with human operators resulted in better correlation with large fires and overall repeatability.

Quantitative methods for evaluating burnback performance have been described by Scheffey et al.[19] and been adopted in ISO/EN and Scandinavian (NORDTEST) test methods. These methods involve the use of radiometers to establish a heat flux during full test-pan involvement. After extinguishment, the radiometers measure the increasing flux as the burnback fire grows. This increasing flux due to burnback is compared against the original flux. A cutoff is established so that the maximum burnback time is the time for the burnback flux to reach some percentage (e.g., 25 percent) of the original full-burning flux.

Critical Application Rates and Correlations between Small- and Large-Scale Tests

The previous section described the application rate differences in standard test methods between AFFF, fluoroprotein, and protein foams. These application rate differences were established based on full-scale testing. For sprinklers, much of the fundamental application rate differences were established during testing conducted by Factory Mutual Research Corporation (FMRC). (See section on foam-water sprinkler systems.) For manual applications, tests in the aviation fire protection field provide the basis for the fundamental application rates. The application rates specified in test standards are usually rates lower than those used in actual practice. (See Table 4-4.3.) There are two reasons for this: (1) a factor of safety is used when specifying rates in actual practice and (2) differences between individual foam agents are more readily apparent at critical application rates. To demonstrate how application rates are developed and how specification tests correlate with large-scale results, an example from aviation fire tests will be used. This example is based on a review of foam fire test standards performed by Scheffey et al. for the Federal Aviation Administration (FAA).[23]

Tests were conducted by the FAA to determine application rates for a single-agent attack to achieve fire control (e.g., 90 percent extinguishment of a fire area) within 1

min under a wide variety of simulated accident conditions. Two factors are important in addition to the application rate required for 1-min fire control: (1) the critical application rate, below which fires will not be extinguished independent of the amount of time an agent is applied; and (2) application density, which is the amount of foam per unit area to control or extinguish a fire.

Minimum application rates were originally developed by Geyer in tests of protein and AFFF agents.[29] These tests involved "modeling" tests with JP-4 pool fires of 21-, 30-, and 43-m (70-, 100-, and 140-ft) diameter. Large-scale verification tests with a B-47 aircraft and simulated shielded fires (requiring the use of secondary agents) were conducted with 34- and 43-m (110- and 140-ft) JP-4 pool fires. All tests were conducted with air-aspirating nozzles. The protein foam conformed to the U.S. government specification, O-F-555b, while the AFFFs used were in nominal conformance with MIL-F-24385 for AFFF. These tests were being performed at the time when the seawater-compatible version of MIL-F-24385 had just been adopted based on large-scale tests.

Figure 4-4.4 illustrates the results of the modeling experiments. The results show that, for a fire control time of 60 s, the application rate for AFFF was on the order of 1.6 to 2.4 lpm/m² (0.04 to 0.06 gpm/ft²), while the application rate for protein foam was 3.3 to 4.1 lpm/m² (0.08 to 0.10 gpm/ft²). The data indicated that the application rate curves become asymptotic at rates of 4.1 lpm/m² (0.1 gpm/ft²) and 8.2 lpm/m² (0.2 gpm/ft²) for AFFF and protein foam, respectively. Above these rates, fire control times are not appreciably improved. Likewise, critical application rates for fire control are indicated when control times increase dramatically. The single test with a fluoroprotein agent indicated that this agent, as expected, fell between AFFF and protein foam.

Large-scale auxiliary agent tests were conducted to identify increases in foam required when obstructed fires
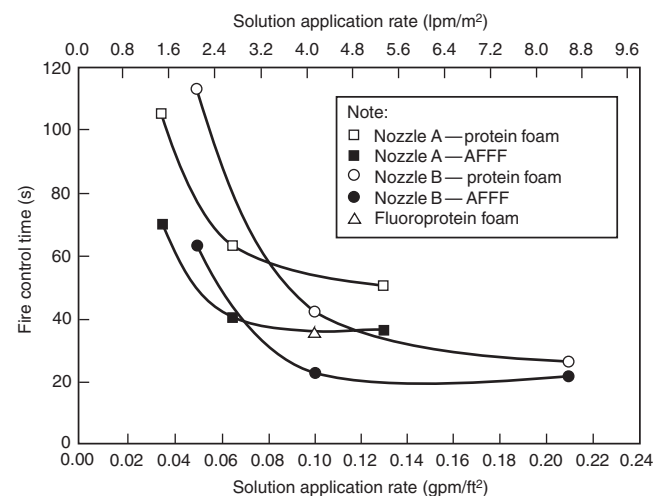
Figure 4-4.4. *Fire control time as a function of solution application rate using protein foam and AFFF on JP-4 pool fires.[29]*

with an actual fuselage were added to the scenario. The results indicated that fire control times increased by a factor of 1 to 1.9 for AFFF and 1.5 to 2.9 for protein foams. It was estimated that the most effective foam solution application rates were 4.9 to 5.7 lpm/m^2 (0.12 to 0.14 gpm/ft^2) for AFFF and 7.5 to 9 lpm/m^2 (0.18 to 0.22 gpm/ft^2) for protein foam. This is the original basis of the recommendations adopted by ICAO of 5.5 lpm/m^2 (0.13 gpm/ft^2) for AFFF and 8.2 lpm/m^2 (0.20 gpm/ft^2) for protein foam. A rate of 7.5 lpm/m^2 (0.18 gpm/ft^2) was subsequently established for fluoroprotein foam. These application rate values are still used by FAA, NFPA, and ICAO to establish minimum agent supplies at airports.

Tests of AFFF alone were conducted by Geyer.[30] These agents, selected from the U.S. Qualified Products List (MIL-F-24385 requirements), were tested on JP-4, JP-5, and aviation gasoline (avgas) fires. Air-aspirating nozzles were used with different AFFF agents. Example results are shown in Figure 4-4.5. Similar data were collected by holding the JP-4 fuel fire size constant at 743 m^2 (8000 ft^2) and varying the flow rates to develop application rate comparisons. These data are shown in Figure 4-4.6.

Additional tests were conducted by Geyer et al. to verify the continuation of the reduction of water when AFFF agents were substituted for protein foam in aviation situations.[1] In 25-, 31-, and 44-m- (82.4-, 101-, and 143-ft-) diameter Jet A pool fires, AFFF, fluoroprotein, and protein foams were discharged with air-aspirating and non-air-aspirating nozzles. The data, summarized in Figure 4-4.7, validated the continued allowance of a 30 percent reduction in water requirement at certified U.S. airports when AFFF is substituted for protein foam.

Although some test criteria in standardized methods do not necessarily correlate directly with actual fire and

Note: No fire control or extinguishment at 0.03 gpm/ft^2

- ● Control time—agent A
- ○ Fire-extinguishing times—agent A
- ■ Control time—agent A
- □ Fire-extinguishing times—agent A

Figure 4-4.6. *Fire control and extinguishing times as a function of solution application rate using AFFF at 250, 400, and 800 gpm on 743-m^2 (8000-ft^2) JP-4 fuel fires.[30]*
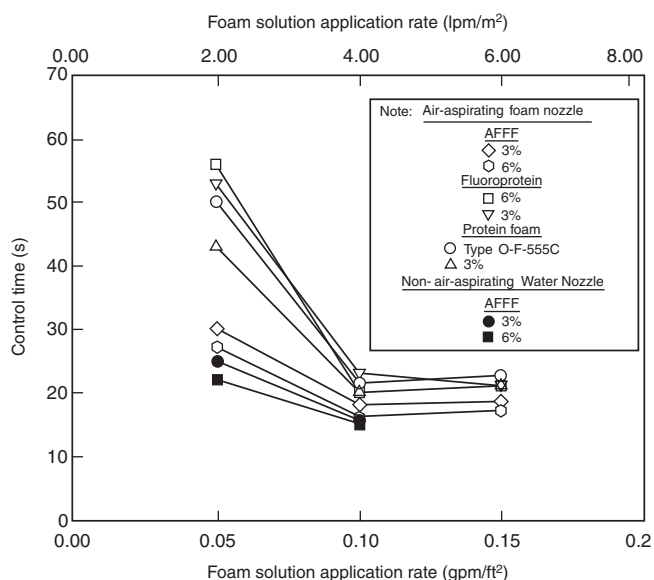
Figure 4-4.7. *Fire control time as a function of solution application rate for AFFF, fluoroprotein, and protein foams for Jet A pool fires.[1]*

Figure 4-4.5. *Fire control and extinguishing times as functions of the foam solution application rate using AFFF at 250 gpm (946 lpm), 400 (1514 lpm), and 800 gpm (3028 lpm) on JP-4, JP-5, and avgas fires.[30]*

burnback performance, small-scale test data for AFFF formulated to the U.S. military specification (MIL-F-24385) has been shown to correlate with large-scale fire test results. This is based on a comprehensive review of small- and large-scale test data.[23] In these data, a key variable

was controlled; that is, all AFFF agents were formulated to meet MIL-F-24385. Ninety percent fire control times were used as the most accurate measure of fire knock-down performance, which were reported in all tests. The use of 90 percent control times eliminates the variability of total extinguishment, which might be dependent on test-bed-edge effects or running fuel fire scenarios. Data for tests using air-aspirated or non-air-aspirated nozzles were combined. Low-flashpoint [less than 0°C (32°F)] fuels were evaluated. The evaluation included only tests where manual application was used, eliminating the variable of fixed versus manual application.

The effects of application rate on control and extinguishment times, as demonstrated in Figures 4-4.4 through 4-4.7, were reconfirmed as shown in Figure 4-4.8. Control time increases exponentially as application rate decreases, particularly below 4.1 lpm/m^2 (0.10 gpm/ft^2). Variability of the data is shown by the first standard deviation.

The scaling of small fires with large fires is shown in Figures 4-4.9 and 4-4.10, which relate the time needed to control the burning fuel surface as a function of fire size. The time needed to control a unit of burning area [s/ft^2 (s/m^2)], designated as the specific control time, is plotted as a function of fire size. For low [1.2 to 2.5 lpm/m^2 (0.03 to 0.06 gpm/ft^2)] and intermediate [2.8 to 4.1 lpm/m^2 (0.07 to 0.10 gpm/ft^2)] application rates, the specific control times decrease linearly as a function of fire area. These data are in agreement with data from Fiala, which also indicate decreasing specific extinguishment control times as a function of burning area for increasing application rates of AFFF.[28] Also, Fiala showed that, for a constant application rate, AFFFs have lower specific extinguishment times as a function of burning area than those of protein and fluoroprotein foams. Obviously, this linear relationship must change at very large areas; otherwise, the specific control/extinguishment time would go to zero. This is evidenced in Figure 4-4.9, where the curve flattens at the high-area end of the plot.

Figure 4-4.9. *Specific control times for AFFF at low application rates.[23]*
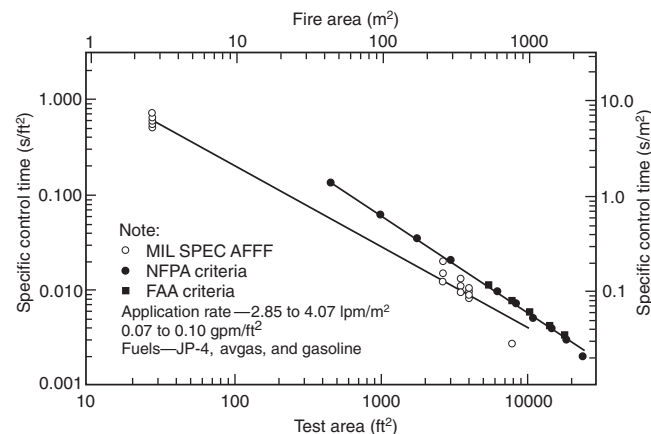
Figure 4-4.10. *Specific control times for AFFF at intermediate application rates.[23]*

Figures 4-4.9 and 4-4.10 show that higher specific control times are required for MIL-F-24385 test fires [2.6 and 4.7 m^2 (50 and 20 ft^2) compared to large fires. This is readily apparent as actual/control extinguishment times for the small fires are on the same order as results from large fires. FAA and NFPA criteria for minimum quantities of agent are also shown in Figures 4-4.9 and 4-4.10. These criteria are expressed in terms of specific control time as a function of area by using the required control time of 60 s and the practical critical fire areas for airports serving different sizes of aircraft. The data indicate that specific control times with MIL-F-24385 agents are roughly equivalent or less than the specific control times established by NFPA and FAA requirements for large fire areas. This relationship is true even with the AFFF discharged at rates 25 to 75 percent below the minimum NFPA/FAA discharge rate of 5.5 lpm/m^2 (0.13 gpm/ft^2). From these data, it can be concluded that a scaling relationship exists between MIL-F-24385 small-scale tests and

Figure 4-4.8. *AFFF control time as a function of application rate.[23]*

actual large-scale crash rescue and fire-fighting applications. The MIL-F-24385 tests are more challenging than the larger tests in terms of specific control time, but this challenging test produces an agent that can meet NFPA and FAA requirements at less than the design application rate. This factor of safety accounts for variables in actual aviation crash situations, for example, running fuel fires, debris that may shield fires, and cross winds that may limit foam stream reach.

Aviation Fire Protection Considerations

Historical Basis for Foam Requirements

The underlying principle in aviation fire protection is to temporarily maintain the integrity of an aircraft fuselage after a mishap to allow passenger escape or rescue. When an aircraft is involved in a fuel spill fire, the aluminum skin will burn through in about 1 min. If the fuselage is intact, the sidewall insulation will maintain a survivable temperature inside the cabin until the windows melt out in approximately 3 min. At that time, the cabin temperature rapidly increases beyond survivable levels.

Aircraft rescue and fire-fighting (ARFF) vehicles are designed to reach an incident scene on the airport property in 2 to 3 min, depending on the standard enforced by the authority having jurisdiction (AHJ). Having reached the scene in this time frame, agent must be applied to control a fire in 1 min or less. The 1-min critical time for fire control is recognized by FAA, NFPA, and ICAO.

Minimum agent requirements on ARFF vehicles are established using the 1-min critical control time plus the anticipated spill area for the largest aircraft using the airport. A "theoretical critical fire area" has been developed, based on tests, and is defined as the area adjacent to the fuselage, extending in all directions to the point beyond which a large fuel fire would not melt an aluminum fuselage regardless of the duration of the exposure. A function of the size of an aircraft, the theoretical critical fire area was amended to a "practical critical fire area" after evaluation of actual aircraft fire incidents. The practical critical area, two-thirds the size of the theoretical critical area, is widely recognized by the aviation fire safety community, including FAA, NFPA, and ICAO. Vehicles must be equipped with sufficient agent and discharge devices to control a fire in the practical critical area within 1 min. Vehicles must also be equipped with secondary agent (dry chemical or Halon 1211) for use in combating three-dimensional fuel fires.

Agent Quantities and Standards

The previous text on critical application rates described the rationale used to develop design application rates used in aviation fire protection. These rates are 5.5 lpm/m² (0.13 gpm/ft²) for AFFF, 7.5 lpm/m² (0.18 gpm/ft²) for fluoroprotein foam, and 8.2 lpm/m² (0.28 gpm/ft²) for protein foam. Using these rates, the practical critical fire area and the 60-s control time criteria,

minimum agent quantities are established for airports serving different size aircraft. These criteria are contained in NFPA 403, *Standard for Aircraft Rescue and Fire-Fighting Services at Airports,* and the FAA Advisory Circular 150/5210-6C, "Aircraft Fire and Rescue Facilities and Extinguishing Agents." ICAO uses similar criteria. NFPA 403 recently adopted the 4.6 m² (50 ft²) fire extinguishment and burnback criteria from MIL-F-24385 for AFFF agents. UL test criteria are acceptable for protein and fluoroprotein foams. Most airports in the United States use AFFF as the primary fire-fighting agent. Recognizing the limitations of its test methods for aviation applications, UL has deleted references to crash rescue fire fighting from the scope of UL 162, *Standard for Foam Equipment and Liquid Concentrates.* NFPA 403 recognizes that the standards for foam that it references are widely recognized throughout North America, but may not be recognized in other areas of the world. In particular, the ICAO test method has significantly different test parameters, including test fuel, application rate, and extinguishment density. The NFPA notes that it is incumbent on the national authority having jurisdiction to determine that alternative test methods meet the level of performance established by NFPA 403 test criteria.

NFPA 412, *Standard for Evaluating Aircraft Rescue and Fire-Fighting Foam Equipment,* provides field test methods to determine the adequacy of foam equipment on crash rescue vehicles. It includes criteria for foam expansion and drainage, and methods to determine foam solution concentration.

Expansion and drainage: Foam expansion and drainage requirements of the current version of NFPA 412, *Standard for Evaluating Aircraft Rescue and Fire-Fighting Foam Equipment,* are shown in Table 4-4.10.

NFPA 412 references a 1600-ml foam sample collector, which was originally adopted by ICAO and ISO/EN. This single method is used to obtain expansion and drainage measurements for all types of foams in hope that similar success could be obtained in using a single fire test method for all foams. The multiple categories of foam test classification in Table 4-4.7 for the ISO/EN method show how difficult this has been to achieve. Given the different methods of foam flow over a fuel surface, it may not be practical to use a common fire test method predicated on the current means of testing. Further development of fundamental foam-extinguishing principles is recommended.

Table 4-4.10 *Foam Quality Requirements from NFPA 412*

Agent	Minimum Expansion Ratio	Minimum Solution 25% Drainage Time (min)
AFFF or FFFP		
Air aspirated	5 : 1	2.25
Non-air-aspirated	3 : 1	0.75
Protein	8 : 1	10
Fluoroprotein	6 : 1	10

The 1600-ml expansion and drainage test method replaced two other methods where a 1000-ml cylinder or 1400-ml pan was used as the collection device. MIL-F-24385 still uses the 1000-ml collection method. This situation, plus other different test methods, makes direct comparison of expansion and drainage data difficult. Tests performed by Underwriters Laboratories (UL) identified differences among the three test methods based on expansion and drainage results.[31] UL found that expansion ratios remained the same but that drainage was quicker using the 1600-ml method compared to the 1000-ml method for film-forming foams. Drainage time increased (i.e., doubled) for the protein foams when the 1600-ml method was used compared to the 1400-ml pan method.

No direct correlations have been established between expansion, drainage, and fire-extinguishing performance. There is a relationship between foam drainage and burnback. Longer drainage times generally result in longer burnback times.

The expansion and drainage data in Table 4-4.10 indicate the inherent differences between air-aspirated and non-air-aspirated film-forming foams. The data in Figure 4-4.7 showed that non-air-aspirated AFFF was more effective at critical application rates than air-aspirated AFFF. This conclusion was verified by Jablonski in tests with U.S. Air Force crash trucks as shown in Figure 4-4.11.[32] Even so, there continues to be debate over aspirated and non-air-aspirated foam for manual applications involving aviation fuel spills.

Under certain conditions, non-air-aspirated AFFF is not as effective as air-aspirated AFFF. The results of the foam tests in the United Kingdom[33,34] and the results from DiMaio et al.[35] described situations where air-aspirated AFFF resulted in better fire extinguishment performance than non-air-aspirated foam.

Given that one-to-one correlation between expansion, drainage, and fire-extinguishing performance is difficult to identify, there appears to be a lower limit where non-air-aspirated AFFF becomes ineffective. This has not been quantified, but it is speculated that poor performance occurs when AFFF expansion ratio is less than 2.5 to 3.0, and drainage is difficult to measure, that is, nearly instantaneous. This is based in part on unpublished data from the Naval Research Laboratory on shipboard bilge AFFF sprinklers[36] and the results of the U.K. tests.[33,34] The importance of this lower limit of foam aspiration is recognized in NFPA 412 criteria.

Foam concentration determination: The most common method of determining foam concentration in the field is by use of a hand-held refractometer. The refractive index, n, is defined as

$$n = \frac{\sin i}{\sin r} \quad (10)$$

where

$\sin i$ = angle of incidence

$\sin r$ = angle of refraction

This is depicted graphically in Figure 4-4.12.

Manufacturers report that the glycols in AFFF formulations create the necessary refractive characteristics to determine concentration. However, they also report that glycol has a potential detrimental impact on overall agent performance. Elimination of this compound might improve (slightly) the performance of AFFF, but the glycol is also needed as a fundamental component of agent mixing.

The refractive index of water at 20°C (68°F) is 1.333 (air has a refractive index of 1.0002926). Since the refractive index of a solution is proportional to the inverse of the solution density, and density is proportional to temperature, then

$$n \propto \frac{1}{T} \quad (11)$$

Figure 4-4.11. *Effects of AFFF aspiration on JP-4 pool fire control times.*[32]

Note:
Refractive index, $n = \dfrac{\sin i \text{ (angle of incidence)}}{\sin r \text{ (angle of refraction)}}$
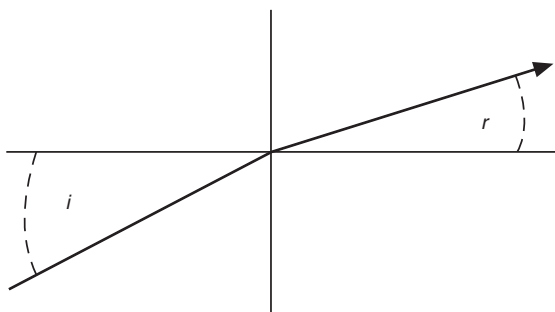
Figure 4-4.12. *Refractive index of solutions.*
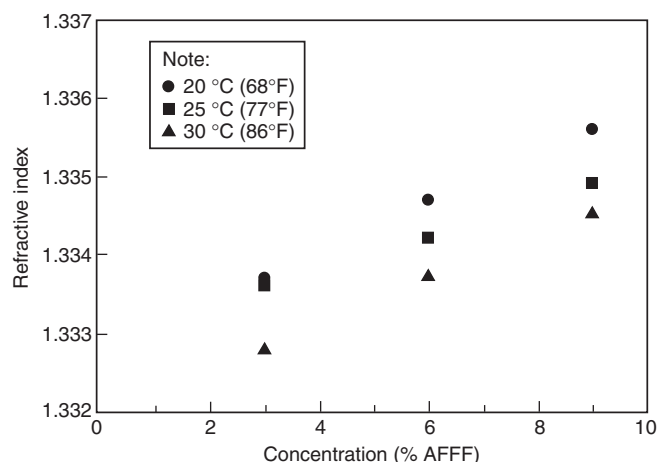
Figure 4-4.13. *Effects of temperature on refractive index.*[37]

Figure 4-4.14. *Refractive indices of 1 percent AFFF solutions in tap water.*

where T is the temperature. This relationship is illustrated in Figure 4-4.13. Any refractive index measurements must be made considering temperature. Some hand-held measurement devices are temperature compensated. It is good procedure to conduct concentration measurements at a constant temperature.

Other scales may be used. For example, the Brix scale is used as a measure of sucrose weight percent concentration. Units with this scale, commonly found in the food product industry, can be used to measure foam concentration. A typical range of a bench or hand-held refractometer is 1.3000 to 1.7000.

NFPA 412, *Standard for Evaluating Aircraft Rescue and Fire-Fighting Foam Equipment,* describes a method to determine foam concentration using the refractive method. In NFPA 412, the preparation of three standard solutions is recommended: one at the nominal concentration, one at one-third more than the nominal concentration, and one at one-third less than the nominal concentration. A plot of the refractive scale reading against the known foam concentration is made on graph paper. This plot establishes a "calibration" curve against which foam samples from a vehicle or system can be judged. Since refractive index is linear, a calibration curve can be created by

$$\text{AFFF } \%_{\text{sample}} = \frac{n_{\text{foam}} - n_{\text{water}}}{n_{\text{concentrate}} - n_{\text{water}}} \times 100 \qquad (12)$$

This method is used by the U.S. Navy for checking proportioning system accuracy onboard ships.

The limitations of the refractive index technique are described by Timms and Haggar.[37] The accuracy of the refractometer can become poor due to the focusing and setting of the refracted light junction on the cross hairs of the viewing window, and the reading of the graduated scale to four decimal places (where the scale is graduated only to three places). This effect is illustrated in Figure 4-4.14, where a calibration curve for a 1 percent AFFF concentrate was established using a straight line through the 50
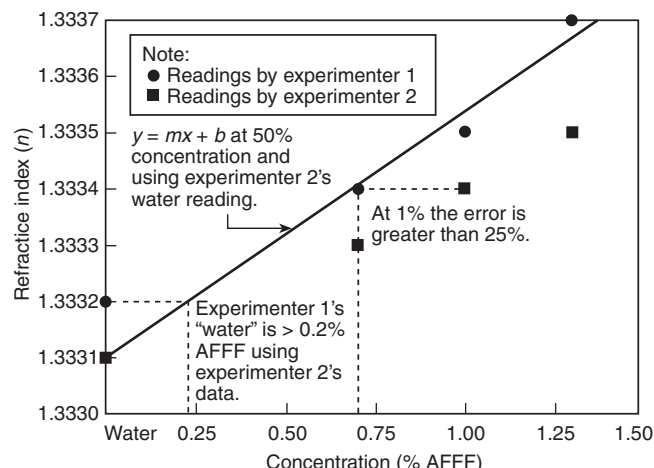
percent concentration point and the "water" reading by one of the experimenters. Note that the error between readings by the two experimenters at 1 percent concentration exceeds 25 percent. In this example, differences in the baseline water reading will create substantial error in the calibration curve. These differences are exaggerated with 1 percent concentrates. At 3 percent or 6 percent, the experimental error in reading the refractometer, for field testing, is generally accepted as adequate.

Alternative methods for measuring AFFF concentration include total fluorine content, optical absorption methods, and electrical conductivity. Since neither the total fluorine content method nor optical absorption method is suited to field use, the conductivity method has been proposed. Since foams contain electrolytes, their conductance, G, can be measured and described as

$$G = \frac{1}{R} \text{ (mhos)} \qquad (13)$$

where R = resistance (ohms). Conductivity, σ, is conductance per unit length:

$\sigma = G/\text{unit length}$

$= \text{mhos/cm}$

$= \text{siemens/cm}$

Since conductivity is directly proportional to temperature, conductivity increases with temperature. (See Figure 4-4.15.) Temperature compensation is appropriate when using this method.

Timms and Haggar showed the influence of the substrate water on both refractive index and conductivity.[37] (See Figures 4-4.16 and 4-14.17.) It is important to note the difference of the characteristic curve for a salt solution. AFFF actually reduces the conductivity of this highly conductive water. Note also that, while conductance may exhibit straight-line characteristics in the area of interest (0 to 10 percent), the overall curves from 0 to 100 percent are nonlinear.
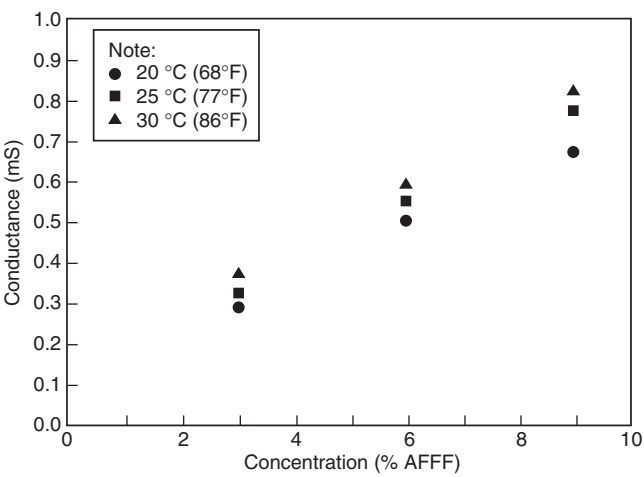
Figure 4-4.15. *Effects of temperature on the conductance of AFFF solutions.*[37]
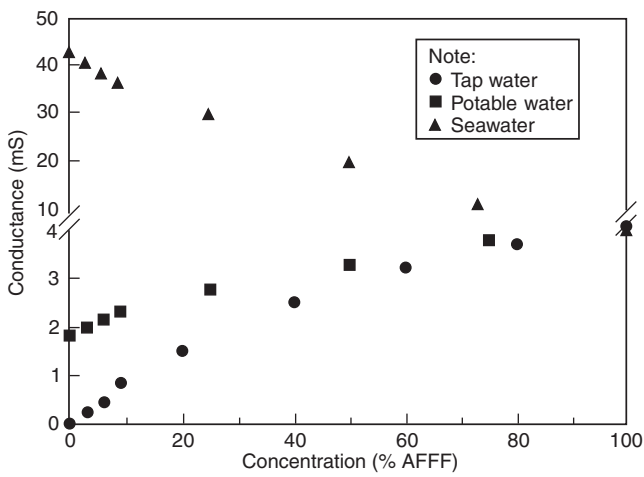
Figure 4-4.17. *Effect of substrate water on conductivity of AFFF solutions.*[37]
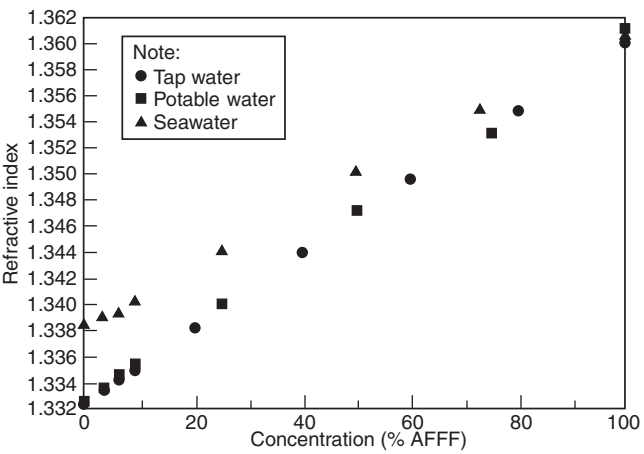
Figure 4-4.16. *Effect of substrate water on refractive index of AFFF solutions.*[37]

Table 4-4.11 *Sensitivity of Refractive Index and Conductivity Methods for Determining Foam Concentration*[37]

	Refractive Index	Conductance (mS)
3%	1.3337	0.318
6%	1.3343	0.558
Difference	0.0006	0.240
"Sensitivity"	0.0005 (0.5 in 1000)	0.43 (430 in 1000)

Table 4-4.12 *Accuracy of Foam Test Measurements*[37]

Solution	Refractive Index	Electrical Conductance	Actual
A	4.5% ± 0.8%	3.5% ± 0.1%	3.50 ± 0.01%
B	5.1% ± 0.8%	5.5% ± 0.1%	5.50 ± 0.01%
C	8.7% ± 0.8%	8.5% ± 0.1%	8.50 ± 0.01%

The "sensitivity" of the two methods (i.e., refractive index and conductivity) was shown by these researchers by comparing the difference between readings for solutions of 3 percent and 6 percent divided by the reading at 6 percent. The sensitivities for tap water show that the conductivity method is more sensitive than the refractive index measure. (See Table 4-4.11.) In repeated readings of refractive index and conductivity, the foam concentration accuracy using conductivity was ± 0.1 percent, where the accuracy of the refractive index method was ± 0.8 percent. (See Table 4-4.12.)

The electrical conductivity method is now recognized in NFPA standards. NFPA 412 cautions against the use of this method for seawater applications. The electrical conductivity method, used for process control in the chemical industry, has recently been adapted for use as a proportioning controller for AFFF systems.

Aircraft Hangar Protection

The two objectives of aircraft hangar protection are (1) protect aircraft and (2) prevent collapse of the hangar roof structure, which is usually unprotected steel. The protection of the aircraft is the principle concern, since its value is generally many times that of the structure. This concern is particularly true for advanced military aircraft. Historically, these protection systems have been deluge-type sprinkler systems with open-head nozzles. They are activated by rapid-response detection systems.

Before the development of foam, water-deluge systems were used. The original foam-water sprinkler systems used protein foam. With the development of AFFF, research was performed to determine appropriate application rates and types of discharge devices. The research work, performed primarily by Factory Mutual Research Corporation (FMRC), provides the basis not only for current aircraft hangar protection criteria, but also for other sprinkler suppression system criteria.

Overhead sprinkler protection: Before the advent of foam, hangars were protected by conventional spray sprinklers using water. Water-deluge systems having discharge rates on the order of 10.4 lpm/m² (0.25 gpm/ft²) were used in conjunction with sloped floors and drains to protect aircraft. Even with these systems, activated by detection systems, burnthrough protection of aircraft fuselages (e.g., 1 min) could not be ensured. Ceiling temperatures in an 18.3-m- (60-ft-) high space on the order of 427 to 816°C (800 to 1500°F) have been recorded for fuel spill fires where this protection was provided. For a 121-m² (1300-ft²) JP-4 fuel fire, 927°C (1700°F) ceiling temperatures have been recorded within 30 s of ignition prior to deluge system discharge.

Protein foam systems, discharging at a rate of 8.2 lpm/m² (0.20 gpm/ft²), were an improvement on the water systems. Air-aspirating sprinklers were required to make effective protein foam. Because of the high centerline velocities of a pool fire plume, the foam flow from the perimeter toward the center of the fire was thought to be the dominant suppression mechanism.[38]

With the development of AFFF, FMRC conducted a series of tests for the U.S. military to establish appropriate design parameters. In a series of baseline comparison tests, FMRC compared AFFF with protein foam. The tests consisted of 83.6-m² (900-ft²) JP-4 pool fires in an 18.3-m-(60-ft-) high space. Air-aspirating, standard upright, and old-style upright sprinklers were evaluated at application rates of 4.1 to 8.2 lpm/m² (0.10 to 0.20 gpm/ft²). In one test, a low-level turret nozzle discharging AFFF was used in conjunction with sprinklers discharging water. Table 4-4.13 summarizes the results of the AFFF tests. A comparison of Tests 4 and 5 with Test 3 indicates improved results from the use of standard sprinklers compared to foam-water sprinklers. At application rates of 6.6 lpm/m² (0.16 gpm/ft²), the standard sprinklers were 1.3 to 1.6 times as effective in achieving extinguishment compared to air-aspirating foam-water sprinklers. At an application rate of 8.2 lpm/m² (0.20 gpm/ft²), the extinguishment times with AFFF from foam-water sprinklers were comparable to results from protein foam tests. Rapid suppression with the turret nozzle [at 8.3 lpm/m² (0.22 gpm/ft²)] combined with an overhead water system was demonstrated in Test 7. No adverse effects were evident from the water discharged from the overhead sprinklers after the foam ran out.

The superior performance of the standard sprinklers was attributed to more effective plume penetration by higher density foam particles. The maximum centerline velocities measured were 23.2 m/s (76 ft/s), with 15.2 m/s (50 ft/s) at the centerline of the fire. The fire plumes tended to bend due to air currents within the test building. Since the terminal velocity of the foam agents was estimated to be on the order of 9.1 m/s (30 ft/s) maximum, the droplets near the centerline never reached the fire. This result supports the theory that extinguishment occurs from the outside perimeter inward. Since foam droplets from standard sprinklers are about twice as dense as air-aspirated particles, the terminal velocities are greater. Greater velocities allow greater penetration of the fire plume. The same mechanisms explain why air-aspirated AFFF provides similar performance to protein foam. When the AFFF is air aspirated, there is no longer any advantage of increased droplet terminal velocity.

Table 4-4.13 *Hangar Deluge System Tests by Factory Mutual Research Corporation[38]*

Test Conditions	Test No. 2	Test No. 3	Test No. 4	Test No. 5	Test No. 6	Test No. 7 (turret nozzle)
Type of Head	Foam-water	Foam-water	Standard	Standard	Standard	Old-style sprinkler
Spacing [m² head⁻¹ (ft² head⁻¹)]	7.4 (80)	9.3 (100)	12.1 (130)	12.1 130	9.3 (100)	9.3 (100)
Application rate [lpm/m² (gpm/ft²)]	8.2 (0.20)	6.6 (0.16)	6.6 (0.16)	6.6 (0.16)	5.2 to 4.4 (0.125 to 0.105)	6.6 (0.16) (water system)
End head pressure [kPa (psi)]	193 (28)	193 (28)	97 (14)	97 (14)	35 (5)	55 (8) (water system)
25% Drainage time (min)	2.5	2.1	0.5–0.8	1.0–1.3	0.5–0.7	No data recorded
50% Drainage time (min)	5.0	4.4	1.3–1.8	1.8–2.3	1.2–1.6	No data recorded
Expansion ratio	4.3 : 1	3.4 : 1	2.2 : 1	1 : 25	2.2 : 1	12 : 1
Extinguishment time (min : s)	2 : 22	2 : 15	1 : 45	2.3 : 1	3 : 05	≈0 : 33

Table 4-4.14 *Estimated Particle Diameter vs. Terminal Velocity[40]*

Particle Diameter [mm (in.)]	Water	Terminal Velocity [m/s (ft/s)]		
		Foam		
		Expansion Ratio 2:1	Expansion Ratio 5:1	Expansion Ratio 10:1
12.7 (0.5)	See note[a]	10.1 (33)	6.7 (22)	4.6 (15)
6.3 (0.25)	10.4 (34)	7.3 (24)	4.6 (15)	3.4 (11)
2.5 (0.1)	6.7 (22)	4.6 (15)	2.7 (9)	—

[a]The breakup of water drops greater than about 6.3-mm (0.25-in.) diameter is highly probable due to instability.

Additional work by FMRC established estimates for the terminal velocity of foam, as shown in Table 4-4.14.[39,40] Plume theory was used to estimate roughly that velocity on the order of 18.3 m/s (60 ft/s) could be expected in an 18.3-m- (60-ft-) high space with an 83.6-m² (900-ft²) JP-4 fire. This estimate was in good agreement with the experimental results. Based on an average foam particle diameter of 6.3 mm (0.25 in.), a maximum terminal velocity of 7.3 m/s (24 ft/s) could be expected. For a JP-4 pool fire, this translates into a 0.7-m²- (8-ft²-) maximum fire size before plume penetration is not possible.

The practical significance of AFFF discharged through non-air-aspirating sprinklers was demonstrated by Breen et al.[40] Air-aspirating sprinklers require 207-kPa (30-psi) nozzle pressure to be effective. Standard sprinklers can discharge effective AFFF solution at pressures as low as 69 kPa (10 psi). This had important retrofit considerations where foam proportioning system losses could be made up through reduced sprinkler pressures.

Additional tests were conducted with closed-head sprinklers in an 18.3-m- (60-ft-) high hangar.[41] Potential cost benefits would have resulted from reduced hardware costs and unwanted discharges from deluge systems. These tests demonstrated that this concept was not feasible for the hangar scenario because of the large number of sprinklers that opened during the 83.6-m² (900-ft²) fire tests.

The superior performance of standard sprinklers compared to air-aspirating sprinklers is reflected in the criteria of NFPA 409, *Standard on Aircraft Hangars.* If standard sprinklers are used with AFFF, the design application rate for overhead deluge systems may be reduced to 6.6 lpm/m² (0.16 gpm/ft²) from 8.2 lpm/m² (0.20 gpm/ft²) required for air-aspirated sprinklers. This decrease represents a 20 percent reduction in foam required when standard sprinklers are used.

Low-level application of AFFF: With the increase in wingspan areas of large aircraft, it was recognized that significant damage could occur before extinguishment of the pool fire underneath the wing. Using overhead sprinklers only, FMRC demonstrated the times required for the foam to spread and extinguish fires. (See Table 4-4.13.) The concept of low-level application of foam, using monitors or turret nozzles, was developed to reduce extinguishment time where shielded fires may occur. This concept was later extended to include side-mounted nozzles and discharge outlets, and flush-mounted nozzles installed in a floor or deck.

These systems are effective because AFFF solution droplets do not have to penetrate the fire plume. They also typically deliver, at spot locations, high densities of foam. A high density allows the foam to gain a "bite" or toehold on the fire. Low-level AFFF systems have been used successfully for over two decades on U.S. Navy air-capable ships, protecting flight decks and special hazard areas.

Table 4-4.15 summarizes fire test data for low-level application of AFFF. As seen, control and extinguishment times are quite rapid. NFPA 409, *Standard on Aircraft*

Table 4-4.15 *Fire Test Data for Low-Level Application of AFFF*

Reference	Test No.	Test Area [m² (ft²)]	Fuel	Nozzle	Nozzle k Factor (gal/psi^0.5)	Maximum Spray Height[a] [m (ft)]	Spray Diameter[a] [m (ft)]	Nominal Application Rate [lpm/m² (gpm/ft²)]	Control and Extinguishment Times
FMRC 1975[39]	3	83.6 (900)	JP-4	Turret nozzle (monitor)	50.3	50-degree arc, 8-s cycle time, 15-degree angle of elevation, 25.9 m (85 ft) from the center of the test pool		4.1 (0.10)	90% in 10 to 15 s 100% in 35 to 40 s
	4	83.6 (900)	JP-4	Turret nozzle (monitor)	50.3	50-degree arc, 8-s cycle time, 15-degree angle of elevation, 25.9 m (85 ft) from the center of the test pool		4.1 (0.10)	90% in 1 min 30 s[b] 100% in ≈ 2 min
	6	83.6 (900)	JP-4	Turret nozzle (monitor)	50.3	50-degree arc, 8-s cycle time, 15-degree angle of elevation, 25.9 m (85 ft) from the center of the test pool		4.1 (0.10)	90% in 20 s 100% in 25 s

Table 4-4.15 *Fire Test Data for Low-Level Application of AFFF (Continued)*

Reference	Test No.	Test Area [m² (ft²)]	Fuel	Nozzle	Nozzle k Factor (gal/psi[0.5])	Maximum Spray Height[a] [m (ft)]	Spray Diameter[a] [m (ft)]	Nominal Application Rate [lpm/m² (gpm/ft²)]	Control and Extinguishment Times
FMRC 1973[38]	7	83.6 (900)	JP-4	Overhead OSS[c] + Turret nozzle	5.0	N/A	N/A	6.6 (0.16)[d] + 9.0 (0.22) — 9.5 (0.38)	Control in 17 s[d] 100% in 33 s
Australia[42]	1	78.5 (846)	Aviation kerosene	P10 Pop-up	4.1	0.8 (2.6)	4.3 (14.1)	5.5 (0.13)	95% in 30 s
	2	78.5 (846)	Aviation kerosene	W-1 Pop-up	3.6	1.5 (4.9)	3.3 (10.8)	4.9 (0.12)	≈90% in 25 s[e]
	3	78.5 (846)	Aviation kerosene	P-10	4.1	0.8 (2.6)	3.3 (10.8)	5.5 (0.13)	98% in 30 s
Naval Weapons Center Phase III 1972[43]	5	697 (7500)	JP-5	Type S flush deck	5.5	1.8 (6)	12.2 (40)	1.6 (0.04)	50% in 30 s 90% in 60 s
	11	697 (7500)	JP-5	Type S flush deck	5.5	1.8 (6)	12.2 (40)	2.4 (0.06)	70% in 30 s 95% in 60 s
	9	697 (7500)	Avgas	Type S flush deck + deck edge	5.5 [114 lpm (30 gpm)	1.8 (6)	12.2 (40)	2.4 (0.06) + 1.6 (0.04) — 4.1 (0.10)	15% in 30 s 50% in 60 s
	15	697 (7500)	Avgas	Type S flush deck + deck edge	5.5 [114 lpm (30 gpm)]	1.8 (6)	12.2 (40)	2.4 (0.06) + 1.6 (0.04) — 4.1 (0.10)	40% in 30 s 70% in 60 s
Naval Weapons Center Pop-Up 1984[44]	10 and 10R	372 (4000)	JP-5	Type SB flush deck	5.1	1.8 (6)	9.1 to 12.2 (30 to 40)	2.4 (0.06)	60 to 90 s for 90% control; 99% in 2 min
	5, 5R, and 5R1	372 (4000)	JP-5	Bete pop-up	5.5	1.8 (6)	9.8 (32)	2.4 (0.06)	60 to 90 s for 90% control; 99% in ≈ 2 min
Naval Weapons Center Weapons Staging Area 1998[45]	I8	48.3 (520)	JP-5	Overhead side-mounted spray nozzles	1.9	NA	NA	8.6 (0.21)	90% in 15 s 99% in 52 s 100% in 57 s
	I11	48.3 (520)	JP-5	Overhead side-mounted spray nozzles	1.9	NA	NA	21.6 (0.53)	90% in 8 s 99% in 15 s 100% in 27 s
	II6[f]	66.9 (720)	JP-5	Low-Level fan	4.7	NA	NA	11.8 (0.29)	90% in 24 s 99% in 52 s 100% in 79 s
	II12[f]	66.9 (720)	JP-5	Low-Level fan	4.7	NA	NA	20.4 (0.50)	90% in 9 s 99% in 16 s

[a]Spray height and diameter at the pressure/flow used in the test

[b]An unplanned 69-kPa (10-psi) pressure drop in FMRC Test 4 caused a 4.6-m (15 ft) reduction in nozzle range, resulting in 90 percent control and extinguishment times 3 to 4 times those observed in Tests 3 and 6.

[c]No wing obstruction over fire test area

[d]The overhead deluge system discharging ordinary water was accidentally activated 12 sec later than the turret nozzle (5 sec before control was attained). The contribution, if any, of the overhead deluge system toward complete extinguishment was judged to be quite small compared to the turret nozzle.

[e]Wind-affected results

[f]Deck pool fire area was obstructed with simulated weapons carts.

Hangars, criterion of 4.1 lpm/m² (0.10 gpm/ft²) for low-level applications is based on a fire control time of 30 s and extinguishment in 60 s. Data indicate that a JP-5 pool fire can be 90 percent controlled in 60 to 90 s and 99 percent extinguished in 2 min when an application rate of 2.4 lpm/m² (0.06 gpm/ft²) is used. The system can be effective at rates as low as 1.6 lpm/m² (0.04 gpm/ft²). For low-flash-point fuels (e.g., avgas), control time increases. Control and extinguishment times can be reduced by increasing the application rates on JP-5 fuel fires. Based on these results, the U.S. Navy adopted an AFFF application rate of 2.4 lpm/m² (0.06 gpm/ft²) for protecting aircraft carrier flight decks.[46]

While they may help control a three-dimensional (spill) fire, low-level application systems cannot be assumed to suppress totally a running fuel fire. Running fuel fires at a spill rate of 189 lpm (50 gpm) are typically used in U.S. Navy flight-deck suppression tests using the flush-deck system. The running fuel fire, shielded by simulated aircraft debris, requires aggressive handline attack for extinguishment.[47]

Obstructions, such as parked vehicles, may block low-level nozzles. Testing for a flight-deck weapons staging area showed that a side-mounted low-level system could be effective even when nozzles are obstructed.[45] In these tests, 5 of the 12 deck-edge nozzles were obstructed to simulate vehicle tires blocking edge-mounted nozzles. Even with 40 percent reduction, the fire was controlled and extinguished in less than 1 min (compared to 15 to 30 s when unobstructed).

Cost of installation, maintainability, and reliability are factors when considering a low-level application system. Reliability issues with turrets/monitors have been identified by both FMRC and the U.S. Navy. The flush-deck system adopted by the U.S. Navy took considerable effort before a high degree of reliability and maintainability could be achieved. This open deluge nozzle, originally installed as a water washdown nozzle, incorporates a ball-check feature in the nozzle orifice to prevent debris from clogging the nozzle. Clean-out traps are installed in system piping for maintenance. Pop-up nozzles have been proposed as an alternative to flush-deck nozzles. These nozzles have their own reliability and maintainability issues. Unless there are very high costs associated with the loss of an aircraft, in-floor or flush-deck nozzles are generally cost-prohibitive for commercial aviation facilities. For high risk/cost applications, in-floor nozzles may be justified. This may be the case for advanced military aircraft; for example, research has been performed on an inverted deluge system that not only can suppress a pool fire, but also can cool exterior combustible components of the airframe. Initial installations have suffered from design and installation problems.[48] Lack of experience with these types of systems was the significant single cause of problems with these systems. Acceptance testing and maintenance were found to be lacking.

Side-mounted nozzles are the most reliable systems, consisting of open-pipe or -spray nozzles. The spreading rate of foam from an aspirated open-pipe system increases control and suppression time. Open-spray nozzles can be very effective, but their reach is limited.

New hangar fire protection design concepts: Issues related to asset protection, reliability of fixed systems, and environmental impact led the U.S. Navy to reevaluate their approach to hangar fire protection systems. A goal was established to install reliable and easily maintained fire protection systems that prevent damage to the hangar structure and to aircraft not directly involved in an initial spill fire ignition. This goal resulted in a multidiscipline study to address all associated technical issues.

All military service branches in North America have been plagued with false activation involving foam-water-deluge sprinkler systems over aircraft with open cockpits. These false activations have been caused by numerous sources including lightning strikes that introduced transient voltage spikes into the fire alarm system; water hammers in aging underground water distribution systems; accidental releases by maintenance personnel; deliberate acts of vandalism; accidental activation of manual pull stations; failure of pressure relief valves at pumping stations; roof-water leakage into overhead heat detection systems; and false activation of fire detection systems. This prompted the pursuit of alternative fire protection designs that would provide the desired level of protection.

Alternative designs included the use of closed-head AFFF overhead sprinkler systems and greater reliance on low-level monitor nozzle AFFF systems as the primary extinguishing component as described in the previous section. Low-level systems were originally designed to provide supplementary protection for the area shadowed from the overhead system by large wing areas. In pursuing these alternative designs, technical and operational issues and limitations of both existing and proposed new systems were identified:

- Thermally activated systems may result in unacceptably high damage to assets prior to fire control/extinguishment, particularly in very high bay hangar ceilings (see Reference 49).
- While it is readily accepted that conventional hangar fire protection systems were not designed to extinguish a three-dimensional fire, some fire protection engineers believed that AFFF extinguishing systems could be designed to control a spill fire and limit the area of the fire to only those aircraft intimate with the initial ignition source.
- Different aviation fuels are now commonly being used, e.g., JP-5 and JP-8 are now the predominant fuels, compared to the lower flashpoint JP-4 previously used.
- Low-level AFFF monitor nozzle systems are
  —Relatively inefficient in terms of pattern distribution
  —Unreliable
  —Susceptible to blockage by equipment
  —Commonly found out of service in the field
- Any new AFFF low-level nozzle should be designed for minimal overspray and should not be significantly impacted by water discharge from any water-only protection system.
- Optical fire detectors are
  —Prone to false alarms
  —Currently tested, listed, and approved using fuels that are not typical in aviation

—Subjected to few if any sources of false alarms in currently recognized approval standards

A concept was developed by the U.S. Navy to meet the desired performance goals. This concept included the following:

- Use of low-level AFFF deluge nozzles, having minimal overspray, to control/extinguish liquid fuel pool spill fires
- Operation of the low-level AFFF system using improved optical detectors designed to
  —Be highly immune to false alarms
  —Rapidly detect JP-5 fuel spill fires
- Installation of a quick-responding, closed-head, wet-pipe sprinkler system in the hangar ceiling
- Implementation of lessons learned from all military hangar design experiences in a comprehensive new, improved design

Most of the research and development associated with the process has been completed and is described in References 49 to 54. Two aspects of U.S. Navy research and development are germane to the performance of AFFF. The first involves the performance of AFFF when subjected to water spray from sprinklers. The second is a developmental effort initiated to design a reliable, low-profile AFFF nozzle that could be installed in the floors of hangars.

Twenty-three full-scale fire tests were conducted to evaluate the effects of overhead water sprinklers on AFFF foam blankets.[51] One AFFF application rate [4.0 lpm/m^2 (0.1 gpm/ft^2)] and two sprinkler application rates [6.5 and 10.2 lpm/m^2 (0.16 and 0.25 gpm/ft^2)] were included in this evaluation. The tests were conducted on a range of spill fires. The spill fires were produced using either JP-5 or JP-8 aviation fuels and were evaluated on a concrete pad with similar drainage characteristics typical of navy hangars. The spill fires continued to burn (i.e., were shielded) during water/foam application. The heating effect on the burnback resistance of foam, with and without sprinkler water application, was evaluated.

The results show that the use of water sprinklers in conjunction with a low level AFFF fire suppression system [with an application rate of 4.0 lpm/m^2 (0.1 gpm/ft^2)] had minimal effects on the ability of the system to suppress the fire and resist burnback. In all tests, the low-level AFFF system was capable of quickly extinguishing the test fire (control ~30 s and extinguishment ~1 min) independent of the sprinkler application rate. The time required for the fire to burnback across the fuel surface was apparently a function of the drainage characteristics of the hangar and was only slightly affected by the application of water through the overhead sprinklers. The tests also show that the flashpoint of the fuel has an effect on the control, extinguishment, and burnback resistance capabilities of the system. Although the burnback times for the lower flashpoint fuels were faster than the higher flashpoint fuels, the duration of protection was not significantly altered. These tests show that overhead water sprinklers have minimal effect on AFFF foam blankets, in-

dependent of the test fuel, particular fire, and sprinkler application rate. A combined low-level AFFF extinguishing system operating in conjunction with an overhead water sprinkler system provided adequate burnback protection during AFFF discharge, but this protection may be lost shortly (a few minutes) after the end of AFFF discharge.

The new low-level fire-extinguishing system was designed to discharge AFFF adequately across a hangar floor, to be less likely to be affected by obstructions, and to reduce the likelihood of damage to exposed aircraft electronic equipment.[53] To achieve these objectives, the nozzle was designed to

- Produce a nominal AFFF application rate of 4.0 lpm/m^2 (0.1 gpm/ft^2)
- Operate at a nominal pressure of 2.8 bar (40 psi)
- Provide coverage to a distance of 7.6 m (25 ft) from a hangar floor drainage trench (centerline of two parallel trenches spaced 15.2 m (50 ft) apart)
- Spray AFFF so that the pattern height does exceed 0.3 m (1 ft) above the deck

The nominal AFFF application rate of 4.0 lpm/m^2 (gpm/ft^2) was selected based on current design practices as described in the previous two sections of the chapter. The nozzle operating pressure was selected based on standard, commercially available pump performance curves and preliminary estimates of friction loss for the system.

Over 50 nozzles were evaluated for this application.[53] Testing of these nozzles indicated that, while a limited number of commercially available nozzles could meet the design requirements, manufacturing, installation, and operation of these nozzles under normal hangar conditions was not feasible. Existing pop-up nozzles were not designed for the high flow rates or spray characteristics required of this application. As a result of these deficiencies, a prototype nozzle was developed. The prototype concept was subsequently developed into a commercially available nozzle. Foam pattern, distribution, and flow tests were conducted by Underwriters Laboratories Inc. on a nozzle with a flow coefficient of 22.6 k (gpm/psi$^{1/2}$).

There is no universal agreement on the proper approach to military hangar fire protection in North America. For example, the U.S. Air Force recognizes the use of high-expansion foam. A number of these systems have recently been installed. The Canadian Ministry of Defense (MoD) is investigating the possible use of compressed-air foam. Additionally, the U.S. Army has evaluated the use of early–suppression fast-response (ESFR) closed-head water sprinkler protection for helicopter hangars.[55] FMRC concluded that both 93°C- (200°F-) temperature-rated ESFR sprinklers discharging at 345 kPa (50 psig) [41 lpm/m^2 (1.0 gpm/ft^2)] and 517 kPa (75 psig) [49 lpm/m^2 (1.2 gpm/ft^2)] and 141°C- (286°F-) temperature-rated, k = 5.6 (gpm/psi$^{1/2}$) quick-response sprinklers at 345 kPa (50 psig) [16 lpm/m^2 (0.40 gpm/ft^2)] can provide adequate fire protection for the hangar against a 61-m^2 (200-ft^2), 473-l (125-gal) JP-4 aviation fuel-pan fire. For some tests, fuel depletion was necessary for the fire to be controlled.

Foam-Water Sprinkler Systems

This chapter has dealt with foam characteristics, foam concentrate, test standards, and manual application techniques. In particular, applications in the aviation industry were described. The text on aircraft hangar protection introduced the concept of fixed foam protection systems. In particular, much of the foam-water sprinkler system test data was originally developed for aircraft hangars. Herein, additional foam-water sprinkler system design criteria are described. Again, emphasis is placed on AFFF systems since they are more effective for extinguishment than protein or fluoroprotein systems.

Codes, Standards, and Regulations

Overhead foam-water sprinkler systems, as specified in the NFPA standards, are generally designed to serve dual purposes: (1) to control and/or suppress a fuel spill fire and (2) when the foam runs out, to cool materials with water. Since the systems are designed to provide protection for flammable/combustible liquid hazards and ordinary combustibles, the specified application rates reflect this dual-protection approach. Table 4-4.3 shows the fundamental application rates used by Underwriters Laboratories on hydrocarbon fuel fires to evaluate sprinklers. The fire must be extinguished within 5 min for AFFF discharged at 4.1 lpm/m² (0.10 gpm/ft²) for standard sprinklers and 6.6 lpm/m² (0.16 gpm/ft²) for agents discharged from foam-water sprinklers (air aspirating). However, since most deluge and closed-head sprinkler systems are installed in industrial occupancies, they must meet highly protected risk (HPR) insurance requirements. As a result, the NFPA standard for deluge and closed-head AFFF systems (NFPA 16, *Standard on the Installation of Deluge Foam-Water Sprinkler and Foam-Water Spray Systems)* requires 6.6-lpm/m² (0.16-gpm/ft²) minimum water application. This water application rate also provides a safety factor over the 4.1 lpm/m² (0.10 gpm/ft²) rate at which AFFF discharged from sprinklers is effective on pool fires. The safety factor is reflected in Table 4-4.3 under the column heading Minimum Application Rate.

Table 4-4.16 summarizes current requirements from NFPA standards and guidelines. NFPA 11, *Standard for Low-Expansion Foam,* is geared toward petroleum and chemical industry protection. Previous requirements from NFPA 11 allowed 4.1 lpm/m² (0.10 gpm/ft²) for loading racks, for example, tank truck loading facilities. The latest requirements for NFPA 11 eliminate this design criterion and reference NFPA 16 requirements, which require 6.6 lpm/m² (0.16 gpm/ft²). In special situations, 4.1 lpm/m² (0.10 gpm/ft²) is permitted by NFPA 11, but only where there is low-level or manual application for a hydrocarbon fuel spill. NFPA 16 is consistent in requiring 6.6 lpm/m² (0.16 gpm/ft²); it references other NFPA standards for special exceptions, for example, NFPA 409, *Standard on Aircraft Hangars,* and NFPA 30, *Flammable and Combustible Liquids Code.* NFPA 409 requirements were previously discussed. Section 4, Chapter 5 provides an example for calculating foam quantities based on design application rates and areas to be protected.

With the publication of the 1998 edition of NFPA 11, marine foam application is now addressed. Foam appli-

Table 4-4.16 *NFPA Standards Related to AFFF Sprinkler Systems*

Standard[a]	Minimum AFFF Application Rate [lpm/m² (gpm/ft²)]	Duration (min)
NFPA 11, (1998) *Low-Expansion Foam*	Indoor storage tank greater than 37 m² (400 ft²) 6.6 (0.16)	30
	Loading rack monitors 4.1 (0.10)	15
	Diked areas Fixed low level (Class II hydrocarbon) 4.1 (0.10)	20
	Monitor 6.6 (0.16)	20
	Undiked areas for AFFF handlines 4.1 (0.10)	15
NFPA 16, *Standard for the Installation of Foam-Water Sprinkler and Foam-Water Spray Systems* (1999)	6.6 (0.16)	10 min; 7 min if above minimum design
NFPA 409, *Standard on Aircraft Hangars* (1995)	Overhead deluge 8.2 (0.20) for aspirated AFFF	10 min; 7 min if above minimum design
	6.6 (0.16) for non-air-aspirated AFFF	
	Supplemental low level (for shielded wing areas) 4.1 (0.10)	10 min

[a]See Additional Readings for complete titles and dates.

Table 4-4.17 *Foam Application Rate for Marine Hydrocarbon Hazards (NFPA 11)*

Type of Hazard	Calculation of Rate
Deck spill	6.50 lpm/m² (0.16 gpm/ft²) or 10% of the cargo block area
Largest tank	9.78 lpm/m² (0.24 gpm/ft²) of the single largest tank area
Largest monitor	3.0 lpm/m² (0.074 gpm/ft²) of the area protected by the largest monitor (not less than 1250 lpm)

cation rates are required to be not less than the greatest of that required for deck spills, the largest tank, or the largest monitor solution flow rate as shown in Table 4-4.17 for hydrocarbon fuels and Table 4-4.18 for polar solvents. For polar solvents, standardized fire tests are used to determine the minimum foam design application

Table 4-4.18 *Foam Application Rate for Marine Polar Solvent Hazards (NFPA 11)*

Type of Hazard	Calculation of Rate
Deck spill	Rate for most hazardous polar solvent × 10% of the cargo block area
Most demanding tank	150% of the highest required foam application rate for the single largest tank
Largest monitor	45% of the highest required foam application rate applied over the area protected by the monitor (not less than 1250 lpm)

rate for the most difficult extinguishment case. Foam concentrates for hydrocarbon fuels must be approved using a 9.29-m² (100-ft²) fire test similar to UL 162. The fixed-nozzle gasoline fire test has an extinguishment application density of 12.2 l/m² (0.30 gal/ft²).

Model building and fire codes in the United States are in the process of adopting AFFF protection criteria for the storage of flammable and combustible liquids. Criteria of insuring authorities [e.g., Industrial Risk Insurers (IRI) and Factory Mutual (FM)] are similar to the NFPA requirements. Insurance authority guidelines should be referenced for specific projects, since there are differences in protection criteria.

Protection of Stored Flammable and Combustible Liquids

Flammable and combustible liquids are stored in containers ranging in size from less than one quart to several hundred gallons. These liquids may be stored for display in a retail outlet or "super store," or stored for distribution in a general-purpose warehouse housing many different combustibles, or stored in "liquid" warehouses containing large quantities of the liquid. NFPA 30, *Flammable and Combustible Liquids Code,* is the applicable NFPA protection document. This code includes requirements for tank storage, piping systems, containers, and operations. Criteria for suppression system protection is addressed in the sections dealing with container storage.

The protection of flammable and combustible liquids is a function of many factors, including the liquid properties, the ignition (which can be a factor of the storage occupancy), the packaging system (e.g., stored in cardboard cartons), the container design and material (e.g., steel, plastic, glass, fiberboard), and the arrangement of storage (e.g., rack versus pallet, storage height, aisle width, and mixture of other combustibles in the array). Based on these factors, a suppression system is provided to control or suppress the anticipated fire and protect the structure. The system may be designed to (1) control a fire so that the fire department can ultimately extinguish or suppress the burning material or (2) suppress the fire. Variables in suppression system design include sprinkler application rate, agent, orifice size, spacing, response time index (RTI), temperature rating, and provision of in-rack protection.

The basis of protection criteria in NFPA 30 is now well documented. Fire test references and associated citations in technical literature are now included with all protection tables.[56] The basis of the protection criteria can now be directly linked to test data or engineering extrapolations of the data. Material in Appendix E of NFPA 30 provides guidance and an example test protocol for evaluating protection of liquids stored in the containers. This includes consideration of the source of the fire, which may be a "point" ignition (i.e., small ignition) or a large spill/three-dimensional fire. Depending on other variables, such as container type and packaging material, one of these scenarios may be more difficult to protect. Appendix E of NFPA 30 provides detailed guidance on this subject.

Stored liquids may be protected using water sprinklers, foam, or other approved methods. Figure 4-4.18 shows a conceptual grouping of water and AFFF protection methods as a function of container type and storage method for water protection of liquids. The reader should consult Reference 56. The basis of AFFF protection is described in the following sections.

Protection of drum and tank storage: Some of the earliest work using AFFF sprinklers involved the protection of 208-l (55-gal) drums. In work conducted at Factory Mutual Research Corporation, sponsored by Allendale Insurance, Factory Insurance Association (FIA), and the 3M Company, the effectiveness of standard sprinklers supplied with AFFF for controlling drum fires was determined.[57] Five fire tests were conducted in simulated flammable liquid-drum storage using two types of storage arrangements. Three tests were conducted with two-, three-, and four-high palletized drum storage, respectively. Two tests were conducted with five-tier high-rack storage of palletized drums.

In all tests, a heptane fuel supply simulated leakage from the upper level of storage. Except for one rack-storage
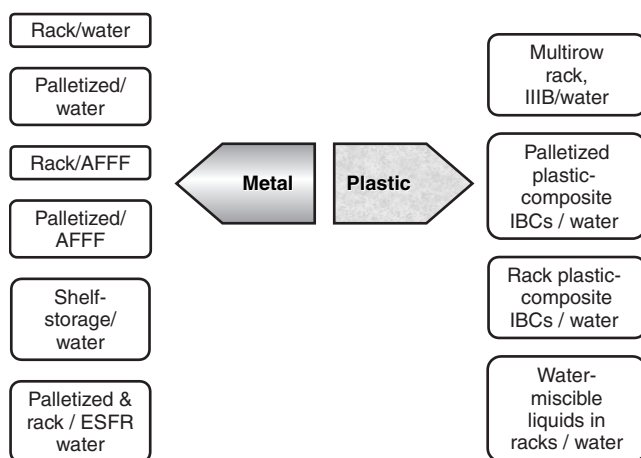
Figure 4-4.18. *Grouping of NFPA 30 protection criteria for liquids.*

test that used a 57-lpm (15-gpm) spill rate, fuel spillage was 7.6 lpm (2 gpm). Ceiling protection employed high-temperature sprinklers at discharge rates of either 12.3 or 24.6 lpm/m² (0.30 or 0.60 gpm/ft²). In-rack supplemental protection for the rack-storage tests was provided at three levels, with ordinary temperature sprinklers each discharging 113 lpm (30 gpm). The success of each test was based on storage stability, that is, no pile collapse, and limitation of drum pressure to 104 kPa (15 psig).

AFFF was effective in controlling spill fires on the floor. The exception was in areas not reached by the discharge from operating sprinklers, where the flow of foam was blocked by pallets. Protection was not effective on the three-dimensional spill fires. Fire exposure and resultant pressure development within drums was more severe with increased clearances between storage and sprinklers due to greater delays in sprinkler operation.

Generally, results were considered good in the rack-storage tests, where in-rack sprinklers were provided in each tier. For palletized storage, the AFFF protection controlled the floor fire although pallets hindered the spread of foam. Ceiling sprinklers alone did not adequately protect palletized storage where an elevated spill resulted in a three-dimensional fire within the pile.

The results of these tests were used, along with engineering judgment, to develop AFFF protection criteria in NFPA 30, *Flammable and Combustible Liquids Code.* AFFF protection of 12.3 lpm/m² (0.30 gpm/ft²) at the ceiling for rack protection of metal drum/tank storage up to 7.6 m (25 ft) high. In-rack protection (e.g., sprinklers in alternating tiers or every tier) is a function of the liquid (flashpoint), container style (relieving vs. nonrelieving), and capacity of the container.

The results of the original Factory Mutual (FM) drum tests were extended in a series of tests conducted by Southwest Research Institute.[58] The objective was to test the effectiveness of relieving-style steel drums and varying degrees of overhead sprinkler protection to mitigate fire hazards associated with the storage of flammable liquids. Nylon plugs inserted in the 5.1-cm (2.0-in.) pour hole and 1.3-cm (0.5-in.) vent hole were designed to melt under fire conditions, allowing the drum to vent any built-up pressure. Heptane, a Class IB flammable liquid, was used as the stored commodity.

Tests were designed to model credible, worst-case loss scenarios involving the 208-l (55-gal) storage of the commodity. The fire modeled the accidental puncture of a full drum, and either an immediate or a delayed ignition source. Sprinkler suppression of the fire was monitored for the duration of the spill, and until flames were either under control or completely extinguished. Commodity was stacked in a 3 × 3 palletized array, to varying heights (2, 3, or 4 high), and protected with varying sprinkler types and densities.

The relieving-style closures were successful at mitigating the hazards associated with overpressurizing drums during a fire. The installed suppression systems were capable of either extinguishing or controlling the fire for the duration of the spill. A summary of the successful protection configurations for the commodity tested is provided in Table 4-4.19.

Table 4-4.19 *Summary of Heptane-Palletized Drum Storage Tests*[58]

Test	Commodity	Protection (nominal application rates)
2 and 3	3 × 3, 2 high	3% AFFF at 12.3 lpm/m² (0.30 gpm/ft²)
5	3 × 3, 2 high	ELO water-based at 24.6 lpm/m² (0.60 gpm/ft²)
7	3 × 3, 3 high	ELO, 3% AFFF at 18.5 lpm/m² (0.45 gpm/ft²)
8	3 × 3, 4 high	ELO, 3% AFFF at 24.6 lpm/m² (0.60 gpm/ft²)

The fuel spill rate (7.6 vs. 56.8 lpm) was found to have a substantial impact on the fire exposure of the drums. When taken in conjunction with the effect of the ignition scenario, the fuel spill rate had a strong influence on the number of initial heads operating and on the duration of the fire exposure. The ignition of the fuel source also played a role in the number of heads actuated during a test. The immediate ignition of fuel (simulating a spill onto an existing ignition source) resulted in a slower growing fire, actuating fewer sprinkler heads. Alternately, an ignition scenario where a 7.6-l spill was allowed to develop prior to ignition resulted in the actuation of four heads within the first minute of fire exposure. A comparable test with the immediate ignition scenario resulted in only two heads operating in a time in excess of 2 min and 30 s. The involvement of fewer sprinkler heads and the prolonged fire exposure implied that the immediate ignition provided a more challenging scenario.

The AFFF system used in the test program was successful in generating a good blanket of foam within 1 to 2 min of actuation (depending on the number of initial heads actuated). The foam quality was such that it was free to flow over drum heads, providing cooling to the tops and sides of drums, and forming a blanket at the floor to suppress pool fires. The foam system (in Tests 6 through 8) was also effective at limiting the fire at the fuel introduction point, periodically extinguishing the source. In general, by the time fuel flow to the array was complete, the foam system had suppressed all pool fires, leaving only small pallet fires for manual suppression.

An initial survey of closure obstruction versus venting phenomenon indicated that there was little or no effect on the obstruction of a plug and its ability to vent. This is indicated by the low number of drums that exhibited bulging during tests. The bulging of a drum indicates an unusual buildup of pressure. This phenomenon was not consistent, even in drums where both closures were obstructed. It was also noted that even partial venting of either opening was sufficient in reducing the pressure within the drum.

Drum deformation was recorded on a subjective basis. Typical deformation involved bulging of the head of the drum by 1.2 to 2.5 cm (0.5 to 1.0 in.). In some cases, deformations were seen on the order of 7.6 to 10.2 cm (3 to 4 in.) with some unfurling of the head chime.

It is difficult to attribute the level of deformation with a corresponding internal pressure. Several drums were deformed to a degree consistent with hydrostatic pressures of 207 to 241 kPa (30 to 35 psi); however, no pressures of this magnitude were recorded. A possible reason for higher levels of deformation at lower pressures may lie in the exposed temperatures of the drums. Several drums were subjected to uneven heating. The uneven heating phenomenon is present where a drum is located directly above a pallet containing venting drums. This scenario sets the subject drum over an isolated flame source, heating it from below.

The results of these tests have been included in the NFPA 30 protection criteria tables for palletized steel drum storage up to four high when protected using AFFF. The use of listed relieving devices is recommended; the exact details of this listing procedure are being developed.

Liquid spill and container storage: Table 4-4.20 summarizes early closed-head AFFF sprinkler testing on a flammable liquid spill.[59] In a 9.1-m- (30-ft-) high ceiling room, *n*-heptane was discharged in a simulated spill to create a three-dimensional spill and a two-dimensional pool fire. Fuel spill rate was varied up to 113 lpm (30 gpm). AFFF application rates were 4.5 to 12.3 lpm/m^2 (0.11 to 0.30 gpm/ft^2). The primary variables were the temperature rating of the sprinkler and the application rate. Non-air-aspirating sprinklers were used. The data show that high-temperature-rated sprinklers activated at about the same time as ordinary temperature sprinklers, controlled the fire in comparable times (roughly 2 min control time), and resulted in significantly fewer sprinklers operating (7 versus 32). An increase in application rate when the high-temperature sprinklers were used resulted in fewer heads operating, but did not decrease overall control and extinguishment time. Fires were controlled, but not totally extinguished as a result of the three-dimensional spill fire. These tests showed the advantage of using high-temperature-rated sprinklers in AFFF closed-head suppression systems.

In response to the concerns related to flammable liquid warehouse protection, the National Fire Protection Research Foundation (NFPRF) initiated the International Foam-Water Sprinkler Research Project. The objectives were to document the performance of foam-water sprinkler systems designed for real-world storage and ignition scenarios and provide a design basis and minimum design parameters for foam-water sprinkler systems. Five tasks were performed, including a literature search, range-finding tests, and large-scale tests involving palletized and rack storage of liquids.

The literature search identified over 1100 sources of information related to flammable liquid fires and foam protection, but a dearth of data related to water and foam-water sprinkler suppression of liquid storage fires.[60] The range-finding tests indicated that the Class IB flammable liquids (heptane) provided a greater challenge than water-miscible fuels (e.g., isopropanol).[61] Breach of steel containers exposed to a flammable liquid pool fire without sprinkler protection occurred over a range of times between 2 and 7.5 min, depending on the particular type of container. Plastic containers were quickly breached and discharged their contents to the exposing pool fire.

Large-scale tests were conducted under an 8.2-m- (27-ft-) high ceiling at the Underwriters Laboratories fire test facility in Northbrook, Illinois.[62] A series of 14 fire tests involving the protection of 3.8- and 18.9-l- (1- and 5-gal-) metal and 18.9-l (5-gal) plastic containers filled with heptane (Class IB flammable liquid) were conducted. The use of closed-head foam-water sprinkler systems for the protection of these fuel packages was investigated. Quantities of fuel used in the fire tests varied from 605 to 7260 l (160 to 1920 gal); fuel storage densities ranged from 160 to 1907 l/m^2 (3.9 to 46.5 gal/ft^2); and storage heights ranged from 4.3 to 42.7 m (1.3 to 13 ft). Each fire test was initiated using a 37.8-l (10-gal) flammable liquid (heptane) spill, recognizing the larger spill ignition scenarios observed in large-loss fires.

Fire tests involving palletized storage of 3.8-l (1-gal) metal F-style containers of heptane, packaged four containers in a corrugated cardboard carton, were conducted. The results indicated that the 37.8-l (10-gal) flammable liquid spill fire could be suppressed by a closed-head foam-water sprinkler system at a 16.4 lpm/m^2 (0.40 gpm/ft^2) design application rate for storage heights up to 3.3 m (10.7 ft) under the 8.2-m (27-ft) ceiling prior to any container breach or fuel loss. Fires involving 18.9-l (5-gal) metal containers of heptane could be suppressed by a closed-head foam-water sprinkler system application rate of 12.3 lpm/m^2 (0.30 gpm/ft^2) for a palletized storage height

Table 4-4.20   *Closed-Head Sprinkler Tests*[59]

Sprinkler Temperature Rating [°C (°F)]	Nominal Application Rate [lpm/m^2 (gpm/ft^2)]	Total Heads Opened	Sprinkler Operation and Control Times (min : s)
71 (160	4.5 (0.11)	34	First sprinkler—0:27 Final sprinkler—1:01 3:50 Control time
71 (160)	7.4 (0.18)	32	First sprinkler—0:22 Final sprinkler—1:08 1:00 to 1:20 for knockdown 2:20 Control time
138 (280)	7.4 (0.18)	7	First sprinkler—0:33 Final sprinkler—0:531 1:50 Control time
138 (280)	7.4 (0.18)	15	First sprinkler—0:28 Final sprinkler—1:44 2:20 Control time
138 (280)	7.4 (0.18)	17 to 19	First sprinkler—0:22 to 0:24 Final sprinkler—1:03 to 1:13 2:00 Control time
141 (286)	12.3 (0.30)	10	First sprinkler—0:24 Final sprinkler—1:10 2:25 Control time

of up to 3.6 m (12 ft). Plastic pour spouts in the 18.9-l (5-gal) tight-head metal containers safety vented and prevented container breaching.

Fires involving 18.9-l (5-gal) plastic containers of heptane could not be suppressed by a preprimed, closed-head foam-water sprinkler system with an application rate of 12.3 lpm/m^2 (0.30 gpm/ft^2), where containers were stacked one high [483 mm (19 in.)], due to container breaching and flammable liquid spillage prior to foam-water discharge.

Rack-storage tests also conducted in the NFPRF International Foam-Water Sprinkler Research Project did not lead to conclusive results.[63]

Based on the results of the NFPRF foam-water sprinkler testing, the FMRC original AFFF drum testing, and engineering judgment/extrapolation, the NFPA 30 Technical Committee adopted protection criteria for palletized and rack storage of liquids in metal containers when protected by AFFF. Variables that affect the specific level of protection include container size, class of liquid stored, inclusion of exterior packaging material, and storage height. Ceiling application rates are on the order of 12.3 to 16.4 lpm/m^2 (0.30 to 0.40 gpm/ft^2). Protection criteria shown in Table 4-4.21 are recommended for palletized storage of small containers that are nonrelieving style (i.e., do not readily vent when exposed to fire). Additional criteria are included in NFPA 30 for foam protection of palletized relieving-style containers based on extrapolation of the NFPRF data and engineering judgment. Where the hazard involves a water-miscible fuel, an alcohol-type foam should be used. The application rate should be at least as great as the rate established by foam listing requirements. AFFF solution should be discharged when four sprinklers are operating.

AFFF protection of flammable and combustible liquids should be used where large spills of low flashpoint fuels are a realistic scenario. Other protection options are available and have recently been adopted or are currently being con-

sidered by NFPA 30 and the model building/fire prevention codes. Designers of warehouse protection should have a thorough knowledge of these criteria and the available test data (including water-only protection) when considering design options for the protection of stored combustible and flammable liquids. Reference 56 and NFPA 30 provide detailed data and guidance for water-only protection. Additional guidance for warehouse protection is available from the Center for Chemical Process Safety.[64]

Foam Environmental Considerations

There has been increasing concern about the consequences of the discharge of foam in the environment. This concern affects the users of foam, the manufacturers of foam agents, the fire safety authority having jurisdiction, and environmental authorities. Quantitative data and methods to evaluate environmental impact are not widely published or well developed. The issue is not a new or unique development but has received increased notice as a result of increased attention to environmental impact of fire-fighting agents.

Factors related to the impact of fire-fighting foam on the environment include

1. Discharge of foam solutions and fuel-contaminated foam solutions to waterways and the potential toxicity to aquatic life
2. Effects on water treatment facilities
3. Persistence and biodegradability of chemicals in foam concentrates and solutions
4. Combustion products of fuel/foam solutions

Perspective on the Use of Foam Agents

In order to assess the impact of foam on the environment, the likely scenarios under which AFFF may be discharged should be considered. Based on these scenarios, the overall impact can be assessed and, where appropriate, potential mitigation strategies can then be developed. Likely scenarios include uncontrolled fires, potential hazardous situations, fire-fighting training evolutions, and fixed or mobile vehicle suppression system discharge testing.

Uncontrolled fires: There are many fires for which foam may be used, including flammable liquid storage, process industry protection, aviation protection, and marine applications. For most fires, the elimination of foam as a suppression agent results in the potential for dramatically increased environmental impact. This impact results from the potential increase in hydrocarbon fuel effluent to the environment (due to smoke from uncontrolled burning and fuel/fire-fighting water effluent). Consider the example shown in Figure 4-4.19. A 929-m^2 (10,000-ft^2) section of a warehouse containing combustible and flammable liquids may be protected using traditional water sprinklers discharging at a rate of 12.3 lpm/m^2 (0.30 gpm/ft^2). If these sprinklers fail to control a large spill fire, the fire may develop and spread past the design area of the sprinklers. The example assumes the fire is contained within the fire wall; this may not always be the case for high-challenge fires. If the fire department aggressively combats the fire, a

Table 4-4.21   *AFFF Sprinkler Protection Requirements in NFPA 30 for Solid-Pile and Palletized Storage of Flammable and Combustible Liquids in Non-Relieving-Style Metal Containers of 18.9-l (5-gal) Capacity or Less*

Package Type	Cartoned	Uncartoned
Class liquid	IB, IC, II	IB, IC, II
Application rate [lpm/m^2 (gpm/ft^2)]	16.4 (0.40)	12.3 (0.30)
Area [m^2 (ft^2)]	186 (2000)	186 (2000)
Temperature rating [°C (°F)]	141 (286)	141 (286)
Maximum spacing [m^2/head (ft^2/head)]	9.3 (100)	9.3 (100)
Orifice size [mm (in.)]	13.3 (0.53)	12.5 or 13.3 (0.5 or 0.53)
Maximum height [m (ft)]	3.4 (11)	3.7. (12)
Hose [lpm (gpm)]	1891 (500)	1891 (500)
Water supply duration (min)	120	120
Foam supply duration (min)	15	15
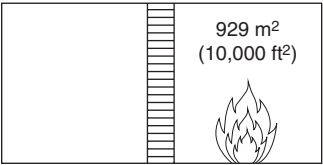
Warehouse storing flammable and combustible liquids

929 m² (10,000 ft²)

Design basis—water

Sprinklers

$$\frac{12.3 \text{ lpm/m}^2 \ (0.3 \text{ gpm/ft}^2) \times 279 \text{ m}^2 \ (3,000 \text{ ft}^2) \times 2 \text{ hr}}{= 408,348 \text{ l} \ (108,000 \text{ gal})}$$

Hose stream

$$\frac{1,891 \text{ lpm} \ (500 \text{ gpm}) \times 2 \text{ hr}}{= 226,890 \text{ l} \ (60,000 \text{ gal})}$$

Total 635,208 l (168,000 gal)

If water sprinklers are inadequate,
the potential water used can be estimated

$$\frac{12.3 \text{ lpm/m}^2 \ (0.3 \text{ gpm/ft}^2) \times 929 \text{ m}^2 \ (10,000 \text{ ft}^2) \times 2 \text{ hours (estimate of suppression time)}}{= 1,361,160 \text{ l} \ (360,000 \text{ gal})}$$

Multiply this times an "efficiency factor" of 35

$$= 48 \text{ l} \ (12.6 \text{ gal}) \times 10^6$$

Design basis—foam

Sprinklers

$$\frac{16.4 \text{ lpm/m}^2 \ (0.4 \text{ gpm/ft}^2) \times 186 \text{ m}^2 \ (2,000 \text{ ft}^2) \times 15 \text{ hr}}{= 45,372 \text{ l} \ (12,000 \text{ gal})}$$

Hose stream

$$\frac{1,891 \text{ lpm} \ (500 \text{ gpm}) \times 30 \text{ min}}{= 56,715 \text{ l} \ (15,000 \text{ gal})}$$

Total 102,087 l (27,000 gal)

Figure 4-4.19.   Example of potential effluent from flammable liquid warehouse fire.

rough estimate of fire-fighting water that may be used is 15 to 50 times the minimum anticipated agent required for suppression.[6,65,66] A rough estimate of the potential fuel-contaminated effluent (neglecting the actual quantities of hydrocarbon liquid) is shown in Figure 4-4.19. In the alternative situation, a properly specified foam-water sprinkler system designed for a high degree of reliability can control or suppress the fire. Using application rates and discharge times based on recent tests and building code requirements, the anticipated fuel/foam/water effluent for this scenario can be estimated. (See Figure 4-4.19.) The use of the foam-water system reduces the potential effluent by a factor of nearly 500 compared to the "unsuccessful" water sprinkler scenario where handlines are used. This reduction neglects the impact of smoke discharged to the atmosphere during the uncontrolled burning in the water-only scenario.

In some cases, it may be possible to collect the effluent from an uncontrolled fire. In other situations, it may not be possible. Any foam solution that has been used in fire suppression is likely to be contaminated with fuel and diluted with water.

Potential hazardous situations: Potential hazardous situations may result from a fuel spill where there is a likely ignition source. In this situation, foam may be applied for ignition prevention. The potential impact of ignition and resulting uncontrolled fire must be assessed against the potential additional environmental impact by discharging foam for ignition prevention. The potential environmental effects from an uncontrolled fire should be considered as described in the previous text. Another consideration is the assessment of any additional impact of foam when applied to a fuel spill. For example, would the resulting fuel with foam have any greater impact on the environment than the fuel alone? If so, how is this impact quantitatively determined?

Training evolutions: Fire-fighting training is usually conducted under conditions conducive to collection of fuel, water, and foam. A separation process might be used to recover fuel. Water/foam solution may then be treated or reused. Alternatively, simulated hydrocarbon fuel spill scenarios might be used, with a simulated foam agent. Propane-fired burners are typically used. The disadvantage of these systems is the potential loss of realism of the simulated fire/agent interaction. These techniques may potentially reduce training effectiveness. Quantitative comparisons have not been performed to assess these differences.

System discharge testing: Facilities protected by foam systems may have containment systems that can hold effluent. Requirements for these containment systems are becoming more widespread in model building and fire codes. An alternative to discharge testing with foam is the use of a simulant that can be measured using concentration determination methods. For example, salt solutions can be used as the "concentrate" to test AFFF systems, with the simulant concentration measured using the conductivity method. Simulators may be more difficult to use for protein-based systems, where viscosity factors influence proportioning system accuracy.

Methods of Assessment

Biodegradability: The primary component of AFFF solution is water. Examples of other components are nonfluorinated surfactants, glycol ethers, and fluorinated surfactants. Freeze-resistant concentrate may contain ethylene or propylene glycol. Alcohol-type foams contain xanthan or similar gums. The fluorinated surfactants are particularly resistant to biodegradation. Further, the less-effective protein-based foams were largely assumed to be nonpolluting because of their "natural" organic base. An early review of the available literature by Factory Mutual Research Corporation indicated that both types of agents, that is, AFFF and protein-based, present inherent environmental issues and that effluents containing either should be processed in some form of sewage treatment facility or diluted prior to discharge into a stream.[39]

A conventional method used to determine the biodegradability of a material is comparison of the chemical oxygen demand (COD) of the material with its biological oxygen demand (BOD). This method is particularly important for waste treatment facilities where the stability of the treatment process may be upset. The method typically used is specified in "Standard Methods for the Examination of Water and Wastewater."[67] BOD measures the amount of oxygen consumed by microorganisms in breaking down a hydrocarbon. COD measures the maximum amount of oxygen that could theoretically be consumed by microorganisms. Therefore, a BOD/COD ratio is representative of the ability of microorganisms to biodegrade the components in a foam. The higher the BOD/COD ratio, the more biodegradable the foam. Results reported for BOD/COD of AFFF range from 0.60 to 0.99. MIL-F-24385 requires a maximum COD of 500,000 mg/l and a minimum 20-day BOD/COD ratio of 0.65 for 6 percent concentrate. AFFF agents have been reported to have higher BOD and COD values than protein foams.[39] AFFF solutions are high-BOD materials compared to the normal influent to treatment plants. Large quantities can "shock load" wastewater treatment facilities.

The fluorochemical-based surfactants in AFFF have a carbon–fluorine chain that apparently does not break down in either the BOD or the COD test. The AFFF might then appear to be completely "biodegradable," even though the carbon–fluorine chain remains.

If nonbiodegradability concerns are based on the persistence of the fluorochemical surfactants, then the environmental impact tests currently used to assess foams do not address this concern. There is speculation that the undegradable material is biologically inert, but no published data confirms this. Since the fluorinated surfactants are required to create surface-tension reduction of the solution, replacement with less persistent chemicals is problematic. There is a need for a more thorough understanding and testing related to the environmental impact of fluorosurfactants and possible alternatives.

The persistence of fluorosurfactants in soil has recently been quantified in a study of fire-training facilities.[68] In a study of training sites having long-term use, perfluorocarboxylates were detected using gas chromatography/mass spectrometry. These chemicals were detected at sites that were inactive for a period of 7 to 10 years. The results are consistent with the view that biodegradation of the long chain perfluorocarbon is unlikely. The influence of the perfluorinated compounds on the biotransformation and transport of other cocontaminants (e.g., training fuel) and other site characterization parameters (e.g., dissolved organic carbon and inorganics) is unknown.

Methods for detecting AFFF in aqueous solutions have been investigated.[69] A Fourier Transform Infrared Spectroscopy (FTIR) method and drain-time test were found to be effective in evaluating the level of AFFF contamination in wastewater and soil. The drain-time method was proposed as a simple, easy-to-use field test. Using these methods, procedures were developed to estimate AFFF contamination levels in wastewater and soil. Analysis of wastewater and soil for AFFF contamination was broken into two groups: nonbiodegraded samples and biodegraded samples. Nonbiodegraded samples were screened for AFFF, then analyzed further if deemed necessary. Samples were initially screened using the drain-time test. Samples with no drain time contain less than a 1:240 dilution of AFFF (5 ppm of fluorosurfactant). If the sample had a drain time, it was recommended that the FTIR analysis be performed on the sample. In solutions with fluorosurfactants, FTIR analysis can provide a quantitative level of AFFF in the sample if the fluorosurfactant source solution is available to develop a calibration curve. Otherwise, FTIR provides a qualitative estimate of the AFFF level in the solution.

Biodegraded wastewater samples were difficult to analyze because the hydrocarbon surfactants and a portion of the fluorosurfactant molecule are degraded. With these foam-making constituents degraded, the drain-time test results were found to be unreliable. However, the fluorine-carbon tail of the fluorosurfactant is not biodegraded, making FTIR analysis on biodegraded samples possible. With biodegraded samples, FTIR analysis can provide a qualitative measure of AFFF levels.

Toxicity: In sufficient concentrations, foams may affect aquatic life. A number of fish toxicity studies have been performed. In tests using fathead minnows, the U.S. Air Force found that these fish could live in a simulated effluent stream containing 250-ppm AFFF without fatality for up to 8 days. LC_{50} values (i.e., the concentration causing deaths of 50 percent of the fish exposed) at 96 and 24 hr were 398 and 650 ppm, respectively.[70] MIL-F-24385

requires AFFF toxicity testing in accordance with ASTM E-729, using dynamic procedures with killifish. LC_{50} of 1000 mg/l for 6 percent concentrate is permitted.

Alone, these values may be considered as having a low degree of fish toxicity using environmental regulation rating scales. Localized concentrations in ponds or streams may exceed the values cited, if there is limited water movement.

Published data do not exist for the phytotoxicity of foam solutions; however, there have been no published reports of plant kills resulting from foam solution discharges.

Manufacturers report that thermal decomposition products from AFFF do not present a health hazard during fire fighting. Again, there are no data published in the literature. Manufacturers' product environmental data for AFFF include references to a test where a layer of AFFF was burned in a pan of gasoline inside an enclosure. Two measurements of hydrogen fluoride recorded above the sample were 0.23 and 0.16 ppm.[71]

Foaming and emulsification of fuels: The surfactants in AFFF solutions can cause foaming in treatment aeration ponds. This foaming process may suspend high BOD solids in the foam. If these are carried over to the outfall of the treatment facility, nutrient loading in the outfall waterway may result. Foam aeration may also cause foam bubble backup in sewer lines.

In uncontrolled fires, spills, and live fire-training scenarios, foams may contain suspended fuels. The fuel may become emulsified in the foam-water solution.

A bench-scale study has been conducted to evaluate the potential inhibitory effects of untreated AFFF wastewater on the biological nutrient removal process.[72] In this study, bench-scale reactors simulating the nitrification process were loaded at various AFFF concentrations, and the influence on process performance was evaluated. The results indicated that AFFF in concentrations between 10 ppm and 60 ppm did not show any inhibition to biological nitrification, and effluent did not exhibit any pass-through toxicity. These range-finding tests did indicate that nitrification inhibition did occur above 60 ppm AFFF. Some reductions in percent COD removal were observed as AFFF concentrations were increased.

Mitigation Strategies

Foam discharges are more easily handled where there is an in-place collection capability. This situation may be available at warehouses, tank farms, and fire-fighting training facilities. Where these facilities are not available, temporary diking is an alternative where time and resources permit.

Investigations have been conducted to develop foam/water separators using aeration and agitation techniques. To date, these techniques have not been optimized.

Discharge to water treatment facilities is recommended by many foam vendors when the solution is uncontaminated by fuel. Metering or dilution may be required to prevent levels of foam that will upset treatment facility reactions or cause excessive foaming. The use of defoamers to reduce aeration has been suggested.

Where fuels contaminate foam solutions, fuel/water separators might be used to skim off the hydrocarbon fuel. AFFF solutions have a tendency to form emulsions with fuels, potentially reducing the effectiveness of fuel/water separators. An alternative is to hold the solution in a pond or tank until the emulsion breaks and the separation process can be used. Agitation should be avoided to prevent the emulsion from reforming. In some situations (e.g., training), the fuel and treated water have been reused. Many fire-training facilities collect foam solution for ultimate discharge to water treatment facilities.

To ensure that unbalanced conditions do not occur in water treatment facilities, foam discharge should be carefully monitored. Different ranges of discharge rates have been suggested. This is an area requiring further investigation. Manufacturers of the foam solution should be consulted in conjunction with the wastewater treatment operator.

The entire area of environmental aspects of foam discharge requires additional evaluation and development of generally recognized guidance. Until generally recognized guidance is promulgated, users must rely on manufacturers' data and guidance. In all situations, discussions with the operator of the wastewater treatment facility and the environmental regulatory authorities are appropriate. Work is continuing in an effort to identify appropriate policy and criteria covering foam discharge for facilities having foam suppression systems. These efforts are focusing on identifying applicable codes and standards, analyzing environmental impact, and evaluating containment options.

Nomenclature

$AFFF\%_{sample}$	percentage of AFFF present in the sample
BOD	biological oxygen demand (mg/l)
γ_a	surface tension of liquid a (dynes/cm)
γ_b	surface tension of liquid b (dynes/cm)
γ_l	interfacial tension between liquids a and b (dynes/cm)
COD	chemical oxygen demand (mg/l)
ΔH_v	combined latent and sensible heads of vaporization (kJ/kg)
δ	viscous boundary layer thickness (cm)
G	conductance (mhos)
g	acceleration of gravity (cm/s²)
h	foam thickness
h_c	critical thickness of the foam layer
i	angle of incidence
k	foam spreading coefficient, dimensionless or nozzle coefficient (lpm/kPa$^{1/2}$)
k_d	foam drainage coefficient, dimensionless
k_e	foam evaporation coefficient, dimenionless
l	length of foam spread
n	refractive index, dimensionless
μ	viscosity (cm²/s)

$\dot{m}_{\text{add}}$	foam addition rate
$\dot{m}_{\text{fuel}}$	fuel mass loss rate
$\dot{m}_{\text{drain}}$	foam mass loss due to drainage
$\dot{m}_{\text{drop}}$	foam loss rate due to drop-out
$\dot{m}_{\text{vap}}$	foam mass loss rate due to vaporization
ν	kinetic viscosity (cm²/s)
n_{water}	refractive index of water, dimensionless
n_{foam}	refractive index of foam solution, dimensionless
$n_{\text{concentrate}}$	refractive index of foam concentrate, dimensionless
P_v	vapor pressure of fuel
ρ_{fuel}	fuel density (g/cm³)
ρ_{foam}	foam density (g/cm³)
$\dot{q}''$	rate of heat transfer
$\dot{q}_{\text{rad}}$	rate of heat transfer due to radiation
q''_{rad}	radiative heat release rate from pool fire
R	resistance (ohms)
r	angle of refraction
σ	spreading coefficient (dynes/cm) or conductivity (mhos)
$S_{a/b}$	spreading coefficient between liquids a and b (dynes/cm)
T	temperature (℃)
t	time (s)
T_i	foam temperature (℃)
T_s	fuel temperature (℃)
V	volume (cm³ or l³)
v_s	spreading velocity of foam (cm/s)

Subscripts

add	addition of foam
drain	drainage of foam
drop	drop-out of foam
rad	radiation
vap	vaporization

Superscripts

·	rate of change, as in $\dot{m}$
″	per unit area

References Cited

1. G.B. Geyer, L.M. Neri, and C.H. Urban, "Comparative Evaluation of Fire Fighting Foam Agents," *Report FAA-RD-79-61,* Federal Aviation Administration, Washington, DC (1979).

2. J.H. Aubert, A.M. Kraynik, and P.B. Rand, "Aqueous Foams," *Scientific American,* 19, 1, pp. 74–82 (1988).

3. V.L. Francen, "Fire Extinguishing Composition Comprising a Fluoroaliphatic and a Fluorine-Free Surfactant," U.S. Patent 3,562,156 (1971).

4. M.J. Rosen, *Surfactants and Interfacial Phenomena,* John Wiley & Sons, New York, Chapters 1, 5, 7 (1989).

5. R.L. Tuve, H.B. Peterson, E.J. Jablonski, and R.R. Neill, , "A New Vapor-Securing Agent for Flammable Liquid Fire Extinguishment," *NRL Report 6057,* Washington, DC (1964).

6. R. Friedman, "Theory of Fire Extinguishment," *Fire Protection Handbook,* 17th ed. National Fire Protection Association, Quincy, MA, pp. 1–74 (1991).

7. C.P. Hanauska, J.L. Scheffey, R.J. Roby, and D.T. Gottuk, "Improved Formulations of Firefighting Agents for Hydrocarbon Fuel Fires," *SBIR Phase I Final Report* Hughes Associates, Inc., Baltimore, MD (1994).

8. B. Persson and M. Dahlberg, "A Simple Model of Foam Spreading on Liquid Surfaces," *SP Report 1994:27,* Swedish National Testing and Research Institute, Boras, Sweden (1994).

9. H. Persson, "Fire Extinguishing Foams—Resistance against Heat Radiation," *SR Report 1992:54,* Swedish National Testing and Research Institute, Sweden (1992).

10. B.Y. Lattimer, C.P. Hanauska, J.L. Scheffey, F.W. Williams, and W. Leach, "Behavior of Aqueous Film Forming Foams (AFFF) Exposed to Radiant Heating," *NRL Ltr Rpt Ser 6180/0013,* Naval Research Laboratory, Washington, DC (2000).

11. S. Ikasson and H. Persson, "Fire Extinguishing Foam—Test Method for Heat Exposure Characterisation," *SP Report 1997:09,* Swedish National Testing and Research Institute, Boras, Sweden (1997).

12. A.M. Kraynik, "Foam Drainage," *Sandia Report SAND-83-0844,* Sandia National Laboratories, Albuquerque, NM (1983).

13. A.M. Kraynik, "Foam Flows," *Annual Review of Fluid Mechanisms,* 20, pp. 325–357 (1988).

14. J.A. Fay, "The Spread of Oil Slicks on a Calm Sea," *Oil on the Sea* (D. P. Hoult, ed.), Plenum, New York, pp. 53–64 (1964).

15. J.A. Fay, and D.P. Hoult., "Physical Processes in the Spread of Oil on a Water Surface," *Coast Guard Final Report,* Massachusetts Institute of Technology, Cambridge, MA (1971).

16. P. Cann, H.A. Spikes, and G. Caporico, "Spreading of Perfluorinated Fluids on Metal Surfaces," *4th International Colloquium on Synthetic Lubricants and Operation Fluids,* Oatfildern, Germany, pp. 631–638 (1984).

17. H.E. Moran, J.C. Burnett, and J.T. Leonard, "Suppression of Fuel Evaporation by Aqueous Films of Fluorochemical Surfactant Solutions," *Naval Research Laboratory Report 7247,* Washington, DC (1971).

18. T. Briggs, and B. Abdo, "Emphasis on Spreading Quality of AFFF Could Be Misleading," *FIRE,* 80, 94, (1988).

19. J.L. Scheffey, R.L. Darwin, J.T. Leonard, C.R. Fulper, R.J. Ouellette, and C.W. Siegmann, "A Comparative Analysis of Film-Forming Fluoroprotein Foam (FFFP) and Aqueous Film-Forming Foam (AFFF) for Aircraft Rescue and Fire Fighting Services," *Hughes Associates, Inc. Report 2108-A01-90,* Hughes Associates Inc., Baltimore, MD (1990).

20. G.B. Geyer, "Status Report on Current Foam Fire Fighting Agents," *International Conference on Aviation Fire Protection,* Interlaken, Switzerland (1987).

21. P.J. Chiesa, and R.S. Alger, "Severe Laboratory Fire Test for Fire Fighting Foams," *Fire Technology,* 16, 1, pp. 12–21 (1980).

22. Underwriters Laboratories Inc., *Standard for Foam Equipment and Liquid Concentrates,* 6th ed., Northbrook, IL (1994).

23. J.L. Scheffey, J. Wright, and C. Sarkos, "Analysis of Test Criteria for Specifying Foam Firefighting Agents for Aircraft Rescue and Firefighting," *FAA Technical Report, DOT/FAA/CT-94/04,* Atlantic City, NJ (1994).

24. International Organization for Standardization, "Fire Extinguishing Media—Foam Concentrates—Part 3: Specification

for Low-Expansion Foam Concentrates for Surface Application to Water-Immiscible Liquids," *Draft European Standard EN 1568-3,* (2000).

25. B.P. Johnson, "A Comparison of Various Foams When Used against Large-Scale Petroleum Fires," Home Office Fire Research and Development Office, *(*1993).

26. W.M. Carey, and M.R. Suchomel, "Testing of Fire Fighting Foam," *Underwriters Laboratories Report No. CG-M-1-81,* Underwriters Laboratories Inc., Northbrook, IL (1980).

27. M.D. Thomas, "UK Home Office Research into Domestic Fire Fighting," *First International Conference on Fire Suppression Research Proceedings,* Stockholm, Sweden, pp. 283–289 (1993).

28. R. Fiala, "Aircraft Post-Crash Firefighting/Rescue," from *AGARD Aircraft Fire Safety Lecture Series No. 123* (1982).

29. G.B. Geyer, "Evaluation of Aircraft Ground Firefighting Agents and Techniques," *Technical Report AGFSRS 71-1,* Tri-Service System Program Office for Aircraft Ground Fire Suppression and Rescue, Wright-Patterson AFB, OH (1971).

30. G.B. Geyer, "Firefighting Effectiveness of Aqueous Film-Forming Foam (AFFF) Agents," *FAA Technical Report FAA-NA-72-48,* DOD Aircraft Ground Fire Suppression and Rescue Unit (ASD-TR-73-13), Washington, DC (1973).

31. W.M. Carey, "Improved Apparatus for Measuring Foam Quality," Underwriters Laboratories Inc., Northbrook, IL (1983).

32. E.J. Jablonski, "Comparative Nozzle Study for Applying Aqueous Film-Forming Foam on Large-Scale Fires," *U.S. Air Force Report, CEEDO-TR-78-22,* Tyndall AFB, Florida (1978).

33. J.A. Foster, "Additions for Hosereel Systems: Trials of Foam on 40 m² Petrol Fires," *Scientific Research and Development Branch Report 40/87,* Home Office, London (1987).

34. P.L. Parsons, "Trials of Foam on Petrol Fires at the Fire Service Technical College," *Scientific Advisory Branch Report No. 14/75,* Home Office, London (1976).

35. L.R. DiMaio, R.F Lange., and F.J. Cone, "Aspirating vs. Non-Aspirating Nozzles for Making Fire Fighting Foams—Evaluation of a Non-Aspirating Nozzle," *Fire Technology,* 20, 1, pp. 5–10 (1984).

36. J.L. Scheffey, "Submarine Bilge AFFF Sprinklers," *Naval Research Laboratory Project, 64561N-S1946-2024000,* unpublished data (1988).

37. G. Timms, and P. Haggar, "Foam Concentration Measurement Techniques," *Fire Technology,* 26, 1, pp. 41–50 (1990).

38. D.E. Breen, "Hangar Fire Protection with Automatic AFFF Systems," *Fire Technology,* 9, 2, pp. 119–131 (1973).

39. L.M. Krasner, D.E. Breen, and P.M. Fitzgerald, "Fire Protection of Large Air Force Hangars," *AFWL-TR-75-119,* Factory Mutual Research Corporation, Norwood, MA (1975).

40. D.E. Breen, L.M. Krasner, B.G. Vincent, and P.J. Chicarello, "Evaluation of Aqueous Film Forming Foam for Fire Protection in Aircraft Hangars," *FMRC Technical Report Ser. No. 21032,* Factory Mutual Research Corporation, Norwood, MA (1974).

41. L.M. Krasner, "Closed-Head AFFF Sprinkler Systems for Aircraft Hangars," *FMRC S. I. 0C6N3.RG, RC 79-T-58,* Factory Mutual Research Corporation, Norwood, MA (1979).

42. "Pop-Up-Type Floor-Mounted Foam Sprinklers for Aircraft Hangars," *Technical Record TR44/153/14(L),* Department of Housing and Construction, Australia.

43. *China Lake CVA Fire Fighting Tests, Phase III,* unpublished data (1972).

44. J.L. Scheffey, "Flow, Pattern, and Fire Performance Characteristics of a Prototype Pop-Up Nozzle for Use on Aircraft Carrier Flight Decks," *Report 2429-17,* Hughes Associates, Inc., Columbia, MD (1985).

45. J.L. Scheffey, and J.T. Leonard, "AFFF Protection for Weapons Staging Areas," *Fire Safety Journal,* 14, 14, pp. 47–63 (1988).

46. Department of the Navy, "General Specifications for Ships of the United States Navy, 1991 Edition," *NAVSEA S9AA0-AA-SPN-010/GEN-SPEC, Section 555,* Department of the Navy, Washington, DC.

47. H.W. Carhart, J.T. Leonard, R.L. Darwin, R.E. Burns, J.T. Hughes, and E.J. Jablonski, "Aircraft Carrier Flight Deck Fire Fighting Tactics and Equipment Evaluation Tests," *NRL Memorandum Report 5952,* Washington, DC (1987).

48. Rolf Jensen and Associates, "Comprehensive Aqueous Film Forming Foam Central Fire Suppression System Analysis/Report, B1-B Aircraft Hangars," *Technical Report A6406,* U.S. Air Force (1989).

49. J.E. Gott, D.L. Lowe, K.A. Notarianni, and W. Davis, "Analysis of High Bay Hangar Facilities for Fire Detector Sensitivity and Placement," *NIST TN 1423,* National Institute of Standards and Technology, Gaithersburg, MD (1997).

50. D.B. Szepezi, G.G. Back, J.L. Scheffey, F.W. Williams, and J.E. Gott, "Aircraft Hangar Fire Suppression System Evaluation—Intermediate Scale Studies," *NRL/MR/6180-99-8422,* Naval Research Laboratory, Washington, DC (1999).

51. G.G. Back, F.W. Williams, J.E. Gott, A.J. Parker, and J.L. Scheffey, "Aircraft Hangar Fire Protection System Evaluation Full Scale Study," *NRL Ltr Rpt Ser 6180/0620,* Naval Research Laboratory, Washington, DC (1998).

52. D.T. Gottuk, J.L. Scheffey, F.W. Williams, J.E. Gott, and R.J. Tabet, "Optical Fire Detection (OFD) for Military Aircraft Hangars: Final Report on OFD Performance to Fuel Spill Fires and Optical Stress," *NRL/MR/6180-00-8457,* Naval Research Laboratory, Washington, DC (2000).

53. A.J. Parker, G.G. Back, J.L. Scheffey, J.J. Schoenrock, J.P. Ouellette, F.W. Williams, J.E. Gott, and R.J. Tabet, "The Development of a Prototype Low-Level AFFF Nozzle System for U.S. Navy Aircraft Hangars," *NRL Ltr Rpt Ser 6180/0004* (2000).

54. J.L. Scheffey, A.J. Wakelin, J.E. Gott, R.J. Tabet, and F.W. Williams, "Aircraft Hangar Fire Suppression System Design Study," *NRL/MR* (in preparation), Naval Research Laboratory, Washington, DC (2000).

55. B.G. Vincent, H.C. Kung, and P. Stavrianidis, "Fire Protection for U.S. Army Helicopter Hangars," *FMRC J.I.OXON1.RA,* Factory Mutual Research Corporation, Norwood, MA (1993).

56. D.P. Nugent, *Directory of Fire Tests Involving Flammable and Combustible Liquids in Small Containers,* 2nd ed., Schirmer Engineering (2000).

57. R.M. Newman, P.M. Fitzgerald, and J.R. Young, "Fire Protection of Drum Storage Using 'Light Water' Brand AFFF in a Closed-Head Sprinkler System," *FMRC Technical Report Ser. No. 22464, RC 75-T-16,* Factory Mutual Research Corporation, Norwood, MA (1975).

58. Southwest Research Institute, "Performance Testing of Automatic Sprinkler Systems in the Protection of Palletized, 55-Gal Storage of Heptane in Self-Relieving Style, Steel Drums," *SwRI Project No. 01-2016-001,* San Antonio, TX (1999).

59. J.R. Young, and P.M. Fitzgerald, "The Feasibility of Using 'Light Water' Brand AFFF in a Closed-Head Sprinkler System for Protection against Flammable Liquid Spill Fires," *FMRC Technical Report RC 75-T-4, Ser. No. 22352,* Factory Mutual Research Corporation, Norwood, MA (1975).

60. Schirmer Engineering Corporation, "International Foam-Water Sprinkler Research Project: Task 1—Literature Search," *Technical Report No. 10-90001-04-00,* National Fire Protection Research Foundation, Quincy, MA (1992).

61. J.P. Hill, "International Foam-Water Sprinkler Research Project: Task 3—Range Finding Tests," *Technical Report OTOR6.RR,*

National Fire Protection Research Foundation, Quincy, MA (1991).

62. Underwriters Laboratories Inc., "International Foam-Water Sprinkler Research Project: Task 4—Palletized Storage Fire Tests 1 through 13," *Technical Report 91NK14873/NC987,* National Fire Protection Association, Quincy, MA (1992).

63. W.M. Carey, "International Foam-Water Sprinkler Research Project: Task 5—Rack Storage Fire Tests," *Technical Report,* National Fire Protection Research Foundation, Quincy, MA (1992).

64. Center for Chemical Process Safety, *Guidelines for Safe Warehousing of Chemicals,* American Institute of Chemical Engineers, New York, (1998).

65. D.J. Rasbash, "The Extinction of Fire with Plain Water: A Review," *Proceedings from the First International Symposium on Fire Safety Science,* (C.E. Grant and P.J. Pagni, eds.), National Institute of Standards and Technology, Gaithersburg, MD, pp. 1145–1163 (1986).

66. J.L. Scheffey and F.W. Williams, "The Extinguishment of Fires Using Low-Flow Water Hose Streams—Part II," *Fire Technology,* 27, 4, pp. 291–320 (1991).

67. American Public Health Association, "Standard Methods for the Examination of Water and Wastewater," 18th ed., Washington, DC (1992).

68. C.A. Moody and J.A. Field, "Determination of Perfluorocarboxylates in Groundwater Impacted by Fire-Fighting Activity," *Environmental Science & Technology*, 33, 16, pp. 2800-2806 (1999).

69. Hughes Associates, Inc., "Development of Detection Method for Aqueous Film Forming Foam (AFFF)," Armstrong Laboratories Environics Directorate, Dayton, OH (1997).

70. National Environmental Health Laboratory, "Biological Treatment of Fire Fighting Foam Waste," *Report No. REHL(K) 67–14,* Kelly AFB, Texas (1967).

71. "Light Water Brand AFFF Waste Disposal Recommendations and Hazard Evaluation," *3M Product Environmental Data Sheet,* 3M Company, St. Paul, MN (1991).

72. M. Enten-Unal, S. Paranjape, G.C. Schafran, and F.W. Williams, "Evaluation of the Effects of AFFF Inputs to the VIP Biological Nutrient Removal Process and Pass-Through Toxicity," *NRL/MR/6180-98-8141,* Naval Research Laboratory, Washington, DC (1998).

Additional Readings

ASTM D1331, *Standard Test Methods for Surface and Interfacial Tension of Solutions of Surface-Active Agents,* American Society for Testing and Materials, Philadelphia, PA (1995).

ASTM E729, "Standard Practice for Conducting Acute Toxicity Tests with Fish, Macroinvertebrates, and Amphibians," American Society for Testing and Materials, Philadelphia, PA (1996).

FAA, "Aircraft Fire and Rescue Facilities and Extinguishing Agents," *FAA Advisory Circular 150/5210-6C,* Federal Aviation Administration, Washington, DC (1985).

ICAO, "Rescue and Firefighting," *Airport Services Guide,* 3rd ed., International Civil Aviation Organization, Montréal, Québec (1990).

NFPA 11, *Standard for Low-Expansion Foam,* National Fire Protection Association, Quincy, MA (1998).

NFPA 13, *Standard for the Installation of Sprinkler Systems,* National Fire Protection Association, Quincy, MA (1999).

NFPA 16, *Standard for the Installation of Foam-Water Sprinkler and Foam-Water Spray Systems,* National Fire Protection Association, Quincy, MA (1999).

NFPA 30, *Flammable and Combustible Liquids Code,* National Fire Protection Association, Quincy, MA (2000).

NFPA 403, *Standard for Aircraft Rescue and Fire-Fighting Services at Airports,* National Fire Protection Association, Quincy, MA (1998).

NFPA 409, *Standard on Aircraft Hangars,* National Fire Protection Association, Quincy, MA (2001).

NFPA 412, *Standard for Evaluating Aircraft Rescue and Fire-Fighting Foam Equipment,* National Fire Protection Association, Quincy, MA (1998).

UL 162, *Standard for Foam Equipment and Liquid Concentrates,* Underwriters Laboratories Inc., Northbrook, IL (1994).

UL Fire Protection Equipment Directory, Underwriters Laboratories Inc., Northbrook, IL (2001).

U.S. Military Specification, MIL-F-24385, Department of the Navy, Washington, DC (2000).

U.S. Government, "Federal Specification, Foam Liquid, Fire Extinguishing, Mechanical," O-F-55B, (U. S. Government Protein Foam Specification), Washington, DC (1964).

CHAPTER 5

Foam System Calculations

Joseph L. Scheffey and Harry E. Hickey

Introduction

Foam agent fire protection is especially suited for the control and extinguishment of flammable and combustible liquid-type fire protection problems.

An impressive array of fire protection problems can be properly addressed using foam classification agents. The NFPA *Fire Codes*® discuss foam fire protection systems as suitable for the protection of numerous fire protection problems.[1] It is important to note that other classifications of fire extinguishing systems, including dry chemicals, wet chemicals, carbon dioxide, halon, and some special agents, may be suitable for similar hazards.

Table 4-5.1 identifies special hazards that may be suitable for adequate fire protection by different types of foam systems. Each special hazard is cross-referenced to one or more classifications of foam fire protection systems that are identified in NFPA standards as being suitable for the stated hazard. This table is useful for examining the scope and limitations of different types of foam application systems for special hazard fire protection. The referenced standards should be consulted concerning specification and design considerations for each specific problem condition.

Foam agent fire protection systems are suitable for Class A fires in ordinary combustible materials in addition to Class B fires (flammable and combustible liquids). Historically, portable foam fire extinguishers provided important fire protection for both Class A and Class B problems. The dual consideration of evaluating foam fire protection systems for both Class A and Class B fire protection problems is important. This consideration is especially important for mixed occupancy storage, which may be suitably protected by foam spray systems, foam water sprinkler or spray systems, or closed head sprinkler systems using aqueous film forming foam (AFFF) type foam agents.

Objective Classification of Fire Problems
for Foam Agent Fire Protection

The following objectives identify five performance areas for evaluating foam agent fire protection. Performance objectives may be combined for specific problem situations. These objectives form important considerations for the hydraulic design of foam agent systems.

Objective 1: Secure the surface of a flammable or combustible liquid that is not burning.

Flammable and combustible liquids emit vapors that may create a hazard condition. Flammable vapors may be suppressed by providing an adequate foam blanket over the surface area. Flammable liquid spills present a fire hazard. This hazard may be mitigated and/or controlled by the use of appropriate foam agent application.

Objective 2: Control and extinguish fires in flammable and combustible liquid hazardous locations in local areas within buildings.

Flammable and combustible liquids are often stored inside buildings in 55-gal (208-l) drums and other types of containers. These liquids are also used in association with manufacturing processes, industrial machinery, heating equipment, experimental activities, and so forth. The use of flammable and combustible liquids inside buildings may result in liquid spill and fuel ignition. Foam agents are appropriate for protecting localized flammable and combustible liquid problems inside buildings.

Objective 3: Extinguish fires in atmospheric storage tanks.

For nearly 100 years, foam agent fire protection has successfully extinguished fires in outdoor vertical atmospheric storage tanks. This type of protection still represents

Joseph L. Scheffey, P.E., is director of RDT&E at Hughes Associates, Inc., Baltimore, Maryland.

Dr. Harry E. Hickey is retired from the University of Maryland where he served as associate professor, Department of Fire Protection Engineering.

Table 4-5.1 *Special Hazard Identification*[1]

| | Protection Reference | | | | NFPA 16 | |
| | NFPA 11 | | | NFPA 11A | | |
	Monitors	Foam Spray	Other Systems	High Expansion Foam	Foam-Water Sprinkler	Closed-Head Sprinkler
Aircraft protection						
1. Aircraft hangars (see NFPA 409)	X	X	X	X	X	X
2. Rooftop heliport construction and protection (see NFPA 418)		X	X		X	
3. Aircraft engine test facilities (see NFPA 423)		X		X	X	
Enclosed stockpiles						
1. Flammable liquids—flash point below 100°C (see NFPA 30)				X[a]		
2. Combustible liquids—flash point of 100°C and above (see NFPA 30)				X[a]		
3. Low-density combustibles (foam rubber, foam plastics, rolled tissue or crepe paper)				X[a]		
4. High-density combustibles—rolled paper (see NFPA 13)				X[a]		
5. Combustibles in containers (cartons, bags, fiber drums)				X[a]		
Nuclear power plants						
1. Fire protection for light water nuclear power plants (see NFPA 803)		X		X	X	
2. Nuclear research reactors (see NFPA 802)		X		X	X	
Protection of commodity storage						
1. Indoor general storage (see NFPA 13)				X		
2. Rack storage of materials (see NFPA 13)				X		
3. Storage of rubber tires (see NFPA 13)				X		
4. Storage of rolled paper (see NFPA 13)				X		
5. Archives and record center storage (see NFPA 232AM)				X		
6. Rack container storage of liquids (see NFPA 30)						X
Marine applications						
1. Machinery spaces		X			X	
2. Deck systems for petroleum and chemical tankers	X					
Special problems						
1. Production, storage, and handling of liquefied natural gas (LNG) (see NFPA 59A)		X		X	X	
2. Fire and dust explosions in chemical, dye, pharmaceutical, and plastics industry (see NFPA 654)		X		X	X	
3. Fires and explosions in wood processing and wood working facilities (see NFPA 664)		X		X		
4. Ovens and furnaces: design, location, and equipment (see NFPA 86)		X				
5. Mobile surface mining equipment (see NFPA 121)		X		X		
6. Tank vehicle and tank car loading and unloading (see NFPA 30)	X	X	X		X	X
7. Automotive service station filling areas (see NFPA 30A)		X				
8. Dipping and coating processes using flammable or combustible liquids (see NFPA 34)		X				
9. Manufacturer of organic coatings (protection of equipment mixers, solvent tanks, and open containers— see NFPA 35)		X		X[a]		
10. Laboratories using chemicals (see NFPA 45)		X			X	X
11. Storage and handling of liquefied petroleum gases at utility gas plants (see NFPA 59)		X		X	X	
Special problems identified in manufacturers' literature and/or identified foam standards and recommended practices						
1. Process structures and equipment		X				
2. Horizontal atmospheric tanks		X				
3. Pump rooms		X				
4. Dip tanks		X				
5. Engine test cells		X				
6. Transformer rooms				X		
7. Dike areas	X		X			

[a]Consider in conjunction with automatic sprinklers

one of the most successful uses of foam agents; in fact, foam agent fire protection is the primary means for the proper protection of atmospheric storage tanks. Foam agents have been successfully used to extinguish flammable and combustible liquid fires in atmospheric storage tanks with diameters up to 200 ft (61 m).

Objective 4: Extinguish fires in outdoor and indoor processing areas.

A large variety of industrial processes utilize flammable and combustible liquids. In most processing plants, these liquids pass through pipelines and are captured in holding tanks. Foam agents, properly selected for the specific hazard, are suitable for controlling and extinguishing fires in process equipment. However, foam agents are not suitable for coping with vertical running fires or fires where the flammable material is flowing from an orifice under pressure.

Objective 5: Protect, prevent, control, and extinguish fire problems in selected special hazards.

In addition to the other specified objectives, foam fire extinguishing agents provide appropriate fire protection for numerous special hazard problems. Some important special hazard conditions that are suitable for foam fire protection are included in the following list: (See also Table 4-5.1.)

> Dike areas
> Engine test cells
> Transformers
> Engine rooms
> Laboratories using chemicals
> Aircraft hangars
> Nuclear research reactors
> High density storage of combustibles
> Rubber tires
> Rack container storage of aerosols
> Loading racks
> Automotive service station filling areas
> Ovens and furnaces

Basic Types of Foam System Protection

Foam fire protection systems are divided into four basic classifications by the National Fire Protection Association. Each of these classifications is briefly identified below. Conditions exist where it may be proper to use more than one classification of protection on a given fire problem. Examples of fixed foam systems are covered under supplemental topics later in this chapter on the hydraulic design of low expansion and high expansion foam systems.

Fixed Foam Systems

These systems are complete installations piped from a central foam station, discharging through fixed delivery outlets to the hazard to be protected. Any required pumping equipment is permanently installed. For example, a fixed system for a vertical atmospheric cone roof storage tank would include the following permanently installed

equipment: water supply lines, foam proportioning equipment, a foam liquid storage tank, foam solution lines to the storage tank, all necessary control valves, a tank solution riser pipe, and one or more topside foam chambers. Other equipment may be added based on the complexity of the problem and associated hydraulic conditions.

Semifixed Foam Systems

Two separate classifications of semifixed foam systems are identified below. The first classification is more predominantly used in the United States, although one major oil company does use applications of the second classification. Common to both classifications is the concept that part of the total system is permanently installed and part of the system is provided by portable elements.

The first classification of semifixed systems indicates a type in which the fire hazard is equipped with fixed discharge outlets connected to piping that terminates at a safe distance. The fixed piping installation may or may not include a foam maker. Necessary foam producing materials are transported to the scene after the fire starts and are connected to the piping.

The second classification of semifixed systems indicates a type in which foam solutions are piped through the area from a central foam station, the solution being delivered through hose lines to portable foam makers such as monitors, foam towers, hose lines, and so forth.

Mobile Systems

Mobile systems basically consist of a unit on wheels that transports all of the required equipment and foam liquid necessary for making finished foam. This concept includes any foam producing unit which is mounted on wheels, and which may be self-propelled or towed by a vehicle. These units may be connected to an available water supply or may use a premixed foam solution. The original concept of a mobile foam system was called a "foam house on wheels," a mobile piece of fire apparatus with a UL-rated fire pump, an integral part of the pumping network, a foam liquid tank, and fire hose. Essentially this unit can double as a structural fire suppression unit. NFPA 11C, *Standard for Mobile Foam Apparatus*, covers the specifications and performance criteria for mobile systems.[1]

Portable Systems

Portable systems represent a rather economical approach to providing basic foam fire protection for small hazards. This classification considers that the foam producing equipment and materials, including the foam liquid, the proportion device(s), the discharge nozzle, the hose, and other required appliances, are transported by hand from a storage location to the incident scene. While portable systems are simple to operate, they are limited by their foam discharge rate capability; they may also be labor intensive to maintain a continuous foam supply over the required duration of discharge. Foam equipment manufacturers can provide technical information on a range of portable equipment.

Protection of Incipient Spills and Related Hazards

Portable fire extinguishers provide one method of protection for small flammable liquid storage hazards, fuel transfer hazards, and incipient spill fires.

Underwriters Laboratories (UL) has classified and listed chemical foam extinguishers. These extinguishers are now generally considered obsolete since their manufacture in the United States was discontinued in 1969. The National Fire Protection Association recommends that these units be replaced with currently available models.

Aqueous film forming foam agent portable fire extinguishers are used to replace the chemical-type foam extinguisher and provide protection for hazard conditions where this type of extinguishing agent is recommended. Extinguishers of this type are usually available in hand portable models of 2½-gal (9 l) capacity and in wheeled models having a liquid capacity of 33 gal (125 l). These extinguishers have ratings of 3A:20B and 20A:160B, respectively. The AFFF portable model closely resembles the stored pressure water extinguisher except for the special type of nozzle. NFPA 10, *Standard for Portable Fire Extinguishers,* should be consulted concerning the selection and placement of portable extinguishers.[1]

Protection for Fixed Roof Atmospheric Storage Tanks

Fixed or cone roof atmospheric storage tanks for the storage of flammable liquids can be protected by fire fighting foam. Several techniques are available for correctly applying foam to a cone roof tank fire. Each technique should be carefully considered with reference to the size of the storage tank, the flammable or combustible liquid being stored in a given tank, and the foam agent classification that is suitable for the hazard. Some fundamental concepts associated with the proper protection for fixed roof atmospheric storage tanks are discussed below. Each individual topic is further developed through design problems on cone roof atmospheric storage tanks.

Foam Monitors

One or more foam monitors may be positioned around the periphery of a cone roof tank to project foam over the tank shell and onto the surface of a burning liquid. This technique has been successfully used on numerous fires. However, NFPA 11, *Standard for Low-Expansion Foam,* clearly indicates that foam monitors may be considered the primary means of protection for fixed roof tanks when the tank is less than 60 feet in diameter. This indication represents a severe limitation on the recommended use of foam monitors for the protection of cone roof tanks.

Foam Handlines

Similar to the concept of providing foam protection with foam monitors, foam handlines may be positioned around the periphery of a cone roof tank to project foam over the tank shell and onto the surface of a burning liquid.

Foam handlines have a flow range from 50 gpm (190 lpm) to less than 300 gpm (1136 lpm) and are only suitable for possible protection of fixed roof tanks with a diameter of less than 30 ft (9 m) and a height not greater than 20 ft (6 m). The selection of foam handline nozzles must be carefully considered to provide the correct total discharge for the flammable liquid problem to be protected.

Foam handlines are very important for supplemental fire protection requirements. Handlines delivering a minimum of 50 gpm (190 lpm) are very useful for extinguishing small spill fires and dike fires in the vicinity of a storage tank. The number of such supplemental foam hose streams is dependent on the diameter of the largest storage tank in the compound to be protected. (NFPA 11 should be consulted.)

Surface Application of Foam

One common and acceptable method of applying foam to the flammable liquid surface of a single roof storage tank is through fixed discharge outlets installed on the tank shell. Two distinct types of foam discharge outlets are available based on the hazard problem and the foam agent. Each type of device may be distinguished as follows:

Type I outlets: These approved discharge outlets will conduct and deliver foam gently onto the liquid surface without submergence of the foam below the flammable liquid surface and agitation of the surface. This type of device was originally intended to apply special alcohol resistant foams to polar solvent fuels. Today, Type I discharge outlets may be used with hydrocarbon fuels. (NFPA 11 should be consulted.)

Two classifications of Type I outlets are commercially available where this device is suitable. A porous tube is a Type I foam discharge outlet. The tube is coarsely woven and rolled up into a foam chamber so that there is an attached end at the foam maker and a free end. When foam is admitted to the tube at the foam chamber, the tube unrolls, dropping into the tank. The buoyancy of the foam causes the tube to rise to the surface, and foam flows out through the pores of the fabric directly onto the liquid surface.

A foam trough represents a second variety of a Type I discharge outlet. The trough consists of sections of steel sheet formed into a chute which is securely attached to the inside of the tank wall so that it forms a descending spiral from the top of the tank to within 4 ft (2 m) of the bottom.

Based upon advances in foam fire protection, porous tubes and foam chutes are rarely installed on new installations for the proper protection of cone roof atmospheric storage tanks.

Type II outlets: These approved discharge outlets do not deliver foam gently onto the liquid surface without submergence of the foam or agitation of the surface. An air foam chamber with a Type II outlet may be attached to the tank shell at the weak seam line. The Type II discharge outlet is positioned on the inside of the tank to permit discharge of the foam down the inside of the tank wall surface onto the flammable liquid surface. The number and discharge capacity of Type II foam chambers for a given

size (diameter) cone roof storage tank are presented in NFPA 11.

Portable foam towers: These devices represent specialized portable equipment that may be fitted with either a Type I or a Type II foam discharge outlet. A tower is a device that is brought to the scene of the fire, erected, and placed in operation for delivering foam to the burning surface of a tank after the fire starts. The Type II discharge outlets are shaped to apply foam inward toward the tank shell. The erection of foam towers adjacent to a burning tank and the operation of the foam towers may present a safety hazard to the personnel working with this equipment. The number of persons required to place foam towers in service is also a problem associated with these devices.

Subsurface Application of Foam

An alternative method of applying foam to a cone roof atmospheric storage tank is through subsurface injection, usually near the base of the tank but above the water bottom in the tank. This application technique involves injecting expanded foam into the flammable liquid near the bottom of the liquid level under controlled velocity conditions. The buoyancy of the foam allows the foam to slowly rise to the flammable liquid surface and spread across the surface to effect fire control and then total extinguishment.

There are three important conditions to consider in subsurface application of foam in fixed and semifixed systems.

1. Subsurface foam application is not considered suitable for the protection of Class IA hydrocarbon liquids.
2. Subsurface foam application is not currently suitable for polar solvent.
3. Subsurface and semisubsurface injection systems are not recommended for *open top* or *covered floating* roof tanks.

Semisubsurface Injection Method

A modified form of subsurface foam injection for cone roof tanks is used in a number of European countries. The modified technique is designated the semisubsurface injection method, based on the equipment used to insert the expanded foam into the tank shell. The semisubsurface injection method has not found any particular application in the United States.

Protection of Floating Roof Storage Tanks

In contrast to single roof tanks, floating roof tanks have a cover or roof over the flammable liquid that floats on the surface of the liquid and moves vertically with the liquid level in the tank. The floating roof may be open to the atmosphere. This physical arrangement of the tank is classified as an "open top floating roof tank." A permanently installed cover may be placed over the entire tank; this second designation is classified as a "covered floating roof tank."

The floating roof has a perimeter seal between the roof cover perimeter and the tank shell. The seal is necessary to prevent flammable vapors from escaping into the atmosphere and collecting over the floating roof. Three types of seal devices may be found on floating roof-type storage tanks: (1) a mechanical shoe seal or a pantograph-type seal, (2) a metal weather shield, and (3) a metal secondary seal.

NFPA 11 should be consulted for a description of each seal device and the physical arrangement of these devices. Some devices also require the use of a foam dam when protected by fixed foam fire protection systems. The requirements for foam dams are also given in the referenced standard.

The fire experience with floating roof tanks appears to be very good. Consequently, fixed foam outlets are not generally required on either open top floating roof tanks or covered floating roof tanks. When an oil company elects to protect these types of tanks or the local fire protection authority requests protection for these types of tanks, three different application techniques may be used for proper protection of open top floating roof tanks. A brief description of each technique follows.

Portable Nozzle Method

The basic fire problem associated with floating roof tanks is a fire burning in the seal area between the cover and the tank shell. Typically, the surface area of this fire is quite small. One technique to extinguish this type of fire is to advance a portable hose line to the top of the tank, supply foam to this hose line, and manually apply foam to the seal area. Personnel operating this hose line should be highly trained in this type of operation and follow established safety practices.

Catenary System Method

The catenary system consists of a series of foam makers at evenly spaced points in the roof near the seal. These foam makers are connected to a common section of piping which in turn is attached to a flexible hose that rides up and down with the access stairway to the roof cover. The stairway is fixed to the top of the tank shell, and the bottom portion of the stairway rides on a set of tracks attached to the floating cover. This arrangement allows the stairway to move both horizontally and vertically as the cover moves with the flammable liquid level.

At the time of a fire, foam solution is pumped under pressure through a vertical pipe and flexible hose to the foam makers. This system can be designed to discharge foam under the seal directly onto the flammable liquid, or foam can be discharged above the seal. Foam equipment manufacturers producing this type of equipment should be consulted for engineering data on design requirements, installation techniques, and hydraulic calculations.

Fixed Foam Maker Method

The fixed foam maker method consists of installing piping around the outside wall of the tank and connecting to it a series of foam makers installed on special mounting shields above the storage tank rim. The circumference of

the tank will determine the number of points needed for foam application. This method requires a foam dam to retain the foam over the seal or weather shield. This dam is normally 12 to 24 in. (305 to 610 mm) in height. Complete construction details of the foam dam may be found in the appendix of NFPA 11.

Covered floating roof tanks generally do not require fixed foam fire protection systems. There may be some cases of substandard installations or locations where local codes require proper protection for this classification of storage tank. The standards for fixed roof tanks should apply where it is required to protect covered floating roof-type tanks.

Protection of Storage or High-Volume Hazards with High-Expansion Foam

High-expansion foam is an agent for the control and extinguishment of both Class A and Class B fires. The classification of foam makes it particularly suitable as a flooding agent for use in confined spaces.

The development and application of high expansion foams for fire fighting purposes started with the work of the Safety in Mines Research Establishment in England concerning the difficult problem of fires in coal mines. It was found that by expanding an aqueous surface active agent solution to a semistable foam of about 1000 times the volume of the original solution, it was possible to force the foam down relatively long corridors, thus providing a means for transporting water to a fire inaccessible to ordinary hose streams. This work was expanded upon by the United States Bureau of Mines immediately after World War II.

Developmental work in the United States on high expansion foam has led to the refinement of specialized high expansion foam generating equipment for fighting fire in confined spaces, for specific applications to fire control problems in both municipal and industrial fire fighting, and for the protection of special hazard occupancies. Medium-expansion foam was developed to cover the need for a more wind-resistant foam than high-expansion foam for outdoor applications.

Concepts and Suitability for Medium- and High-Expansion Foams

Medium- and high-expansion foams are aggregations of bubbles that are mechanically generated by the passage of air or other bases through a net, screen, or other porous medium which is wetted by an aqueous solution of surface active foaming agents. Under proper conditions, fire fighting foams of expansions from 20:1 to 1000:1 can be generated. Such foams provide a unique agent for transporting water to inaccessible places, for total flooding of confined spaces such as basements, and for volumetric displacement of vapor, heat, and smoke. Extensive tests have demonstrated that under certain circumstances high expansion foam, when used in conjunction with water sprinklers, will produce more positive fire control and extinguishment than either extinguishment system by itself; this appears to be especially true with high rack storage of mixed commodities (e.g., high piled storage of paper stock and mixed storage of Class A and Class B materials). Optimum efficiency of high-expansion foam in any one type of hazard is dependent to some extent on the rate of application and also the foam expansion and stability.

Personal Safety

Persons should not enter a space filled with high-expansion foam without wearing full protective gear, self-contained breathing apparatus, an attached lifeline, and operating in a "buddy" system. A person who is immersed in high-expansion foam can experience disorientation and other psychological and personal discomforts. Foam entering any of the body cavities may cause severe irritation and membrane swelling.

Special Considerations

The proper design and application of high-expansion foam systems are directly related to a number of special system considerations. Special design factors include maximum submergence time and location of foam generating equipment.

A maximum time needs to be specified for filling the enclosed space to the proper depth with expanded foam. The time, expressed in minutes, is a function of the type of combustible material and the arrangement of the combustible material. An important consideration in maximum submergence time is whether stock material should be considered at a constant storage level in the space to be protected. Also of importance is whether the stock is protected by automatic sprinklers in addition to the high expansion foam. The basic objective is to control a developing fire before the fire has an opportunity to spread vertically over the face of a storage pile.

Fixed installations using high-expansion foam fire protection will probably involve the use of customized foam generating equipment to produce the cubic feet per minute requirement of foam discharge. The following points should be observed in the selection and placement of high-expansion foam generating equipment:

1. Two generators positioned remotely from each other are more effective and efficient than a single generator.
2. Generating equipment should be top mounted to avoid back pressures on the foam making equipment. Generators are normally mounted on external towers or special roof supports.
3. Generating equipment should be so positioned as to avoid product-of-combustion air intake. Induced smoke into the generating equipment can significantly reduce the quality and quantity of the foam produced.
4. To effectively dampen convection currents from a developing fire in an area to be protected, the capacity of each required foam generator should be the same.

All of the above information on types and classifications of foam systems serves as the background for actually designing a specific foam fire protection system. Some important limitations concerning both low- and high-expansion foam systems are presented in the following section before some problem examples.

Limitations of Foam Fire Protection Systems

This section discusses both low- and high-expansion foam systems. The limitations of foam fire protection must be addressed relative to each of these two system classifications. The following points should be reviewed during the proper selection and design of foam-type fire protection.

Limiting Factors for Low-Expansion Foam Systems

1. Low-expansion foam application is limited to the extinguishment of horizontal or two-dimensional fire problems. This type of foam application is not suitable for three-dimensional fires.
2. Low-expansion foam systems are limited by foam agent suitability for the defined flammable or combustible liquid. Basically, foam agents are suitable for either hydrocarbon fuels or polar solvents. Alcohol resistant-type foams may be approved for both hydrocarbons and polar solvents.
3. Different types and brands of foam concentrates may be incompatible and should not be mixed in storage.
4. Foam solution consists of 90 percent or more water. Foam system limitations should be evaluated with respect to the proper use of aqueous based agents on flammable materials and the electrical conductivity of the application method.
5. Foam systems are limited by the equipment appliances and devices used to proportion the foam and to deliver the finished foam onto a given hazard or fire problem. Equipment limitations pertaining to flow rate, operating pressure ranges, and proportioning ranges should be carefully considered in the selection and application of foam systems.

Limiting Factors for High-Expansion Foam Systems

1. Medium- and high-expansion foams are finding applications for a broad range of fire protection problems. However, unlike low-expansion foam systems, medium- and high-expansion foam fire protection systems should be specifically evaluated for each type of hazard condition. The fact that each system requires a feasibility study and individual design may be considered a form of limitation when contrasted to the design concepts for low-expansion foam systems.
2. NFPA 11A, *Standard for Medium- and High-Expansion Foam Systems*,[1] states that "under certain circumstances it may be possible to utilize medium and high expansion foam systems for control of fires involving flammable liquids or gases under pressure, but no general recommendations can be made in this standard due to the infinite variety of particular situations which can be encountered in actual practice." This statement is considered to be a design limitation.
3. Medium- and high-expansion foam systems should not be used on fires in the following hazards unless competent evaluation, including tests, indicates acceptability:

(a) Chemicals, such as cellulose nitrate, which release sufficient oxygen or other oxidizing agents to sustain combustion
(b) Energized unenclosed electrical equipment
(c) Water reactive metals, such as sodium and potassium (Na, K)
(d) Hazardous water reactive materials, such as triethylaluminum and phosphorous pentoxide
(e) Liquefied flammable gas

Hydraulic Calculation for Atmospheric Storage Tanks Protected by Low-Expansion Foam Systems

This section of the chapter is concerned with the proper design and associated hydraulic calculations for foam fire protection systems protecting atmospheric storage tanks with low-expansion foam systems. The material presented is limited to fixed protection systems using either top mounted foam chambers or subsurface injection, as discussed in the first section of this chapter. A single flammable liquid storage tank problem is presented for developing the appropriate methods and techniques for computing the foam agent requirements, system hardware requirements, and the necessary hydraulic calculations to properly deliver the required rate of foam to the subject hazard. The single example will be calculated using topside application of foam and subsurface injection of foam. This approach permits comparison and contrast of the system design and hydraulic requirements between the two foam application methods.

EXAMPLE 1:
Problem statement. The single outside storage tank depicted in Figure 4-5.1 is to be protected by a completely fixed foam system. The topside foam chamber arrangement is used in this problem. Note that the foam system is connected to a domestic water supply. The water supply curve is illustrated in Figure 4-5.2. For this problem, consider that the water available for the foam system is limited to the street main flow characteristics. A foam system job work sheet and a complete set of hydraulic calculations are to be prepared for this problem.

SOLUTION:
Procedure statements. A systematic outline follows for the proper design and hydraulic assessment associated with the stated problem; reference is made to criteria established in NFPA 11. This standard should serve as a companion guide to the systematic evaluation of each problem scenario. Individual item information is transferred to the referenced problem job sheet (Figure 4-5.3) and the associated hydraulic calculation sheet (Figure 4-5.4).
Problem assessment. In addition to the physical layout of the design problem, information is required on the hazard to be protected. The nature of the hazard drives the problem design. The following steps identify the hazard and standard requirements associated with the hazard:
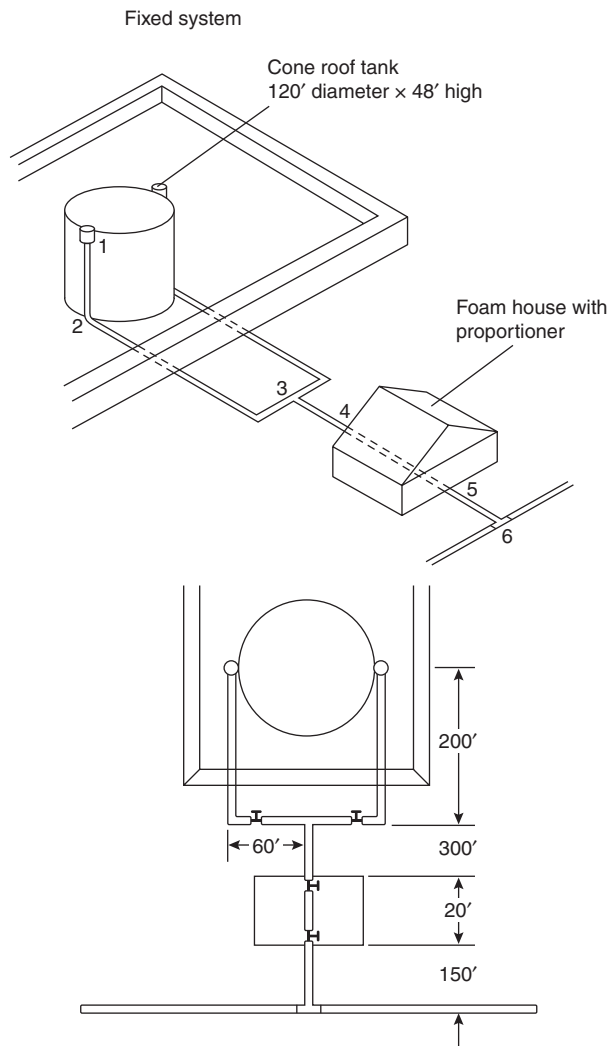
Figure 4-5.1. *Single storage tank with fixed foam system protection. The numbers 1 through 6 in the top portion of the drawing represent the reference points for hydraulic calculations for Example 1.*

Step 1: Installation identification.

Refer to Figure 4-5.1. One vertical atmospheric storage tank is positioned in a dike area. The tank is protected by a fixed foam fire protection system and connected to the domestic water supply.

Step 2: Hazard classification.

Flammable liquid atmospheric storage tank

Step 3: Type of protection.

Fixed protection systems

Step 4: Hazard description.

120-ft diameter outdoor cone roof flammable liquid storage tank

Step 5: Flammable or combustible liquid area to be protected.

Calculate the flammable liquid surface area: Area $= 0.7854d^2$:

$$A = 0.7854(120)^2 = 11,310 \text{ ft}^2$$

Step 6: Flammable liquid or combustible liquid identification.

Gasoline—Sg. 0.72

Step 7: Foam application method.

Top mounted fixed foam chambers—Type II

Step 8: Description, number, and placement of foam application devices.

Several factors need to be simultaneously considered in responding to this step. The description should reference a given manufacturer's foam chamber because the flow and pressure characteristics of the foam chamber *may be* a factor or present options for the system design. Manufacturer's literature and the UL listing of foam equipment should be consulted on this matter.

For proprietary reasons, the selected foam chamber for this problem will be identified as an FMA chamber with an operating pressure range of 40 to 80 psi and a flow range from 300 to 700 gpm of foam solution.

The foam standard (NFPA 11) requires a minimum of two foam chambers for a 120-ft diameter tank. More foam makers may be used based on hydraulic considerations, or economies of scale based on equipment costs. Individual manufacturers of foam equipment must be consulted on these options.

Placement of foam makers should consider equal spacing around the upper tank perimeter and placement of the foam solution feed lines. If possible, maintain constant flow and pressure requirements of each device.

Step 9: Foam agent selected.

A 3 percent fluoroprotein foam is selected for the defined hazard. Note that the type of foam agent selected for a particular design problem may affect other variables or consideration in the foam system design. This caution is reflected in Step 10.

Step 10: Foam solution application rate.

Foam solution application rates for storage tanks containing liquid hydrocarbons should be at least 0.1 gpm/ft^2 of liquid surface area of the tank to be protected. It should be noted that other types of foam protection (e.g., portable nozzles) may require different application rates. Also, flammable and combustible liquids not classified as hydrocarbons may require different foam solution application rates. Reference should be made to NFPA 11 concerning design application rates.

The foam solution application rate for the stated problem is calculated as follows:

rate (gpm) = 0.1 gpm/ft^2 $\times$ 11,310 ft^2 = 1131 gpm
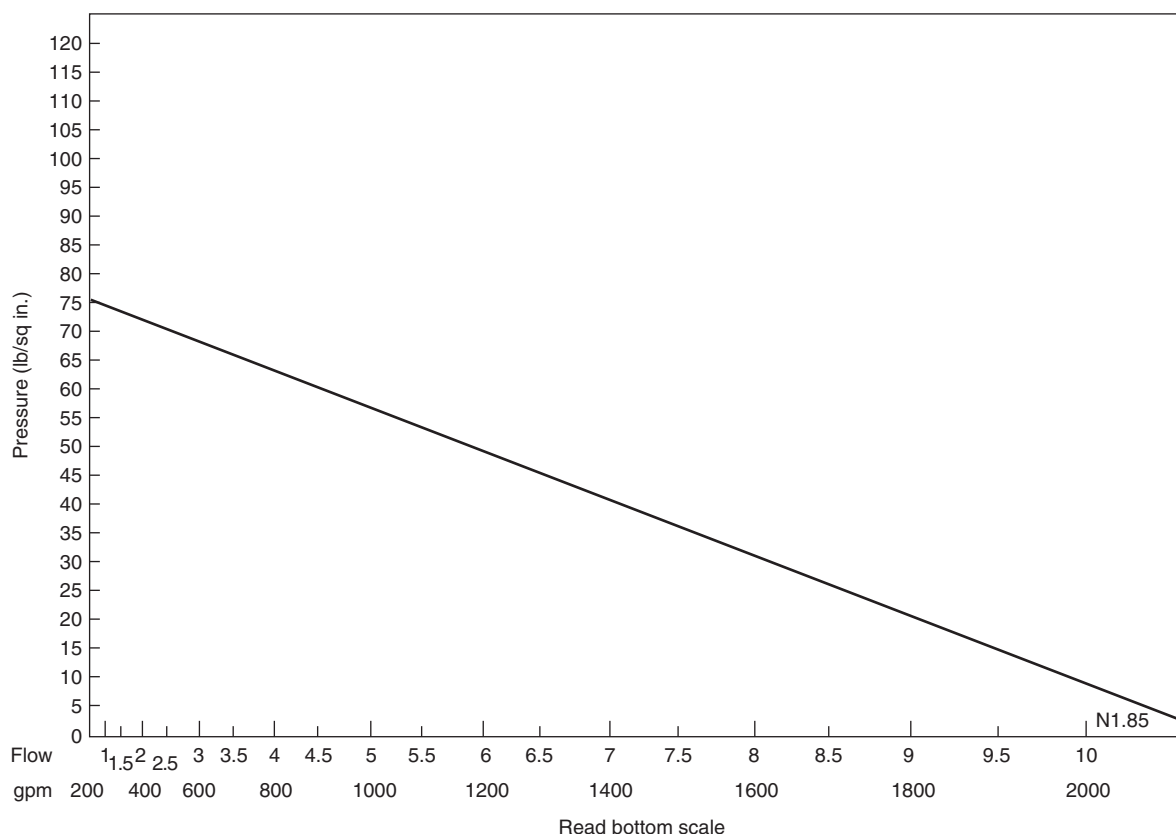
Figure 4-5.2. *Water supply curve for fixed foam system for Examples 1 and 2.*

However, the total rate is divided equally between two foam makers so it is appropriate to specify a rate of 1132 gpm, or 566 gpm per foam maker.

Step 11: Foam concentrate rate.

The foam concentrate rate is based on the foam agent proportioning rate. A 3 percent fluoroprotein foam is selected for this problem (see Step 9). In other words, 3 percent of the calculated solution rate is the foam concentrate rate. This rate may be determined as follows:

$$\text{foam concentrate rate} = 0.03(\%) \times 1132 \text{ gpm}$$
$$= 34 \text{ gpm}$$

Note that a continuous supply of foam agent (concentrate) must be available at a rate of 34 gpm for the required duration of discharge (see Step 13).

Step 12: Water application rate.

Quite simply, the water application rate is the foam solution rate minus the foam concentrate rate. The water application rate proceeds as follows:

$$\text{water application rate} = 1132 \text{ gpm} - 34 \text{ gpm}$$
$$= 1098 \text{ gpm}$$

The water application rate can also be determined as 97 percent of the "solution" rate when using a 3 percent foam concentrate.

Step 13: Duration of discharge.

A minimum foam solution discharge time is specified in NFPA 11 to control and extinguish a fire in a cone roof atmospheric storage tank. Duration of discharge is dependent on the classification of flammable or combustible liquid and the *type* of discharge outlet. Information for the given problem is contained in NFPA 11. The requirement for protecting gasoline with Type II foam chambers is 55 min. of continuous foam solution discharge.

Step 14: Gallons of foam required.

The required foam supply for any given problem should properly consider a primary supply and a reserve supply. The primary supply is computed by multiplying the determined rate of foam agent required by the duration of discharge as follows:

$$\text{foam agent required} = 34 \text{ gpm} \times 55 \text{ min} = 1870 \text{ gal}$$

The authority having jurisdiction may require that equal quantity of foam be placed in reserve for a second fire.

FOAM SYSTEM JOB WORK SHEET

Sheet: ___1___ of: ___1___

Designer: ___Staff___   Date: ___1986___

Installation identification: ___Ourville Oil Company___

Hazard classification: ___Flammable liquid atmospheric storage tank___

Type of protection: ___Fixed protection system___

Hazard description: ___120 ft diameter outdoor cone roof flammable liquid storage tank___

Flammable or combustible liquid area to be protected: ___11,310 ft²___

Flammable or combustible liquid identification: ___Gasoline___
___Sq. 0.72___

Foam application method: ___Type II—fixed chambers___

Description, number, and placement of foam application devices: ___2—Chambers equally spaced___

Foam agent selected: ___Fluoroprotein—3%___

Foam solution application rate: ___0.1 gpm per sq ft or 1131 gpm___

Foam concentration rate: ___34 gpm___

Water application rate: ___1098 gpm___

Duration of discharge: ___55 min___

Gallons of foam required: ___1870 gallons___

Gallons of water required: ___60,390 gallons___

Water supply information: ___See Figure 4-5.2___

Special foam design considerations: _____

Figure 4-5.3.   *Foam system job work sheet.*

Step 15: Gallons of water required.

The basic procedure follows the concept presented in Step 14. The water requirement is the product of the water rate times the time.

water required = 1098 gpm × 55 min = 60,390 gal

While the above calculation is straightforward, the answer may come as a surprise. Fixed foam protection systems for atmospheric storage tanks require a large quantity of water. The total quantity of water must be available at the site to assure foam delivery over the required time.

Step 16: Special foam system design considerations.

The first 15 steps in this problem analysis focus on fundamental considerations required to determine foam agent and water supply requirements. It is now appropriate to examine a series of special considerations that directly relate to the hydraulic design factors associated with this problem. Other design factors may be appropriate for different problems. However, the basic considerations outlined below should serve to guide similar calculations for other design problems.

1. Pipe size selection.
   Water supply pipe and foam solution pipe may be sized to minimize head loss between identified supply and demand points; pipe may also be designed on the basis of a mean velocity flow in a given section of pipe. A flow velocity of 10 ft per second may be used in the absence of other specific criteria for the determination of both water supply pipe and foam solution pipe. Pipe will be sized in this manner for the stated problem.

2. Valves in the pipe system.
   (a) The laterals of each foam chamber or fixed roof tank should be separately valved outside of the dike installation.

HYDRAULIC CALCULATIONS

Subject: _Example problem 1_

Job no.: _____

Sheet no.: _____ Of: _____

By: _____ Date: _____

Chkd by: _____ Date: _____

Application rate: _0.1_ gpm per sq ft   Area: _11,130 sq ft_

Minimum solution rate: _1131 gpm_   Actual solution rate: _1132 gpm_

Foam maker pressure and rate: _50 psi—566 gpm_   Foam system: _Chamber type 2_

Water data: _____   Ref. drawing: _Figure 4-5.1_

Foam maker type and location	Added gpm	Total gpm	Pipe size (in.)*	Pipe & equivalent fitting lgth. (ft)**	Friction psi/ft C=100	Friction Total psi	Static psi	Propor-tioner psi	Req'd pres gpm

Starting point: _1_   Elevation: _48 ft_   Pressure at foam maker: _50 psi_

Foam maker type and location	Added gpm	Total gpm	Pipe size (in.)*	Pipe & equivalent fitting lgth. (ft)**	psi/ft C=100	Total psi	Static psi	Propor-tioner psi	Req'd pres gpm
1	566	566							50
1–2		566	5.047	48'+(1E)8.6'=56.6'	0.0420	2.4	20.8		73.2
2–3		566	5.047	260'+(1GV)2'=(1T)25'					–
(2–3)				Σ = 287'	0.0420	12.1	–		85.3
3–4	566	1132	8.071	300'+(1GV)2'=302'	0.154	4.7	–		90.0
4–5		1132	8.071	18'+(1GV)2'=20'	0.154	0.3		4.0	94.3
5–6		#1098	8.071	150'=(1T)35'=185'	0.145	2.7			97.0
Σ at 6		1098							97.0

\#   Water only

*   "X" indicates extra hvy.—std. wt. otherwise

** See sheet for tabulation of pipe and fittings

Figure 4-5.4.   *Hydraulic calculation work sheet.*

(b) The water line to each proportioner inlet should be separately valved.
Note: Valves are properly shown in Figure 4-5.1.

3. Foam proportioner selection.
Several different foam proportioners are available from equipment manufacturers. It is very important to select foam proportioning equipment that meets the following requirements:
(a) Proper proportioning over the range of desired flows.

(b) Minimum or acceptable head loss across the proportioning device.
(c) Suitability for the foam agent selected.
(d) Capability of overcoming any back pressure limitations.

4. Water pumps.
The water supply in a given case may require a pressure boost to meet the foam chamber discharge requirements. Where a water pump is required, consideration must be given to the pump capacity, the

pressure profile, the pump horsepower requirement, and the pump intake-discharge positions with respect to the total installation of pipe.

Hydraulic analysis for Example 1: The supporting documentation above provides a foundation for conducting a hydraulic design for the problem depicted in Figure 4-5.1. The design parameters and associated calculations are presented in sequential steps below. All reference points conform to Figure 4-5.1. Computations are also charted on a hydraulic calculation sheet as shown in Figure 4-5.4.

Step 1: Starting point.

The design objective is to provide each of the two foam chambers with the required pressure to discharge the calculated quantity of foam solution. The stated problem requires a foam maker discharge of 566 gpm at 50 psi. An orifice plate is supplied by the foam equipment manufacturer to provide the correct discharge at the design pressure (50 psi). The design pressure is a function of the range of pressures that can be used with a specific manufacturer's foam chamber.

Step 2: Design tank riser.

The vertical pipe supplying the foam chamber (reference points 1–2) is sized on the basis of a maximum flow velocity of 10 feet per second. The pipe size is determined as follows:

Formula:

$$\text{Velocity} = \frac{0.40852 \times \text{gpm}}{d^2}$$

a. Solve for d

b. $10 \text{ fps} = \dfrac{0.4085 \times 566 \text{ gpm}}{d^2}$

c. $d^2 = 23.12$ in.

d. $d = 4.8$ in.

e. 5-in. pipe is selected. (Note: The authority having jurisdiction may require a 6-in. pipe.)

Step 3: Enter hydraulic calculation from reference points 1-2.

1. Friction loss, FL, is determined by the Hazen-Williams formula

$$\text{FL} = \frac{4.52 \times Q^{1.85}}{C^{1.85} \times d^{4.87}}$$

where

$Q = 566$ gpm

$C = 100$

$d = 5.047$ (internal diameter of pipe)

FL = 0.0420 psi/ft

2. Note: All friction losses and head losses are summed in the required pressure column.

3. The head loss, H_L, for 48 ft of elevation difference between reference points is computed as follows:

$$H_L = 0.433 \text{ psi/ft} \times 48 \text{ ft} = 20.8 \text{ psi}$$

4. The pipe section includes one standard elbow at reference point 2. For hydraulic calculations, fittings are treated as equivalent feet of pipe in accordance with NFPA 13, *Standard for the Installation of Sprinkler Systems.*[1]

Step 4: Enter hydraulic calculations from reference point 2 (bottom of tank) to reference point 3.

1. The flow is constant (566 gpm) so the pipe size remains the same at 5 in.

2. Pipe fittings include a globe valve outside the dike area and a standard tee at reference point 3.

Step 5: Enter hydraulic calculations from reference point 3 to the foam house (reference point 4).

1. The total foam solution flow (1132 gpm) is supplied by line 2-3.

2. Determine the pipe size based on a maximum flow velocity of 10 ft/s.

3. velocity $= \dfrac{0.4085 \times \text{gpm}}{d^2}$

$$10 \text{ fps} = \frac{0.4085 \times 1132 \text{ gpm}}{d^2}$$

$$d = 6.8 \text{ in.}$$

4. An 8-in. pipe is recommended between the foam house and reference point 3.

5. The friction loss in the stated line includes the linear distance plus the gate valve.

6. It should be observed that the required pressure at the discharge side of the foam house is 90.0 psi.

Step 6: Enter the hydraulic calculations in the foam house.

1. To the left of the top view, bottom half, Figure 4-5.1, is an illustration of the foam proportioning ratio controller inserted into the water line. The proportioning device selected for this problem has a friction loss of 4 psi at a solution flow rate of 1132 gpm. Foam equipment manufacturers should be consulted on head loss characteristics for specific devices. The ratio controller takes up a lineal distance of 2 ft leaving 18 ft of straight run pipe in the foam house.

2. The calculations provided do not include provisions for a water pump.

Step 7: Enter the hydraulic calculations from the foam house to the street main.

1. The flow rate in line 5-6 is 1098 gpm. Note the change in friction loss.

2. An 8-in. main is used to connect the street main to the foam house.

Step 8: Summary.

1. The water demand requirement at reference point 6 is 1098 gpm at 97.0 psi.

2. The hydraulic demand has been calculated to provide a foam solution flow of 566 gpm at 50 psi for *each* designated foam chamber.

3. The water supply curve referenced as Figure 4-5.2 shows 1098 gpm available at 53 psi. Therefore, a water

pump is required in the pump house to boost the pressure from 50 psi (loss of pressure from reference points 6 to 5 is approximately 3 psi) to 97 psi or approximately 50 psi. A pump can be engineered for this specific application.

EXAMPLE 2:

Overview statement. The flammable liquid storage tank presented as Example 1 is also presented as Example 2; only the method of fire protection changes. Example 2 considers the depicted 120-ft diameter storage tank to be protected with subsurface application of foam to the described hazard. The subsurface application technique requires new design considerations with respect to foam equipment and hydraulic calculations. The following principles should be observed in the design of subsurface application foam systems:

1. Foam solution is expanded outside of the dike area by a "high back pressure" foam maker. A typical foam expansion of 4:1 is achieved at the foam maker.
2. The expanded foam flows through a carefully designed pipeline from the foam maker to an opening in the tank shell just above the water bottom in the tank. In accordance with NFPA 11, *Standard for Low-Expansion Foam,* the foam velocity at the point of discharge into the tank contents shall not exceed 10 ft/s for Class IB liquids and 20 ft/s for other type liquids. An excessive input velocity to the tank can cause the foam to be saturated with fuel pickup.
3. Foam entering the product rises to the fuel surface by natural buoyancy.

Problem statement. A single outside storage tank illustrated in Figure 4-5.5 is to be protected by a completely fixed foam system. The subsurface foam application method is used for this problem. The Figure 4-5.2 water supply curve is to be applied with this problem. Consider that the water available for the foam system is limited to the street main flow characteristics. A foam system job work sheet and a complete set of hydraulic calculations are to be prepared for this problem.

Procedure statements. A systematic outline follows for the proper design and assessment associated with Example 2. Reference is made to criteria established in NFPA 11 by paragraph reference. NFPA 11 should serve as a companion guide to the systematic evaluation of each problem scenario. Individual item information is transferred to the referenced problem sheet (Figure 4-5.6) and the associated hydraulic calculation sheet (Figure 4-5.7).

Problem assessment. In addition to the physical layout of the design problem, information is required on the hazard to be protected. The nature of the hazard is identical to Example 1; only the method of protection changes. Some of the following steps are repeated for maintaining a sequence to the problem solution. New material will be explained in detail. Calculations for similar material are referenced to Example 1.

Step 1:   Installation identification.
    Refer to Figure 4-5.5. One vertical atmospheric storage tank is positioned in the dike area. The tank is pro-
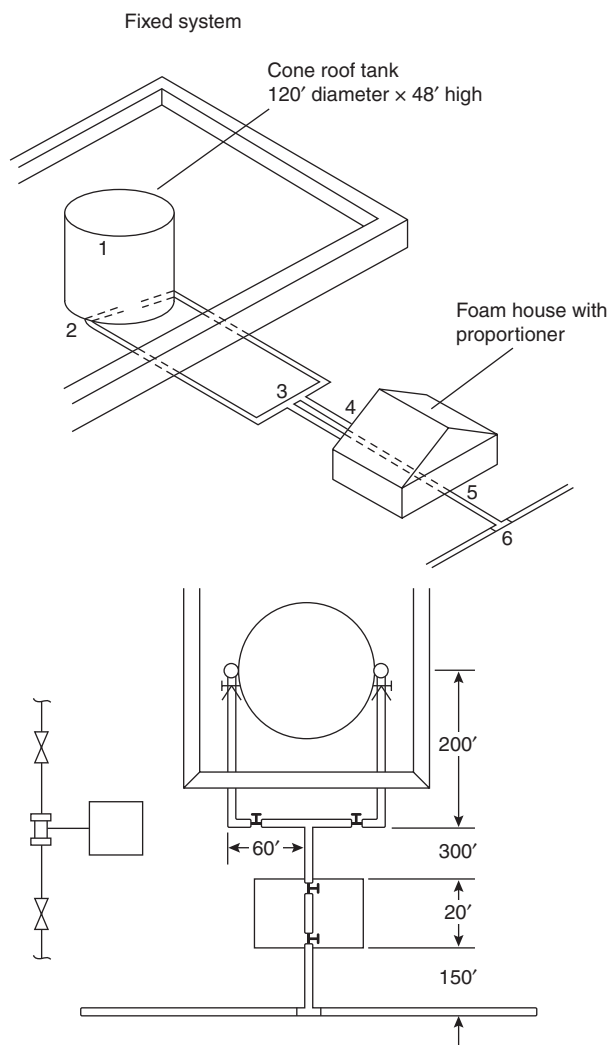
Figure 4-5.5.   *Subsurface application foam system with reference points used in Example 2.*

tected by a fixed subsurface injection foam fire protection system and connected to the domestic water supply.

Step 2:   Hazard classification.
    Flammable liquid atmospheric storage tank

Step 3:   Type of protection.
    Subsurface application to fixed roof storage tanks (Re: NFPA 11, Section 3-2.4)

Step 4:   Hazard description.
    120-ft-diameter outdoor cone roof flammable liquid storage tank

Step 5:   Flammable or combustible liquid area to the protected.
    11,310 ft² (See Step 5—Example 1)

Step 6:   Flammable liquid or combustible liquid identification.
    Gasoline—Sq. 0.72

FOAM SYSTEM JOB WORK SHEET

Sheet: ___1___ of: ___1___

Designer: ___Staff___   Date: ___1986___

Installation identification: ___Ourville Oil Company___

Hazard classification: ___Flammable liquid storage tank___

Type of protection: ___Subsurface application to fixed roof storage tank___

Hazard description: ___120 ft diameter outdoor cone roof flammable liquid storage tank___

Flammable or combustible liquid area to be protected: ___11,310 ft²___

Flammable or combustible liquid identification: ___Gasoline — sq. 0.72___ ___sq. 0.72___

Foam application method: ___Subsurface application to a liquid hydrocarbon___

Description, number, and placement of foam application devices: ___Two subsurface injection points positioned equal and opposite on the tank shell. A PHB foam maker is used.___

Foam agent selected: ___3%___

Foam solution application rate: ___1132 gpm___

Foam concentration rate: ___34 gpm___

Water application rate: ___1098 gpm___

Duration of discharge: ___55 min___

Gallons of foam required: ___1870___

Gallons of water required: ___60,390___

Water supply information: ___See Figure 4-5.2___

Special foam design considerations: ___Foam injection piping to be sized for a maximum fluid velocity of 10 fps___

Figure 4-5.6. *Foam system job work sheet.*

Step 7: Foam application method.

Subsurface application to a liquid hydrocarbon (Re: NFPA 11, Section 3-2.4)

Step 8: Description, number, and placement of foam application devices.

Several equipment design variables must be considered simultaneously in this step. Again, reference must be made to a specific foam manufacturer's equipment offerings or the conduct of a comparative analysis between two or more manufacturers of suitable equipment. The manufacturer's literature and the UL listing of foam equipment should be consulted on this matter.

The following substeps outline the key features of the design to be evaluated and computed at this overall step in the design development. Each substep may impact on other substeps and therefore all substeps must be evaluated before selecting a set of equipment and associated calculations.

Step 8(a): Velocity of approach into the storage tank.

Gasoline is a Class IB liquid, and therefore the injection velocity of the expanded foam into the product tank should not exceed 10 ft/s. This does not mean that the velocity of foam between the foam maker and the injection point has to be controlled to a maximum of 10 ft/s. Rather, the foam velocity at the physical point of entry to the product is the key consideration.

Remember that the foam is expanded at the entry point to the product. Special flow curves must be examined to determine velocity characteristics with expanded foam. These curves are not available in the current edition

HYDRAULIC CALCULATIONS

Subject: _Example problem 2_

Job no.: _____

Sheet no.: _____ Of: _____

By: _____ Date: _____

Chkd by: _____ Date: _____

Application rate: _0.1_ gpm per sq ft   Area: _11,130 sq ft_

Minimum solution rate: _1132 gpm_   Actual solution rate: _1132_

Foam maker pressure and rate: _PHB—159 psi—566 gpm_   Foam system: _Subsurface_

Water data: _Figure 4-5.2_   Ref. drawing: _____

Foam maker type and location	Added gpm	Total gpm	Pipe size (in.)*	Pipe & equivalent fitting lgth. (ft)**	Friction psi/ft C=100	Friction Total psi	Static psi	Propor- tioner psi	Req'd pres psi
Starting point: _1_				Elevation: _48 ft_			Pressure at foam maker: _50 psi_		
1		2264	10"				15		15
1–2		2264	10"	20	0.20	0.4			15
2–3				560+1CV(55)1GV(5)	0.40	24.8			40
				620					
Σ3									40

Note: The demand pressure at 3 is less than the allowable pressure of 64.0 psi

* "X" indicates extra hvy.—std. wt. otherwise

** See sheet for tabulation of pipe and fittings

Figure 4-5.7. *Hydraulic calculations.*

of NFPA 11; one must turn to manufacturer's literature on this topic.

A set of flow curves for expanded foam in various pipe diameters are included in the Appendix of the chapter with approval of National Foam System, Inc. Figure 4-5A.3 is consulted for this problem element.[2]

Table 3-2.4.2 of NFPA 11 indicates that two discharge outlets must be provided for a 120-ft-diameter tank. The foam solution rate for each outlet is given in Step 10 of this example and is equal to the calculations for Example 1: 566 gpm per outlet. However, the foam is expanded at the high back pressure foam maker using a ratio of 4:1. The expanded foam flow rate at each outlet is 2264 gpm. This is the value used when checking foam velocity.

A 10-in. pipe is required to maintain a foam velocity less than 10 ft/s when the rate of expanded foam is 2264 gpm (see Figure 4-5.A3). The pipe length upstream from the discharge point must be at least 20 times the

diameter of the pipe to establish uniform velocity. Therefore, a straight run of 10-in. pipe at least 17 ft in length is necessary.

The foam outlet is not required to be at the tank shell. Note that the 10-in. pipe is actually inserted into the tank. This design approach permits economizing the pipe sizes between the tank and the high back pressure foam maker. The high back pressure foam maker is to be positioned outside of the dike area. A gate valve and a check valve are installed adjacent to the tank shell.

Step 9: Foam agent selected.

A 3 percent fluoroprotein foam is selected for the defined hazard. The foams should be listed for subsurface injection.

Step 10: Foam solution application rate.

For tanks containing liquid hydrocarbons, the foam solution rate must be at least 0.10 gpm/sq ft of liquid surface area of the tank to be protected. The maximum rate must be 0.20 gpm/sq ft. (Re: NFPA 11, Table 3-2.4.3.)

The foam solution application rate for Example 2 is the same foam solution rate calculated for Example 1; the application rate is 1132 gpm.

Step 11: Foam concentrate rate.

The foam concentrate rate is determined in the same manner as set forth for Example 1. Using a 3 percent fluoroprotein foam, the requirement is 34 gpm for a total solution rate of 1132 gpm. This requirement impacts on Step 14 of this example.

Step 12: Water application rate.

The water application rate is also determined in the same manner as set forth in Example 1. The water application rate is the foam solution rate minus the foam concentrate rate: the water rate is 1098 gpm.

Step 13: Duration of discharge.

The minimum discharge time for subsurface application of foam is identical to the requirement for Type II application. (Re: NFPA 11, Section 3-2.4.3.) Gasoline product requires a total discharge time of 55 minutes.

Step 14: Gallons of foam required.

The gallons of foam required is computed in the same manner as set forth in Example 1. The primary foam supply is computed by multiplying the determined rate of foam agent by the duration of flow, which indicates a requirement of 1870 gal.

Step 15: Gallons of water required.

The water requirement is the product of the water rate times the discharge time, or 60,390 gal.

Step 16: Special foam system design considerations

One special design consideration is presented in Step 8(a) and involves the pipe requirements for injecting foam into the base of a storage tank under controlled velocity conditions. Other special conditions that apply specifically to subsurface injection of foam to storage tanks are given below.

1. *High-back-pressure foam maker.* A high-back-pressure foam maker is designed for capability to make foam and discharge the foam against considerable back pressure. The high-back-pressure foam maker selected for the example problem is designed to operate satisfactorily at inlet pressures of 100 to 300 psi and produce foam of 2:4 expansion against back pressures not exceeding 40 percent of the inlet pressure. With an inlet pressure of 150 psi, for example, 60 psi is available at the discharge for forcing the foam through a hose and/or piping into the storage tank and to overcome the fuel head in the tank. Manufacturers of high-back-pressure foam equipment should be consulted for obtaining flow and pressure characteristics and back pressure limitations. Two high-back-pressure foam makers are used with Example 2. The two foam makers are located in the foam house and are arranged for parallel operations. (See Figure 4-5.5.)

2. *Pipe size selection.* Expanded foam flowing in conduit (pipe) does not follow the head loss characteristics expressed in the Hazen-Williams formula. A set of flow curves have been developed for determining friction loss for expanded foam discharge by a high-back-pressure foam maker.[2] A set of these curves is provided in the Appendix to this chapter with the permission of National Foam System, Inc. (See Figures 4-5A.1 and 4-5A.2.)

   A flow velocity of 10 ft/s is used for the determination of pipe sizes flowing foam solution and water. If necessary, water supply pipe and foam solution pipe may be sized to minimize head loss between identified supply and demand points.

3. *Valves in the pipe system.* (Re: NFPA 11, Section 3-2.6.3.) For subsurface application, each foam delivery line must be provided with a valve and check valve, unless the latter is an integral part of the high-back-pressure foam maker or pressure generator to be connected at the time of use. When product lines are used for foam, product valving must be arranged to ensure foam enters only the tank to be protected.

4. *Foam proportioner selections.* The practices and procedures outlined in Example 1 apply to Example 2. However, to accommodate the pressure requirements associated with a high-back-pressure foam maker, a balanced proportioner would appear to provide the best level of constant proportioning over designated pressures.

5. *Water pumps.* The required pressure at the intake to the high-back-pressure device is approximately 150 psi. The static pressure on the water system is only 75 psi. Therefore, a water pump is required to boost the water-solution pressure in the foam hose. The most efficient approach to designing a required water pump installation is to select or design a pump-driver combination that will boost the available residual pressure to the required residual pressure at the demand flow. In

other words, with the right capacity pump, the driver horsepower is calculated to raise the pressure over the differential range. Other criteria must be used if a standard fire pump is required by the authority having jurisdiction.

Hydraulic analysis for Example 2: The information above provides a foundation for conducting a hydraulic design for the problem depicted in Figure 4-5.5. The design parameters and associated calculations are presented in sequential steps below. All reference points conform to Figure 4-5.2. Computations are also charted on a hydraulic calculation sheet, designated as Figure 4-5.7.

Step 1: Precalculation for high-back-pressure foam maker.
The hydraulic characteristics of the high-back-pressure foam maker must be considered before the computations start. A high-back-pressure foam maker delivering 550 gpm at 150 psi is selected for each finished foam line to the tank.

a. Determine a K value for the specified unit:

$$Q = K\sqrt{150}$$
$$K = 44.9$$

b. Required discharge per foam maker is 566 gpm.

c. Determine the required input pressure for a flow of 566 gpm:

$$566 \text{ gpm} = 44.9\sqrt{P}$$
$$P = 159 \text{ psi}$$

d. The available back pressure becomes 40 percent of 159, or 64.0 psi.

Remember: Head loss converted to psi between the foam maker discharge and the foam discharge outlet to the tank, plus the product head, must not exceed 64 psi.

Step 2: Size foam injection pipe to tank.
Step 8(a) under problem assessment for Example 2 establishes that a 10-in. pipe is required to maintain a flow velocity under 10 ft/s.

Step 3: Determine head loss from production storage.
Finished foam rising through the product must overcome the product head. Gasoline is the product for this series of problems with a Sq. = 0.72.

$$\text{psi loss} = 48 \text{ ft} \times 0.433 \text{ psi/ft} \times 0.72 \text{ Sq.}$$
$$\text{psi loss} = 15$$

Step 4: Size the foam supply line from the tank shell to the foam house.
The stated pipe is selected on the basis of the allowable friction loss of 64 psi minus the product head loss which equals 15 psi. Therefore, 49 psi (64 psi − 15 psi) can be dissipated from the tank to the foam maker through 500 ft of pipe and be used as an initial estimator; the flow rate is 2264 gpm. Figure 4-5.8 indicates a 6-in. pipe is required. A 6-in. check valve and a 6-in. gate valve will be installed on the foam supply line adjacent to the tank in

GSA warehouse

Rate of foam discharge

$R = (V/T + R_s) \times C_N \times C_L$ where

R = Rate of discharge—cfm
v = Submergence volume—cubic feet
T = Submergence time—minutes
R_s = Rate of foam breakdown by sprinklers
C_N = Compensation for normal shrinkage (1.15)
C_L = Compensation for leakage (1.2)

$R = S \times Q$ where

S = Foam breakdown in cfm per gpm of sprinkler discharge. S shall be 10 cfm/gpm

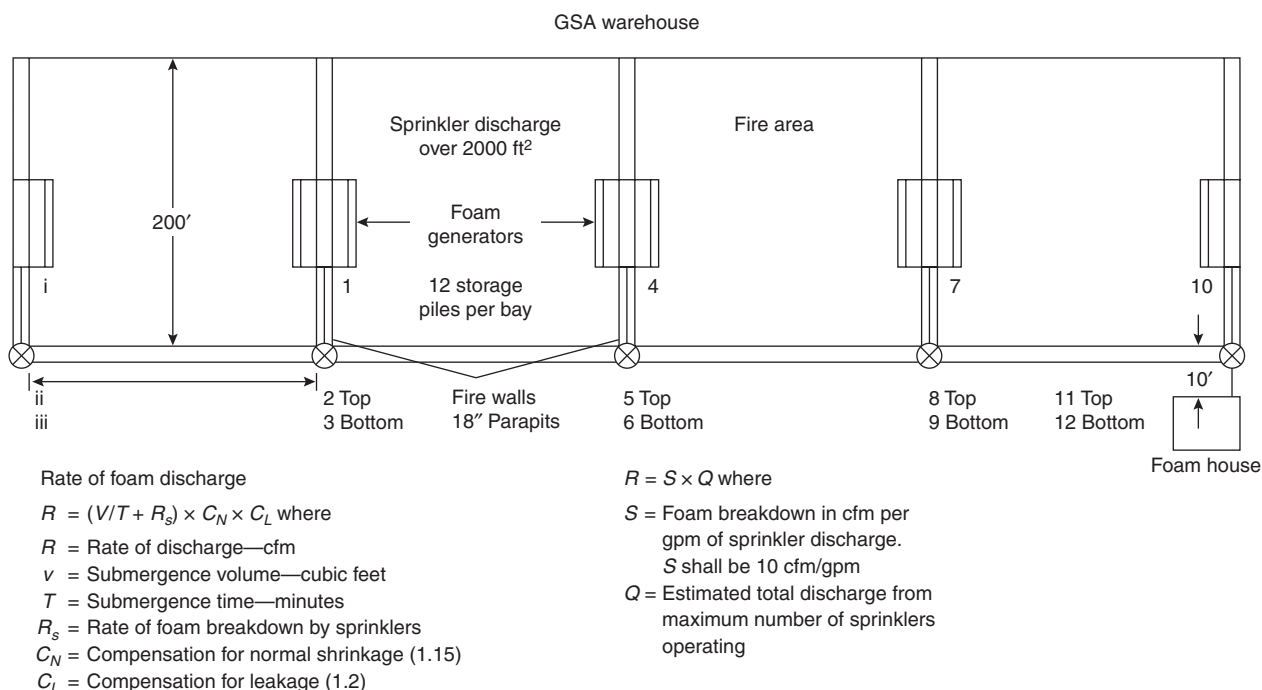Q = Estimated total discharge from maximum number of sprinklers operating

Figure 4-5.8. *Typical four-bay warehouse complex.*

the dike area. The required friction loss calculations are presented in Figure 4-5.7.

Calculation note: Subsurface foam system hydraulics actually divide into two separate calculation sets, as follows: (1) the hydraulics between the high-back-pressure foam maker and the storage tank and (2) the hydraulics between the street main supply and the high-back-pressure foam maker.

Step 5: Street main to fire pump calculation.
  The lateral supply line will be designated at a velocity of 10 ft/s. Recall that only water is moving through this line.

$$\text{Velocity} = \frac{0.4085 \times \text{gpm}}{d^2}$$

a. Solve for d

b. $10 \text{ ft/s} = \dfrac{0.4085 \times 1098 \text{ gpm}}{d^2}$

c. $d^2 = 44.85$ in.
d. $d = 6.69$ in.
e. Use an 8-in. pipe

Step 6: Piping in foam hose.
  8-in.-diameter pipe will be used in the foam house to connect between the water pump, the foam proportioner, and the high-back-pressure foam maker.

High-Expansion Foam Systems

Many of the fundamental hydraulic concepts presented with low-expansion foam system design problems also apply to high-expansion foam systems. Some similarities and differences between the hydraulic design for high-expansion foam systems and low-expansion foam systems are presented in Table 4-5.2. In this analysis, a low-expansion foam system using top-mounted foam chambers is compared to an elevated high-expansion foam generator installation.

Example 3 considers the use of a high-expansion foam system in conjunction with automatic sprinkler protection for fire control and suppression in a specified government warehouse. Be careful to note the generator flow rates, foam concentrate rates, and water supply rates. One of the advantages for considering high-expansion foam for the protection of confined space hazards is the low rate of foam application and associative water rate when compared to other aqueous types of systems.

EXAMPLE 3:
  Problem statement. An owner has elected to protect a number of warehouse complexes with a combination of automatic sprinklers and high-expansion foam. A typical four-bay warehouse complex is illustrated in Figure 4-5.8. The storage item is crude rubber piled 12 ft 6 in. high in 2000 ft² pile areas. The installed sprinkler design is 0.2 gpm/ft². The location of the high-expansion foam generators is illustrated on the 12-in. wide brick fire walls. Each foam generator is equipped with a set of remote-controlled baffels that permits directional flow of foam into adjacent fire areas. Custom generators are used that have a foam solution rate requirement of 1.83 gpm per 1000 ft³ of foam production. Three percent foam proportion with a UL-listed high-expansion foam is used for this system.
  Procedure statements. The key consideration in high-expansion foam system design is the proper sizing of the foam-generating equipment to be used for a specific application. A special job work sheet is provided to systematically calculate the foam generation requirements. (See Figure 4-5.9.) Individual item information is transferred from the referenced job sheet to the associated hydraulic calculation sheet. (See Figure 4-5.10.) Reference is made to criteria established in NFPA 11A, *Standard for Medium- and High-Expansion Foam Systems.* This standard should serve as a companion guide to the systematic evaluation of the warehouse protection problem.
  Problem assessment. The fundamental considerations of the hazard to be protected establish the elements of the

Table 4-5.2   *Comparison of Design Criteria for Low-Expansion and High-Expansion Foam Systems*

Design/Hydraulic Step Function	Low-Expansion Foam System—Top Chamber	High-Expansion Foam System—Top Generator
Starting point	Foam chamber(s)	Foam generator(s)
Second determination	Foam solution requirement per chamber (gpm)	Expanded foam requirement per chamber (cfm)
Third determination	Foam solution delivery rate between foam maker and foam house	Same determination
Fourth determination	Size pipe from foam maker(s) to foam house	Size pipe from foam generator(s) to foam house
Fifth determination	Determine type and size of foam proportioner	Same determination
Sixth determination	Determine hydraulic requirements in foam house	Same determination
Seventh determination	Evaluate water supply/demand requirement at foam house	Same determination
Eighth determination	Assess requirement for water pump in foam house; recalculate hydraulic requirements in foam house	Same requirement

HIGH-EXPANSION FOAM SYSTEM JOB WORK SHEET

Sheet: __1__ of: __1__

Designer: __Staff__

Date: __1986__

Installation identification: __GSA Defense Materials Warehouse__

Hazard classification: __High density combustibles__

Type of protection: __Dry pipe automatic sprinkler—fixed HI-X foam__

Hazard description: __Crude rubber in piles__

Rate of discharge determination:

1. Submergence volume (cubic feet)

   v = floor area __40,000__ sq ft × foam depth __14.5 ft__ = __580,000__ cu ft

2. Submergence time (minutes) T = __5__

3. Rate of foam breakdown by automatic sprinklers: $R_s = S \times Q$ where

   S shall be 10 cfm/gpm and Q shall be total discharge from operating sprinklers

   R_s = 10 cfm × __400__ gpm = __4000__ cfm

4. Compensation for normal foam shrinkage—C_N: C_N = __1.15__

5. Compensation for leakage—C_L; C_L range is from 1 to 1.2: C_L = __1.1__

6. Rate of discharger (cfm) = $(v/T + R_s) \times C_N \times C_L$ = __151,800__

Description, number, and placement of foam generators: __2—80,000 cfm foam generators__
__per storage bay. Placement on fire walls as shown__

Foam solution rate: __146 gpm/generator × 2 = 292 gpm__

Foam concentration rate: __3% proportion × 292 gpm = 9 gpm__

Duration of discharge: __15 minutes of full operation__

Gallons of foam required: __Main and reserve = 270 gals__

Gallons of water required: __4,245__

Water supply information: __Adequate for demand curve__

Special foam system design considerations: __System is activated by automatic__
__sprinkler system dry pipe trip.__

Figure 4-5.9. *High-expansion foam system job work sheet.*

problem design. In the case of high-expansion foam, some subjective criteria needs to be established due to the lack of specific information in NFPA 11A. Subjective criteria will be fully noted in the problem development. The following steps identify the hazard and the standard calculations associated with the hazard.

Step 1: Installation identification.
Refer to Figure 4-5.8, a defense materials warehouse.

Step 2: Hazard classification.
High density combustibles. Note: The actual storage material is crude rubber provided in irregular flat sheets.

This commodity is not specifically specified in Table 2-3.4 of NFPA 11A. Therefore, some judgment must be made when selecting foam submergence time as required for the calculations below.

Step 3: Type of protection.
The warehouse is protected by a drypipe automatic sprinkler system with a maximum discharge capability of 0.2 gpm/ft^2 over 2000 ft^2. This discharge density is not considered adequate protection for crude rubber in 2000 ft^2 piles. The automatic sprinkler protection is supplemented by a fixed high-expansion foam system. The foam generators are mounted on the coping section

HYDRAULIC CALCULATIONS

Subject: _GSA Warehouse_

Job no.: _Sample problem 3_

Sheet no.: _1_   Of: _1_

By: _Staff_   Date: _1986_

Chkd by: _____   Date: _____

Application rate: _NH_ gpm per sq ft

Area: _40,000 ft_

Minimum solution rate: _1.83 gpm/1000 ft³_

Actual solution rate: _185 gpm/1000 ft³_

Foam maker pressure and rate: _50 psi @ 146 gpm_

Foam system: _Fixed_

Water data: _____

Ref. drawing: _____

Foam maker type and location	Added gpm	Total gpm	Pipe size (in.)*	Pipe & equivalent fitting lgth. (ft)**	Friction psi/ft C=100	Total psi	Static psi	Propor- tioner psi	Req'd pres psi
Starting point: _1_				Elevation: _22 ft_			Pressure at foam maker: _50 psi_		
1	146	146							50
1–2–3		146	3.068	212'+E(7')=1 T(15)	.0387	9.1	9.5		68.6
				234'					
2 @ 3									68.6
3–6		146	4.026	200'	.0103	2.06			70.7
6–9–12	148	294	4.026	400'	.0375	15.0			85.7
Foam house		294						4.0	89.7
System demand		294							90.0

*   "X" Indicates extra hvy.—std. wt. otherwise

**   See sheet for tabulation of pipe and fittings

Figure 4-5.10.   *Hydraulic calculations.*

to the fire walls that divide the warehouse into fire areas. Generators positioned on the internal fire walls are arranged to discharge foam into whichever compartment, as required.

Step 4:   Hazard description.

The fundamental considerations associated with the hazard are given under Step 1. It should be further noted that 12 storage piles of 2000 ft² each are located in the designated fire areas. Each individual pile is approximately 12 ft 6 in. high. Due to the piling arrangement of the rubber and the burning characteristics of rubber, no deduction is made for "stock" in the rate discharge determination.

Step 5:   Rate of discharge determination.

The basic design objective is to determine the rate of expanded foam discharge in cubic feet per minute to sub-

merge the hazard in a defined period of time. This determination can be accomplished by applying a rate formula developed by the NFPA Foam Committee. The formula is given in Figure 4-5.9, under sub-item 6. The formula can be applied by first calculating and then assigning values to the formula variables.

1. *Submergence volume* (Re: NFPA 11A, Section 2-3.3).
   Floor area: 200 ft $\times$ 200 ft = 40,000 ft^2
   Foam Depth:
   (a) 1.1 $\times$ height = 1.1 $\times$ 12.5 = 13.75 ft
   (b) Height + 2 ft − 12.5 ft + 2 ft = 14.5 ft
   Use the larger of the two values or 14.5 ft for calculations.
   Volume = area $\times$ depth
   Volume = 40,000 ft^2 $\times$ 14.5 ft = 580,000 ft^3
   (See Step 4—no deduction is made for stock)
2. *Submergence time* (Re: NFPA 11A, Section 2–3.4).
   5 minutes for high density materials with sprinkler protection
3. *Rate of foam breakdown for sprinklers* (Re: NFPA 11A, Section 2-3.5.2).
   (a) Discharge from sprinklers:

   $$Q = 0.2 \text{ gpm/ft}^2 \times 2000 \text{ ft}^2 = 400 \text{ gpm}$$

   (b) Apply formula:

   $$R_s = 10 \text{ cfm} \times 400 \text{ gpm} = 4000 \text{ cfm}$$

4. *Compensation for shrinkage.* Set at 1.15 as a constant (Re: NFPA 11A, Section 2-3.5.2).
5. *Compensation for leakage.* Use 1.1 to allow for some leakage around doors (Re: NFPA 11A, Section 2-3.5.2).
6. Apply formula:

   $$\text{cfm} = (v/T + R_s) \times C_N \times C_L$$

   $$\text{cfm} = (580,000 \text{ ft}^3/5 \text{ min} + 4000 \text{ cfm}) \times 1.15 \times 1.1$$

   $$= 151,800 \text{ cfm}$$

Note: The foam breakdown from sprinklers is a relatively small value compared to the total cfm rate.

Step 6: Description, number, and placement of generators.
   Custom-built foam generators will be required for this problem. Each generator will have a capacity of 80,000 cfm with a foam solution rate of 146 gpm. (See given information with problem statement.) Five generators will be required to protect the entire warehouse. Generators mounted on interior fire walls will be equipped with baffels arranged to discharge foam into either adjacent compartment; electrical controls will be operated from the foam house. Generators are actually mounted 22 ft above the finished floor.

Step 7: Foam solution rate.
   The foam solution rate per generator is given in Step 6. The solution rate requirement is 1.83 gpm per 1000 ft^3 of foam production.
   Solution rate = 80,000 ft^3/1000 ft^3 $\times$ 1.83 gpm = 146 gpm
   Two generators require 292 gpm.

Step 8: Foam concentrate rate.
   The foam selected for this problem proportions at 3 percent. Therefore, the concentrate rate is 3 percent $\times$ 292 gpm = 9 gpm.

Step 9: Duration of discharge.
   Duration of discharge for the foam systems should be checked with the authority having jurisdiction. A basic minimum discharge time is 15 minutes of continuous operation.

Step 10: Gallons of foam required.
   It is assumed that enough foam will be placed in storage to meet both a main and a reserve requirement: 9 gpm $\times$ 15 min $\times$ 2 = 270 gal.

Step 11: Gallons of water required.
   The primary water supply must provide a rate of 283 gpm for 15 minutes or 4245 gal. A like amount must be supplied for the secondary demand.

Step 12: The problem considers that the water supply to the foam house is adequate to meet the calculated demand for the system.

Step 13: The foam system is arranged to be activated by the automatic sprinkler system when the drypipe valve trips due to a sprinkler head operating. The system can also be activated manually.

Hydraulic analysis for Example 3

Step 1: The inlet pressure requirement for the foam generator is 50 psi.

Step 2: The foam solution line supplying each foam generator and the riser pipe to the top of the fire wall are sized on the basis of a maximum flow velocity of 10 ft/s.

$$\text{Velocity} = \frac{0.4085 \times \text{gpm}}{d^2}$$

a. $10 \text{ fps} = \dfrac{0.4085 \times 146 \text{ gpm}}{d^2}$
b. $10d^2 = 59.64$
c. $d^2 = 5.96$
d. $d = 2.44$
e. Use a 3-in. pipe

   Since the same size pipe is used from the foam generator to ground level, the hydraulic analysis can go from reference point 1 to reference point 3. The elevation head to be considered is 22 ft.

Step 3: The flow and pressure demand at the base of each riser supplying a foam generator is the same, since the generator sizes are equal. It is necessary to calculate a flow constant at this location so the pressure points upstream can be correctly adjusted for higher pressure values developed by friction loss between supply points. The demand constant is calculated as follows:
   (reference point 3)
   $Q = K\sqrt{P}$
   146 gpm = K 68.6

Step 4: The ground-level cross-main connecting the foam generator risers is sized on the basis of a maximum flow velocity of 10 ft/s. The flow from two generators is used for the flow computations.

$$\text{Velocity} = \frac{0.4085 \times \text{gpm}}{d^2}$$

a. $V = \dfrac{0.4085 \times 292 \text{ gpm}}{d^2}$

b. $10d^2 = 119.282$

c. $d^2 = 11.928$

d. $d = 3.45$

e. Use a 4-in. pipe

Step 5: Determine the actual flow characteristics for the high-expansion foam generator at reference point 4.

Use the K value (constant) determined in Step 3 to calculate the actual supply to the second foam generator at reference point 4. The new pressure at the riser base is (reference point 6) 70.7 psi from the hydraulic calculation sheet. The higher pressure is used with the K value to determine the actual flow for the second high-expansion foam unit.

$$Q = K\sqrt{P}$$
$$Q = 17.6\sqrt{70.7}$$
$$Q = 148$$

The actual flow increases by 2 gpm for the second generator.

Step 6: Determine the flow and pressure requirements at the foam house. Determine the friction loss for the total flow back to the foam hose and add in 4 psi for the foam proportioner.

Step 7: System demand.

The final system demand is 294 gpm at 90.0 psi at the foam proportioner inlet to supply the two high-expansion foam generators. The water supply to the foam house must meet this demand.

The Advent of Class A Foams

Class A foams have been used extensively in wildland fire suppression. The success of Class A foam for the confinement, control, and extinguishment of natural cover fuel fires suggests that this type of foam may be effective for structural fire protection as foam solution in fire streams. Initial research has been conducted to quantify the fire fighting efficiency of Class A foams to improve the operating efficiency of these foams when compared to plain water fire streams. The National Fire Protection Research Foundation has published research findings on Class A foam effectiveness: one in December 1993[3] and one in November 1994.[4] A synopsis of the findings are presented below.

The National Fire Protection Research Foundation (NFPRF) sponsored a research program with Underwriters Laboratories, Inc. (UL), to investigate the effectiveness of Class A foams by means of three discharge devices: (1) a standard spray nozzle, (2) an air-aspirated spray nozzle, and (3) by injecting compressed air into the Class A foam solution. This research investigation has two objectives: (1) to develop test data related to the fire fighting effectiveness of Class A foam solutions as compared to water only and (2) to conduct laboratory analysis of the Class A foam concentrate used in the performance tests.

Briefly, the initial fire test plan included a Class 20A wood crib fire with foam solution concentrates selected at 0.1, 0.3, and 0.5 percent. Adjunct variables included nominal expansion ratios of 5 for a standard nozzle at 15 gpm, 7.5 for an air-aspirated nozzle at 15 gpm, and 7.5 for injecting compressed air into the Class A foam solution.

The wood crib fire tests were conducted at UL's test facility located in Northbrook, Illinois, and are reported in the December 1993 publication.

In summary, the initial set of fire tests provide support of the following conclusions by the Technical Advisory Committee (TAC):

- Handheld hoselines supplied with Class A foam solutions provide enhanced fire fighting performance when compared to handheld hose lines supplied with water only.
- The best foam quality, as measured by retention and exposure protection tests, was achieved with compressed air foam.
- Results of the wood crib fire tests indicated superior characteristics in terms of fire control time for Class A foams when compared to water application only.
- Fire tests conducted with the air-aspirated test nozzle had the longest reignition times, while tests conducted with the Compressed Air Foam had the lowest crib weight losses.
- Exposure protection test results demonstrated the ability of the Class A foam to lengthen the ignition time of a combustible surface when compared to cribs protected by the same rate and duration of water.
- Retention-of-weight tests demonstrated that wood cribs exposed to Class A foam retain more weight than cribs treated with water.

The testing program outline above was very controlled in a laboratory setting. Foam applications were not subjected to many real world variables that could include wind, weather conditions, fuel geometry, pre-burn times, and human factors in the foam application. Despite such conditions, the reported testing program clearly supports a number of advantages for using Class A foam on structural type fires.

The Phase II research project report of 1994 reviews the conduct of structural fire suppression tests. These tests were also conducted at UL's test facilities in Northbrook, Illinois. A test cell measuring 30 by 36 by 30 ft was used for the Class A foam comparative analysis tests. Two fuel package scenarios were used as follows:

- The Series I UL 1626 residential fuel package consisted of a wood crib and simulated furniture positioned in one corner of the enclosure.
- The Series II fuel package consisted of a corner upholstered sofa scenario.

Fire test monitoring of the enclosure included measurements of the Class A foam solution or water flow rate; room temperature gradients at distances of 2, 9, 18, 24, 33, 48, and 72 in. below the ceiling; rate of heat release; oxygen content; smoke density; and heat flux. In each test series, observations were made of fire knockdown and damage to the walls of the enclosure and the fuel package.

Upon ignition, the fuel package was allowed to burn until flashover was achieved in the enclosure. Five seconds after flashover, a water application or a Class A foam solution was applied to suppress the fire using either a direct or indirect application method. The direct application method consisted of discharging the agent directly onto the walls of the enclosure and the fuel package. In contrast, the indirect application method consisted of discharging the agent first onto the ceiling and walls and then onto the fuel package.

The 1994 Class A Foam Study Report divides the summary information according to the Series I and II testing programs. The Series I abbreviated findings are summarized as follows:

- Class A foam using a direct application method took less time and quantity of agent to lower heat release to 500 KW than plain water.
- Class A Compressed Air Foam (CAF) using the indirect application method was more effective in reducing heat release values down to 500 KW.

The Series II abbreviated findings are limited to the following selective observations:

- The test results using Class A foam solutions generally provided for a reduced amount of total heat release from the fire and less damage to the sofa.
- Class A Compressed Air Foam applied at 7 gpm using the direct application method demonstrated the shortest time period and the lowest quantity of agent required to reduce the rate of heat released to 500 KW.
- The direct application method provides for a reduced amount of total heat release and less damage to the sofa when compared to the same tests conducted using the indirect application method.

Both reports recommend additional research on the application of Class A Foams with special attention given to hardware devices that include handheld fixed nozzles, proportioning equipment, and foam-generating equipment.

Additional research has been conducted by the National Institute of Standards and Technology.[5] The effectiveness of Class A foams on Class A and Class B fire threats were characterized. Four representative Class A foams were chosen for evaluation. A series of Class B fire suppression tests were conducted in conformance with UL 162 *Standard for Foam Equipment and Liquid Concentrates*. These tests utilized a 4.6-m² (50-ft²) heptane pool fire and consisted of the suppression of the fire and then testing for reignition and burnback resistance. Agent was applied at 2.44 and 4.88 lpm/m² (0.06 and 0.12 gpm/ft²), which is one and one-half and three times the rate required by the standard for AFFF application. The higher flow rates were used because the agents could not extinguish the fire at the standard AFFF application rate. The four agents had fire knockdown (control) times similar to AFFF, but two of the agents did not completely extinguish the fire in all the tests. AFFF had a higher resistance to burnback and longer time to re-ignition than the other four agents.

Full-scale fire experiments were conducted with 92.9-m² (1000-ft²) gasoline pool fires. Agent application was made with a 454 lpm (120 gpm) hose stream (i.e., 4.88 lpm/m² [0.12 gpm/ft²]). Two application techniques were used with each of the four agents in the large-scale tests. One application was made with a self-aspirating tube nozzle, and one application was made with a non-aspirating adjustable fog nozzle. AFFF and water were used as benchmark agents for these tests. Plain water could not extinguish this fire. AFFF exhibited better fire control and extinguishment characteristics, and substantially better burnback resistance, than those of the Class A foams.

In tests conducted for the U.S. Air Force, the Naval Research Laboratory assessed a compressed air foam system for possible use for aircraft hangar scenarios involving JP-8 fuel.[6] The breadboard unit used AFFF as the fire extinguishing agent. It was found that a commercial off-the-shelf non-air-aspirating nozzle was as effective as the air-aspirating nozzle provided with the unit. Air injection for aeration of the AFFF stream before discharge from the nozzle was found to be unnecessary.

Nomenclature

C	Hazen-Williams coefficient (constant)
C_L	foam leakage correction factor
C_N	normal foam shrinkage factor
d	internal pipe diameter (in.)
FL	friction loss (psi/ft)
K	nozzle discharge coefficient (gpm/psi$^{1/2}$)
Q	flow (gpm)
R	total foam generator capacity (cfm)
R_s	total rate of foam breakdown [$S \times Q$] (cfm/gpm)
S	rate of foam breakdown by sprinklers per gpm of sprinkler discharge (cfm/gpm)
T	submergance time (min)
V	velocity (ft/s)
v	submergence volume (ft³)

References Cited

1. *National Fire Codes,* National Fire Protection Association, Quincy, MA.
2. "Flammable Liquid Storage Tank Protection," *National Foam Engineering Manual,* Section 6, National Foam, Lionville, PA (n. d.).
3. W.M. Carey, *National Class A Foam Research Project Technical Report,* National Fire Protection Research Foundation, Quincy, MA (December 1993).
4. W.M. Carey, *National Class A Foam Research Project Technical Report, Phase II,* National Fire Protection Research Foundation, Quincy, MA (December 1994).
5. D. Madrzykowski and D.W. Stroup, "Demonstration of Biodegradable, Environmentally Safe, Non-Toxic Fire Suppression Liquids," *NISTIR 6191,* National Institute of Standards and Technology Report, Gaithersburg, MD (1998).
6. S.A. Hill, J.L. Scheffey, F. Walker, and F.W. Williams, "Tests of Alternative Fire Protection Methods for USAF Hangars," *NRL/MR/6180-99-8337,* Naval Research Laboratory Report, Washington, DC (1999).

Appendix
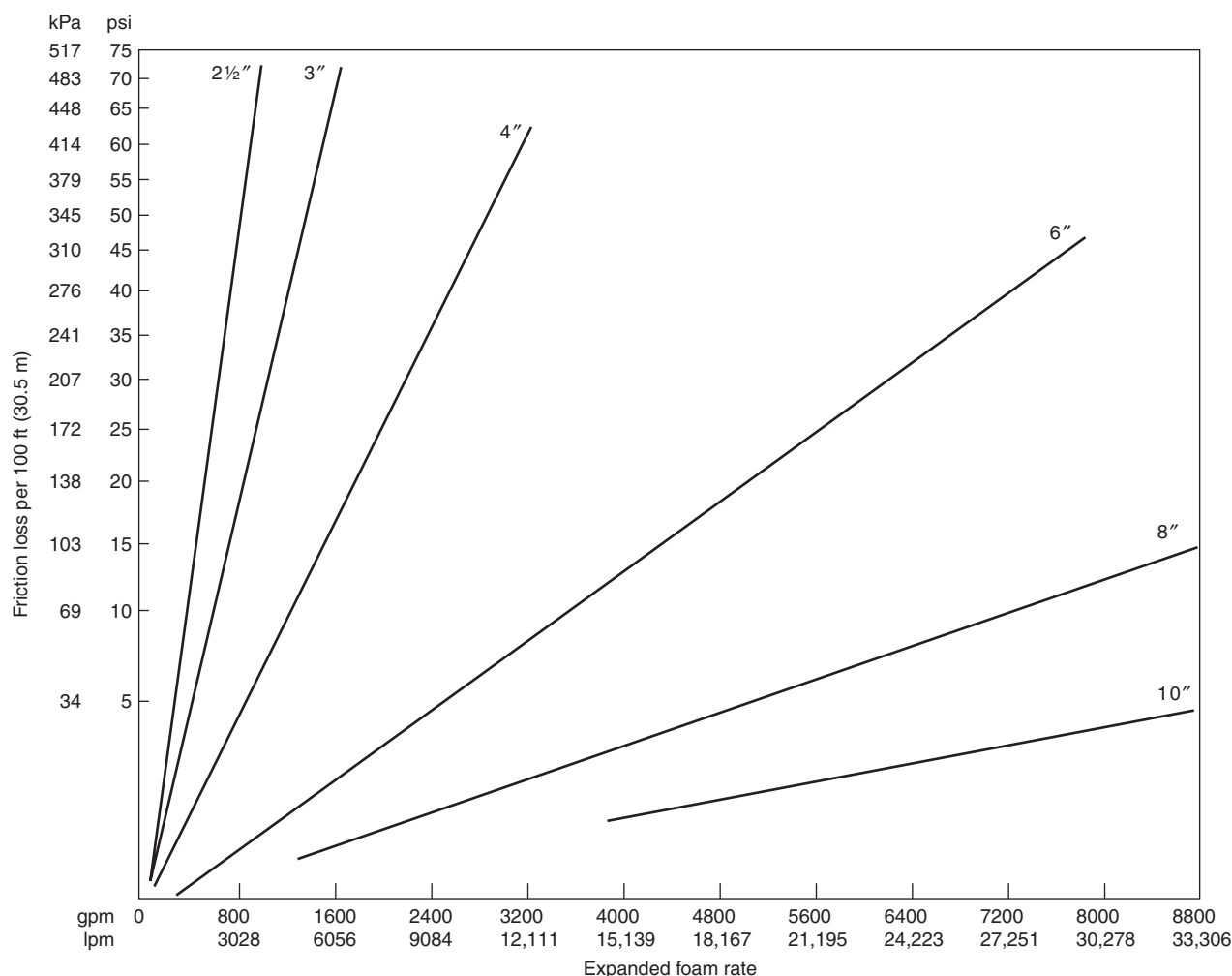
Figure 4-5A.1. *Foam friction losses—4:1 expansion (2½", 3", 4", 6", 8", and 10" pipe).*
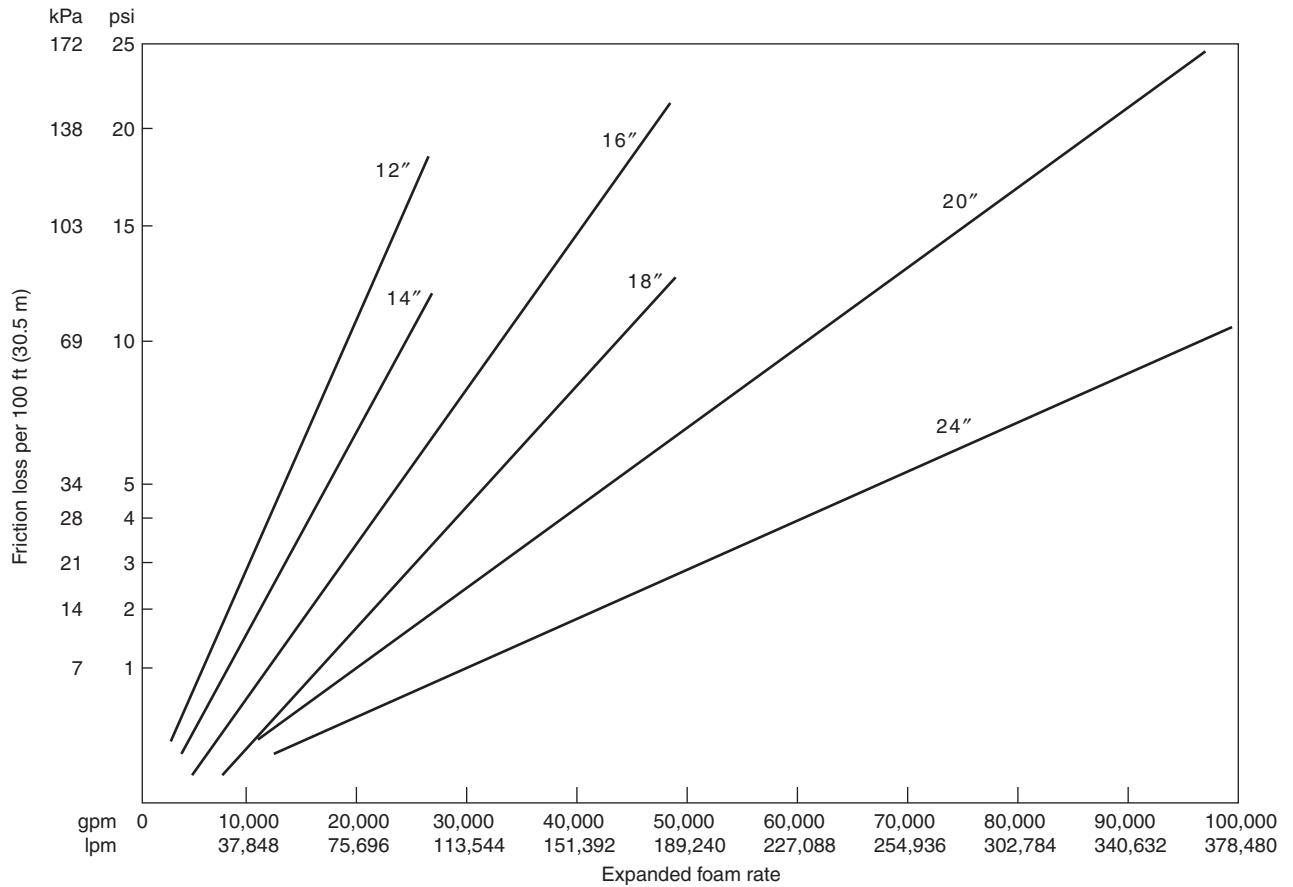
Figure 4-5A.2. *Foam friction losses—4:1 expansion (12", 14", 16", 18", 20", and 24" pipe).*
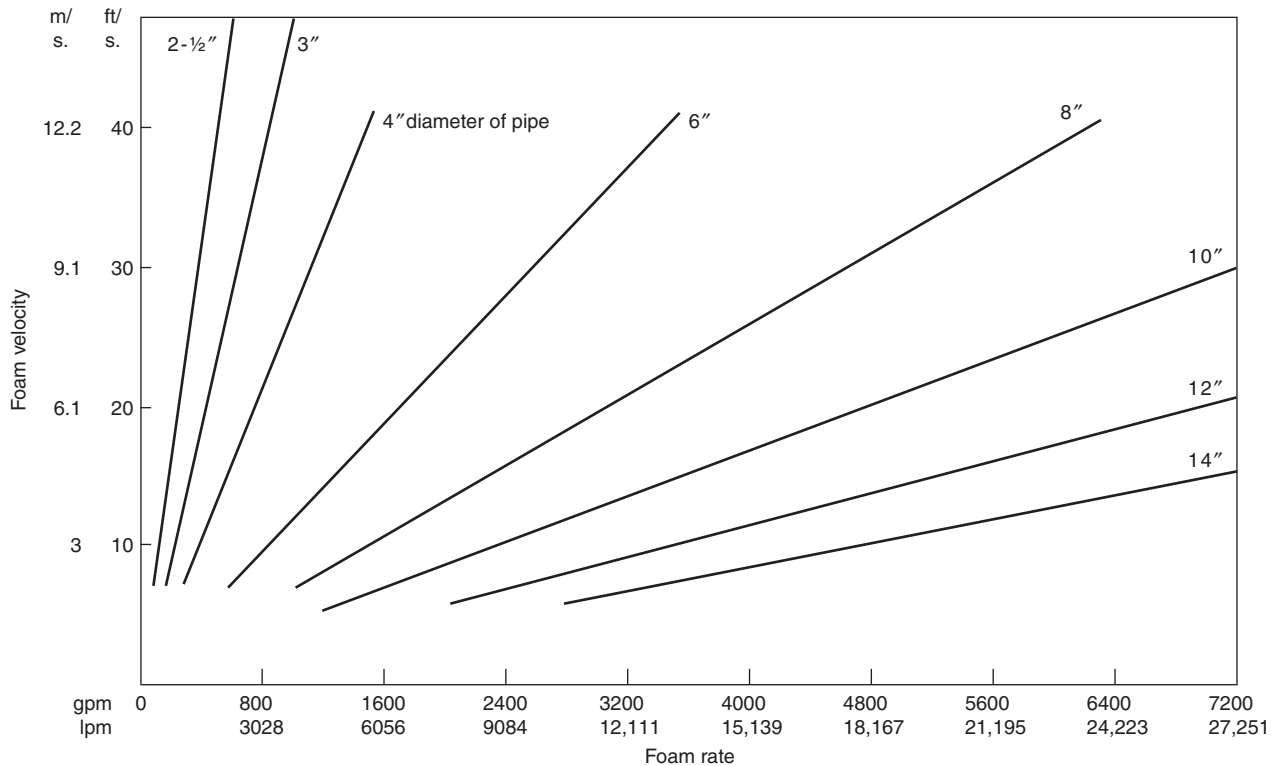

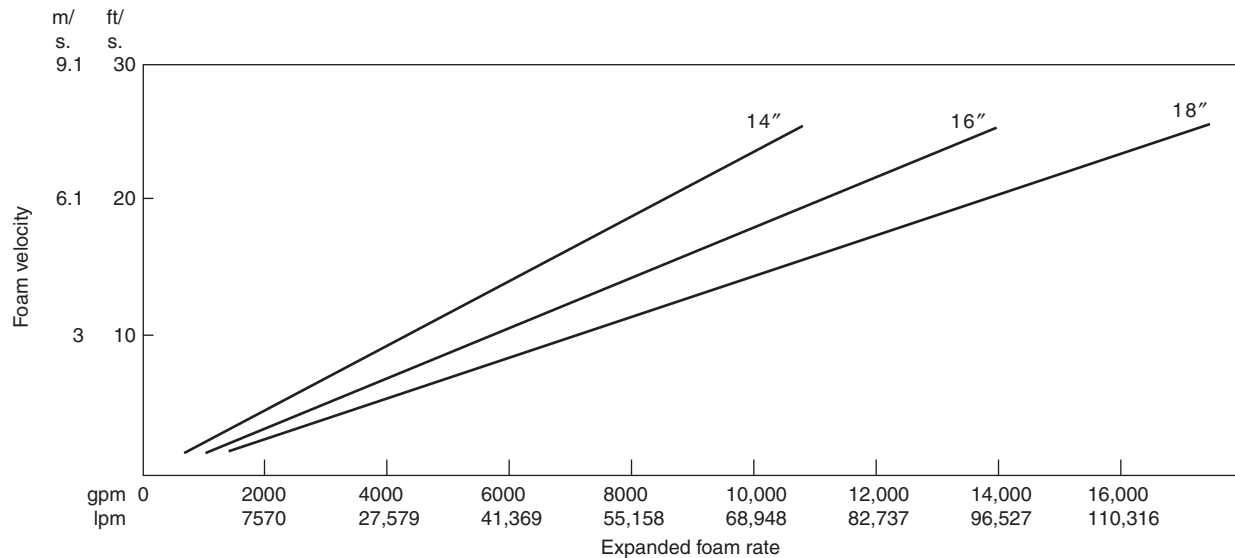**Figure 4-5A.3.** *Foam velocity versus pipe size (2½", 3", 4", 6", 8", 10", 12", and 14" pipe).*

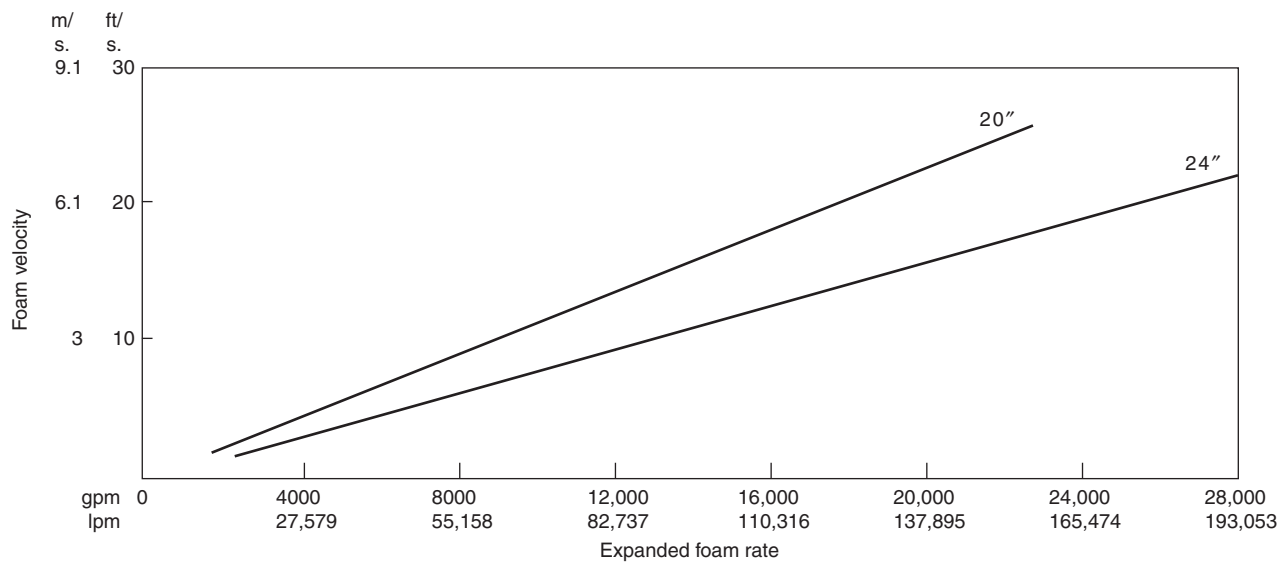**Figure 4-5A.4.** *Foam velocity versus pipe size—Schedule 40 pipe (14", 16", and 18" pipe).*

Figure 4-5A.5. *Foam velocity versus pipe size—Schedule 40 pipe (20" and 24" pipe).*

CHAPTER 6

Halon Design Calculations

Casey C. Grant

Introduction

Halogenated agent extinguishing systems are a relatively recent innovation in fire protection, but, despite this, they already face extinction. As of January 1, 1994, the global production of fire protection halons in many countries ceased.

The obvious question is, "Why maintain this chapter on halon design calculations?" Although global production of fire protection halons essentially ceased on January 1, 1994, it is expected that this technology will continue for an extended period of time to address the modification and maintenance of existing systems, and new essential systems that will use recycled surplus stock.

The stratospheric ozone layer depletion issue is a problem confronting the global community unlike any other. Late in 1987, the United States and 24 other countries (including the European Economic Community) signed the Montreal Protocol to protect stratospheric ozone.[1] Originally, the protocol restricted the consumption of ozone-depleting chlorofluorocarbons (CFCs) to 50 percent of the 1986 use levels by 1998, and halon production was to be frozen in 1993 at 1986 production levels. But the November, 1992, Copenhagen revision to the Montréal Protocol accelerated this, such that all production of the chemicals ceased worldwide as of January 1, 1994.

The Montreal Protocol is based on unprecedented trade restrictions and is the first time nations of the world have joined forces to address an environmental threat in advance of fully established effects. The trade restrictions concern nations not participating in the agreement (the nonsignatories). Within one year of the agreement taking effect, each party shall ban the import of the bulk chemicals from the nonsignatory nations. About four years after

the effective date of the agreement, imports of products containing the identified chemicals from nonsignatory nations would be banned. Within five years, products made with the chemicals (but not containing them) would be banned or restricted. This is truly significant since many products, including many electronic components, are currently manufactured using CFCs.

Today, high technology demands new and different fire protection techniques for which halon systems have proved ideal.

Characteristics of Halon

Background, Definition, and Classifications of Halon Compounds

Although there are a variety of methods available for applying halogenated agents, the most common is the total flooding system. The most popular halogenated agent is Halon 1301, with its superior fire extinguishing characteristics and low toxicity. Halogenated agent extinguishing systems are a promising tool for the fire protection engineer and have great potential for solving many of our fire protection problems now and in the future.

Halogenated extinguishing agents are hydrocarbons in which one or more hydrogen atoms have been replaced by atoms from the halogen series: fluorine, chlorine, bromine, or iodine. This substitution confers flame extinguishing properties to many of the resulting compounds that make them ideal for certain fire protection applications.

The halogenated extinguishing agents are currently known simply as halons, and are described by a nomenclature that indicates the chemical composition of the materials without the use of chemical names. This simplified system was proposed by James Malcolm at the U.S. Army Corps of Engineers Laboratory in 1950 and avoids the use of possibly confusing names.[2] The United Kingdom and parts of Europe still use the initial capital "alphabet" system, that is, bromotrifluoromethane (Halon 1301) is BTM

Casey C. Grant, P.E., is Secretary, NFPA Standards Council. He is a former member of the NFPA Technical Committee on Halogenated Fire Extinguishing Agent Systems and was previously supervisor of systems design engineering at Fenwal Incorporated.

and bromochlorodifluoromethane (Halon 1211) is BCF. The number definition for the chemical composition of Halon 1301, perhaps the most widely recognized halogenated extinguishing agent, is 1 (carbon), 3 (fluorine), 0 (chlorine), 1 (bromine), and 0 (iodine).

By definition, the first digit of the number represents the number of carbon atoms in the compound molecule; the second digit, the number of fluorine atoms; the third digit, the number of chlorine atoms; the fourth digit, the number of bromine atoms; and the fifth digit, if any, the number of iodine atoms. Trailing zeros in this system are not expressed. Figure 4-6.1 graphically demonstrates this concept by illustrating Halon 1301 in comparison to methane.

There are three halogen elements commonly found in halon extinguishing agents used for fire protection: fluorine (F), chlorine (Cl), and bromine (Br). Compounds containing combinations of fluorine, chlorine, and bromine can possess varying degrees of extinguishing effectiveness, chemical and thermal stability, toxicity, and volatility. In general, the relevant properties of these three halogen elements are characterized as shown in Table 4-6.1.

Due to the many chemical combinations available, the characteristics of halogenated fire extinguishing agents differ widely. It is generally agreed that the agents most widely used for fire protection applications are Halon 1301, Halon 1211, Halon 1011, and Halon 2402. Also somewhat common is Halon 122, which has been used as a test gas because of its economic advantages. However, because of its widespread use as a test agent, many individuals have wrongly assumed that Halon 122 is an effective fire extinguishing agent. Table 4-6.2 illus-

Table 4-6.2   *Halons Commonly Used for Fire Protection*

Chemical Name	Formula	Halon Number
Methyl bromide	CH_3Br	1001
Methyl iodide	CH_3I	10001
Bromochloromethane	CH_2BrCl	1011
Dibromodifluoromethane	CF_2Br_2	1202
Bromochlorodifluoromethane	CF_2BrCl	1211
Dichlorodifluoromethane[a]	CF_2Cl_2	122
Bromotrifluoromethane	CF_3Br	1301
Carbon tetrachloride	CCl_4	104
Dibromotetrafluoroethane	$C_2F_4Br_2$	2402

[a]A popular test gas without substantial fire extinguishing properties.

trates the halogenated hydrocarbons most likely to be used today.

History

The earliest halogenated fire extinguishing agent known to be used for industrialized fire protection was carbon tetrachloride (Halon 104).[3] First becoming available as early as 1907, it was most widely used in hand-pump portable extinguishers and was popular due to its low electrical conductivity and lack of residue following application. Also referred to as "pyrene" extinguisher fluid, Halon 104 caused a number of accidental deaths and serious injuries due to its toxicity, and eventually its use was halted during the 1950s.

Methyl bromide (Halon 1001) gained popularity after it was discovered in the late 1920s to be a more effective extinguishing agent than carbon tetrachloride. Due to its high toxicity, it was never used in portable extinguishers even though it was used extensively in British and German aircraft and ships during World War II. Interestingly, methyl bromide possesses a narrow "flammability" range between 13.5 and 14.5 percent in air, though above and below this range it is an efficient fire extinguishant. Germany developed bromochloromethane (Halon 1011) in the late 1930s to replace methyl bromide, but it failed to enjoy widespread use until after World War II.[4]

Thus, prior to World War II, three halogenated fire extinguishing agents were available: Halon 104, Halon 1001, and Halon 1011. Yet because of their inherently high toxic nature, these agents slowly disappeared from typical system applications. By the mid-1960s Halon 104 and Halon 1001 were no longer being used, and Halon 1011 was only in limited use for specialized explosion suppression applications. Figure 4-6.2 represents a chronology chart that indicates the usage of these early halons as well as the halons more commonly used today.

Joint research was undertaken in 1947 by the U.S. Army Chemical Center and the Purdue Research Foundation to evaluate the fire suppression effectiveness and toxicity of the large number of available agents.[2] After testing more than 60 new agents, 4 were selected for further study: dibromodifluoromethane (Halon 1202), bromochlorodifluoromethane (Halon 1211), bromotrifluoromethane (Halon 1301), and dibromotetrafluoromethane

Figure 4-6.1.   *Molecular composition of methane and Halon 1301.*

Table 4-6.1   *Contributing Characteristics of Fluorine, Chlorine, and Bromine*

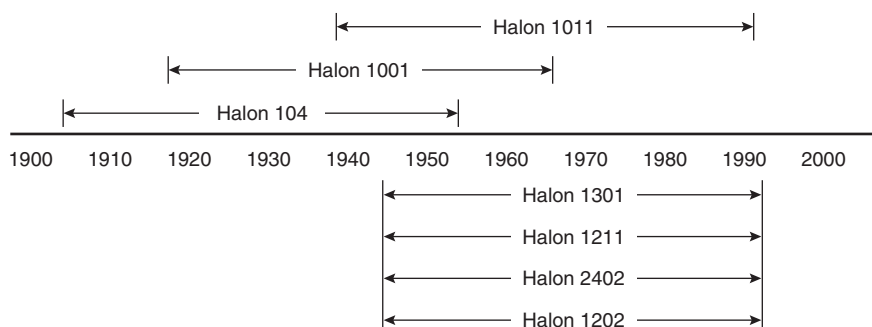|	Fluorine	Chlorine	Bromine
Stability to compound	Enhances	—	—
Toxicity	Reduces	Enhances	Enhances
Boiling point	Reduces	Enhances	Enhances
Thermal stability	Enhances	Reduces	Reduces
Fire extinguishing effectiveness	—	Enhances	Enhances

Figure 4-6.2. *Time span usage of selected halons.*

(Halon 2402). Further testing revealed that Halon 1202 was the most effective yet also most toxic, while Halon 1301 was the second most effective and least toxic. As a result of this testing, the use of halon to provide fire protection for modern technology took on new dimensions. Halon 1202 was used by the U.S. Air Force for military aircraft engine protection while the Federal Aviation Administration (FAA) selected Halon 1301 for a similar application in commercial aircraft engine nacelles.[5] Portable extinguishers using Halon 1301 were implemented by the U.S. Army. The use of total flooding systems originated in 1963, and in the following five years several total flooding systems were installed based on carbon dioxide system technology.

In 1966, attention began to focus on the use of Halon 1301 for the protection of electronic data processing equipment. That year, the NFPA organized a Technical Committee (NFPA 12A) to standardize the design, installation, maintenance, and use of halon systems. Their resulting work was officially adopted by the NFPA membership as a standard in 1968.[6] Subsequent recognition that there were differences among the halon agents made it apparent that separate standards would be necessary. The initial halon standard, NFPA 12A, *Standard for Halon 1301 Fire Extinguishing Systems* (hereinafter referred to as NFPA 12A), focused on the use of Halon 1301 due to its high desirability and growing popularity.[7] Work on an additional standard, NFPA 12B, *Standard on Halon 1211 Fire Extinguishing Systems,* concerning the use of Halon 1211, was started in 1969 and was officially adopted by the NFPA as a standard in 1972.[8] A tentative standard on the use of Halon 2402 (NFPA 12CT) was established, but has not been officially adopted.[9]

Another NFPA committee directly concerned with the use of halon is the NFPA Committee on Electronic Computer/Data Processing Equipment (NFPA 75, *Standard for the Protection of Electronic Computer/Data Processing Equipment).*[10] Even though this standard was adopted in 1961, the use of halon was not considered until after 1972, when extensive testing by several major companies demonstrated that the use of Halon 1301 was suitable for protecting electronic computer and data processing equipment.[11] Halon 1301 eventually became the most widely used extinguishing agent for this purpose in the United States and throughout much of the world. However, certain areas of Europe have preferred Halon 1211 and 2402.

In anticipation of the worldwide production phaseout of fire protection halons, which eventually settled at January 1, 1994, for developed countries, a new committee was established during 1992 within the NFPA standards-making system designated as the Technical Committee on Alternative Protection Options to Halon. The committee's first document is NFPA 2001, *Standard on Clean Agent Fire Extinguishing Systems,* which addresses the design, installation, maintenance, and operation of total-flooding fire extinguishing systems that use halon replacement agents.[12]

Halon 1301

Attributes and limitations: Of all the halogenated extinguishing agents used in fire protection today, Halon 1301 is by a wide margin the most commonly used. The primary use of this agent is for the protection of electrical and electronic equipment, flammable liquids and gases, and surface-burning flammable solids such as thermoplastics. Areas normally or frequently occupied, air and ground vehicle engines, and other areas where rapid extinguishment is important or where damage to equipment or materials or cleanup after use must be minimized are also ideally protected by this agent. However, Halon 1301 is not a panacea, and it is appropriate to recognize its limitations as well as its attributes. The benefits of Halon 1301 are: fast chemical suppression, penetrating vapor, clean (no residue), noncorrosive, compact storage volumes, nonconductive, and colorless (no obscuration). There are also limitations to using Halon 1301: it has minimal extinguishing effectiveness on reactive metals and rapid oxidizers, it may have unfavorable side effects on deep-seated Class A fires, the agent is expensive, and it is potentially harmful to the environment. Obviously, the most significant limitation is the detrimental effect that the halons have on the earth's stratospheric ozone layer.

Because Halon 1301 inhibits the chain reaction of the combustion process, it chemically suppresses the fire very quickly, unlike other extinguishing agents that work by removing the fire's heat or oxygen. Stored as a liquid under pressure and released at normal room temperature as a vapor, Halon 1301 gets into blocked and baffled spaces readily and leaves no corrosive or abrasive residue after use. A high liquid density permits compact storage containers, which on a comparative weight basis, makes Halon 1301

approximately 2.5 times more effective as an extinguishing agent than carbon dioxide. Since it is virtually free of electrical conductivity, Halon 1301 is highly suitable for electrical fires. Halon 1301 is a colorless vapor when discharged into a hazard volume, though it sometimes temporarily clouds the volume due to the chilling of any moisture in the air. But of all its attributes, the most promising is that of people compatibility, for unlike other extinguishing agents, Halon 1301 is essentially nontoxic in the concentrations usually required for fire suppression.

There are several types of flammable materials on which Halon 1301 is ineffective and not recommended. Reactive metals such as potassium, Nak eutectic alloy, magnesium, sodium, titanium, and zirconium burn so intensely that they overpower the agent's extinguishing abilities.[5] Included with these are the metal hydrides such as lithium hydride, and petroleum solvents such as butyl-lithium. Autothermal decomposers and fuels that contain their own oxidizing agent will also burn freely in the presence of halon agents. These latter substances, such as gunpowder, rocket propellants, and cellulose nitrate, have an oxidizer physically too close to the fuel, and the agent cannot penetrate the fire zone fast enough. Halon is also not effective in preventing the combustion or reaction of chemicals capable of autothermal decomposition such as hydrazine or organic peroxides. Even though Halon 1301 is effective with certain surface-burning flammable solids such as thermoplastics, deep-seated Class A fires typically require relatively high agent concentrations for long soaking periods. When exposed to deep-seated fires for long periods of time, Halon 1301 may decompose into toxic and corrosive products of decomposition. Therefore, it is important that the agent be dispersed while the fire is small. The expense necessary to purchase, install, and maintain a properly functioning Halon 1301 system for more specific Class A hazards is often not economically justified. Halon 1301 fire suppression systems are usually not associated with everyday commodities, but instead are found in applications pertaining to highly valued risks.

Properties

Physical properties: On the average, Halon 1301 requires 10 percent less agent on a gas-volume basis than does Halon 1211 to extinguish any given fuel.[2] However, both agents are approximately 2.5 times more effective on a weight-of-agent basis than carbon dioxide. Halon 1301 is a gas at 70°F (21°C) with a vapor pressure of 199 psig. Although this pressure would adequately expel the material, it decreases rapidly to 56 psig (4 bar) at 0°F (–18°C) and to 17.2 psig (1.2 bar) at −40°F (−40°C). Therefore, it is necessary to increase the container pressure with dry nitrogen either to 360 or 600 psig (25 or 41 bar) at 70°F (21°C), ensuring adequate performance at all temperatures. Figure 4-6.3 demonstrates the temperature-pressure profile for Halon 1301 and Halon 1301 superpressurized with dry nitrogen.

Halon 1301 is normally stored in a pressure vessel as a liquid before it is released to occupy the hazard volume as a vapor. With a boiling point of −72°F (−58°C), it is ap-
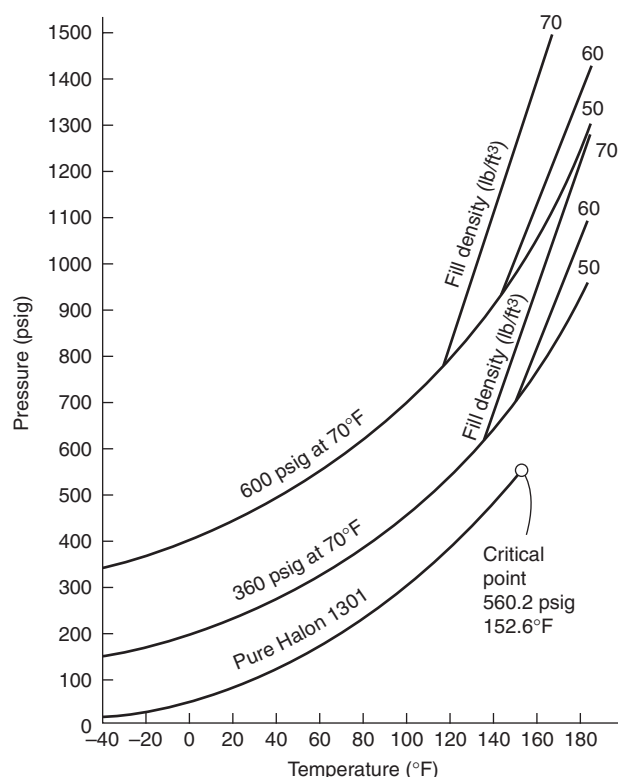
Figure 4-6.3. *Temperature-pressure relationship for pure Halon.*

proximately 1.5 times more dense than water in its liquid phase and approximately 5 times heavier than air in its vapor phase. Thus, Halon 1301 vapor will typically escape through openings in the low portions of a totally flooded volume. Other physical properties are shown in Table 4-6.3.

Traditionally, there were three distinct elements assumed for combustion: heat, fuel, and oxygen. Known as the fire triangle, this theory had to be modified as halons became more widely used and better understood. Typical fire extinguishment involves either removing the fuel from the fire, limiting oxygen to the fire (smothering), or removing the heat (quenching). The halons do not extinguish fire in any of these ways, but instead break up the uninhibited chain reaction of the combustion process. The tetrahedron of the fire, as it is now called, is shown in Figure 4-6.4.

Table 4-6.3 *Selected Physical Properties of Halon 1301*

Boiling point	−72.0°F
Freezing point	−270.4°F
Specific gravity of liquid (@70°F)	1.57
Specific gravity of vapor (@70°F)	5.14
Liquid density @70°F	98.0 lb/ft³
Vapor density @70°F	7.49 lb/ft³ (standard)
Critical temperature	152.6°F
Critical pressure	575 PSIA
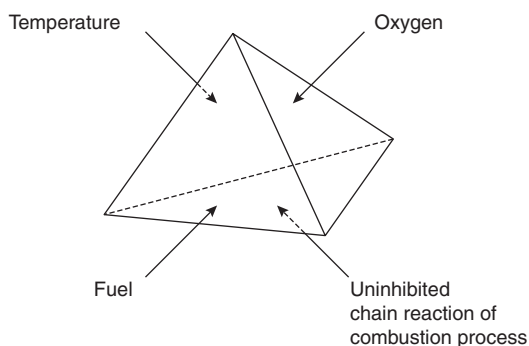
Figure 4-6.4. *The tetrahedron of fire.*

The extinguishing mechanism of the halogenated agents is not completely understood, yet there is definitely a chemical reaction that interferes with the combustion process. The halogen atoms act by removing the active chemical species involved in the flame chain reaction. While all the halogens are active in this way, bromine is much more effective than chlorine or fluorine. With Halon 1301 (54 percent by weight bromine), it is the bromine radical that acts as the inhibitor in extinguishing the fire. Yet the fluorine in the molecule also serves a specific task since it is the fluorine that gives the agent thermal stability and keeps Halon 1301 from decomposing until approximately 900°F (480°C).[13]

Extinguishing effectiveness: As shown in Figure 4-6.5, the four types of fire are ordinary combustibles (Class A), flammable liquids and gases (Class B), electrical (Class C), and reactive metals (Class D).[5]

It was previously mentioned that Halon 1301 is ineffective on Class D fires and is not as desirable as other agents in extinguishing deep-seated Class A fires. The effectiveness of Halon 1301 on Class A fires is not as predictable as with other classes of fire. It depends to a large extent upon the burning material, its configuration, and how early in the combustion cycle the agent is applied. Most plastics behave as flammable liquids and can be extinguished rapidly and completely with 4 to 6 percent concentrations of Halon 1301.[7]

Other materials, particularly cellulosic products, can in certain forms develop deep-seated fires in addition to flaming combustion. The flaming portion of such fires can be extinguished with low 4 to 6 percent Halon 1301 concentrations, but the glowing deep-seated portion of the fire may continue under some circumstances. Even so, the

deep-seated fire can be controlled since its rate of burning and consequent heat release will be reduced. Considerably higher concentrations (18 to 30 percent) of Halon 1301 are required to achieve complete extinguishment, but these levels are seldom economical to apply and their application may result in unwanted products of decomposition. However, the concept of controlling deep-seated fires with halogenated agents has been accepted in the respective NFPA standards.[7]

It is Class B and Class C fires for which halon is particularly well suited. The most common applications involve Class C electrical hazards, with the increase in popularity of Halon 1301 keeping well in stride with the development of high technology. Typically, electrical and electronic equipment are protected with a concentration of 5 percent Halon 1301 by volume, though a significantly lower concentration will suitably extinguish a potential fire.[14] The concentrations necessary to extinguish Class B fires have been the subject of much testing with results that vary widely. The effectiveness of halogenated agents on flammable liquid and vapor fires is quite dramatic, especially in total flooding systems. Rapid and complete extinguishment is obtainable with low concentrations of the agent.[7] To be effective, the fire must be contained (such as inside a building) so that the agent can react with it; Halon 1301 applied to large exterior running pool fires dissipates into the atmosphere without penetrating the flame zone.

Corrosive effects of undecomposed halons: Unlike Halon 1301 and Halon 1211, the early nonfluorinated halogenated agents had significant corrosive problems. Laboratory tests by DuPont in a 44-month exposure period with aluminum, magnesium, steel, stainless steel, titanium, and brass exposed to undecomposed Halon 1301 support the fact that this agent will not corrode these metals, which may all commonly be used in fixed fire extinguishing systems.[13] This is not surprising from a chemical standpoint because the presence of the fluorine atom in a molecule generally reduces its chemical reactivity and corrosive properties and increases its stability.

The presence of free water in systems containing Halon 1301 should be avoided. Free water is defined as the presence of a separate water phase in the liquid halon. When present in a small quantity, free water can provide a site for concentrating acid impurities into a corrosive liquid.[15] Free water should not be confused with dissolved water, which is not a problem in a Halon 1301 system.

Halon 1301 is inert toward most elastometers and plastics. In general, rigid plastics that are normally unaffected include polytetrafluorethylene, nylon, and acetal copolymers. Most of the commonly used plastics undergo little, if any, swelling in the presence of Halon 1301, with the exception of ethyl cellulose and possibly cellulose acetate/butyrate. Elastomers are particularly suitable when exposed to Halon 1301 for extended periods of time with the notable exception of silicone rubber.[13] Halons decomposed at high temperatures during suppression produce halogen acids and free halons that can be corrosive.
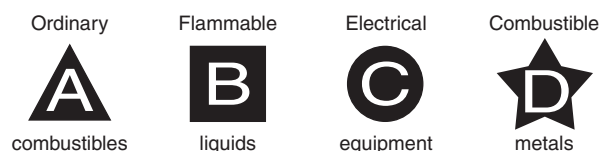

Figure 4-6.5. *The four classes of fire.*

Toxicity

General toxic properties: The relative safety of Halon 1301 has been established through more than 30 years of medical research involving both humans and test animals. No significant adverse health effects have been reported from the proper use of Halon 1301 as a fire extinguishant since its original introduction into the marketplace.[7]

Early studies by the U.S. Army Chemical Center on Halon 1301 determined the approximate lethal concentration for a 15-minute exposure to be 83 percent by volume.[2] Animals exposed to concentrations below lethal levels exhibit two distinct types of toxic effects. Concentrations greater than 10 percent by volume produce cardiovascular effects such as decreased heart rate, hypotension, and occasional cardiac arrythmias.[16] Concentrations of Halon 1301 greater than 30 percent by volume result in central nervous system changes including convulsions, tremors, lethargy, and unconsciousness. Effects are considered transitory and disappear after exposure.[17]

Human exposure to concentrations of Halon 1301 greater than 10 percent by volume have shown indications of pronounced dizziness and a reduction in physical and mental dexterity.[18] With concentrations between 7 and 10 percent by volume, subjects experienced tingling of the extremities and dizziness, indicating mild anesthesia. Exposure to Halon 1301 concentrations less than 7 percent by volume have little effect, with the exception of a deepening in the tone of voice caused by a higher density in the medium between the vocal chords. The effects at all levels of concentration disappear quickly after removal from the exposure. Testing of Halon 1301 for potential teratogenic (i.e., altering the normal process of fetal development) and mutagenic (a carcinogen in humans) effects have indicated that no serious problems exist.[5]

Most fire protection applications today have a design concentration of 5 percent by volume, thus the question of toxicity is not usually a serious concern. Exposure limitations for Halon 1301 (indicated by NFPA 12A) are summarized in Table 4-6.4.[7]

In addition to possible toxic effects, liquid Halon 1301 (including the spray in the immediate proximity of a discharge) may freeze the skin on contact and cause frostbite. However, direct contact is necessary for this to occur and is unlikely, since with engineered Halon 1301 fire extin-guishing systems the discharge nozzles are typically distant from all occupants.

Products of decomposition: Consideration of the life safety of Halon 1301 must also include the effects of breakdown products which have a relatively higher toxicity than the agent itself. Upon exposure to flames or hot surfaces above approximately 900°F (480°C), Halon 1301 decomposes to form primarily hydrogen bromide (HBr) and hydrogen fluoride (HF).[19] Trace quantities of bromine (Br_2), carbonyl fluoride (COF_2), and carbonyl bromide ($COBr_2$) have been observed, but the quantities are generally too small to be of concern. Although small amounts of carbonyl halides (COF_2 and $COBr_2$) were reported in early tests, more recent studies have failed to confirm the presence of these compounds. Table 4-6.5 summarizes the predominant products of decomposition for Halon 1301.[20]

The primary toxic effect of the decomposition products is irritation. Even in concentrations of only a few parts per million, the decomposition products have characteristically sharp, acrid odors. This characteristic provides a built-in warning system since the irritation becomes severe well in advance of truly hazardous levels. In addition, the odor also serves as a warning that carbon monoxide and other potentially toxic products of combustion may be present. Prompt detection and rapid extinguishment of a fire will produce the safest post-extinguishment atmosphere.

Other Halons

Physical properties: The predominant halogenated agent in existence today for total flooding fire extinguishing systems is Halon 1301, though some areas of Europe have utilized Halon 1211 for this purpose. One reason for this use of Halon 1301 (besides toxicity) is the ability of the agent to vaporize and penetrate all portions of the hazard volume. Table 4-6.6 shows that Halon 1301 has the lowest boiling point and Halon 1211 has the second lowest.

With the discharge of a halon system at ambient temperature, Halon 1301 flashes to a vapor almost instantaneously, while Halon 1211 tends to pool momentarily. Agents with boiling points exceeding the temperature of the hazard volume will stay liquid until heated by the fire itself. These high boiling point halogenated agents have two distinct attributes: they can be projected in a liquid stream and they have a quenching effect in addition to

Table 4-6.4   *Permitted Exposure Time for Halon 1301*

Concentration (percent by volume)	Permitted Time of Exposure
Normally occupied areas	
0–7%	15 min
7–10%	1 min
Above 10%	Not permitted
Normally unoccupied areas	
0–7%	15 min
7–10%	1 min
10–15%	30 s
Above 15%	Prevent exposure

Table 4-6.5   *Predominant Halon 1301 Decomposition Products*

Compound	Formula	ALC[a] for 15-min Exposure ppm by Volume in Air
Hydrogen fluoride	HF	2500
Hydrogen bromide	HBr	4750
Bromine	Br_2	550
Carbonyl fluoride	COF_2	1500
Carbonyl bromine	$COBr_2$	—

[a]Approximate lethal concentration

Table 4-6.6 *Selected Physical Properties of Typical Halogenated Fire Extinguishing Agents*

Halon Number	Type of Agent	Approximate Boiling Point (°F)	Approximate Freezing Point (°F)	Specific Gravity of Liquid (@70°F)
104	Liquid	170	–8	1.59
1001	Liquid	40	–135	1.73
1011	Liquid	151	–124	1.93
1202	Liquid	76	–223	2.28
1211	Liquefied gas	25	–257	1.83
1301	Liquefied gas	–72	–270	1.57
2402	Liquid	117	–167	2.17

breaking the uninhibited chain reaction. Thus, portable extinguishers generally use Halon 1301 as a propellant for other halon agents.

Toxicity

One of the primary reasons that Halon 1301 is the most preferred of the halogenated agents is its relatively low toxicity, as discussed earlier. Table 4-6.7 compares the approximate lethal concentration of both the natural and decomposed vapors for a variety of fire extinguishing agents. Included with this list of halon agents is carbon dioxide for sake of comparison. As a natural vapor, Halon 1301 is the least toxic halogenated agent. Carbon dioxide may appear to compare favorably with Halon 1301, yet high concentrations of carbon dioxide are necessary for fire extinguishment, which also makes the hazard volume lethal to human occupants.

Halon in the Fire Protection Spectrum

Halogenated agent extinguishing systems are only one segment of the total fire protection spectrum. Good engineering judgment is necessary when trying to determine the applicability of halon and whether it should be used instead of, or in addition to, other fire protection measures. It must be clearly understood that halogenated agent extinguishing systems are not the panacea for all fire hazards, yet they do offer a safe method to extinguish

Table 4-6.7 *Approximate Lethal Concentrations (ppm) for 15-min Exposure to Vapors of Various Fire Extinguishing Agents*

Formula	Halon Number	Natural Vapor	Decomposed Vapor
CCl_4	104	28,000	300
CH_3Br	1001	5,900	9,600
CH_2ClBr	1011	65,000	4,000
CF_2Br_2	1202	54,000	1,850
CF_2ClBr	1211	324,000	7,650
CF_3Br	1301	832,000	14,000
$C_2F_4Br_2$	2402	126,000	1,600
CO_2	—	658,000	658,000

Table 4-6.8 *Necessary Control Measures for Computer Room Fire Stage Sequence*

Fire Stage	Control	Serious Danger Concern
1. Pre-ignition	Good housekeeping practices, control combustible furnishings and interior finish	
2. Initial pyrolysis	Smoke detection system	Occupants and business interruption
3. Incipient	Portable fire extinguishers, Halon 1301 automatic suppression system	Occupants and contents
4. Pre-flashover	Automatic sprinklers	Occupants and structure
5. Post-flashover	Fire walls, compartmentalization	Surrounding structures

certain fires in their very early stages. Thus, these systems are commonly applied to situations where even the smallest fire is absolutely unthinkable.

As an example, total computer room fire protection might involve several different control measures addressing different possible fire conditions. Table 4-6.8 illustrates this concept, based on the different stages of a growing fire. The table is not a rigid description of the fire protection requirements of every computer room, but instead an example of how total fire protection is the overall objective when approaching a design situation.

An important factor of developing halogenated agent extinguishing systems is the interaction of all concerned individuals. To design, install, maintain, and operate a halon system requires a cooperative effort from a number of different groups. As shown in Figure 4-6.6, these individuals include the end users, consultants, manufacturers, installers, insurance representatives, and other selected authorities. Representatives from all these groups work together to develop and enhance model codes, which provide guidance and understanding for proper halon system usage.

System Configurations

Detection

The three primary parts of every halogenated agent extinguishing system are detection, control panel, and agent delivery. Since there is no single type of detector that offers the ultimate for every application, consideration must be given to the types of combustibles and combustion that are likely to occur in the protected area.

Photoelectric and ionization smoke detectors have different response characteristics to fires and can be susceptible to false or unwanted alarms. Thermal detectors, although more reliable, react more slowly to fire conditions. In certain applications, speed is critical and optical detectors would be required.

Figure 4-6.6. *Typical inter-relationship of halon fire protection interests.*

To optimize the speed and reliability of detection systems, it is important to use two different types of detectors on two separate detection loops within the hazard area. This method is referred to as cross-zone detection. Each detection loop functions independently to provide both added reliability with a comforting degree of redundancy.[21]

Control Panels

Features: As its name implies, the control panel is the device that controls system operation and allows the system to function as designed. When a control panel protects more than one area, each individual area is referred to as a zone of protection. Each zone of every halon control panel has three different types of circuits: initiating, signaling, and release. A fire alarm zone and halon zone are compared in Table 4-6.9 to illustrate the differences between these circuit types. It is unusual for a single halon control panel to protect more than five zones at once due to the high number of circuits required. Fire alarm control panels, on the other hand, may have dozens of individual zones.

Initiating circuits provide the input into the panel and support automatic detectors, manual pull stations, and other initiating devices. Automatic detectors are normally cross-zoned, which implies two separate detection circuits. One circuit is required for prealarm and both circuits are necessary for halon release. The signaling circuits, sometimes referred to as bell or auxiliary circuits, are used for audible/visual alarms and other auxiliary functions. The release circuits allow the halon to release from the containers and are sometimes referred to as firing, solenoid, initiator, dump, or halon circuits.

Modes of operation: At any time, a halon control panel and the halon system could be in one of four modes of operation; as shown in Table 4-6.10 these include unpowered, normal, alarm, and trouble condition. The alarm condition is further definable with prealarm, prerelease, release, and postrelease condition. Typical systems utilizing cross-zoning detection activate, when required, into prealarm and/or release condition, but this often becomes more complicated with time delays, abort switches, and other auxiliary functions. Unless otherwise specified, manual pull stations activate all alarm conditions, override abort switches, if present, and immediately release the halon. These different alarm conditions provide a convenient mechanism for sequential operation

Table 4-6.9 *Typical Control Unit Features*

	Halon Zone	Fire Alarm Zone
Initiating circuit	Two cross zone detection circuits	One circuit for detection
Signaling circuit	Multiple signaling sequence	Multiple signaling sequence
Release circuit	One circuit	None

Table 4-6.10 *Modes of Control Panel Operation*

Unpowered condition	Off
Normal condition	On
Alarm condition:	
Prealarm	One detector activates.
Prerelease	Two cross-zoned detectors activate. Time delay starts.
Release	Time delay ends or manual pull station activates. Halon is released.
Postrelease	Halon has been released.
Trouble condition	Failure or disruption of field wiring. Insufficient power input.

of audible/visual signaling, equipment shutdown, fire service notification, and other auxiliary functions.

Control panel economics: As halogenated agent extinguishing systems become more numerous, the frequency of large-scale projects with multiple halon zones in a single facility is increasing. Today, entire data processing centers and telecommunications buildings are protected with Halon 1301 systems. To protect a large building with many halon zones, it may appear that the most effective way of configuring the system is by using a single large control panel with the capacity for all required halon zones. This is not true, since there is a limitation to the number of halon zones that any one halon panel can effectively manage. Figure 4-6.7 illustrates an alternative method, where the individual halon zones of a large building each have their own halon panel wired to give an alarm or trouble signal to a central fire alarm panel.

A typical halon zone requires an average of 12 wires to support all the necessary system functions. Thus, the cost of running multiple wires and large conduit instead of only two wires (for interpanel communication) often

offsets the cost of smaller, more numerous panels located near the halon zones. This configuration offers flexibility for future consolidations or additions, which are common for high technology facilities. Aesthetics are enhanced at the master control location, and system operation is simplified. Installation checkout and servicing is easier when the halon control panel is within the hazard area. Finally, the overall system is more reliable due to less wiring, lack of design complexity, simplified maintenance, and multisource dependence.

Agent Delivery

In addition to the control panel and detection, the other primary part of every halogenated agent extinguishing system is agent delivery. The agent delivery includes the discharge nozzles, agent storage container(s), release mechanism, and associated piping. As shown in Table 4-6.11, three methods of agent delivery exist: (1) central storage, (2) modular, and (3) shared supply. Central storage has the container(s) centrally located, with the agent piped accordingly. This method is popular due to its similarity with carbon dioxide system technology (which helped develop early systems), along with usually having the lowest initial cost. Modular systems use smaller containers strategically located throughout the hazard area, with minimal piping. The high reliability of modular systems is based on lack of dependancy on piping integrity, negligible piping calculations, total system supervision, multisource dependence, and the inherent ability to be heat actuated regardless of catastrophic system failure. Modular systems are simple to design, are relatively easy to install, and have a high degree of future flexibility. Systems utilizing shared supply are essentially central storage systems with container(s) shared by more than one hazard volume. Even though fewer containers are used, directional valves and extensive piping do not often allow shared supply systems to be cost effective.
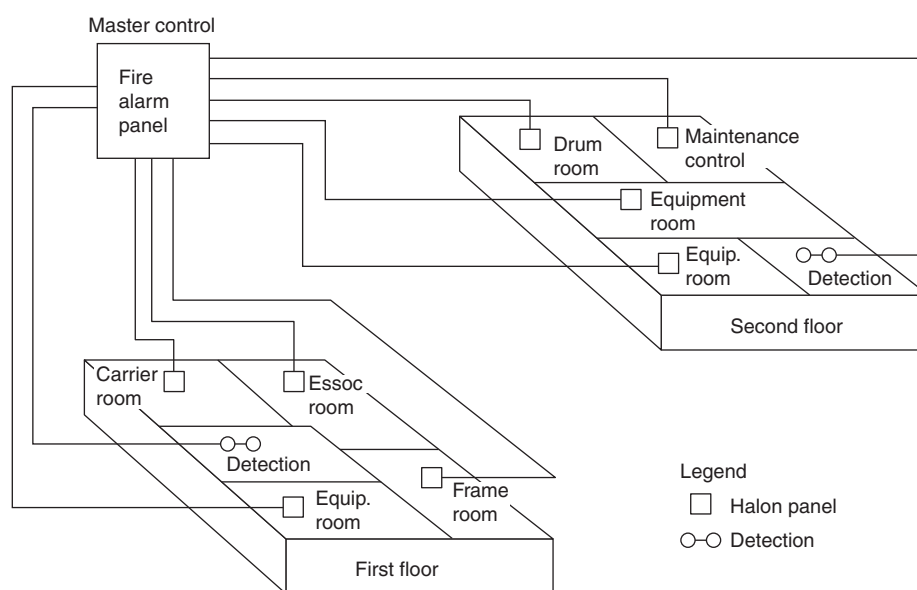

Figure 4-6.7. *The network concept of control panel interface for a typical halon application.*

Table 4-6.11 *Comparison of Different Methods of Agent Delivery*

	Central Storage	Modular	Shared Supply
Hardware cost	Moderate	High	Moderate
Installation cost	Moderate	Low	Moderate
Design simplicity	Difficult	Simple	Difficult
Installation simplicity	Difficult	Medium	Difficult
Operation and maintenance simplicity	Medium	Medium	Medium
Reliability	Moderate	High	Low
Future flexibility	Low	High	Low

Halon System
• 1 Control Unit
• 1–5 Zones
• ~12 Wires per Zone

Fire Alarm System
• 1 Control Unit
• 1–100 Zones
• ~4 Wires per Zone

Halon Zone
• Volume of Halon Zone Coverage
• Release Circuit Equals Halon Zone

Fire Alarm Zone
• Area of Detection Zone Coverage
• Detection Circuit Equals Fire Alarm Zone

Figure 4-6.8. *Halon/fire alarm differences.*

Adding to its unpopularity are its design and installation complexity, low reliability, and impaired future flexibility. When a shared supply halon system activates for one hazard, the remaining hazards become unprotected until the system is completely recharged.

Design Concepts and Methodology

Definitions and Terminology

Halogenated agent extinguishing systems are typically classified as either total flooding or local application systems. A total flooding system is designed to develop and maintain a concentration of halon that will extinguish fires in combustible materials located in an enclosed space. Local application systems are designed to apply the agent directly to a fire that may occur in an area or space that is not immediately enclosed. In addition to these, there are specialized applications, which may include combination total flooding/local application or partial flooding. The vast majority of installed halon systems today are the total flooding type using Halon 1301.

The definitions of halon system and halon zone are often confusing. This is especially true to individuals closely associated with the fire alarm industry, since fire alarm terminology is similar. Figure 4-6.8 defines the basic features of a halon system and halon zone and offers a comparison with each respective fire alarm counterpart.

A halon zone usually equates to an area of halon coverage functioning on a single release circuit, while the zones in a fire alarm system typically are each detection circuit. As an example, one halon zone could be a single computer room, whereas a fire alarm zone could be the entire floor of a building. A halon system also has much fewer (though more comprehensive) zones than a fire alarm system.

Halon Design Guidelines

The design process necessary for total flooding systems is easily quantified. The procedure can be separated into five definable steps: (1) hazard identification, (2) determination of agent quantity, (3) specification of operating requirements, (4) determination of hardware requirements, and (5) generation of postdesign information.

The initial step is to provide a definition of the hazard. This includes determining the fuels involved, the di-

mensions and configuration of the enclosure, the maximum and minimum net volumes, the status of occupancy, the expected hazard area temperature range, and possible unclosable openings. Based on this information, the minimum design concentration can be established. Next, the agent quantity is determined based upon the design concentration, the volume, minimum expected temperature, leakage due to ventilation or unclosable openings, and altitude above sea level. Usually, the gross volume is used to calculate the agent quantity to allow for extra agent to replace that lost through normal building leakage. However, agent concentrations must conform with the applicable toxicity criteria with respect to the minimum net volume and maximum temperature. The operating specifications are then required if they have not already been established. These will indicate how the system is to operate, the modes of operation, the type of agent delivery, and so forth. When these are known, the necessary hardware requirements must be obtained and the design of the system completed. The final step is to generate the postdesign information necessary for others to install, test, operate, and maintain the system. Postdesign information should contain all design calculations (including hydraulic calculations), complete blueprint drawings, and detailed information describing the testing, operation, and maintenance of the system.

Local Application and Special Systems

Local application systems are often installed to extinguish fires involving flammable liquids, gases, and surface burning solids. Such systems are designed to apply the agent directly to a fire that may occur in an area or space not immediately enclosed. They must be designed to deliver halon agent to the hazard being protected in such a manner that the agent will cover all burning surfaces during discharge of the system. Because of its lower volatility, Halon 1211 may be better suited than other forms of halon for local application systems. The lower volatility, plus a high liquid density, permits the agent to be sprayed as a liquid and thus propelled into the fire zone to a greater extent than is possible with other vaporized agents. Examples of areas protected by local application are spray booths, dip and quench tanks, oil-filled electric transformers, printing presses, heavy construction equipment, and vapor vents. An example of a local application system is shown in Figure 4-6.9.
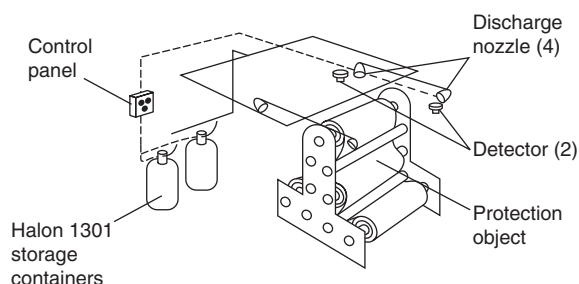
Figure 4-6.9. *Local application system.*

Currently, NFPA standards do not set a minimum limit on the discharge time for a local application design. The rate of discharge and the amount of agent required for a given application must be determined by experimentation and evaluation. The most critical components of these systems are the discharge nozzles; the discharge velocity and rate must be sufficient to penetrate the flames and produce extinguishment but not be so great as to cause splashing or spreading of fuel and thus increase the fire hazard. The minimum design discharge quantity should not be less than 1.5 times the minimum quantity required for extinguishment at any selected design rate.[20] Also of critical importance are type and location of detectors.

As with other types of gaseous suppression systems, local application systems can be designed according to the rate-by-volume method or the rate-by-area method. The rate-by-area method determines nozzle discharge rates based on the exposed surface area of the hazard being protected. This method is less popular than the rate-by-volume method, which requires discharge rates sufficient to fill (within the discharge time) a volume whose imaginary boundaries extend a limited distance from the protected hazard. This method is favored since it performs similarly to total flooding systems. Important factors to be considered in the design of a local application system are the rate of agent flow, the distance and area limitations of the nozzles, the quantity of agent required, the agent distribution system, and the placement of detectors.

Unlike total flooding systems, only the liquid portion of the discharge is effective for local application systems. The computed quantity of agent needed for local application must be increased to compensate for the residual vapor in the storage container at the end of liquid flow. An additional 25 percent storage capacity is required in the absence of an enclosure that would prevent gas dissipation. Systems should also compensate for any agent vaporized in the pipe lines due to heat absorption from the piping. The heat transfer is important when the piping is at a higher temperature than the agent. The following equation determines the amount of agent increase necessary to compensate for this effect:[7]

$$W_x = \frac{2\pi k L (T_p - T_a)(t)}{3600 h (\ln r_o/r_i)} \qquad (1)$$

where

W_x = amount of agent increase, kg (lb)

k = themal conductivity of the piping, W/m·K (Btu·t/hr·ft²·°F)

L = linear length of the piping, m (ft)

T_p = pipe temperature, °C (°F)

T_a = agent temperature, °C (°F)

t = system discharge time

h = heat of vaporization of the agent at T_a, kJ/kg (Btu/lb)

r_o = outside pipe radius, mm (in.)

r_i = inside pipe radius, mm (in.)

Specialized systems using a variety of agents are in wide use throughout the world to protect hazards such as aircraft engine nacelles, military vehicles, emergency generator motors, earth moving equipment, and racing cars. The characteristic common to all these systems is that they can only be applied to the specific hazard for which they were designed and tested. One unusual concept used to protect aircraft flight simulator areas is known as partial flooding, where only the volume containing the simulator equipment receives the total flooding concentration, and not the expansive open areas above it. A design concentration of 7 percent is recommended to achieve a 5 percent concentration in the hazard area and should provide for a minimum agent height level relative to the agent concentration of approximately 1.5 m (5 ft) above the highest part of the hazard. The placement of the nozzle is critical and should be designed to direct agent discharge approximately 30 degrees below the horizontal plane. As shown in Figure 4-6.10, the savings associated
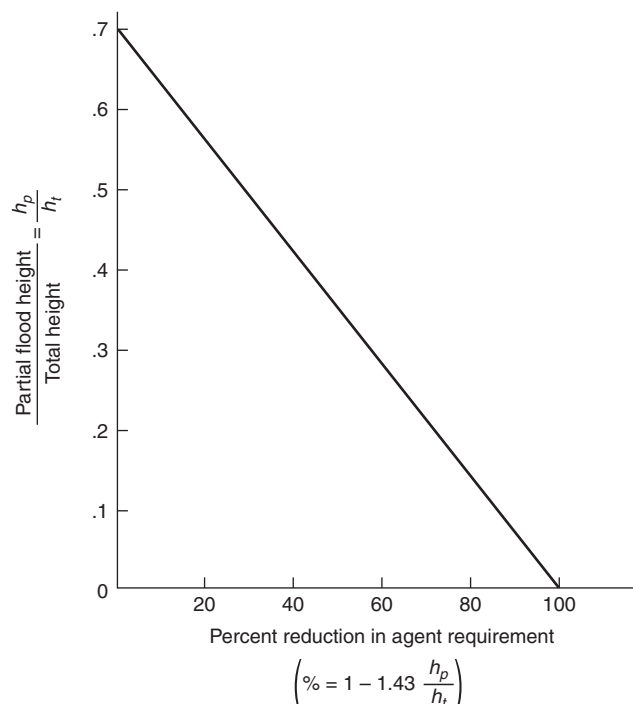
Figure 4-6.10. *Agent reduction associated with partial flooding systems.*

with partial flooding systems can be substantial, especially in areas with very high ceilings.[19]

Agent Requirements: Total Flooding

Design Concentrations: Solid Fuels

Flammable solids may be classified as those that do not develop deep-seated fires and those that do. Class A combustible solids that develop deep-seated fires do so after exposure to flaming combustion for a certain length of time, which varies with the material. Some materials may begin as deep seated through internal heating such as spontaneous ignition. With respect to Halon 1301 total flooding systems, a fire is considered deep seated if a 5 percent concentration will not extinguish the fire within 10 min after agent discharge.[7] Materials that do not become deep seated undergo surface combustion only and may be treated much the same as those in a flammable liquid fire.

The presence of Halon 1301 in the vicinity of a deep-seated fire will extinguish the flame and reduce the rate of burning, yet the quantity of agent required for complete extinguishment of all embers is difficult to assess. Often it is impractical to maintain an adequate concentration of Halon 1301 for a sufficient time to ensure the complete extinguishment of a deep-seated fire. Factors affecting this concentration include

1. Nature of fuel
2. Time during which it has been burning
3. Availability of oxygen within the enclosure

4. Ratio of burning surface area to the volume of the enclosure
5. Geometric characteristics of the fuel
6. Fuel distribution within the enclosure

Table 4-6.12 illustrates the extinguishing concentrations of selected flammable solid fires as indicated by six different halon industry groups.[22]

Even where the fire has inadvertently become deep seated, application of a low Halon 1301 concentration has two benefits. First, all flaming combustion is halted, preventing rapid spread of the fire to adjacent fuels. Second, the rate of combustion is drastically reduced. These two characteristics justify the ability of Halon 1301 to control, if not extinguish, deep-seated fires. However, Halon 1301 systems that are specifically designed to extinguish deep-seated fires are seldom economical to apply and may not be as effective in these fires as other types of extinguishing systems.

Design Concentrations: Liquid and Gas Fires

There are two general types of flammable liquid or gas fires. First, a flammable or explosive mixture of vapors exists that must be prevented from burning, and second, fuel is burning that must be extinguished. Associated with each of these conditions is a minimum level of Halon 1301 extinguishing concentration, respectively known as inerting and flame extinguishment. When determining the halon design concentration, proper consideration must be given to the quantity and type of fuel

Table 4-6.12   *Extinguishing Concentrations of Selected Flammable Solid Fires*

	Halon 1301 Concentration (percent by volume)					
	Factory Mutual	Fenwal	Ansul	DuPont	Safety First	Underwriter Labs
Surface Fires						
Polyvinyl chloride		2.0		2.6	3.8	
Polystyrene		3				
Polyethylene		3				
Stacked computer printout			5.1			
Polyester computer tape		5			3.8	
Wood crib 30 pcs. $\frac{3}{4}$" × $\frac{7}{8}$"	3					
Wood crib 24 pcs. 2" × 2" × 18"					3.8	
Wood crib 1A 50 pcs. 2" × 2" × 18"					3.8	3.88
Excelsior loose on floor					3.8	6.0
Shredded paper loose on floor					3.8	
Polyurethane foam				3	3.8	
Cotton lint					3.8	
Crumpled paper	3	6			3.8	
Wood pallets—stack of 10	3					
Deep-Seated Fires						
Shredded paper in wire basket					20	18.0
Polyester computer tape loose in open wire basket		10				
Charcoal	13					
Parallel wood blocks	20					
Glazed fox fur					6.5	

involved, the conditions under which it normally exists in the hazard, and any special conditions of the hazard itself. If certain hazards have explosion potential either before or following a fire due to the presence of volatile, gaseous, or atomized fuel, then special consideration should be given to vapor detection and explosion suppression measures.

As its name implies, the flame extinguishment concentration assumes that the given fuel is burning and that Halon 1301 injected into the air surrounding the fuel at the stated concentration will extinguish the fire.[7] Design concentrations for flame extinguishment are given in Table 4-6.13. These concentrations are not considered effective with premixed flames or explosive mixtures of fuel vapor in air, but instead apply to diffusion flames, where the flames emanate from pure fuel vapor, and oxygen suffuses into the flame zone from the outside. If the possibility of a subsequent reflash or explosion exists, then the flame extinguishing concentration is not sufficient. NFPA 12A[7] defines these conditions as "when both:

1. The quantity of fuel permitted in the enclosure is sufficient to develop a concentration equal to or greater than one-half of the lower flammable limit throughout the enclosure, and
2. The volatility of the fuel before the fire is sufficient to reach the lower flammable limit in air (maximum ambient temperature or fuel temperature exceeds the closed cup flash point temperature) or the system response is not rapid enough to detect and extinguish the fire before the volatility of the fuel is increased to a dangerous level as a result of the fire."

Most fuels exhibit about a 30 to 40 percent higher concentration for inerting than for flame extinguishment. The minimum inerting concentration suppresses the propagation of the flame front at the "flammability peak" or stoichiometric fuel/air composition and inerts the enclosure so that any fuel/air mixture will not burn. The higher inerting concentration is often considered safer to use even if the flame extinguishment concentration is feasible, yet the sacrifices include higher system cost and higher concentrations to which personnel may be exposed. (See Table 4-6.14.)

Table 4-6.13   Design Concentration for Flame Extinguishment

Fuel	Minimum Design Concentration (percent by volume)
Acetone	5.0
Benzene	5.0
Ethanol	5.0
Ethylene	8.2
Methane	5.0
n-Heptane	5.0
Propane	5.2

Table 4-6.14   Halon 1301 Design Concentrations for Inerting

Fuel	Minimum Concentration (percent by volume)
Acetone	7.6
Benzene	5.0
Ethanol	11.1
Ethylene	13.2
Hydrogen	31.4
Methane	7.7
n-Heptane	6.9
Propane	6.7

Includes a safety factor of 10 percent added to experimental values

It is possible to calculate whether the flame extinguishing concentration is acceptable by determining if the fuel present in the hazard will permit attainment of the one-half lower flammable limit of the fuel. The equation to determine the maximum allowable fuel loading (*MFL*) for flame extinguishment concentrations is

$$MFL = \frac{(K_c)(LFL)(MW)}{T} \qquad (2)$$

where

MFL = maximum allowable fuel loading, kg/m^3 (lb/ft^3)

K_c = conversion factor, 0.06093 (0.00685)

LFL = lower flammable limit of fuel in air, percent volume

MW = molecular weight of fuel

T = temperature, K (R)

This can be compared with the actual fuel loading (*FL*), which is calculated by

$$FL = \frac{(VF)(W_{h_2O})(SG)}{V} \qquad (3)$$

where

FL = fuel loading, kg/m^3 (lb/ft^3)

VF = volumetric quantity of fuel, m^3 (ft^3)

W_{h_2O} = specific weight of water, 997.9 kg/m^3 (62.3 lb/ft^3)

SG = specific gravity of fuel

V = volume of enclosure, m^3 (ft^3)

If the fuel loading, *FL*, exceeds the maximum allowable fuel loading, *MFL*, then the inerting concentration for the particular fuel should be used. Most applications involve a variety of fuels within a single enclosure. If the sum of the actual fuel loadings, *FL*, is greater than any single maximum allowable fuel loading, *MFL*, then the most stringent inerting concentration is recommended. If it is determined that a flame extinguishment concentration is sufficient, the value for the fuel requiring the greatest concentration is most applicable.

Calculation of Agent Quantity

The calculations necessary for determining the Halon 1301 total flooding quantity are dependent on temperature, volume of the enclosure, agent concentration, altitude with respect to sea level, and losses due to ventilation and leakage. Most applications are based on a static volume enclosure with all openings sealed and all ventilation systems shut down prior to discharge. This simplifies the calculation significantly. Often the ventilation system does not shut down but instead is dampered to allow recirculating air (without makeup air) to continue cooling sensitive electronic equipment and promote the mixing of halon and air. Total flooding quantities are still based on a static volume for these applications. However, in this instance, it may be necessary to include the volume of the ventilation ductwork in addition to the volume of the enclosure. The equation to determine the Halon 1301 total flooding quantity is

$$W = \frac{(V)(C)(A_c)}{S(100 - C)} \qquad (4)$$

where

W = 3 weight of Halon 1301 required, kg (lb)

C = Halon 1301 concentration, percent by volume

A_c = altitude correction factor—(Refer to Table 4-6.15)

S = specific vapor volume based on temperature, m³/kg (ft³lb)

$S = 0.14781 + 0.000567T; T$ = Temperature °C

$S = 2.2062 + 0.005046T; T$ = Temperature °F

Application Rate

Discharge time and soaking period: When designing a Halon 1301 total flooding system, it is important to determine the system discharge time and soaking period.

As indicated in NFPA 12A, "the agent shall be completed in a nominal 10 seconds or as otherwise required by

Table 4-6.15 *Correction Factors for Altitudes*

Altitude		Correction Factor
Feet	Meters	
3000	914	0.90
4000	1219	0.86
5000	1524	0.83
6000	1829	0.80
7000	2134	0.77
8000	2438	0.74
9000	2743	0.71
10000	3048	0.69
11000	3353	0.66
12000	3658	0.64
13000	3962	0.61
14000	4267	0.59
15000	4572	0.56

the authority having jurisdiction."[7] The reasons for a rapid discharge time include keeping unwanted products of decomposition to a minimum and achieving complete dispersal of agent throughout the enclosure. Sometimes a much faster application rate is required due to the possibility of a fast spreading fire; yet, discharge times longer than 10 s are sometimes necessary for areas such as museums requiring that turbulence be kept to a minimum, or areas with unavoidably difficult piping configurations.

The soaking time is another important requirement for a Halon 1301 total flooding system. This is especially true for deep-seated fire or fires that may reflash. The most common application today for total flooding systems is the protection of valuable electronic equipment. Fires in these applications are almost always extinguished within a few seconds by the Halon 1301 agent, yet a 10-min soaking period is usually required. This estimated time period allows responsible individuals to arrive at the scene to take follow-up action. It is important to remember that halogenated agent extinguishing systems in most cases have only a single chance to control an unwanted fire.

Effects of ventilation: When Halon 1301 is discharged into a total flooding enclosure that is ventilated, some agent will be lost with the ventilating air. Assuming that ventilation must continue during and after discharge, a greater amount of agent is required to develop a given concentration. Also, to maintain the concentration at a given level requires continuous agent discharge for the duration of the soaking period. If an enclosure initially contains pure air, the Halon 1301 discharge rate required to develop a given concentration for agent at any given time after the start of discharge is[7]

$$R = \frac{(C)(E)}{(S)(100 - C)\left[1 - e^{(-Et_1/V)}\right]} \qquad (5)$$

where

R = Halon 1301 discharge rate, kg/s (lb/s)

E = ventilation rate, m³/s (ft³/s)

t_1 = discharge time, s

e = natural logarithm base, 2.71828

The Halon 1301 discharge rate necessary to maintain a given concentration of agent is[7]

$$R = \frac{(C)(E)}{(S)(100 - C)} \qquad (6)$$

After the agent discharge is stopped, the decay of the agent concentration with respect to time is[7]

$$C = C_0 e^{(-Et_2/V)} \qquad (7)$$

where

C_0 = agent concentration at end of discharge, percent volume

t_2 = time after stopping discharge, s

Compensation for leakage: Occasionally a Halon 1301 total flooding system is designed for an enclosure that has openings that cannot be closed. An example may be a conveyor belt penetrating an enclosure wall, yet even these openings can sometimes be closed using inflatable seals. Halon 1301 discharged into an enclosure for total flooding will result in an air/agent mixture that has a higher specific gravity than the air surrounding the enclosure. Therefore, any openings in the lower portions of the enclosure will allow the heavier air/agent mixture to flow out and the lighter outside air to flow in. Fresh air entering the enclosure will collect toward the top, forming an interface between the air/agent mixture and fresh air. As the leakage proceeds, the interface will descend toward the bottom of the enclosure. The space above the interface will be completely unprotected, whereas the lower space will essentially contain the original extinguishing concentration. There are two methods of compensating for unclosable openings: initial overdose and extended discharge.

The initial overdose method provides for an adequate overdose of Halon 1301 to ensure a preestablished minimum of agent at the end of the desired soaking period. Mechanical mixing is required within the enclosure to prevent stratification of agent concentration and a descending interface. Also caution must be used to prevent personnel exposure to the high initial concentrations. The necessary initial concentration depends upon the extended protection time required, the opening height, the opening width, and the volume of the enclosure. Referring to Figure 4-6.11, the equation used to determine the initial concentration for a final concentration of 5 percent is[7]

$$G = \frac{(K)(W_o)(2g_cH^3)^{1/2}}{3V} \qquad (8)$$

where

G = geometric constant

K = orifice discharge coefficient, 0.66

W_o = opening width, m (ft)

g_c = acceleration due to gravity, 9.81 m/s^2 (32.2 ft/s^2)

H = opening height, m (ft)

The other method used to compensate for unclosable openings is extended discharge. This involves at least two separate piping systems: one to achieve the initial agent concentration, and the other to provide a continuous addition of Halon 1301 at a rate which will compensate for leakage out of the enclosure during the soaking period. The agent must be discharged in such a way that uniform mixing of agent and air is obtained. This mixing is often difficult due to the extremely low flow rates being discharged over the entire soaking period, occasionally resulting in small nozzles freezing due to air moisture. Based on the design concentration and opening height, Figure 4-6.12 can be used to determine the Halon 1301 makeup rate per unit opening width.

Assuming the design concentration of Halon 1301 is established in the enclosure initially, the time required for
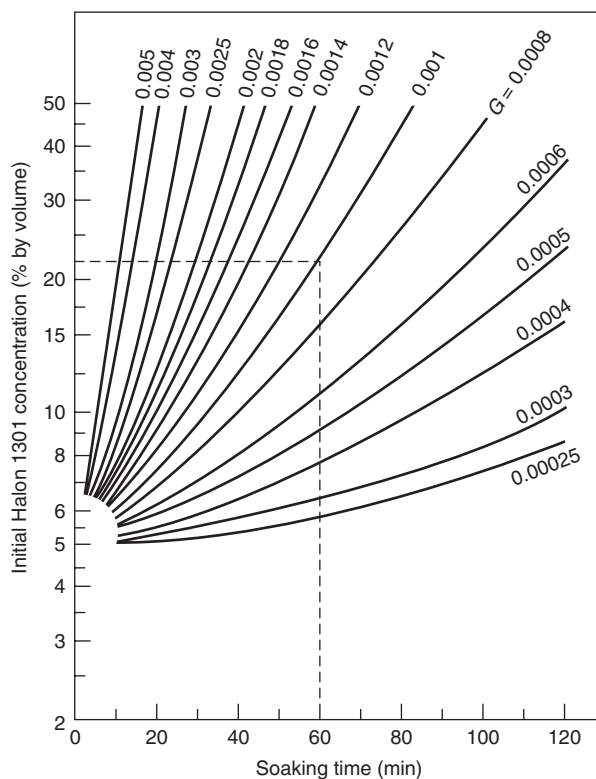
Figure 4-6.11. *Initial amount of Halon 1301 to produce a 5 percent residual concentration in enclosures equipped for mechanical mixing.*

the interface to reach half-way down the enclosure height can be calculated. Referring to Figure 4-6.13, the geometric constant previously calculated for intial overdose is used to find the soaking time based on the initial design concentration.

Flow Calculations

Piping Theory

The overall objective of designing a Halon 1301 piping system is to properly disperse the required concentration of Halon 1301 throughout the hazard volume within the specified time period. Systems must be engineered to operate quickly and effectively. The discharge time (usually a nominal 10 s as indicated by NFPA 12A) is a critical system constraint and is measured as the interval between the first appearance of liquid at the nozzle and the time when the discharge becomes predominantly gaseous.[7] The hydraulic calculations are considered to be the most difficult part of the entire design process, and are almost always calculated with the aid of computer programs due to the tedious nature of manual calculations.

As illustrated in Figure 4-6.14, the primary components of a Halon 1301 piping system are the agent storage
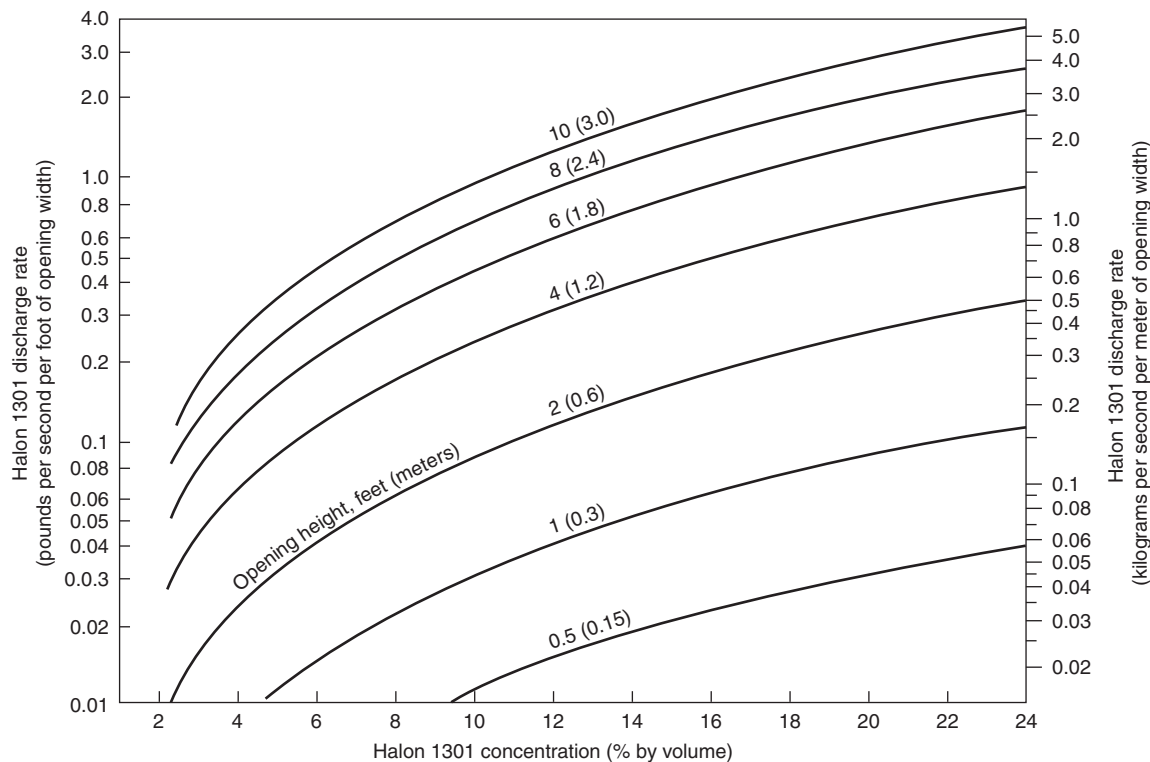
Figure 4-6.12. *Extended discharge rate of Halon 1301 to maintain constant concentrations in enclosures with openings.*

container, the discharge nozzle, and the pipe. Often, more than one nozzle is required, complicating the calculations significantly. An attempt should always be made to keep the piping system simple and if possible, balanced. A balanced system has the actual and equivalent pipe lengths from container to each nozzle within ± 10 percent of each other and has equal design flow rates at each nozzle.[7]

As with sprinkler systems or other systems involving fluid flow, the methodology for solving Halon 1301 piping calculations involves seeking terminal characteristics based on property changes encountered due to the movement of the fluid. The system hydraulics are controlled by the selection of the orifice area at the discharge nozzle. This orifice area is calculated from the nozzle pressure, which is based on the starting pressure in the container and pressure losses in the pipe. Because the flow of Halon 1301 is nonsteady and has a change in phase from liquid to vapor, the calculations become highly complex. To simplify calculations, the average discharge conditions are determined so that they might reasonably represent the entire discharge time span. This time-independent model is based on the moment in time when half the liquid phase of the agent has left the nozzle. All the calculations for a 10 s discharge condition shown in Figure 4-6.15 would be solved at the mid-discharge condition (5 s). Hence, the critical characteristics that vary with dis-

charge, such as the storage container pressure and the pressure-density relationship in the pipeline, are replaced with average time-independent values.[23]

By the time half of the liquid agent is out of the nozzle, the original pressure in the storage container has dropped considerably. To calculate the mid-discharge storage container pressure, the percent of agent still within the pipe must be determined. Also, the initial drop in pressure immediately after the start of discharge is nonlinear. As seen in Figure 4-6.16, the pressure recovery is due to the nitrogen vigorously boiling out of the halon/nitrogen mixture within the storage container.

Unlike water-based fluid flow, the pressure drop occurring when Halon 1301 flows through a pipe is nonlinear and is dependent on the pipeline agent density, not the distance traveled. The pipeline flow is two phase, with a mixture of liquid and vapor agent. As the agent travels in the pipe, the pressure and density decrease, which increases the velocity and the amount of halon vapor. Interestingly, the evolution of the nitrogen from the halon/nitrogen mixture in the storage container causes the halon to drop in temperature and become more dense. This phenomenon fortunately is not a factor in the calculations since a time-independent model is being used. The increase in density at any one location over the entire time span should not be confused with the decrease in density that occurs when the agent flows from one location to another.
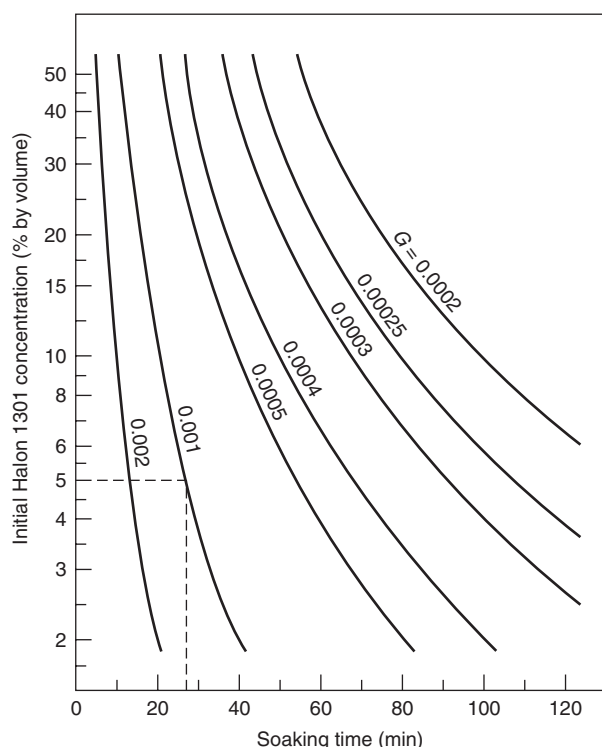
Figure 4-6.13. *Time required for interface between effluxing Halon 1301/air mixtures and influxing air to descend to center of enclosures not equipped for mixing.*
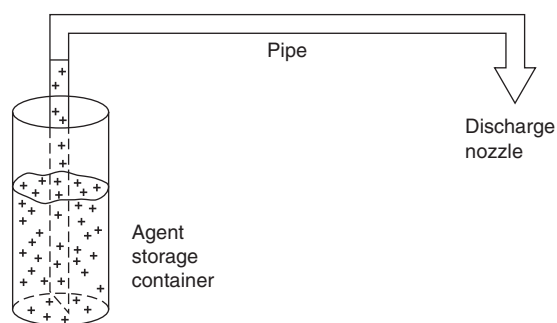
Figure 4-6.14. *Primary components of a Halon 1301 piping system.*

Figure 4-6.15. *Summary of Halon 1301 discharge conditions based on a 10-s discharge.*

Guidelines and Limitations

Unrealistic distribution networks often fail to perform to specifications and are difficult if not impossible to predict from a calculation standpoint. As the piping system becomes more unrealistic, the calculations become more unreliable. To aid in the development of accurate calculations, certain fundamental limitations are necessary to ensure proper system design. These limitations are especially important with respect to computer programs since these programs have a tendency to be operated abusively with high expectations. Summarized below are the design constraints for Halon 1301 hydraulic calculations.[24]

1. Good design practice
2. Discharge time $\leq$ 10 s
3. Favorable system temperature
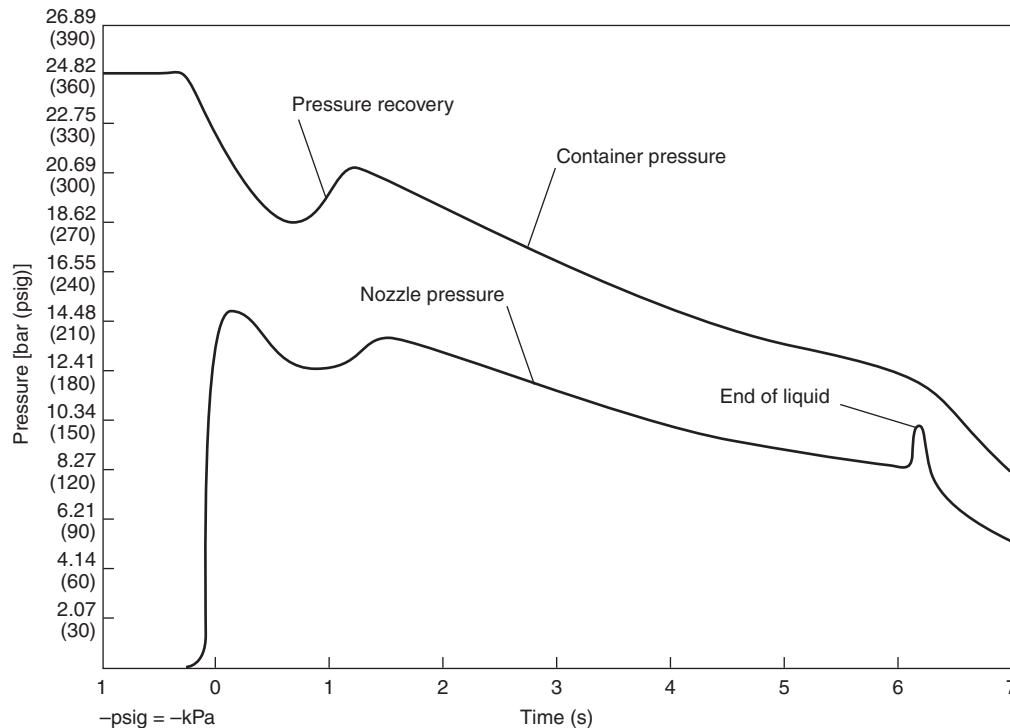
Figure 4-6.16.   *Pressure profile during system discharge.*

4. Initial container pressure = 2482.2 kPa (360 psig) or 4137.0 kPa (600 psig)
5. Initial container fill density ≤ 1121.4 kg/m³ (70 lb/ft³)
6. Percent in pipe ≤ maximum value
7. Turbulent flow ≥ minimum value
8. Nozzle pressure ≥ minimum value
9. Actual nozzle area ≤ percentage of feed pipe area
10. Actual nozzle area = calculated nozzle ±5 percent

Good design practice includes such items as favoring balanced systems, keeping the degree of flow/split imbalance below a maximum value, avoiding vertically installed tees, and avoiding nozzles on different floor levels which may separate the halon gas/vapor mixture. The values for some of the constraints are determined by the individuals developing computer programs that are verified by approval agencies through testing.

Calculation Procedure

The piping calculations comprise four steps:

1. Determining the necessary input data
2. Calculating the average storage container pressure
3. Calculating the nozzle pressure at each nozzle, and
4. Calculating the nozzle orifice areas

Pipeline calculations are performed for each segment of pipe having both a constant flow rate and a uniform pipe diameter; thus the piping network is divided into sections called junctions. Each discharge nozzle is also

identified. The forms necessary for the input data, pressure calculations, and nozzle calculations are contained in Figures 4-6.17 and 4-6.18. Assuming the appropriate input data are known, the average storage container pressure is determined from Figure 4-6.19 based on the percent agent in pipe, which itself is determined by[7]

$$\% \text{ in pipe} = \frac{K_1}{\left(W_i/V_p\right) + K_2} \tag{9}$$

where

W_i = initial charge weight of Halon 1301, lb

V_p = internal pipe volume, ft³ (See Table 4-6.16)

K_1 and K_2 = constants (See Table 4-6.17)

Once the average storage container pressure is known, Figures 4-6.18 and 4-6.20 and Equations 10 through 22 can be used to determine the nozzle orifice areas for a 360 psig system. Usually the calculations are based on a 10-s discharge time, though this is sometimes changed slightly to produce flow rates in accordance with Table 4-6.18. Turbulent pipeline flow can also be achieved by using smaller pipe sizes. Pipe diameters that are too small result in unacceptably high pressure losses; therefore, care must be used in pipe size selection. It is important to recognize that approximations have been made for Y and Z factors and nozzle coefficients. The calculation procedure presented here is only intended to demonstrate the current methodology and not to provide a rigorous solution. The necessary equations are[7,25]

System Halon weight _ _ _ _ _ _ _ _ _ _ _ _ _ _ _ _ lb
Container fill density _ _ _ _ _ _ _ _ _ _ _ _ _ _ _ _ _ lb/ft3
Discharge time _ s

Form I: System summary

N1: _ _ _ _ _ _ _ _ _ _ lb   N3: _ _ _ _ _ _ _ _ _ lb   N5: _ _ _ _ _ _ _ _ _ lb
N2: _ _ _ _ _ _ _ _ _ _ lb   N4: _ _ _ _ _ _ _ _ _ lb   N6: _ _ _ _ _ _ _ _ _ lb

A	B	C	D	E	F	G	H	I	W	X	Y
					Inputs					Outputs	
Junction number	Nozzle number	Flow rate Q	Pipe type	Pipe diameter D	Actual pipe length L	Fittings, equivalent length L	Total length L	Elevation change h	Junction pressure P (starting of from Form II)	Density at orifice r (Fig. 4–6.20)	Orifice area F (Eq. 22)

Figure 4-6.17. *Halon 1301 piping calculation summary form.*

$$P_e = \frac{rL_e}{144} \tag{10}$$

where
P_e = elevation pressure, psig
r = agent density, lb/ft3
L_e = pipe elevation length, ft

$$A = 1.013D^{5.25} \tag{11}$$

where
A = pipe size factor
D = actual pipe diameter, in.

$$B = \frac{7.97}{D^4} \tag{12}$$

where
B = pipe size factor

$$Y_1 = -\left(\frac{a}{3}p_0^3 + \frac{b}{2}p_0^2 + cP_0 + d\right) \tag{13}$$

where
Y_1 = first Y factor
P_0 = junction starting pressure, psig
$a, b, c,$ and d = constants (See Table 4-6.19)

Form II: Pressure calculations

J	K	L	M	N	O	P	Q	R	S	T	U	V
		Initial pressure						Final pressure				
	Elevation		Corrected starting pressure P_0	Pipe size factors		1st Y factor Y_1 (Table 4–6.19, Eq.13)	1st Z factor Z_1 (Eqs. 14–17)	Temporary Y factor Y_t (Eq. 18)	Temporary pressure P_t (Table 4–6.19, Eq.19)	2nd Z factor Z_2 (Eqs.14–17)	2nd Y factor Y_2 (Eq. 20)	Final junction pressure P (Table 4–6.19, Eq. 21)
Junction pressure	Density r (Fig. 4–6.20)	Pressure P_e (Eq. 10)		A (Eq. 11)	B (Eq. 12)							

Figure 4-6.18.   *Halon 1301 pressure calculation summary form.*

Average Storage Cylinder Pressure vs. Percent of the Agent Supply Needed to Fill the Pipeline
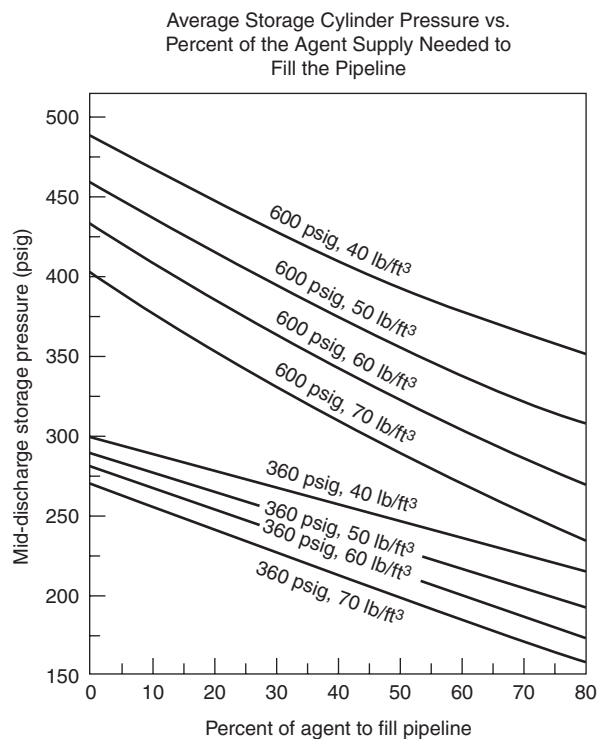
Figure 4-6.19.   *Mid-discharge storage container pressure.*

$$Z = 1.01790 - 0.01179(P - 160) \quad \begin{array}{l}\text{for 70 lb/ft}^3 \\ \text{fill density}\end{array} \quad (14)$$

$$Z = 0.96913 - 0.01098(P - 170) \quad \begin{array}{l}\text{for 60 lb/ft}^3 \\ \text{fill density}\end{array} \quad (15)$$

$$Z = 0.96412 - 0.01051(P - 175) \quad \begin{array}{l}\text{for 50 lb/ft}^3 \\ \text{fill density}\end{array} \quad (16)$$

$$Z = 0.95900 - 0.01008(P - 180) \quad \begin{array}{l}\text{for 40 lb/ft}^3 \\ \text{fill density}\end{array} \quad (17)$$

where

Z = Z factor

P = pressure, psig

$$Y_T = Y_1 + L\left(\frac{Q^2}{A}\right) \quad (18)$$

where

Y_T = temporary Y factor

Q = flow rate, lb/s

$$P_T^3 + \left(\frac{3b}{2a}\right)P_T^2 + \left(\frac{3c}{a}\right)P_T = -\left(\frac{3}{a}\right)Y_T - \left(\frac{3d}{a}\right) \quad (19)$$

where

P_T = temporary pressure, psig

Figure 4-6.20. *Pipeline density/pressure relationship for a 360 psig system.*

Table 4-6.16 *Internal Volume of Steel Pipe*

Nominal Pipe Diameter (in.)	Schedule 40 Inside Diameter (in.)	ft³/ft	Schedule 80 Inside Diameter (in.)	ft³/ft
1/4	0.364	0.0007	0.302	0.0005
3/8	0.493	0.0013	0.423	0.0010
1/2	0.622	0.0021	0.546	0.0016
3/4	0.824	0.0037	0.742	0.0030
1	1.049	0.0060	0.957	0.0050
1 1/4	1.380	0.0104	1.278	0.0089
1 1/2	1.610	0.0141	1.500	0.0123
2	2.067	0.0233	1.939	0.0205
2 1/2	2.469	0.0332	2.323	0.0294
3	3.068	0.0513	2.900	0.0459
3 1/2	3.548	0.0687	3.364	0.0617
4	4.026	0.0884	3.826	0.0798

$$Y_2 = Y_T + B\left(Z_2 - Z_1\right)Q^2 \qquad (20)$$

where

Y_2 = second Y factor

$$P^3 + \left(\frac{3b}{2a}\right)P^2 + \left(\frac{3c}{a}\right)P = -\left(\frac{3}{a}\right)Y_2 - \left(\frac{3d}{a}\right) \qquad (21)$$

$$F = 1.5Q[1/f(rp)^{1/2}] \qquad (22)$$

where

F = nozzle orifice area, in.²
f = nozzle coefficient (approximation = 0.7)

Table 4-6.17 *Constants to Determine Percent of Agent in Piping*

Storage (psig)	Filling Density	K_1	K_2
600	70	7180	46
600	60	7250	40
600	50	7320	34
600	40	7390	28
360	70	6730	52
360	60	6770	46
360	50	6810	40
360	40	6850	34

Table 4-6.18 *Minimum Design Flow Rates to Achieve Turbulent Pipeline Flow*

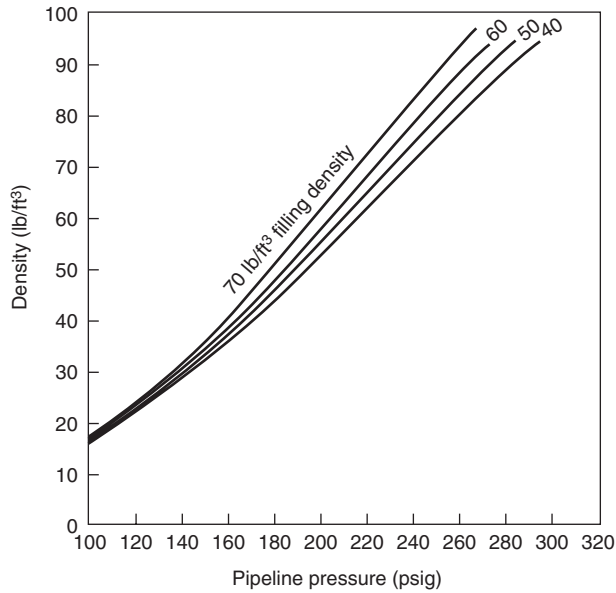| Nominal Pipe Diameter (in.)	Schedule 40 Minimum Flow Rate (lb/s)	Schedule 80 Minimum Flow Rate (lb/s)
1/8	0.20	0.11
1/4	0.34	0.24
3/8	0.68	0.48
1/2	1.0	0.79
3/4	2.0	1.9
1	3.4	2.8
1 1/4	5.8	4.8
1 1/2	8.4	7.5
2	13	13
2 1/2	19.5	17
3	33	26
4	58	48
5	95	81
6	127	109

For SI units: 1 lb/s = 0.454 kg/s

Table 4-6.19 *Constant for Y Factor/Pressure Equations*

P Storage (psig)	Fill Density (lb/ft³)	a	b	c	d
360	70	3.571 × 10⁻⁴	0.6971	−63.50	−5921
360	60	4.018 × 10⁻⁴	0.6913	−64.01	−6333
360	50	3.125 × 10⁻⁴	0.6238	−56.90	−7386
360	40	3.720 × 10⁻⁴	0.6187	−55.55	−8120

Postdesign Considerations

Postdesign considerations are divided into two categories: system documentation and inspection/acceptance practices. Good halon system design is not complete until full documentation is provided for installation, acceptance, and eventual end user operation. Proper documentation is especially important to prevent the inadvertent discharge of a halon system for other than a fire, since replacement of the halon agent could be very difficult with future availability being dependent on recycled stock.

System Documentation

System documentation should include the items listed below. This material is necessary for others to install, test, operate, and maintain the system. Information can be recorded entirely on system drawings or in both a written manual and system drawings.

System manual

1. Design Data
   (a) Functional and operational description
   (b) Halon 1301 weight calculations
   (c) Hydraulic piping calculations
   (d) Special considerations
2. Installation, Maintenance, and Inspection Instructions

As-built system drawings

1. Floor Plan Layout
   (a) Suitable dimensions
   (b) Equipment locations
   (c) Special installation details
2. Electrical Schematic
3. Equipment Identification
4. Special Notes

Inspection and Acceptance

After installation, each system should be inspected and tested by technicians trained by the equipment manufacturer covering the items listed below:

1. Test system wiring for proper connection, continuity, and resistance to ground
2. Check system control unit in accordance with factory recommended procedures
3. Calibrate and test each detector in accordance with factory recommended procedures
4. Test each releasing circuit for proper resistance by means of a current-limiting meter
5. Test the operation of all ancillary devices such as alarms, dampers, magnetic closers, and so on.
6. Obtain a certificate of inspection signed and dated by the installing contractor and the authority having jurisdiction

An installation checklist is often used, which expands on the above items in complete detail.[26] These checklists are available from agent and equipment manufacturers, installers, insurance groups, and consultants.

When accepting a newly installed halon system, it is important to determine compliance with design specifications. In previous years, a full discharge test was required to provide unquestionable evidence of performance, yet this could be a costly and sometimes unnecessary burden carried by the end user. End users with multiple systems would often prove system acceptance based on the performance characteristics of their other systems.

The primary reason for discharge test failure, when it was performed, was because the hazard enclosure would not hold the design concentration over the entire soaking period.[27] Checking the enclosure for possible halon leak-age points has always been difficult and is the only questionable part of the acceptance/inspection procedure. A method referred to as the enclosure integrity test has proved to be very effective for this problem, and validates the integrity of the protected enclosure.[7] This technique shows much promise and has potential for substantially enhancing the reliability of proper system operation.

The most immediate and effective use of fan pressurization techniques is for leakage path indication.[28] This involves pressurizing or depressurizing the enclosure with the fan pressurization apparatus and using an indicating device, such as a smoke pencil or acoustic sensor, to determine leakage paths. The installers' visual inspection of the enclosure now becomes very effective since even the smallest cracks can be located. Due to low cost and simplicity, a smoke source is usually the most desirable method for locating leaks, but an excellent alternative is the use of a directional acoustic sensor that can be selectively aimed at different sound sources.[29] Highly sensitive acoustic sensors are available that can detect air as it flows through an opening and are sensitive enough to clearly hear a human eye blink.[30] Openings can also be effectively detected by placing an acoustic source on the other side of the barrier and searching for acoustic transmission. Another method is to use an infrared scanning device if temperature differences across the boundary are sufficient.[31] These techniques are not quantitative, but they are effective, inexpensive, and easily performed.

Environmental Considerations

Scientific evidence indicates that fire protection Halon 1301 is one of several man-made substances adversely effecting the earth's ozone layer.[32] Ozone exists naturally as a thin layer of gas in the stratosphere that blocks the sun's harmful ultraviolet rays and thus is vital to life on earth. Several adverse environmental and direct health effects are linked to ozone layer depletion, and its preservation is of paramount concern to mankind. It's believed that Halon 1301 (and other chlorofluorocarbons) chemically destroy ozone when emitted into the atmosphere.

Earlier, the phase-out of full system discharge tests that were used to verify enclosure integrity received special attention since they accounted for a proportionately large percentage of fire protection halon emissions. Fortunately, the amount of fire protection Halon 1301 released for actual fires is relatively small. Testing a system by performing a full discharge test allows the release of Halon 1301, which on a cumulative basis may be potentially harmful to the environment and depletes relatively precious stocks of halon agent that should be dedicated to suppressing fires. The release of Halon 1301 should be minimized.

With regard to ozone layer depletion, halons used for fire protection are different than halons used for other industrial applications.[33] Fire protection halons are unique because of their essential mission to prevent the loss of life, minimize the loss of irreplaceable property, assure the continuity of vital operations, and reduce the amount of fire byproducts polluting the atmosphere. Efforts have

been made to minimize the release of fire protection halons for noncritical tasks like training, testing, and research. It is assumed that halon systems will remain in existence for many more years, despite the present worldwide restriction on their production.

Nomenclature

a	constant (see Table 4-6.19)
A	pipe size factor
A_c	altitude correction factor—(refer to Table 4-6.15)
b	constant (see Table 4-6.19)
B	pipe size factor
c	constant (see Table 4-6.19)
C	Halon 1301 concentration, percent by volume
C_0	agent concentration at end of discharge, percent by volume
d	constant (see Table 4-6.19)
D	actual pipe diameter, in.
e	natural logarithm base, 2.71828
E	ventilation rate, m^3/s (ft/s)
f	nozzle coefficient (approximation = 0.7)
F	nozzle orifice area, $in.^2$
FL	fuel loading, $kg/m^3(1b/ft^3)$
g_c	acceleration due to gravity, $9.81\ m/s^2$ ($32.2\ ft/s^2$)
G	geometric constant
h	heat of vaporization of the agent at T_a, kJ/kg (Btu/lb)
H	opening height, m (ft)
k	thermal conductivity of the piping, $W/m\cdot K$ ($Btu\cdot t/hr\cdot ft^2\cdot f$)
K	orifice discharge coefficient, 0.66
K_c	conversion factor, 0.06093 (0.00685)
L	linear length of piping, m (ft)
L_e	pipe elevation length, ft
LFL	lower flammable limit of fuel in air, percent volume
MFL	maximum allowable fuel loading, kg/m^3 (lb/ft^3)
MW	molecular weight of fuel
P	pressure, psig
P_0	junction starting pressure, psig
P_e	elevation pressure, psig
P_T	temporary pressure, psig
Q	flow rate, lb/s
r	agent density, lb/ft^3
R	Halon 1301 discharge rate, kg/s (lb/s)
r_i	inside pipe radius, mm (in.)
r_o	outside pipe radius, mm (in.)
S	specific vapor volume of Halon 1301 based on temperature, m^3/kg (ft^3/lb)
SG	specific gravity of fuel
t	system discharge time
T	temperature, K (R)
t_1	discharge time, s
t_2	time after stopping discharge, s
T_a	agent temperature, C (F)
T_p	pipe temperature, C (F)
V	enclosure volume, m^3 (ft^3)
VF	volumetric quantity of fuel, m^3 (ft^3)
V_p	internal pipe volume, ft^3 (See Table 4-6.16)
W_x	amount of agent increase, kg (lb)
W_{h_2O}	specific weight of water, $997.9\ kg/m^3$ ($62.3\ lb/ft^3$)
W	weight of Halon 1301 required, kg (lb)
W_o	opening width, m (ft)
W_i	initial charge weight of Halon 1301, lb
Y_1	first Y factor
Y_2	second Y factor
Y_T	temporary Y factor
Z	Z factor

References Cited

1. C.C. Grant, "Fire Protection Halons and the Environment: An Update Symposium," *Fire Technology,* 24, p. 1 (1988).
2. "The Halogenated Extinguishing Agents," *NFPA Quarterly,* 48, 8, Part 3 (1954).
3. D. Wharry and R. Hirst, *Fire Technology: Chemistry and Combustion,* Inst. of F. Engrs., Leicester, England (1974).
4. R. Strasiak, "The Development of Bromochloromethane (CB)," *WADC Technical Report 53–279,* Wright Air Development Center, Dayton, OH (1954).
5. *Fire Protection Handbook, Seventeenth Edition,* National Fire Protection Association, Quincy, MA (1991).
6. NFPA 12A-T, *Standard on Halogenated Fire Extinguishing Agent Systems,* National Fire Protection Association, Quincy, MA (1968).
7. NFPA 12A, *Standard on Halon 1301 Fire Extinguishing Systems,* National Fire Protection Agency, Quincy, MA (1992).
8. NFPA 12B, *Standard on Halon 1211 Fire Extinguishing Systems,* National Fire Protection Association, Quincy, MA (1990).
9. NFPA 12C-T, *Tentative Standard on Halon 2402 Fire Extinguishing Systems,* National Fire Protection Association, Quincy, MA (1983).
10. NFPA 75, *Standard for the Protection of Electronic Computer/Data Processing Equipment,* National Fire Protection Association, Quincy, MA (1992).
11. C. Ford, *Halon 1301 Computer Fire Test Program—Interim Report,* DuPont Co., Wilmington, DE (1972).
12. NFPA 2001, *Standard on Clean Agent Fire Extinguishing Systems,* National Fire Protection Agency, Quincy, MA (1994).
13. "DuPont Halon 1301 Fire Extinguishant," *Technical Bulletin B-29E,* DuPont Co., Wilmington, DE.
14. *Evaluation of Telephone Frame Fire Protection,* GTE/Fenwal, Holliston, MA (1970).
15. "Handling and Transferring 'Freon' FE 1301 Fire Extinguishing Agent," *Technical Bulletin FE-2,* DuPont Co., Wilmington, DE (1969).
16. D.G. Clark, *The Toxicity of Bromotrifluoromethane (FE 1301) in Animals and Man,* Ind. Hyg. Res. Lab., Imperial Chemical Industries, Alderley Park, Cheshire, England (1970).
17. R.D. Stewart, P.E. Newton, A. Wu, C. Hake, and N.D. Krivanek, *Human Exposure to Halon 1301,* Medical College of Wisconsin, Milwaukee, unpublished (1978).

18. The Hine Laboratories, Inc., *Clinical Toxicologic Studies on Freon Fe-1301, Report No. 1,* San Francisco, CA, unpublished report (1968).

19. J.L. Bryan, *Fire Suppression and Detection Systems,* Macmillan, New York (1982).

20. N. Sax, *Dangerous Properties of Industrial Materials,* Section 12, 2nd ed., Reinhold, New York (1963).

21. G.J. Grabowski, *Fire Detection and Actuation Devices for Halon Extinguishing System, An Appraisal of Halogenated Fire Extinguishing Agents,* National Academy of Sciences, Washington, D.C. (1972).

22. C. Ford, "Extinguishment of Surface and Deep-Seated Fires with Halon 1301," *Symposium of an Appraisal of Halogenated Fire Extinguishing Agents,* National Academy of Sciences, Washington, D.C. (1972).

23. H.V. Williamson, *Halon 1301 Flow Calculations—An Analysis of a Series of Tests Conducted by FEMA at the Fenwal Test Site,* Chemetron Corp., Hanover (1975).

24. C.C. Grant, "Computer Aided Halon 1301 Piping Calculations," *Fire Safety Journal,* (1985).

25. *Flow in Pipes—Pyroforane Halon 1301,* Produits Chimiques Ugine Kuhlmann, Corbevoie, France.

26. J.J. Brenneman and M. Charney, "Testing a Total Flooding Halon 1301 System in a Computer Installation," *Fire Journal,* 68, p. 6 (1974).

27. S.A. Chines, "Halon System Discharge Testing—An Authority Having Jurisdiction Point of View," *Seminar Paper for Fire Protection Halons and the Environment, NFPA Annual Meeting,* Cincinnati (1987).

28. C.C. Grant, "Controlling Fire Protection Halon Emissions," *Fire Technology,* 24, p. 1 (1988).

29. D.N. Keast, and H.S. Pei, "The Use of Sound to Locate Infiltration Openings in Buildings," *Proceedings of the ASHRAE-DOE Conference on the Thermal Performance of the Exterior Envelope of Buildings,* Orlando, FL, p. 85 (1979).

30. *Ultraprobe 2000 Data Sheet (acoustic sensor),* UE Systems, Elmsford, NY (2000).

31. A.K. Blomsterberg, and D.T. Harrje, "Approaches to Evaluation of Air Infiltration Energy Losses in Buildings," in *ASHRAE Transactions, Vol. 85, Pt. 2,* p. 797 (1979).

32. S.O. Andersen, "Halons and the Stratospheric Ozone Issue," *Fire Journal,* p. 56 (May/June 1987).

33. G. Taylor, "Achieving the Best Use of Halons," *Fire Journal,* 81, 3, p. 69 (1987).

CHAPTER 7

Halon Replacement Clean Agent Total Flooding Systems

Philip J. DiNenno

Introduction

The regulation of Halon 1301 under the Montreal Protocol and its amendments culminated in the phaseout of production of halons in the developed countries on December 31, 1993. This regulation engendered tremendous research and development efforts across the world in a search for replacements and alternatives. Over the past several years, several total flooding, clean agent alternatives to Halon 1301 have been commercialized, and development continues on others. In addition to clean total flooding gaseous alternatives, new technologies, such as water mist and fine solid particulate, are being introduced. This chapter focuses on total flooding clean agent halon replacements.

Table 4-7.1 is a summary of the most important halocarbon and inert gas extinguishing agents developed to date. The table gives the chemical name; trade name; American Society of Heating, Refrigerating, and Air-Conditioning Engineers, Inc. (ASHRAE) designation (for halocarbons); and chemical formula.

Characteristics of Halon Replacements

Clean fire suppression agents are defined as fire extinguishants that vaporize readily and leave no residue.[1] Clean agent halon replacements fall into two broad categories: (1) halocarbon compounds and (2) inert gases and mixtures. Halocarbon replacements include compounds containing carbon, hydrogen, bromine, chlorine, fluorine, and iodine. They are grouped into five categories: (1) hydrobromofluorocarbons (HBFC), (2) hydrofluorocarbons (HFC), (3) hydrochlorofluorocarbons (HCFC), (4) perfluorocarbons (FC or PFC), and (5) fluoroiodocarbons (FIC).

Philip J. DiNenno, P.E. is president of Hughes Associates Inc., a fire protection engineering research and development firm. He has been actively involved in the testing and development of halon replacement chemicals and alternative fire suppression technologies.

Table 4-7.1 *Commercialized Halon Replacement Nomenclature*

Chemical Name	Trade Name	ASHRAE Designation	Chemical Formula
Perfluorobutane	CEA-410	FC-3-1-10	C_4F_{10}
Heptafluoropropane	FM-200	HFC-227ea	CF_3CHFCF_3
Trifluoromethane	FE-13	HFC-23	CHF_3
Chlorotetrafluoroethane	FE-24	HCFC-124	$CHClFCF_3$
Pentafluoroethane	FE-25	HFC-125	CHF_2CF_3
Dichlorotrifluoroethane (4.75%)	NAF-SIII	HCFC Blend A	$CHCl_2CF_3$
Chlorodifluoromethane (82%)			$CHClF_2$
Chlorotetrafluoroethane (9.5%)			$CHClFCF_3$
Isopropenyl-1-methylcyclohexene (3.75%)			
N_2/Ar/CO_2	Inergen	IG-541	N_2 (52%) Ar (40%) CO_2 (8%)
N_2/Ar	Argonite	IG-55	N_2 (50%) Ar (50%)
Argon	Argon	IG-01	Ar (100%)

While the characteristics of halocarbon clean agents vary widely, they share several common attributes:

1. All are *electrically nonconductive.*
2. All are *clean agents;* that is, they vaporize readily and leave no residue.
3. All are *liquefied gases* or display analogous behavior (e.g., compressible liquid).
4. All can be stored and discharged from typical Halon 1301 hardware (with the possible exception of HFC-23, which more closely resembles 600 psig [40 bar] super-pressurized halon systems).
5. All (except HFC-23) use nitrogen superpressurization in most applications for discharge purposes.

6. All are less efficient fire extinguishants than Halon 1301 in terms of storage volume and agent weight. The use of most of these agents requires increased storage capacity.
7. All are total flooding gases after discharge. Many require additional care relative to nozzle design and mixing.
8. All produce more decomposition products (primary HF) than Halon 1301, given similar fire type, fire size, and discharge time.
9. All are more expensive at present than Halon 1301 on a weight (mass) basis.

Inert gas alternatives include nitrogen and argon, and blends of these. One inert gas replacement has a small fraction of carbon dioxide. Carbon dioxide is not an inert gas, because it is physiologically active and toxic at low concentrations (approximately 9 percent). Inert gas clean agents are stored as pressurized gases. They are electrically nonconductive, form stable mixtures in air, and leave no residue.

Extinguishing Mechanisms

Halocarbon clean agents extinguish fires by a combination of chemical and physical mechanisms, depending upon the compound. Chemical suppression mechanisms of HBFC and HFIC compounds are similar to Halon 1301; that is, the Br and I species scavenge flame radicals, thereby interrupting the chemical chain reaction. Other replacement compounds suppress fires primarily by extracting heat from the flame reaction zone, thereby reducing the flame temperature below that which is necessary to maintain sufficiently high reaction rates by a combination of heat of vaporization, heat capacity, and the energy absorbed by the decomposition of the agent.

Oxygen depletion also plays an important role in reducing flame temperature. The energy absorbed in decomposing the agent by breaking fluorine and chlorine bonds is quite important, particularly with respect to decomposition production formation. There is undoubtedly some degree of "chemical" suppression action in flame radical combustion with halogens, but it is considered to be of minor importance since it is not catalytic (e.g., one F radical combines with one H flame radical).

The lack of significant chemical reaction inhibition in the flame zone by HCFC, HFC, and FC compounds results in higher extinguishing concentrations relative to Halon 1301. The relative importance of the energy sink represented by breaking halogen species bonds results in higher levels of agent decomposition relative to Halon 1301.

Inert gas acts by reducing the flame temperature below thresholds necessary to maintain combustion reactions. This condition is created by reducing the oxygen concentration and by raising the heat capacity of the atmosphere supporting the flame. The addition of a sufficient quantity of inert gas to reduce the oxygen concentration below 12 percent (in air) will extinguish flaming fires. The agent concentration required is also a function of the heat capacity of the inert gas added. Hence, there are differences in minimum extinguishing concentration between inert gases.

Flame Suppression Effectiveness

Flame suppression effectiveness of total flooding halon replacement agents has been evaluated in a number of ways. The predominant small-scale test method for establishing flame extinguishing concentrations for liquid and gaseous fuels is the ICI cup burner or variations thereof.

Figure 4-7.1 is a schematic of the ICI cup burner. A small laminar flame is established above a "cup" of fuel surrounded by a cylindrical chimney. An air/agent mixture flows up the chimney surrounding the flame. The minimum concentration of agent (in air) at which the flame is extinguished is the minimum extinguishing concentration (MEC). There are many variations of the basic device as used by different laboratories. These variations include cup and chimney diameter, different mixing and measuring methods, chimney height, and agent/air mixture velocity past the flame.[2] Table 4-7.2 gives some indication of the variation in cup burner extinguishing concentration for a range of extinguishment concentrations for a range of agents with *n*-heptane as the fuel.
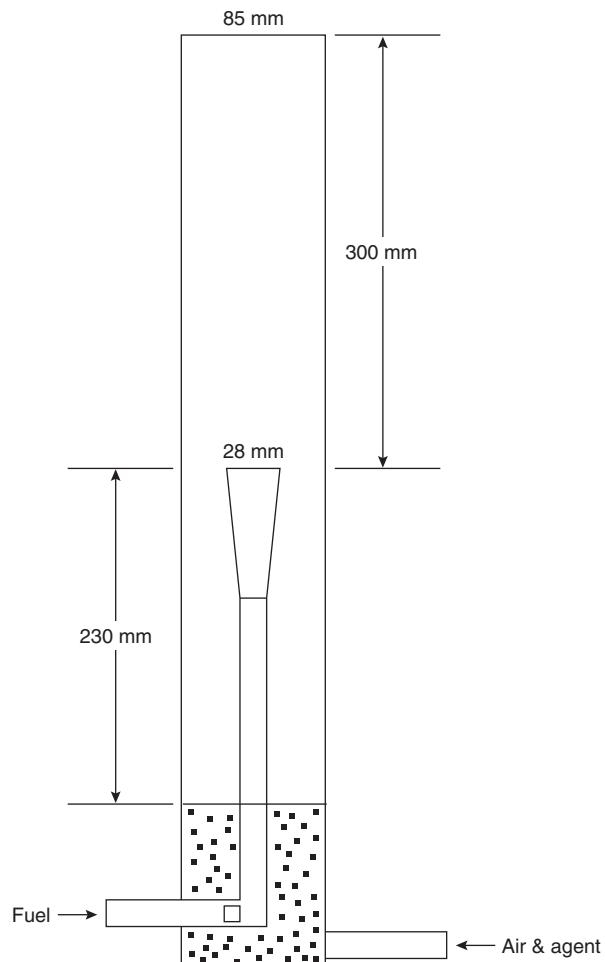

Figure 4-7.1. *Schematic of ICI cup burner apparatus.*[2]

Table 4-7.2 *n-Heptane Cup Burner Extinguishing Values from Various Investigators (from NFPA 2001,[1] except as noted)*

Reference	Nitrogen	FC-3-1-10	HFC-227ea	HFC-23	Halon 1301
Sheinson	30[3]	5.2	6.6	12	3.1
3M		5.9	—	—	3.9
NMERI[a]		5.0	6.3	12.6	2.9
Senecal, Fenwal		5.5	5.8	12 (13)	3 (3.5)
Robin			5.9	12.7	3.5
NIST[b]	32	5.3	6.2	12	3.2

[a]New Mexico Engineering Research Institute

[b]National Institute of Standards and Technology

Table 4-7.3 *Agent Fraction in the Oxidizer Stream at Extinction of n-Heptane Cup Burner Flames[3]*

Agent Type	Agent	Mass Percent	Volume Percent
Inert	N_2	31	32
	CO_2	32	23
	He	6.0	31
	Ar	38	41
Nitrogen containing	NF_3	a	a
Silicon containing	SiF_4	36	13
Sodium containing	$NaHCO_3$ (10–20 μm)	3.0	b
Hydrofluorocarbons	CF_3H	25	12
	CF_2H_2	c	c
	CF_2H_2/C_2HF_5	30	15
	CH_2FCF_3	29	10
	CHF_2CF_3	29	8.7
	$CF_3CH_2CF_3$	27	6.5
	C_3HF_7	28	6.2
Fluorocarbons	CF_4	37	16
	C_2F_6	30	8.1
	C_3F_6	29	7.3
	C_3F_8	30	6.3
	$c\text{-}C_4F_8$	32	6.3
	C_4F_{10}	32	5.3
Chlorine containing	CHF_2Cl	28	12
	$CHCl_2F$	32	11
	CH_3CF_2Cl	c	c
	$CF_2 = CHCl$	c	c
	$CF_2 = CFCl$	31	10
	$CHFClCF_3$	26	7.0
Bromine containing	CF_3Br	14	3.1
	CF_2Br_2	16	2.6
	CH_2BrCF_3	17	3.5
	$CH_2 = CHBr$	c	c
	$CF_2 = CFBr$	27	6.3
	$CF_2 = CHBr$	24	6.0
Iodine containing	CF_3I	18	3.2

[a]Acted as an oxidizer, promoted flame stability

[b]Solid powder not expressed in volume percent.

[c]Agent observed to be flammable.

Given the wide variation in test methods, the minimum extinguishing concentrations measured from these different devices are reasonably close.

The cup burner can also be used to establish the MEC for inert gases; Ansul obtained a value of 2.91 percent for IG-541. This result is in contrast to concentrations of 32, 41, and 23 percent by volume measured by the National Institute of Standards and Technology (NIST) for nitrogen, argon, and carbon dioxide, the components of Inergen.

NIST has conducted investigations on a wide range of halon replacement chemicals for aviation use. In order to give a wider perspective on the type and range of chemicals being evaluated for fire suppression use, Table 4-7.3 is included. The table gives cup burner *n*-heptane flame extinction data for a wide range of potential halon replacements.

Table 4-7.4 presents cup burner MEC for a range of fuels and agents taken from various sources. Where multiple values of the MEC were found, they are given. The nitrogen data are presented as representative inert gas values. Argon/N2 blend MEC values would be higher. These data should not be used for design purposes without ensuring that the concentrations are consistent with system manufacturer requirements and third-party approvals.

Table 4-7.5 presents cup burner and full-scale data from VdS. Table 4-7.6 is a compilation of "best values" of cup burner data from a range of sources compiled by Tapscott.

In addition to the cup burner apparatus, researchers at NIST have utilized an opposed-flow diffusion flame (OFDF) apparatus to rank halon replacements for fire extinguishing effectiveness. The OFDF burner is commonly used for combustion research. It has many advantages as a research tool for fundamental combustion studies. Its primary advantage is in its ability to relate the results to fundamental predictions of flame structure and conditions at flame extinction. The oxidizer (and suppressant) stream is forced down onto the fuel surface, exhaust gases are drawn down through an annulus or jacket around the fuel cup, and a flat flame is established. Water cooling is provided for the fuel cup and exhaust gas.

The OFDF burner can vary the turbulence intensity or strain rate of the flame. For most applications of clean agent fire suppression, the strain rate is not a major concern, but in specialized applications, such as engine nacelles with high fuel and oxidizer flow rates or in high-pressure spray or jet fires, the strain rate will substantially impact the minimum condition for extinguishment. Figure 4-7.2 is a sample plot showing the variation of the mole fraction of extinguishing agent versus the strain rate at extinction for n-heptane fuels for a range of suppressants. For typical natural fires, the strain rate is approximately 25 s^{−1}. At high strain rates, the flame is extinguished at lower agent concentrations.

Figure 4-7.3 shows the relationship between MEC for the cup burner and OFDF apparatus. As expected, the cup burner concentration is quite similar to the OFDF concentration at a low strain rate (25 s^{−1}), typical of natural fires. In all cases, the MEC of agent is much lower for high strain rate flames. This further reinforces the value of

Table 4-7.4 *Cup Burner Minimum Extinguishing Concentrations*

Fuel	Cup Burner Extinguishment Concentration (Vol %)				
	HFC-227ea[b]	FC-3-1-10	HFC-23	HCFC Blend A	N_2
Acetone	6.8	5.5[e]			
Acetonitrile	3.7				
AV gas	6.7				
n-Butanol	7.1				
n-Butyl acetate	6.6				
Cyclopentanone	6.7				
Diesel no. 2	6.7				
Ethanol	8.1	6.8[e]			
Ethyl acetate	5.6				
Ethylene glycol	7.8				
Gasoline (unleaded)	6.5				
n-Heptane	6.0[a]	5.2[c]	12.0[c]	12.6[d]	32[a]
	5.8–6.6[c]	5.0[d]	12.6[d]		
Hydraulic fluid	5.8	4.3–4.5[a]			22–26[a]
JP-4	6.6				
JP-5	6.0[a]	4.8[a]			27[a]
	6.6[c]				
Methane	6.2				
Methanol	10.0	9.4[e]			
Methyl ethyl ketone	6.7				
Methyl isobutyl ketone	6.6				
Morpholine	7.3				
Propane	6.3	6.0[a]			32.5[a]
i-Propanol	7.3				
Pyrrolidine	7.0				
Tetrahydrofuran	7.2				
Toluene	5.8				
Turbo hydraulic oil 2380	5.1				
Xylene	5.3				

[a]From Reference 3
[b]From Reference 4
[c]From Reference 5
[d]From Reference 6
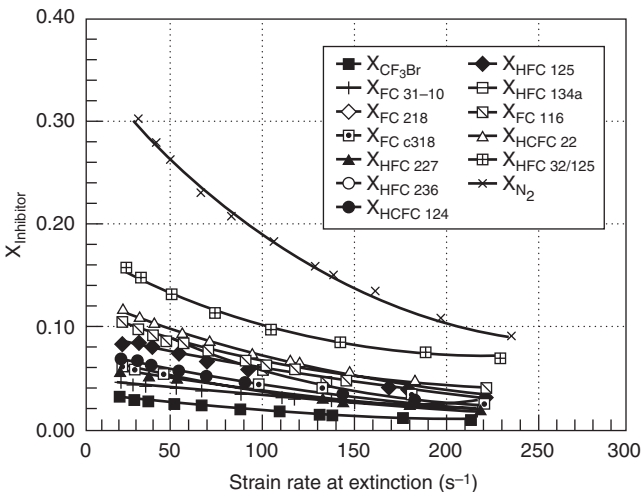[e]From Reference 7

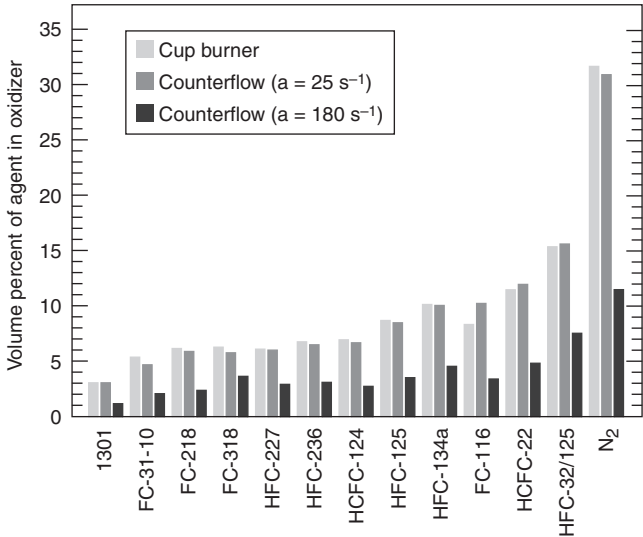**Figure 4-7.2.** *Mole fraction of various suppressants as a function of strain rate at extinction for n-heptane.*[3]

Figure 4-7.3. *Comparison of n-heptane extinction results for the cup burner and OFDF apparatus at two strain rates.*[3]

Table 4-7.5   *Inert Gas Extinguishing Concentration Data from VdS[8]*

Extinguishant Gas	Fuel	ISO Cup Burner		VdS Large Cup Burner (percent by volume gas)	Room Fire	
		Fuel Unheated (percent by volume gas)	Fuel Heated (percent by volume gas)		Extinguished (percent by volume gas[a])	Not Extinguished (percent by volume gas[a])
CO_2	Acetone	18.7	19.4	21.4		
	Diethyl ether	—	23.0			
	Ethanol	20.8	23.0			
	n-Heptane	19.6	21.1	23.3	24.1	23.1
	n-Hexane	20.4	21.3			
	Methanol	27.5	28.5	31.3		
	n-Pentane	—	21.6			
	Toluol	15.9	16.7			
	Polypropylene			21.5		
	Polyethylene			20.8		
	Wood crib				26.8	24.4
Argon	Acetone	37.8	38.8	43.7		
	Diethyl ether	—	44.8			
	Ethanol	41.4	44.1			
	n-Heptane	40.9	41.4	45.0	40.8	38.7
	n-Hexane	40.0	41.5			
	Methanol	52.2	55.6	54.5		
	n-Pentane	—	41.7			
	Toluol	32.7	35.5			
	Polypropylene			40.6		
	Polyethylene			37.8		
	Wood crib				30.7	29.0
Inergen	Acetone	29.4	31.7	35.9		
	Diethyl ether	—	35.7			
	Ethanol	32.8	35.5			
	n-Heptane	33.0	33.8	37.2	37.0	33.0
	n-Hexane	31.6	34.8			
	Methanol	41.1	43.8	47.3		
	n-Pentane	—	32.9			
	Toluol	25.7	28.1			
	Polypropylene			35.8		
	Polyethylene			31.3		
	Wood crib				28.1	26.6
Nitrogen	Acetone	28.5	29.9	33.2		
	Diethyl ether	—	33.8			
	Ethanol	32.1	34.5			
	n-Heptane	30.9	32.3	35.6	36.6	33.8
	n-Hexane	30.6	32.6			
	Methanol	38.5	41.2	44.8		
	n-Pentane	—	32.4			
	Toluol	22.2	28.0			
	Polypropylene			34.7		
	Polyethylene			30.8		
	Wood crib				28.6	27.7

[a]Calculated on the basis volume of discharged extinguishant

the cup burner and OFDF apparatus for evaluation of minimum extinguishing concentration.

Extinguishing concentrations for Class A fuels were traditionally developed using wood cribs as part of the equipment listing/approval process. Further, the minimum Class A extinguishing concentration used for design purposes was required to be greater than or equal to the minimum extinguishing concentration for heptane. Recently, additional tests utilizing plastic sheet arrays of polymethylmethacrylate (PMMA), acrylonitrile-butadiene-sytrene (ABS), and polypropylene (PP) have been required.[9,10] Typical results are shown in Figure 4-7.4

Table 4-7.6 *"Best Values" of Cup Burner Concentrations (vol %)[11]*

Fuel	Halon 1301	FC-3-1-10	FIC-13I1	HCFC Blend A	HCFC-124	HFC-125	HFC-227ea	HFC-23	HFC-236fa	IG-01	IG-100	IG-541	IG-55
70% isopropanol in water													26 (1)
80% methanol/ 20% n-heptane	5.8 (1)a	5.2 (1)					8.3 (1)a						
Acetone				10.0 ± 0.7 (2)a			6.8 ± 0.1 (2)a			38 (1)	29 (1)	29 ± 0.90 (3)	31 (1)
Acetonitrile				7.0 (1)a						33 (1)a			16 (1)
Aviation gas, 100 octane, low lead				11.4 ± 0.1 (2)a						32 (1)a		30 (1)	26 (1)
Benzene	2.4 (1)	3.4 (1)					4.8 (1)	10.6 (1)			31(1)		
n-Butanol				12.2 (1)a						36 (1)a			33 (1)
n-Butyl acetate				9.8 (1)a									36 (1)
Carbon disulfide													49 (1)
Cyclohexane				10.1 ± 0.3 (2)a						36 (1)a			32 (1)
n-Decane	3.9 (1)										34 (1)		
Diesel					6.8 (1)a								
Diesel no. 2				8.9 (1)						27 (1)a			26 (1)
Diethyl ether										45 (1)	34 (1)	36 (1)	
n-Dodecane	3.7 (1)										33 (1)		
Ethanol	4.3 ± 0.0 (2)	6.9 ± 0.0 (2)					8.5 ± 0.2 (2)	16.0 ± 0.0 (2)		41 (1)	35 ± 2.7 (3)	35 ± 3.3 (2)	30 (1)
Ethyl acetate				10.6 (1)a						35 (1)a			30 (1)
Ethylene glycol				11.1 (1)a						31 (1)a			30 (1)
Exxon Turbo Oil													16 (1)
Gasoline (unleaded)				9.7 (1)a	7.5 (1)a					37 (1)a			26 (1)
Heptane (commercial)	3.2 (1)						6.5 ± 0.2 (1)	12.6 ± 0.5 (2)				32 (1)	
n-Heptane	3.4 ± 0.0 (2)	5.4 ± 0.1 (3)	3.2 (1)a	9.9 (1)	6.7 ± 0.3 (3)a	8.9 (1)	6.6 ± 0.0 (5)	13.0 ± 0.2 (3)	6.3 ± 0.4 (3)a	42 ± 1.4 (3)	33 ± 1.6 (3)	31.2 (5)	35 ± 3.7 (2)
n-Hexane				11.0 ± 0.1 (2)a						40 (1)	31 (1)	31 ± 0.4 (2)	29 (1)
Hydraulic oil (Mobil Fluid 350)										26 (1)a			21 (1)
Hydrogen				20 (1)a									
Isobutanol													29 (1)
Isooctane				9.8 (1)a			5.9 (1)	11.3 (1)					
Isopropanol				10.6 (1)a			7.2 ± 0.2 (1)			35 (1)a		28 (1)	28 (1)
Jet A/JP-5				9.0 (1)a	6.9 (1)a					32 (1)a			26 (1)
JP-4				10.1 (1)a						32 (1)a			
JP-8				9.7 (1)									
Kerosene	3.4 (1)	5.0 (1)					6.4 (1)	12.5 (1)			30 (1)	31 (1)	
Methane				13.7 (1)a						35 (1)a			25 (1)
Methanol	7.8 (1)	8.0 (1)		17 (1)			10.2 ± 0.4 (3)	19 (1)	8.0 (1)a	52 (1)	41 ± 3.5 (2)	41 (1)	39 (1)
Methyl isobutyl ketone				9.4 (1)a									
Morpholine				13.7 (1)a						38 (1)a			
Natural gas				12.4 (1)a									
Nitromethane										34 (1)a			32 (1)
n-Octane	3.4 (1)										34 (1)		
n-Pentane											30 (1)a		
Propane				12.6 (1)a						40 (1)a			34 (1)
n-Propanol				10.6 (1)a									
Pyrrolidine				10.1 (1)a									31 (1)
Tetrahydrofuran				12.0 (1)a			4.8 ± 0.3 (4)	9.7 ± 0.0 (2)					32 (1)
Toluene	2.3 ± 0.0 (2)	3.6 ± 0.0 (2)		6.8 (1)			6.6 (1)	12.8 (1)		33 (1)	25 ± 2.0 (3)	25 ± 0.5 (2)	26 (1)
Transformer oil	2.3 (1)	5.4									27 (1)	28 (1)	
n-Undecane			3.8 (1)								33 (1)		
Xylene				8.7 (1)a						26 (1)a			24 (1)

Number in parentheses indicates the number of different data sources.
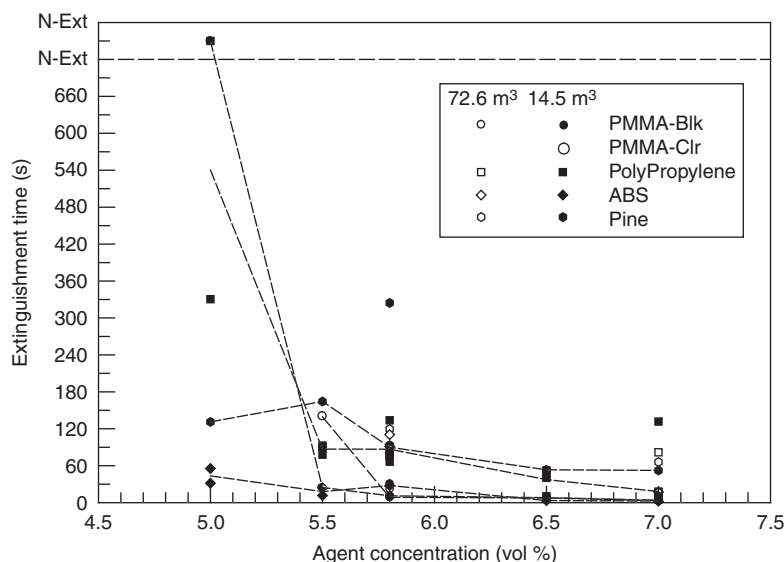
aNonstandard cup burner

Figure 4-7.4. *Typical Class A extinguishment results for HFC-227ea.*

for two different room sizes. The results of these tests indicate that for extinguishment times exceeding 3 min, the extinguishing concentrations for these materials are below the heptane cup burner value and in general well above the 10-min extinguishment time value for wood cribs.

Clean agent systems are widely used in electronic equipment areas where fires involving electrically energized cables and equipment are often encountered. Extinguishment tests involving PMMA heated externally with Nichrome wire indicated that agent concentrations substantially higher than those typical for plastic fuels were required. For example, extinguishing concentrations of 9.5, 9, and 20 percent were required for FC-3-1-10, HFC-227ea, and HFC-23, respectively.

Extinguishment tests on actual wire and cable materials were reported by McKenna et al.[12] Three types of tests were conducted: ohmic heating, conductive heating, and printed wiring board arcing. The ohmic heating tests involved deliberate electrical overheating of the conductor. These results are summarized in Table 4-7.7 for HFC-227ea. Note that even under severe overcurrent conditions, all cable assemblies were extinguished at 5.8 percent, a typical Class A extinguishing concentration. The one exception was the 18 AWG polyethylene (PE) coaxial cable, which is generally not used in power applications. The striking difference between these results and those discussed earlier for PMMA probably lies in the fire-retardant nature of real electrical wire and cable assemblies.

Results for cable assemblies heated at the ends by conduction, a situation simulating an overheated connection, showed results similar to the ohmic heating tests for Hypalon and PVC cables.

Tables 4-7.8 and 4-7.9 summarize the fire suppression capability of halon replacement agents relative to Halon 1301 for halocarbon and inert gas agents, respectively. Agent mass and storage volume ratio equivalents for Halon 1301 are given as 1. All comparisons are based on 120 percent of the agent manufacturer's recommended

MEC, based on the cup burner. The design values used are as provided by the manufacturer. Design values for HCFC Blend A and Argon are problematic, because these values are below the MEC as measured by the cup burner.

Note that all clean agent alternatives require at least 60 percent more agent by weight and storage volume. This requirement is a consequence of the elimination of bromine in the compounds and subsequent level of catalytic recombination of flame radicals. These data should be taken as representative values, as there are variations between hardware manufacturers.

The storage volume equivalents are based on the maximum fill density permitted in a storage cylinder with a pressure rating as recommended by the manufacturer. The approximate 10 : 1 storage volume requirement for inert gases is a consequence of the inability to liquefy these gases at ambient temperature.

The storage volume equivalent does not translate directly to a required area or volume for storage cylinders. The relative "footprint" of these storage volume equivalents will vary with the volume of the space protected and the maximum storage cylinder size offered by a manufacturer for a particular gas. In general, the floor area required for storage of inert gases exceeds 10 : 1 for large protected volumes.

Explosion Inerting

One of the most important application areas of total flooding fire suppressants is explosion inertion. The inerting concentration of an agent is the concentration required to prevent unacceptable pressure increases in a premixed fuel/air/agent mixture subjected to an ignition source. Inertion concentrations are typically measured in small laboratory-scale spheres, with an electric spark initiator.

The measured inerting concentration of an agent is dependent on the details of the test apparatus used, particularly the ignition source strength and "allowable" pressure rise. The allowable pressure rise is a surrogate

Table 4-7.7   *Summary of Ohmic Heating Tests with HFC-227ea*

Test	Sample	Current (A)	Orientation	Ignition Source	% C$_3$HF$_7$ (FM 200)	Time to Extinguish (s)
EEE035		350	Horizontal	Pilot	5.8	9
EEE036		350	Horizontal	Pilot	5.8	9
EEE046		350	Horizontal	Pilot	5.8	10
EEE049	8 AWG XLPE,	350	Horizontal	Pilot	5.8	13
EEE037	5 wire bundle,	350	Horizontal	Pilot	5.8	13
EEE038	center wire energized	350	Vertical	Pilot	5.8	8
EEE039		350	Vertical	Pilot	5.8	8
EEE054		350	Vertical	Pilot	5.8	10
EEE055		350	Vertical	Pilot	5.8	10
EEE040		350	Vertical	Pilot	5.0	11
EEE047		600	Horizontal	Pilot	5.8	11
EEE050	12 AWG SJTW-A,	600	Horizontal	Pilot	5.8	11
EEE053	6 cable bundle,	600	Horizontal	Pilot	5.8	9
EEE041	4 of 18 conductors	600	Horizontal	Pilot	5.5	9
EEE043	energized	600	Horizontal	Pilot	5.5	8
EEE044		600	Horizontal	Pilot	5.0	11
EEE056	8 AWG PVC,	325	Horizontal	Pilot	5.8	12
EEE059	7 cable bundle,	325	Horizontal	Pilot	5.8	10
EEE062	center wire energized	325	Horizontal	Pilot	5.8	13
EEE068		350	Horizontal	Pilot	6.8	12
EEE069		350	Horizontal	Pilot	6.8	13
EEE071		350	Horizontal	Pilot	6.5	15
EEE075		350	Horizontal	Pilot	6.5	11
EEE079	18 AWG chrome	350	Horizontal	Pilot	6.5	16
EEE076	PVC, over PE,	350	Horizontal	Pilot	6.2	DNE
EEE077	4 cable bundle,	350	Horizontal	Pilot	6.2	15
EEE078	12 conductors	350	Horizontal	Pilot	6.2	DNE
EEE058	energized	350	Horizontal	Pilot	5.8	12
EEE061		350	Horizontal	Pilot	5.8	DNE
EEE065		350	Horizontal	Pilot	5.8	10
EEE066		350	Horizontal	Pilot	5.8	11
EEE067		350	Horizontal	Pilot	5.8	DNE
EEE057	16 AWG neoprene	500	Horizontal	Pilot	5.8	3
EEE060	over rubber, 9 of 12	500	Horizontal	Pilot	5.8	6
EEE064	conductors energized	500	Horizontal	Pilot	5.8	6
EEE031		475	Horizontal	Self-ignited	6.8	14
EEE033		475	Horizontal	Self-ignited	6.8	14
EEE048	18 AWG PE,	475	Horizontal	Self-ignited	6.8	14
EEE029	4 parallel wire array,	475	Horizontal	Self-ignited	6.5	DNE
EEE030	all wires energized	475	Horizontal	Self-ignited	6.5	DNE
EEE028		475	Horizontal	Self-ignited	5.8	DNE
EEE026		475	Horizontal	Self-ignited	5.7	DNE

Time to extinguish is taken from the beginning of discharge.
DNE: did not extinguish

measurement of the distance the flame front travels inside the constant volume sphere prior to suppression. Inerting concentration is not appropriate for use in deflagration or detonation (explosion) suppression.

Small-scale sphere data are used to develop flammability diagrams for various fuel/oxidizer/agent concentrations. Section 2, Chapter 7, which addresses flammability limits, gives an excellent introduction to the subject. There is a wealth of data in the combustion literature on flamma-

bility limits for inert gases, such as nitrogen and argon, for a variety of fuels available.

Table 4-7.10 provides inerting concentration data for several agents and fuels, taken from small-scale inertion spheres.[13–15] There are some substantial differences in results. Heinonen[16] has identified both ignition source type and strength as important variables with differences of ±40 percent for Halon 1301 inerting concentrations reported. Figure 4-7.5 shows flammability

Table 4-7.8   Weight and Storage Volume Equivalent Data for New Technology Halocarbon Gaseous Alternatives

Trade Name	Designation	Formula		BP (°C)	Cup Burner (% V/V)[g]	Minimum Design Concentration . (% V/V)	Ratio Agent Mass Required to H 1301[e]	Ratio Agent Storage Volume Required to H 1301[f]	Storage Pressure (psi) 20°C
Halon 1301	Halon 1301	CF_3Br		−58	2.9–3.9	5[d]	1.0	1.0	360
CEA-410	FC-3-1-10	C_4F_{10}		−2	5.0–5.9	6[a,b]	1.9	1.7	360
FM-200	HFC-227ea	C_3F_7H		−16.4	5.8–6.6	7[a,b]	1.7	1.6	360
FE-13	HFC-23	CHF_3		−82.1	12–13	16[a]	1.7	2.2	609
FE-25	HFC-125	H_2HF_5		−48.5	8.1–9.4	10.9[a]	1.9	2.3	166
NAF-S-III	HCFC Blend A	HCFC-22	82%	—	>11	8.6[c]	1.1	1.4	360
		HCFC-123	4.75%						
		HCFC-124	4.5%						
		Organic	3.75%						
CF_3I	Halon 1301	CF_3I		−22.5	2.7–3.2	5.0	~1	~1	—

[a]Based on 120 percent of cup burner value for *n*-heptane

[b]Based on 120 percent of cup burner value verified by listing/approval tests

[c]Based on listing/approval tests

[d]Minimum design concentration per NFPA 12A, *Standard on Halon 1301 Fire Extinguishing Systems,* 1992 edition; cup burner value approximately 3 percent

[e]Ratio of halon design concentration 20.6 lb/ft³ at 70°C to new agent

[f] Ratio of halon storage volume required at minimum design concentration (max. fill density 70 lb/ft³) to new agent

[g]Range of independently established values

Table 4-7.9   Agent Weight and Storage Volume Equivalent Data for New Technology Inert Gas Alternatives

Trade Name	Designation	Formula		Cup Burner (% V/V) (*n*-heptane)	Minimum Design Concentration (% V/V)	Ratio Agent Mass Required to H 1301[b]	Ratio Agent Storage Volume Required to H 1301[d]	Storage Pressure (psi [bar]) 20°C
Halon 1301	Halon 1301	CF_3Br		2.9–3.9[c]	5[a]	1	1	360 (25)
Inergen	IG-541	N_2	52%	29.1[c]	35[f]	2.0	10.0[e]	2180 (150)
		Ar	40%					
Argonite	IG-55	CO_2	8%					
		N_2	50%	30[e]	~36[f]	2.0	10.0[e]	2220 (153)
Argon	IG-01	Ar	50%					
		Ar	100%	30[e]	~36[f]	2.0	8.0[e]	2370 (163)

[a]Minimum design concentration per NFPA 12A, *Standard on Halon 1301 Fire Extinguishing Systems,* 1992 edition; cup burner value approximately 3 percent.

[b]Ratio of halon design concentration 20.6 lb/ft³ at 70°C to new agent.

[c]Range of independently established values.

[d]Ratio of halon storage volume required at minimum design concentration (max. fill density 70 lb/ft³) to new agent.

[e]Manufacturers' values. MEC for argon is approximately 41 percent (see Reference 3).

[f] Based on 120 percent of cup burner value for *n*-heptane.

diagrams derived from small-scale inertion data such as that presented in Table 4-7.10, along with points taken from a large-scale (22.5 m³) explosion vessel. While the small- to large-scale agreement is reasonable, there are scale effects.

Explosion Suppression

Explosion suppression systems employ rapid delivery of agent following very early detection of an ignition. Such systems employ significantly higher agent quantities (than flame suppression or inertion), delivered at higher rates. The total agent delivery time is on the order of 100 milliseconds.

Explosion suppression systems must be specifically designed for a particular application. There are no generic design requirements or standards currently available for such systems.

Senecal[17] and Senecal et al.[18] report on explosion suppression testing in occupied armored fighting vehicles and aerosol filling rooms. Results were obtained on premixed fuel droplet sprays. In contrast to flame suppression or inerting, suppression or deflagration requires significantly more agent. The aerosol filling room tests employed 20 kg of HFC-227ea, FC-3-1-10, and HFC-236fa, and 10 kg of water in an 80-m³ test room to suppress a 90-g propane release in a simulated aerosol filling station. Suppression of the propane-air deflagration was achieved, and the maximum
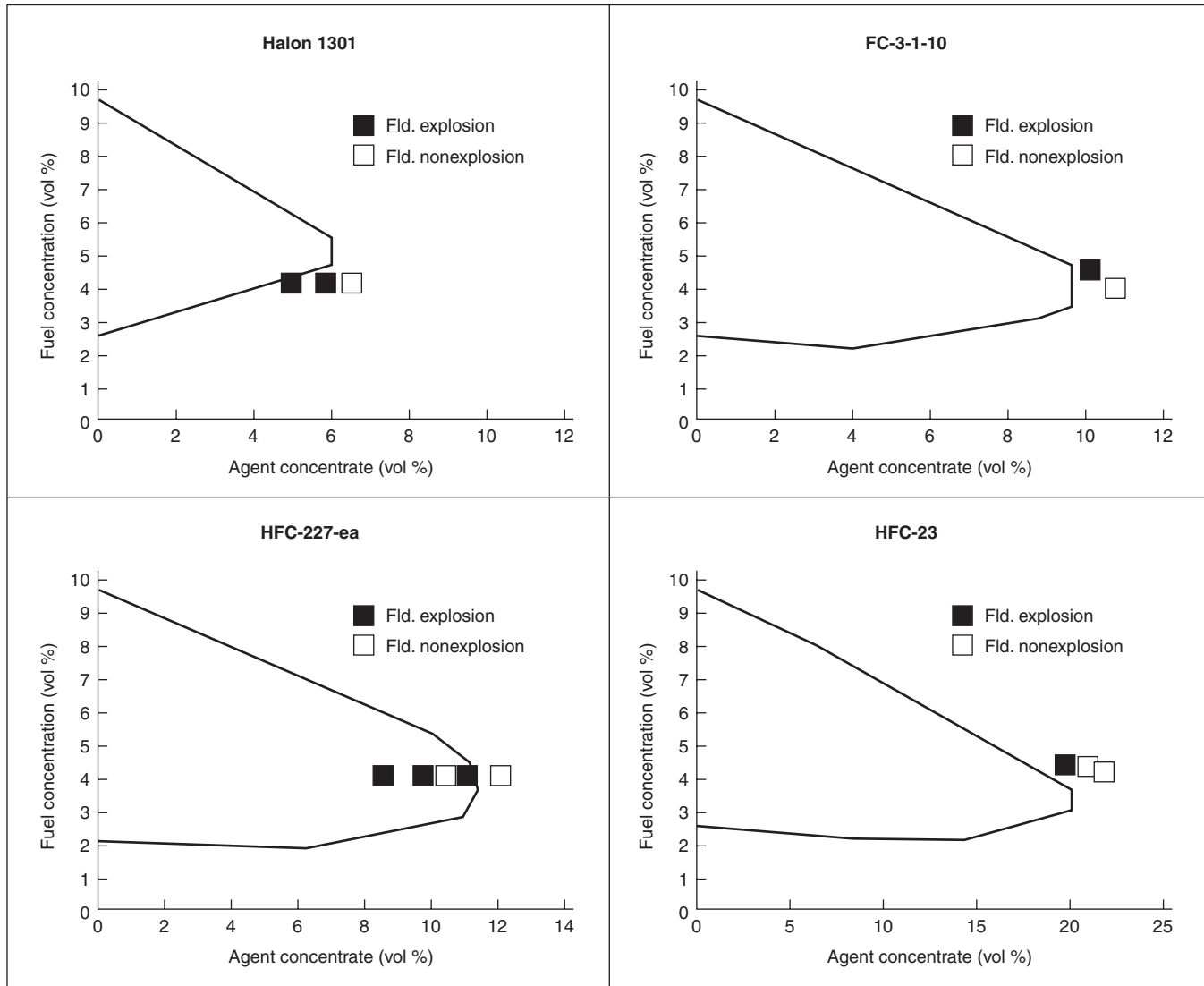
Figure 4-7.5. *Small-scale flammability diagrams for propane and several replacement agents. Squares denote explosion/nonexplosion points in large-scale 22.5 m³ chamber.*[19]

flame front extension was approximately 4 ft. Suppression tests of heated diesel fuel droplet cloud deflagrations were conducted in simulated armored fighting vehicle crew compartments.

Table 4-7.11 summarizes typical data for flame suppression, inertion, and deflagration suppression concentrations. Note these values are for comparison purposes only. They should not be used in any way for design purposes.

Suppression of detonations requires substantially higher agent concentrations. An excellent discussion is given in Reference 3.

Toxicity

A major factor in the use of a clean agent fire suppressant in a normally occupied area is toxicity. While all halocarbon agents are tested for long-term health hazards, the primary end point is acute or short-term exposure. The primary acute toxicity effects of the halocarbon agents described in this chapter are anesthesia and cardiac sensitization. For inert gases, the primary physiological concern is reduced oxygen concentration.

Halocarbon agents: Cardiac sensitization is the primary short-term toxicity problem for fire suppression applications. Cardiac sensitization is a term describing the sudden onset of cardiac arrhythmia in the presence of a concentration of an agent, caused by sensitization of the heart to epinephrine. The presence of epinephrine is critical to the onset of arrhythmia. This knowledge is important in fire protection applications because production of epinephrine is increased by the body under stress.

Table 4-7.10 *Explosion Inerting Concentrations, Small-Scale Inertion Sphere*

Agent	Inerting Concentration (vol %) of Fuel			
	Propane	Methane	*i*-Butane	Pentane
FC-3-1-10	10.3[b]	~7.8[d]	—	
	9.5[d]			
HFC-227ea	12.0[d]	8.0[d]	11.3[b]	11.6[a]
	11.6[a]			
HFC-23	20.2[b]	20.2[b]	—	
	19.8[d]	14.0[d]		
IG-541	49.0[c]	43.0[c]	—	
HCFC Blend A	18.0[d]	13.3[d]		

[a]From Reference 4
[b]From Reference 13
[c]From Reference 14
[d]From Reference 15

Table 4-7.11 *Comparison of Concentrations for Flame Extinguishment, Inertion, and Deflagration Suppression*

Agent	Volume (%)		
	Typical Value Flame Suppression	Inerting Concentration in Propane	Diesel Fuel Droplet Deflagration Suppression
Halon 1301	3	6–7	12
FC-3-1-10	5.5	10.3	8
HFC-227ea	5.8	~12	11
HFC-23	12	20.2	—
IG-541	29	49.0	—

The two toxicity end points used to describe cardiotoxicity and allowable exposure levels are (1) no observed adverse effect level (NOAEL) and (2) the lowest observed adverse effect level (LOAEL). The NOAEL is the highest concentration of an agent at which no "marked" or adverse effect occurred. The LOAEL is the lowest concentration at which an adverse effect was measured.

The procedures used to evaluate cardiac sensitization vary somewhat. The procedure involves intravenous dosing of male beagle hounds with epinephrine for 5 min. Continuous inhalation exposure to the agent follows for 5 min. Following this inhalation exposure, the hound is dosed again with epinephrine and monitored for 5 min to determine the effect of the agent and epinephrine. The protocol is performed at higher doses until an effect occurs.

Effects are monitored by electrocardiograph (EKG) measurements. An adverse effect is generally considered to be the appearance of five or more arrhythmias or ventricular fibrillation. The data from these tests are evaluated by medical experts, and the appropriate NOAEL and LOAEL values are reported by the Environmental Protection Agency (EPA) under the Significant New Alternatives Policy (SNAP) program.

There is no direct correlation between the experimental results from hounds to humans. It is generally accepted, due to the combination of the high doses of epinephrine in the tests and the similarity in cardiovascular function between hounds and humans, that the results can be applied to humans.

In addition to the short-term chronic exposure limits of interest in fire suppression system design, the EPA evaluates longer term inhalation data for these compounds. Table 4-7.12 summarizes NOAEL, LOAEL, and LC_{50} values. Note that the LC_{50} (the concentration lethal to 50 percent of a population) values greatly exceed the NOAEL at typical fire extinguishing concentrations.

Recently, the exposure limits for halocarbon agents have been modified. Physiologically based pharmacokinetic modeling (PBPK) for evaluation of acute exposure to

Table 4-7.12 *Toxicity Data for Halocarbon Clean Agent Fire Suppressants*

Trade Name	Designation	Formula		NOAEL % V/V[a]	LOAEL % V/V[a]	LC_{50} or ALC[b]
CEA-410	FC-3-1-10	C_4F_{10}		40	>40[c]	>80%
FM-200	HFC-227ea	C_3F_7H		9.0	>10.5	>80%
FE-13	HFC-23	CHF_3		50	>50[c]	>65%
FE-24	HCFC-124	C_2HClF_4		1	2.5	23–29%
FE-25	HFC-125	H_2HF_5		7.5	10.0	>70%
NAF-S-III	HCFC Blend A	HCFC-22	82%	10	>10	64%
		HCFC-123	4.75%			
		HCFC-124	4.5%			
		Organic	3.75%			
CF_3I	Halon 1301	CF_3I		0.2	—	—

[a]From EPA SNAP documents

[b]From NFPA 2001 *Standard on Clean Agent Fire Extinguishing Systems,* 1994 edition

[c]Maximum concentration before oxygen depletion

halocarbon agents has been used to establish alternative exposure limits for halogenated agents.[20] PBPK modeling attempts to account for the time-dependent uptake rate of halocarbons in the body and establishes exposure limits based on the rate of uptake.[21–25] The limits are based on the concentration of agent and the time at which the concentration of agent in the blood equals that of the LOAEL. Typical PBPK results for safe exposure times for HFC-227ea and HFC-125 are given in Table 4-7.13. Note that exposure above the NOAEL limits and up to the LOAEL is permitted.

These limits were derived and supported by the EPA, which has the primary regulatory authority for health and toxicity associated with halon replacements. The use of the PBPK approach partially accounts for the differences between laboratory animal tests and humans. The laboratory results form the basis of the end points (LOAEL) and are still conservative due to the nature of epinephrine dosage used during the animal tests.[26]

Where PBPK modeling data do not exist, the use of halocarbon agents in occupied areas is subject to the constraint that the design concentration must be less than the NOAEL. While it is recommended that all systems employ predischarge alarms and that personnel evacuate prior to system actuation, it is understood that inadvertent discharges and short-term exposures will occur, hence the limitation. It is expected that emergency exposures for up to several minutes at or below the NOAEL are reasonably safe. In no case should systems be designed or installed where intentional exposure of any duration is anticipated.

It has been proposed by the EPA that agents be permitted for use at concentrations up to the LOAEL where evacuation will occur in less than 60 s. This proposal has not been integrated into design standards to date due to the uncertainty of accidental exposure conditions.

Table 4-7.13   *Exposure Limits Derived from PBPK Modeling for HFC-227ea and HFC-125*[20]

HFC-227ea Concentration			HFC-125 Concentration		
% V/V	ppm	Human Exposure Time (min)	% V/V	ppm	Human Exposure Time (min)
9.0	90,000	5.00	7.5	75,000	5.00
9.5	95,000	5.00	8.0	80,000	5.00
10.0	100,000	5.00	8.5	85,000	5.00
10.5	105,000	5.00	9.0	90,000	5.00
11.0	110,000	1.13	9.5	95,000	5.00
11.5	115,000	0.60	10.0	100,000	5.00
12.0	120,000	0.49	10.5	105,000	5.00
			11.0	110,000	5.00
			11.5	115,000	5.00
			12.0	120,000	1.67
			12.5	125,000	0.59
			13.0	130,000	0.54
			13.5	135,000	0.49

Based on the limitation that the design concentration must be below the NOAEL, it can be seen from Table 4-7.12 that three agents are acceptable for use in normally occupied areas for flame extinguishant purposes: HFC-227ea, HFC-23, and FC-3-1-10.

Inert gas agents: Inert gas agents are, in effect, physiologically inert. The primary physiological problem with these agents is the reduced oxygen concentration caused by the high agent design concentrations. One inert gas blend employs a low concentration of CO_2 (which is not physiologically inert) in order to counter the effects of the reduced oxygen concentration. The mechanism of this effect is discussed in Reference 27.

Current limitations on exposure limits for inert gases are as follows: for gas concentrations up to 43 percent (a residual oxygen concentration of 12 percent), exposure time is limited to 5 min. For agent concentrations between 43 and 52 percent (12 and 10 percent residual oxygen concentration), the exposure time is limited to 3 min. For concentrations greater than 52 percent, exposure time is limited to 30 s.

There is strong indication that small concentrations of CO_2 added to inert gases (such as IG-541) substantially reduce hypoxic effects and improve human performance at low oxygen levels. Regulatory authorities have not yet differentiated between such agents and other inert gases or blends.[27]

Environmental Factors

The evaluation of clean agent fire suppressants includes a consideration of environmental factors. International, national, and local government regulations control the use of any alternatives in this regard. The primary environmental consideration is ozone depletion potential (ODP). ODP is a measure of a chemical's ability to deplete stratospheric ozone, with CFC-12 as a basis with an ODP of 1. All chemicals with non-zero ODP are subject to phaseout under the Montreal Protocol and its amendments. Table 4-7.14 summarizes environmental impact data for halocarbon alternatives. Note that FC and HFC compounds have zero ozone depletion potential. The HCFC compounds have quite low ODP. Other HCFC compounds are widely used as CFC replacements for refrigerants.

Other environmental factors that are potentially important in a regulatory context are global warming potential (GWP) and atmospheric lifetime. GWP is a measure of the contribution of a gas to the so-called greenhouse effect. It is a function of atmospheric lifetime and the ability of the gas to absorb infrared radiation. The evaluation of GWP is an extremely complex issue, and, currently, none of these compounds are regulated on that basis in the United States. Long atmospheric lifetime, a measure of the persistence of a chemical in the atmosphere, is of concern not only as it relates to GWP, but also due to the uncertainty of the effects of chemicals for long time periods in the atmosphere. The EPA currently has use restrictions on FC-3-1-10 based primarily on its long atmospheric lifetime. These restrictions permit the use of this chemical

Table 4-7.14 *Environmental Factors for Halocarbon Clean Agents*

Trade Name	Designation	Formula		ODP	GWP (100 yr)	Atmospheric Lifetime (yr)
Halon 1301	Halon 1301	CF_3Br		16	5800	100
CEA-410	FC-3-1-10	C_4F_{10}		0	5500	2600
FM-200	HFC-227ea	C_3F_7H		0	2050	31
FE-13	HFC-23	CHF_3		0	9000	280
FE-24	HCFC-124	C_2HClF_4		0.022	440	7
FE-25	HFC-125	H_2HF_5		0	3400	41
NAF-S-III	HCFC Blend A	HCFC-22	82%	0.05	1600	16
		HCFC-123	4.75%			
		HCFC-124	4.5%			
		Organic 3	3.75%			
CF_3I	Halon 1301	CF_3I		<0.2	0	—

in applications where no other alternative is technically feasible.

Thermophysical Properties

Tables 4-7.15 and 4-7.16 give thermophysical properties of clean agent replacements from NFPA 2001,[1] in English and SI units, respectively. Table 4-7.17, extracted from Reference 28, gives independent data and estimates for some thermophysical properties. Additional thermophysical and transport property data can be found in Reference 4 for FM-200, and Reference 28 for a range of halocarbon alternatives.

Isometric diagrams for halocarbon agents HFC-227ea, pressurized at 360 and 600 psig at 70°F with nitrogen, and HFC-23 are given in Figures 4-7.6, 4-7.7, and 4-7.8, respectively. Note that HFC-23 is not pressurized with nitrogen. Figure 4-7.9 gives the pressure/temperature relationship

Table 4-7.15 *Thermophysical Properties of Clean Halocarbon Agents (English units)*

	Units	FC-3-1-10	HCFC Blend A	HCFC-124	HFC-125	HFC-227ea	HFC-23	IG-541	IG-55	IG-01
Molecular weight	—	238.03	92.90	136.5	120.2	170.03	70.01	34.0	33.95	39.9
Boiling point @ 760 mm Hg	°F	28.4	−37.0	12.2	−55.3	2.6	−115.7	−320	−310.2	−302.6
Freezing point	°F	−198.8	<−161.0	−326.0	−153	−204	−247.4	−109	−327.5	−308.9
Critical temperature	°F	235.8	256.0	252.0	150.8	215.0	78.6	—	−210.5	−188.1
Critical pressure	psia	337	964	524.5	521	422	701	—	602	711
Critical volume	ft³/lbm	0.0250	0.0280	0.0283	0.0281	0.0258	0.0305	—	—	—
Critical density	lbm/ft³	39.3	36.00	35.28	35.68	38.76	32.78	—	—	—
Specific heat, liquid @ 77°F	Btu/lb·°F	0.25	0.30	0.270	0.301	0.2831	0.370	—	—	—
Specific heat, vapor @ constant pressure (1 atm) & 77°F	Btu/lb·°F	0.192	0.16	0.177	0.191	0.2054	0.176	0.195	0.187	0.125
Heat of vaporization at boiling point	Btu/lb	41.4	97	83.2	70.8	57.0	103.0	94.7	77.8	70.1
Thermal conductivity of liquid @ 77°F	Btu/h·ft·°F	0.0310	0.052	0.0417	0.0376	0.040	0.0450	—	—	—
Viscosity, liquid @ 77°F	lb/ft·hr	0.783	0.508	0.723	0.351	0.443	0.201	—	—	—
Relative dielectric strength @ 1 atm @ 734 mm Hg 77°F (N_2 = 1.0)	—	5.25	1.32	1.55	0.955 @70°F	2.00	1.04	1.03	1.01	1.01
Solubility of water in agent @ 70°F	—	0.001% by weight	0.12% by weight	0.07% by weight @ 77°F	0.07% by weight @ 77°F	0.06% by weight	500 ppm @ 50°F	0.015%	0.006%	0.006%
Vapor pressure @ 77°F	psi	38.8	1.37	56	199	66.4	686.0	2207	—	—

Table 4-7.16   *Thermophysical Properties of Clean Halocarbon Agents (SI units)*

	Units	FC-3-1-10	HCFC Blend A	HCFC-124	HFC-125	HFC-227ea	HFC-23	IG-541	IG-55	IG-01
Molecular weight	—	238.03	92.90	136.5	120.2	170.03	70.01	34.0	33.95	39.9
Boiling point @ 760 mm Hg	°C	−2.0	−38.3	−11.0	−48.5	−16.4	−82.1	−196	−190.1	−185.9
Freezing point	°C	−128.2	<−107.2	−198.9	−102.8	−131	−155.2	−78.5	−199.7	−189.4
Critical temperature	°C	113.2	124.4	122.2	66.0	101.7	25.9	—	−134.7	−122.5
Critical pressure	kPa	2323	6647	3614	3595	2912	4836	—	4150	4860
Critical volume	cc/mol	371	162	241.6	210	274	133	—	—	—
Critical density	kg/m³	629	577	565	571	621	525	—	—	—
Specific heat, liquid @ 25°C	kJ/kg°C	1.047	1.256	1.13	1.260	1.184	1.549	—	—	—
Specific heat, vapor @ constant pressure (1 atm) & 25°C	kJ/kg°C	0.804	0.67	0.741	0.800	0.8082	0.737	0.574	0.782	0.523
Heat of vaporization at boiling point	kJ/kg	96.3	225.6	194	164.7	132.6	239.6	220	181	162.2
Thermal conductivity of liquid @ 25°C	W/m°C	0.0537	0.0900	0.0722	0.0651	0.069	0.0779	—	—	—
Viscosity, liquid @ 25°C	centipoise	0.324	0.21	0.299	0.145	0.184	0.083	—	—	—
Relative dielectric strength @ 1 atm @ 734 mm Hg 25°C ($N_2 = 1.0$)	—	5.25	1.32	1.55	0.955 @ 21°C	2.00	1.04	1.03	1.01	1.01
Solubility of water in agent @ 21°C	—	0.001% by weight	0.12% by weight	0.07% by weight @ 25°C	0.07% by weight @ 25°C	0.06% by weight	500 ppm @ 10°C	0.015%	0.006%	0.006%
Vapor pressure @ 25°C	kPa	267.5	948	386	1371	457.7	4729	15,200	—	—

Table 4-7.17   *Selected Properties of Agents[28]*

	FC-3-1-10	HFC-227ea	HCFC-124	HFC-125	HFC-23
Boiling point @ 0.101 MPa (°C)	−2.0	−16.4	−13.2	−48.6	−82.1
Critical temperature (°C)	113.2	101.7	122.5	66.3	25.6
Critical pressure (MPa)	2.32	2.9	3.65	3.62	4.82
Vapor pressure @ 25°C (MPa)	0.27	0.47	0.38	1.38	4.73
Liquid density at 25°C (kg/m³)	1497	1395	1401	1245	669
Liquid heat capacity @ boiling point (kJ/kg·K)	0.951	1.074	1.080	1.107	1.269
Liquid heat capacity at 25°C (kJ/kg·K)	1.047	1.184	1.111	1.26	1.55
Latent heat of vaporization at boiling point (kJ/kg)	96	132.6	194	160	240

for inert gases IG-541, IG-55, and IG-01, pressurized to 2175 psig, at 70°F. This display is the pressure/temperature relationship for an ideal gas.

Clean Agent System Design

Once the agent has been selected, the general discussion on clean agent system design presented by Grant in Section 4, Chapter 6 should be reviewed. The basic process is outlined below:

1. Determine the design concentration.
2. Determine the total agent quantity.
3. Establish the maximum discharge time.
4. Select piping material and thickness consistent with pressure rating requirements.
5. Design piping network and select nozzles to deliver required concentration at required discharge time to ensure mixing.
6. Evaluate compartment over/underpressurization and provide venting if required.
7. Establish minimum agent hold requirements and evaluate compartments for leakage.

These attributes apply only to the mechanical design of the system.

The detection and actuation systems are critical and integral parts of a clean agent system design. The detection system should be designed to actuate the system, with ap-
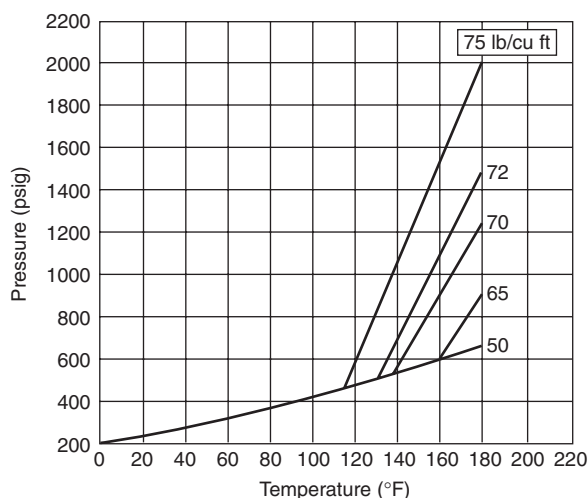
Figure 4-7.6. *Isometric diagram of HFC-227ea, pressurized to 360 psig with N$_2$, at 70°F.*[4]
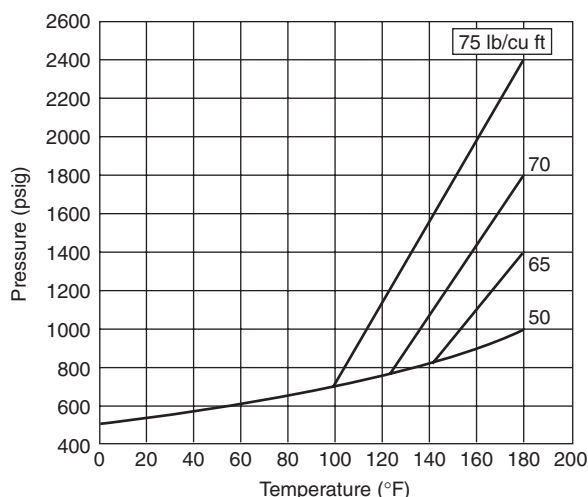

Figure 4-7.7. *Isometric diagram of HFC-227ea, pressurized to 600 psig with N$_2$, at 70°F.*[4]

propriate pre-discharge alarms, before unacceptable thermal or nonthermal damage occurs. This aspect is particularly important where the thermal decomposition products of halocarbon clean agents are a concern. Section 4, Chapter 1 provides engineering methods and calculation procedures for this purpose.

In addition to the detection, actuation, and alarm systems, the enclosure itself is critical in the design of any total flooding suppression system. The most important considerations are that the enclosure be of sufficient integrity to (1) prevent preferential agent loss during discharge and (2) prevent excessive agent/air mixture loss after discharge to ensure adequate hold time.

As a general rule, all openings, notably doors and ventilation fans and/or openings, must be secured prior to discharge in conjunction with the detection and alarm
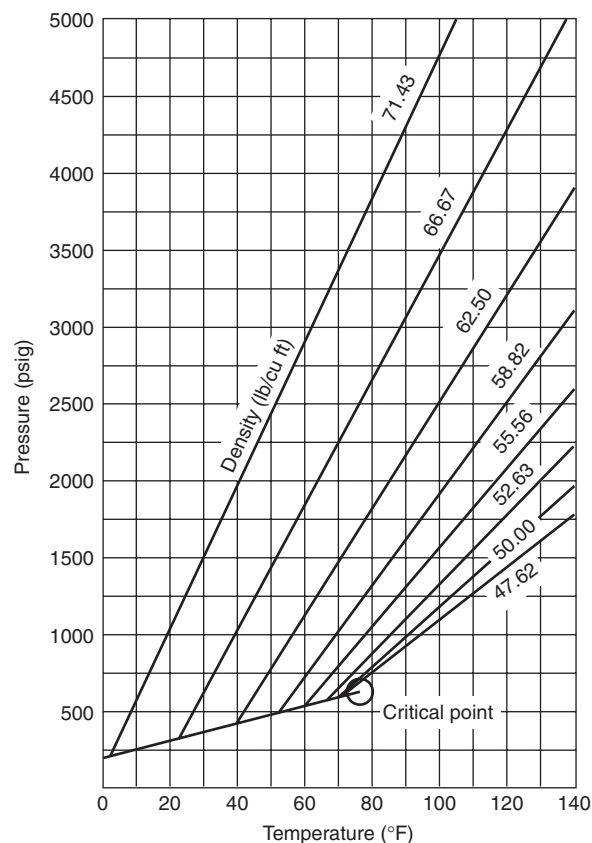
Figure 4-7.8. *Isometric diagram of HFC-23.*[1]

systems. Agent system installation in rooms with unclosable openings should not be attempted unless sufficient test data are available to ensure adequate concentrations. Some enclosures, such as very tightly sealed low EMF emission electronics spaces, require additional care to avoid compartment damage due to over/underpressurization during agent discharge.

Design Concentration

Flame extinguishment: Design concentrations for various agents and fuel combinations are generally determined by a combination of small-scale testing, large-scale testing, independent laboratory approval of hardware, and addition of design safety factors.

Historically, minimum design concentrations for Halon 1301 were set by the cup burner extinguishing concentration plus a 20 percent safety factor. A minimum Halon 1301 design concentration of 5 percent was also established for all applications. For heptane, the cup burner value was approximately 3 percent; with a 20 percent safety factor, a design concentration of 3.6 percent is obtained. At the minimum design concentration set by NFPA 12A, *Standard on Halon 1301 Fire Extinguishing Systems*, 1992 edition, of 5 percent, a 66 percent safety factor was achieved. For fuels with cup burner extinguishing concentrations greater than 4.2 percent, the safety factor remained at 20 percent.
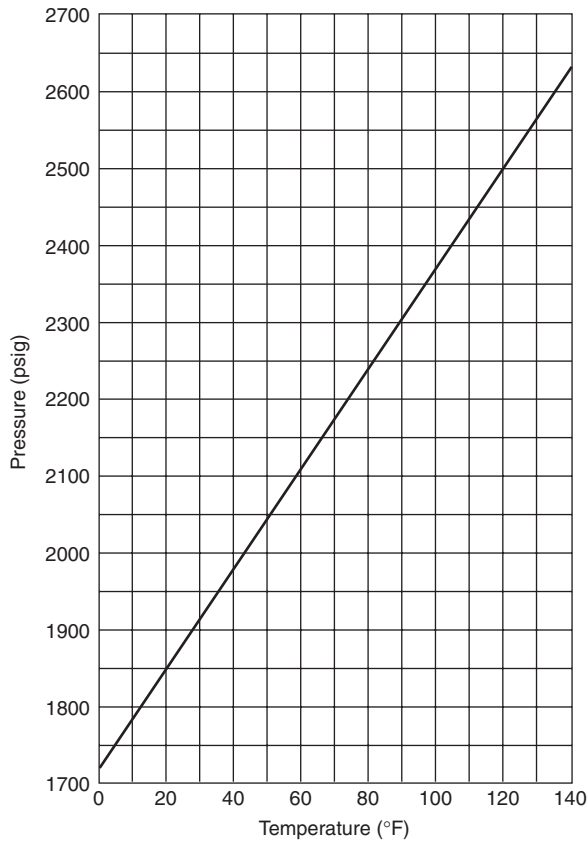
Figure 4-7.9. *Isometric diagram of inert gases and blends, treated as ideal gases, pressurized to 2175 psig, at 70°F.*[1]

The basic requirement for determining the design concentration of clean agents in NFPA 2001, *Standard on Clean Agent Fire Extinguishing Systems,* 1994 edition, is two-fold. First, the minimum extinguishing concentration as determined by the cup burner must be established. Second, after this minimum is established by the *system* manufacturer, full-scale third-party approval testing is conducted using the manufacturer's hardware on heptane, wood crib, and selected flammable liquids. These tests are performed at the cup burner minimum extinguishing concentration, not the design concentration. Further, they are conducted with flooding factors lower than utilized in design. Hence, the minimum set by the cup burner or equipment manufacturer, whichever is higher, is tested in full scale as part of the approval/listing process for the agent/system combination. Often, hardware manufacturers will establish a minimum concentration greater than the cup burner value to account for nozzle inefficiency.

There has been some full-scale test work that indicates that the 20 percent safety factor may be insufficient. Sheinson et al. noted significant improvement in extinguishing time performance with a safety factor of 40 percent.[29] Brockway noted similar results, with no performance improvement beyond a safety factor of 40 percent.[30]

Analysis by Schlosser[31] indicated that the probability of failure of a system was reduced from approximately 15

to 10 percent when the safety factor increased from 20 to 30 percent. In addition to these data, the variation in cup burner values used as a basis for design concentration was significant due in part to a lack of standardization in the method. Some full-scale test results[32] also indicated a need for higher design concentrations.

Based on these factors, the first edition of ISO 14520-1 required a minimum safety factor of 30 percent.[33] The current edition of NFPA 2001[20] requires a 30 percent safety factor for Class B hazards and for any system actuated by manual means only.

In addition to increased safety factors, the concept of design factors was introduced into the 2000 edition of NFPA 2001. A design factor is used to increase the agent quantity for a specific installation or design that has attributes for which the minimum safety factor may not be sufficient. The only variable for which design factors have been quantified is for systems with multiple flow splits protecting more than four enclosures simultaneously. The motivation for a design factor in these rare cases is the uncertainty in the split of agent mass flow at unbalanced tee junctions and the compound of that uncertainty with more than four tees in series.

It has also been noted by several investigators that higher safety factors result in lower thermal decomposition products.[29,30,34] None of the above referenced investigations utilized listed or approved hardware for the specific agents tested; as in most cases, the tests were performed before such hardware was available.

There is an exception in NFPA 2001, to the general rule that a minimum extinguishing concentration be established by the cup burner method. It was alleged that reliable cup burner data were not available for HCFC Blend A due to the fact that (1) the agent was a blend and (2) one of the blend components heats at a low vapor pressure. In the case of this agent, a minimum extinguishing concentration of 7.2 percent and, hence, a design concentration of 8.6 percent was established through limited full-scale testing. Since at the time insufficient data were available to evaluate the claim, the exception that requires full-scale testing at minimum extinguishing concentration consistent with UL 1058, *Halogenated Agent Extinguishing System Units,*[35] was invoked. Since that time, reliable cup burner data were obtained for the blend from several laboratories. The data are consistent with MEC values for the blend components, primarily HCFC 22. Furthermore, some full-scale testing has indicated that the design concentration of 8.6 percent may be inadequate.[36] This issue is, however, unresolved at the present time.

For Class A fires, NFPA 2001 requires full-scale testing and third-party approval for evaluating design concentration on solid polymeric materials. In many cases, the MEC for heptane is used as a practical minimum.

There has been no systematic evaluation of these agents under so-called "deep-seated" fire scenarios. Part of the problem is the circular definition of deep-seated fires in NFPA 12A. However, the Underwriters Laboratories Inc. (UL) and Factory Mutual Research Corporation (FMRC) listing procedures require testing on wood cribs subsequent to long preburn times (approximately 5 min). Under these tests, surface oxidation and char reactions do occur.

Design concentrations for fire scenarios involving long preburn times in thick arrays of cellulosic fuels will require additional testing. For most applications where incidental quantities of cellulosic materials may be involved and preburn times are relatively short (<5 min) time frames (i.e., automatic actuation), the flame extinguishing concentrations for Class A fuels will be less than, or equal to, that of n-heptane and can be used. Surface oxidation or charring reactions do not occur with most polymers; hence, so-called "deep-seated" fires are not a concern where Class A fuels are involved.

IG-541 is used at 37.5 percent minimum design concentration where Class A materials are involved. Other inert gases should have similar or higher minimum design concentrations.

As previously discussed, the minimum design concentration is a function of the fuel, the agent, and the delivery systems. Design concentrations for specific hazards must be determined in accordance with the system manufacturer's approval or listing.

Agent Quantity

Once the design concentration is established, the quantity of agent necessary to achieve that concentration is determined. The quantity of halocarbon agent necessary is determined by the following equation:

$$w = \frac{V}{S}\left(\frac{C}{100 - C}\right) \tag{1}$$

where

V = net volume of protected space

C = design concentration (%)

w = specific weight of agent required

S = specific volume [ft³/lb (m³/kg)] and is determined by

$$S = k_1 + k_2(T) \tag{2}$$

where T is the minimum ambient temperature of the protected space, and k_1 and k_2 are constants. Values for k_1 and k_2 used in Equation 2 are given in Table 4-7.18.

The flooding factor in Equation 1 $[C/(100 - C)]$ implies that the agent/air mixture "lost" during discharge is well mixed and has an agent concentration of C. This formula makes no assumption regarding leakage of the enclosure. During UL/FMRC approval testing, the agent is evaluated with a flooding factor of $(C/100)$, essentially assuming that losses during discharge are 100 percent air.

For inert gases, the following formula is used:

$$X = 2.303 \frac{V}{S} \log\left(\frac{100}{100 - C}\right) V_s \tag{3}$$

where

X = volume of inert gas required at 70°F

V_s = specific volume at 70°F

V = net protected hazard volume

S = specific volume at ambient temperature in protected volume (from Equation 2) = $k_1 + k_2 (T)$

Table 4-7.18 *Specific Volume Constants*

Agents	°F		°C	
	k_1	k_2	k_1	k_2
FC-3–1-10	1.409	0.0031	0.0941	0.0003
HCFC Blend A	3.612	0.0079	0.2413	0.00088
HCFC-124	2.352	0.0057	0.1578	0.0006
HFC-125	2.724	0.0063	0.1701	0.0007
HFC-227ea	1.885	0.0046	0.1269	0.0005
HFC-23	4.731	0.0107	0.2954	0.0012
IG-541	9.7261	0.0211	0.649	0.00237
IG-01	8.514	0.0185	0.5685	0.00208
IG-55	10.0116	0.0217	—	—

The flooding factor used here, log $[100/(100 - C)]$, is derived assuming that leakage from the compartment during discharge occurs with a varying concentration of agent from zero to C from beginning to the end of discharge. It is identical to the expression used in CO_2 system design. It assumes that the displaced atmosphere is freely vented from the enclosure.

Discharge Time

The maximum discharge time permitted for halocarbon clean agent systems is 10 s. This discharge time is taken to be the moment where all liquid agent has cleared the nozzle. The total discharge time will be longer as agent vapor and nitrogen are expelled from the system.

The 10-s discharge time limitation for halocarbon agents is designed to aid four objectives:

1. Provide high flow rates through nozzles to ensure adequate mixing of agent with air inside the enclosure.
2. Provide sufficient velocity through pipes to ensure homogeneous flow of liquid and vapor.
3. Limit the formation of agent thermal decomposition products.
4. Minimize direct and indirect fire damage, particularly in fast-developing fire scenarios.

The most important of these objectives relative to discharge time is the minimization of agent thermal decomposition product formulation. Items 1 and 2 alone are determined by the piping system design.

The discharge time requirement for inert gases is currently 60 s.[1] Longer discharge times are typically used for these systems in Europe. The two primary reasons to constrain the discharge time of inert gas agents that form no thermal decomposition products are (1) to limit the direct and indirect fire damage and (2) to minimize the length of time that the fire burns in a depleted oxygen atmosphere. As more information is developed on the effect of discharge time on inert gas agent performance, this 60-s limit may be increased for certain applications.

In some applications, such as flammable liquid hazards and explosion inerting, it is necessary to discharge the agent quickly to minimize direct fire damage or to ensure that the agent concentration is achieved prior to the lower explosive limit (LEL) being reached.

Thermal Decomposition Products

All of the halocarbon replacement agents form higher levels of thermal decomposition products than Halon 1301 under similar conditions. For a given fuel, the two primary variables determining the level of decomposition products are (1) the size of the fire at the time of discharge and (2) the time required to reach an extinguishing concentration in the compartment.

The dependence of thermal decomposition product formulation on discharge time and fire size has been extensively evaluated.[29–34,36–39] Figure 4-7.10 from Reference 36 is a plot of peak HF concentration as a function of fire size to room volume ratio. Similar data for 10-min average HF concentrations are given in Figure 4-7.11. Data are given for Halon 1301, HFC-23, HFC-227ea, FC-3-1-10, and HCFC Blend A from three series of fire tests done at different room scales. The data are for a total discharge time of 15 s, which is analogous to a 10-s discharge time based on nozzle liquid runout. The data are for heptane pool or heptane pool and spray fires.

The first observation is that the quantity of HF formed is approximately five to ten times higher for all halocarbon replacements relative to Halon 1301. There may be differences between the various HFC/HCFC compounds tested, but it is not clear from these data whether such differences (1) occur, (2) are attributable to agent mixing and distribution, or (3) are attributable to locally high velocities or concentrations of agent from the nozzle. In all of the data reported, the fire source, that is, heptane pans of varying sizes, was baffled to prevent direct interaction with the agent jet.

These data were taken with an FTIR spectrometer at a location approximately 1 m from the floor, or about mid-flame height, near the wall. The method used was correlated to grab sample and ion-specific electrode (ISE) methods.[37] In all cases, the agreement was good, except for the HCFC blend. In this case, the HF concentration inferred from the treated grab sample was significantly
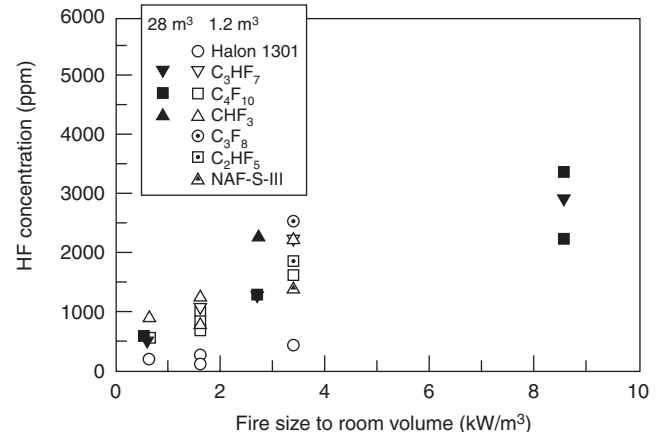

Figure 4-7.11. *Average HF concentration resulting from extinguishment of heptane pool or heptane pool and spray fires with nominal 15-s total discharge time.*[37]

(>50 percent) higher than that measured using the FTIR. Since the HCFC blend contains an HF "scrubber," it is postulated that treatment of the grab sample with a basic solution, as required for the ISE measurements, caused formation of additional HF by reentry with F loosely bound up by reaction with the scrubber. Hence, the FTIR data presented for HCFC Blend A represent a significantly lower quantity of HF than would actually be expected if the product was hydrolyzed. This condition is also consistent with the fact that the agent was tested at the manufacturer's recommended design concentration, which is approximately 40 percent lower than the basis for all other agents.

The effect of long discharge times or delayed extinguishing times is shown in Figure 4-7.12.[37] The variation between the HFC/HCFC alternatives and Halon 1301, relative to HF production, is approximately the same as that shown in Figure 4-7.11 for different fire sizes.
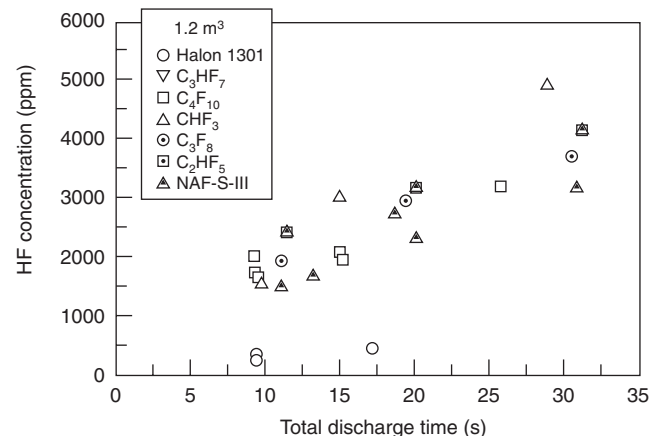

Figure 4-7.10. *Maximum HF concentration resulting from extinguishment of heptane fires with nominal 10–15 s total discharge times.*[36]

Figure 4-7.12. *Maximum HF concentration resulting from extinguishment of 4.0-kW heptane fires.*[37]

Although other thermal decomposition products have been identified in some cases, it appears that HF is the primary thermal decomposition product of interest relative to human safety and equipment damage.

HF, like HCl, is an irritant gas, detectable at very low concentrations. For HF there are very large differences between the approximate lethal concentration (ALC) and human detection and severe sensory irritant thresholds (approximately two and three orders of magnitude, respectively).

Fire size necessary to generate short-term lethal concentrations of HF in an enclosure (on the order of >1000 ppm) can, in some cases, pose a greater hazard to personnel in the protected space during a discharge in a fire incident, due to the fire and its effects, than the secondary impact of agent thermal decomposition products. This, however, should be verified for a particular application under a range of fire scenarios, using engineering methods discussed by Hanauska[40] and Hanauska et al.[41]

The production of HF and other agent decomposition products forms a potential hazard for occupants. Table 4–7.19[20] summarizes potential health effects in healthy individuals. Note that exposure above 200 ppm may begin to impair escape particularly at exposure times exceeding 5 min.

Emergency Response Planning Guidelines (ERPG) values, developed by the American Industrial Hygiene Association, for 10-min exposures, are as follows: ERPG-2, a level at which mitigating steps such as evacuation should be taken is 50 ppm, and ERPG-3, the maximum non-lethal exposure concentration for 10 min is 170 ppm. The ERPG values are in contrast to an analysis by Melchrum,[42] which indicates that a dose of 12,000 ppm/min has 1 percent lethality in exposed animals. Additional health-effect and risk-assessment data are given in References 43 to 46.

The impact of thermal decomposition products on electronics equipment is another area of concern. There are not sufficient data at present to predict the effects of a given HF exposure scenario on all electronics equipment. Several evaluations of the impact of HF on electronics equipment have been performed relative to the thermal decomposition of Halon 1301, where decomposition products include HF and HBr. One of the more notable was a NASA study where the shuttle orbital electronics were exposed to 700, 7000, and 70,000 ppm HF and HBr.[40] In these tests, exposures up to 700 ppm HF and HBr caused no failures. At 7000 ppm, severe corrosion was noted; there were some operating failures at this level.

Dumayas exposed IBM-PC-compatible multifunction boards to environments produced by a range of fire sizes as part of an evaluation program on halon alternatives.[47] He found no loss of function of these boards following a 15-min exposure to postfire extinguishment atmosphere up to 5000 ppm HF, with unconditioned samples stored at ambient humidity and temperature conditions for up to 30 days. Forssell et al.[48] exposed multifunction boards for 30 min in the postfire extinguishment environment; no failures were reported up to 90 days posttest. HF concentrations up to 550 ppm were evaluated.

While no generic rule or statement can be made at present, it appears that short-term damage (<90 days) resulting in electronics equipment malfunction is not likely for exposures of between 500 to 1000 ppm HF for up to 30 min. This result, however, is dependent on the characteristics of the equipment exposed, postexposure treatment, exposure to other combustion products, and relative humidity. Important equipment characteristics include its location in the space, existence of equipment enclosures, and the sensitivity of the equipment to damage.

All HCFC and HFC clean agents form more thermal decomposition products than Halon 1301, given similar fire sizes and discharge times. The primary variable controlling the quantity of thermal decomposition products is the size of the fire at the time of agent discharge. Through evaluation of the fire size at the time of system actuation, using engineering methods described in Section 4, Chapter 1, and subsequent design of the detection system, the potential hazard posed can be managed adequately.

Hanauska[40] and Hanauska et al.[41] have indicated that the degree of thermal decomposition products of agents can be managed safely. Full-scale testing with typical Class A fuel packages, in conjunction with typical detection system installation,[48] has shown that the level of thermal decomposition products is acceptable in typical computer/electronics spaces. For installation in hazard areas where very rapidly developing large fires are likely, the degree of thermal decomposition formation should be

Table 4-7.19 *Potential Human Health Effects of Hydrogen Fluoride in Healthy Individuals[20]*

Exposure Time	Hydrogen Fluoride (ppm)	Reaction
2 min	<50	Slight eye and nasal irritation
	50–100	Mild eye and upper respiratory tract irritation
	100–200	Moderate eye and upper respiratory tract irritation, slight skin irritation
	>200	Moderate irritation of all body surfaces, increasing concentration may impair escape
5 min	<50	Mild eye and nasal irritation
	50–100	Increasing eye and nasal irritation, slight skin irritation
	100–200	Moderate irritation of skin, eyes, and respiratory tract
	>200	Definite irritation of tissue surfaces, will impair escape at increased concentrations
10 min	<50	Definite eye, skin, and upper respiratory tract irritation
	50–100	Moderate irritation of all body surfaces
	100–200	Moderate irritation of all body surfaces, escape-impairing effects likely
	>200	Escape-impairing effects will occur, increasing concentrations can be lethal without medical intervention

evaluated in the context of the hazard posed by the fire and the performance of alternative fire protection systems.

Hydraulic Flow Characteristics

All halocarbon replacement agents exhibit two-phase flow behavior. Since all, except HFC-23, are used in cylinders pressurized to 360 or 600 psig, they are also multiple-component flows. Inert gas mixtures are single-phase gas flows with one or more components. As in the case of engineered Halon 1301 systems, all flow calculation procedures used must be listed or approved by the authority having jurisdiction, and be within the limitations of the flow calculation method determined during the engineered system approval process.

The characteristic that differentiates two-phase pipe flow from incompressible fluid (e.g., water) pipe flow is the existence of gas and liquid phases simultaneously in the pipe network. This aspect, coupled with the relatively short flow times, results in significant challenges to correctly predicting the flow. Among the important factors are the change in density of the fluid with pressure, the release of nitrogen in the cylinder and pipe as the fluid pressure and temperature change, differences in agent mass delivered caused by the flow time imbalances between nozzles, and preferential distribution of phases (and subsequently agent mass) at tee splits.

The need for accurate flow predictions is driven by three design requirements:

1. Control of agent discharge time
2. Maintenance of adequate nozzle flow and pressure to ensure agent distribution and mixing at the listed coverage area
3. Delivery of adequate, but not excessive, agent quantities to different rooms within the same protected area, when such rooms are flooded simultaneously

In addition, agent flow rate and thermodynamic state properties are necessary for estimating compartment pressurization levels during agent discharge.

For pre-engineered systems, limits on discharge time and nozzle pressure are built into the limits on piping system geometry. Agent distribution is handled by constraining pre-engineered systems to balanced flow conditions (i.e., the same agent mass is distributed from each nozzle). For adequate design of engineered systems, accurate methods for predicting these elements are required.

Figure 4-7.13 is an idealized plot of cylinder and nozzle pressure during discharge. Throughout the discharge process the amount of agent vapor and liquid, as well as dissolved and gaseous nitrogen, varies. As the pressure decreases in the cylinder and piping system, more agent is vaporized and nitrogen is released from the solution in the agent. The formation of additional vapor and nitrogen bubbles lowers the average density of the fluid. The rapid vaporization of agent is more pronounced in low boiling point/high vapor pressure agents. The fluid temperature also varies with time and along the length of the piping network. The fluid temperature also impacts the degree of agent vaporization and nitrogen release as well as liquid agent density. The discharge process can be divided into five sections.
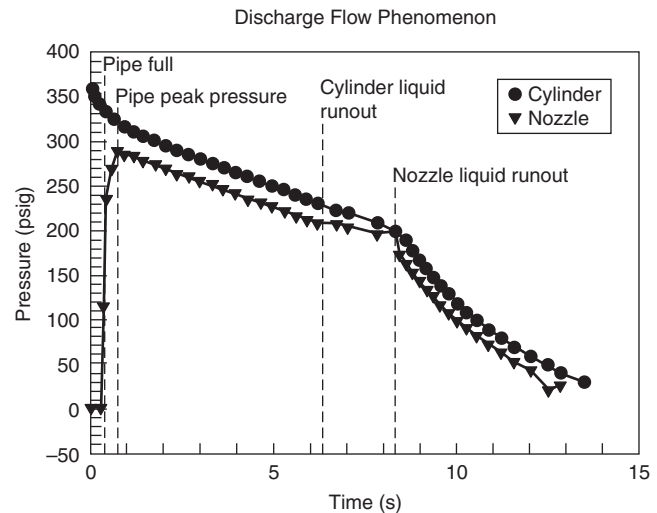

Figure 4-7.13. *Idealized cylinder and nozzle pressure time curves for halocarbon agents.*

The first is the process of filling the pipe with agent. The rate at which this process occurs is driven by the speed of the agent interface moving through the network. This speed is determined by either the sonic velocity at the agent interface or the discharge of displaced air through the nozzle. This phase determines the time at which the agent discharges from each nozzle. For systems with high degrees of imbalance in terms of flow path length or large pipe volume differences between nozzles, there can be significant delay in agent reaching one nozzle before another. This delay has a dramatic effect on the distribution of mass from each nozzle.

Once the agent reaches the nozzle and is compressed in the pipeline, the so-called nozzle peak pressure is reached. At this moment, agent is discharging from each nozzle.

The next step in the discharge process is the so-called quasi-steady agent flow regime. This step is generally the longest portion of the discharge, particularly for systems with low pipe volume to agent volume ratios. This period of the discharge process is the basis for the simplified pressure drop calculations embodied in NFPA 12A for balanced Halon 1301 systems.

The next milestone during the discharge process is cylinder liquid runout, where no liquid agent remains in the cylinder. At this moment, an interface between liquid agent and nitrogen/agent vapor forms and travels through the network.

When the trailing liquid/vapor interface reaches the first nozzle, nozzle liquid runout occurs. This runout is important in two ways. First, liquid runout occurs at different times during the discharge for each nozzle and can significantly impact the quantity of agent flowing from any given nozzle. Second, it is possible in many circumstances to discharge sufficient vapor/gas mixture from the first nozzle at NLRO (nozzle liquid runout) to reduce the pressure in the piping below that necessary to flow the remaining agent in the network. This aspect is

especially important for low vapor pressure agents and for nozzle designs requiring relatively high minimum operating pressures.

Once all of the nozzles have been cleared of liquid agent, the system is discharging a combination of nitrogen and agent vapor. This regime is usually ignored since most (>95 percent) of the agent has already been delivered through the nozzles.

The importance of the pipe filling and nozzle runout with these alternatives is relatively more critical with low vapor pressure alternatives due to (1) the inability of the agent to deliver significant pressure to the system by boiling and (2) the higher fluid densities that occur in the piping relative to Halon 1301.

Figures 4-7.14(a) through (d) illustrate the stages of the agent discharge network.

Flow regime: If the flow velocity of the agent in the piping is not high enough, the flow may separate into two distinct phases in the piping. This occurrence causes severe problems at tee splits and in evaluating pressure drops. Therefore, minimum flow rates that ensure a homogeneous mixture of agent liquid and vapor/nitrogen bubbles must be maintained. Various flow regimes are illustrated in Figures 4-7.15 and 4-7.16 for horizontal and vertical pipe, respectively. One of the objectives of approval testing of flow calculation procedures is to ensure

► Pressure decrease

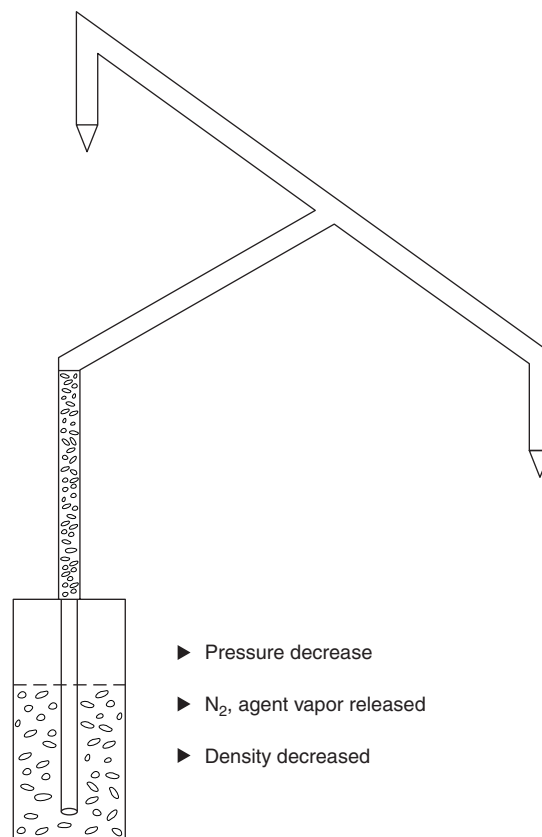► N_2, agent vapor released

► Density decreased

Figure 4-7.14(b).   *Valve open, pipe filling.*

that homogeneous flow regimes are maintained in the piping throughout the discharge process. In Figures 4-7.15 and 4-7.16, these are denoted as dispersed bubble and bubble flow regimes, respectively.

Flow division at tees: For a single-component, single-phase flow condition, the flow split at a tee junction is determined by the flow rate of the nozzles downstream of the tee. For two-phase fluids, flow distribution occurs at tees that are sensitive to the velocity of the flow along each branch of the tee, the orientation of the tee, the pressure at the tee, and the phase distribution of the fluid (gas or liquid) entering the tee.

The primary cause of preferential flow splits at tees is the inertia of the liquid versus vapor/gas phase. This condition is most readily envisioned for side-flow tees where one branch of the flow is required to turn 90 degrees. Gas/vapor bubbles with lower momentum relative to the liquid agent will make this change of direction more readily. This change results in relatively less mass flow down the side-flow branch at approximately the same volumetric flow rate or velocity. For bullhead tees, the same problem applies, except that it is more subtle and involves velocity differences through each branch of the tee. For evenly split (50 percent/50 percent) flows, the velocity is identical in both directions, resulting in no flow split correction; as the split becomes greater the velocity
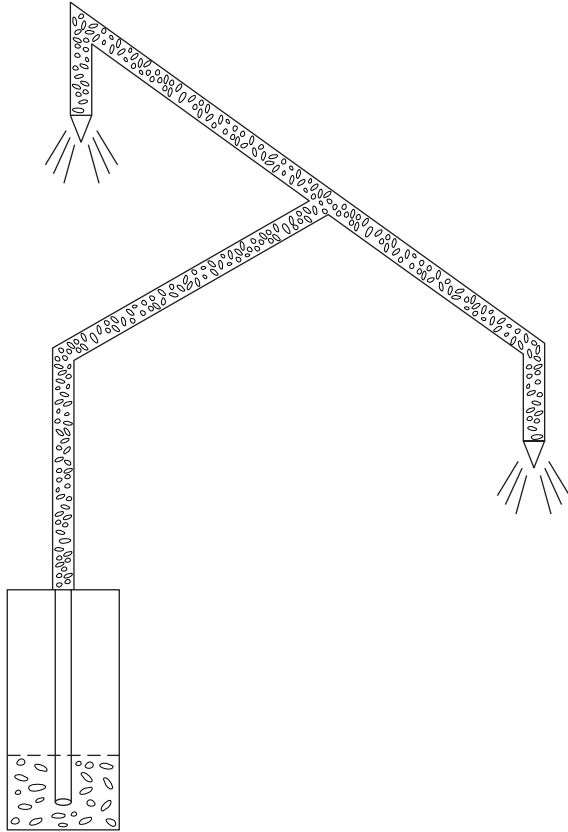

Nozzle

Nozzle

Valve

Agent vapor / N_2

Agent vapor / N_2 (dissolved)

Cylinder

Figure 4-7.14(a).   *Initial conditions.*

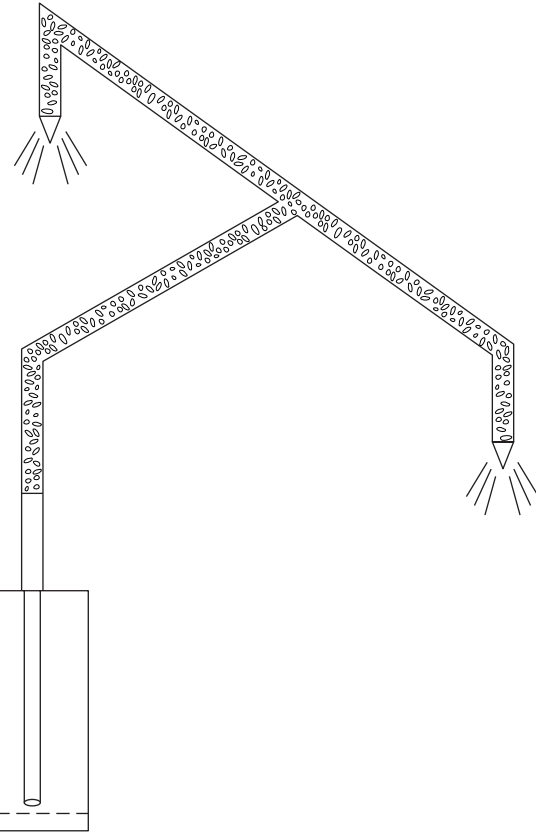**Figure 4-7.14(c).** *Quasi-steady flow, liquid throughout network.*

Figure 4-7.14(d). *Cylinder liquid runout.*

differences are greater, and inertial effects of the gas/vapor relative to the liquid cause significant redistribution of mass through each branch of the tee.

The dependence was understood for Halon 1301 and described in detail by Williamson.[49] Similar processes occur in all two-phase flows including air/water, steam/water, and refrigerant flows. In the context of clean agent system design calculations, this flow distribution is dealt with using empirical factors that redistribute the flow relative to the pure pressure-driven flow distribution which would occur without preferential phase distribution at tees.

Figures 4-7.17 and 4-7.18 illustrate these correction factors for Halon 1301 flows in bullhead and side-flow tees, respectively.[49] All of the halocarbon agent flow predictions require similar treatment. Side-flow tees and bullhead tees require independent empirical correction factors. One of the most important limitations to any flow calculation procedure is the maximum flow split allowed for each type of tee. For a bullhead tee, as one moves farther away from 50 percent/50 percent splits, the correction factor becomes greater, and at some point usually in the range of 80 percent/20 percent, it becomes so large that the prediction becomes unreliable. For side-allowable flow splits, ranges between 75 percent/25 percent and 90 percent/10 percent are typical. This correction

of flow splits at tees is one reason that final approval of engineered system designs should be constrained to calculation methods that have undergone testing within the range of flow splits required.

Pressure drop due to friction loss: The pressure drop caused by friction in the pipeline is calculated differently for two-phase fluids. The presence of agent vapor and gas affects the pressure drop per unit length of pipe. There are numerous methods for dealing with two-phase fluid pressure drop.[50,51] Those typically used for fire suppression agent calculations involve either (1) correcting the pressure drop estimated for single-phase fluid as a function of liquid to vapor/gas volume fraction or (2) empirical correlations of the pressure drop to average fluid density. Figure 4-7.19 illustrates the dependence of pressure drop on liquid volume fraction. In all cases for purposes of design of fire protection systems, the pressure drop is calculated on the basis of a homogeneous flow assumption where changes in the liquid fraction are seen as density changes in the homogeneous fluid.

Testing and approval of design methods: The approval or listing of a two-phase flow calculation procedure is part of the approval granted for engineered systems. Since some aspects of two-phase flow calculations are em-
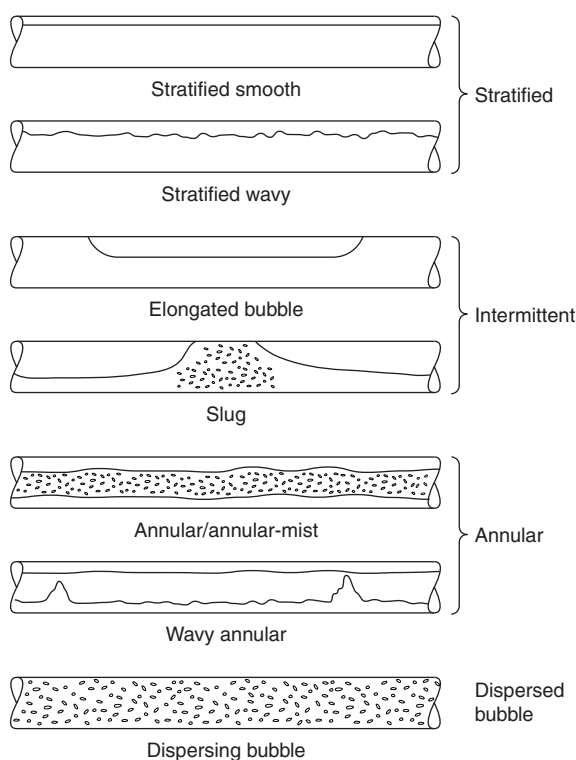
Figure 4-7.15. *Horizontal pipe flow regimes.[52]*

Figure 4-7.16. *Vertical pipe flow regimes.[52]*

pirically based (e.g., flow regime, pressure drop, and flow splits) and all calculation procedures have some bounds on their validity, testing is performed to verify the predictions and establish the limits of the calculation procedure. These limitations are crucial in helping to ensure that system designs do not exceed verified limits of calculation.

One of the most rigorous approval procedures used in verifying design methods is outlined by Underwriters Laboratories Inc.[35] UL 1058, *Halogenated Agent Extinguishing System Units,* was used for evaluating engineered Halon 1301 systems, but the same approach is taken for all clean agent alternatives. Design method limitations are described by the following ten parameters:

1. Percent of agent in piping (maximum)
2. Minimum and maximum discharge times
3. Minimum pipeline flow rates
4. Variance of piping volume to each nozzle
5. Maximum variance of nozzle pressures within a piping arrangement
6. Maximum ratio of nozzle diameter to inlet pipe diameter
7. Arrangement most likely to exhibit vapor time-imbalance condition at nozzle
8. All types of tee splits, including through tees, bullhead tees, and so forth
9. Minimum and maximum container fill density
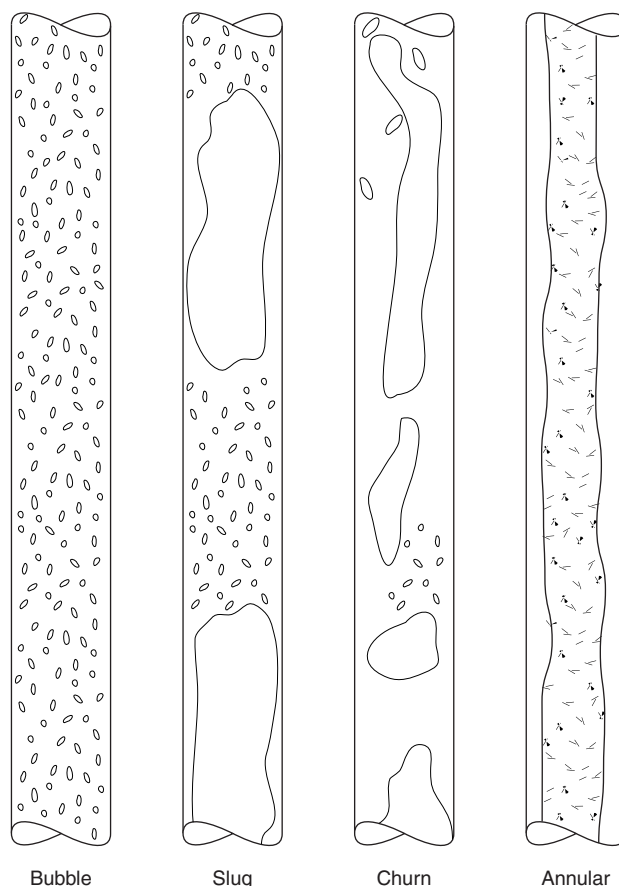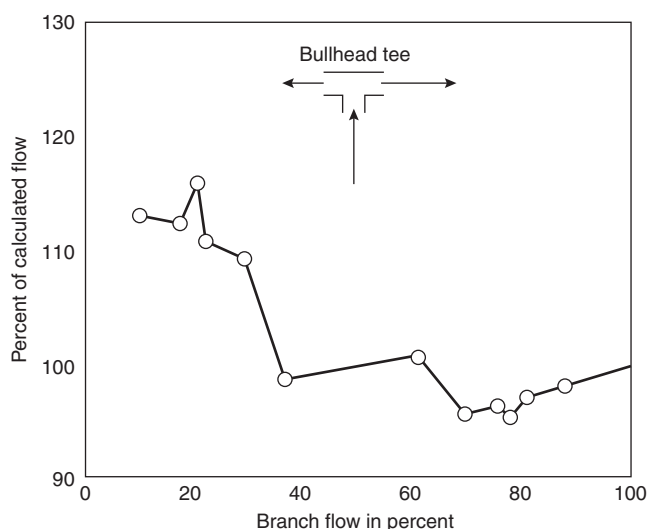10. Minimum and maximum flow split for each type of tee

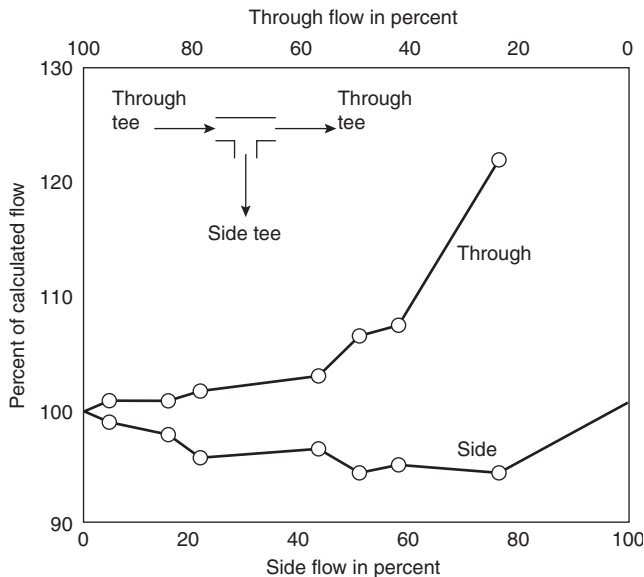**Figure 4-7.17.** *Bullhead-tee-flow split corrections for Halon 1301.[49]*

Figure 4-7.18. *Side- and through tee-flow split corrections for Halon 1301.*[49]
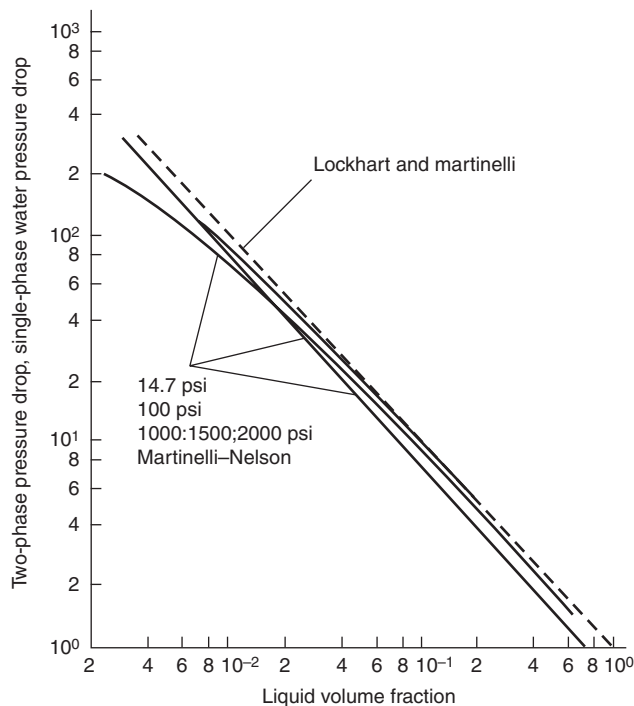

Figure 4-7.19. *Pressure drop versus liquid volume fraction.*[51]

These parameters are related to the important attributes of the agent discharge process previously discussed. Full-scale testing is performed to evaluate the performance of the design method. The limits on flow calculation method performance are as follows:

1. Actual versus predicted discharge time ±1 s
2. Actual versus predicted nozzle pressure ±10 percent
3. Actual versus predicted mass flow through a nozzle, −5 + 10 percent

Testing in conjunction with a particular manufacturer's hardware is important. Ensuring that pressure drop through a particular valve assembly is calculated properly and nozzle orifice discharge coefficient evaluation are two critical hardware-dependent verifications.

Several generic flow calculation routines have been developed.[37,53–56] Of these, two are directed at single-nozzle systems with very short discharge times[55] or relatively simple balanced networks.[54] It is not recommended that any generic calculation procedure be used for final design purposes, unless it has been tested with the specific hardware to be installed and the system is within the limitations derived by tests.

In order to preserve a 10-s discharge time, the mass flow rate of these clean agents must be higher than Halon 1301. The increased density of some of the alternative agents in the piping, caused by lower vapor pressures and nitrogen solubility differences, may result in high enough mass flow rates to retrofit existing Halon 1301 systems. While agent cylinders and nozzles will require replacement, it is often possible to preserve the existing Halon 1301 pipe network. Preservation often requires the use of lower fill density cylinders to increase the average system pressure throughout the discharge time. Any such retrofit using existing Halon 1301 piping must be carefully evaluated with respect to hydraulic performance, with particular care given to preserving minimum required nozzle pressures and flow divisions at tees.

Nozzle Area Coverage and Height Limitations

One of the most important requirements of a gaseous total flooding fire suppression system is the ability of the system to deliver a uniform concentration of agent throughout the protected enclosure. The nozzle design and minimum nozzle pressure are critical in ensuring this distribution of agent. The performance of the nozzle is evaluated by full-scale approval testing, such as UL 1058.[35] The basic testing performed to evaluate nozzles is as follows:

1. Establish minimum nozzle pressure and maximum nozzle height by ensuring extinguishment of heptane fires located throughout a space with a height equal to the maximum allowable, at the minimum allowable nozzle pressure.
2. Establish maximum nozzle coverage area by extinguishing tests in a plenum at the minimum height (generally less than 0.5 m) at the maximum nozzle coverage area (on the order of 100 m²) and minimum nozzle operating pressure.

There are substantial differences between hardware manufacturers relative to minimum nozzle pressure, maximum ceiling height, and maximum average coverage. All nozzle orientations should be evaluated. In general, maximum nozzle heights are on the order of 4 to 5 m, nozzle area coverage on the order of 9 to 10 m², and minimum nozzle pressure between 3 and 6 bar. It is critical to

ensure that the nozzle spacing, height, and minimum pressure limits are not exceeded for a particular manufacturer's hardware in a specific design.

The flow, mixing, and distribution of an agent from a nozzle into an enclosure can be predicted theoretically for relatively simple nozzle designs using sophisticated computer models.[54] Further development of such methods for complex nozzle designs and compartment geometries may eventually form the basis of a design procedure. At present, however, the primary means of ensuring adequate nozzle performance is the hardware approval process and real-scale testing.

Since many of the halocarbon replacements have lower vapor pressures than Halon 1301, there is often a much higher percentage of liquid at the nozzle. This liquid makes the task of vaporizing and mixing the agent in the compartment more difficult. In general, nozzle designs used for Halon 1301 systems are not adequate for the halocarbon replacement agents. Due to the increased liquid fraction at the nozzle, it is critical to ensure that no unenclosed openings exist along the trajectory of the nozzle orifices. Increased liquid fraction may result in significant preferential loss of agent through these openings. This condition further emphasizes the need for third-party approval testing of nozzle performance. In any retrofit situation, the nozzles will need to be replaced even if the piping is adequately sized to deliver adequate agent flow rates.

Compartment Pressurization

The rapid discharge of agent into a compartment will cause rapid changes in the compartment pressure. Depending on the agent and rate of discharge, the initial pressure change may be negative. Figure 4-7.20 is a plot of compartment pressure versus time for the discharge of HFC-227ea into a 28-m^3 room with a 360-cm^2 (56-in.^{2}) leakage area.[37] Immediately after discharge, the pressure in the compartment drops below ambient to a minimum of −0.3 kPa; at approximately 1.5 s after discharge began,
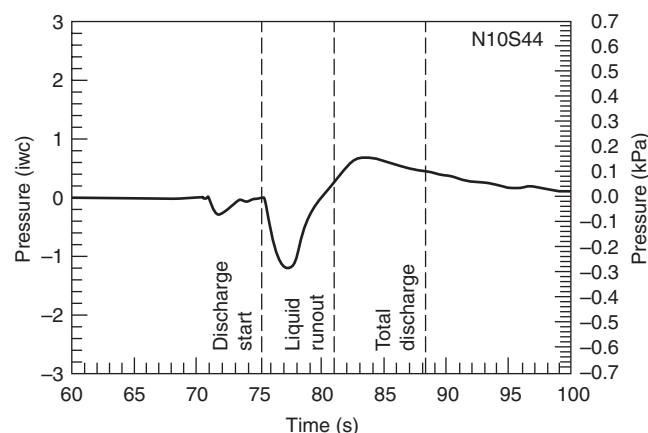
the pressure then begins to increase to a maximum of approximately 0.14 kPa after nozzle liquid runout. Similar results were obtained for FC-3-1-10. HFC-23 discharge exhibited much higher compartment overpressurization, without the marked initial negative pressure. The maximum overpressure for HFC-227ea and FC-3-1-10 discharge was similar to that of Halon 1301.

As the halocarbon agent is discharged into the space, it vaporizes rapidly, cooling the compartment and lowering the pressure. As the agent/air mixture gains heat from the walls or other objects in the space, the pressure recovers and, as additional agent is added, the pressure increases over ambient as mass is added to the compartment.

The expected maximum and minimum compartment pressure during discharge will be a function of the following:

1. Thermodynamic state of the agent at the nozzle
2. Nozzle design
3. Compartment volume and wall surface area
4. Size of fire
5. Initial conditions in space
6. Leakage area from compartment
7. Agent flow rate

For inert gases, significant compartment overpressurization can occur during discharge, unless adequate free vent area is provided. Calculation of required open area for venting is a part of the design manual for IG-541 systems.[57]

No generalized design procedure for calculating under/overpressurization has been established. Forssell and DiNenno[37] have developed a procedure for estimating the compartment pressure as a function of agent, agent flow rate, agent thermodynamic state at the nozzle, compartment volume, and surface area and leakage area. The method has not been sufficiently tested for general application.

Agent Hold Time and Leakage

Traditionally, total flooding gas systems were required to maintain a minimum concentration for a specified time period (10 to 20 min) after discharge. The minimum required hold time was based on the following:

1. Soak time required for deep-seated Class A fuels
2. Response time of emergency personnel
3. Prevention of reflash due to presence of hot surfaces and other reignition sources, particularly in flammable and combustible liquid applications

Currently, there is no specified minimum hold or soak time for clean agents. The variables described above will vary between installations, and there is no significant database on the performance of these agents on deep-seated fires other than wood cribs. The designer will be required to specify the minimum soak time consistent with the requirements of the hazard being protected.

The ability of a compartment to maintain adequate agent concentrations is a function of the leakage of the compartment. Historically, this was done with Halon 1301 through the use of discharge tests. Discharge testing for

Figure 4-7.20. *Pressure measured in 28-m^3 enclosure during C_3F_7H discharge, with nominal 15-s discharge time and 5-cm pan of n-heptane.*[37]

this purpose was rendered unnecessary by the introduction of door fan pressurization leakage tests. Appendix B of NFPA 2001 describes a complete procedure for evaluating agent hold time as a function of compartment leakage measured by the door fan pressurization method.

The only difference between alternative agents and Halon 1301 in this regard is the density of the agent/air mixture, which is the driving force for leakage in quiescent environments. The mixture density can be estimated as follows:[1]

$$\rho_m = V_d \frac{C}{100} + \left[\frac{\rho_a(100 - C)}{100} \right]$$

where

ρ_m = clean agent/air mixture density (kg/m³)

ρ_a = air density (1.202 kg/m³)

C = clean agent concentration (%)

V_d = agent vapor density at 21°C (kg/m³)

Agent vapor densities at 21°C are given below:

FC-3-1-10	9.85 kg/m³ (0.615 lb/ft³)
HBFC-22B1	5.54 kg/m³ (0.346 lb/ft³)
HCFC Blend A	3.84 kg/m³ (0.240 lb/ft³)
HFC-124	5.83 kg/m³ (0.364 lb/ft³)
HFC-125	5.06 kg/m³ (0.316 lb/ft³)
HFC-227ea	7.26 kg/m³ (0.453 lb/ft³)
HFC-23	2.915 kg/m³ (0.182 lb/ft³)
IG-541	1.43 kg/m³ (0.089 lb/ft³)]
Halon 1301	6.283 kg/m³ (0.392 lb/ft³)

All agents, except inert gases, have higher mixture densities than Halon 1301 at 5 percent when used at their design concentrations. This will require slightly more leak-tight enclosures to maintain the same hold time.

Summary

A wide range of inert gas and halocarbon total-flooding clean agents has been introduced over the past several years. More will be commercialized in the near future. The use of an agent must be consistent with applicable environmental regulations. The selection of an agent is driven by its fire performance characteristics, agent and system space and weight concerns, toxicity (particularly for use in occupied areas), and the availability of approved system hardware.

The design of clean agent systems must be carefully done in accordance with third-party listing and approval limitations on both agent and hardware. Given the relative lack of experience with systems employing these new agents, particular care in design, installation, inspection, testing, and maintenance is warranted. Design and installation standards, such as NFPA 2001 form the minimum requirements for these new technologies.

As generalized design methods and more detailed requirements evolve, the ability to design and install systems on a performance basis will increase. A critical part of the installation process is post-installation inspection and testing. NFPA 2001 contains requirements for the approval and post-installation inspection and test of clean agent systems. Bearing in mind the relative complexity of these systems and the importance of the detection system and enclosure integrity, post-installation inspection and testing should be rigorously performed.

References Cited

1. NFPA 2001, *Standard on Clean Agent Fire Extinguishing Systems,* National Fire Protection Association, Quincy, MA, 1994 edition.

2. T.A. Moore, "Cup Burner Analysis," *Halon Substitute Program Review,* (1993).

3. A. Hamins et al., "Flame Suppression Effectiveness," in *Evaluation of Alternative In-Flight Fire Suppressants for Full-Scale Testing in Simulated Aircraft Engine Nacelles and Dry Bays,* NIST SP 861, National Institute of Standards and Technology, Gaithersburg, MD (1994).

4. M.L. Robin, "Properties and Performance of FM-200™," in *Proceedings of the Halon Options Technical Working Conference 1994,* New Mexico Engineering Research Institute, Albuquerque, NM, pp. 531–542 (1994).

5. R. Sheinson et al., "Halon 1301 Total Flooding Fire Testing, Intermediate Scale," in *Proceedings of the Halon Options Technical Working Conference 1994,* New Mexico Engineering Research Institute, Albuquerque, NM, pp. 43–53 (1994).

6. T.A. Moore et al., "Intermediate Scale (645 ft³) Fire Suppression Evaluation of NFPA 2001 Agents," in *Proceedings of the Halon Options Technical Working Conference 1993,* New Mexico Engineering Research Institute, Albuquerque, NM, pp. 115–127 (1993).

7. M.J. Ferreira et al., "Thermal Decomposition Product Results Utilizing PFC-410," in *Proceedings of the Halon Options Technical Working Conference 1992,* New Mexico Engineering Research Institute, Albuquerque, NM (1992).

8. "Extinguishing Behavior of Inert Gases," *Final Report,* VdS, Cologne, Germany (1998).

9. UL 2166, *Halocarbon Clean Agent Extinguishing System Units,* Underwriters Laboratories Inc., Northbrook, IL (1999).

10. UL 2127, *Inert Gas Clean Agent Extinguishing System Units,* Underwriters Laboratories Inc., Northbrook, IL (1999).

11. R.E. Tapscott, "Best Values of Cup Burner Extinguishing Concentration," in *Proceedings of the Halon Technical Options Technical Working Conference 1999,* New Mexico Engineering Research Institute, Albuquerque, NM, pp. 27–29 (1999).

12. L.A. McKenna et al., "Extinguishment Tests of Continuously Energized Class C Fires," in *Halon Options Technical Working Conference 1998,* New Mexico Engineering Research Institute, Albuquerque, NM (1998).

13. J.A. Senecal, "Agent Inerting Concentrations for Fuel-Air Systems," *CRC Technical Note No. 361,* Fenwal Safety Systems, (1992).

14. F. Tamanini, *Determination of Inerting Requirements for Methane/Air and Propane/Air Mixtures by an Ansul Inerting Mixture of Argon, Carbon Dioxide, and Nitrogen,* Factory Mutual Research Corp., Norwood, MA (1992).

15. E. Heinonen, "Laboratory-Scale Inertion Results," *Halon Substitutes Program Review,* (1993).

16. E.W. Heinonen, "The Effect of Ignition Source and Strength on Sphere Inertion Results," in *Proceedings of the Halon Options Technical Working Conference 1993,* Albuquerque, NM, pp. 565–576 (1993).

17. J.A. Senecal, "Explosion Protection in Occupied Spaces: The Status of Suppression and Inertion Using Halon and Its Descendants," in *Proceedings of the 1993 International CFC and Halon Alternatives Conference,* Washington, DC, pp. 767–772 (1993).

18. J.A. Senecal, D.N. Ball, and A. Chattaway, "Explosion Suppression in Occupied Spaces," in *Proceedings of the Halon Options Technical Working Conference 1994,* Albuquerque, NM, pp. 79–86 (1994).

19. T.A. Moore, "Large-Scale Inertion Evaluation of NFPA 2001 Agents," in *Proceedings of the 1993 International CFC and Halon Alternatives Conference,* Washington, DC (1993).

20. NFPA 2001, *Standard on Clean Agent Fire Extinguishing Systems—2000 Edition,* National Fire Protection Association, Quincy, MA, 2000 edition.

21. A. Vinegar and G.W. Jepson, "Cardiac Sensitization Thresholds of Halon Replacement Chemicals Predicted in Humans by Physiologically-Based Pharmacokinetic Modeling," *Risk Analysis,* 16, 4 (1996).

22. A. Vinegar, G.W. Jepson, and J.H. Overton, "PBPK Modeling of Short Term (0 to 5 min) Human Inhalation Exposures to Halogenated Hydrocarbons," *Inhal. Toxicol.,* 10, pp. 411–429 (1998).

23. A. Vinegar, *Performance of Monte Carlo Simulations of Exposure to HFC-227ea,* ManTech Environmental Technology, Inc., Dayton, OH (1999).

24. A. Vinegar, G.W. Jepson, M. Cisneros, R. Rubenstein, and W. J. Brock, "Setting Safe Exposure Limits for Halon Replacement Chemicals Using Phyiologically Based Pharmacokinetic Modeling," *Inhal. Toxicol.* (in press).

25. A. Vinegar, and G. Jepson, "Pharmacokinetic Modeling for Determining Egress from Exposure to Halon Replacement Chemicals," in *Proceedings of Halon Options Technical Working Conference 1998,* New Mexico Engineering Research Institute, Albuquerque, NM (1998).

26. A. Vinegar, and G. Jepson, "Ephinephrine Challenge for Cardiac Sensitization Testing versus Endogenous Ephinephrine," in *Proceedings of the Halon Technical Working Conference 1999,* New Mexico Engineering Research Institute, Albuquerque, NM (1999).

27. "Research Basis for Improvement of Human Tolerance to Hypoxic Atmospheres in Fire Prevention and Extinguishment," *EBRDC Report 10.30.92,* Environmental Biomedical Research Data Center, Institute for Environmental Medicine, University of Pennsylvania, Philadelphia, PA (1992).

28. J.C. Yang and B.D. Bruel, "Thermophysical Properties of Alternate Agents," in *Evaluation of Alternative In-Flight Fire Suppressants for Full-Scale Testing in Simulated Aircraft Engine Nacelles and Dry Bays,* NIST SP 861, National Institute of Standards and Technology, Gaithersburg, MD (1994).

29. R.S. Sheinson et al., "Halon 1301 Replacement Total Flooding Fire Testing, Intermediate Scale," in *Proceedings of Halon Options Technical Working Conference 1994,* New Mexico Engineering Research Institute, Albuquerque, NM, pp. 43–53 (1994).

30. J.C. Brockway, "Recent Findings on Thermal Decomposition Products of Clean Extinguishing Agents," 3M Report presented to NFPA 2001 Committee, Ft. Lauderdale, FL (1994).

31. I. Schlosser, "Reliability and Efficacy of Gas Extinguishing Systems," in *Proceedings of Conference on Fire Extinguishing Systems,* VdS, Cologne, Germany (1998).

32. *Halon Alternatives, A Report on the Fire Extinguishing Performance Characteristics of Some Gaseous Alternatives to Halon 1301, LPR6: July 1996,* Loss Prevention Council, Hertfordshire, UK (1996).

33. ISO 14520-1, *Gaseous Fire Extinguish Systems—Physical Properties and System Design, Part 1: General Requirements,* International Standards Organization, (2000).

34. T.A. Moore et al., "Intermediate Scale (645 ft³) Fire Suppression Evaluation of NFPA 2001 Agents," in *Proceedings of Halon Options Technical Working Conference 1993,* New Mexico Engineering Research Institute, Albuquerque, NM, pp. 115–128 (1993).

35. UL 1058, *Halogenated Agent Extinguishing System Units,* Underwriters Laboratories Inc., Northbrook, IL (1984).

36. G.G. Back et al., "Draft Report: Full-Scale Machinery Space Testing of Gaseous Halon Alternatives," USCG R&D Center, Groton, CT (1994).

37. E.W. Forssell and P.J. DiNenno, "Evaluation of Alternative Agents for Use in Total Flooding Fire Protection Systems," Contract NAS 10-1181, National Aeronautics and Space Administration, John F. Kennedy Space Center, FL (1994).

38. P.J. DiNenno et al., "Thermal Decomposition Testing of Halon Alternatives," in *Proceedings of the Halon Alternatives Technical Working Conference 1993,* New Mexico Engineering Research Institute, Albuquerque, NM (1993).

39. D.S. Dierdorf et al., "Decomposition Product Analysis During Intermediate Scale (645 ft³) Testing of NFPA 2001 Agents," in *Proceedings of the Halon Alternatives Technical Working Conference 1993,* New Mexico Engineering Research Institute, Albuquerque, NM (1993).

40. C.P. Hanauska, "Hazard Assessment of HFC Decomposition Products," presented at *1994 International CFC and Halon Alternatives Conference,* Washington, DC (1994).

41. C.P. Hanauska et al., "Hazard Assessment of Thermal Decomposition Products of Halon Alternatives," in *Proceedings of the Halon Alternatives Technical Working Conference 1993,* New Mexico Engineering Research Institute, Albuquerque, NM (1993).

42. M. Meldrum, *Toxicology of Substances in Relation to Major Hazards: Hydrogen Fluoride,* Health and Safety Executive (HSE) Information Centre, Sheffield, England (1993).

43. W. Dalby, *Evaluation of the Toxicity of Hydrogen Fluoride at Short Exposure Times,* Stonybrook Laboratories, Inc., Pennington, NJ, sponsored by the Petroleum Environmental Research Forum (PERF), PERF Project 92–90 (1996).

44. W. Machle and K.R. Kitzmiller, "The Effects of the Inhalation of Hydrogen Fluoride, II. The Response Following Exposure to Low Concentrations," *J. Ind. Hyg. Toxicol.,* 17, pp. 223–229 (1935).

45. W. Machle, F. Tharnann, K.R. Kitzmiller, and J. Cholak, "The Effects of Inhalation of Hydrogen Fluoride, I. The Response Following Exposure to High Concentrations," *J. Ind. Hyg. Toxicol.,* 16, pp. 129–145 (1934).

46. W.J. Brock, "Hydrogen Fluoride: How Toxic is Toxic? (A Hazard and Risk Analysis)," in *Proceedings of the Halon Options Technical Working Conference 1999,* New Mexico Engineering Research Institute, Albuquerque, NM, pp. 27–29 (1999).

47. W.A. Dumayas, "Effect of HF Exposure on PC Multifunction Cards," Senior Research Project, University of Maryland, College Park (1992).

48. E.F. Forssell et al., "Draft Report: Performance of FM-200 on Typical Class A Computer Room Fuel Packages," Hughes Associates, Inc., Columbia, MD (1994).

49. H.V. Williamson, "Halon 1301 Flow in Pipelines," *Fire Technology,* 13, 1, pp. 18–32 (1976).

50. D. Chisholm, "Predicting Two-Phase Flow Pressure Drop," in *Encyclopedia of Fluid Mechanics, Vol. 3* (N.P. Cheremisinoff, ed.), Gulf Publishing Company, Houston, TX (1986).

51. Y.Y. Hsu and R.W. Graham, *Transport Processes in Boiling and Two-Phase Systems,* Hemisphere Publishing Corporation, Washington, DC (1976).

52. D. Barnea and Y. Taitel, "Flow Pattern Transition in Two-Phase Gas-Liquid Flows," in *Encyclopedia of Fluid Mechanics, Vol. 3 (*N.P. Cheremisinoff, ed.), Gulf Publishing Company, Houston, TX (1986).

53. P.J. DiNenno et al., "Modeling the Flow Properties and Discharges of Halon Replacement Agents," in *Proceedings of the Halon Options Technical Working Conference 1994,* New Mexico Engineering Research Institute, Albuquerque, NM (1994).

54. E.B. Bird et al., "Development of Computer Model to Predict the Transient Discharge Characteristics of Halon Alternatives," in *Proceedings of the Halon Options Technical Working Conference 1994,* New Mexico Engineering Research Institute, Albuquerque, NM (1994).

55. T.G. Cleary et al., "Flow of Alternative Agents in Piping," in *Proceedings of the Halon Options Technical Working Conference 1994,* New Mexico Engineering Research Institute, Albuquerque, NM (1994).

56. W.M. Pitts et al., "Fluid Dynamics of Agent Discharge," in *Evaluation of Alternative In-Flight Fire Suppressants for Full-Scale Testing in Simulated Aircraft Engine Nacelles and Dry Bays, (*Grosshandler et al., eds.), NIST SP 681, National Institute of Standards and Technology, Gaithersburg, MD (1994).

57. Ansul Co., *Inergen System Design Installation and Maintenance Manual,* Ansul Co. (1994).

Additional Readings

P.J. DiNenno, "Content and Relevance of ISO and NFPA Guidelines," in *Proceedings of Conference on Fire Extinguishing Systems,* VdS, Cologne, Germany (1998).

M.R. Driscoll and P.E. Rivers, "Clean Extinguishing Agents and Continuously Energized Circuits: Recent Findings," in *Proceedings of the Halon Options Technical Working Conference 1997,* New Mexico Engineering Research Institute, Albuquerque, NM (1997).

NFPA 12A, *Standard on Halon 1301 Fire Extinguishing Systems,* National Fire Protection Association, Quincy, MA (1992).

R. Nieman, et al., "Evaluation of Selected NFPA 2001 Agents for Suppressing Class 'C' Energized Fires," in *Proceedings of the Halon Options Technical Working Conference 1996,* New Mexico Engineering Research Institute, Albuquerque, NM (1996).